UNCLASSIFIED

AD NUMBER
AD234626
LIMITATION CHANGES
TO: **Approved for public release; distribution is unlimited.**
FROM: **Distribution authorized to U.S. Gov't. agencies and their contractors; Administrative/Operational Use; OCT 1959. Other requests shall be referred to Bureau of Aeronautics (Navy), Washington, DC.**
AUTHORITY
NAVAIR ltr, 22 Apr 1980

THIS PAGE IS UNCLASSIFIED

~~26.2~~

DTM

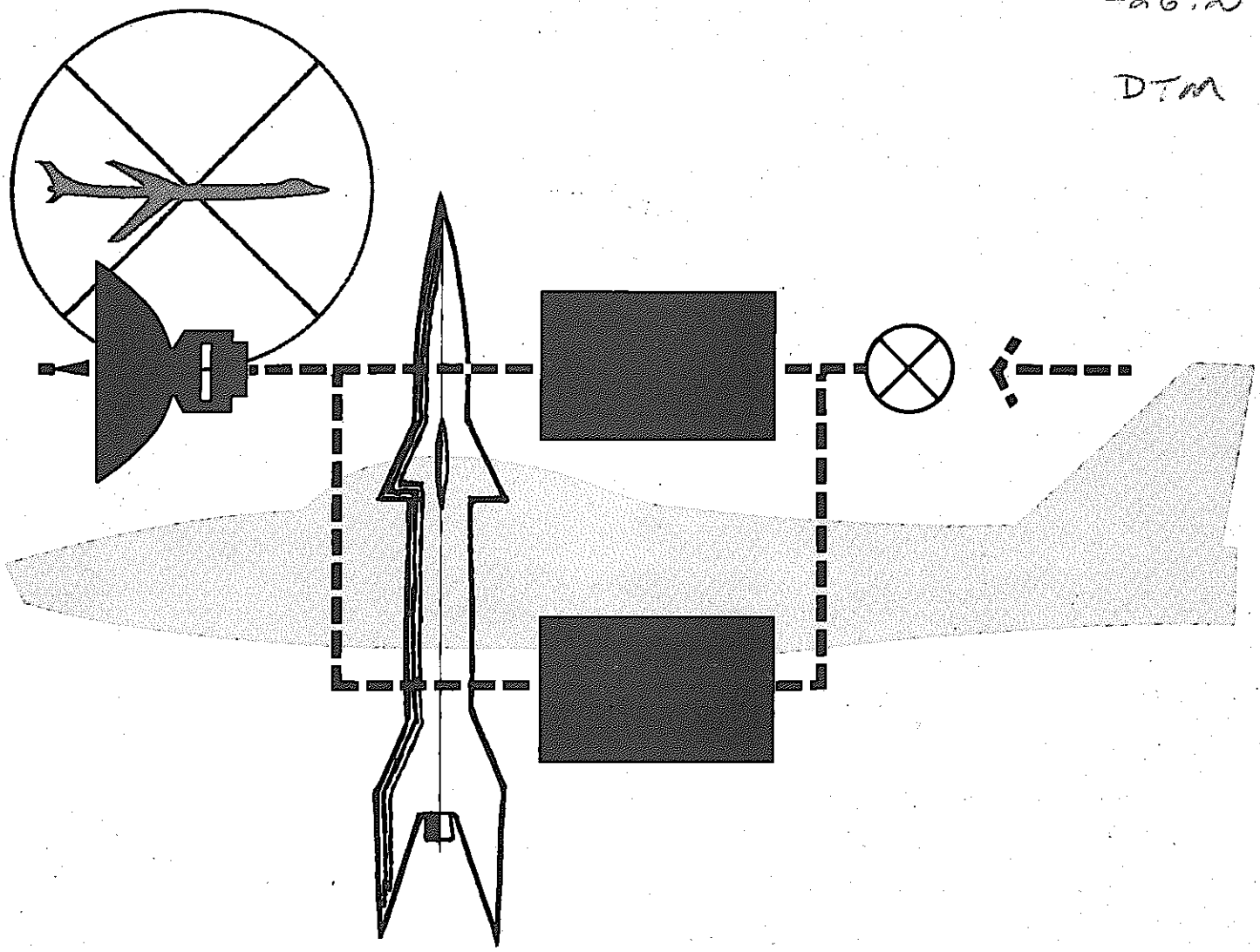

METHODS OF DESIGN AND EVALUATION OF INTERCEPTOR FIRE CONTROL SYSTEM

AE-6-4-VII

NORAIR A DIVISION OF NORTHROP CORPORATION

1 AUGUST 1969 THE IDENTIFICATION OF THIS DIVISION CHANGED TO:

Northrop Corporation
Aircraft Division

BuAer

Report AE 61-4-VII

VOLUME VII

METHODS OF DESIGN AND EVALUATION OF INTERCEPTOR FIRE CONTROL SYSTEMS

October 1959

NORAIR Division
Northrop Corporation

Prepared Under Sponsorship
of
BUREAU OF AERONAUTICS, NAVY DEPARTMENT

PREFACE

Early planning for this volume of the BuAer series was undertaken in 1952 when Northrop Corporation published the first six reports in this detailed study of Piloted Aircraft Systems. This latest book attempts to summarize a few of the ideas contained in the previous six volumes by extending these ideas to the complete fire control system. Although this is the only volume of the series to deal directly with fire control, much of the discussion has been curtailed by limitations on space, security classification and other factors.

The volume is intended only as a general treatise of the subject, system engineering of fire control systems, and concerns itself with the major concepts of evaluation and design. The actual design of fire control hardware, to provide more room for theoretical discussion, has been intentionally omitted.

Combat conditions establish the true operational criteria for the fire control system, and this means that the methods of evaluation covered in this volume indicate only a theoretical, noncombat study of the airborne fire control system and its key parameters. Actual combat would play a major part in tightening, or extending, these parameters. Although the volume is theoretical, the author has dedicated much effort toward reconciling the detailed, extensive literature of fire control systems with the main purpose of such a system--the destruction of a live target.

The major element of this volume presents system engineering concepts for design and evaluation of airborne fire control systems. A survey of existing fire control systems has been made in order to establish a sound basis for the methods described here. In numerous instances means are suggested for improving existing fire control system design by illustration of detailed advanced fire control concepts. The methods of system engineering are provided for the engineer concerned with systems analysis aspects of fire control design, that is, for the engineer who is required to incorporate fire control systems into airborne vehicles. To the technician attempting to comprehend the intricacies of a modern, complex interceptor weapon control system, this volume demonstrates the theoretical basis on which the myriads of hardware can be developed. To these individuals,

and to the many others concerned with the detailed, specialized aspects of airborne fire control, who wish to gain understanding of the complete system concept, this volume is respectfully dedicated.

The authors are indebted to those individuals and companies whose active and tacit support by publication of technical reports, books, and verbal reports, have made this volume possible.

Special appreciation is due to E. Rawlinson Jr. and R. L. Seifer for their diligence in preparing the manuscript for publication, to Nancy D. Standiford for her untiring efforts in preparing typewritten copy, and to M. G. Cornford, charged with the project implementation. The task of writing this book has been made possible by the continued interest and able consultation of C. B. Solloway.

C. J. Savant, Jr. Chief
Airborne Electronics Systems

J. L. Taylor, Chief
Weapon Systems Analysis

Compiled and Edited by

N. Almond

Contributing Authors

S. Moglewer
E. E. Veeveant
N. Almond

BUAER SERIES

1.	AE-61-4 I	Methods of Analysis and Synthesis of Piloted Aircraft Flight Control Systems
2.	AE-61-4 II	Dynamics of the Airframe
3.	AE-61-4 III	The Human Pilot
4.	AE-61-4 IV	The Hydraulic System
5.	AE-61-4 V	The Artificial Feel System
6.	AE-61-4 VI	Automatic Flight Control Systems for Piloted Aircraft

TABLE OF CONTENTS

			Page
		PREFACE	iii
CHAPTER	I	INTRODUCTION	1
Section	1	Purpose of the Volume	1
Section	2	Scope of the Volume	1
CHAPTER	II	THE TACTICAL ENVIRONMENT-DESIGN OBJECTIVES	5
Section	1	Introduction	5
Section	2	The Air Defense System	5
Section	3	The Threat	6
	(a)	Bombers	6
	(b)	Missiles	7
Section	4	Possible Enemy Tactics and Their Effect on Fire Control System Requirements	7
Section	5	Early Warning Systems	10
Section	6	Determination of Fire Control System Equipment Functions from Practical and Tactical Considerations	11
Section	7	Tactics and Counter-Countermeasures	13

Contents

			Page
Section	8	Summary of Fire Control System Requirements	15
Section	9	A Proposed System	16
Section	10	Description of a Typical Interception	17
CHAPTER	III	ARMAMENT	23
Section	1	Introduction	23
Section	2	The Guided Missile as a Part of the Fire Control System	24
Section	3	Guided Missile Classification	25
Section	4	Determination of the Optimum Interceptor-borne Missile Type	26
Section	5	The Warhead and Fuse	29
Section	6	Fundamental Differences between Missile and Interceptor Guidance and Control Systems	30
Section	7	Missile Auxiliaries	32
Section	8	Stowage and Launching	33
Section	9	The Proposed Guided Missile Armament	34
Section	10	General Constraints Imposed on the Fire Control System by the Missile Armament	35

			Page
CHAPTER	IV	THE RADAR	37
Section	1	Introduction	37
Section	2	General Radar Requirements	38
Section	3	Synthesis of a Fire Control Radar	40
Section	4	Search Radar Requirements	41
	(a)	Search Radar Range	41
	(b)	Search Radar Angular Coverage	43
	(c)	Search Radar Pattern Parameters	45
Section	5	Properties of the Transmitted Signal	52
	(a)	Pulse Radar	53
	(b)	CW Radar	56
	(c)	Comparison of Pulse and CW Radar	59
	(d)	Pulse-Doppler Radar	60
	(e)	Pulse-Doppler Filter Considerations	62
Section	6	Effect of the Type of Transmitted and Received Signal on Search Radar Design	72
Section	7	Search Radar Design - Miscellaneous Considerations	78
Section	8	Search Radar Range	80
Section	9	The Acquisition and Lock-On Phase	82

Contents

			Page
Section	10	Automatic Tracking	87
	(a)	Angle Tracking	89
	(b)	Range Tracking	95
	(c)	Velocity Tracking	98
	(d)	Other Loops	99
	(e)	Performance Specifications for the Tracking Radar	101
	(f)	Discrimination Against Range Ambiguity	102
	(g)	Track-While-Scan	102
	(h)	The Jam-Track Mode	102
Section	11	Identification Systems	102
Section	12	Block Diagram of the Proposed System	103
Section	13	Tracking Characteristics	105
Section	14	Detailed Discussion of the Various Blocks in the Proposed System	106
	(a)	Transmitter	106
	(b)	Indicators and Display System	106
	(c)	Duplexer	107
	(d)	Receiver	108

			Page
	(e)	Automatic Alert Unit	110
	(f)	Track-While-Scan Unit.	110
	(g)	Interrogator and Responsor (AAI) Units. .	110
	(h)	Lock-On and Recycle Unit.	111
	(i)	Search and Search-Stop Units	111
	(j)	The Range-Track Unit	111
	(k)	Velocity-Track Unit.	113
	(l)	Angle-Track Unit	115
	(m)	Antenna Drive and Angle - Search Units.	117
	(n)	The Antenna	118
	(o)	Radome	119
	(p)	Local Oscillator and Automatic Frequency Control.	119
CHAPTER	V	THE COMPUTER	121
Section	1	Introduction	121
Section	2	Computing and Control Requirements . . .	123
Section	3	Computer Functions.	124
Section	4	The Fire Control Problem	127

			Page
Section	5	The Computer Tracking Problem.	140
	(a)	Attack Phase	141
	(b)	Navigation Phase.	144
Section	6	Fire Control Computing Systems	151
Section	7	Attack Computer Requirements for a Proposed System	157
Section	8	Derivation of Attack Computer Equations.	159
Section	9	Mechanization of the Attack Computer as an Analog Computer	173
Section	10	The Digital Mechanization of the Attack Computer	179
	(a)	The Ballistics Program	180
	(b)	The Steering Program	185
	(c)	The Launching Program	189
CHAPTER	VI	INFRARED FIRE CONTROL SYSTEMS . . .	191
Section	1	Introduction	191
Section	2	Basic Components of the Infrared Systems	192
	(a)	Infrared Detectors.	192
	(b)	The Optical Subsystem	199
	(c)	Infrared Domes.	204

			Page
Section	3	Types of Infrared Systems	205
	(a)	Search Systems	205
	(b)	Track Systems	206
	(c)	Search - Track Systems	206
Section	4	Factors Affecting the Infrared System	206
	(a)	Atmospheric Transmission	206
	(b)	Target Radiation	207
Section	5	Infrared System Evaluation	210
CHAPTER	VII	ANALYSIS OF THE FIRE CONTROL SYSTEM	215
Section	1	Introduction	215
Section	2	Tracking System Radar Analysis	218
	(a)	Introduction	218
	(b)	The Antenna Tracking Loop	220
Section	3	The Velocity Tracking Loop	248
	(a)	Introduction to Velocity Tracking	248
	(b)	General Problems	250
	(c)	Detailed Design Considerations	258

			Page
Section	4	Ideal Servo Analysis in the Absence of Noise	259
	(a)	A Comparison of Frequency-and Phase-Locked Loops in the Absence of Noises	266
	(b)	Servo Analysis in the Absence of Noise	275
	(c)	Simplified Noise Analysis of a Frequency-Locked Loop	283
	(d)	The Range Tracking Servo	298
	(e)	Miscellaneous Considerations	321
	(f)	Range and Velocity Tracking Comparison	322
	(g)	Extraction of Angle Information from Scan Modulation	324
	(h)	Automatic Gain Control Considerations	325
	(i)	Phase Detector Operation	327
	(j)	Antenna Beam Distortion	333
CHAPTER	VIII	EVALUATION OF FIRE CONTROL RADARS	337
Section	1	Introduction	337
	(a)	General Evaluation Considerations	337

			Page
Section	2	Effectiveness of an Interceptor Fire Control Radar	340
	(a)	Radar Range Considerations	343
	(b)	Increasing the Radar Range.	348
Section	3	Evaluation by Theoretical Analysis.	350
	(a)	Pulse-Doppler Radar Evaluation Summary	350
	(b)	Range Performance	355
	(c)	The Pulse-Doppler Radar Phase Jitter . .	357
	(d)	Continuous Wave (CW) Radar.	358
	(e)	Side-Looking Radar	362
	(f)	Lobing Techniques.	363
	(g)	Evaluation of Range Rate Techniques . . .	366
	(h)	Tracking Radar.	370
Section	4	Range of Tracking Radar.	375
Section	5	Evaluation of Tracking Radar	381
Section	6	Effect of Noise on Detection.	386
Section	7	Evaluation of Ground Testing.	398
	(a)	Radar Self-Test Evaluation - General . . .	398
	(b)	Analog and Digital Computers in System Test and Evaluation.	400

			Page
Section	8	Evaluation by Airborne Testing	408
	(a)	Airborne Fire Control Systems Testing. .	408
	(b)	Development of the Cumulative Probability Curve from Flight Test Data .	414
	(c)	Flight Test Evaluation of Laboratory Model Pulse-Doppler Radar.	416
	(d)	Flight Data Compilation Techniques	417
	(e)	Evaluation of Radar Detection from Flight Data.	418
	(f)	Role of the Airborne Digital Computer in Advanced Fire Control System Evaluation	421
	(g)	Mission Effectiveness	422
	(h)	Airborne Attack Test Simulation	423
Section	9	Results of Evaluation Studies.	424
CHAPTER	IX	TECHNIQUES OF ESTIMATING WEAPON SYSTEM EFFECTIVENESS	427
Section	1	Weapon-Target Parameters	427
Section	2	Weapon Systems Analysis	429
	(a)	Maneuver Barrier	432
	(b)	Antenna Scan Barrier.	435
	(c)	Sector Barrier	437

			Page
	(d)	Lock-On Barrier	437
	(e)	Maximum Time Barrier	438
	(f)	Nortam Formulation	439
	(g)	Comparison of Barrier and Simulation Techniques	444
	(h)	Missile Simulation Techniques	444
Section	3	Mission Effectiveness	445
Section	4	Force Effectiveness	448
APPENDIX A		Associated Fire Control Subsystems	453
APPENDIX B		Example of a Weapon System Interception Model	463
APPENDIX C		Discussion of Fire Control Radar Errors and Correlation	491
APPENDIX D		Noise and Fire Control Systems	499
APPENDIX E		Nonlinear Theory of Conical Scanning	513
APPENDIX F		Angular Scintillation Theory	523
APPENDIX G		Prediction and Filtering Problem	533
BIBLIOGRAPHY			547

CHAPTER I

INTRODUCTION

SECTION 1 — PURPOSE OF THE VOLUME

This volume proposes to describe: first, the system considerations that must be made in the design of fire control systems; second, evaluation techniques for the designed system; and finally, methods for estimating weapon system effectiveness. The fire control discussions are limited specifically to the case in which the carrier is an interceptor to be used against bomber targets. The basic weapons carried by the interceptor are assumed to be air-to-air guided missiles. The fundamental fire control problem is that of launching missiles from the interceptor at a target in a manner that will ensure a high probability of target kill.

The ideal way to design an optimum system is by synthesizing it from the design objectives and the performance specification. This report proposes a basic system, then analyzes this system in order to optimize the parameters. This procedure, although not purely one of synthesis, will yield the best fire control system in the least time.

SECTION 2 — SCOPE OF THE VOLUME

Since the purpose of the fire control system is target kill, the order in which the subject is discussed begins with the tactical environment of the weapon. The next topic is the armament, and discussion of it starts with the warhead and fuse. Because the type of warhead strongly affects the fire control system design, this consideration precedes the main discussion of fire control system principles. The implementation of a system follows and includes both radar- and infrared-type tracking systems. Less material is devoted to infrared than to radar, because much of the same equipment and design philosophy can be used in both types of systems. The principal difference occurs in the front end of the fire control system (where an optical system and infrared detector are used in the infrared system in place of the conventional radar antenna). Once the control signals have been developed by either IR or radar means, the remainder of the fire control system can be identical in both cases.

The over-all problem is treated as though the engineer were faced with the problem of designing a complete all-weather interceptor armed with guided missiles and capable of completely automatic operation from takeoff to touchdown, including navigation, attack and launching, target kill, return to base, and landing. Naturally, any or all of these phases could be carried out by manual operation of the interceptor. The key divisions in the over-all system are the radar and the computer. These subdivisions receive principal attention in this volume. Appreciable analysis is also included in the design and evaluation studies. Procedures for optimizing the fundamental parameters of importance in the tracking and control systems are also developed. Several concepts which include noise and information theory are detailed in the appendices. To coordinate and illustrate the principles of the analysis being developed, a specific example, referred to as the proposed or "illustrative" fire control system, is carried throughout the chapters on design. This fire control system consists of a pulse-doppler radar system with either semiactive radar or passive infrared air-to-air missile armament.

The completed work may be used as a text or reference book on airborne fire control systems for guided armament. The specific organization and scope of the material can be found from an investigation of the table of contents.

Following the introductory chapter, Chapter 2 includes a discussion of the tactical environment, and the design requirements imposed by this environment. The principal purpose of the volume is to describe technically a suitable design of a fire control system; the design is effectively dictated by the tactics available to the enemy. Of importance also are the tactics available to the interceptor and other friendly aircraft. The tactical situation is, therefore, presented from the point of view of its effect on the design philosophy of the basic fire control system. The subject of Chapter 3 deals with the armament. The detailed design of the armament is not explained, since such a discussion is beyond the scope of this volume. Nevertheless, the end purpose of the fire control system is the proper launching of the armament to maximize the probability of target kill and, consequently, a general discussion of the armament is in order. This chapter precedes the principal fire control discussion since the choice of type of armament affects the design philosophy and objectives of the fire control system.

The two principal components of the fire control system, the radar and the computer, are considered in detail. The radar system is treated in Chapter 4. The radar, which serves as the "eyes" of the system, develops the required angle, range, and velocity information needed to guide the interceptor to the proper course for missle launching and to provide the proper prelaunch and firing signals to the guided armament. The radar section is divided into two categories: first, the design of a search radar with acquisition and lockon phases; and second, the design of a tracking radar. The proposed system tracks in range and velocity as well as in angle. Following the discussion of general philosophy, a block diagram of a proposed system is presented along with a detailed discussion of the blocks.

Chapter 5 discusses the other principal component of the fire control system, namely, the computer. This chapter includes discussion not only of the computing and control function requirements, but also of the geometric problem of tracking and the general problem of navigation, particularly during the attack phase. The navigation equations which are used to control the interceptor are derived in this chapter, and navigation systems and principles are discussed. Subsequently, an attack computer is developed and mechanized both as an analog and a digital computer.

Chapter 6 considers the basic principles of infrared (IR) fire control systems. Chapter 7 is a fire control system analysis. An overall systems analysis and a detailed analysis of the various principal components in the tracking system, the computer, and the aircraft control system are given in this chapter. Particular emphasis is made of the optimum design of the principal tracking loops in the radar. These tracking loops include the angle tracking system, the range tracking system, and the velocity tracking system. In the analysis, an electromagnetic-type radar is assumed as the subject; however, the analysis applies equally well to infrared systems. In the analyses, a procedure is outlined for determining the optimum parameters for the expected type of input signals. The chief parameters for the radar system design are maximum radar range and accuracy compatible with tactical considerations. The principal difficulty encountered in attempting to increase range lies in the contamination of the input signal by noise, jamming, and other undesirable random influences. Included in Chapter 7 is a discussion of computer types and an analysis of the general prediction problem in fire control radar. The chapter also contains a discussion of the search radar and,

in particular, applications of information theory to the determination of optimum search radar parameters so that the radar can accept information at the maximum rate.

The material through Chapter 7 outlines considerations required in the design of a fire control system and in analyzing the system to optimize its parameters. Chapter 8 uses a designed system to present methods of field evaluation to determine whether the optimum design has been attained. Chapter 9 investigates techniques of estimating weapon effectiveness. This represents another phase of evaluation and includes a discussion of mission effectiveness. To present some of the basic background material necessary for a noise analysis of the system, certain appendices are included. These include appendices on information theory, noise, conical scanning, and angular scintillation theory.

A diagram of the fundamental blocks of the fire control system is shown in Figure 1-1. Inputs to the fire control computer include signals from the radar, the inertial navigator, and air data computer. The outputs from the tracking system and the flight instruments are applied to the computer. The computer makes the necessary computations to guide the aircraft on a course suitable for missile launch, and supplies appropriate prelaunch and launch signals for guided missile armament.

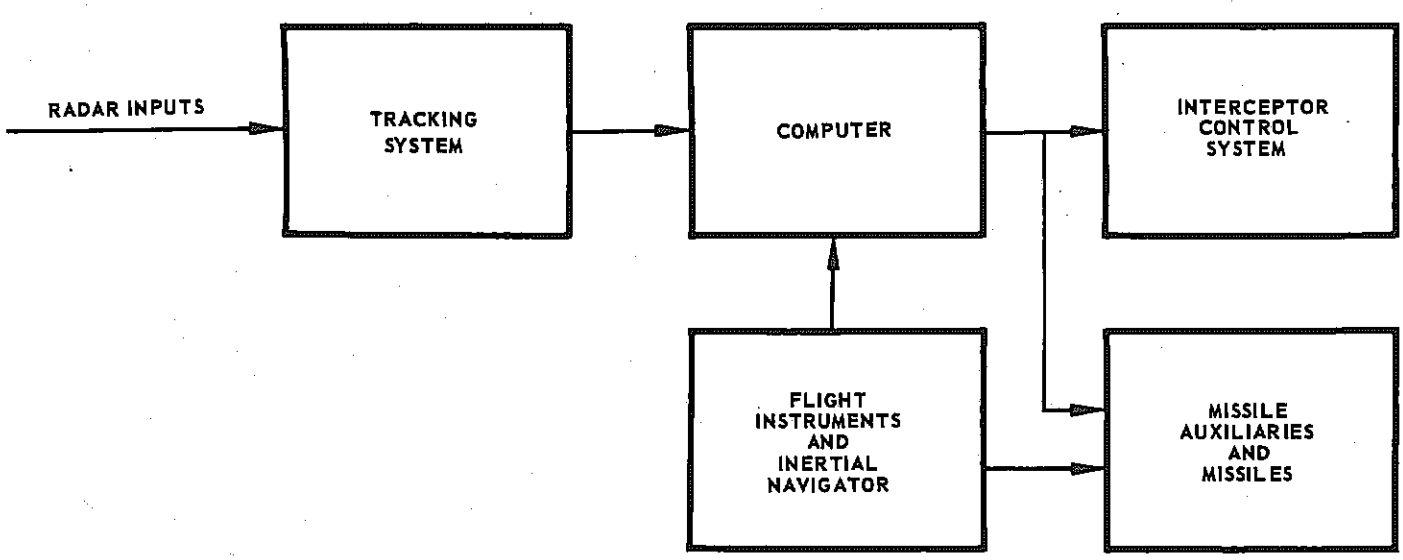

FIGURE 1-1. BASIC BLOCK DIAGRAM OF THE OVER-ALL FIRE CONTROL SYSTEM

CHAPTER II

THE TACTICAL ENVIRONMENT - DESIGN OBJECTIVES

SECTION 1 — INTRODUCTION

Although the principal purpose of this book is to provide a technical description of fire control systems, the proper design of not only the fire control equipment but the entire weapons system is dictated by the tactics available to the enemy. Consequently, time will be spent describing the tactical environment, which includes the friendly interceptor and the enemy aircraft (assumed to be a bomber).

It is assumed that no prior knowledge of enemy tactics is available and that the enemy will use all feasible tactics.

SECTION 2 — THE AIR DEFENSE SYSTEM

The defense of a vast complex is extremely complicated by the large variety of possible attacks. The defense complex consists of the interceptor-weapon systems, the auxiliary ground and airborne warning and control systems, and the target. The purpose of any air defense system is to destroy the greatest possible number of enemy aircraft before they come within lethal range of their target. The intercepting tactics are determined by a number of factors, including (1) speed, range, altitude, and maneuverability of the target, (2) the formations and approaches used by the enemy, (3) the offensive armament possessed by the enemy, (4) the targets which the enemy has selected, (5) the countermeasures the target can be expected to employ, and (6) the defensive weapons carried by the target. The enemy will attack in whatever way necessary to minimize the effectiveness of the defense and still inflict the greatest damage on the selected target. In order to destroy an enemy attack, the air defense system must be capable of detecting the enemy, alerting the appropriate interceptors, scrambling the fighters and vectoring them into the desired attack area, launching the weapons with a high probability of kill, and returning the interceptors safely to the base. Other schemes for the defensive situation than that just described could be designated; for example, the use of ground-to-air or long range guided missiles. But, since this book is concerned primarily with airborne fire control systems, the

emphasis will be on airborne defense systems, rather than on the more complex problems of complete territorial defensive systems. In this volume, a manned-interceptor is assumed to be the fire control system carrier. The interceptor will be assumed to be completely automatic and essentially a guided device. Many of the fire control system problems encountered and the solutions suggested are, therefore, directly applicable to guided missile design.

Because of the diverse characters of possible enemy attacks, great versatility is demanded of the air defense system. Since a single enemy aircraft equipped with high lethal radius weapons can inflict vast damage on potential targets, the air defense system must be virtually impregnable. This impregnability requires perfection of the reliability and efficiency of the defense system. These general requirements are made somewhat less abstract by a knowledge of specific enemy equipment and tactical constraints. However, dependence on intelligence information alone is not sufficient defense. Such knowledge only puts broad general bounds on the problem as described.

SECTION 3 — THE THREAT

Intelligent design of weapon systems demands that the threat be defined, at least within general bounds. Although the idea of a single weapon system for use against all possible enemy threats is a very attractive one, it is unrealistic. In general, the fewer the demands put on a weapon system, the more efficient it will be. A compromise is made, based on the tactical environment, technical, and "state-of-the-art" limitations, and the defense system is tailored to the enemy threat.

Unfortunately, much specific data on both defensive and enemy tactical capabilities are classified. However it is not unreasonable to assume that the following weapons might be operational.

(a) BOMBERS

A high Mach manned bomber which is operational at altitudes up to 100,000 feet and still supersonic at sea level. Countermeasures, evasive maneuvers, and defensive armament can be expected.

(b) MISSILES

Ground-to-air and air-to-air missiles capable of high Mach speeds at altitudes in excess of 100,000 feet are possible. Both passive and active (or semiactive) homing can be expected and nuclear warheads are quite likely.

SECTION 4 — POSSIBLE ENEMY TACTICS AND THEIR EFFECT ON FIRE CONTROL SYSTEMS REQUIREMENTS

To maximize the effectiveness of an interceptor defense system, it is necessary to make a reasonable estimate of possible enemy tactics. This requires a study of likely target areas, the tactical environment, etc. The fundamental defense objective is the maximization of enemy attrition to prevent defense penetration. The results of such a study set the requirements for base location, number of bases, early-warning system capabilities, interceptor performance, etc., as well as for fire control system design. So far as the interceptor fire control system is concerned, the desired tactical properties it should possess include:

(a) Ability to attack high speed, high altitude targets.
(b) Long detection and tracking ranges for combating enemy attacks for which there is adequate early warning.
(c) Ability to track at high relative target-missile velocities and angular rates.
(d) Ability to operate properly from any attack aspect.
(e) Ability to tolerate large vectoring errors and evasive target maneuver.
(f) Good capability against multiple targets and decoys.
(g) Good capability against chaff, ECM, and other countermeasures.
(h) Good capability against low altitude targets - good surface clutter and background noise rejection.

All of these abilities contribute to a high probability of target kill.

The enemy tactics which determine some of the above-mentioned system requirements will be considered in greater detail. Enemy bombers can be expected at altitudes up to 100,000 feet. The range of altitudes and velocities is much more restricted if the bombers are to optimize their range and fuel consumption. The most likely attack is probably one

in which the optimum bomber velocity and altitude are maintained until the defended area is approached. At this time, range and fuel economy are sacrificed by either climbing to very high altitudes to make interception difficult, or descending to very low altitudes to make radar detection and early warning difficult. In the target vicinity, high bomber velocities are quite likely. The low altitude detection problem is particularly difficult because of absence of early warning, and deterioration of both interceptor and missile radar performance.

When adequate early warning exists, it is desirable to launch the defensive armament as early as possible, so that the enemy weapon and bomber are destroyed as far from the defended area as possible. Obviously this is particularly important when the enemy is carrying atomic or nuclear bombs. This requirement demands that the search, lockon, and tracking systems in the interceptor be capable of operating over long ranges at low signal-to-noise ratios. This basic technical problem is considered in detail in this volume. It is also desirable that the interceptor armament have as long a range as possible in order that the interceptor be afforded the greatest possible time for protective maneuvering.

The interception of high performance bombers by aircraft implies that high interceptor-target relative velocities and angular rates exist. These conditions set minumum requirements on fire control system accuracy, especially on tracking accuracy. High velocities demand good range and velocity tracking capability; high angular rates demand good angle tracking capability.

High probability of kill imposes the requirements not only of high system reliability and high performance weapons, but also of optimum launching and control of the weapon. Optimum launching implies minimum directional error, optimum range, and good lockon for the missile at launch. If postlaunch control or target illumination is required by the missile, the fire control system must sustain high-accuracy missile performance while the interceptor remains at the greatest possible distance from the kill locality.

The bomber interception may occur at any target-interceptor relative aspect and, therefore, the fire control system should be capable of locking on, tracking, and launching missiles at corresponding aspects. This

requirement is difficult to achieve and depends to a great extent on interceptor capability.

The typical interceptor mission is one in which the interceptor is vectored into the target area from the ground. GCA radar and other ground equipment may supply vectoring information which is lacking in accuracy. In spite of this, the fire control system must be able to locate and lock onto the suspect target. After lockon, the interceptor must track the target, which may maneuver and perform other evasive operations.

The enemy can employ multiple bomber formations in a raid on a defended area. The fire control system and the missile must distinguish individual bomber targets to prevent tracking of and launching at a "group center" of the formation. Bombers can be spaced in formation and the velocities of the bombers can be controlled relative to each other so as to make range and/or velocity discrimination difficult. The bombers can be located sufficiently close together to make angular resolution difficult and yet sufficiently far apart to make the probability of kill from small or even medium kill-radius warheads small. These conditions impose a requirement for high resolution capability of the interceptor radar. If a formation occupies a finite fraction of the radar field of view, randomness in direction of arrival of the received signal, i.e., "angular scintillation," creates another source of noise in the presence of which the fire control system must operate satisfactorily. This effect also occurs with single targets which similarly occupy a finite portion of the field of view. Multiple targets, therefore, represent a form of enemy countermeasure. The enemy can also employ passive countermeasures such as decoys. These can be unarmed expendable aircraft or simple reflectors which provide large radar cross sections for the tracking radar system.

The enemy can also employ active as well as passive electronic countermeasures. Chaff can be fired in any direction and at various rates. The fire control system must be capable of distinguishing chaff from true targets and of discriminating against the chaff. Various active countermeasures such as noise jamming using either "barrage" jamming (noise spread over a wide band) or "spot" jamming (high density noise in a localized frequency region) should be considered in the fire control system design. The fire control system and all of the interceptor electronic equipment must be designed to minimize the effect of the possible enemy countermeasures.

The radar detection range for early warning systems as well as airborne fire control systems is limited by ground clutter effects. The enemy can implement the bomber attack at low altitudes so that the radar signal return is confused by ground or sea clutter. The radar horizon limits early detection and lockon, especially for ground based equipment. Ground target return signals give rise to a multiple target noise problem. The radar fire control system must be able to discriminate against this surface clutter. The fire control system must further be capable of distinguishing true targets from false targets, clutter, and background noise, and be able to track the target with a low probability of target loss.

The preceding paragraphs have described some of the possible enemy tactics which determine the character of the defense system in general, and the airborne fire control system in particular.

SECTION 5 — EARLY WARNING SYSTEMS

The interceptor is one part of the over-all defense complex. Ground-based early warning equipment is equally important to the success of the defense. Limitations of the ground control equipment will greatly affect the design of the airborne fire control system.

A minimum defense system for the continental U. S. consists of the following elements:

(a) The DEW radar line located partly within the arctic circle protecting the northernmost reaches of North America. This line provides early warning target position and heading information.

(b) The McGill fence in Canada which reports target position. Between the DEW and McGill lines are located radars and other observing stations.

(c) Continuous radar coverage of at least 500 miles outside the boundary of the U. S. including the Canadian Pinetree line, AEW aircraft, picket ships, off-shore Texas Towers and shore-based heavy radars.

(d) The SAGE system. In this system, the U. S. is divided into sectors, each of which contains a direction center and command post. Information is sent from each radar to the direction center for processing. Incoming data are presented on scopes and monitors. This information is sent to computers which compare it with information from known aircraft in the area. If the identification is unfriendly, the weapons

director makes a decision as to the type of interception required and "scrambles" a flight of interceptor aircraft.

The fire control system must be coordinated within this defense system. The interceptor must have a data link for interceptor vectoring, target acquisition, etc. The interceptor system design is a function of the range of the ground based radar as well as the accuracy of vectoring and target data available to the interceptor. Since interceptor performance is degraded by weight, as many of the necessary electronic functions as possible should be performed on the ground.

SECTION 6 — DETERMINATION OF FIRE CONTROL SYSTEM EQUIPMENT FUNCTIONS FROM PRACTICAL AND TACTICAL CONSIDERATIONS

The effect of enemy tactics on fire control system design has been considered thus far in generalized aspects. A brief description of early warning systems and their effect on fire control design has also been included. It is necessary now to assign tasks to the various parts of the interceptor control system. A principal function of the interceptor system is to receive or derive target information and process that information into control signals. By this means, the interceptor can be flown to positions from which guided missiles can be launched with high probability of kill.

Some of the functions necessary to attain the interception objective can be performed by human operators, both in the aircraft and on the ground, to avoid the need for excessive amounts of interceptor equipment, which can degrade aircraft performance.

In general, as much equipment as possible should be ground-based, where it may be maintained conveniently and is not subjected to the severe interceptor environment. Of even greater importance is the fact that the interceptor aerodynamic performance is penalized by excessive equipment. The equipment required by the interceptor can be determined by considering first the necessary armament for enemy kill.

If the missile armament is passive (infrared, for example) or active (containing transmitting and receiving equipment), no control from interceptor to missile is needed after launch. If, however, semiactive seekers (no missile-borne transmitters) are employed, the target must be radar

illuminated until the target is destroyed. Assume that both semiactive and passive missiles are carried, the interceptor must illuminate the target with the fire control radar in order to guide the semiactive missiles after launch.

From the missile requirements, the missile launching and prelaunch equipment can be determined. Although well-designed missiles can correct in flight for some initial launching error, excessive error appreciably decreases the probability of kill. The accuracy of the interceptor data provided by ground stations which may be many miles from the point of interception is comparatively poor so that at the time of missile launch it is necessary to have control provided by the airborne radar. The airborne radar must not only illuminate the target during the period from launch until impact, but must also track the target for a time prior to launch. The term "tracking" as used here includes the selection or "gating" of a specified target from other targets and noise, and the maintaining of this condition as the target signal strength varies with time. It can thus be seen that data must be supplied at the proper time by the tracking radar to control the interceptor system. The target must first be located and then locked onto in order for the radar to track. Target location data provided by the ground system are usually so inaccurate that a search mode must be included in the interceptor radar. The search and lockon functions generally must take place in angle, in range and in velocity. Tracking in range and/or velocity improves signal-to-noise ratio and also discriminates against multiple targets and countermeasures. Range and velocity tracking also provides for the determination of the optimum missile firing time, appreciably improving the missile probability-of-kill.

Since the interceptor receives data from the ground control system, it must have data link and voice communications systems. Because the data from ground stations are comparatively inaccurate, they must be combined with information obtained from interceptor fire control system measurements of the same data; the combined data are processed in the airborne computer for use in the interceptor control system, the missile launching system, and the missile. Although much of this information can be displayed for use by the pilot, the conditions at supersonic speeds cause human reactions to be slow and human judgment subject to gross error so that the decisions required during the attack must be made by a computer. The computer thus provides the required computational data to the control systems, to the pilot's display, and to the missile.

The equipment which the interceptor must carry includes the missile and launcher, missile auxiliaries, radar, computer, and auxiliaries such as power supplies. Additional essential equipment includes automatic aircraft control equipment, pilot's display, air-to-ground communications system, data link, and other equipment. Other equipment which is sufficiently important to be included consists of a decoder for coded ground-to-air data transmissions, equipment for automatic landing systems and for air-traffic control devices, identification, equipment, and navigational equipment for enroute navigation.

The interceptor must eventually depend on its own data gathering capability, at least for the short period from the time of airborne radar lock-on to target kill. The other interception operational phases (namely takeoff, navigation to target area, turn, return to base, and landing) can be controlled from the ground. These phases require a ground radar system capable of tracking and maintaining surveillance, not only on all of the targets approaching the defended area, but on all of the interceptors as well. The interceptors must be supplied with target and interceptor position and heading, and information about the optimum target in a group of targets. Information regarding other aircraft in the vicinity must also be provided from the ground radar system. The ground system must also be capable of multiple target "tracking and scanning" and must be able to correlate information gained from each of the various aircraft in its area of search. This information must be collected and processed by a ground computer, which finally transmits the computed data to the proper interceptor.

One general technique used in deciding what equipment should be included in the interceptor fire control system requires the interceptor to carry sufficient equipment to make the aircraft as independent of ground control as possible. At the same time it is required that the interceptor be sufficiently light and compact so as not to degrade aircraft performance to the point where successful interceptions are limited or prevented.

SECTION 7 — TACTICS AND COUNTER-COUNTERMEASURES

The design of a fire control system depends not only on the bomber tactics, but also the interceptor tactics and capability. The probability of success of a mission may be considered as the product of three

probabilities: (1) the probability of intercept, i.e., the probability of reaching the combat zone and detecting the target, (2) the probability of detecting the target sufficiently early for the interceptor to bring its missiles into readiness for firing, and (3) the probability of weapon effectiveness.

The first probability is determined by the "early-warning" detection, which is a function of the time required by the ground systems to (1) process the information, (2) make a decision, and (3) "scramble" the interceptors. This probability is also determined by the interceptor performance (rate of climb, speed, range, maneuverability, etc.).

The second probability is determined by the ground vectoring accuracy, the accuracy and extent of the interceptor fire control system capability (especially radar detection range), aircraft maneuverability, and armament ballistics.

The third probability, that of weapon effectiveness, depends on the type of armament selected, particularly its range, aerodynamic performance capability, fuse, and warhead.

All the probabilities assume perfect functioning of the equipment involved. Equipment reliability is a very important factor in determining the probability of mission success and kill.

This chapter is not concerned with the calculation of tactical regions within which successful attacks can be made, but instead, it attempts to show the interrelationship of tactics and performance and, in a general way, indicates a choice of design parameters. It is important, however, to discuss the relative importance of various design and functional parameters which are set primarily by tactical considerations. For example, fire control system limitations produce regions in the vicinity of the target where attack is impossible. Such limitations include maximum radar tracking scan angle, maximum antenna slewing rates, maximum radar detection (also acquisition and lockon) ranges, maximum information processing and computing time, and armament preparation time. Great effort should be made to optimize parameters which affect these limitations. The most important parameter to be maximized is radar range. Considerable time will be spent in later chapters on this problem. Another important parameter to be optimized is the maximum antenna

look-angle and field-of-view. In order to detect targets outside of the search field-of-view and in order to track targets which exceed the antenna look-angle, the interceptor must turn. Maneuvers expend valuable time and delay weapon launching. It is important to have a high angular tracking capability as well as high relative velocity tracking capability because large maneuvers of either the target or the interceptor may produce excessively high angular rates.

The interceptor fire control system must be able to counteract enemy jamming and saturation tactics. A saturation raid contains more targets than the ground system can handle simultaneously. Methods of combating such tactics might consist of interceptor mid-course guidance methods such as inertial navigation, celestial navigation, or the use of a special computer for extrapolative prediction of the course based on past information.

Enemy tactics which use decoys and chaff may be conteracted by the use of infrared (IR) and electromagnetic radars aboard the interceptors. Various other electronic countermeasures and chaff can be combated by appropriate counter-countermeasure equipment carried by the interceptor. These anticountermeasure techniques in general require additional equipment and cause delay in the weapon launch. The interceptor may carry countermeasure equipment to jam the bomber's electronic equipment.

SECTION 8 — SUMMARY OF FIRE CONTROL SYSTEM REQUIREMENTS

The summary of major fire control system requirements given in the following paragraphs is based on the tactical considerations previously discussed.

(a) Reliability and maintainability- The equipment must be combat-ready at all times, and must have a high probability of proper operation in combat. In case of malfunctions, the system must be made operative with little delay; this requires that the system be easily maintainable. The requirements can be satisfied by the use of reliable components which have been tested under the environmental conditions similar to those expected in the operational environment.

(b) Maximum radar detection range- As a consequence of the tactical and countermeasure environments which cause appreciable time delay, it is necessary to increase the time between target detection and

missile launch by increasing the radar range to a maximum consistent with other requirements.

(c) Maximum possible radar antenna field-of-view and look-angle-These quantities limit the regions about the target from which a successful attack can be made; they should, therefore, be made large.

(d) Maximum tracking rates in angle and velocity-This requirement stems from the many possible directions and speeds of the target.

(e) Ability to navigate without ground information-This requirement demands extrapolative computer functions and auxiliary navigating equipment such as an inertial navigator.

(f) Counter-countermeasure capability-This includes multiple target discrimination, low altitude target detection, and tracking capability, as well as other active and passive countermeasure discrimination features. Good ground- and weather-clutter rejection capabilities add immeasurably to the over-all fire control system capability.

(g) Small size, weight, and power consumption-These quantities seriously affect the interceptor's aerodynamic qualities.

(h) Capability to launch various types of armament, both singly and in salvos-The fire control system must satisfy the launching, preparation, control illumination, and other requirements imposed by the armament.

SECTION 9 — A PROPOSED SYSTEM

Heretofore, the discussion has dealt in a general manner with system requirements and tactics. Although it is convenient to consider in broad outline the major factors affecting the design of all fire control systems, much can be learned by the quantitative consideration of the design for a specific system. The treatment of material in this chapter will continue to be qualitative, but a specific block diagram for the fire control system will be proposed. The proposed system will still be general since the representative blocks are actually systems in themselves. Some of the blocks will be considered in detail, especially the radar and the computer. A detailed discussion of these subsystems will be included in subsequent chapters, which will include quantitative analyses wherever they are considered pertinent.

The block diagram (Figure 2-1) represents a proposed system in which the following assumptions hold:

(a) The carrier is a manned interceptor.
(b) The fire control system obtains information both from the ground and from the interceptor radar.
(c) The principal system armament consists of air-to-air guided missiles.

The automatic portions of the fire control system may be manually overridden at the pilot's discretion. The display-and-control panel provide the pilot with a complete indication of the flight and tactical conditions at any instant of time; the panel includes warning devices to indicate malfunctions.

Inputs to the fire control system consist of target data and air-to-air identification information from the radar antenna, ground control information from the GCA center via data link to the airborne receiving antenna, distance and bearing information from ground navigation stations for mid-course guidance, and air-traffic control and landing control signals from the ground, and voice communications. The inputs other than voice communications are received as shown in the block diagram and processed into signals suitable for use by the computer. An inertial navigator is to be used as an adjunct to the ground navigational aids in case of failure or jamming. Flight sensing instruments supply aerodynamic data to the computer, inertial navigator, and pilot's display. The computer processes the input data, supplying computer output information to the interceptor automatic flight control system and to the missile auxiliaries for missile preparation. The cockpit display panel displays the data required to enable the pilot to monitor the tactical situation.

SECTION 10 — DESCRIPTION OF A TYPICAL INTERCEPTION

To illustrate how the proposed system operates, consider a hypothetical high altitude interception. After early warning detection and identification have been established, "scramble" orders are sent to the readied pilots. The interceptors leave according to planned procedure. Although the pilot may take the interceptor off and fly it manually, it will be assumed here that the entire procedure is mechanized. The automatic takeoff system is actuated and locked onto the proper takeoff path

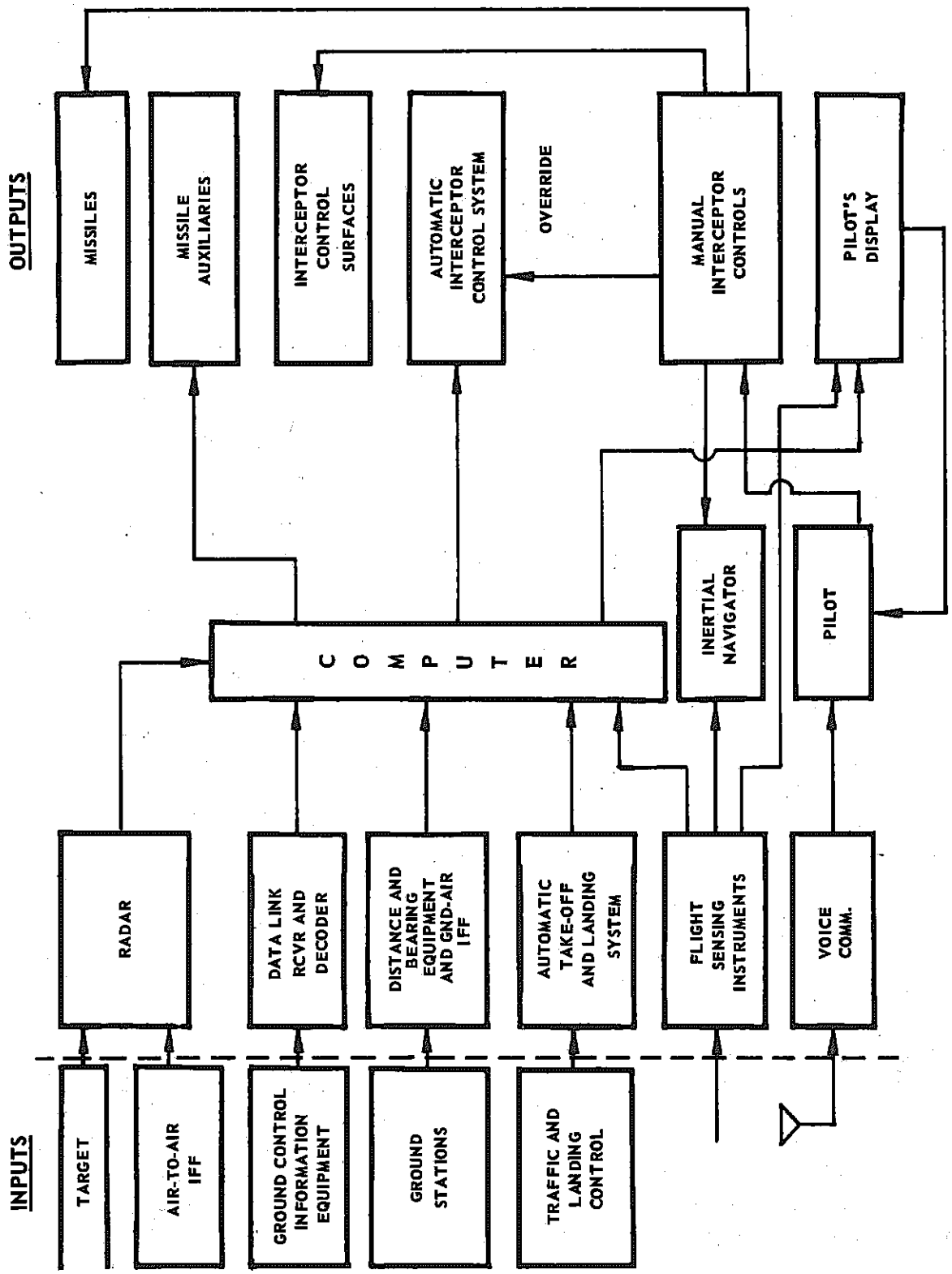

FIGURE 2-1. BLOCK DIAGRAM OF PROPOSED FIRE CONTROL SYSTEM

by a terminal traffic beacon and control system. The ground control station immediately begins supplying coded data for ground vectoring along the optimum flight path computed by the ground-based computers (i.e., along that path which takes the minimum time to interception). In addition to standard instruments, the pilot's control panel contains instruments which indicate airspeed and rate of climb for the optimum flight path. The monitored flight path can be compared by the pilot with the measured airspeed and rate of climb to determine how well the automatic equipment is functioning. After the interceptor arrives at altitude, it is flown at an optimum airspeed for maximum fuel economy for long range interceptions. This speed is determined by the computer. The throttle may be manually or automatically controlled. The steering signal and artificial horizon on the display allow the pilot to monitor the operation of the automatic steering system. The scope gives a PPI-type display for the "track-while-scan" presentation during the search operation. Immediately after takeoff, the radar operates in the search mode. The scope display should afford flexibility in the choice of azimuth angles and ranges to be covered, so that areas of particular interest can be examined. Identification information can be obtained from the PPI display by coding the displayed targets.

Upon detection the target can be automatically selected by permitting radar to lock on in angle and search the lockon in velocity, range, or both. Manual selection of a specific target may be most suitable where multiple targets exist, since the automatic search may cause the radar to lock onto an undesired target. If for example velocity search is used, the automatic system may lock onto the highest velocity target, which could be the one at greatest range. Furthermore, the tactical situation may make it undesirable to start tracking immediately after detection. A "lock-on control" should be provided for lockon, accomplished either manually or automatically, so that the time of lockon is at the pilot's discretion. After lockon, precise angle, range, and/or velocity information are provided by the automatic tracking radar. The interceptor is then automatically held on a proper course for launching the missiles. The course is determined by the computer, which supplies corresponding input signals to the flight control system for control of the interceptor control surfaces. Special conditions which call for launchings at altitudes below or above the target cause the computer to solve for the necessary climbing or descending trajectory. The computer supplies the missile auxiliaries with the necessary prelaunch information and determines the proper

launch time. The firing time is normally at the maximum effective range of the missile and depends to a great extent upon the altitude, as well as other factors.

After missile launch the interceptor is automatically programmed onto a controlled turn to escape the target area as quickly as possible. The controlled turn is not necessarily the one with the shortest radius. If semiactive missiles are used, the rate of turn is limited by the requirement that the interceptor radar continue to illuminate the target until the missile has reached the target. If the missile requires a reference signal from the interceptor radar, this must continue to be supplied after launch. After target destruction the interceptor is no longer constrained by the missile requirements and may again be operated in the search mode. Finally, the interceptor may proceed to a home base or to a traffic control point from which a ground system will vector it homeward. The automatic landing control system assumes control in the vicinity of the base. It is desirable for the pilot to have an indication of the terrain clearance at all times, particularly during the low altitude and landing phases.

The design goal indicated in the preceding discussion is to mechanize the entire interception as much as possible, so that the number of operations the pilot must perform are few and simple. The pilot's principal duties are to monitor the tactical situation and to take over control of the interceptor in case of equipment failure.

Provisions have been made for extended flights during the navigation phases before target detection and after target kill. Distance and bearing-measuring equipment are used for this prupose. Ground navigation beacons supply the necessary data when selected by the pilot in accordance with the organized flight plan. Cockpit controls and indicators must be provided for the navigational flight. Since the principal concern of this book is centered about the radar and computer portions of the fire control system, the problems associated with navigational flights are considered only briefly.

In case of failure or jamming of the ground control link, the interceptor is navigated by inertial guidance with the computer or by dead reckoning. If data link loss occurs before missile launch, the pilot may possibly locate the target with the interceptor search radar.

If data link loss occurs in midcourse, navigation can be predicted by the computer on the basis of the previous history of target position and heading relative to the interceptor.

The pilot should have "antijam" capabilities available to him. The radar transmitting and repetition frequency should be capable of being changed as required. Radar and radio antijamming features should be built into the equipment. Safety features such as "weapon jettison" and "destruct" controls for destroying faulty missiles after firing should be included.

Low altitude operation introduces special problems which include: loss of ground-to-air communication because of radio horizons, danger from terrain features such as mountains in the vicinity of attack area, reduction of aerodynamic range by drag at low altitudes, and reduction of radar range by ground and altitude clutter. In this type of interception, airborne early warning systems equipped with radar capable of distinguishing moving targets can be used to provide the interceptor with vectoring information. Airborne early warning systems may also be used as intermediate repeaters for ground-to-interceptor voice communication and data link.

In low altitude interceptions the same problems plague both the radar missile and the interceptor radar. Under certain conditions (discussed in Chapter IV) the guided missile should not be used. In these special cases, auxiliary rocket armament may be satisfactorily employed.

Detailed discussions of the various blocks in the proposed system appear in later chapters. Since this volume is intended to be a study and analysis of the more important problems associated with fire control system design, and not a proposal, no attempt will be made to invent clever ways of instrumenting the various blocks. However, a thorough understanding of the basic problems involved will be illustrated by specific equipment. It therefore becomes necessary to describe the principal constituents of each block in the proposed system. This will be done with major emphasis on the radar and the computer.

CHAPTER III

ARMAMENT

SECTION 1 — INTRODUCTION

The ultimate purpose of the airborne fire control system is to fire the interceptor's weapons in a manner that will assure maximum probability of target kill and, at the same time, provide maximum probability of interceptor safety. It is the purpose of this chapter to describe the properties of various types of armament to maximize the probability of weapon effectiveness.

The solution to the defense problem must yield the best method of defending a target complex. The solution must minimize enemy penetration and maximize enemy attrition, all at a minimum cost of friendly manpower and equipment. Although the best defense may be a good offense, offensive and strategic weapons will not be considered here. The concept of using accurate surface-to-air and air-to-air long range guided missiles is very attractive, even though technological development production costs per missile are high. The limiting factor, however, is not cost but time. Until long range missiles with high probabilities of kill are in production, the interim choice remains the interceptor armed with weapons which can provide the desired probability of kill.

The decision of armament type for use by the interceptor must be made. The principal weapons considered include: machine guns, airborne artillery and air-launched bombs, rockets, and guided missiles. If guns are to be effective at supersonic speeds, they must be controlled by radar gun directors. Even when correct firing direction and optimum firing range are determined, the dispersion of bullets at the required ranges is so great as to make guns ineffective. Unguided rockets may also be fired under control of rocket directors. Since rockets have longer ranges and greater firepower than bullets, the probability of kill at the required ranges is greater than that for guns, but is still inadequate in most cases. One case in which rocket armament proves to be effective is at short range and low altitude where ground effects limit the usefulness of many types of guided missiles.

The minimum safe interceptor range is determined by a hypothetical surface about the target, outside of which, the probability of interceptor kill by the bomber weapons is small. In most cases, the air-to-air guided missile appears to be the optimum choice for interceptor armament. It can be designed to give a high probability of kill at reasonable ranges.

The missile offers not only the greatest offensive capability of the weapons considered, it also provides the largest probability of survival for the interceptor. This follows since, if the target aircraft is armed with guided missiles, the interceptor must have armament of greater range and accuracy than the target aircraft. This constraint alone requires that at least part of the interceptor armament be guided missiles. Since interceptor weight and volume are critical items, the smallest and lightest possible weapon equipment consistent with the requirements of long range and high probability of kill must be chosen. In many cases the guided missile armament best satisfies these requirements.

SECTION 2 — THE GUIDED MISSILE AS A PART OF THE FIRE CONTROL SYSTEM

Although basically the missiles are not part of the fire control system, the optimizing of the performance of these weapons represents the purpose of the system. Consequently, the nature of the problems associated with missile armament will be discussed before the design of the fire control system is undertaken. As an illustration, consider the effect of two different missile design philosophies on the fire control system: (1) a missile with a small conventional warhead and simple contact fuse is used. This missile requires accurate guidance and an actual hit to accomplish target kill; and (2) a missile employing a powerful warhead and proximity fusing, but using relatively simple guidance, is used. In the first case, the fire control system must be accurate in order to launch the missile at the precise time with small launching error; in the second case, the radar and the control system associated with missile launch can be relatively crude.

The choice of missile type affects the interceptor flight trajectory and, therefore, the fire control system design. A bomber side view offers the largest radar cross-section. Hence, the optimum computed course for radar missiles is one which launches the missiles in a side attack. The greatest infrared intensity occurs off the tail of jet bombers, and so an optimum course for IR missiles is one which launches the

missile closer to a tail attack. These general conclusions are greatly affected by other considerations, such as the missile's speed advantage over the target, maneuverability, and type of warhead.

SECTION 3 -- GUIDED MISSILE CLASSIFICATION

Guided missiles are generally classified according to their tactical application and type of guidance. There are four major guided missile types: (1) air-to-air, (2) air-to-ground, (3) ground-to-air, and (4) ground-to-ground. The first two types are generally smaller, shorter range missiles than the latter two, since the air-launched missile and its associated control equipment must be carried by the aircraft. The air-to-ground and ground-to-ground types are especially vulnerable to radar and IR ground-return interference during the terminal phases of their flights. All four types suffer from target scintillation, and from receiver noise, especially at long ranges.

One or more types of guidance may be employed during a missile flight. The principal guidance types are: (1) command, (2) beam-rider, (3) homing, and (4) inertial guidance systems. On a single flight in which ground-to-ground and ground-to-air missiles are used, two or more types of guidance often will be employed. For example, a ground-to-ground missile might employ beam-rider guidance during launch and the early part of the flight and then, after exceeding the radar range of the beam, it might use inertial mid-course guidance, and, finally, switch to homing guidance for the terminal phases of the flight. Radar or infrared techniques are usually employed for the first three types of guidance. Type 4 does not depend on external target and reference signals and, hence, is inherently jam-free. In the ground-to-ground missile, the course is set by dead reckoning and maintained by accurate inertial references (usually gyroscopic). Since the effectiveness of this missile depends on the accuracy and reliability of mechanical devices such as gyros and accelerometers, errors created by external effects such as accelerations and friction cause misses which increase with the length of the flight. The first three types of guidance are associated either directly or indirectly with target radar reflection and IR radiations. Guidance types 1 and 2 also suffer increased degrees of missile miss with increasing range. Type 3 increases in accuracy with closing missile-target range, with a resultant smaller miss distance.

SECTION 4 — DETERMINATION OF THE OPTIMUM INTERCEPTOR-BORNE MISSILE TYPE

Missile guidance for use in interceptors logically falls into categories 1 and 2 (see Section 3). However, any one or combination of the various types of guidance can be used on air-launched missiles. Command, beam-rider, and other types of guidance which originate at the interceptor are less suitable than homing guidance for the following reasons: Target location and heading information must be obtained by the interceptor radar and then communicated to the missile, either by command or by means of the interceptor radar beam. Using the interceptor radar beam, the missile tracks the beam or scan axis of the interceptor radar antenna pattern and corrects flight deviations when the interceptor is "off the beam." Because of interceptor radar tracking errors, there is always some initial launching error for this type of missile guidance. For a given angular error, the target miss increases linearly with range in missiles which obtain target data by way of the interceptor radar. For the same initial angular launching error, homing missiles, which obtain target information directly from the target, tend to decrease this error as the target is approached. After launch, interceptor tracking error has relatively little effect on the semiactive missile tracking error, and no effect on passive or active missile tracking error. Another fact which augments the preceding conclusions is that, at launch, the signal-to-noise ratio available for command, beam-rider, and similar type missiles is good but progressively worsens as the missile moves farther away from its source of information and approaches the target. Thus, in addition to interceptor beam-tracking errors, the degraded signal-to-noise ratio of the missile control signals increases the miss. Contrastingly, homing missiles are launched at poor signal-to-noise ratios, but the ratio continually improves as the missile approaches the target (which is the homing missile's source of information).

From the preceding argument, it might appear that the homing missile should be selected over the command or beam-rider missile. Generally this is true, except in cases where the launching range is so great that the signal-to-noise ratio at launch reduces the probability of kill below that required. In this case, it may be necessary to launch the missile with beam-rider, command, or inertial guidance, and switch it to the homing phase during flight. Disadvantages of the latter procedure stem from the fact that the angular error at switchover is often greater than at launch (it is possible for the target to be entirely outside the missile's field of view at switchover). The process of switchover is a complicated

one requiring increased system complexity and resulting in a lowered reliability. Inertial guidance alone is not too practical for use against moving targets. The typical inertial guidance scheme involves the prelaunch determination of a trajectory. The trajectory is programmed and deviations from the program prior to launch are corrected. Obviously the prelaunch program will be in error if the target deviates from the planned trajectory after launch. Inertial guidance is feasible for use in an air-to-ground missile if the program is computed for a specific launch point against a fixed target. Changes in target position could be relayed to the inertial guidance system for correction of the program, but then the system would no longer be considered entirely inertial. The great advantage of the inertial system over the other guidance systems is the fact that it cannot be jammed. Countermeasures can degrade, confuse, or destroy external source-to-missile information links. Radiations generated by the target, reflected from the target, transmitted to the missile from the interceptor, or from the ground, can all be jammed. When no external sources of information are required by the missile, the missile may be considered jam-free. The major advantage of the inertial guidance system is also its major weakness; since it receives no radiated information during flight, it is essentially an open-ended system with no means for detecting and nulling errors resulting from target maneuvers.

The fire control system of the preceding section will be assumed to incorporate radar and IR air-to-air missiles. It will be further assumed that the missiles employ homing guidance all the way to the target. The radar missiles employed may be active, semiactive, or passive. Radar missiles that home on target radiations are often called antiradiation missiles. A useful feature which can be employed in semiactive and active missiles is a technique that switches the missile from normal operation to passive tracking when a jamming source is sufficiently powerful to cause normal tracking to be difficult or impossible. The disadvantage of this technique is that a decoy jammer, rather than the target, may be the source of the jamming radiation. Even if the jammer is on the target aircraft, it may jam only until target track is lost, leaving the missile with no source of signal to track. IR passive tracking is considerably more reliable than electro-magnetic radiation passive tracking, since it is very difficult for a target (particularly a jet aircraft) to mask its heat sources; it is, however, relatively simple for the target to mask its electromagnetic radiation sources. The simplest means for masking electromagnetic radiation is by simply turning off the specific radiating equipment. Active radar missiles have one advantage. They require no link with the interceptor after launch. This permits

the interceptor to leave the combat area at the earliest moment. The active missile and the interceptor radar frequency can be different so that the active missile radiation can be jammed only during the short period of missile flight. This missile, therefore, has good antijamming qualities. The active missile design, however, presents some serious practical difficulties. It is difficult to prevent the missile radar transmitter from saturating the associated missile receiver, particularly when the system must transmit and receive simultaneously as in a CW system. The transmitter, which is required in an active system, considerably increases the missile size, weight, and power consumption. These disadvantages are particularly serious in an airborne system. The active missiles are appreciably larger than corresponding semiactive missiles, not only because of extra equipment and power requirements, but also because the extra weight makes a larger motor and greater aerodynamic surface necessary. Additional missile size and weight complicate stowage and launching problems on the interceptor, and generally degrade interceptor performance. For these reasons, semiactive radar missiles and passive IR missiles will be the assumed armament for the illustrative interceptor.

Semiactive missiles also suffer from various effects. The missile's dependence on interceptor radar illumination of the target up to the time of target kill is a serious handicap, since any stoppage of the interceptor's radar signal causes the missile to be "blind." The interceptor is thus forced, after missile launch, to limit its turn, which delays its departure from the target area. The radius and rate of the interceptor turn are limited by the interceptor radar antenna's field of view, and by limitations in angular tracking rate respectively.

In order to track the target in angle, an antenna lobing or scanning technique is used. The target reradiation fluctuates, not only as a consequence of the irregular vibrating reflecting surface of the target, but also as a result of variations in magnitude of the radiation incident on the target. These variations are made worse by increased tracking error resulting from high interceptor angular rates and from target evasive maneuvers. The amplitude of the received signal at the interceptor antenna varies in a random manner as a consequence of these effects (this variation is termed "amplitude scintillation"). As a consequence of the scintillation effects, the angle-of-arrival direction of the received wavefront varies randomly, producing "angular scintillation" and apparent target range and velocity variations which produce "range and velocity scintillation." Although all radar signals scintillate, the scintillation is perhaps worse in semiactive than passive or active systems. In addition

to random scintillation, the interceptor radar scanning frequency, repetition rate (if pulsed), and other modulations are received by the missile and add confusion to the received signal.

SECTION 5 — THE WARHEAD AND FUSE

The warhead and fuse comprise the payload of the guided missile. The choice of warhead affects the design of the fuse, missile tracking system, and interceptor fire control system. A principal decision that must be made is whether to use a large kill-radius warhead or a small kill-radius conventional warhead. The proper one for use is determined by the tactical situation, as well as by related factors. It is not axiomatic that the largest possible kill-radius warhead should be used. Large kill-radius warheads are expensive to construct, dangerous to handle, difficult to maintain, and require special facilities for storage and handling. The triggering and fusing mechanisms are generally more complicated and less reliable than those of conventional warheads. The payload becomes a large percentage of the total missile weight and volume. Large kill-radius warheads are especially effective in tactical situations where multiple targets are closely spaced. Since spacing bombers widely is a simple form of countermeasure, it is assumed that enemy aircraft will be so spaced. Under these conditions, destruction of a single target by a large kill-radius warhead is unwarranted. Considering other aspects of the problem, the accuracy and refinement of the missile and interceptor radars and control systems are a function of the warhead kill radius. A compromise is made to optimize the weapon effectiveness. If a small warhead is employed, the additional available space and weight in the missile can be used for additional control equipment to make the missile more accurate. Advantages of simplicity and reliability in the missile guidance and interceptor fire control systems are gained by the use of large kill-radius warheads which diminish the required guidance accuracy. This advantage can be lost if the missile fuse is extremely complex. Large misses can be expected when simple guidance systems are used; however, misses up to the kill radius of the warhead can be tolerated. If the warhead is to be triggered at the optimum point (not necessarily the closest approach to the target), a suitable proximity fuse must be used.

Various radar techniques are used in the design of proximity fuses which make use of the received signal frequency doppler shift. An efficient proximity fuse is a complete radar system, which may or may not make use of the tracking and other functions from the missile tracking system. The fuse can be jammed by high-power jamming and confused by chaff and

decoys. Intelligent jamming, however, is difficult because of the short time allowed the jammer to determine the salient properties of the fuse.

A contact-type fuse is worthless unless physical contact is made; hence, a missile guidance system employing such a fuse must be sufficiently accurate to give a high probability of actually hitting the target. If the target can be hit by the missile, a relatively small conventional warhead is adequate for weapon-carrier kill. The choice of warhead size and fuse type determine whether simple or complex guidance and fusing systems are required.

SECTION 6 — FUNDAMENTAL DIFFERENCES BETWEEN MISSILE AND INTERCEPTOR GUIDANCE AND CONTROL SYSTEMS

The specific function of a "fire control" system in an interceptor is to launch the missiles in an optimum direction and time. To accomplish this, information about the target and missile characteristics is applied to the fire control system computer, which generates preparation, firing, and control signals for the missile. The missile and interceptor guidance and control systems are similar in many respects.

The missile computing functions are, however, relatively simple compared to those which must be performed by the interceptor fire control system. If a homing missile is used, it can be locked onto the target before launch by means of information from the interceptor radar. If the missile signal-to-noise ratio at launch is sufficiently great to allow it to track through the boost period, the only "computing" the missile guidance system must do is that required for target tracking in angle. The angular position and rates of change of angular position can be determined from the tracking signal. If the missile turning rate is made proportional to the angular rate of change of the line of sight (LOS) between the missile and the target, the missile will navigate toward a collision course with the target.

The missile "computing" functions are analog in nature and are mechanized accordingly. The interceptor computing can also be carried out by analog operations, but the nature of the input data and type of computation desired make a digital computer a more suitable choice.

The differences between the missile and interceptor guidance and control systems are largely differences of degree. Because of space

requirements, small air-to-air missiles must employ miniaturized components. Environmental conditions under which the missile operates are more severe than those under which the interceptor operates; the missile equipment must withstand greater acceleration, vibration shock, and more rapid temperature changes. The missile must also be capable of operating within wider parameters. For example, the missile is subject to lateral accelerations several times as great as those imposed on the interceptor. Missile roll rates and boost accelerations greatly exceed interceptor roll rates and longitudinal accelerations. Because of the low moment of inertia about its longitudinal axis, the missile is subject to high rates and perturbations in roll. Since roll causes crosstalk between pitch and yaw control channels, roll and roll-rate stabilization is required. Air-to-air missiles tend to be highly underdamped in pitch and yaw, so that stabilization in these coordinates is also necessary. These conditions cause the design of missile electronic tracking circuits to be more difficult and critical than those of the corresponding interceptor radar circuits.

The variation in signal strength at the missile will generally be much greater than that seen by the interceptor radar. Even though both systems begin tracking at relatively low signal-to-noise ratios, the interceptor turns away from the target before the target signal reaches saturation values. A missile with contact fusing can be subjected to signal strengths sufficiently great to saturate not only the receiver, but even to burn out the mixer crystal. For this reason the missile AGC design problem is more difficult than that of the interceptor radar receiver. The proximity of the missile to the target just before impact creates other problems such as accentuation of the angular scintillation effect. If the radar illumination is pulsed and the missile tracks in range, the missile is blind for a range roughly equal to a time corresponding to the pulse width. During this so-called "blind range," the missile is unguided.

Another requirement of the semiactive missile is the reference signal needed for tracking. The "active" interceptor radar can determine range or velocity by use of the time delay or doppler shift, respectively, between transmitted and received signals. The semiactive missile, however, has no transmitter and requires a reference signal from the interceptor radar. This reference signal must be transmitted from the interceptor radar to the missile rear-reference system link. If absolute measurement of missile range and velocity is unnecessary, the rear-reference system requirement is deleted. A missile radar seeker which performs purely tracking operations need not obtain absolute range or

velocity information to track, but merely the rate of change of the range or velocity. Missile reference frequency variations from the transmitter frequency appear to the missile as doppler shifts and are tracked accordingly. Thus, a portion of the total missile tracking capability is wasted in following reference drifts and other fluctuations which are not a result of missile-target relative motion. The more tracking capability used up in meaningless tracking, the lower will be the probability of kill. It is important, if no rear-reference link is used, that the missile reference and the radar transmitted frequency be as stable as possible.

In connection with this problem, one of the difficult radar design problems is that of developing stable reference frequencies. The higher frequency and more power demanded from the oscillator, the more difficult the frequency stabilization problem becomes. The maintaining of pulse-to-pulse frequency and phase coherence in a pulsed transmitter is particularly difficult. However, the alternative of an interceptor-missile rear-reference link is not desirable. Even though the average signal-to-noise ratio at the rear-reference receiver may be high because of one-way transmission, the signal level fluctuates randomly if the radar target-tracking beam is used for the interceptor-missile link. The missile flies through the nulls and peaks of the radar antenna pattern with consequent variation in received signal strength. The tactical situation may be such that the missile lies in an antenna null sufficiently long to cause target tracking loss because of a lack of reference signal. These problems can be solved by the addition of an auxiliary tracking system with an illuminating antenna for the purpose of tracking the missile. This added complication is very undesirable since it requires additional equipment with all the attendant problems.

SECTION 7 — MISSILE AUXILIARIES

The probability of kill increases as the number of missiles fired in a salvo, or consecutively, at a particular target is increased. A compromise is made in determining the number of missiles to be carried by the interceptor. Besides increased weight and volume required for each additional missile, more complex circuitry is required for launching and firing. The tactical situation might demand simultaneous salvos, or a pattern of successive firings ("ripple" firing). The firing circuitry must be capable of implementing these variations. Each missile must be launched so as to not only maximize the probability of target kill, but also to minimize the probability of locking onto other missiles, friendly aircraft, decoys and chaff.

Each missile must be prepared for launching. A typical preparation procedure might require that the following conditions occur in the missile: (1) gyro and motors energized and brought to speed, (2) antenna slaved to the expected missile-target LOS, (3) batteries and power supplies energized, (4) range and velocity tracking gates locked on, and (5) guidance and control parameters set for the particular flight and tactical situation. The missile is then fully prepared to be armed and fired. The fire control system must provide the following prelaunch items in order to effect missile preparation: (1) antenna pointing information, (2) target range and velocity information, (3) signals to set the various missile gain-levels and parameters, (4) lockon signals for range and range rates, (5) arming and firing signals, and (6) prelaunch missile power. The armament auxiliary equipment obtains the required information principally from the radar and the computer, and processes it to provide the missile with proper signal forms, proper signal impedances, and required power levels for missile firing. The missile prelaunch signals must occur at precisely the required time. This need is evidenced by the missile battery requirements. These batteries must not be energized too early because of their limited energy storage capacities. Energizing the batteries too late prevents the missile tracking system from being fully warmed and operating efficiently at the time of launch.

SECTION 8 — STOWAGE AND LAUNCHING

The missile must be stowed in the interceptor in an efficient manner. Stowage space must be small and readily accessible for movement of missiles from the stowed to the launching position. The space problems can be somewhat alleviated by using folded-fin missiles. Considerations of rocket motor blast and electrical and hydraulic connections must be properly taken into account. The missile is launched from rails which may also be used to position the missile prior to launch.

If the various missile tracking functions are slaved to the radar prior to launch, the transition between the slaved and the active tracking conditions may cause the target to be lost. This problem can be solved by employing suitable "memory" in the missile tracking circuitry. External pods with radomes or simple under-the-wind open storage devices can be used to allow the missile to track before launch. These "external" methods are aerodynamically undesirable since they degrade interceptor performance. Inertial stowage is preferable but requires mechanisms for opening the interceptor bay doors and moving the missile

out of the fuselage for unobstructed firing. After firing, suitable rail-retracting and bay-door-closing mechanisms are required.

The design of an efficient launching mechanism can be critical. It is important that the launching operation add little error to the existing errors due to "jump-angle" and "tipoff" effects. Jump angle error occurs at the instant the missile is launched into the airstream, and tipoff error is caused by angular momentum imparted to the missile when it separates from the launcher. The effect of these two errors must be compensated for by the missile guidance system prior to launch.

SECTION 9 — THE PROPOSED GUIDED MISSILE ARMAMENT

To continue the fire control system example, a proposed guided missile including a system block diagram and the general physical layout is presented in Figure 3-1. The possible physical layout for a small air-to-air missile (with no booster) is shown in Figure 3-2. The numbered units in Figure 3-2 are identified as follows:

(1) Radome and antenna (radar) or irdome and telescope (IR).
(2) Guidance unit - antenna or telescope positioning.
(3) Converter unit - crystal mixer, local oscillator, and rf for radar missile, or chopper disk and IR-sensitive cell for an infrared system.
(4) Electronics unit - receiver, range and velocity track, control and positioning circuits.
(5) Warhead and fuse.
(6) Sensing gyros, accelerometers, etc.
(7) Power supply and umbilical plug.
(8) Rocket Motor
(9) Control surfaces

The missiles used may be either semiactive radar or passive IR homing-all-the-way missiles. Items 1, 2, and 3 can be made interchangeable for either type of missile so that the same missile can use either a radar or an IR front end.

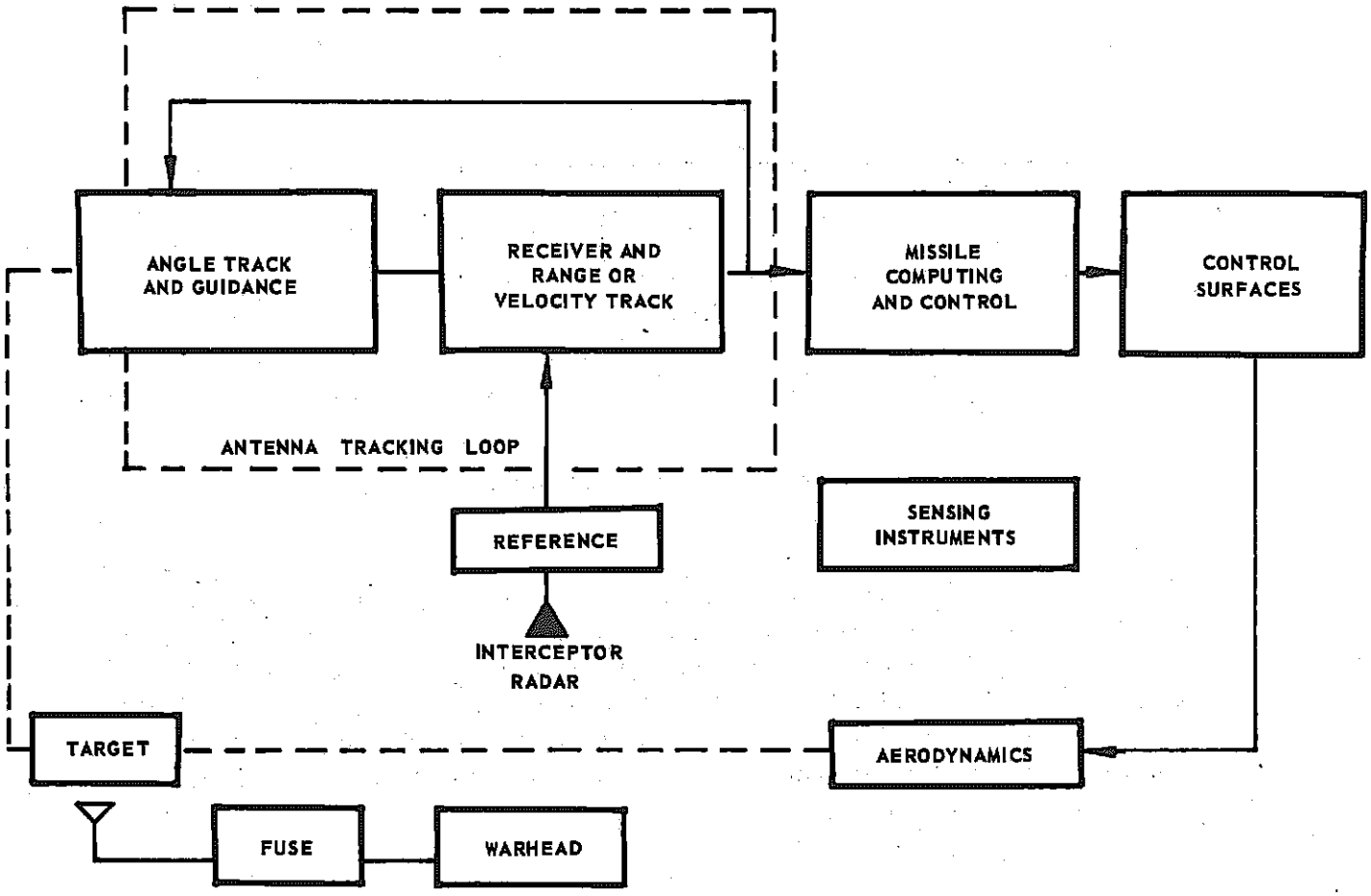

FIGURE 3-1. BLOCK DIAGRAM OF MISSILE CLOSED-LOOP GUIDANCE AND CONTROL SYSTEM AND PAYLOAD

SECTION 10 — GENERAL CONSTRAINTS IMPOSED ON THE FIRE CONTROL SYSTEM BY THE MISSILE ARMAMENT

The basic fire control system requirement imposed by the missile is that the launch signal be at the optimum target range with a minimum launching error. This dictates that an accurate interceptor radar and computer be used. Missile preparation time imposes a requirement for additional radar range. The target tactics and missile performance capabilities define the requirements for the interceptor flight path. The need for target illumination and a rear-reference link for semiactive

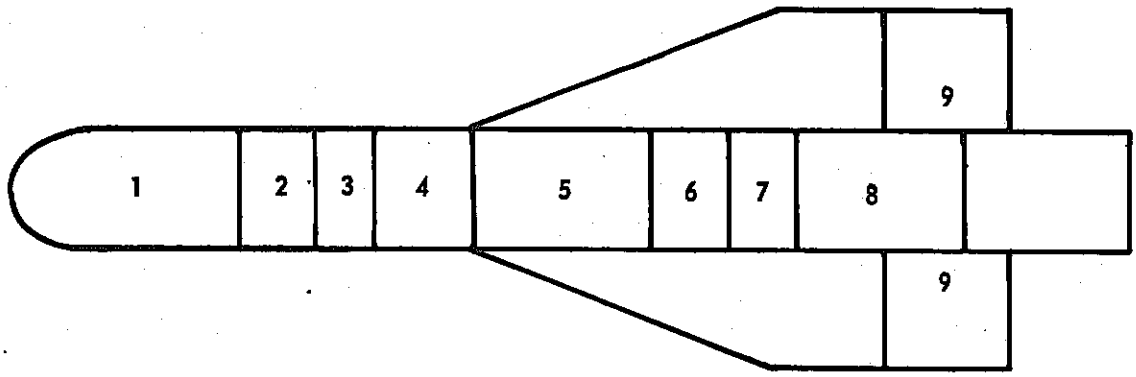

FIGURE 3-2. PHYSICAL LAYOUT OF MISSILE

missiles affects the radar design and interceptor flight path. The missiles must be stowed, cooled, powered, and launched by the interceptor and its fire control system. The types of warheads and fuses used determine to a large extent the accuracy and complexity of the fire control system. Obviously, the fire control system cannot be designed without a thorough knowledge of the limitations described and the requirements of the missile armament.

CHAPTER IV

THE RADAR

SECTION 1 — INTRODUCTION

The radar is the "eye" of the fire control system whose specific purpose is to search, detect, lock onto, and track the desired target. The information gained from tracking the target is used to prepare the missile armament, fly the interceptor on the proper course for missile launching, and launch the missiles on the proper course at the proper time. The radar also illuminates the target during missile flight when semiactive armament is used. The radar provides visual indication of the tactical situation to the pilot at all times. The radar may also serve as a navigational aid, air traffic and weather indicator, terrain clearance indicator, landing and takeoff aid, etc. The radar "eye" and the computer "brain" are the two most important elements in the fire control system.

The design specifications, component parts, and parameter values of a radar system are set by the output requirements and the nature of the input signal. The input signal is affected by the type of radiation reflected (or emitted) by external reflectors (or sources). The nature of the reflected energy depends upon the type and quantity of energy transmitted by the radar. Consequently, the receiver design is a function of the transmitter design.

Once the types of information needed and the form in which this information must appear at the radar outputs are decided upon, the general design requirement is that the useful information rate be as great as possible.

Although the radar may be used as a navigational aid or for other purposes, its most important contribution to the success of the mission occurs during the attack phase of the interception. The "attack" phase includes that portion of the mission from target detection to target kill. The "vectoring" phase includes the remainder of the mission. A brief qualitative discussion of the vectoring phase (approach and return stages)

will be included here. It is desirable for the pilot to have the tactical situation displayed to him during this phase. This information is probably best obtained from the radar operating in its search function. The resulting information is probably best displayed on an off-center PPI (plan-position indicator) scope. The PPI uses polar coordinates with r equal to range and θ equal to azimuth angle. This type of presentation is the closest to that seen by the human eye. The off-center feature makes better use of the forward hemisphere search volume of the radar than the centered display. This type of presentation is particularly convenient when the pilot is flying in formation and must maintain spacing from the other aircraft. In order to retain the realistic picture presented in level flight when in nonlevel attitudes, the search pattern should be stabilized in pitch and roll. The search parameters such as azimuth and pitch angular coverage, search rate and pattern, etc., must be specified. These problems are considered in detail later. It is important that the parameters which are optimum for the attack phase be employed, or at least be compatible with, those used during the approach phase. Although the problems associated with radar and computer design for operation during the vectoring phase are as formidable as, or more formidable than, those associated with the attack phase, little emphasis will be placed on vectoring phase problems. The reason is that radar, computer, and associated equipment, strictly speaking, become a fire control system only during the attack phase of the mission. During the remainder of the mission, this equipment forms what might be called a navigation system. The remainder of this chapter will therefore be concerned with airborne radar design for use during the attack phase (unless otherwise specified). This condition will henceforth be understood and hence not mentioned.

SECTION 2 — GENERAL RADAR REQUIREMENTS

The attack portion of the mission can be divided into three principal phases:

(1) Search and target acquisition
(2) Prelaunch attack run
(3) Postlaunch turn and illumination

The radar subsystem has the following principal functions during these phases, namely (in order of their occurrence):

(1) Automatic search - to scan an appropriate volume of space so as to detect and acquire (i.e., lock onto) the target and thereby initiate the interception.

(2) Automatic track - to obtain position, rate, and possible rate-derivative information on the selected target for use by the rest of the fire control system (particularly the armament and interceptor control system).
(3) Illumination - to illuminate the target for semiactive missiles.

The principal radar performance requirements during these phases are:

(1) Maximum radar range - both detection and tracking ranges
(2) All altitude operation - particularly extremely low and high altitude lock-on and tracking capability
(3) Adequate anticountermeasure capability
(4) Adequate tracking accuracy

In addition, the usual requirements on reliability, ease of maintenance, size, weight, and power consumption must be satisfied.

The principal parameters which must be specified for an active radar include:

(1) Transmitted signal parameters

(a) Type and frequency of carrier
(b) Type of modulation
(c) Power

(2) Antenna parameters

(a) Type and size
(b) Beamwidth
(c) Side and back lobes
(d) Boresight error

(3) Scanning parameters - search phase

(a) Type of search pattern
(b) Search rates
(c) Type and accuracy of angular lock-on
(d) Angular coverage

(4) Scanning parameters - tracking phase

(a) Type and rate of beam lobing
(b) Angular tracking accuracy
(c) Field of view
(d) Maximum angular tracking rate

(5) Receiver parameters

(a) Type of receiver
(b) Receiver noise figure, gain, and sensitivity
(c) Receiver bandwidth and dynamic range

(6) Search and lock-on parameters

(a) Types of search
(b) Search rates
(c) Lock-on method and threshold setting
(d) Lock-on range and signal-to-noise ratio

(7) Tracking circuit parameters

(a) Types of tracking servos
(b) Servo properties - particularly open loop gain and closed loop bandwidth
(c) Tracking accuracy and probability of target loss
(d) Multiple-target, extraneous input, and anticountermeasure capability
(e) Minimum signal-to-noise ratio for reliable tracking range

(8) Display parameters

SECTION 3 — SYNTHESIS OF A FIRE CONTROL RADAR

The optimum radar design would be a pure synthesis procedure, in which the desired inputs and outputs are specified and the system synthesized analytically from the input-output specifications alone. Practical difficulties render this idealized procedure impossible. The radar system itself can be divided into two main parts:

(1) The transmitter, including carrier generator, modulator, transmitting antenna (the transmitting antenna usually also serves as the receiving antenna), and power supply.

(2) The receiver, which is here generalized to include not only the receiving antenna, local oscillator (LO), and amplifier, but also the search, lock-on, and tracking circuitry. These two parts cannot be synthesized independent of each other, since the type of transmitted signal to be used depends on the type of receiver used, and likewise the receiver design depends on the nature of the input signal and consequently on the properties of the transmitted signal. Thus, the input specifications cannot be prescribed independent of the output specifications.

The radar contains many "unalterable" components whose characteristics do not meet the requirements of an idealized synthesis because of "state-of-the-art" limitations. Furthermore, input-output specifications are only one of several constraints the radar must satisfy. For practical reasons, then, in this chapter an attempt is made to lay out a block diagram for the radar based on qualitative arguments and estimates of the bounds on important system parameters. This will be done by considering various possible types of radars and choosing one for the example by a process of elimination based on the general system requirements enunciated in the last section. The block diagram of the chosen system will be developed by a systematic consideration of what components are needed to implement the chosen radar. Crude estimates of the important parameters will then be made on the basis of requirements set by a hypothetical tactical situation and assumed armament. Detailed mathematical techniques for the determination of optimum system parameters will be deferred until Chapter 7.

SECTION 4 – SEARCH RADAR REQUIREMENTS

Once the system requirements have been stated generally, more detailed requirements for each phase of the attack may be considered.

(a) SEARCH RADAR RANGE

It is desired to intercept the enemy from all approaches and aspects. Search range will be defined as the range at or before which a target of a given radar cross section has a specified probability of detection. The entire problem of maximum radar range is a statistical one.

At the stated search range, a certain percentage of the targets will remain undetected and, therefore, during a certain percentage of the time the stated range will not be realized. The system should be designed to minimize these percentages and, consequently, the probability of enemy penetration of the defense perimeter.

The minimum search range can be determined from the time required for the necessary operations between target detection and missile launch, the maximum missile range, and the maximum expected target velocity relative to the interceptor. A table of the principal time-consuming operations and the estimated time required for an hypothetical fire control system follows.

Operation	Time Designation	Time Estimate
Search Acquisition	t_s	10 sec
Target Identification	t_i	20 sec
Search-to-track Lock-on	t_e	10 sec
Prelaunch Track	t_t	20 sec
	Total -	60 sec

Assume a bomber maximum velocity of Mach 2 and an interceptor maximum velocity of Mach 3 at medium altitudes. The target velocity relative to the interceptor is maximum for head-on approaches and is Mach 5, or approximately one mile per second. Assume a missile maximum range of approximately 20 miles. The prelaunch operations require approximately 60 miles in the worst case. A minimum search range of the order of 80 miles is indicated. This estimate is probably the greatest lower bound since the worst case of maximum relative velocity and maximum prelaunch operation time was assumed. Unfortunately, near head-on interceptions are not unlikely, particularly when the early warning is adequate. The operation times are a function of the input signal-to-noise ratio and hence of the target cross section. The prelaunch operation time may be appreciably reduced for large, clearly defined targets. The probability of detection at the minimum allowable search range for the minimum expected target cross section should be high, say, at least 80 percent. The maximum range is then set by the minimum allowable probability of detection P_{dc} which must be less than or equal to the P_{dc} at the minimum search range. The range of a

given target is highly dependent on the required probability of detection. In the vicinity of 50% probability of detection, a small reduction in range (say, 3%) may appreciably increase the probability of detection (say, from 50 to 60%).

A brief discussion of the various prelaunch operations and factors significantly affecting the time of operation is in order. "Search acquisition" is the actual appearance of the target on the search display, or as a system input which is distinguisable from the noise. The time required for this operation depends on the search scan frame time, the number of "looks" at the target per frame time, target scintillation and resolvability, signal-to-noise ratio, etc. "Target identification" is the automatic and/or manual identification and selection of the desired target. The pilot has an override option on automatic target identification and selection in which he may identify and select the target manually from the scope presentation. The human decision-making time increases t_i appreciably, but human judgment is often quite essential at this stage of the interception. "Search-to-track lock-on" is the automatic switchover from the search to the track condition once the target selection has been made. This operation is quite complicated. The antenna search pattern mechanical motion must be stopped, beam lobing and angle tracking initiated, and all of the tracking circuits locked on. This operation depends greatly on the signal-to-noise ratio. The lock-on time can be quite short (less than 5 seconds) for good signal-to-noise ratios. At poor signal-to-noise ratios the lock-on operation is not only slower, but the likelihood of false lock-on increases. False lock-on requires that the search cycle be re-initiated with a consequent increase in true target lock-on time. "Prelaunch track" is essential to correct the errors in interceptor trajectory from the proper missile launching trajectory. Correction of these errors normally introduces flight and system transients which must be effectively damped out before launch. After lock-on, the missile prelaunch operations commence. This missile preparation time sets an absolute minimum on the prelaunch track time and may be the limiting factor if the interceptor happens to be close to the proper missile launching trajectory at lock-on.

(b) SEARCH RADAR ANGULAR COVERAGE

If the entire volume of space about the interceptor were searched, the complete tactical situation would be available at all times. Aside from the extreme practical difficulty in instrumenting such an isotropic

search scheme, extensive search coverage, particularly in the rear hemisphere, is unnecessary. If the ground vectoring information were sufficiently accurate, only a very small volume of space would need to be scanned. Ground information may be appreciably in error, particularly at long ground-radar target ranges. Enemy countermeasures may also appreciably degrade ground vectoring information. Some reasonable region of space must therefore be searched. Since the likelihood of bomber targets appearing in the rear hemisphere about the interceptor longitudinal axis is small (assuming adequate early warning), a region of space extending in azimuth over the forward hemisphere, and over an elevation angle which extends from the ground to the maximum expected target altitude at the search ranges expected, should be adequate. Suppose the total prelaunch operations consumes 15 seconds. The minimum radar search range would be approximately 35 miles. At this range, altitudes 60,000 feet below and 60,000 feet above the interceptor altitude would be covered by an elevation coverage of $\pm 20^{\circ}$ about the horizontal. The minimum azimuthal coverage is set by the maximum expected antenna "look" angle (angle between the interceptor longitudinal axis and antenna axis) for the typical interception. Maximum probability of kill requires a missile launch toward the side of the target which will require large look angles before lock-on and trajectory correction for near head-on interceptions. Estimate this maximum angle to be 60° for the hypothetical system. A possible specification for this system angular search coverage might therefore be $\pm 20^{\circ}$ elevation by $\pm 70^{\circ}$ azimuth.

The entire search pattern should be capable of being shifted, particularly in elevation. Search and track line-of-sight angles relative to the interceptor axis might be considerably depressed below -20° elevation for low flying targets, for example. It is also desirable that certain sectors of the search area be capable of being isolated and searched in more detail. This decrease in searched area should be accompanied by an increase in angular resolution.

At any given instant of time, the volume of space seen by the radar is within the antenna main beam (disregarding the sidelobe structure). Although the beam is limited in angle, targets lying in the beam at any range up to the maximum radar range are seen simultaneously. If these targets are capable of being resolved in range (as in a pulsed radar), it may be desirable to "gate" in range, that is, select a portion of the search volume bounded by two ranges. This gated range could then be expanded on the scope to provide additional range discrimination between multiple targets, and to combat countermeasures.

(c) SEARCH RADAR PATTERN PARAMETERS

Once the volume of space to be searched is decided upon, the other parameters of the pattern must be chosen. Some of these parameters include antenna beamwidth, type of search pattern, search rate, frame time, pattern stabilization and control. Analytical techniques for determining these quantities will be presented in Chapter 7 — for the present, consider some of the general conditions which affect the choice of parameter values. Let the main antenna beam be defined as essentially a surface of revolution about the beam axis whose cross section through the beam axis might be as shown in Figure 4-1.

The beam shown in Figure 4-1 is a normalized plot of received field intensity as a function of angle measured relative to the beam axis. The power is proportional to the square of the field intensity; when the "power" is down to one-half of its value on the beam axis, the angle at the half-power point is called the "beamwidth", β. Two targets can be considered to be resolved in angle when they are roughly a beamwidth apart. From the view point of good angular resolution, then, the beamwidth should be as small as possible. Narrowing the beamwidth has the additional advantage of increasing the tracking range of the radar because, if the target is "in the beam" (i.e., its angular separation from the beam axis is less than β) as is the case when the system is tracking in angle, the intensity at every point in the beam is increased. This follows since, for the same power transmitted, reducing β elongates the beam, i.e., it increases the antenna "gain." The gain is defined as the ratio of the intensity on the beam axis to the intensity in any direction if the same power were radiated isotropically. One disadvantage of narrowing the beam is caused by the resulting increase in the number and

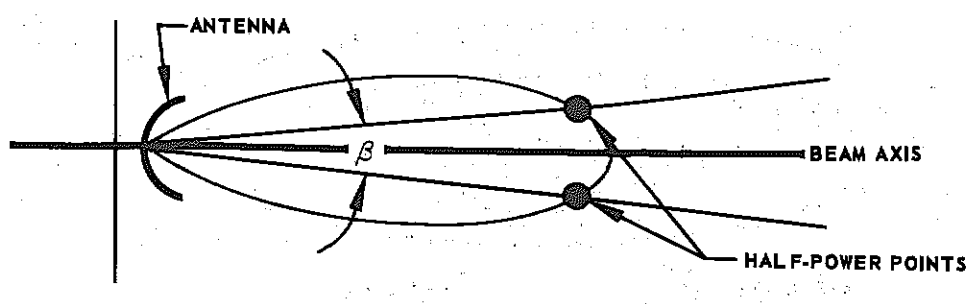

FIGURE 4-1. THE ANTENNA BEAM

intensity of sidelobes. Another is the increase in antenna size required to narrow the beam. However, the principle disadvantage of too narrow a beam is that, if the time required to cover the region of space to be searched is fixed, the frame time -- the time during which a given region in space is illuminated by the beam -- becomes exceedingly small. The search rate is essentially the velocity at which the beam moves in sweeping out the search volume. The search area is defined as the area enclosed by the elevation and azimuth angular bounds on the surface of a sphere, centered at the radar and with a radius equal to the maximum radar range. This search area can be considered to be composed of many adjacent circles whose radii subtend the beamwidth angle β at the center of the sphere. The geometrical arrangement is shown in Figure 4-2. Consider a sweep in azimuth. The narrower the beam, the more beamwidths per azimuth angle, and the greater the rate in beamwidth per second for a given search rate. Suppose a target lies within one of the beamwidth circles. The time during which the target is illuminated decreases with decreasing beamwidth. The target energy returned per frame time is correspondingly reduced. A given signal-to-noise ratio is required during the time the target is illuminated in order to distinguish the target from the noise (detection signal-to-noise ratio) and another signal-to-noise ratio to stop the search and lock onto the target for tracking (lock-on signal-to-noise ratio). To attain the signal-to-noise ratio the decrease in energy return per frame resulting from narrowing the beamwidth must be compensated for by decreasing the maximum search acquisition (detection) range and lock-on range. These ranges are generally exceeded by the tracking range. The detection range is therefore the critical one and every effort should be made to maximize it.

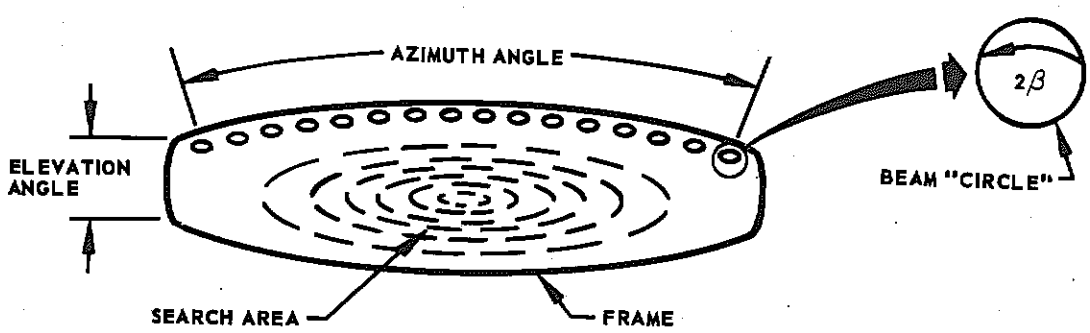

FIGURE 4-2. SEARCH AREA GEOMETRY

From the aforementioned conflicting requirements the proper beamwidth must be chosen. All of the search pattern parameters are interrelated. The other search pattern parameters are also determined from considerations similar to those used in choosing the beamwidth. For example, the time spent in sweeping across each beamwidth circle can be maintained constant when the beamwidth is narrowed by reducing the search rate. The detection range is still reduced, however, since the corresponding increase in frame time reduces the overage received energy per unit time. The only way the frame time can remain unchanged is through reduction of the size of the search area and thereby the tactical effectiveness of the interceptor weapon system. The frame time and search rate are affected not only by the search area and beamwidth, but also by the search pattern. The most common search pattern is a TV-type raster (no interlace). This scheme suffers from wasted flyback time from sweep to sweep as well as from frame to frame. The ideal pattern wastes no time which could be spent actually seaching.

In addition to the proper choice of parameters, the search pattern should be stabilized. If the search pattern remains in interceptor coordinates, there is elevation-azimuth crosstalk during interceptor banks. The elevation coverage becomes azimuth coverage and vice-versa in a 90-degree bank. To avoid the serious reduction in azimuth coverage during a bank and yet avoid the penalty of widening the elevation coverage, the search pattern should be stabilized in roll. To avoid distortion and maintain target separation in elevation, the search pattern should also be stabilized in pitch.

There are fundamental limitations involved in the determination of the various search and track parameters. These limitations are a result of the fact that all information obtained by a radar with an ordinary receiving antenna is contained in the time-behavior of a single electrical signal. All the useful data must be extracted from this single signal. This is quite different from a nonelectrical type of receiving system such as the human eye, which is capable of receiving many different signals simultaneously and is, therefore, analogous to a multichannel receiver. Once specific search range and angular coverage have been decided upon, the important parameter to maximize is the probability of detection of a specific target in a volume of space within a given time. The limit of this probability depends only on the average power transmitted and the sensitivity of the receiver. It may be stated in a qualitative manner that the transmitting antenna gain does not affect probability since the beamwidth is decreased as the antenna gain is increased. Consequently, although more

signal is returned during the period of time that the target is illuminated, this time period is correspondingly reduced, resulting in the average received energy per target "look" remaining independent of the transmitter antenna gain.

In addition to the preceding considerations, the effect of choice of beamwidth on sidelobe structure and antenna diffraction pattern must be determined. Briefly, the antenna is a function of shape of the antenna aperture (antenna feed and reflector) and of the feed pattern. The far-field antenna pattern is found by adding the contributions at a distant point from each element of the aperture. The major effects which determine the antenna pattern are the relative phase and amplitude of the signal strength at the point in question; the relative phase and amplitude in turn depend upon the phase and amplitude of the elements in the aperture, as well as the relative phase shift produced by the distance the waves travel from the different elements. For example, a uniform excitation of a square antenna of side L produces an antenna pattern given by $E(\theta,\psi)$, the relative field strength,

$$E(\theta,\psi) \cong \frac{\sin\left(\frac{\pi \ell \theta}{\lambda}\right)}{\frac{\pi \ell \theta}{\lambda}} \quad \frac{\sin\left(\frac{\pi \ell \psi}{\lambda}\right)}{\frac{\pi \ell \psi}{\lambda}} \tag{4-1}$$

$$\theta << 1 \quad , \quad \psi << 1$$

where θ is the angle between the direction of radiation and the perpendicular to the plane source in one dimension and ψ is a corresponding angle in the orthogonal direction.

Equation 4-1 may be interpreted to show that the pattern is approximately $\frac{\sin X}{X}$ in orthogonal planes defined by the angle θ. The antenna pattern has the approximate shape shown in Figure 4-3. Points in Figure 4-3 where the antenna pattern goes to zero are called the "nulls" of the pattern. The main beam is that portion of the pattern which lies between the first null to the left of zero degrees and the first null to the right of zero degrees. The distance between these two nulls is $\frac{2\lambda}{\ell}$. The successive nulls thereafter occur at multiples of λ/ℓ and the peaks at distances halfway between successive nulls. The peaks (except for the main beam peak at $\theta = 0^{\circ}$) are the sidelobes. The strongest sidelobes are the ones adjacent to the main beam. These are about 13 db below the intensity of the main lobe. Note that even for $\theta = 180^{\circ}$, some radiated energy still

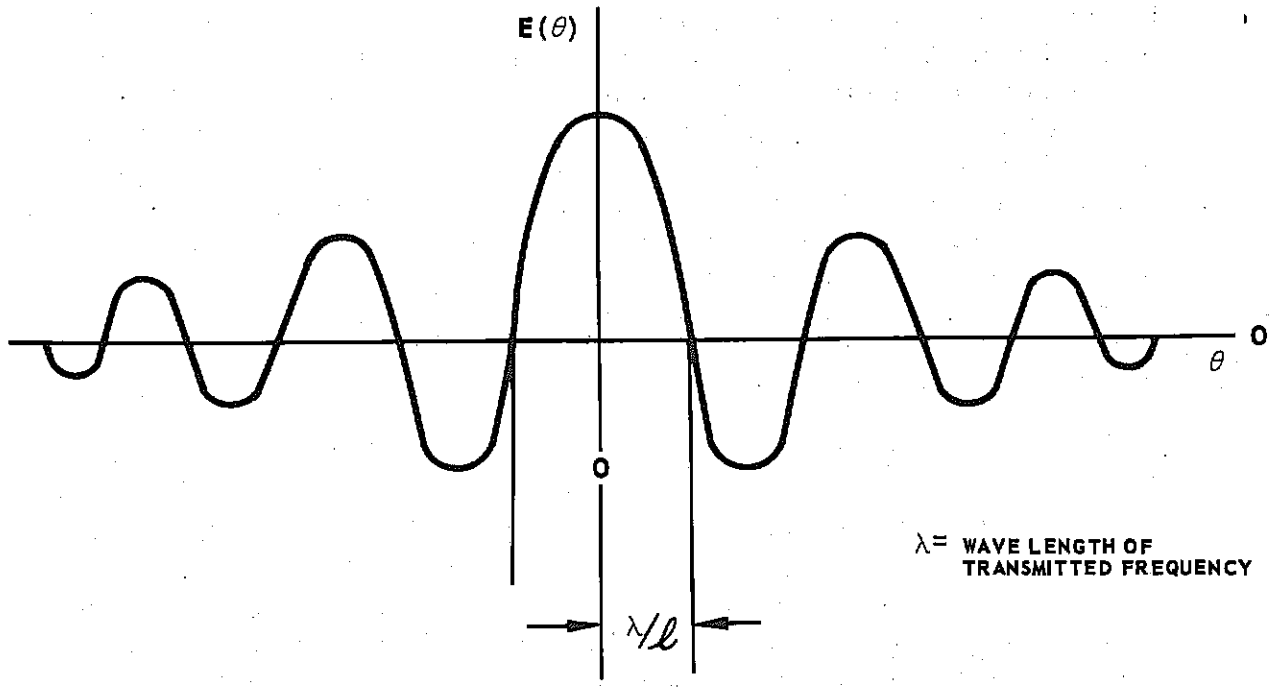

FIGURE 4-3. ANTENNA PATTERN PHASE AND AMPLITUDE

remains. This shows that energy is not only radiated toward the front and sides of the pattern, but toward the rear as well. It is important to note that the width of the main beam (with respect to antenna size) is inversely proportional to the length of the reflector. Thus, a narrow beam indicates the requirement for a large antenna; however, the number and intensity of the sidelobes are correspondingly increased.

A major problem in radar antenna design is the reduction of the number and amplitude of the sidelobes. For example, when a target is received on a sidelobe, the returned energy intensity for certain target aspects is comparable to that received from the main lobe. Unless the search pattern and presentation can discriminate against signals returned from the sidelobes, it may be erroneously assumed that sidelobe targets are actually in the main beam, resulting in very large angular error. A similar effect occurs in tracking systems, where it results in severe ambiguity. If the tracking system erroneously indicates the target to be in the main beam, the angular tracking error is disproportionately large. Angular resolution considerations are further complicated by the presence

of sidelobe energy. If, for example, two targets are in the field of view, even though the two targets are resolved in angle so far as the main beam is concerned, one target may appear in the main beam and the second in the sidelobe. If the target in the sidelobe is larger or comparable in size to that in the main lobe, an automatic tracking system may lock onto and track the wrong target. The ground-return problem is also made more severe by the effect of the sidelobes. Even though the antenna may be directed above the horizontal plane, a very large return may be obtained from the ground because of the large clutter area exposed to the radar beam. Many of the lower sidelobes will be reflected as ground-return clutter energy, confuse the system, and obliterate essential ground targets. Means for discriminating against ground clutter are described in a subsequent section. Sidelobe radiation also creates a problem for the radar-guided missile employing a rear-reference system, after it has been launched. For this particular case, the receiver uses energy from the radar tracking antenna to supply a signal for velocity and range reference. The fluctuation in intensity of the received main and sidelobe signals will cause sharp variances as the missile flies through the combined antenna pattern. This creates a severely fluctuating reference signal which then must be controlled by fast AGC or limiter circuits. If the intensity of the received reference signal is low compared to other extraneous signals and noise, the effect of limiting or fast AGC may appreciably worsen the signal-to-noise ratio, thereby reducing the effectiveness of the missile. Fortunately, however, the signal-to-noise ratio for the reference signal is usually quite good because of one-way transmission.

For the reasons stated as well as other considerations, it is desirable that the antenna pattern be controlled to minimize the number and amplitude of the sidelobes. The detailed configuration of an antenna pattern can be adjusted over a considerable range by proper controlling of the aperture excitation. For example, the sidelobes can be reduced relative to the main lobe by tapering the amplitude of the feed pattern near the edges of the aperture or antenna reflector. The disadvantage of this tapered-feed pattern is that the main lobe tends to increase in width when the main-beam gain is reduced. A typical parabolic antenna has a half-power beamwidth of about $\frac{1.2\lambda}{\ell}$, with the first sidelobes 20 db below the main beam. A cross-section taken through a main lobe generated by a circular aperture is very much like the $\frac{\sin X}{X}$ structure shown in Figure 4-3.

For some applications, the antenna beam pattern may be modified to result in a more complex beam. In PPI search sets or ground surface search, a fan beam may be required. Fan beams are narrow in one dimension and broad in the orthogonal dimension. For example, a fan beam which is narrow in azimuth gives good azimuth resolution, yet is wide in elevation and may be used to detect airplanes over a wide altitude range. This type of antenna pattern is designed by making the antenna aperture long horizontally and short vertically. Although it is entirely possible that optimum antenna patterns for search and tracking operations may be different, the assumption is made that the fundamental antenna pattern is unchanged in going from one phase to another. Since highly directional antenna patterns are needed at least for the tracking phase, such an antenna pattern will also be used in the other modes of operation.

As a first estimate of several of the antenna search pattern parameter requirements, suppose that a 3-degree main beamwidth (between half-power points) is adequate to give good angular resolution while searching the required range in ample time. From the preceding considerations, it may be concluded that a 3-degree beamwidth can be attained with a 27-inch parabolic reflector. This dish diameter is not unreasonable for present interceptor space accommodations, which allow the reflector to be satisfactorily positioned in the aircraft nose section. If the dish diameter were appreciably larger than 2-2$\frac{1}{2}$ feet, either the interceptor fuselage diameter would have to be increased, or the dish would have to be moved back to the point where it would interfere with other aircraft functions. A typical interceptor installation might place a 27-inch dish approximately 3 feet from the leading edge of the aircraft nose. The region in front of the dish must consist of a radome which passes electromagnetic waves with little or no attenuation. If the 3-degree beam is swept or scanned at a rate of approximately 100 degrees per second, a 70- by 20-degree search area will be scanned in about five seconds. If an interval of 10 seconds is allowed for target detection, the radar will have at least two "looks" at the target during the detection phase.

The search radar is then capable of providing angular-position and rate information. By determining the angular position of the axis of the beam or the antenna axis when a target appears at the receiver, the position of the target (in angle) relative to the coordinate system of the interceptor can be determined. The target's change in angular position from one frame to the next provides a measure of the angular rate, resulting in target trajectory information. This rate information is

nonprecise if the frame time is long and the number of "looks" during the search phase is few. Some measurement of angular rate and target heading can be found during the period of time in which the target is being illuminated by the beam. This illumination interval is on the order of 30 milliseconds for the assumed system. Direction information obtained during target illumination can (in principle) be found from the variation in received signal strength. If the interceptor-target relative velocity is small, the number of frames during which the interceptor radar is still in the search phase may be very large. In this case the progressive motion of the target can be recorded in several ways. For example, the information contained on successive frames may be transmitted back to the ground-control-interception (GCI) station, where the trajectory can be plotted by automatic means. On the basis of the past information it is possible to predict future locations of the target and thereby employ a "track-while-scan" feature. The track-while-scan feature is a useful one during the search phase and will be discussed in some detail in a later section. Thus, fairly precise angular-position information and nonprecision angle time derivative information are available during the search phase of the radar. Information such as range and range-rate data are useful during the search period. In the radar tracking phase, range and/or range-rate information are required. A method of determining range or time derivatives of range information, as well as considerations in design that the method entails, will be developed.

SECTION 5 — PROPERTIES OF THE TRANSMITTED SIGNAL

The measured angular position of the target in space is dependent upon the mechanical position of the antenna when a target signal is received, and not upon the nature of the transmitted radiation. Range and range-rate are inherent in, and available from, the target signal. This information is dependent on the nature of the transmitted signal; specifically, the spatial relationship of target and interceptor can be measured by determining the elapsed time between the transmission of a pulsed signal and its reception. Thus, if the transmitted carrier has some sort of time (or phase) modulation imposed on it, the absolute range between the interceptor and the target can, in principle, be measured. Similarly, the range-rate or velocity of the target can be measured from a knowledge of the rate-of-change of phase or frequency of the carrier compared to the frequency of the received signal (the so-called "doppler" effect). The radar may be instrumented to simultaneously measure range and velocity. Higher range derivatives such as acceleration and rate-of-change of

acceleration, could also be measured but usually do not add enough useful information to make the additional circuit complexity worthwhile. One of the principal ways of distinguishing radar types is by means of the modulation imposed upon the carrier. Several radar types, which are designated by the kind of modulation imposed on the transmitted signal, are described in the following paragraphs.

(a) PULSE RADAR

Pulse radars emit short bursts of rf energy at intervals. Pulses illuminating the target are reflected and some are received back at the radar receiver. The elapsed time between the transmission of a specific pulse and its reception is a measure of the range between the target and the interceptor. A simple range-measuring radar would consist of a transmitter which transmits a pulse of energy at a given instant of time and a receiver which receives the echo pulse a given instant later. Both the transmitted pulse or "main bang" and the echo or received pulse are displayed on the same indicator in such a manner that the time interval between the main bang and the echo pulse can be measured. The transmitted energy packet is shaped by the antenna beamwidth radially and by the pulsewidth longitudinally.

The rf wave energy is propagated at the velocity of light, C. If the target-interceptor range is denoted by "R," the time required for the transmitted pulse to reach the target and the time for the reradiated pulse to reach the radar receiving antenna is R/C. The total elapsed time between the transmission and reception of a given pulse is therefore

$$t = \frac{2R}{C} \qquad (4\text{-}2)$$

The value of C is approximately 1,000 feet per microsecond.

If the time t is known, the range R can be calculated. Time t can be measured by means of the scope, presenting both the main bang and echo on a scaled range. For the case where an A scope is used (the receiver output presented vertically against time horizontally), the time between the main bang pulse and echo pulse is the time t in Equation 4-2. During the search phase, range information can be presented on an oscilloscope indicator for use by the pilot. The same information may also be transmitted back to the ground control station. Since the pulsewidth of a pulse radar can be made extremely small compared to the interval of time

between the transmitted and received signals, very accurate measurements of range are theoretically possible. The pulse radar transmission is formed from a continuous wave (CW) carrier by turning the carrier on for a period of time τ, and then off for a time T, resulting in a train of rf pulses when the process is continuously repeated (see Figure 4-4)

where τ = pulsewidth; $T = \frac{1}{fr}$, and fr is the pulse repetition frequency;

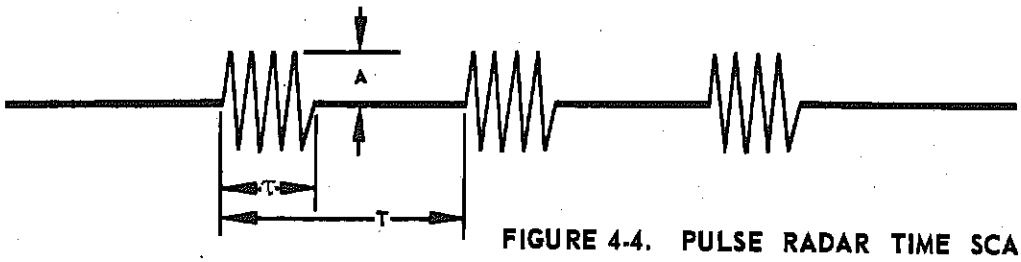

FIGURE 4-4. PULSE RADAR TIME SCALE

A = the pulse amplitude.

The train of rf pulses is received at the antenna, amplified, and demodulated so that only the video pulse envelope remains. The video as well as the mainbang pulse T are depicted in Figure 4-5.

Figure 4-5 is idealized since only the transmitted and received pulses are considered; noise and extraneous signals being excluded, and both the main bang and received pulse are assumed to be square. The echo pulse is much attenuated compared to the main transmission.

The presence of multiple targets in the antenna beam creates a problem of range resolution similar to the angular resolution case. If targets differ in range by less than $\frac{C\delta}{2}$ the received pulses will overlap, tending to obscure the separate identities (see Figure 4-6).

The range resolution can be improved to some extent by narrowing the pulsewidth. This narrowing, however, cannot be carried too far since the average power transmitted is proportionately decreased, which decreases the probability of detecting a target. Decrease of the pulsewidth can be offset by an increase in the transmitted pulse amplitude.

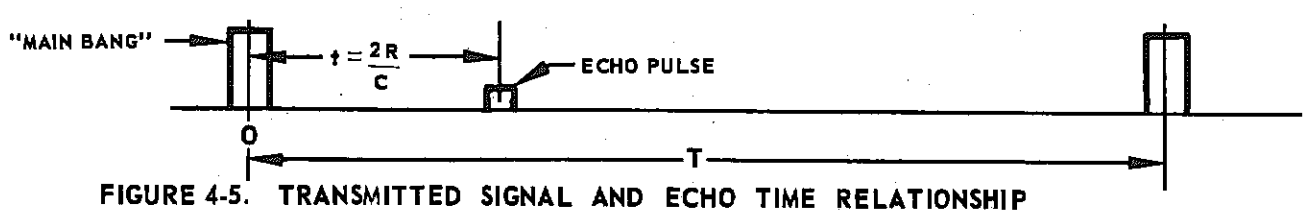

FIGURE 4-5. TRANSMITTED SIGNAL AND ECHO TIME RELATIONSHIP

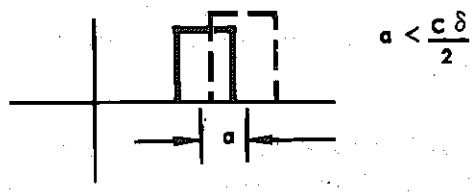

FIGURE 4-6. RECEIVED PULSE OVERLAP

Power increase is limited by voltage breakdowns which occur in waveguides and transmitting tubes. Another way to increase the average power while maintaining good range resolution consists of increasing the duty cycle by reducing the repetition period T. This procedure may produce the range ambiguity effect, which is the effect of receiving return echos not from the last transmitted pulse but from preceding pulses. The principal range ambiguity effect is usually from the preceding pulse with negligible contributions from pulses two or more previous to the return echo desired. Range ambiguity should be removed. A simple method for accomplishing this is to make the interpulse interval T as large as possible so that targets at ranges as great as $\frac{CT}{2}$ are presented without ambiguity. Increasing T has the effect of decreasing average power and, therefore, the detection probability will be reduced. The minimum radar range problem can occur even when only a single target appears in the field of view. By referring to Figure 4-5 it can be seen that when

$$R \leq \frac{C\delta}{2} \tag{4-3}$$

the main bang and echo pulse overlap as in the case shown in Figure 4-6. This effect causes the pulse radar to have a minimum range. Targets closer than the minimum range cannot be observed. The minimum-range effect is not as important in fire control radars as in guided missile minimum-range considerations. A missile equipped with contact fusing must enter the so-called "minimum range" (where the missile will not track) for target kill.

Other types of radar modulation than pulse modulation can be used for measuring range. For example the continuous wave (CW) rf signal can be frequency-modulated so that the variation or change in frequency of the transmitter which occurs between the transmission and return of an echo is a measure of the range between the target and the aircraft. Such systems are called FM-CW systems (i.e. frequency-modulated continuous wave systems) and are discussed in detail in another section.

An advantage of this type of system lies in the elimination of the minimum-range problem of pulse radar.

Measurement of target velocity is possible from information available in the pulse radar system. For example, if the change in position of the echo pulse is observed as a function of time, the approximate velocity of the target can be determined. This method has the disadvantage of providing a discontinuous velocity measurement, since the measurement can only be made over intervals approximating the duration of the repetition period.

(b) CW RADAR

Using the CW technique, a continuous measure of the relative velocity between target and radar is possible because of the doppler-shift effect of the received and transmitted frequencies. Although the doppler-shift effect also exists in the pulsed radar case and could therefore be used to measure velocity, the power available at the carrier-plus-doppler-shift frequency of the received signal is considerably reduced because of the low duty cycle in the pulsed case. The doppler shift is given by

$$f_d = \pm \frac{2v_r}{\lambda} \tag{4-4}$$

where f_d is the doppler shift, v_r is the radial component of target velocity relative to the radar, and λ is the wavelength of the transmitted radiation. Equation 4-4 can be interpreted to indicate that, as the target recedes from the radar by one half wavelength, one full cycle of returned radiation is denied the receiver as a result of the time required for energy to travel the additional half-wavelength and back. The sign in Equation 4-4 will, therefore, be negative if the direction of the target relative to the radar is away from the radar, and positive if the direction of the radial component of the target velocity vector is in the direction of the radar. The frequency of the doppler-shifted echo can be detected and measured by heterodyning the returned echo against the transmitted signal frequency.

A disadvantage of CW doppler systems is that there is now no convenient method for measuring range because of the lack of absolute time or phase information. This disadvantage can be offset by modulating the CW in some way such as by frequency, commonly referred to as FM-CM. Some of the desirable properties of CW doppler systems are thus diminished. For example, one of the advantages of CW doppler systems is

the ability of the system to discriminate against ground clutter. The reason for this can be seen from Figure 4-7, where it is shown that ground targets will return doppler frequencies extending all the way from zero up to f_g, where

$$f_g = \frac{2 v_g}{\lambda} \tag{4-5}$$

In Equation 4-5, f_g is the radar velocity relative to the ground. This equation indicates that the maximum doppler frequency which can be returned from ground clutter is the relative ground-interceptor velocity. For the case of head-on closing conditions, the target doppler frequency exceeds f_g since the relative target to radar velocity exceeds that of the ground to radar. This condition is shown in Figure 4-8, where it can be seen that the doppler line lies outside the ground return spectrum. In the search phase, the operator or automatic detection device can distinguish the doppler frequency shift from the ground return spectrum by using a spectrum analyzer. The doppler shift can be utilized during the tracking phase to discriminate against ground return spectrum by use of a velocity tracking gate. The desirable conditions depicted in Figure 4-7 do not exist for receding targets, for in this case the target doppler line lies within the ground return spectrum. This is a condition not likely to occur tactically if the interceptor has a speed advantage over the target. If the CW doppler spectrum shown in Figure 4-7 is frequency-modulated so as to yield range as well as velocity information, the spectra shown are necessarily smeared, thus increasing the possibility of overlap. When the spectral line is smeared out to a distance from f_d equal to or greater than a frequency $\frac{f_d - f_g}{2}$, the spectra will overlap and the desirable isolation which existed in the CW case will no longer exist. The range

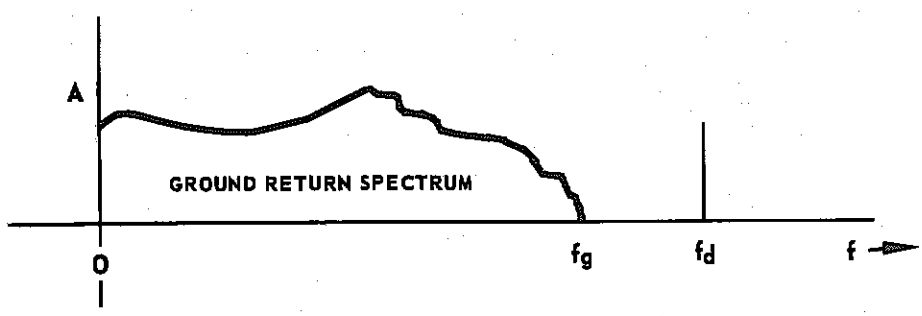

FIGURE 4-7. DOPPLER FREQUENCY GROUND DISCRIMINATION

accuracy and range resolution capabilities of a modulated CW system increase with increases in spectral width; but, unfortunately, increases in spectral width decrease the ground-clutter rejection capability. Thus it appears that in a simple, modulated CW system, good range accuracy and resolution are not compatible with velocity accuracy and resolution requirements. Figure 4-7 indicates that a CW doppler system is effective not only for discrimination in the presence of ground clutter, but also for the detection of low flying targets and for the detection of moving targets in the midst of stationary clutter. The clutter rejection capability of the CW system can thus be seen to have great tactical value.

In a conventional pulsed radar, ground clutter extends all the way from the range (altitude) of the radar above the ground to greater ranges, with the clutter amplitude being generally greatest at the altitude of the interceptor. (See figure 4-8.)

Figure 4-8 indicates that, if the range of the target from the radar were greater than the altitude of the interceptor above the ground, the target would lie in the ground return. Since it is difficult to differentiate the target from ground returns when R exceeds R_a, range radars are primarily useful against targets at lesser ranges than the interceptor's altitude (R_a). The ground return problem becomes particularly difficult when the target being tracked is flying at a lower altitude than the interceptor. The CW-doppler case depicted in Figure 4-7 has a distinct advantage over the pulsed range radar situation depicted in Figure 4-8, since the doppler line remains separated from the ground return frequency spectrum regardless of the range, provided only that the interceptor is overtaking the target. Further, there is no minimum velocity or

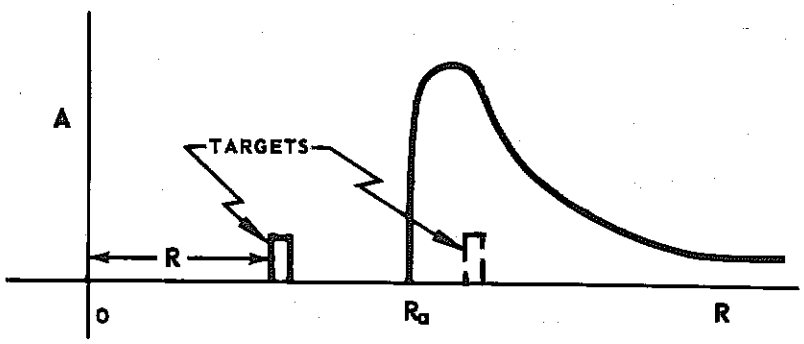

FIGURE 4-8. ALTITUDE - RANGE GROUND CLUTTER EFFECT

velocity ambiguity problem such as is found in the conventional pulse radar. There is, however, a velocity resolution problem as can be seen, for example, in the case where targets lying in the same beam return doppler only if the targets differ in their relative velocities with respect to the radar. The signal differences can be isolated by means of filters, but the closer together the signal frequencies are, the greater the resolving capability of the filters must be. Practical filters must span the expected velocity rates.

(c) COMPARISON OF PULSE AND CW RADAR

In an active CW radar, target echoes received simultaneously with a transmitted signal cause distortion of the returned signal. This is a difficult practical problem which has not been completely solved. A second CW radar difficulty results from the requirement for an extremely stable oscillator, since any shift in the transmitted carrier or the local oscillator frequency appears in the receiver as a target doppler shift. In an active system, differential frequency shifts between transmitter and the receiver local oscillator can be compensated for by locking the local oscillator to the transmitter. In semiactive systems, differential frequency shift problems can be solved in one of two ways. One method is by use of a "brute force" technique, that is, by designing very stable equipment. The required degree of stability for many applications has not yet been reached. A second technique for solving the problem is by transmitting a reference frequency signal to the semiactive receiver and locking the receiver local oscillator frequency to the transmitted rf signal. The latter technique can, for example, be advantageously applied to a semiactive CW missile.

CW systems have an inherent average power advantage over comparable pulse radars. For a given peak voltage breakdown the CW system can transmit an amount of power equal to a corresponding pulse system times the reciprocal of the duty cycle. Since duty cycles of the order of 1/1000 are common, the implication is that for the same voltage breakdown, the average power transmitted by a CW system will ultimately be on the order of 1000 times as great as that of the pulse system.

A comparison of a velocity-tracking CW system and a range-tracking pulse system illustrates the frequency-time duality which exists throughout physics. For example, in order to get good range resolution, the range radar employs short pulses but the corresponding frequency spectrum which results is broad, as is shown by the character of the

frequency-time duality of the Fourier transform pair. A more complete discussion of spectra and frequency-time duality appears elsewhere. Good range resolution indicates a liklihood of frequency functions of the two pulses that overlap. Similarly, to obtain greater velocity resolution, relatively narrow frequency spectra with correspondingly broader time functions are required, so that eventually the two time functions will overlap. In the CW case, the frequency spectra are lines and the corresponding time functions are sinusoids extending indefinitely into time. The phenomena may also be viewed as a problem in multiplexing. A range radar can be considered a device which uses time multiplexing; that is, the received and transmitted signal can be distinguished on the basis of time separation. Similarly, the velocity tracking, or CW doppler, system can be viewed as a frequency multiplexing system in that the received signal is separated from the transmitted signal on the basis of frequency. It is interesting to speculate whether or not it might be possible to simultaneously make use of both frequency and time multiplexing, taking advantage of the useful properties of both types of radar.

(d) PULSE-DOPPLER RADAR

Although it may appear from the preceding discussion that a combined system with a high degree of range and velocity resolution and accuracy is impossible, this is not the case. For example, consider a pulsed radar in which use is made of both time and doppler-shift information. The latter is inherently available because of doppler shifts in the pulse repetition frequency lines of the pulse train frequency spectrum. In the practical pulse range radar case, the difficulty is that the phase of the carrier from one pulse to the next is not coherent, in other words, the starting phase of the carrier during each pulse is not the same. The lack of phase coherency causes the fine structure of lines in the corresponding frequency spectrum to be smeared and made indistinguishable so that the doppler shifts associated with the lines in the pulse frequency spectrum are not distinguishable from the carrier lines. If the pulses were generated by successively starting and stopping a stable continuous CW oscillator, the pulse-to-pulse phases would be coherent and the fine line structure would exist with no smearing. In this case, the doppler-shifted lines would interlace with the transmitted lines and the difference frequency could be detected. If multiple targets existed, the various doppler frequencies would give rise to lines which interlaced the lines of targets of other velocities. The desired target could then be resolved in velocity by means of a comb filter, i.e., a filter whose rejecting bands lie between the spectral lines of the desired signal. An alternative technique would be to

select the proper target in range by means of a range gate, and reject targets outside of the range. This scheme makes use of the range resolution properites of the system. The output of the range gate can then be passed through an appropriate comb filter which selects the desired target by resolving in velocity those few targets which were unresolved in range by the range gate. In principle, this combination of range and velocity gating yields a better degree of resolution than either one separately. The combined system has the further advantage of the receiving signal occurring only when the transmitted signal is off, thus obviating many practical difficulties discussed in connection with CW radars.

A disadvantage found in the combined range and velocity discrimination system is due to a velocity ambiguity similar to the range ambiguity previously described. As a consequence of pulse modulating the CW carrier in the pulse-doppler radar, the single doppler-shifted line is periodically repeated. The time periodicity gives rise to range ambiguity of

$$R_{amb} = \frac{ncT}{2} \tag{4-6}$$

Similarily, the periodicity of the frequency lines in the doppler spectrum also gives rise to an ambiguity given by

$$V_{amb} = \frac{n\lambda}{4T} \tag{4-7}$$

where n is an integer.

When the doppler-shifted return signal is heterodyned with the transmitted signal there will result signals whose doppler velocities with respect to the carrier are

$$f_d + \frac{2}{\lambda}\,\frac{\lambda}{4T},\ f_d + \frac{2}{\lambda}\,\frac{2\lambda}{4T},\ \ldots\ldots\ldots\ldots\text{etc.}$$

Thus, the doppler shift is detected by beating the returned echo with the stable oscillator which generates the rf carrier. The heterodyning process is the same regardless of whether the carrier is above or below one of the spectral lines of the echo. Since unambiguous range and velocity measurements are desired, both quantities in Equations 4-6 and 4-7 should be large. In order for R_{amb} to be large, T must be large; whereas, for V_{amb} to be large, T must be small. It is impossible for

both quantities to be simultaneously large. A system will be described later that works properly in the presence of ambiguity in either (but not both) of the two parameters.

Because of the many desirable properties of a pulse-doppler system, it is the recommended system. As previously mentioned, pulse-doppler systems should be made coherent by locking the receiver local oscillator to the transmitter. The latter problem is solved by means of automatic frequency control. A CW transmitter-oscillator is modulated by a train of pulses which effectively gates the CW oscillator on and off at a regular rate. The desired frequency stability of the transmitter is difficult to maintain when the oscillator is turned on and off. It is preferable, therefore, to keep the CW oscillator operating continuously, opening and closing the line leading from the transmitter oscillator to the antenna. Ferrite switches which capably perform this function have been developed. Coherent pulses may also be developed by starting with a low frequency (as compared to the desired transmitted frequency) and then employing frequency multipliers to multiply it to the final output frequency. The switching required to provide a pulsed output may be performed before or after frequency multiplication.

(e) PULSE-DOPPLER FILTER CONSIDERATIONS

Pulse-doppler radar is employed to permit targets to be distinguished from clutter created by ground, sea, or weather returns. One characteristic that distinguishes the target from clutter is velocity. Because of the doppler effect, velocity differences appear as frequency or spectral differences in the return signal.

The first step in separating the target from unwanted echoes is by filtering the total return. Not all of the noise can be eliminated by filtering the region of the target spectrum, since there will always be at least receiver noise and usually clutter. The filter employed should be no wider than the target spectrum. In a simple tracking system, a single range gate can be made to track the variations of the received target range and a velocity gate made to track the velocity variations of the desired target. In the search mode, targets at all ranges and velocities must be presented. One way of providing information while still using the desirable properties of range and velocity gating is by using a series of range gates (a filter bank) which divide the interpulse or repetition period into n_r contiguous range intervals. Each of the successive range gates can be followed by a corresponding range doppler filter to divide the

expected range of doppler frequencies into n_v frequency bands. Each of the doppler filters should be followed by a threshold device which distinguishes whether the signal present in the filter is noise or signal-plus-noise, and further indicates when the threshold is exceeded. A block diagram of the proposed arrangement appears in Figure 4-9. The receiver must be blanked during the period of the transmitted pulse to prevent the transmitted pulse from entering the receiver and confusing the logic processing circuitry. The logical arrangement shown in Figure 4-9 can be used for indicating the velocity of a target relative to the interceptor for a specific range interval. After the signal has been range-gated, there is still a finite strip of return ground area that is passed by the gate. In this strip the velocity of ground targets relative to the interceptor can vary from $+V_i$, to $-V_i$, where V_i is the interceptor velocity. This ground return gives rise to doppler shifts relative to the carrier frequency of $\frac{\pm 2V_i}{\lambda}$. This ground doppler spectrum might be as shown in Figure 4-10. The ground return clutter is, in general, more intense on the side in which the target return appears because the main beam is pointed toward the target. As shown in Figure 4-10, if the velocity of the target relative to the interceptor is closing, the doppler-shifted frequency is greater than the carrier frequency (positive shift). The main-beam clutter also comes from ground return, which generally has a velocity that is closing relative to the interceptor. Side- and backlobe clutter give rise to that portion of the ground clutter spectrum which has opening velocities relative to the interceptor. The width of the target spectrum is approximately equal to the reciprocal of the time it takes for the beam to sweep across the target. When the target is being tracked, the resulting spectrum is narrowed appreciably. In the case shown in Figure 4-10, the velocity of the target relative to the interceptor is closing (decreasing) so that the interceptor is being overtaken by the target. As indicated in connection with CW radar, a relative closing velocity vector (between target and interceptor) insures that the target lies outside of the ground clutter spectrum centered about f_o. For a pulse-doppler system, the spectrum about f_o is repeated periodically at the pulse repetition frequency as shown in Figure 4-10. Thus, the velocity at which the interceptor is overtaking the target must not be so great that the doppler-shifted received frequency lies in the side- and backlobe clutter spectrum centered about the fixed repetition frequency component.

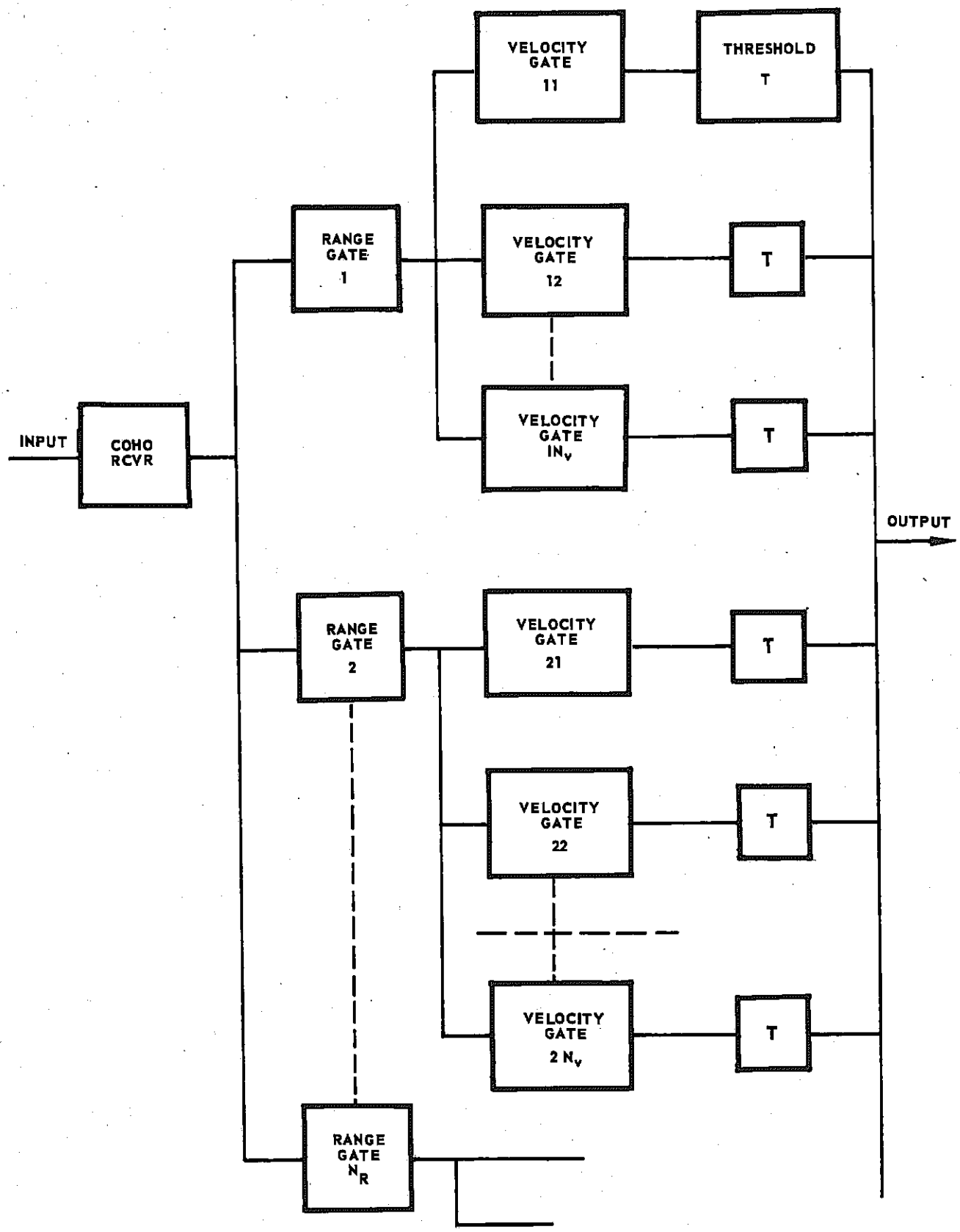

FIGURE 4-9. PULSE DOPPLER LOGIC BANK

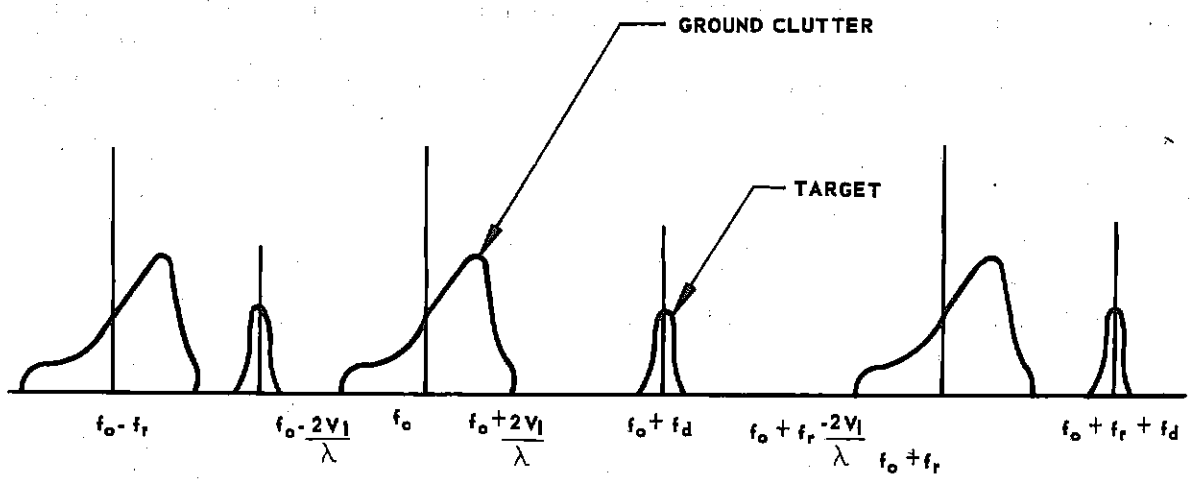

FIGURE 4-10. GROUND DOPPLER SPECTRUM

The condition required for the target doppler to be clutter-free is (neglecting the width of the target doppler spectrum)

$$f_o + \frac{2V_I}{\lambda} < f_o + f_d < f_o + f_r - \frac{2V_I}{\lambda} \tag{4-8}$$

or

$$\frac{2V_I}{\lambda} < f_d < f_r - \frac{2V_I}{\lambda} \tag{4-8A}$$

Equations 4-8 and -8A indicate that a lower limit is set on the repetition frequency of

$$f_r \geq \frac{4V_I}{\lambda} \tag{4-9}$$

where V_I is the interceptor velocity. For the condition where the equality sign holds in Equation 4-9, the ground clutter spectra about the successive repetition frequency lines are contiguous and no clutter-free signal

line can be passed. If a doppler frequency range from zero to $f_{d_{max}}$ is needed because of the tactical requirements, then the minimum repetition frequency must be

$$-f_{d_{max}} \leq f_d \leq f_{d_{max}}$$

$$f_r \geq \frac{4V_I}{\lambda} + \left(f_{d_{max}} - \frac{2V_I}{\lambda}\right) = \frac{2V_I}{\lambda} + f_{d_{max}} \tag{4-10}$$

where

$$f_{d_{max}} > \frac{2V_I}{\lambda}$$

In Equation 4-10 the equality sign implies clutter and target overlapping because of the finite spectral width of the target doppler return. Equation 4-10 allows an estimate to be made of the minimum repetition frequency. Assume the maximum interceptor velocity to be Mach 3 and the maximum target velocity to be Mach 2. At 35,000 feet the velocity of the interceptor is

$$V_I \cong 3000 \text{ feet per second}$$

and the velocity of the target is

$$V_T = 2000 \text{ feet per second}$$

The maximum doppler frequencies corresponding to these velocities are

$$f_{d_I} = \frac{2V_I}{\lambda} = \frac{2(3000)}{.1} = 60\text{kc} \quad f_{d_T} = 40 \text{ kc}$$

$$f_{d_{max}} = f_{d_I} + f_{d_T} = 100 \text{ kc}$$

$$\therefore f_r \geqq f_{d_I} + f_{d_{max}} = 160 \text{ kc}$$

It therefore follows that a repetition frequency of at least 160 kc is required in the case cited. This greatly exceeds the conventional pulse radar repetition rate. From Equation 4-6, the target range from which the first ambiguous signal results, is

$$R_{amb} = \frac{C}{2f_r} = \frac{10^9 \text{ ft/sec}}{3.20 \times 10^5 \text{ cycles/sec}} \cong 3000 \text{ feet}$$

If the repetition period is held constant, this ambiguity is quite serious, since all targets beyond the desired target at multiples of 3,000 feet enter the range gate. This gate must be at least wide enough to pass the pulse. If the pulse selected is 1/2 microsecond, the gate should also be a minimum of 1/2 microsecond, which corresponds to 500 feet. Since 500 feet is only one-twelfth of the interpulse interval, range-gating discriminates against only eleven-twelfths of the extraneous targets and eleven-twelfths of the noise distributed throughout the interpulse interval. Obviously, the relatively high duty cycle selected (one-twelfth) did not lead to efficient range resolution and did result in a high probability of range ambiguity. A method for removing range ambiguity is by jittering the repetition rate. The repetition period, $T = f_r$, can be varied about some average value. Echoes that return during the range sweep, triggered by the corresponding transmitted pulse, will appear at specific ranges, while echoes returned from prior transmissions will be scattered over random regions of the sweep under consideration. This serves to identify the extraneous echoes but does not remove them. If there are a large number of pulse returns from the target per scan, the jittered returns from ambiguous ranges will tend to be further discriminated against by the process of integration. Just as for the conventional pulse radar, this shows why a large number of pulses returned per scan is advantageous. An additional benefit to be derived from jittering the repetition rate is that of decreasing the deleterious effects of interference from other radar transmitters and certain kinds of electronic jamming. For example, a jamming signal which sends back signals resembling the echoes but at false ranges cannot easily be synchronized with the randomly transmitted repetition frequency. A suitable jittered repetition frequency might have a mean value of about 160 kc and, for this case, the jitter should not exceed approximately 500 feet of range.

Assume that 5 seconds are required for a scan to be completed and let the antenna scan rate be 100 degrees per second. With a 3-degree beamwidth, the time on target is approximately 30 milliseconds, requiring a doppler-filter bandwidth or velocity gate of approximately 35 cycles per second. This filter has a bandwidth that is wide enough to allow the target signal to build up during the time the beam is actually on the target, and yet which is sufficiently narrow to reject a large amount of noise. The doppler frequencies of interest vary from 60 to 100 kilocycles. It therefore follows that associated with each of the 12 range gates there must be more than 1,000 velocity gate filters to completely fill the band. This number of doppler filters is too great for a practical system. Reducing the number of velocity gates to say, 50, reduces the velocity resolution to 40 feet per second. A signal-to-noise ratio degradation factor of 20 is also introduced by decreasing the number of filters from 1000 to 50. The signal-to-noise ratio can, however, be improved by integrating the signal after it has passed through the velocity gate. With the assumed 50 velocity gates for each of the 12 range gates, there are, then, 600 velocity gates. The signal-to-noise ratio required for a low false alarm rate (for example, one per minute) is set by the threshold and the detector following the velocity gate. The setting of the threshold thus adjusts for the required signal-to-noise ratio in the velocity gate to assure a given probability of detection in a single scan. When the acceptable false alarm rate and probability of detection are specified, it is possible, from Equation 4-11, to calculate the required signal-to-noise ratio in the doppler filters and, consequently, determine the required average transmitted power. For this application, the quantity B in Equation 4-11 represents the bandwidth of the velocity gate. The solution of Equation 4-11 shows an excessive value, since no consideration was made for power loss due to blanking of the receiver during pulse transmission. Jittering the repetition period broadens the doppler return spectrum. But, since it is necessary to reduce the total number of velocity gates anyway, jittering the transmitted frequency has little effect in determining the required average power transmitted. As an example of the calculation of transmitted power, assume that the signal-to-noise ratio required at the output of the doppler filter is unity. This should give a reasonably high (i.e., 50 percent) probability of detection in a single scan, with a low false alarm rate. The equation for average power can now be solved

$$P_{avg} = \frac{4\pi R^4_{max} \lambda^2 \gamma k T B_v}{L \sigma A^2} \qquad (4\text{-}11)$$

$$P_{avg} = \frac{4\pi (4 \cdot 10^5)^4 \, (.01) \, (10) \, (4.2) \, (10^{-21}) \, (300) \, (800)}{5 \, (10) \, (\pi^2) \, (1.1)^2}$$

$$P_{avg} \cong 5 \text{ kw avg pow}$$

$$P_{peak} \cong 60 \text{ kw}$$

Thus, the value of 5 kw represents a first estimation of the required average power. Because of the large duty cycle capability of this system, the peak (60 kw) power is not as difficult to obtain as the average power. The same peak rf power required may be obtained by a proportionate increase in the size of the antenna, since the average power required varies inversely as the fourth power of the dish diameter. Thus, if the dish diameter is increased to 40 inches and a correspondingly smaller area is searched (while the time of dwell remains constant) on each target, the average power could be reduced to 1 kilowatt. The estimate made here is probably somewhat low since the combined range and velocity gating improves the apparent signal-to-noise ratio. With improved signal conditions an operator may successfully detect targets displayed on the face of the scope at signal-to-noise ratio values lower than one.

It may be questioned whether the addition of FM modulation to a CW radar system to accomplish range gating actually improves the over-all accuracy and resolution capability. It appears to be a corollary that, for an improvement in range accuracy and resolution, there is a degradation of velocity accuracy and resolution, and conversely. Principal deterrent to the use of a CW system is the practical difficulty of simultaneous transmission and reception of signals with a single antenna. The problem might conceivably be solved by using two antennas, but because of the large size of the antenna needed for angular accuracy and resolution, this seems impractical. Further, without modulation the CW system has no range measuring capability. The range information could be obtained from auxiliary range-measuring radar equipment, but such an approach would require more equipment and complexity than the pulse-doppler scheme. The suggested design approach has been to produce a system with good velocity resolution and accuracy. This results in poorer range

accuracy and resolution. A multiple gate system has been suggested for improving signal-to-noise ratio and discriminating against ground clutter and noise. One of the principal techniques used in conventional pulse radars to discriminate against ground clutter is the moving target indicator (MTI) or the airborne moving target indicator (AMTI). The coherent MTI system operates on the principle that successive return echo signals in a system employing a stable pulse-to-pulse phase coherent transmitting frequency show a difference in the return from stationary and moving targets. Stationary targets remain unchanged in amplitude on successive sweeps, whereas moving targets vary in amplitude, blurring the composite picture for the moving target only. An analysis of the technique follows:

For a target which is stationary relative to the radar,

$$R = \text{constant, and } V_R = \frac{dR}{dT} = 0, \text{ and } f_d = 0 \tag{4-12}$$

For a target moving at a constant velocity V_{R_1} relative to the target,

$$f_d = \frac{2V_R}{\lambda} \tag{4-13}$$

During a transmitted pulse of carrier frequency f_o, the pulse can be represented by

$$y_R(t) = y_o \cos 2\pi f_o t \tag{4-14}$$

The received target pulse may be represented as

$$y_R(t) = y_o \cos 2\pi f_o (t-T) \tag{4-15}$$

where $T = \frac{2R_s}{c}$ for the stationary target at range R_s and

$$T = \frac{2R_m}{c} = \frac{2}{c}\int_o^t V_R dt + \frac{2R_v}{c} = \frac{2}{c}\left(V_R t + R_v\right) \tag{4-16}$$

for the moving target whose range was R_v at $t = 0$. The return from the stationary target is therefore

$$y(t) = y_o \cos 2\pi f_o \left(t - \frac{2R_s}{c}\right) \tag{4-17}$$

and when beat against the transmitted signal, the resulting video pulse amplitude is

$$y = \frac{y_T\, y_r}{y_o} = \frac{y_o}{2}\left[\cos\,(2t-T)\,2\pi f_o + \cos 2\pi f_o T\right] \tag{4-18}$$

After filtering the double frequency term

$$y = \frac{y_o}{2}\cos 2\pi f_o T = \frac{y_o}{2}\cos\frac{4\pi f_o R_s}{c} \tag{4-19}$$

which is a pulse of constant amplitude. For the moving target,

$$y = \frac{y_o}{2}\cos\frac{4\pi f_o}{c}\left[V_R t + R_v\right] = \frac{y_o}{2}\cos\left(2\pi f_d t + \frac{4\pi R_v}{\lambda}\right) \tag{4-20}$$

A sinusoidal varying video results from the moving target, the rate of variation corresponding to the doppler frequency. The moving target can be distinguished from the stationary target by delaying the echo signal one pulse repetition period and subtracting the return which is stationary in the period, thus leaving only the moving target. This process depends on the moving target return pulse varying from one pulse interval to the next, and therefore depends upon a high degree of pulse-to-pulse transmitter frequency stability. When the radar is moving relative to the ground, some means must be provided to compensate for the velocity of the system if a coherent MTI system is to be used. One method is to change the phase of the reference signal at the same rate at which the phase of fixed echoes is being changed by the motion of the radar. The effect is to give the radar a virtual velocity which cancels the actual velocity.

Another AMTI method which is very applicable to airborne radar is the noncoherent method. A target moving in clutter produces an echo that varies in both amplitude and phase. The amplitude variations of the target signal can be detected by a nonlimiting receiver. For this case, ground clutter itself acts as a reference signal. Since a coherent reference oscillator is

not used, the method is referred to as a noncoherent method of detecting moving targets. Here the local oscillator does not have to be stabilized since phase changes are not to be detected as in the coherent case. The transmitter still must maintain good stability as in the coherent case because overlapping ground clutter would set up frequency beating as the transmitter frequency varied from pulse to pulse. Since this system is sensitive only to amplitude fluctuations, whereas the motion of the radar causes mainly phase changes in the received echoes, this method will work even though the radar is moving. The main disadvantage of the noncoherent method is that a moving target can be detected only when there is ground clutter at the same range and azimuth as the target (the target is lost in the clear areas). It is possible to overcome this disadvantage by providing noncoherent operation for short ranges and low altitudes where ground clutter is quite sure to occur and coherent operation for areas where ground clutter is not likely to occur.

To summarize, AMTI that is suitable under all conditions is relatively complex and is relatively no better in discriminating against ground return than the multiple gate system previously described. The multiple range gate approach does offer additional improvement in the signal-to-noise ratio even when clutter is not the main source of noise. The multiple gate method is also useful against jamming techniques. The principal disadvantage of the multiple gate system is the large number of filters required to give adequate resolution. One way of reducing the number of velocity gate filters is by using a sweep oscillator to scan the repetition frequency interval with the velocity gates. The action then is similar to the multiple gating procedure. The velocity gate must not sweep by the target so fast that the threshold fails to trigger, yet it must sweep sufficiently fast to cover the entire expected doppler range during a repetition period. The minimum rate for a 40-cycle filter, for example, is 1000 cycles per repetition period, or 160 megacycles per second. This high sweep rate is impracticable and, if a wider velocity gate is used to reduce this rate, the receiving system becomes inferior to the multiple gate system in both resolution and accuracy. It is recommended, therefore, that a proposed system use a multiple range and velocity gate system such as described.

SECTION 6 —EFFECT OF THE TYPE OF TRANSMITTED AND RECEIVED SIGNAL ON SEARCH RADAR DESIGN

In Section 4, the effect of search radar angular coverage and antenna pattern was discussed. The discussion indicated a choice of parameters

for a practical system. Further considerations must be made when range is introduced.

Consider that, during the search phase operation of a range-measuring pulse radar, not only must the scan be capable of covering the entire required angular space, but the rate must be such that many pulses are returned during the period of time that the target is illuminated. The detection probability is dependent on the various search parameters, especially the pulse repetition frequency and the speed of scan. It is highly desirable that the beam dwell on the target long enough to allow at least several pulses to be received. The maximum target detection range for many pulses is appreciably greater than that for a single pulse. To attain more returned pulses from the target during the interval in which the target is illuminated, the antenna scan rate must be slowed. A conflicting demand requires that the entire search area be covered as rapidly as possible, hence, a compromise must be made. The number of pulses striking the target during one scan is given by N, where

$$N = \frac{f_r \beta}{\omega_{sc}} \tag{4-21}$$

and

f_r = the repetition frequency

β = the antenna beamwidth

ω_{sc} = the angular scan frequency

It follows that $\frac{\beta}{\omega_{sc}}$ is the time of target illumination (between half-power points) and f_r is the number of pulses per second. An example for the case where one pulse is returned from the target per scan, N=1 (assuming a beamwidth of 3 degrees and a scan rate of 100 degrees/sec), the required pulse repetition frequency is

$$f_r = \frac{\omega_{sc}}{\beta} N = \frac{100^\circ/\text{sec } 1 \text{ pulse}}{3^\circ} \cong 33 \text{ pulses/sec}$$

A common repetition frequency used in pulsed radar lies in the vicinity of 2000 pulses per second. At this rate (other parameters remaining the same) approximately 60 pulses would be returned per target look. For high velocity resolution pulse-doppler radar requirements, it is desirable to go to even higher repetition frequencies than the above example. In the pulse-doppler radar, the higher repetition frequency more closely approximates the pure CW system, thus providing improved velocity accuracy and resolution over the conventional pulsed radar. The rate at which the radar collects information can be computed. Consider the diagram in Figure 4-11.

If Ω is the total solid angle scanned, and ω is the solid angle included in the beam, and T is the total scanning time, then T must be equal to the number of beamwidths in the angular coverage area times the beamwidth search rate in beamwidths per second, or

$$T = \frac{\Omega}{\omega} \text{ beamwidths} \cdot \frac{\beta \text{degrees/beamwidth}}{\omega_{sc} \text{degrees/sec}} = \frac{\Omega}{\omega} \frac{N}{f_r} \qquad (4\text{-}22)$$

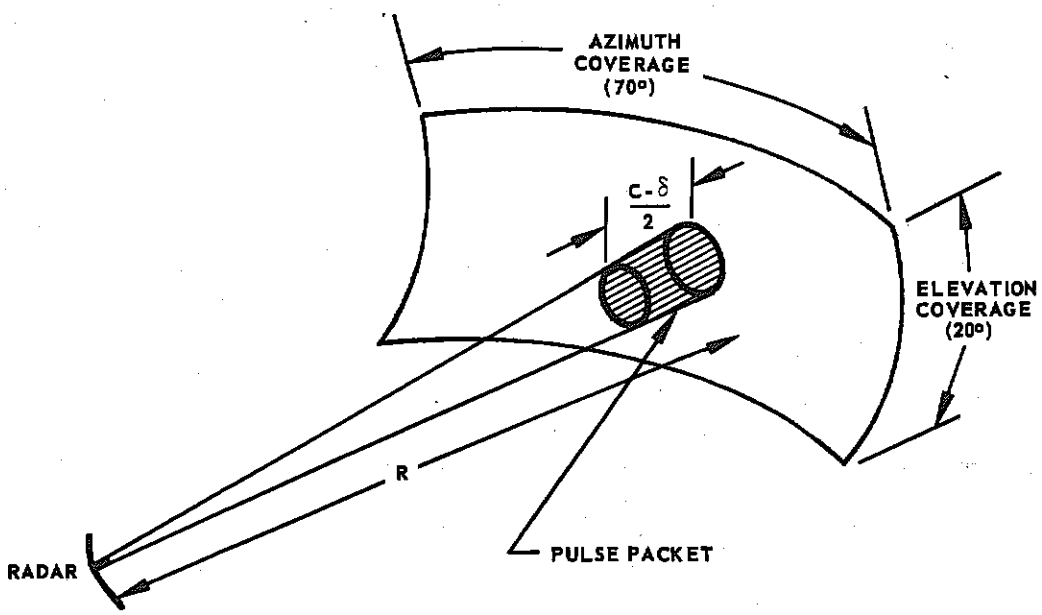

FIGURE 4-11. SCAN - BEAM WIDTH RELATIONSHIP

and the maximum repetition frequency $f_{r_{max}}$ is

$$f_{r_{max}} = \frac{1}{t} = \frac{c}{2R} \tag{4-23}$$

The maximum repetition frequency $f_{r_{max}}$ is one which is just sufficient to allow the transmitted pulse to be received at the range R. If the repetition frequency were any greater than this, a second pulse would be transmitted before the first was received and range ambiguity would result. Thus, for no range ambiguity, the maximum repetition rate must again be

$$f_{r_{max}} = \frac{1}{t} = \frac{c}{2R}$$

Then substituting Equations 4-10 and 4-11 yields

$$T = \frac{\Omega}{\omega} Nt = \frac{\Omega}{\omega} N \frac{2R}{c} \tag{4-24}$$

Defining a pulse packet as the smallest discrete volume from which echoes can be received, the packet dimensions are determined by the angular size of the beam and the radial distance, $\frac{C\delta}{2}$. The number of pulse packets in the volume scanned is

$$P_{pac/vol} = \frac{\Omega}{\omega} \cdot \frac{R}{\frac{c\delta}{2}} = \frac{\Omega}{\omega} \frac{2R}{c\delta} \tag{4-25}$$

where Ω = beamwidth

ω = volume

R = packets

$\frac{c\delta}{2}$ = beamwidths

The number of packets examined per second is

$$\frac{P_{pac}}{sec} = \frac{\frac{\Omega}{\omega} \cdot \frac{2R}{c\delta}}{T} = \frac{\Omega}{\omega} \frac{2R}{c\delta c} = \frac{1}{N\delta} \tag{4-26}$$

where T has dimensions of seconds per volume.

Equation 4-26 may be called the information rate of the radar, which is the number of units of information per unit time received. The unit of information is defined as the pulse packet and may be assumed to carry one bit of information, namely, that the packet either contains or does not contain a target. In classical information theory, the information rate is given by the expression

information rate = information/sample • samples/second

The number of samples per second which can be transmitted is fixed by the bandwidth of the communication channel, which in this case is the bandwidth of the radar receiver. The bandwidth of the radar receiver is approximately

$$B \cong \frac{1}{\delta} \tag{4-27}$$

If the signal-to-noise ratio is large, the number of pulses needed to yield the information desired is only one. The maximum information rate, or channel capacity, is therefore simply $\frac{1}{\delta}$. However, since more than one pulse is received per look at the target, the maximum rate is not achieved — in fact, an N-fold redundancy resulting in an information content per sample of 1/N is introduced. This redundancy reduces the information rate for high signal-to-noise ratios but is very useful for combating the noise at low signal-to-noise ratios, since it is a type of integration or filtering. Thus, a lower information rate than that possible at high signal-to-noise ratios is acceptable in order to combat noise. The preceding is a very simple example of some of the simplest and most fundamental concepts of information theory. Assuming a system in which there are 161 beamwidths per volume for a range of 80 miles and a 1/2 microsecond pulse width, the information bandwidth contains

$$I_p/BW = \frac{2R}{C} = \frac{2 \times 80}{18{,}000}\ 1/2 \times 10^{-6} = 1800\ \frac{\text{packets}}{BW}$$

or in terms of packets per volume

$$I_{p/vol} = 161\ \frac{BW}{vol} \cdot 1800\ \frac{\text{packets}}{BW} = 300{,}000\ \frac{\text{packets}}{vol}$$

The number of packets examined per second will then be the number of packets per unit volume, divided by the time it takes to scan the volume (assume 5 seconds in the example), then

$$P_{\frac{ex}{sec}} = \frac{1}{N} = \frac{300{,}000}{5} = 60{,}000$$

For a pulse width of one-half microsecond,

$$N = \frac{1}{P_{\frac{ex}{sec}}} = (60{,}000)\ 1/2\ .10^{-6} = .3$$

This shows that the number of pulses needed to strike the target per scan is only one to adequately scan the specified volume. One returned pulse per scan is the maximum information rate. Thus, in the absence of noise, it is possible for the whole system to scan at the optimum rate. However, in order to detect targets at long ranges, the number of pulses required per look will be very much greater than one.

To determine the information rate for a CW radar which has the same maximum range as the corresponding pulse radar, consider the following. A CW radar can theoretically be converted from the pulse radar by simply increasing the pulse width and correspondingly reducing pulse amplitude so that the same average power is transmitted from both systems. Thus the peak power is reduced by the duty cycle when the pulse width δ is increased to the reciprocal of the repetition frequency, $1/f_r$. Equation 4-14 then becomes

$$\text{Information rate} = \frac{f_r}{N} \cdot \qquad (4\text{-}28)$$

The maximum rate with one pulse returned per look at the target is simply the repetition frequency f_r. Thus, for the same range, the CW radar is not capable of yielding information at as high a rate as a pulse radar. But, for the case where high information rate is of lesser importance, a CW radar system may be entirely adequate. It may be questioned why the area under consideration is not scanned at a higher rate in order to obtain maximum information. One reason is that, since the beam is on the target for a finite time only, even a single frequency doppler signal will be spread out over a band whose extent will be roughly the reciprocal of the time the beam is on the target. For very high rates, the CW anticlutter capabilities would be degraded. Again, the inability of the CW radar to handle high information rates can be partially offset by the use of a pulse-modulated doppler system. In this regard the pulse-doppler system again overcomes a disadvantage of one of the component systems used alone. It retains the desired useful antiground clutter capability, and further resolves the practical problem of transmission and reception of signals at the same time. It improves the over-all resolution problem by resolving targets both in range and velocity. There are relatively few restrictions on the relationships between the doppler and repetition frequencies, although it is difficult to design a system which is undisturbed by either range or velocity ambiguities. Parameters which are now to be determined are the pulse width and the repetition frequency. A pulse width equal to one-half microsecond represents a reasonable choice based on pulse amplitude and high average transmitted power considerations. A one-half microsecond pulse imposes a 500 foot "blind" range which is not detrimental for most interceptor radar applications. Generation and reception of half-microsecond pulse current are not severe parameter requirements. The determination of repetition frequency is not easy. As indicated previously, the repetition frequency affects the number of target looks per scan and, consequently, the noise rejection capability of the system. The problem of range and velocity ambiguity is also inherently related to the choice of repetition frequency.

SECTION 7 — SEARCH RADAR DESIGN - MISCELLANEOUS CONSIDERATIONS

The fire control radar system's total effectiveness would be considerably enhanced by the addition of "track-while-scan" capability. From maximum detection considerations, the target is detected and locked on at the maximum possible range. This immediately causes the system to go into the tracking mode, which prevents further detection of targets

which may be in the area. The track-while-scan technique enables the system to continue searching even though locked-on in the tracking mode and allows the interceptor to attack while still surveying the radar search volume. Another value of the track-while-scan technique lies in its counter-countermeasure capability. It is likely that the target will not employ electronic countermeasures until it is sure it is under attack, it is possible for the interceptor and the missile to track on the bombers countermeasure radiation. Thus, if during the major portion of the interception, the radar mode of operation is unchanged, a manned target receives little indication that it is under attack. It is desirable, from this consideration, to delay lock-on to the last possible moment.

Two desirable features which modern radars should incorporate are (1) automatic alerting and (2) target identification. The pilot is normally unable to concentrate his attention continuously on the radar scope, and he should, therefore, be alerted to the appearance of targets on the display. The alerting problem is actually one of dealing with threshold signals. The threshold must be set so that there is a high likelihood of alerting on a true signal and a small likelihood of alerting on a false signal or noise. The second tactical requirement which needs to be satisfied is the identification of other aircraft. Thus, some sort of IFF (identification, friend or foe) system must be incorporated in the fire control system.

One of the most serious problems facing the fire control radar system designer is the inclusion of appropriate counter-countermeasure equipment. The enemy will have certain natural countermeasures to aid him. These include multiple targets, ground return, scintillation, etc. The most likely artificial countermeasure that will be carried for use against radar-type missiles and interceptor radars is chaff. It is quite possible that bombers carrying high-yield armament will be surrounded by a screen of chaff at the proper time. The coherent pulse doppler radar has considerable counter-countermeasure capability against chaff. Other electronic countermeasures might include the use of barrage jamming or repeaters. Barrage jamming may confuse the whole search area, and repeaters may confuse the search problem in that many apparent targets will appear in the search field of view. Both of these electronic countermeasures can be discriminated against by incorporating in the radar and the missile the ability to track through jamming of the type described. One of the most difficult countermeasures to discriminate against is the decoy target. A suitable decoy could be provided by a diversionary bomber. If the decoy

bomber carries armament as well as countermeasures, the destruction of the decoy is, of course, worthwhile.

SECTION 8 - SEARCH RADAR RANGE

The most important fire control radar specification is the maximum range of detection. It is also important that the lock-on and tracking ranges be equally great. The maximum tracking range can be greater than either the detection or lock-on range. Since lock-on occurs at a time later than detection, the range between target and radar will be less than at detection. A system designed to provide adequate detection range should have adequate lock-on and tracking ranges and, in many instances, the maximization of the search range does maximize the lock-on and tracking ranges. In the search case, the beam sweeps by the target and reflects a limited number of pulses back to the antenna during the scan period. The returned signal must have sufficient energy that it may be distinguished from noise at the radar scope. The most likely way in which a target will be selected is by the pilot observing it on the radar scope. It is, therefore, important that the target signal be readily distinguishable from the noise. If automatic detecting or alerting devices are used, the signal must be of sufficient strength to operate the threshold bias.

A "brute force" way to obtain maximum radar range is by increasing transmitter power. The upper limit on average transmitted power is set primarily by practical considerations. Airborne radar transmitters which exceed one-megawatt power capabilities are generally large and bulky and require large amounts of power. These considerations make them unsuitable for airborne application. The disadvantage of excessively high peak powers lies in the danger of breakdown, not only in the transmitter oscillator, but also in the waveguide and other rf equipment. Breakdown is mainly a function of the distance between conductors of different potentials and of the dielectric material separating these conductors. One way to solve voltage breakdown problem is to make use of waveguide components of sufficiently large dimensions. The size of the waveguide is, however, limited to dimensions of the frequency employed.

Previous estimates of antenna size have been based on an assumed use of the X-band frequency of approximately 10,000 megacycles per second. This represents a good choice for transmitted frequency; it is based on X-band component development, as well as size. Higher

frequencies make possible the use of even smaller components with a subsequent reduction in size and weight, but with a corresponding increase in the voltage breakdown problem. There is also the problem of losses of rf energy through absorption by various gases and vapors in the atmosphere. These absorption bands are quite resonant, and their number increases with increase in frequency above X-band. If frequency is decreased to reduce the voltage breakdown problem, the size of components increases, making them less suitable for airborne application. More important to the over-all fire control problem than the considerations mentioned thus far, are the frequency effects upon the angular resolution and accuracy. Higher frequencies make possible the fulfillment of the narrow antenna beamwidth requirement. Since a beamwidth of from one to three degrees is a desirable width for angular resolution and accuracy, frequencies appreciably lower than X-band are not considered. The antenna size required and the mechanical problems involved in scanning and in the installation of the system in fighter aircraft increase when lower frequencies are used. It might be that a higher frequency would increase the antenna gain but, as pointed out previously, no actual improvement in the probability of detection is obtained.

Another method of increasing the radar range is to increase the radar receiver sensitivity. Tracking range can also be increased by judicious design of the automatic tracking servos. For the case of search radar, no tracking servo is employed during the detection process and the problem is strictly one of maximizing and optimizing receiver sensitivity and average transmitted power. The receiver sensitivity is reflected in the noise figure, where this figure is a measure of quality of the receiver and, hence, is an important factor in determining the minimum receivable signal at the antenna. Signal, as considered here, must be distinguishable from noise at the indicator.

Since the system must operate over long ranges (80 miles for the example case considered here), the reflected echo energy from the farthest targets can be expected to be small compared to the magnitude of transmitted signal energy. The transmitted signal power has been attenuated from 10^{-12} to 10^{-15} by the time a return signal echo is received from the longest ranges. If additional extraneous or disturbing signals (noise) were not present, the range of the radar could be made infinitely large by adding sufficient gain to the receiver to amplify the smallest signal. Unfortunately, the receiver itself is a source of much noise. Thermal noise originates primarily in resistors; random motion of electrons in vacuum tubes generates shock noise, and semiconductor

devices such as crystal diodes and transistors also operate with some random motion of electrons and other particles that create noise. By suitable circuit design in the receiver, noise levels can be reduced to less than micro-microwatt levels. Even at this low signal level, after amplifications of 120 db or more, there is still an appreciable noise level (perhaps as much as a fraction of a volt). At long ranges, the amplitude of the returned echo signal may be comparable to or even smaller than these noise (RMS) voltages. At distant ranges, the echo signal is difficult to distinguish from noise, and it is the ultimate inability to resolve a signal from the noise that sets a limit on maximum obtainable radar range. Noise can be discriminated against on the basis of known differences between noise and signal voltages; for example, on the basis of the spectral difference characteristics of noise and signal. Appropriate filtering may be used to appreciably improve the signal-to-noise ratio. The nonlinearities of receivers operating at low signal-to-noise ratios also degrade the signal-to-noise ratio. Some nonlinearities such as dynamic range limitations are undesirable, but also unavoidable. It may be said that nonlinearities in amplifiers degrade the signal-to-noise ratio when the input signal-to-noise ratio is below unity. Despite the best efforts made to extend the dynamic range of an amplifier, there will always be cut-off and saturation limit effects. Dynamic ranges and other types of nonlinearities are improved by the use of properly designed AGC systems. These AGC systems have, however, thresholds below which the system tends to maintain constant gain of noise rather than signal. This effect occurs at very low signal-to-noise ratios and may appreciably degrade the system noise-rejection capability. Other nonlinearities are deliberately introduced; these nonlinearities described are usually associated with modulators and demodulators. For optimum detection processes the signal-to-noise ratio will remain unchanged, and in most practical detection processes the signal-to-noise ratio is degraded. The design of detectors to minimize signal-to-noise ratio degradation is, therefore, of great importance in extending radar range.

SECTION 9 – THE ACQUISITION AND LOCK-ON PHASE

The duties of an interceptor pilot require not only the carrying out of flight procedures connected with the combat flying mission, but also the viewing of the radar display, locking the interceptor onto targets, and various other duties connected with the fire control interception.

For any proposed fire control system, the use of automatic target detecting and pilot alerting equipment should be considered. Because of

the known fallibility of automatic devices, the equipment should have a manual override to permit the pilot to take over control of the interceptor. After automatic target detection and pilot alerting have taken place, the target must be acquired (locked onto) to permit tracking. At this point, the need for human judgment (in selection of the proper target) is greatest. Once the proper target has been selected, automatic lock-on and tracking should begin.

The radar is essentially locked onto in four aspects: azimuth, elevation, range, and velocity. Since the search radar is already searching in elevation and azimuth coordinates, automatic lock-on in these two dimensions requires only a lock-on device. Range and velocity are not searched during the search phase; hence, automatic lock-on in these coordinates requires not only a detection device, but also a corresponding searching arrangement.

Present techniques for searching and locking on by a human radar operator are much simpler than the suggested automatic schemes. The operator is required to inspect the radar scope, select the proper target by use of a cursor, and manipulate cockpit controls to lock onto the target. This operation automatically stops the antenna search. The antenna beam axis is then aligned to the cursor position in azimuth and elevation. In another arrangement, the position of the cursor relative to the target of interest can be used to designate the target to the track-while-scan system, which stores the coordinates of the target. Thereafter, the target is tracked automatically, even though the scanning operation continues.

An automatic detection and alerting device is inherently available in the multiple-gating scheme. This technique can be made particularly effective against barrage or noise jamming. At each velocity gate output, there is a threshold detector which will not indicate the presence of a signal until the threshold is exceeded. The threshold is set so that the false alarm rate is small and the probability of detection is large. This simple procedure works well in the presence of receiver noise and other noise sources. If jamming noise is applied, however, the false alarm rate will increase unless the receiver gain is appropriately decreased. A fast acting AGC would be required to overcome the noise, since the

level fluctuates rapidly over wide limits as a result of antenna scanning and other phenomena. A fast AGC may, however, blank out a true target. By making the AGC dependent upon the average of the outputs of all or a large number of the filters, a true signal in one filter would produce only a small change in the average gain and, consequently, true signals would not be blanked under such a condition. At the same time, the automatic gain control could limit the noise outputs of all the filters. When the target signal spectrum is narrow compared to the noise spectrum, band-pass limiting can be employed. In this scheme, the signal plus the noise is passed through an ideal amplitude limiter and then through a band-pass amplifier centered on the signal input spectrum. It will be shown that the usual degradation in signal-to-noise ratio caused by nonlinearities is minimized by band-pass limiting. Not only is the degradation small for small signal-to-noise ratios, but there is an actual gain for large input signal-to-noise ratios. Furthermore, the output power density for small input signal-to-noise ratios is a constant and is independent of the input noise power. The band-pass limiter effectively acts as an AGC on the noise, obviating the necessity for control of receiver gain. Furthermore, the AGC action is essentially instantaneous compared to the finite time lag introduced by an ordinary AGC. The band-pass limiting is a very attractive scheme for reliable automatic alerting, even in the presence of jamming noise. With the multiple gate scheme, the searching problem is simplified, since the searching device can scan the outputs of the velocity gate threshold detectors and lock onto the velocity gate which indicates a target presence. The scanning device automatically selects the range gate associated with a bank of velocity gates and locks on in range. This method is satisfactory for a single target. In the multiple target case, the first target to be locked onto is determined by the manner in which the search scheme is mechanized.

Velocity search starts with the highest velocity, searching downward to the lowest velocity; a higher velocity target would therefore be locked onto first. The highest velocity target might not, however, be the suspect target. This particular difficulty is avoided in the multigate system by simultaneously searching in velocity each of the range gate velocity filters and choosing, first, the target at the closest range.

Tactically, neither the highest velocity nor the closest target may be the desired one. The weapon-carrying target may fly at intermediate ranges and velocities so as to be protected by decoys, chaff dispensing aircraft, and electronic countermeasures. Obviously, the problem of complete automatic detection and lock-on is not solved and, therefore, requires a manual override control.

A difficulty in designing automatic search schemes is caused by the requirements for the system to scan until a target is located and then stop when a target appears. A compromise among search rate, reliability of detection, and search stop must be made. An excessively high search scan rate gives a lower probability of target detection than does a slow rate. Upon indication that the sweep is to be stopped, the signal must be suitably precessed. This makes additional circuitry necessary and expends valuable time in the tactical situation. When the search operation is stopped, that is, after automatic target lock-on, verification of valid target acquisition should be determined. If the target locked onto subsequently proves to be not a true target but simply noise or jamming, the search operation should be recycled to begin again. The recycling is more easily accomplished for range and velocity scanning by electrical than by mechanical techniques. For the automatic elevation and azimuth lock-on, recycling is best accomplished by mechanically stopping the antenna scanning motion on the line-of-sight. System complexity is increased considerably if automatic search and lock-on in range, velocity, elevation, and azimuth are provided. Furthermore, the search lock-on signal-to-noise ratio and, consequently, the search lock-on range are considerably poorer than the corresponding characteristics for the tracking case. This follows

since, in the tracking mode, target parameters are measured continuously; whereas, in the search scheme, only brief looks are taken at potential targets. During these short look times, the search system must logically conclude if a signal is a true target or not, and then it must act on this information by either stopping sweep and locking onto the true target or recycling if the target is false.

SECTION 10 — AUTOMATIC TRACKING

Tracking a target in a specific coordinate (range velocity, elevation, or azimuth) may be defined as the process of selecting the desired target in the presence of other targets, jamming, and noise so that the output of the tracking device designates the true target. The position of the target may be tracked in the three coordinates which may be used to define the position in space; namely, azimuth, elevation and range. Similarly the time rate of change of a point (target) in space may be tracked by tracking the azimuth, elevation and range rates of the target. Similar higher time derivatives of the position may be tracked. The combined tracking of a target in azimuth and elevation is usually termed "angle tracking." Angular rates can usually be found directly from the angle tracking by simply differentiating the azimuth and angle signals. Since the azimuth and angle signals are generally continuous functions of time, the corresponding derivatives will also be continuous functions of time. In principle, range-rate or velocity tracking could also be derived from range tracking information. In the typical pulsed range radar, the information which yields the range is not continuous, but is, rather, sampled (discrete). Velocity information then can be derived only by differencing. Since the pulse-to-pulse change in position is relatively small, particularly for high pulse repetition frequencies, this method for obtaining velocity is not difficult. However, because velocity information is inherently available in the doppler shift, it is preferable to make use of this phenomenon for determining velocity. Knowledge of velocity information is sufficient to determine range by use of the process of integration. The constant of integration is required for determining the initial range and must be determined by other means than pure velocity tracking. If the velocity information is appreciably more accurate than the range information, range may be more accurately predicted by integrating the velocity information (if the initial constant of integration is known) than by direct measurement of range information. Continuous range information may be obtained by integrating velocity and using the resulting range information for the initial range as well as for continous corrections to the range as the flight progresses.

Many of the problems of the tracking radar are the same as those of the search radar. Accuracy resolution and maximum range are desired in both cases. Maximum range depends upon the noise associated with the signal and the signal-to-noise ratio. In this regard, the principal difference between the search and tracking cases is in the ultimate application of the information; for search the output is presented on an

indicator, and for tracking it is directed to automatic detection and alerting devices. The purpose of the search radar is to present a fairly large field of view of the tactical situation to the pilot, and to alert the pilot when a true target enters the field of view. The purpose of the tracking radar, on the other hand, is to actually track the target in its various coordinates so that an accurate measurement of these coordinates and their rates can be presented to the computer. Although the track-while-scan feature is a desirable one, it is unlikely that track-while-scan will be employed continuously until weapon firing. Consequently, ordinary tracking techniques are considered before track-while-scan techniques. This section on automatic tracking is divided into three principal parts: (1) angle tracking, (2) range tracking, and (3) velocity tracking. Tracking systems other than the three listed could also be used. Any type of automatic control device may be considered a tracker. For example, automatic gain control and automatic frequency control are both automatic control and tracking devices and come under the category of the feedback devices referred to as servomechanisms. An automatic tracking radar is, in essence, a complicated multiple-loop servo. The servo outputs provide information to the computer, which ultimately controls the flight of the aircraft, as well as weapon preparation, arming, and firing.

A target coordinate tracker is a special type of servo whose block diagram generally falls into the type of servo indicated in Figure 4-12.

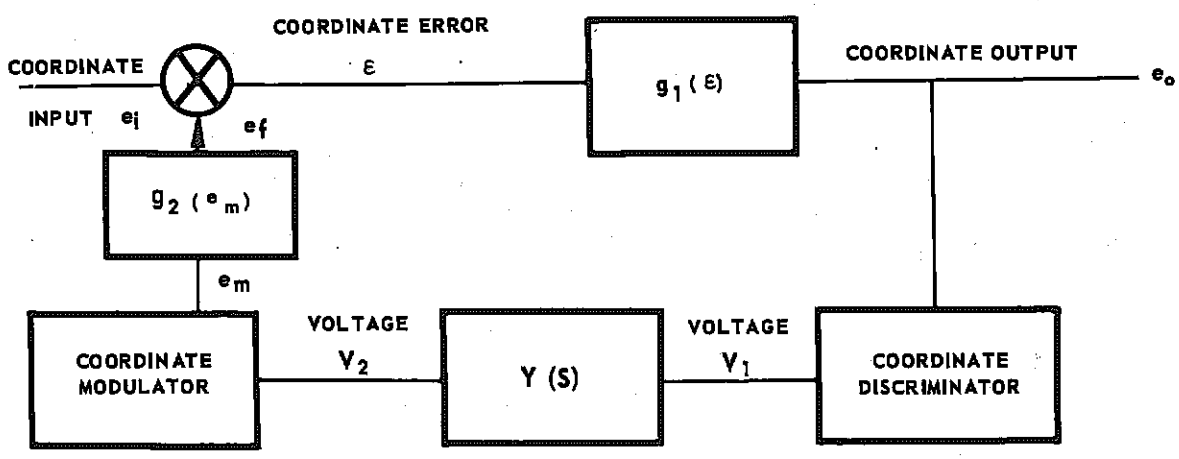

FIGURE 4-12. COORDINATE DISCRIMINATOR SERVO

Referring to Figure 4-12, the coordinate input appears as a parameter of a time. This parameter, which is proportional to the coordinate to be tracked, may be the amplitude, frequency, phase, etc., of the time waveform. The input coordinate is compared in some way with the feed-back coordinate so that the coordinate "error," defined as the difference between the input and the output, is small. As long as this coordinate error remains sufficiently small, it is considered that the coordinate is being tracked. To generate the required feed-back coordinate, the error must be operated upon. The block $g_1(\epsilon)$ indicates an operation on the coordinate error. This operation usually includes a gating or selective device which selects the desired target from other targets and noise. The output of this device is used at the computer input. The selected target signal is then passed on to a coordinate discriminator or demodulator, which develops at the output a voltage linearly proportional to the coordinate output. The discriminator output voltage is operated on by the transfer function, indicated as Y (S), whose purpose is to introduce the proper servo parameters into the system. These parameters consist of gain, equalization, integration for memory, and other parameters as required. The output of the Y (S) block is applied to a coordinate modulator, which inverts the demodulation process to provide an output proportional to the voltage from Y (S). The coordinate modulator output can be further processed by another block, indicated as $G_2(e_m)$, which supplies output to be fed back for comparison with the input coordinate of the comparator. Although trackers may vary considerably from the described servo, the basic system of most trackers can be described in terms of Figure 4-12.

(a) ANGLE TRACKING

The coordinate input in Figure 4-12 represents, for this case, the angle the antenna scan axis makes with a line connecting the radar antenna and the target. This line is called the line of sight (LOS). If the antenna scan axis is pointing directly along the line of sight, the system is said to be tracking in angle. Angular error is usually divided into azimuth angular error and elevation angular error, where azimuth and elevation correspond to orthogonal coordinates in the interceptor coordinate system. The angular error between the antenna axis and the line of sight can be measured in the interceptor by using a frame of reference fixed to the interceptor; the elevation error is referred to in the interceptor elevation plane, and the azimuth error in the interceptor azimuth plane. Angular error must be measured in

some way. A simple measurement of variation and return intensities is not sufficient to give good angle tracking. The reason for this is that the target itself varies in aspect and, hence, effective cross-sectional area. The target may indicate a larger return off the main beam axis than it does on the main beam axis. Such effects introduce appreciable angular error in tracking. Further, the apparent cross-sectional area varies in a random manner due to scintillation and glint effects. What is needed is a means for measuring the direction of arrival of the wavefront when the normal to the wavefront passes through the source of radiation.

The angle tracking error will be zero when the antenna axis is aligned with the normal to the wave front. The method of determining this normal is called antenna lobing. The lobing process amounts to bracketing the target in direction by moving the antenna beam or lobe around in space. Comparison of the relative strength of the receiver signal with the lobe in different positions is used by the antenna tracking loop to cause the antenna drive mechanism to move the antenna in the proper direction to follow the target. One method of doing this consists of switching the lobe from one angular position to another while observing the return signal from each position. The result of this lobing is an amplitude-modulated signal in the receiver, which derives an error signal used in the tracking loop. In this lobing method the beam axis never points directly at the target when the angle tracking system is tracking perfectly. In Figure 4-13 the cross-section of the antenna beam in the

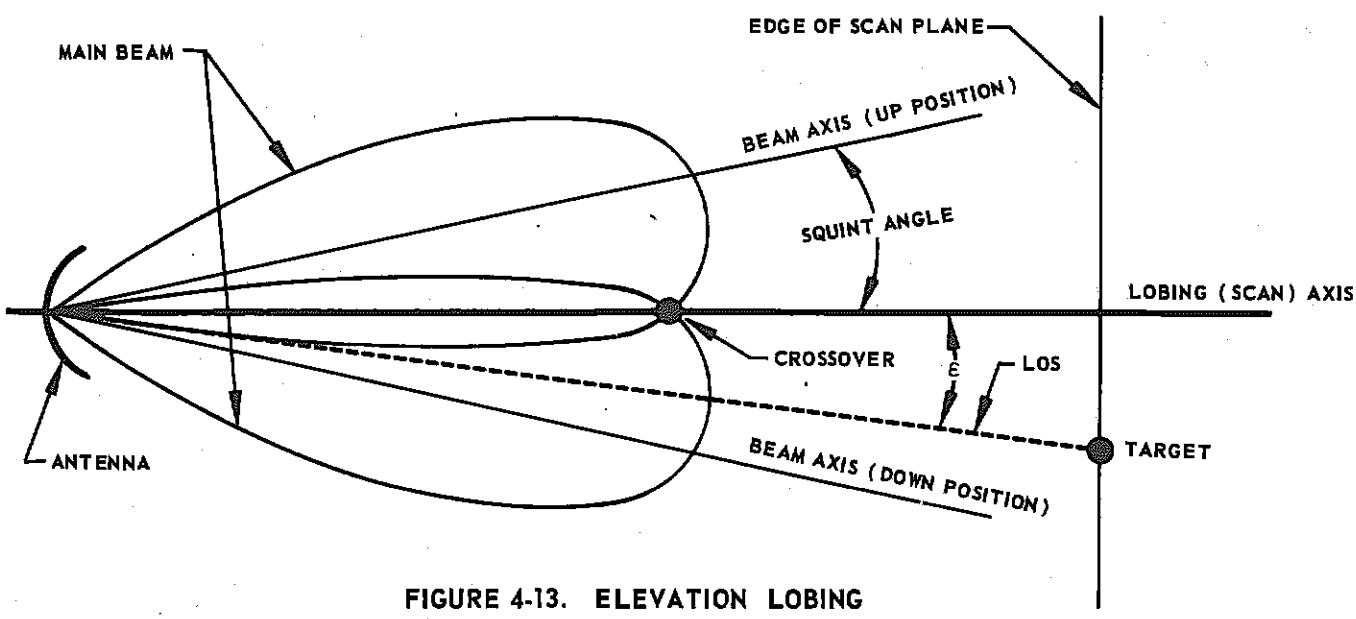

FIGURE 4-13. ELEVATION LOBING

elevation plane is shown in two positions, namely, the maximum up and down positions relative to the axis of symmetry or lobing (scan) axis. Thus, if the beam is switched, or lobed, alternately between the up and down positions as shown, it can be determined whether the target is above or below the lobing axis by the average intensity returned from the up position of the beam compared to that returned from the down position. Note that the two beams cross over at a given point and the line connecting the antenna to the cross-over point is called the lobing, or scan axis. The word lobing is preferred over scanning for this type of operation, since the word scanning was used in connection with the search radar, which scanned the volume of space. The purpose of the antenna motion in this case is not to search space but, rather, to provide a means for determining the direction of arrival of the wave-front from the target. The maximum angle that the axis of symmetry of the beam makes with respect to this lobing axis is called the squint angle. Clearly, the arrangement shown in Figure 4-13 will indicate whether the target is up or down with respect to the lobing axis, and may even indicate the actual angular displacement of the target from the lobing axis in the elevation plane, but it yields no information whatsoever about the component of angular displacement in the azimuth plane. If the antenna beam were similarly switched in azimuth, the corresponding indication in the azimuth plane could be determined. If four such switched positions for the antenna beam were used, the antenna beam could progress sequentially in either clockwise or counterclockwise direction in a plane around the lobing axis. The time required for the antenna beam to switch or lobe to the other positions and return to its original position is called a scan period, and the complete operation is called a scan cycle. It appears that the minimum number of lobing positions per scan cycle needed to give information in both azimuth and elevation must be slightly greater than two. The preceding conclusion can be deduced from some very basic concepts in information theory.

Rather than perform discrete switching operations in which the beam axis travels in discrete steps from one point on a cone to the next, the lobing operation is generally performed in a continuous motion. The lobing axis forms the principal axis of the cone and the beam axis the directrix of the cone. The time taken for the beam axis to complete a 360-degree rotation is called the scan period, and the reciprocal of the scan period is called the scan frequency. The entire process is called conical scanning, although it more correctly might be called conical lobing. Mechanically, conical lobing can be produced by using a fixed antenna dish with the feed rotating around the lobing axis,

or, conversely, by using a fixed feed on the lobing axis, tilting the dish axis with respect to the lobing axis, and then rotating the offset dish about the lobe axis. As in the case of the search scan, there is a minimum scan rate set by the need for unambiguous angle information. In particular, there must be a minimum of slightly more than two looks at the target per scan cycle; that is, slightly more than two return pulses per scan cycle. It therefore follows that

$$\frac{1}{f_r} < \frac{1}{2f_s} \tag{4-29}$$

or

$$f_r > 2f_s \tag{4-29a}$$

where f_s is the scan frequency and f_r is the pulse repetition frequency. The repetition frequency must be at least twice the scan frequency. Scan frequencies exceeding 1000 cycles per second are uncommon because of the difficulty of rotating mechanical components at these rates. Electronic means can be used effectively to increase the scan rate. It is advantageous to have as high a scan rate as practical, since the amplitude scintillation spectrum is of the low-pass type; the higher scan frequencies restrict amplitude scintillation, increasing the angular accuracy of the target measurement. Conical scanning is a type of time-sequential scanning in which the direction of the target is determined after at least one scan cycle has been completed. The direction is then determined by an averaging process. It is possible to lobe in such a way that the direction of the target is determined instantaneously from each pulse of returned energy. Such systems are called simultaneous-lobing or monopulse systems. In a monopulse system, multiple antennas are used to determine the direction of arrival of the wavefront from a single measurement obtained from the information in a single returned pulse. This method has several advantages, one of which is that mechanical motion of the antenna is unnecessary, even while tracking. Another advantage of monopulse technique is that amplitude fluctuations of the return signal do not affect monopulse systems to as great an extent as they affect conical scanning systems. This is particularly true of phase monopulse systems, in which the phase of the return signal is used to indicate direction of arrival of the wavefront. The phase monopulse measurement of the direction of arrival of the wave front is essentially independent of the amplitude of the return signal, depending only on its phase. In conical scanning systems, the

amplitude of the error signal derived is proportional to the amplitude of the return signal. The monopulse principle can be ascribed to the co-existence of two lobes. The position of the targets relative to the lobing axis can be found by determining which beam has the greater return intensity. This lobing scheme is called amplitude monopulse. Considering phase monopulse, two antennas are physically separated so that a target off the lobing axis will return the signal to the nearer antenna first. A measure of the phase delay in the time of arrival of the wavefront at the second antenna compared to the time of arrival at the first antenna is the measure of the angular error. Note that the directional information acquired by the monopulse system is simultaneous rather than sequential, and may be considered a type of time multiplexing.

In the tracking system of the radar, the angular tracking error is resolved into the angular error in the azimuth plane, and the angular error in the elevation plane. In principle, two tracking servos of the type shown in Figure 4-12 must be employed, and their outputs combined to yield the actual angular position of the target. In actual practice some of the operations are common to both loops. For example, the angle-gating operation is implemented by the antenna pattern. Targets whose angular displacements from the lobing axis exceed the squint angle plus a half-beamwidth of the antenna are effectively attenuated or discriminated against so that the antenna pattern acts as an angle gate. If the output signals are arranged to yield positive output voltage for targets lying above the lobing axis and negative output voltages for targets lying below the axis, then, as the target moves in angle relative to the lobing axis, an S-shaped discriminator-like curve is traced out with the crossover occuring at the antenna beam crossover. Thus, in a sense, the antenna pattern also acts as an angle discriminator with the peaks occurring at approximately the squint angle from the crossover or lobing axis. A sketch of a discriminator characteristic appears in Figure 4-14.

In an amplitude-comparison monopulse system, this S-shaped curve is actually the coordinate discriminator shown in Figure 4-12. For a conical scanning system, the situation is somewhat more involved. The electrical signal modulated by the pulsed carrier as a result of the conical scanning process has an amplitude that is proportional to the displacement of the target from the scan axis, and a phase proportional to the angular displacement of the target from some reference (for example, from the azimuth plane). The geometrical relationship can be demonstrated for the scan plane, where the scan plane is defined as a

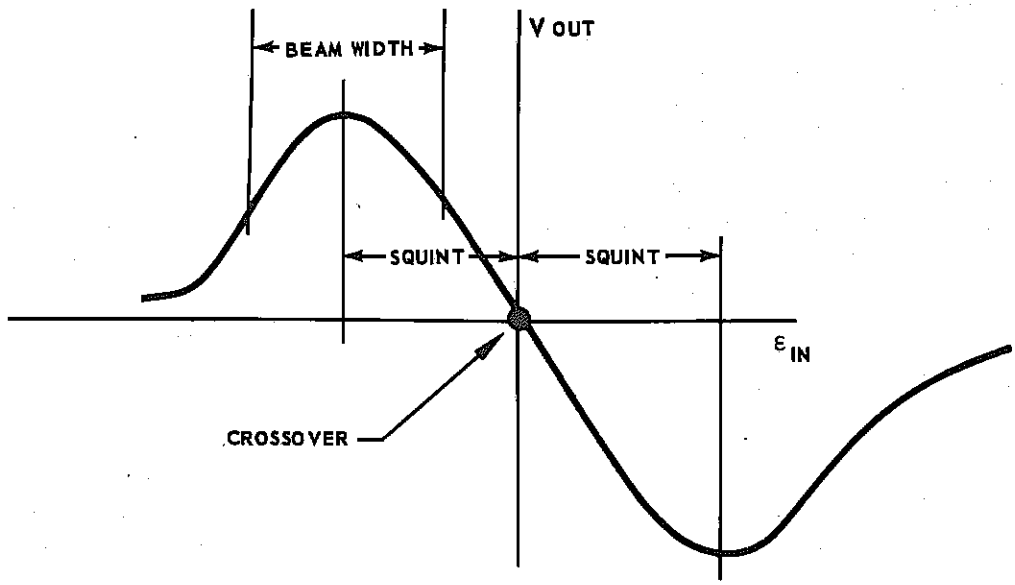

FIGURE 4-14. DISCRIMINATOR CHARACTERISTICS

plane which passes through the target and is normal to the lobing axis (see Figure 4-15).

The antenna pattern may be considered in terms of the coordinate discriminator of Figure 4-12, since the magnitude is determined by the beam pattern. The angular position of the target is found by orienting, with respect to a reference plane, the plane that contains the scan axis and passes through the target. The vector error signal has a phase which

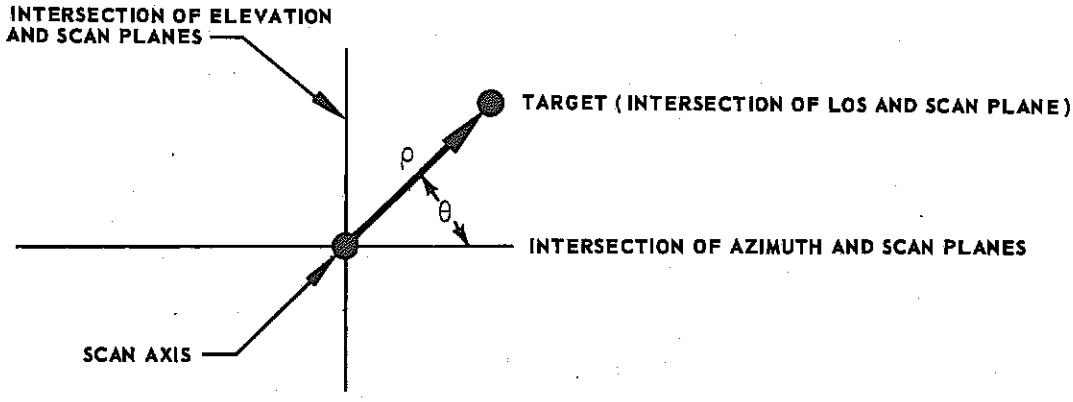

FIGURE 4-15. POLAR COORDINATE SYSTEM

is proportional to the dihedral angle between these two planes. A phase detector can then resolve the vector error signal, V_s, in Equation 4-30.

$$V_s = k_\rho \sin(\omega_s t + \theta) \tag{4-30}$$

into the two component errors given in equations 4-31 and 4-32.

$$V_{AZ} = k_\rho \cos\theta \tag{4-31}$$

$$V_{EL} = k_\rho \sin\theta \tag{4-32}$$

At the phase detector, the angle tracking channel is split into two channels. The necessary servo operations are then performed and the signal is amplified and divided to provide two signals to the antenna-drive mechanism. The transducer converts these voltages into torques, which are applied to position the scan axis. It is of basic importance in the design of the tracking radar to optimize the antenna, as well as the tracking loop parameters. The design of optimum tracking loops in presence of noise is a subject of considerable importance and will be discussed in Chapter VII.

(b) RANGE TRACKING

The coordinate input for range tracking is represented by the range of the target from the radar. Assume that the target return signal has been amplified and the rf pulses train demodulated into a video pulse train. The displacement in time between the transmitted and received pulses is a measure of the range between the target and the radar. The desired target signal can be selected from undesired targets, clutter, and noise by means of a range gate whose width is comparable to the pulse width. Assume the range gate to be initially locked-on after first sweeping a bank of range gates. The gated output can be used as the input to the velocity tracking system. If range gating alone were used, the gated output could be fed directly to the angle tracking system. The advantage of gating is not only that it discriminates against multiple targets and chaff, but that it appreciably improves the signal-to-noise (S/N) ratio. For noise spread over the interpulse interval, the improvement in S/N ratio is roughly the reciprocal of the duty cycle. In practice, the gate is generated at the servo output and is applied to gate the input video signal. The gated output video goes to a time discriminator which is a coordinate discriminator. The time discriminator measures the

degree of coincidence of the gate and the video pulse. Circuitry is so arranged that, when the gate and the pulse are in full coincidence, the output is zero, corresponding to the crossover of the discriminator characteristic. The displacement of the center of the pulse from the gate center represents a measurement of the error. In the vicinity of crossover, the discriminator output is proportional to that area of the pulse not in coincidence with the gate. To illustrate how the S-shaped curve representing the time discriminator characteristic is developed in a typical range tracking comparator, consider the so-called split-gate tracking system. The split gate samples the echo by two shorter time gates, the "early" and "late" gates, each of which is half of the total range gate. The range gating circuits constitute the time discriminator. Signals passed by these two gates are subtracted, and the resultant error signal is fed back by a servo loop to advance or retard the phase of the range gate. If the gate occurs early, more of the echo will lie in the late gate and vice versa. The servo attempts to cause the gate and echo pulse to coincide so that as much energy lies in the late gate as in the early gate. These concepts are illustrated in Figure 4-16.

The upper illustration in Figure 4-16 indicates the idealized characteristic derived from the gate position shown in the lower illustration. The height of the discriminator characteristic is equal to the area of coincidence of the early gate minus the area of coincidence of the late gate. At crossover, there is complete coincidence and, therefore, zero discriminator output. When the target is in coincidence with the early gate only, a maximum positive voltage is developed. Similarly, when there is coincidence with the late gate only, maximum negative voltage is developed, and zero voltage is developed when there is no coincidence. The variation in the difference of these areas is, for square pulses, a linear function of the error between the center of the range gate and the center of the pulse. The actual characteristic is S-shaped, as shown in Figure 4-16, the reason for this being that the pulses and gates are not square as shown, but are, instead, rounded. The split gate comparator is, therefore, a time discriminator corresponding to the coordinate discriminator shown in Figure 4-12. The range tracking servo behavior is fitted to the required system performance. For example, it might be desirable to incorporate velocity memory which causes the gate to continue to move at a constant velocity, even in the absence of signal. This is a desirable tracking servo property, since most targets are subjected to appreciable return signal fluctuations (target scintillation) which may cause temporary signal loss. When there is no coincidence between the target and the gate, the tracking servo is said to have "lost" the target. If the tracking loop servo loses the target for an appreciable period of time, the search and

acquisition process must again be performed. Position and velocity memory are essential if the loop is to regain track after the signal has faded. Ideal velocity memory requires two open loop integrations. Integration generally requires equalization in the loop. The coordinate modulator of Figure 4-12 corresponds to the gate generator in the range-gate system. The output of the transfer function Y (S), which depends on the time discriminator voltage V, triggers a gate delayed from the main bang. This trigger is used to generate the early and late gates which are combined to form the actual range gate. The coordinate modulator may also measure the time delay between the main bang and the gate position.

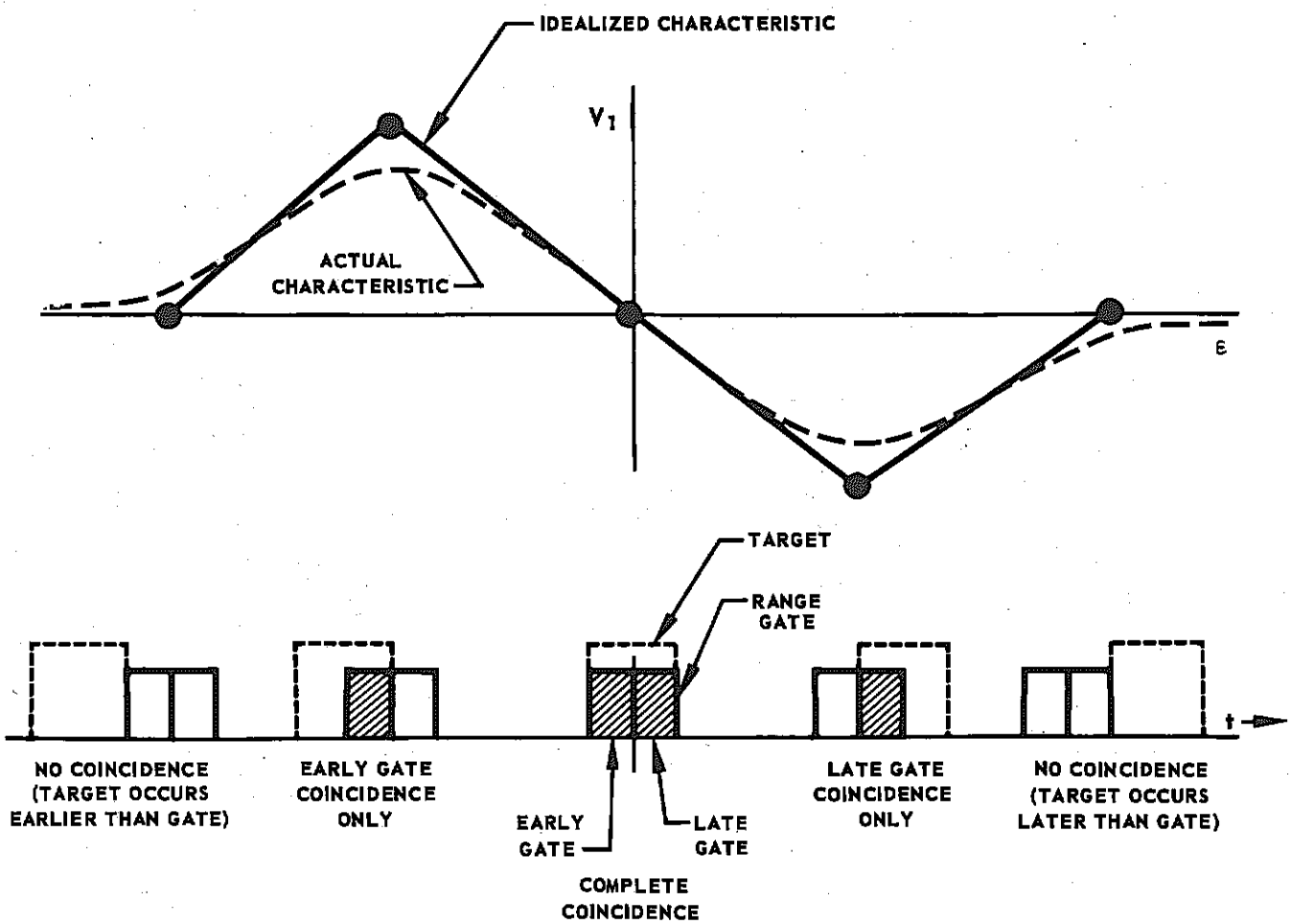

FIGURE 4-16. GATE AND DISCRIMINATOR TIME COMPARISON

This can be accomplished by triggering a delay generator from the main bang at the time the gate delay has been reached. The time interval between the main bang and the gate is then a measure of the range.

Determination of optimum parameters for range tracking is as difficult as for the corresponding problem in angle tracking. A determination of the optimum parameter settings will be given after a more detailed analysis of the range tracking loop.

(c) VELOCITY TRACKING

The range-gated signal is passed on to the velocity tracking system. The input to the velocity tracking servo is a train of pulses whose repetition frequency components have been shifted by the doppler effect. Doppler spectral components can be selected by velocity gates to provide velocity discrimination and tracking. There is appreciable absolute power loss if only one of the spectral components is selected; the loss factor is approximately equal to the reciprocal of the duty cycle. This loss can be avoided by using a "comb" filter as velocity gate. The teeth of the comb are separated by an amount equal to the repetition frequency. This process is unduly complicated if sufficient signal level can be derived from one spectral component to drive the servo. The signal-to-noise ratio is unaffected by the number of spectral components gated. Consider, therefore, the input to the velocity servo as a single doppler signal which is slowly varying in frequency as a result of changes in target velocity. This may be the case if filtering separates the range and velocity tracking loops. Even if no filtering is used between the tracking loops, a single velocity gate will eliminate all but the one component of interest.

Referring to Figure 4-12, the servo may now be assumed to have a velocity input. The time function parameter which is proportional to velocity is the CW doppler frequency component. The doppler component can be tracked by means of a moving filter which acts as a velocity gate. This velocity gate filter rejects noise, clutter, and extraneous targets which lie outside the filter bandpass. Since it is difficult to instrument actual shifts in the center frequency of the filter, the same effect is accomplished with an automatic frequency control system. In Figure 4-12, the doppler frequency appears at the input and is compared with the output doppler frequency to yield an error frequency. The time function at the error frequency is amplified and passed through a narrow velocity gate filter. This imposes a restriction on the width of the velocity gate filter, since it must not be narrower than the amplitude modulation

spectrum carrying the angle information. The frequency of the gated output signal can also be used as a measure of the absolute velocity of the target. The gated output signal containing the angle modulation provides the input to the angle tracking system. The gated output drives the coordinate discriminator which, in this case, is the typical S-shaped frequency discriminator. The discriminator crossover frequency must be the same as the center frequency of the velocity gate. In general, the crossover frequency will not be zero. Input frequencies which differ from the discriminator crossover frequency generate voltages which are operated upon in a manner similar to that of the range tracking loops. The output of the transfer function drives a frequency modulator which is needed to translate the feed-back voltage into the frequency domain for comparison with the input frequency. A typical modulator would consist of a voltage controlled oscillator (VCO) whose output frequency is proportional to the input control voltage. The output frequency of the voltage controlled oscillator is adjusted so that, in the absence of a control voltage, the difference between the input frequency and the feed-back frequency (which is the output of the modulator) is exactly the center frequency of the velocity gate. Thus, the input frequencies are heterodyned to the center of the gate in a manner similar to that of automatic frequency control. It is desirable from considerations of noise, clutter, and extraneous target discrimination to make the velocity gate as narrow as possible, although too narrow a velocity gate increases the probability of target loss. Loss of target results from small frequency errors occurring in a short time span and causing the signal frequency to lie outside the velocity gate. When loss occurs, the loop is open-ended, similar to the condition described in the range tracking case. The requirement for a high signal-to-noise ratio (narrow filter) at the gated output must be balanced against the necessity for a low probability of loss (wide filter). The determination of the optimum parameters for the velocity tracking loop is discussed again in the section on tracking loops.

(d) OTHER LOOPS

In addition to the principal tracking coordinate loops, there are other loops which perform useful operations. The received echo may vary over wide ranges as a consequence of change in range and fluctuations in the apparent crossection of the target. If the signal is to have some specified amplitude at the output, the amplification of the receiver must be adjusted to the signal being tracked. If the signal becomes too large, the receiver or some other portion of the system will saturate and cause

the overall tracking system to become inoperative. Automatic gain control (AGC) provides this needed function. Even if the system does not saturate the tracking loops, the range and velocity loops, are sensitive to changes in amplitude and, unless otherwise instrumented, the open loop gain is directly proportional to the absolute signal level. This follows in the range tracking case because, in the split gate comparitor, the slope of the discriminator characteristic is determined by the difference in areas caused by the degree of coincidence between the two halves of the gates. The larger the target, the greater the proportionate rate at which the areas of coincidence differ. Similarly, in the velocity tracking loop, the typical frequency discriminator characteristic is proportional to the input amplitude. Thus, if the input signal to either one or both of the tracking loops is fluctuating, the open-loop gain of the loops will also fluctuate, and the whole system becomes time-varying. Since, in theory, the time discriminator output is dependent on time differences only and, similarly, the frequency discriminator output is proportional to frequency errors only, this amplitude dependence is undesirable. Limiting may be used in place of AGC in some instances, but it is merely a special case of a very fast AGC. The design of automatic gain control systems, of which there will be at least one in any proposed system, is important because the detailed behavior of the AGC loop in the presence of noise appreciably affects the behavior of the other servos.

Another important tracking loop in the radar is the automatic frequency control (AFC). Since receiver local oscillator frequency varies as a function of time in relation to the transmitter frequency, these variations generate an apparent doppler shift. If the doppler shift is sufficiently great, it is possible for the pulsed signal to lie partially or completely out of the AFC bandpass. The consequent distortion of the target signal strongly affects the behavior of all the loops. These variations can, however, be controlled by an automatic frequency tracking loop similar to the velocity tracking loop previously discussed. An automatic frequency control system heterodynes a portion of the reference (transmitter) signal with the local oscillator frequency in a mixer. The output, which is near the IF frequency, is sent through a frequency discriminator and used to control the local oscillator frequency in order to maintain a constant IF frequency. Both the AGC and AFC functions are required during the search and acquisition phases as well as during the tracking phase. In addition to the loops described, there are other fire control system loops which incorporate the entire radar as a single block; for example, there is the loop composed of the radar, computer, aircraft control system, external aerodynamics and flight geometry. That this

complex loop exists can be illustrated by a change of target position, which causes a variation in the line of sight, which in turn affects the received signal, resulting in a change in the coordinate developed by the radar. These coordinate changes are processed by the computer and applied to the control surfaces of the aircraft, changing the attitude and orientation of the aircraft and, finally, closing the loop by again affecting the line of sight.

(e) PERFORMANCE SPECIFICATIONS FOR THE TRACKING RADAR

Now that the general nature of the automatic tracking radar and its specific objectives have been discussed, it is worthwhile to consider some of the performance specifications which might be established for such a system. For a proposed system, assume the tracking range to be approximately 80 miles. The angular tracking accuracy required with guided armament is not nearly so stringent as that required with unguided armament. If the guided missile armament can tolerate large launching errors, the accuracy requirements of some of the fire control system parameters may be eased. The radar tracking system, however, must be sufficiently accurate to provide for allowable launching error and missile antenna pointing error within required tolerances. Since the antenna in semiactive missiles or the telescope in infrared (IR) missiles can be slaved to the radar antenna, the radar antenna must point with sufficient accuracy along the line of sight so that prelaunch error can be readily corrected by the missile angle tracking loop. This restriction is more severe for the IR than the radar missile because of the restricted IR field of view. A reasonable performance specification for radar antenna alignment accuracy is $\pm$ 2 to 3 degrees. This implies that the target must be tracked by the radar with at least one-degree accuracy. On the other hand, a missile launching error as great as five degrees is not unreasonable. The launching error accuracy is set not only by angular tracking error but also by range tracking error. The launching error tolerance usually is broad for both types of homing guided missiles. Also, the range and range rate accuracy requirements are not too great. This is convenient, generally, since the velocity tracking system is appreciably more accurate than the range-tracking system. Probably the measurement most difficult to maintain with a given accuracy is the angular rate. The maximum angular rate error that can be permitted without exceeding the allowable RMS armament miss distance is 1/2 degree per second.

(f) DISCRIMINATION AGAINST RANGE AMBIGUITY

As previously mentioned, the use of very high repetition frequencies introduces range ambiguity problems. A solution suggested for this problem consists of jittering the repetition frequency. It is also possible to obtain two ranges by jittering the repetition frequency in a specific fashion, for example by sinusoidal and pulse modulation, where the pulses are coded. If the PRF is jittered in a random manner, true pulse coding is not obtained. Random jittering is probably a better choice for determining range since the range tracking loop will tend to discriminate against the spreadout of random frequency pulses by treating them as noise.

(g) TRACK-WHILE-SCAN

Track-while-scan techniques can be implemented by use of a computer. Initial range may be determined without ambiguity by permitting several sweeps of the jittered repetition frequency signal to be repeated. The initial range is stored in the computer along with initial values of azimuth, elevation, and relative velocity. As the system continues scanning, the values of azimuth, elevation, and velocity are corrected by the latest data from the radar receiver. The gates are repositioned from both target data and predicted (computed) target information. The predicted position of the target can be computed by means of polynomial extrapolation (see Chapter 7). The computed outputs can then be used for presentation on the display and for controlling various interceptor control functions.

(h) THE JAM-TRACK MODE

Because electronic countermeasures must be expected, the fire control system should be capable of operating in the presence of jamming by using the electromagnetic jamming radiations emitted by the jammer itself for tracking purposes. If the direction of the jammer's wave-front can be determined, the radar can at least track the jammer in angle. The detailed design of a track-on-jamming system depends on the nature of the jamming.

SECTION 11—IDENTIFICATION SYSTEMS

Two types of identification may be considered necessary for the fire-control interceptor system; namely, ground-to-air and air-to-air identifaction functions. The problem of ground-to-air identification is solved

by the interceptor replying correctly to a coded query from the ground interrogator. This function is provided by an airborne transponder designed to respond automatically to the ground interrogation system. Air-to-air identification requires equipment for interrogating radar targets and equipment for replying to interrogations from friendly aircraft. It is important that targets be identified at very near the maximum detection range because of the limited time available and the long firing ranges to be expected from the target armament. The identification system must have high angular and range resolution capabilities to be able to distinguish an individual target in the midst of multiple targets. If the angular resolution were not adequate, an enemy aircraft might appear to be friendly as a result of a reply from a friendly aircraft at the same range but at a slightly different angle. The enemy can be expected to employ countermeasures against the identification system. The counter-countermeasure, in this case, consists of the use of complex coding, with the resultant degradation in system reliability. It is necessary that coding schemes be flexible enough to permit required changes without extensive equipment modifications.

Air-to-air identification can be accomplished by using an interrogator-responsor. The coded interrogation signal is sent to aircraft within range of the interceptor radar. Friendly aircraft equipped with the proper transponder will return a coded reply. If the correct reply is received by the interceptor, a specific identification-characteristic appears on the display. If the reply is incorrect or no reply is received, the aircraft is not identified and must be suspected as unfriendly. The radar antenna may be used by the transponder for transmitting and receiving identification signals if suitable duplexing is employed. Interrogation rates may be lower than the highest radar repetition rate used. Low repetition rates should be used in order to avoid range ambiguities. The interrogation problem is complicated by the fact that the receiver is blanked during the radar transmission. To avoid a series of blind intervals in range which could not be interrogated, there must be sufficient isolation between the radar transmitter and responsor-receiver so that the responsor can receive signals during the transmitted pulse.

SECTION 12—BLOCK DIAGRAM OF THE PROPOSED SYSTEM

An overall block diagram of a radar system described in the text appears in Figure 4-17. The block diagram indicates the three major modes of the radar: (a) search, (b) acquisition and lock-on, and (c) track. The switchover from search to track is illustrated in part by the

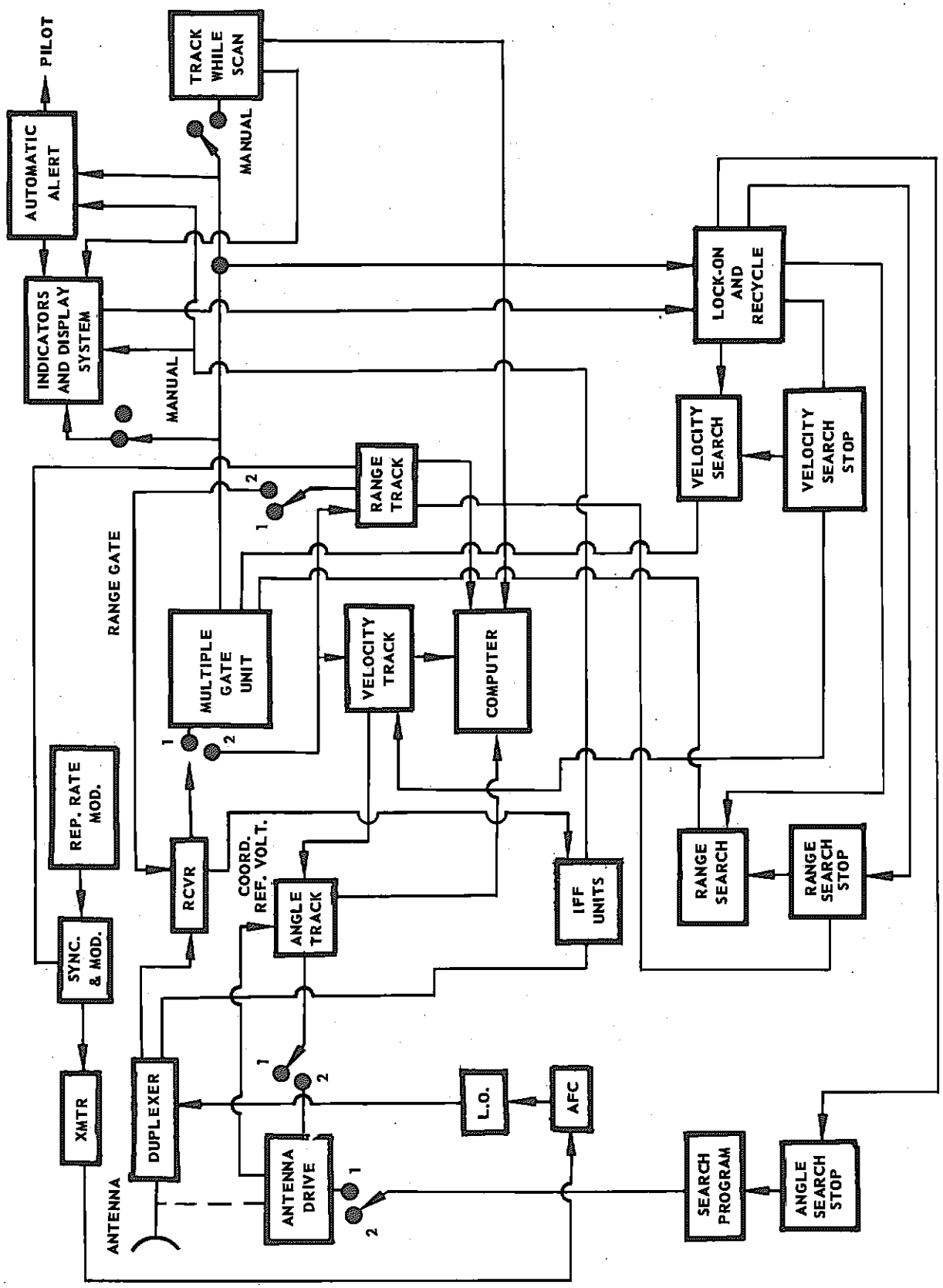

FIGURE 4-17. RADAR SYSTEM BLOCK DIAGRAM

switching operation shown; switch position 1 corresponds to the search function, and switch position 2 corresponds to the track function.

In the search program, the antenna drive is required to follow a specific search pattern. The transmitter repetition period is synchronized from the synchronizer while the repetition rate is jittered by the repetition rate modulator. As pointed out, the repetition rate modulator attempts to overcome the effects of range ambiguity. The repetition rate synchronizer also provides a reference signal for the range track. The suggested transmitter is a stable pulse-to-pulse coherent transmitter consisting of a CW oscillator which is pulse-modulated. The detailed block diagrams of the transmitter, angle tracking unit, receiver, etc., appear later in this chapter. Coherent rf pulses are applied through the TR tube and isolator located in the antenna duplexer. The returned signal is received at the antenna, passed through the duplexer, and into the receiver. The receiver amplifies and demodulates the signal and also provides AGC. In the search mode, the receiver output drives the multiple gate unit. The output of the gate unit is presented on the indicator and drives the automatic alert function as well as the track-while-scan. The track-while-scan feature must be used in conjunction with a memory device.

SECTION 13 — TRACKING CHARACTERISTICS

In addition to, or instead of, a track-while-scan mode, precision tracking (that is, tracking in which the target is constantly illuminated) is provided. This mode is required for use with semiactive missiles. Continuous automatic tracking is provided in azimuth, elevation, range, and velocity. The angular tracking limits are the same as those for search. The upper velocity tracking limit is the maximum expected target-interceptor velocity. The antenna is stabilized to counteract the effect of interceptor maneuvers. The radar angle-tracking servo must, therefore, follow only the inertial space motion of the line of sight. Again the azimuth, elevation, velocity, and range of the target being tracked are available for cockpit display and for processing by the computer. Range information is continuous and nonambiguous. The radar also supplies the missile auxiliaries with information such as angular position, angular rate, range, and range rate, which are needed for missile lock-on.

SECTION 14—DETAILED DISCUSSION OF THE VARIOUS BLOCKS IN A PROPOSED SYSTEM

A detailed discussion of various blocks in Figure 4-17 follows.

(a) TRANSMITTER

A block diagram of the principal elements in the transmitter appears in Figure 4-18.

The transmitter (power-amplifier block) shown in Figure 4-18 is the rf high power amplifier and may be a traveling-wave tube or a klystron. The tube should cover a wide band of frequencies and should have high gain. The block titled pulse modulator consists of switch tubes which simply turn the input CW drive signal on and off. The CW oscillator is required to be extremely stable and must be isolated from the modulator so that the gating modulation does not affect the CW frequency. To attain the required stability at the transmitted frequency it is necessary to generate the CW at a lower frequency and employ stable frequency multipliers.

(b) INDICATORS AND DISPLAY SYSTEM

The principal pilot's display is a radar scope showing elevation versus azimuth, with provisions for coding the target signal to display additional information such as target velocity. In addition, other

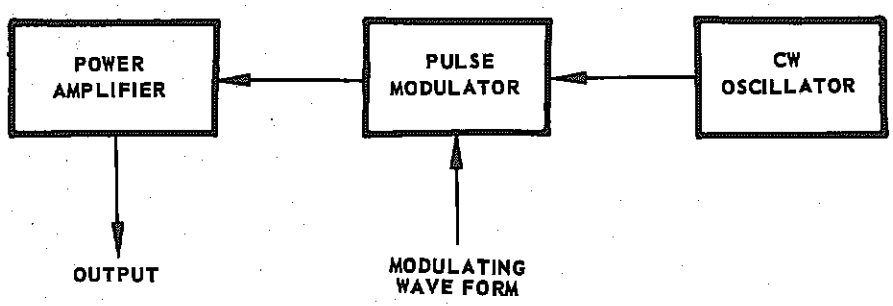

FIGURE 4-18. PRINCIPAL TRANSMITTER ELEMENTS

information relevant to the attack may be displayed on this indicator. An off-center PPI display should be available for the pilot to use in conjunction with a printed map of the region when the interceptor is operating in the ground-mapping mode. There is a wide choice of displays and cockpit arrangements which would be useful to the pilot. The principal information which must be presented to the pilot includes: interceptor position and heading, ground vectoring information and heading, range remaining, target position, map of the area, altitude, ground vectoring altitude and target altitude, rate of climb or descent, bank angle, vertical flight path angle, instrument landing system information, error information, deviation from desired heading, radar attack steering information, indicated air speed, angle of attack, Mach number, maximum safe Mach number, ground vectoring Mach number, slip indication, throttle indication, and computer program indication. On the radar display, required information includes: azimuth and elevation of targets, velocity of targets, range of targets, target identification data, and radar attack information such as vertical and horizontal steering commands, time until firing, range rate, pull-out collision warning, etc.

(c) DUPLEXER

The transmitter output is passed through a duplexer before being transmitted. The duplexer is essentially a mixer and electronic switch which connects the antenna to the transmitter during the transmitting period and to the receiver the rest of the time. This allows a single antenna to be used for both transmitting and receiving. The older radar types employ a TR tube for the switching action. This tube depends on ionization of the gas by electric fields set up in a resonant circuit by the transmitter main bang to prevent transmitter energy from entering the receiver directly. Received echoes are too weak to cause ionization of the TR gas. If the switch is not in operation, the received energy passes directly to the receiver. For a high repetition rate, the use of a high-speed switch is required. Gas-type TR tubes are not as suitable for this purpose as ferrite switches. The duplexer also contains the mixer cavity where a fraction of the transmitted energy is mixed with the local oscillator energy to give the control signal for the automatic frequency control loop. The duplexer actually contains two mixers: one for the automatic frequency control loop, and another for the received signal. The received signal is mixed with the local oscillator energy and the difference frequency is passed on to the receiver. The receiver mixer may be considered part of the receiver, as well as being considered part of the duplexer.

(d) RECEIVER

The essential elements of a receiver are shown in Figure 4-19. The ratio of transmitted-to-received power for the minimum receivable signal may be on the order of 10^{18} or more. The principal purpose of the receiver is to amplify weak received echoes to a useful level. This requires voltage amplifications of 10^{6} or more. The received echoes are amplified with a superheterodyne receiver such as the one shown in Figure 4-19. The rf energy at the antenna is passed through the duplexer and into the receiver mixer. The receiver mixer cavity mixes the received energy and the local oscillator energy in a detector, usually a crystal, and passes it through a coupling network to the intermediate-frequency amplifier. This amplifier is tuned to the difference frequency between

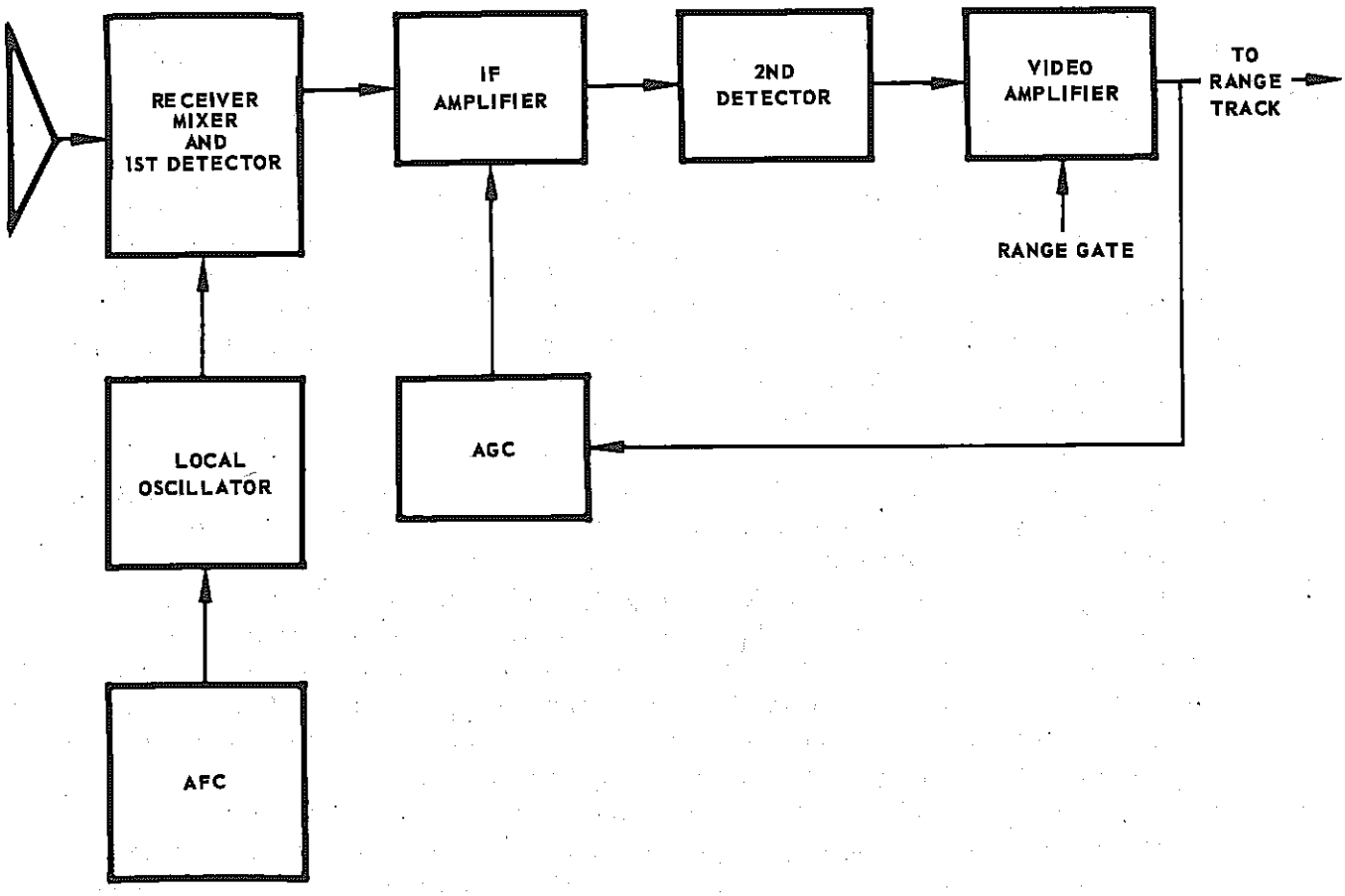

FIGURE 4-19. PRINCIPAL RECEIVER ELEMENTS

the incoming rf energy and the local oscillator frequency. The difference frequency is maintained by adjusting the local oscillator frequency with an automatic frequency control. The intermediate-frequency amplifier provides the major voltage gain for the received signal. It is possible to dispense with the local oscillator intermediate-frequency amplifier arrangement simply by immediately detecting the audio or video signals modulated on the carrier and by usinga high gain video amplifier (a so-called "crystal video receiver"). This process is impractical for the high gains required. High gain video amplifiers that are effective to low frequencies are not as easily designed as high gain bandpass intermediate frequency amplifiers; also, the noise figure of crystal video receivers is appreciably worse than that of superheterodyne receivers. One of the principal reasons for the poor noise figure in crystal video receivers is that the first detector crystal noise is substantially greater at low frequency outputs than it is at higher frequency outputs. In ordinary radar systems, the AFC input is often taken from the IF amplifier output. The local oscillator frequency adjustment should not be derived from the output of the IF amplifier, since the local oscillator must be locked and stable with respect to the transmitted frequency. This is required so that differential shifts added to the fixed difference between the local oscillator frequency and the transmitter frequency do not appear as doppler shifts in the velocity tracking unit. A restriction on the bandwidth of the IF amplifier is that it be wide enough to pass not only the pulses, but the pulses plus the additional doppler shift. Since the bandwidth required for passing half-microsecond pulses is at least 2 megacycles, the additional 100 kc bandwidth necessary for doppler shifts is inconsequential. The necessity for tracking the doppler shift puts stringent requirements on local oscillator stability. In an active radar, an easy way to satisfy this stability requirement is by locking the local oscillator to the transmitted frequency. The optimum IF bandpass is determined by the spectral content of the signal and the noise spectrum. The bandpass should be designed to pass the necessary spectral components of the signal to give the desired rise time and time characteristics while rejecting much of the noise. The signal in the IF amplifier consists of a train of doppler-shifted intermediate frequency pulses. The output of the IF amplifier, then, drives the second detector, which yields the video envelope of this train of pulses. The output of the video amplifier drives the range track unit and also develops the voltage for the AGC which automatically controls the gain of the IF amplifier. The amplified video signal is gated by range circuitry so that the signal fed to the range tracking unit has already been gated by the gate it generates.

The advantages accruing from range gating include multiple target resolution, clutter discrimination, and improved signal-to-noise ratios.

(e) AUTOMATIC ALERT UNIT

The automatic alert unit is simply a thresholding device which alerts the pilot and provides a coded mark on the indicator and display system to show the presence of a target. The presence of targets in the multiple gate outputs are used as triggers for the automatic alert unit. The multiple-gate unit output supplies display information for the indicator, which shows the positions of the targets in angle, range, and velocity.

(f) TRACK-WHILE-SCAN UNIT

The presence of targets in the velocity gates of a track-while-scan system is indicated by the threshold detectors associated with each velocity gate. If a threshold bias is exceeded, the output of the corresponding gate is presented on the indicator. The gate output also triggers the automatic alert and presents this information to the track-while-scan unit. The track-while-scan unit processes the signal and supplies it to the computer for use in predicting the future position of the target on the basis of present and past position data. The computer determines the trajectory of the target and presents it on the indicator. The track-while-scan unit is further discussed in connection with the fire control computer.

(g) INTERROGATOR AND RESPONSOR (AAI) UNITS

The AAI (Air to Air Identification) system is a part of the radar auxiliary equipment. The AAI interrogation signal is passed through the duplexer and out the common interceptor antenna. If the interrogated aircraft are friendly, a coded signal is returned to the radar antenna. This signal passes through the duplexer and receiver and is recovered by the AAI decoder unit. Each friendly aircraft is equipped with an AAI transponder for coded response to other friendly aircraft interrogations. If there is no response to the interrogation, the automatic alert system is triggered by the AAI transponder unit. If correct coded reply is received from an aircraft transponder, coded symbols are placed on the indicator to identify the friendly aircraft.

(h) LOCK-ON AND RECYLE UNIT

The lock-on and recycle unit is actuated by the pilot. When the pilot moves the cursor onto the desired target and pushes the lock-on button, the lock-on unit stops the angle search by providing control signals to the angle-search-stop unit, which slaves the antenna scan axis in the direction indicated on the scope display. The lock-on also initiates operation of the velocity and range search units to start searching the multiple gate unit output in velocity and range for the desired target. Once targets are found, the velocity-search- and range-search-stop units are actuated, stopping the search on the approprate target. If a recycle function is included, then the lock-on and recycle units will also contain a target checking facility for determining whether or not the target is a true one or is simply noise. If it is a true target, the recycle unit is not actuated. If the suspected target is simply noise or jamming, the recycle unit reinitiates velocity and range search, and reinitiates angle search automatically or indicates to the pilot that the target is false. The latter indication allows the pilot to manually reinitiate angle search.

(i) SEARCH AND SEARCH-STOP UNITS

The angle-search-stop unit is activated by the lock-on signal. The antenna is slaved to the proper position, which is determined by the location of a cursor. Velocity search and range search units both examine the outputs of the multiple range and velocity gate units for presence of targets. The searching will cease at the first gate containing a target. Each bank of velocity gates, corresponding to the various range gates, is searched simultaneously. The range search then selects the proper bank of velocity gates when the signal is encountered and the search stop is energized. The target chosen is then compared in range and velocity with the corresponding target on the scope display. If the target is one located by the cursor, the switch shown in Figure 4-17 is automatically switched from position 1 to position 2 and automatic tracking is initiated. If the target chosen does not coincide with the target indicated by the cursor, then the velocity search moves to the next target in the chosen range gate bank and the process is repeated. The search continues until the target selected corresponds to the suspected one. The velocity search should logically start with the highest velocity, shortest range target.

(j) THE RANGE-TRACK UNIT

A block diagram of the range-track unit appears in Figure 4-20.

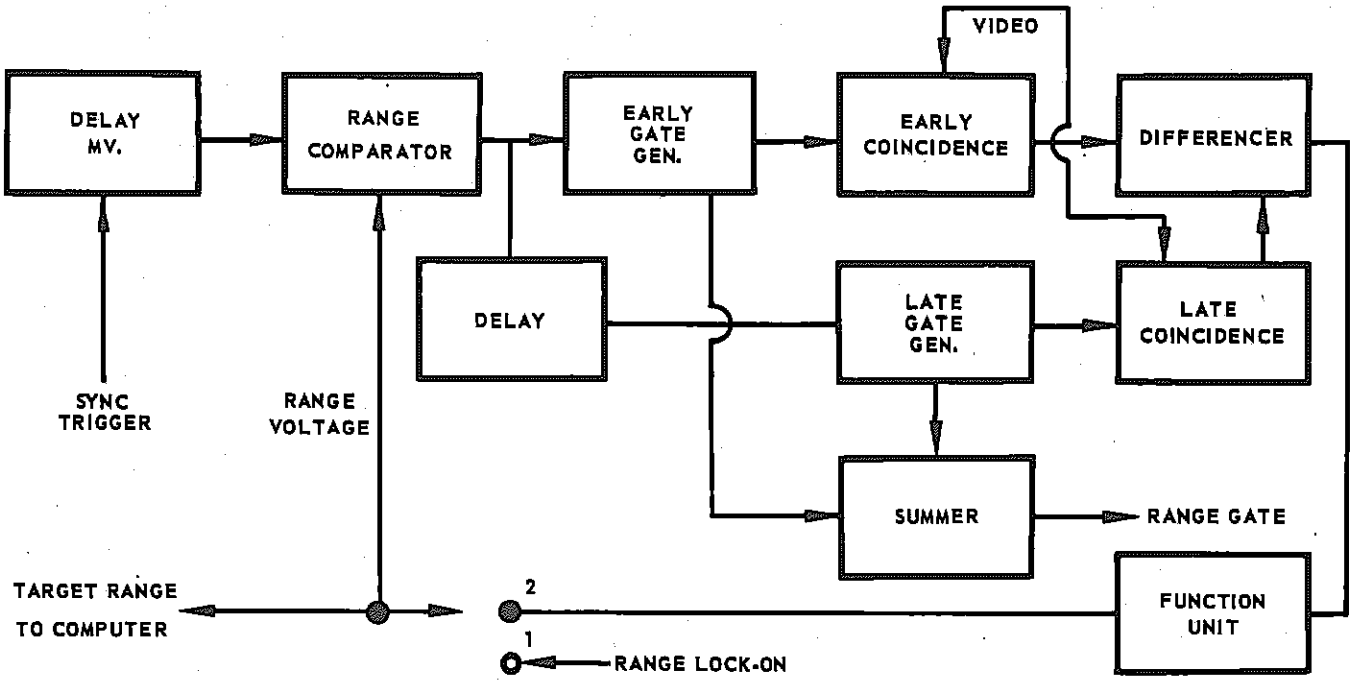

FIGURE 4-20. RANGE - TRACK UNIT

The block diagram illustrates one possible mechanization of the range-track function. The synchronizing trigger from the transmitter triggers a one-shot delay multivibrator, or linear delay unit, the output of which is compared with the feed-back range voltage in the range comparator circuit. When the range voltage and the linearly rising sweep voltage from the delay multivibrator coincide, a trigger is generated by the range comparator to trigger the early and late gates as shown. The early and late gate outputs go to coincidence circuits which permit the portion of the video that coincides with the respective gate to pass to the differencer. A voltage proportional to the difference in the two areas of coincidence is generated by the differencer. This voltage, which is proportional to the servo error, is the output of the time discriminator. The error voltage then goes to a servo unit where integration, amplification, and equalization are performed. The output, consisting of a slowly varying dc voltage, is fed back to the range comparator. This range voltage provides a measure of the absolute target range from the interceptor and is fed as an analog signal to the computer. The early and late gates are combined in a summer which compiles the total range gate for use in gating the receiver. The video input signal, which drives both the range and velocity track units, has already been range-gated. The range lock-on voltage is determined by the range-search-stop unit

output, which is obtained from the range gate that selected the desired target. When the lock-on button is depressed, or when the recycle function has verified the target to be a true one, the range lock-on converts to the tracking position. During the search function, the range gate is not connected to the receiver.

(k) VELOCITY-TRACK UNIT

A block diagram of the velocity-track unit appears in Figure 4-21.

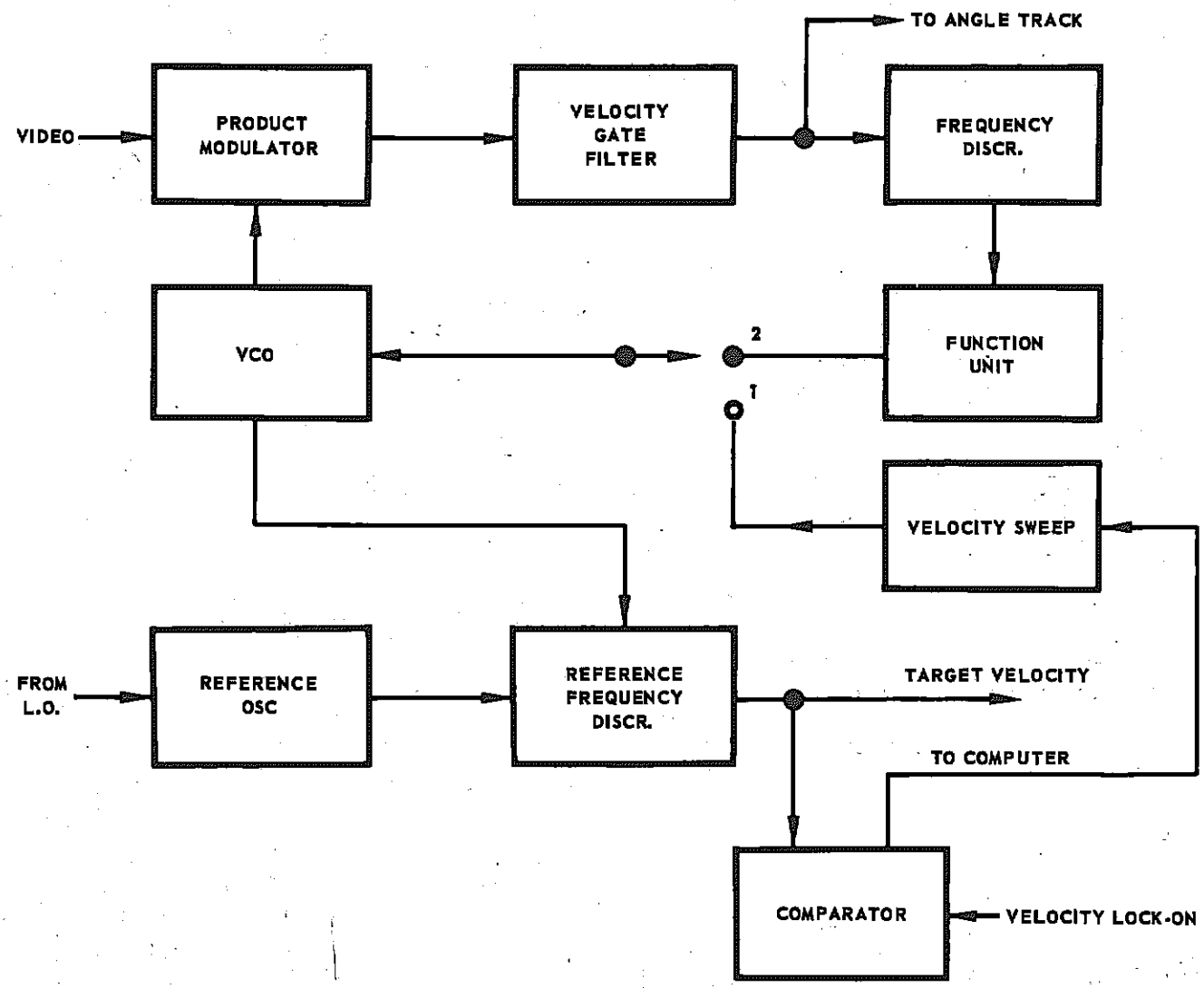

FIGURE 4-21. VELOCITY - TRACK UNIT

The velocity-track unit accepts the range-gated video and compares it with the output of a voltage-controlled oscillator (VCO) in the product modulator. The output voltage from the product modulator has a frequency proportional to the difference of one video input (the doppler-shifted repetition rate frequency components) and the VCO output. The VCO is adjusted so that the difference between the output frequency and the video doppler-shifted input frequency lies at the center frequency of the velocity gate filter. The output of the narrow velocity gate filter is an amplitude-modulated ac signal used for the angle track signal. The angle track signal has been range and velocity gated for maximum target resolution, signal-to-noise ratio, signal-to-clutter ratio, and signal-to-jamming ratio. The output of the velocity gate filter is applied to a frequency discriminator whose crossover frequency is turned to the exact center frequency of the velocity gate filter. The voltage out of the frequency discriminator drives a servo unit in which the appropriate integration, equalization and amplification are performed. The output of the servo (a slowly varying dc voltage) controls the VCO frequency in the tracking mode. The VCO frequency is adjusted so that it is at the velocity gate filter center frequency (which is above a specific repetition rate component of the received video) when the control voltage from the servo unit is zero. A reference oscillator is locked to the corresponding repetition rate component of the transmitter by means of frequency locking from the local oscillator or the transmitter. When there is no doppler shift on the input video, the difference between VCO frequency and the reference oscillator frequency is the crossover of the frequency discriminator. Thus, when the VCO shifts as a result of doppler shift on the video with respect to the transmitted frequency, the reference frequency discriminator develops an output voltage proportional to the absolute target velocity with respect to the interceptor. This voltage is fed to the computer for velocity information. A possible arrangement for velocity lockon in shown in Figure 4-21. Since the VCO control voltage is not a measure of absolute velocity, but is zero for some fixed voltage when the loop is tracking, lock-on must be accomplished by sweeping the VCO frequency during the lock-on phase. Frequency sweeping continues until the VCO output frequency (when compared with the reference oscillator and the reference frequency discriminator) generates a voltage equal to the velocity lock-on voltage from the multiple gate unit. The velocity lock-on voltage is then compared with the actual target velocity indicated by the velocity sweep until the two voltages are equal. When equality occurs, the comparator generates a sweep-stop signal, which stops the velocity sweep by simply switching to the tracking mode. The tracking loop then operates in normal fashion. It should be noted that the sweep and

sweep-stop arrangement must be used in the velocity tracking unit because no absolute reference to zero relative velocity is used in the tracking loop. In other words, the tracking loop tracks changes in relative velocity without ever making an absolute measure of target velocity relative to the interceptor. It is only because of the initial lock-on problem and the need for an absolute target velocity measurement for the computer that the additional components are included. It is interesting to note that the range tracking unit could be built in a manner similar to the velocity tracking unit. In other words, it is possible to build a synchronous range tracking unit in which there is no absolute reference. As shown in Figure 4-20, the synchronizer and delay multivibrator supply the absolute reference for zero range. The tracking range could be found by observing the changes in range indicated by integrating the doppler shift in much the same manner as the described velocity tracking loop. If the range-track loop were so mechanized, absolute range would have to be determined by auxiliary equipment comparable to that indicated in Figure 4-21. Additionally, a lock-on problem would be encountered. The arrangement of Figure 4-20, which makes use of an absolute range measurement, could be used for velocity tracking by measuring absolute velocity. This technique could be implemented with a linear sweep which begins at a frequency corresponding to the interceptor velocity and continues to the maximum expected interceptor-target relative velocity. An output VCO frequency, which is always the velocity gate frequency above this absolute frequency reference, is then developed. When the video frequency and the swept frequency coincide, a generator stops the linear increase in frequency and tracking ensues. The type of servo employed in Figure 4-20 can be considered a nonsynchronous absolute range measuring tracking unit, while the system described in Figure 4-21 might be considered a synchronous nonabsolute velocity measuring tracking unit.

(1) ANGLE-TRACK UNIT

The angle-track loop (see Figure 4-22) actually includes the antenna, target, duplexer, receiver, range and velocity track unit, angle track unit, and antenna drive. These units can be considered the antenna tracking servo. When there is angular error between the antenna scan axis direction and the line-of-sight, a scan modulation voltage is developed and carried as modulation through the duplexer and the receiver. The output of the receiver is a video pulse train which is still amplitude-modulated by the angle modulation. The range-gated video is then applied to the velocity tracking unit, which develops an essentially sinusoidal amplitude-modulated carrier in the velocity tracking gate. This sinusodial amplitude-modulated signal is applied to the angle tracking

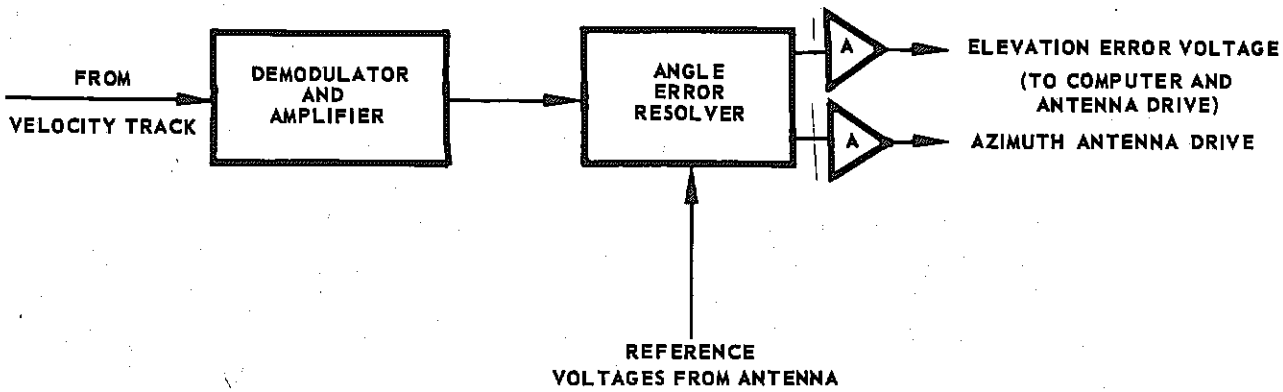

FIGURE 4-22. ANGLE - TRACK UNIT

unit. Output of the angle tracking unit consists of two slowly varying dc voltages, one each in azimuth and elevation. These control voltages are applied to the antenna drive unit, which positions the antenna in both elevation and azimuth to reduce the angular error between the line-of-sight and the antenna scan axis.

The function of the angle-track unit is to demodulate the amplitude-modulated velocity track output signal and to resolve the scan modulation into azimuth and elevation control voltages. The velocity track output is an amplitude-modulated signal about a carrier at the velocity gate center frequency. This signal is applied to an amplitude demodulator, which recovers the ac scan modulation and amplifies it. The output of this demodulator is sent to the angle error resolver, which is effectively a phase detector. In order that the angular scan modulation may be resolved into elevation and azimuth components, a reference must be derived from the interceptor coordinate system. One way that this reference signal can be derived is by means of pip coils mounted relative to the antenna or antenna feed (depending on which is being rotated for the scan modulation). A pip magnet is mounted on the antenna (or feed) to denote an arbitrary zero-phase reference. When this pip magnet passes the pip coil, a trigger is generated to mark the azimuth plane and the elevation plane in interceptor coordinates. The error resolver forms a product between the reference waveform and the

error waveform. From this product, a resulting phase can then be determined. The output voltage corresponding to the cosine of the angle between the phase of the input and the azimuth phase reference is developed in the azimuth channel. The voltage corresponding to the sine of the phase angel between the input signal phase and the azimuth reference phase (or the cosine of the angle between the input signal phase and the elevation reference phase) is applied with the output voltage to the elevation error channel. These dc output voltages, which are slowly varying, are amplified by power amplifiers. The resulting signals are used to control the antenna drive mechanism and to provide elevation and azimuth voltage measurements. Essentially the error resolver is a bidirectional two-switch circuit, commutated by the reference pip voltages. Mathematically, the operation amounts to multiplication of the signal voltage by the reference voltages.

(m) ANTENNA DRIVE AND ANGLE-SEARCH UNIT

The antenna drive unit is essentially an electro-mechanical transducer which transforms the electrical signals from the angle-track unit to mechanical control torques which move or precess the antenna. The mechanism for establishing control of this operation is the torqued gyro. A gyro tends to maintain its position in space unless torques are applied to the precession axes. The voltages out of the angle-track unit can be used to position mechanical torquers which precess the gyro spin axis. The gyro spin axis is slaved to the antenna scan axis by means of mechanical linkage, a mechanical servo, or by mechanically linking the antenna to the antenna drive gyro. When precession error signals are generated by the angle tracking unit, the antenna precession axis will be torqued and the antenna scan axis will precess toward the line of sight. When the error signal is zero, the angle tracking servo output precession voltages become zero. The torques are no longer applied to the antenna gyro and drive unit, and the antenna motion stops. In the search mode, the precession voltages are properly programmed to make the antenna search the required volume. The angle-search stop, which is actuated by the lock-on device, stops the sweeping precession control voltages at the value which corresponds to the selected position of the cursor on the indicator scope. The antenna is then properly positioned for initiation of angle tracking. When the recycle check is finished, the system is changed from the search to the track operation and the antenna drive is controlled by the automatic angle tracking servo.

(n) THE ANTENNA

The antenna scan axis is aligned with the gyro spin axis, which requires that the axis of the antenna be offset with respect to the spin (or scan) axis by approximately half of the squint angle. It is assumed that the antenna is parabolic and receives illumination from the antenna feed during transmission, and from return echo radiation during reception. The returned radiation is focused onto the feed, thus reversing the process for the reception. Either the antenna feed or the antenna must rotate to provide the appropriate scan modulation for a mechanical scanning scheme. In either case, the antenna feed must nutate in order to remain aligned with the scan axis. The antenna pattern must be stabilized with respect to pitch and roll. If the antenna is not stabilized with respect to roll, the received radiation will not necessarily lie in the plane of polarization of the transmitted radiation. This results in a loss roughly proportional to the cosine of the angle between the received and the transmitted polarization planes. If the plane of polarization is revolved through 90 degrees between transmission and reception, the received energy is zero. The signal tends to become depolarized because of complex reflection paths and propagation effects, which introduce losses in the received signal. An antenna should be designed to have high gain, narrow beamwidth, and low sidelobe energy transmission. Sidelobe suppression is desired, since this energy could be converted to main beam energy. Sidelobe energy produces large ground return signals at ranges shorter than the main beam, and covers a wider range of doppler frequencies than the main beam signal. Backlobes pick up main bang energy, thus increasing the minimum-range problem. Back and sidelobes pick up doppler modulations from the aircraft and other sources. These modulations may enter the velocity tracking system and result in possible false lock-on. A beamwidth as narrow as practical is desirable from the standpoint of improved angular resolution, increased radar range, and system gain. If the beam is too narrow, however, initial angular lock-on becomes more difficult, and the frame-time is increased for a given angular coverage. It is important that the beam be symmetrical in order to reduce amplitude errors and to avoid cross-talk between the azimuth and elevation planes.

If simultaneous lobing (monopulse) is used, the antenna configuration will differ since more than one feed is used. The monopulse receiver differs because matched receivers are used for the paired antenna waveguide. The fundamental operations of the various units are essentially unchanged. A detailed discussion of the types of antenna search

scans and antenna-track lobing techniques will be found in Chapter VII.

(o) RADOME

Some of the most difficult problems in the design of airborne radar systems are those concerned with distortion of the microwave beam. Such distortion introduces crosstalk, azimuth and angular error, nonlinearities, increased transmission and reception loss, increased angular scintillation, and other adverse effects. A principal source of distortion is so-called "radome error." Radome error is an effect which causes the apparent line of sight to the target to differ from the true line of sight. This effect occurs because of the electrical, as well as the mechanical, properties of radome materials. The received and transmitted waves are both reflected (producing energy loss) and refracted (producing angular error between the line ofsight and the radar scan axis). The most serious effect of radome error is not the direct effect but, rather, the resulting effects of the error. The signal developed with the radome error present depends not only on angular position data but also on turning, precession, and roll rates. Radome error effects are reduced by stabilizing the antenna relative to the radome. A signal appearing in one interceptor coordinate plane introduces a degree of crosstalk or undesired signal in the other channel. Mismatch in the microwave circuitry reflects the incoming wave back through the waveguide, where it is reradiated and rereflected by the radome. This reflective wave sets up standing waves, which further degrade the desired signal. Reflections also tend to adversely affect the local oscillator frequency. Radome mismatch is reduced as much as practical by radome design, while the local oscillator frequency stability is improved by suitable decoupling.

(p) LOCAL OSCILLATOR AND AUTOMATIC FREQUENCY CONTROL

It is imperative that the transmitter frequency be stable in order that pulse-to-pulse coherency may be maintained for use in doppler tracking. The local oscillator must maintain a constant frequency difference between itself and the transmitter in order that differential shifts between transmitter and local oscillator frequencies will not appear to the velocity tracking system as doppler shifts. To maintain an absolute frequency differential, the local oscillator can be locked to the transmitter frequency by means of an automatic frequency control (AFC). This may be accomplished by having the transmitter generate a CW signal at a frequency lower than the transmitted microwave frequency. The CW

oscillator frequency is then multiplied up to the transmitter frequency for transmission and up one or more harmonics higher to develop the local oscillator frequency. The intermediate frequency used in the receiver is then equal to, or a harmonic of, the basic CW oscillator frequency in the transmitter. One disadvantage to this system is the possibility of CW feedthrough from the transmitter of the receiver. This problem can be alleviated by suitable attenuation of the transmitter-to-receiver path. For the types of accuracies desired in a proposed system, local oscillator and transmitter short-term frequency stability should be approximately one part in 10^8. The received signal will be offset from the IF center frequency by the doppler shift with this type of AFC, but since the IF bandpass is wide compared to the IF doppler shift, this effect is negligible.

Additional information concerning associated fire control subsystems can be found in Appendix A.

CHAPTER V

THE COMPUTER

SECTION 1 — INTRODUCTION

The radar and most of the other components of the fire control system (excluding the armament) are devices whose main function is to track and measure certain physical quantities. Somehow this measured information must be operated on and translated into useful data forms for controlling the aircraft and firing the armament. The component that accepts this information, operates on it in the desired manner, and provides the needed output information is the computer. Basically, a computer is a device which possesses memory and is able to perform simple arithmetical operations. The fire control system computer must accept inputs, usually in analog form, such as radar range and direction, gyro or accelerometer data, air pressure, airspeed, and angle of attack. The output of the computer must supply signals to the interceptor control system and to the armament system. This information is usually required in analog form. The operations to be performed and equations to be solved are determined by the navigation scheme and control mechanisms, and by the instructions which are required for the armament system.

The computational device used in the fire control system may be either an analog or a digital computer, or a hybrid of the two types. A digital computer performs mathematical operations with digits which can assume only discrete values. The accuracy of the result depends on the number of digits the machine can handle. An analog computer converts numbers into physically measurable quantities (usually voltages or shaft positions) and performs computations by suitably interconnecting physical elements. A significant disadvantage of the analog computer when compared with a corresponding digital machine is that the accuracy of the former depends on the precision with which its component parts have been fabricated. Theoretically, the accuracy of digital computer results can be made as high as practical requirements demand by addition of suitable digital equipment. Additional equipment, however, implies a decrease in

reliability and simple analog computers may turn out to be more reliable than their more complicated digital counterparts.

Since most digital computers perform mathematical calculations by successive additions, some operations, such as transcendental ones which require a converging series summation or equivalent, may be more time-consuming and complex than the same computation in an analog computer where the operation is performed by simple rotation of a resolver shaft. Because of round-off errors and loss of significant figures, the computer, carries along larger numbers than are actually needed. For these reasons, the digital computer tends to be larger, heavier, and more complex, and is possibly less reliable than an analog computer counterpart.

Until recently, the principal disadvantage of digital computers intended for airborne applications has been their excessive size and weight. Technical improvements such as subminiaturization techniques have now made these computers suitable for airborne fire control systems. Other examples of digital computer component improvements include: the use of magnetic cores for reliable quick-access memory; the use of transistors in place of vacuum tubes because of improved transistor reliability (i.e., the latest transistors are less environment-sensitive and consume less power than earlier types); and the use of printed circuitry in conjunction with small semiconductor diodes for the accomplishment of much computer logic.

Another problem associated with the digital fire control computer is that created by the requirement for analog-to-digital input equipment and digital-to-analog output equipment. This requirement stems from the fact that the radar and other airborne instruments provide their information in analog form, and also because the aircraft control system and missile auxiliaries require analog signals. It appears that the airborne digital computer must, of necessity, be a hybrid digital-analog computer system. Despite the described apparent disadvantages of the digital computer, its use is rapidly becoming widespread for fire control system applications. Both types of computers will be considered in this chapter. Following a discussion of general fire control problems and navigation, the necessary equations will be derived. Two possible computer designs for a proposed system will then be described. One system will exemplify an all-analog computer, the other an all-digital computer.

SECTION 2 — COMPUTING AND CONTROL REQUIREMENTS

The computing and control system instrumentation problems can be divided into two categories, those related to the attack phase, and those which deal with the navigation phase. The navigation phase is as important as the attack phase in terms of the over-all success of the mission; but the attack phase is of primary concern in design of fire control systems. The major emphasis will, therefore, be placed upon the satisfaction of requirements for the computer during the attack phase. Once the computer and control requirements have been set, it is essential that the computer satisfy the speed and capacity requirements demanded by the interceptor control system and missile armament. The target information available from the radar must be operated on, and an automatically generated attack course computed. This course must be computed whether the information comes from continuous-tracking radar or from a track-while-scan radar. The computer must also be capable of generating the proper course on the basis of the ground control system information.

The type of course to be flown depends upon the navigation scheme chosen. It will be shown that an optimum course is a lead collision attack course that results in minimum-time interception. In addition to providing the information for flying the proper course, the computer must also supply information to arm and fire automatically the armament selected by the pilot. The computer will fire the armament along the proper lead collision course if sufficient time is available. If sufficient time is not available, the computer should still be able to fire the armament in the optimum way permitted by the dynamic situation. The computer must provide the pilot with an indication of the tactical situation and also preclude firing of high level explosive armament if sufficient clearance time is not available. In addition to these fundamental operations, the computer must provide the system with the necessary computed information to provide the inertial navigation subsystem with precession rates, correction terms, etc. Additionally, the computer must be capable of selecting the required armament, and computing preparation timing, parameter setting, etc.

During the navigation phase, a considerable number of additional requirements are imposed on the computer. In particular, it must process information from the ground in order to correct computations from celestial, inertial, or other guidance equipment. Many of the computations required by the interceptor can be performed by a ground system

computer and transmitted to the aircraft. The airborne computer must determine the proper flight path required to bring the aircraft into the attack area in the minimum time and yet not exceed a maximum safe pull-out period. Additionally, the computer must compute the proper course for either minimum time or minimum fuel consumption. The computer must also determine the proper takeoff and landing paths. The computer can also act as a decoder for ground-to-air information from the data link and communication systems. The computer accepts measured information pertaining to the aerodynamic conditions such as air density, air pressure, and Mach number. This information is operated on to adjust properly the pitch, trim, and control surface effectiveness, and to maintain aircraft stability, etc. The computer may also be used to operate as a nonlinear filter to discriminate against unwanted signals and jamming.

SECTION 3 — COMPUTER FUNCTIONS

By using information from the radar, the computer can solve for position and velocity of the target to permit a continuous display of the target position to the pilot. These same data are required by the computer for determination of the proper flight trajectory. As indicated, the computer receives target information not only from the radar, but also from the ground via the data link. The target's last known velocity can be used by the computer to extrapolate target position in the absence of other data. This capability is particularly useful under severe jamming conditions. Information transmitted from the ground station via data link should be coded for security and decoded in the interceptor control system. Optimum coding represents a separate study requirement (see Appendix). Target position is determined by the computer using dead reckoning in the intervals between data transmissions and in the absence of continuous radar information. The radar supplies information while in either a track-while-scan mode or a continuous tracking mode. In the track-while-scan mode, the radar provides, once each scan frame, the following: range rate, ambiguous range, and angular position of the antenna. While in the continuous tracking mode, the radar supplies the digital computer with unambiguous range, range rate, angular position, and angular rate of the line of sight (LOS).

In addition to information pertaining to the tactical situation supplied from either the ground system or from the airborne radar interceptor, position data must be supplied to the computer. The interceptor may contain an inertial navigator that provides the computer with information to

derive the interceptor position, the ground velocity of the interceptor, and the interceptor's attitude. This information is necessary for the determination of the interceptor flight trajectory. Air velocity and wind direction are also required to compute heading. The air velocity, Mach number, temperature, and other aerodynamic data can be obtained from flight sensing instruments. The inertial navigation system serves as an attitude sensor. The inertial reference system in space can be used to measure aircraft pitch, roll, and yaw relative to the inertial system; in other words, it can be used to determine the relative orientation between an inertial coordinate system and the aircraft coordinate system.

The usual inertial system operates by sensing acceleration along the platform axes, integrating acceleration to obtain velocity, and then integrating a second time to obtain position in inertial coordinates. This information is then used to precess the platform axes to correct for earth rotation and aircraft movement over the earth. These corrections may be effected by applying rate signals to platform gyro torquers. Computation of the corrective torquing signals necessary to compensate properly for aircraft motion and the earth's rotation is a major difficulty in the design of a fire control system. Proper orientation of the inertial coordinate system requires accuracies of about 0.01 percent and, hence, accuracies of this order are required of the computer. Such accuracies are not readily attainable with analog computers, but are feasible with digital computers.

With present state-of-the-art developments, the use of a digital computer in conjunction with the inertial navigator appears practical.

If for some reason the inertial platform position and velocity outputs are in error or are unavailable, the computer should still be able to obtain an estimate of the interceptor position by dead reckoning. This can be done by integrating the aircraft velocity vector from a known initial position. Other miscellaneous functions which the computer must perform are: determination of armament ballistics, computation of true airspeed, etc. The ascertainment of these quantities requires air data inputs such as static pressure, impact temperature, Mach number, and angle of attack. These inputs change relatively slowly compared to the basic time constants in the computer and, consequently, are suitable for airborne computer inputs.

As mentioned previously, the primary duties of a computer in the attack phase are to steer the interceptor on an optimum trajectory and to prepare and launch the armament in order to maximize the probability of kill. The type of course to be chosen depends upon the countermeasure and tactical environment. In the absence of countermeasures and with adequate early warning time, a lead collision course is an optimum one; however, countermeasures or inadequate early warning time may prescribe a course varying between lead collision and pursuit. The course is also determined by the type of armament to be used. If a semi-active missile is to be launched, the computer must not only fire the missiles on the correct course, but also determine the aircraft flight trajectory to ensure target illumination until destruction occurs. The selected course also depends on the type of warhead. If a highly destructive warhead is used on a missile, more launching error can be tolerated than for the case of a smaller destructive radius warhead missile. In either case, the trajectory must be chosen to maximize the kill probability, taking into consideration pilot and aircraft safety. The computer also provides the necessary signals to prepare the armament for optimum aerodynamic performance prior to launching the armament at the proper time. Although the computer is able to operate with track-while-scan information from the radar, the pilot must convert to the continuous-tracking mode prior to launching the armament in order to provide required lock-on and slaving signals for the missile. The computer must provide the radar system with a signal when the minimum time has been reached in order to convert to continuous tracking. An important function that the computer must perform is the prediction of the future position of the target, based on past information (See Chapter VIII). This prediction of future target position is required to determine properly the course and trajectory for the aircraft and launching course for the missile. It is particularly advantageous to have the capability to extrapolate the range, position, and velocity of the target when tracking information is lost as a result of jamming or other causes. The computer not only provides the information for the proper interceptor course, but also determines the launch time for a missile lead collision trajectory. As well as supplying information preparatory to firing, the computer also determines the time to fire and introduces certain correction factors such as those required because of missile jump.

It is essential that the computing system be highly reliable. One method for improving system reliability is to include system self-test features. The self-test function can be provided by both inflight and

preflight checks. A discussion of system test and self-evaluation appears in Chapter VIII.

SECTION 4 — THE FIRE CONTROL PROBLEM

The fire control problem deals with a basic situation, namely, the launching of a projectile from a moving weapon carrier at a target (that, in general, will also be moving) so as to maximize the probability of target kill. The fire control problem for air-to-air projectiles is depicted in Figure 5-1.

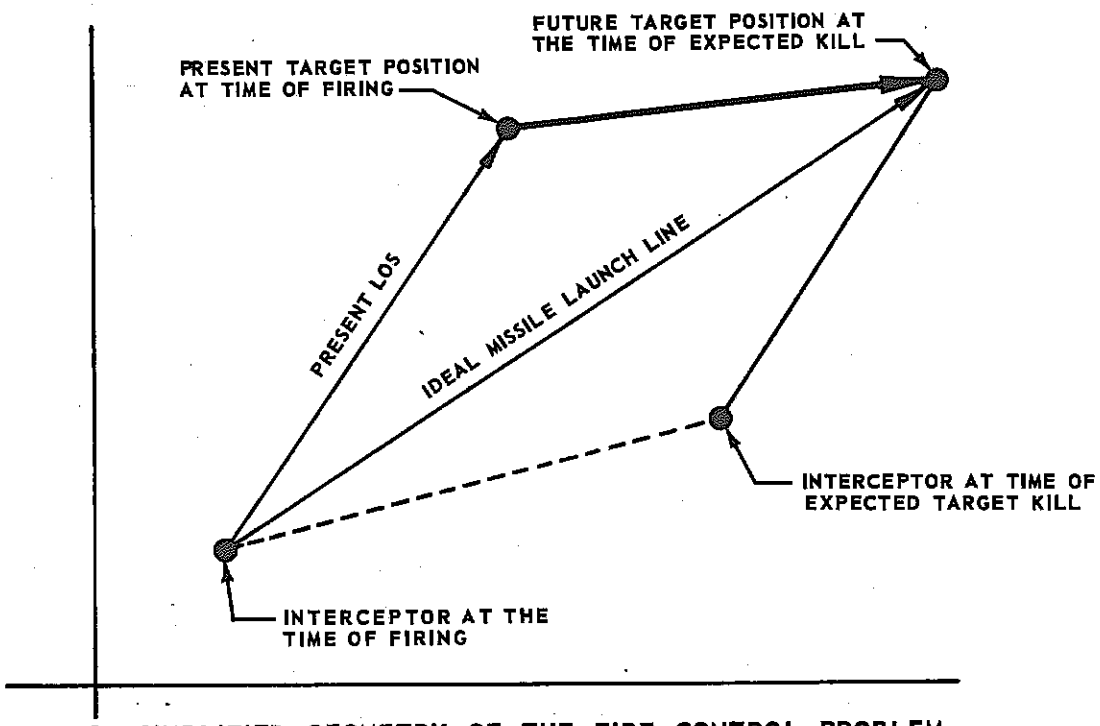

FIGURE 5-1. SIMPLIFIED GEOMETRY OF THE FIRE CONTROL PROBLEM

There are various miss-producing effects which may prevent target destruction. The interceptor fire control system attempts to reduce these miss-producing effects as much as possible; the guidance and control system in the missile attempts to reduce them further. Some of the major causes of missed targets include target motion, curvature of the projectile trajectory, and aerodynamic launch jump. If the latter two effects were not present, the missile could be fired along the ideal launch line shown in Figure 5-1. Clearly, the fire control system must predict the position of the target after further interceptor and missile flight time. Even if the future position of the target is predicted properly by the fire control system, the curvature of the missile trajectory must be taken into account, especially if the projectile is unguided. If the projectile is guided, curvature-producing effects and misalignment of launch direction effects should still be minimized. This prediction must be made so that the missile guidance and control system will function in its linear range of operation to produce smaller miss distances. The trajectory perturbations are caused by gravity, wind, and apparent terms due to acceleration of the observer's reference. "Jump" is an effect produced as a result of a combination of factors that cause the apparent initial velocity of the missile to differ from the direction in which the missile was aimed. As a result of the perturbations, it is necessary for the fire control system to apply a set of corrections for these miss-producing effects. Lead angle must be introduced to compensate for target motion during the time of flight; further curvature correction must be introduced, particularly for unguided missiles, to compensate for inflight forces acting on the projectile. Lastly, jump correction must also be introduced to compensate for initial velocity effects.

As can be seen from Figure 5-2, the LOS from the interceptor to the target is not the line along which the missile should be fired. The "ideal" direction for missile launching is along the LOS to the target after the missile time of flight, i.e., on an ideal collision course. The lead angle, θ_e, shown in Figure 5-2, is the angle between the present LOS and the LOS to the target at the time of impact, with respect to the interceptor position at the time of firing. The missile is not actually fired along this collision course line because of the curvature of the missile during its unguided phase (normally during the power boost period) and because of the initial jump. As shown in Figure 5-2, the curvature correction, θ_c, and jump correction, θ_j, modify the launching direction so that the final

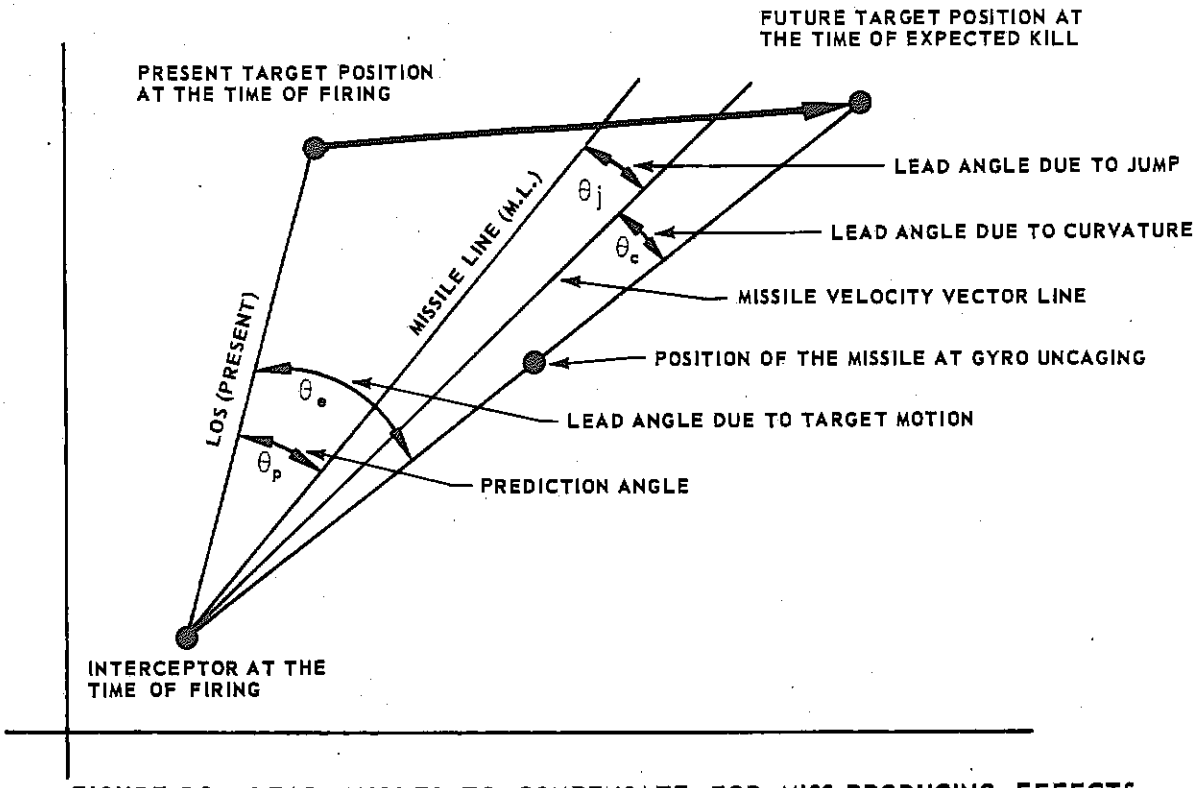

FIGURE 5-2. LEAD ANGLES TO COMPENSATE FOR MISS-PRODUCING EFFECTS

line along which the missile is fired, the "missile line" (ML) is at the prediction angle, θ_p. All of these angles are measured in the plane defined by the present and future positions of the target and the interceptor at the time of firing. The geometrical problem may be set up mathematically (refer to Figure 5-3).

Consider a unit vector $\bar{r}_e$ along the LOS and a second unit vector $\bar{r}_m$ along the missile line (ML). The prediction angle vector $\bar{\theta}_p$ can then be defined as

$$\bar{\theta}_p = \bar{r}_e \times \bar{r}_m \quad \frac{\theta_p}{\sin \theta_p} \tag{5-1}$$

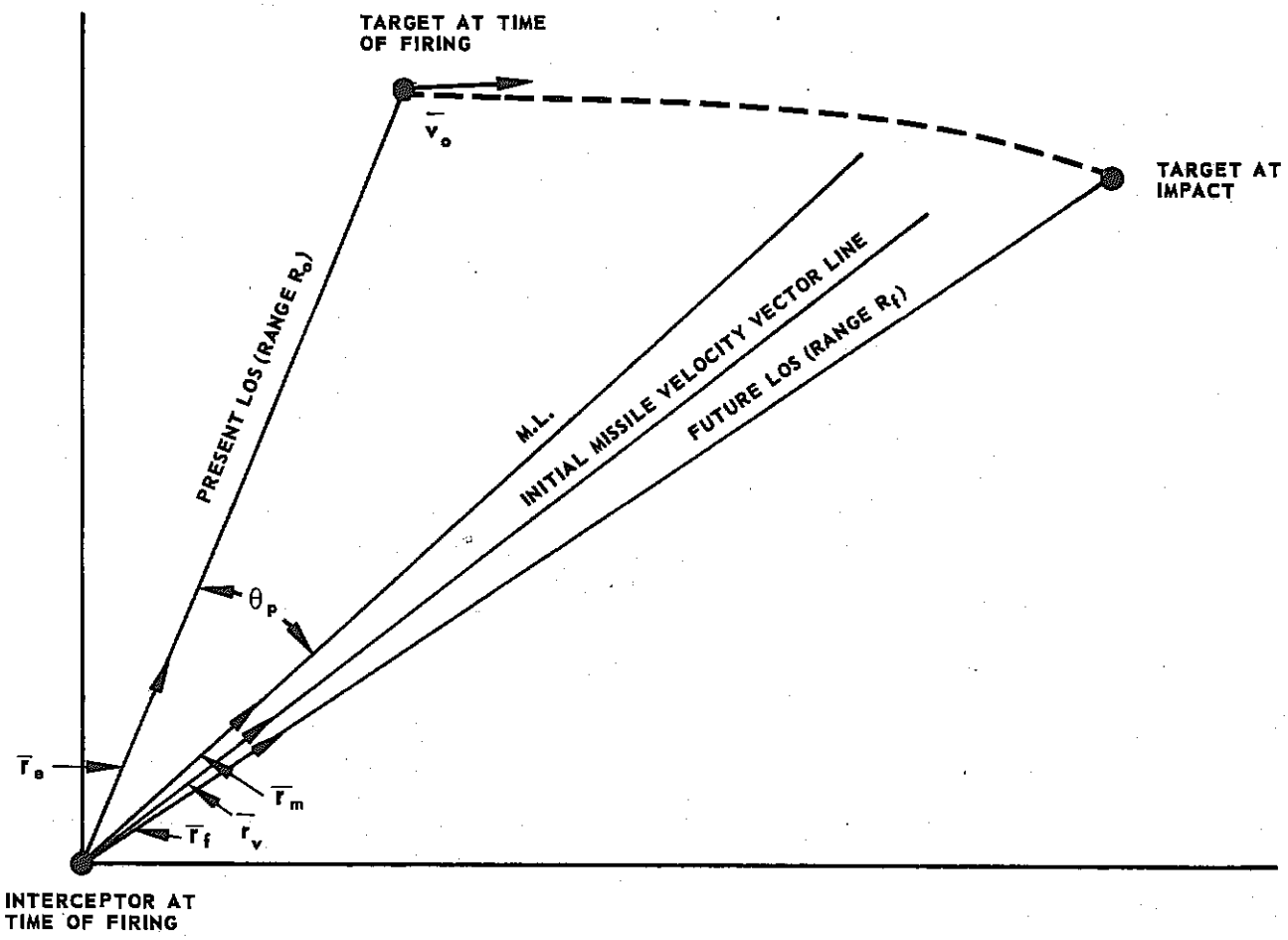

FIGURE 5-3. VECTOR GEOMETRY OF THE PROBLEM

Equation 5-1 follows, since

$$\bar{r}_e \times \bar{r}_m = r_e\, r_m \sin \theta_p\, \bar{r}_p = \bar{r}_p \sin \theta_p \tag{5-2}$$

where $\bar{r}_p$ is a unit vector in the direction of the vector angle $\bar{\theta}_p$ (normal to the plane of $\bar{r}_p$ and $\bar{r}_e$) and the magnitudes $r_e = r_p = r_m = 1$. If θ_p is sufficiently small $\sin \theta_p \cong \theta_p$ holds, in which case, Equation 5-1 becomes

$$\bar{\theta}_p = \bar{r}_e \times \bar{r}_m \tag{5-3}$$

Observe that the prediction angle defined in Equation 5-3 is invariant with the coordinate system used because the present LOS and the ML are determined by quantities that are unaffected by the choice of reference system. The prediction angle is composed of the lead angle, the curvature correction angle, and the jump angle correction according to

$$\bar{\theta}_p = \bar{\theta}_e - \bar{\theta}_c - \bar{\theta}_j \tag{5-4}$$

Observe that the curvature correction is a function of the time of unguided flight, the jump correction is a function of initial conditions only, and the lead correction is a function of the launching error and the time of flight. As in the case of the prediction angle, the angular errors and corrections can be represented by vectors. Thus,

$\bar{\theta}_e$ = vector representing the lead angle correction

$\bar{\theta}_c$ = vector representing the curvature angle correction

$\bar{\theta}_j$ = vector representing the jump angle correction

Let $\bar{r}_e$ be the unit vector along the present LOS and $\bar{r}_f$ the unit vector along the future LOS. Let R_o be the present target range and $\bar{R}_f$ be the vector range plus the vector motion of the target during the time of flight t_f. Thus,

$$\bar{R}_f = \bar{R}_o + \bar{v}_{otf} + \int_o^{t_f} dt \int_o^{t} \bar{a}(x)dx \tag{5-5}$$

where v_o is the target velocity at the time of firing and a(x) is the target acceleration. The missile will hit the target if

$$R_f = v_{avg}\, t_f \tag{5-6}$$

Note that

$$\bar{r}_f = \frac{\bar{R}_f}{R_f} \tag{5-7}$$

and

$$\bar{\theta}_\ell \cong \bar{r}_e \times \bar{r}_f \tag{5-8}$$

where v_{avg} is the average missile speed during the time of flight. Substituting Equations 5-5, 5-6, and 5-7 into Equation 5-8 yields

$$\bar{\theta}_\ell = \frac{\bar{r}_e \times \bar{R}_f}{v_{avg}\, t_f} \doteq \frac{\bar{r}_e \times \bar{v}_o}{v_{avg}} + \frac{\bar{r}_e}{v_{avg}\, t_f} \times \int_o^{t_f} dt \int_o^{t} \bar{a}(x)dx \tag{5-9}$$

The initial target velocity is not measurable, but may be found by measuring the angular velocity of the LOS. Thus,

$$\bar{\omega}_\ell = \dot{\bar{\sigma}}_\ell = \frac{\bar{r}_e \times \bar{v}_o}{R_o} \tag{5-10}$$

where ω_ℓ is the angular velocity of the present LOS due to target motion and σ is the angle that the present LOS makes with the space reference. The target motion component of the LOS angular velocity also may not be directly measurable. The total angular velocity and the interceptor component of angular velocity are measurable.

Referring to Figure 5-3, it can be seen that

$$\bar{\omega} = \dot{\bar{\sigma}} = \bar{\omega}_\ell + \bar{\omega}_r \tag{5-11}$$

also,

$$\bar{\omega}_r = -\frac{\bar{r}_e \times \bar{v}_i}{R_o} \tag{5-12}$$

where $\bar{v}_i$ is the vector velocity of the interceptor in interceptor coordinates. If, in the proposed system, the interceptor coordinates are fixed to the interceptor frame (for example the X-axis in the plane of the wings, the Y-axis normal to the X-axis and the longitudinal axis and passing through their intersection, and the Z-axis which is the longitudinal axis

of the interceptor), then $v_i = 0$ and $\omega = \omega_\ell$. Where ω_ℓ is the angular velocity of the present LOS in interceptor coordinates, ω_r is the angular velocity of the present LOS in interceptor coordinates due to interceptor motion and ω is the total angular velocity of the LOS. Substituting Equations 5-10, 5-11 and 5-12 into Equation 5-9 yields

$$\theta_\ell = \frac{R_o \bar{\omega}_\ell}{v_{avg}} + \frac{\bar{r}_e}{v_{avg}} x \int_o^{t_f} dt \int_o^t \bar{a}(x)dx$$

$$= \frac{R_o \bar{\omega}_\ell}{v_{avg}} + \frac{\bar{r}_e \times \bar{v}_i}{v_{avg}} + \frac{\bar{r}_e}{v_{avg}} x \int_o^{t_f} dt \int_o^t \bar{a}(x)dx \qquad (5\text{-}13)$$

If the measurements are made with respect to an inertial coordinate system, such as might be provided by a free gyro coordinate system, then Equation 5-13 becomes

$$\theta_\ell = \frac{R_o}{v_{avg}}(\bar{\omega}_i - \bar{\omega}_t) + \frac{\bar{r}_e \times \bar{v}_i}{v_{avg}} + \frac{\bar{r}_e}{v_{avg}} x \int_o^{t_f} dt \int_o^t \bar{a}(x)dx \qquad (5\text{-}14)$$

where

$$\bar{\omega}_i = \bar{\omega} + \bar{\omega}_t \qquad (5\text{-}15)$$

where ω_i is the angular velocity of the present LOS with respect to an inertial coordinate system, ω_t is the present angular velocity of the interceptor coordinate system with respect to the inertial coordinate system, R_o is the present range, v_{avg} is the average missile speed during the time of flight $\bar{r}_e \times \bar{v}_i$ is the interceptor velocity in interceptor coordinates normal to the present LOS, $\bar{a}(t)$ is the target acceleration during the time of flight, and t_f is the time of flight of the missile.

The lead is the angle between the present and future lines of sight. Present line of sight is, by definition, the direction from the interceptor to the target at the instant of firing and, consequently, is invariant with the observer's reference space. Future line of sight is the direction that an

observer in the interceptor would view the target at impact from a position on the interceptor at the time of firing. The future line of sight and, therefore, the lead angle are functions of the coordinate system chosen. The coordinate system shown in Figure 5-3 is called the "interceptor coordinate system at the time of firing" or simply, the "interceptor coordinate system."

The target motion normal to the present line of sight requires lead correction. This motion is very nearly the normal component of the average target velocity over the time of flight. It can thus be set equal to the velocity at the time of firing and the integrated effect of target acceleration during the time of flight. As can be seen from Equation 5-14, the terms which comprise the lead angle include: that due to the total angular velocity of the present line of sight with respect to an inertial coordinate system, that due to the interceptor velocity (in interceptor coordinates normal to the present line of sight), and that due to the target acceleration term. The target acceleration in any coordinate system is equal to its acceleration in an inertial coordinate system less an amount equal to its apparent acceleration due to the earth's rotation measured in inertial coordinates, less another quantity equal to the target's apparent acceleration due to the motion of the interceptor in the earth's coordinate system. Assume a coordinate system consisting of a fixed coordinate system centered at the point of firing, an earth coordinate system fixed in the earth and centered at the earth's center, and an inertial coordinate system which is fixed relative to the universe. The vector displacement of the target from the origin of interceptor space is

$$\bar{R}_i = \bar{R}_e - \bar{R}_t \tag{5-16}$$

where $\bar{R}_i$ is the displacement of the target from the origin in interceptor space, $\bar{R}_e$ is the displacement of the target from the origin of the earth coordinate system, and $\bar{R}_t$ is the displacement of the center of the interceptor coordinate system from the center of the inertial coordinate system. The target acceleration in interceptor space is then

$$\bar{a}(t) = \ddot{\bar{R}}_i \tag{5-17}$$

which can be written in terms of acceleration relative to the earth coordinate system as

$$\bar{a}(t) = \ddot{\bar{R}}_e - \left\{ \bar{\omega}_e \times (\bar{\omega}_e \times \bar{R}_i) + 2\bar{\omega}_e \times \bar{v}_i + \dot{\bar{\omega}}_e \times \bar{R}_i \right\} \tag{5-18}$$

The first term in Equation 5-18 is the acceleration of the target relative to the inertial coordinate system, the second term is the centripetal acceleration, the third term is the Coriolis acceleration, and the fourth is the tangential acceleration.

$\bar{\omega}_e$ is the angular velocity of the interceptor coordinate system relative to the earth coordinate system. Taking the second derivative of Equation 5-16 with respect to earth coordinates yields

$$\ddot{\bar{R}}_e = \ddot{\bar{R}}_{ie} + \ddot{\bar{R}}_{te} \tag{5-19}$$

Equation 5-19 can be substituted into Equation 5-18, which can then be written as

$$\bar{a}(t) = \ddot{\bar{R}} - \left\{ \bar{\omega}_{ie} \times (\bar{\omega}_{ie} \times \bar{R}_e) + 2\bar{\omega}_{ie} \times \bar{v}_e \right\}$$
$$- \left\{ \ddot{\bar{R}}_{te} + \bar{\omega}_e \times (\bar{\omega}_e \times \bar{R}_i) + 2\bar{\omega}_e \times \bar{v}_i + \dot{\bar{\omega}}_e \times \bar{R}_i \right\} \tag{5-20}$$

where

$\ddot{\bar{R}}$ = the inertial acceleration of the target equal to the force per unit mass acting on the target,

$\bar{\omega}_{ie}$ = the angular velocity of the earth relative to inertial space,

$\dot{\bar{\omega}}_{ie}$ = the angular acceleration of the earth relative to inertial space and must be zero, and

$\bar{v}_e$ = the velocity of the target relative to the earth

The acceleration of the target in the interceptor coordinate system can, therefore, be divided into three parts: the acceleration of the target relative to an inertial coordinate system, the apparent acceleration of the target due to the earth's rotation in the inertial coordinate system, and the apparent acceleration of the target due to the motion of the interceptor coordinate system in the earth's coordinate system. The terms involving earth rate and rotation relative to the inertial coordinate system will be neglected because the times of flight to be considered in the

example are short. These terms are usually important only in long range firings.

Target acceleration is quite difficult to treat and to compute in the fire control system. The most common approach to the problem is to assume that the target acceleration is zero, so that the target is considered to be moving in a straight line at constant speed. This assumption will be used in the example. The second assumption is that the target acceleration is constant. The third assumption includes estimates of anticipated maneuvers based on the probabilities of various target courses. This last estimate is quite difficult to determine in advance and is therefore difficult to mechanize. For the case of bomber defense, it may be assumed that the target is following a lead pursuit course directed toward the interceptor. In this case, the integrated acceleration term becomes

$$\int_0^{t_f} dt \int_0^t a(x)dx = \frac{1}{2} a_o t_f^2 + \int_0^{t_f} dt \int_0^t dx \int_0^t \dot{a}(y)dy \qquad (5\text{-}21)$$

The principal mathematical difficulty in predicting future acceleration of the target is caused by the fact that a power series expanded about time of firing is valid only if no arbitrary motion of the target occurs during the time of flight. This does not, however, describe the typical practical case. A second approach is based on prediction using statistical concepts. The subject of target prediction is detailed in Chapter VIII. The proper statistical procedure considers an ensemble of possible target motions and assigns probabilities to each of these motions. One approach might determine the most likely future position of the target based on probability distribution. The principal difficulty lies in assigning weights to the various probabilities. Since data concerning randomness of target acceleration are generally poor, little effort is expended in determining possible positions of the target based on acceleration effects. Since missiles, during periods of guidance, continually correct for changes of target position due to acceleration and any other causes, consideration of these points is unnecessary. The effects of changing target position become vitally important when firing unguided projectiles such as rockets.

Curvature correction may be defined in terms of curvature angle in much the same manner used for lead and prediction angle. Curvature correction is necessary for angular correction in order to compensate

for the effect of forces acting on the projectile during its flight. The curvature and jump correction as shown in Figure 5-2 is the angle between the future line of sight and the missile line. The missile line coincides with the missile initial velocity vector at the time of firing. Boundaries of the curvature and jump correction angles are dependent therefore on the reference coordinate system. Curvature correction in the absence of jump is defined as

$$\bar{\theta}_c \cong \bar{r}_m \times \bar{r}_f \tag{5-22}$$

$$\bar{r}_m = \frac{\bar{v}_o}{\bar{v}_a} \tag{5-23}$$

$\bar{\theta}_c$ is the curvature correction, $\bar{r}_m$ is the unit vector along the missile line, and $\bar{v}_a$ is the missile velocity at the time of firing. The range at the end of boost is given by

$$\bar{R}_b = \bar{v}_o t_b + \int_o^{t_b} dt \int_o^t \bar{a}(x)dx \tag{5-24}$$

where $\bar{a}(x)$ is the missile acceleration, and t_b is the time of boost. The range at the end of boost is also given by

$$\bar{R}_b = \bar{r}_f \, v_{avg} \cdot t_b \tag{5-25}$$

When Equations 5-25 and 5-24 are inserted into Equation 5-22, the result is

$$\bar{\theta}_c \cong \frac{\bar{r}_m \times \bar{v}_o}{v_{avg}} + \frac{\bar{r}_m \times \int_o^{t_b} dt \int_o^t \bar{a}(x)dx}{v_{avg}\, t_b} \tag{5-26}$$

In the preceding equations it is assumed that the missile terminates boost on the future LOS.

Again, the apparent missile acceleration can be resolved into inertial effects and effects due to the acceleration of the earth and of interceptor space. The principal forces acting on the missile during the boost period are (1) gravity, (2) aerodynamic drag, which is proportional to the air velocity of the missile, (3) the drift force per unit mass, which is the interaction of the torque produced by the rotating aerodynamic lift vector acting at the center of pressure with the angular momentum of a spinning projectile when its trajectory is curved by the action of gravity, (4) the lift when the projectile is self-propelled, (5) the thrust when the projectile is self-propelled, and (6) the kinetic reaction, which is the apparent force due to acceleration of interceptor space. As will be shown, the forces exerted on the missile by all of the aforementioned forces except gravity can be neglected in a proposed system if the missile boost time is short (for example, on the order of 2 seconds). The components of several of these forces are normal to the missile line and therefore result in curvature of the trajectory. Components parallel to the missile line affect the time of flight. The principal term affecting the curvature of the missile is that due to the force of gravity. The aerodynamic effect is due to deflecting winds and is usually of minor importance. The third-listed force arises as a consequence of the spin of the projectile. This is unimportant in missiles that are guided. The fourth and fifth force effects are due to the missile propulsion system and lift forces. Finally, there are effects which result as a consequence of the acceleration of the missile reference system relative to inertial space. The effect of deflecting winds, drift, and accelerating coordinate system forces can be completely neglected in view of the short duration of missile boost. Errors in the direction of the flight caused by the propulsion and aerodynamics of the missile are considered briefly. The principal error, namely that due to gravity, is considered in detail, and even though a gravity drop correction is included in the computation, it is shown that the effect of curvature can be completely neglected for the short boost times considered. The missile can tolerate limited initial launching error. If the fire control system does not correct for curvature, the initial rms launching error may still be within the allowable rms error, for which the missile is able to correct.

Jump correction must be added to the angular correction term since the missile velocity vector does not lie along the missile line as indicated by target motion and curvature effects alone. The angle between the future LOS and the missile line is therefore determined by jump as well as curvature effects. The missile line, or line parallel to the longitudinal axis of the missile, is generally not aligned with the initial

velocity vector of the missile because of launcher tipoff and because the wind vector and the missile velocity vector are misaligned. The jump correction is not invariant with respect to the coordinate system. When jump angle is considered, Equation 5-21 no longer applies. Defining $\bar{r}_v$ as the unit vector along the initial missile velocity vector (see Figure 5-3), the jump and curvature correction terms become

$$\bar{\theta}_j \cong \bar{r}_m \times \bar{r}_v \tag{5-27}$$

$$\bar{\theta}_c = \bar{r}_v \times \bar{r}_f \tag{5-28}$$

Although an empirical jump correction term is included in the computation for a proposed fire control system, this type of correction can be neglected because the jump error is usually small. The prediction angle is determined by the following: the line-of-sight angular velocity, the rotation of the reference coordinate system relative to the earth inertial coordinate system, the interceptor velocity, the target acceleration, gravity drop, aerodynamic drag, drift, lift and thrust acceleration of the reference coordinate system, velocity jump, and windage jump. The curvature correction terms (gravity drop, aerodynamic drag, drift, lift and thrust, and acceleration of the reference space) can be lumped into the curvature correction term.

The various jump effects can be included in a single jump term. From Equations 5-14 and 5-4, taking into account the preceding discussion, the equation for the prediction angle can be written

$$\bar{\theta}_p = \frac{R_o \bar{\omega}_i}{v_{avg}} - \frac{R_o \bar{\omega}_t}{v_{avg}} + \frac{\bar{r}_e \times \bar{v}_i}{v_{avg}} + \frac{\bar{r}_e}{v_{avg}} \times \int_o^{t_f} dt \int_o^t \bar{a}(x)dx - \bar{\theta}_c - \bar{\theta}_j \tag{5-29}$$

The first term in Equation 5-29 is the principal one and it describes the inertial LOS angular velocity; the second term accounts for rotation of the reference space; the third accounts for the interceptor velocity in the reference system in which $\bar{\theta}_p$ is measured; the fourth takes into account target acceleration; the fifth is the curvature correction, which

includes gravity, drag, drift, lift, thrust and reference space acceleration; and the sixth term is the jump correction, which includes velocity jump (due to a component of the missile velocity normal to the missile line) and windage jump. The computer equations which may be mechanized are a special case of Equation 5-29 and a time-of-flight equation. The time of flight is determined by the various forces acting on the missile during its flight, as well as by the missile velocity, acceleration, initial velocity, and future position of the target. The future position of the target may be computed from the present range by addition of range increments which are a result of target motion. The average missile velocity can then be determined from the ratio of the final range less the initial range to the time of flight. The accuracy of the time of firing computation is not too critical for the guided missiles as compared to the case of unguided armament. A fairly wide tolerance in guided missile launching range is allowable, requiring only that the launching range be great enough to allow correcting the initial launching error before the missile reaches the target vicinity without exceeding the missile aerodynamic or radar range.

SECTION 5 — THE COMPUTER TRACKING PROBLEM

The general fire control problem has been stated in the previous section. The solution to the fire control problem will now be considered. The radar and fire control system auxiliaries require certain measurements of motion and direction in space associated with the target, the interceptor, and other factors. The data are processed by the computer to derive values for time and direction of missile launch. Additionally, the computer navigates the aircraft during the attack phase. To establish a correspondence between the geometry of the fire control problem and the measurements required for its solution, a discussion of the general tracking problem is in order.

Assume that the search, lock-on, and acquisition phases of the attack have been completed, and that the radar is tracking the target. This implies that the antenna tracking loop of the radar is functioning, that the scan axis of the radar is aligned with the line of sight (LOS) from the interceptor to the target, and that the radar is developing control voltages which are applied to the computer input for the solution of the fire control problem. As a result of servo errors, the scan axis of the antenna will deviate from the true LOS by the angular tracking error. Since the aircraft navigates using the scan axis of the radar antenna pointing direction as the true LOS, the resulting error will give navigational errors in the control of the aircraft, and launching error in the missile at the time

of firing. In the proposed system, the "missile line," or line along the direction in which the weapon is fired, coincides with the longitudinal axis of the aircraft; i.e., the missiles are so oriented in the launcher that the missile axis is aligned with the longitudinal axis of the aircraft. Assume the longitudinal axis of the aircraft to be one of the coordinate directions of the interceptor coordinate system. The scan axis direction is measured with respect to the interceptor coordinate system. The computer accepts voltages which are proportional to the position of the target in space relative to the interceptor coordinate system, and the angular and radial rates of the target relative to the interceptor coordinate system.

(a) ATTACK PHASE

The computer inputs are operated upon in such manner as to determine the correct prediction angle, the angle between the present interceptor-target LOS and the proper line for zero launching error. The zero launching error or missile line and the prediction angle are not directly available in the system but can be determined within the accuracies of the system by measurement of other system parameters. Parameters available for measurement are the actual interceptor coordinate system and the computed prediction angle relative to it. Since the radar system already contributes to the error or difference between the computed and correct prediction angle, the computer must be designed to introduce as little additional error to the measurements as possible if accurate flight trajectory and weapon firing time are to be obtained. The geometrical relationships between the various lines are shown in Figure 5-4. Note that the angle between the computed missile line and the correct missile line is not necessarily equal to the angle between the scan axis direction and the LOS. The angle between the LOS and the scan axis is a tracking error in the radar alone, whereas the error between the correct missile line and the computed missile line consists of the error due to misalignment of the scan axis and the LOS, plus miss-producing effects such as target motion, curvature of the missile trajectory, and jump. Since the true LOS and the correct missile line are not available as references, either the missile or the scan axis line can be considered as the reference and the prediction angle can be computed from this reference. In either case, the indicated prediction angle is the angular difference between the scan axis and the computed missile line. This prediction angle is sometimes called the "lead" angle, although lead angle has been defined as the angle between the

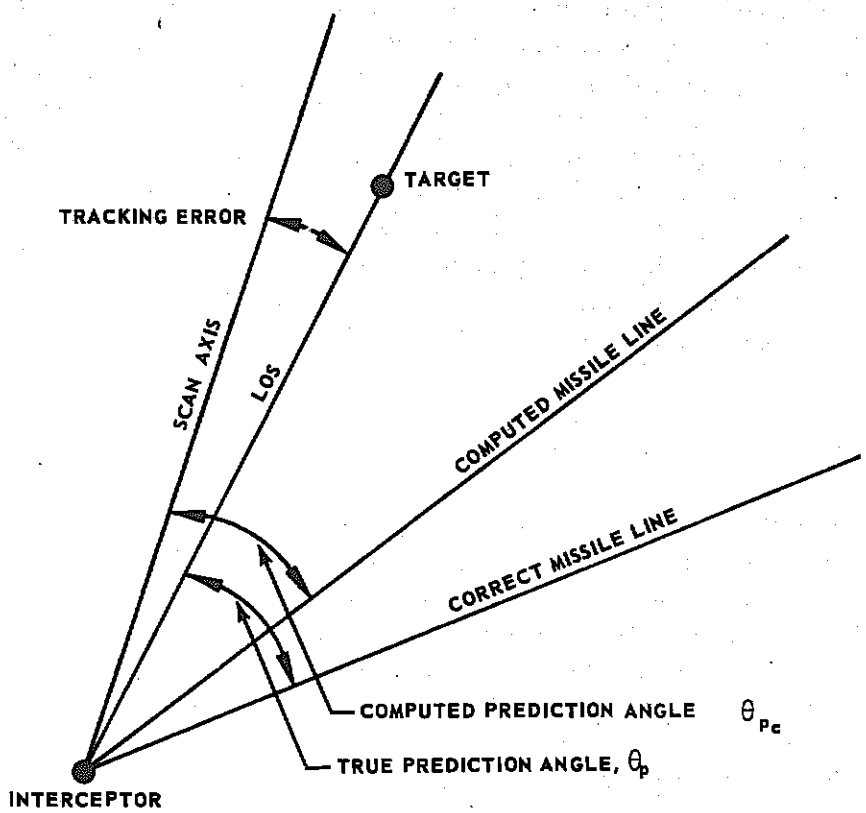

FIGURE 5-4. EFFECT OF TRACKING ERRORS ON FIRE CONTROL GEOMETRY

present LOS (the true LOS) and the line connecting the target position at impact and the interceptor at the time of firing.

The tracking problem requires nulling of the angular error to obtain the scan axis line. There are various ways in which this can be done. For example, the tracking error signal, which is proportional to the tracking line correction, can actuate the tracking antenna drive so as to null the error (i.e., to reduce the tracking error to zero). Alternatively, the tracking error signal may be used to actuate the weapon drive and thereby null the error.

A system may use an inertial reference line and measure the angular velocity of the scan axis line in order to compute the prediction angle. The angle tracking loop in the radar attempts to reduce the tracking error to zero. Even though tracking error is the principal one, the computed launching direction would not necessarily coincide with the

true missile line, even if the tracking error were zero, because of computer and interceptor control system errors and lags. If the missile axes are aligned with the interceptor axis, the computed launching direction coincides with the interceptor longitudinal axis.

Inputs for computing prediction can be used in several ways; for example, the computed lead angle may be based on the scan axis angular velocity or on the missile line angular velocity less the rate of change of the computed prediction angle. Computed lead angle may also be based on the computed scan axis angular velocity referenced to the indicated prediction angle.

The solution of the fire control problem depends upon the input data and the reference coordinate system with respect to which the input data are measured. If corrections to the tracking line are referred to inertial space, any non-inertial characteristics of the coordinate system in which the computation takes place must be accounted for in the mechanization of the fire control problem. For instance, the interceptor may roll, pitch, and yaw with respect to the reference coordinate system used. These motions have nothing to do with the measurement of the proper prediction angle and should be removed. One method for removing these interfering motions depends on stabilization of certain parts of the fire control equipment as, for example, by use of a gyro stabilized platform. As can be seen, the problem is one of maintaining in the presence of disturbing influences, a fixed direction in inertial space which can, however, be changed in response to a command signal. In the case of radar tracking, the correction to the tracking line causes the scan axis to rotate into alignment with the LOS. This angular rotation is a vector quantity which is specified without reference to any particular coordinate system since it depends only on the LOS and the scan axis. The corrected scan axis direction then implicitly defines the reference for an inertial coordinate system. The inertial tracking correction must be converted to signals which are referenced to the interceptor coordinate system to align the longitudinal axis of the aircraft with the proper missile launching trajectory at the correct time. A coordinate transformation between inertial space and the interceptor or computation space must be included in the fire control system. An inertial three-dimensional coordinate system may be set up by using two free gyros with their spin axes mounted normal to each other. If the gyros were mounted in an ideal frictionless gimbal system so that the speed of the gyros could be maintained constant and the gyros were unaffected by gravity and other disturbing influences, then an inertial coordinate system would remain stable throughout the

flight of the aircraft. Since none of these ideal conditions are attainable in a practical system, the spin axes will precess and the gyro inertial coordinate system itself will be in error. Coordinate transformation between the inertial and interceptor coordinate system can be accomplished by mounting instrumentation devices such as potentiometers between the gyro gimbal axes and the interceptor frame. In a practical system the antenna scan axis may be aligned with the antenna gyro spin axis. Each gyro of the inertial system maintains a fixed direction in inertial space unless torqued. The torquing signals are applied so as to align the antenna scan axis with the true line of sight. It turns out that the torque-to-precession rate relationship is invariant with respect to the coordinate system so that the problem of coordinate transformation does not arise in this type of antenna tracking system. Such a transformation is required, however, for the interceptor control system inputs. Antenna tracking gyro alignment with the scan axis (with respect to inertial space) provides the fire control computer with a basic input of the angular velocity measurement of the line of sight.

In the most general type of fire control system, the problem of fire control prediction is separate and distinct from that of navigation. When, however, the interceptor has fixed armament such as missiles (whose axes are fixed relative to the interceptor coordinate system), the problem of navigation is synonymous with the problem of fire control prediction. Once the scan axis approximation to the LOS is determined and its angular rate measured, the problem of computing the prediction angle and directing the missile properly through space becomes simply the problem of navigating the aircraft along the proper trajectory for missile launch. Part of the solution to the fire control problem becomes simply the determination of the proper navigation scheme for the interceptor during the attack phase. A complete solution to the problem must also include the determination of the proper instant of firing plus the proper preparation of the armament prior to firing.

(b) NAVIGATION PHASE

The types of navigation of principal interest in aircraft and missile guidance are (1) pursuit courses, (2) proportional navigation courses, and (3) lead collision courses. A pursuit course is one in which the interceptor maintains a specified angle with the LOS during the time of flight. In a pure pursuit course the interceptor velocity vector is aligned with the present LOS. In a "lead pursuit" course (see Figure 5-5) the velocity vector is directed along a line forming the instantaneous computed prediction angle with the LOS. The computation of a lead pursuit

course differs from that of the pure pursuit course since the prediction angle must be computed in the former. In a pure pursuit course, no computation is required because the interceptor velocity vector is simply aligned with the scan axis of the radar antenna.

It should be emphasized that the longitudinal axis of the aircraft is, in general, not aligned with the instantaneous velocity vector of the aircraft because of the aircraft angle of attack. A proportional navigation course is one where the aircraft turning rate is proportional to the angular velocity of the line of sight. Eventually, the aircraft velocity vector may point toward a future target position where collision occurs. If this happens, the angular velocity of the line of sight approaches zero. The rate at which it approaches zero depends upon the proportionality factor. When the velocity of the line of sight becomes zero, the aircraft is said to be on a "collision" course. A collision course is often referred to as a "constant bearing" course since the prediction angle, or more properly, the angle between the aircraft velocity vector and the LOS, remains constant. A collision course should result from the final stage of a proportional navigation course. It is important to note that the requirement for proper missile launching is <u>not</u> that the interceptor fly an <u>interceptor</u> collision course with the target, but rather, that the interceptor fly a <u>missile</u> collision course with the target. In other words, if a proportional navigation scheme is to be used in the missile, the launching error is said to be zero when the missile is launched along an "ideal" trajectory, which is a missile collision course. The optimum navigational method for homing missiles can be shown to be proportional navigation. If this type of navigation is used, the trajectory which the aircraft should follow just prior to and at the time of launch, is a missile collision course. The optimum interceptor course to bring the missile onto the missile collision course at launch time will be shown to be a lead collision course. The interceptor is assumed to be missile-armed and attacking a bomber which is flying with a constant velocity vector. The target future positions t_{fi}, are shown in Figure 5-5 at successive intervals during the attack. The angles θ_{pi} are the computed predicted angles. In a pure pursuit course, these angles would all be identically zero.

Figure 5-6 illustrates a collision course. The target is again assumed to be flying with a constant velocity vector, as is the missile. The missile-target line and the LOS are shown at successive equally spaced intervals during the attack. Note that prediction angle remains constant; that is, the target has a constant bearing relative to the missile during the attack.

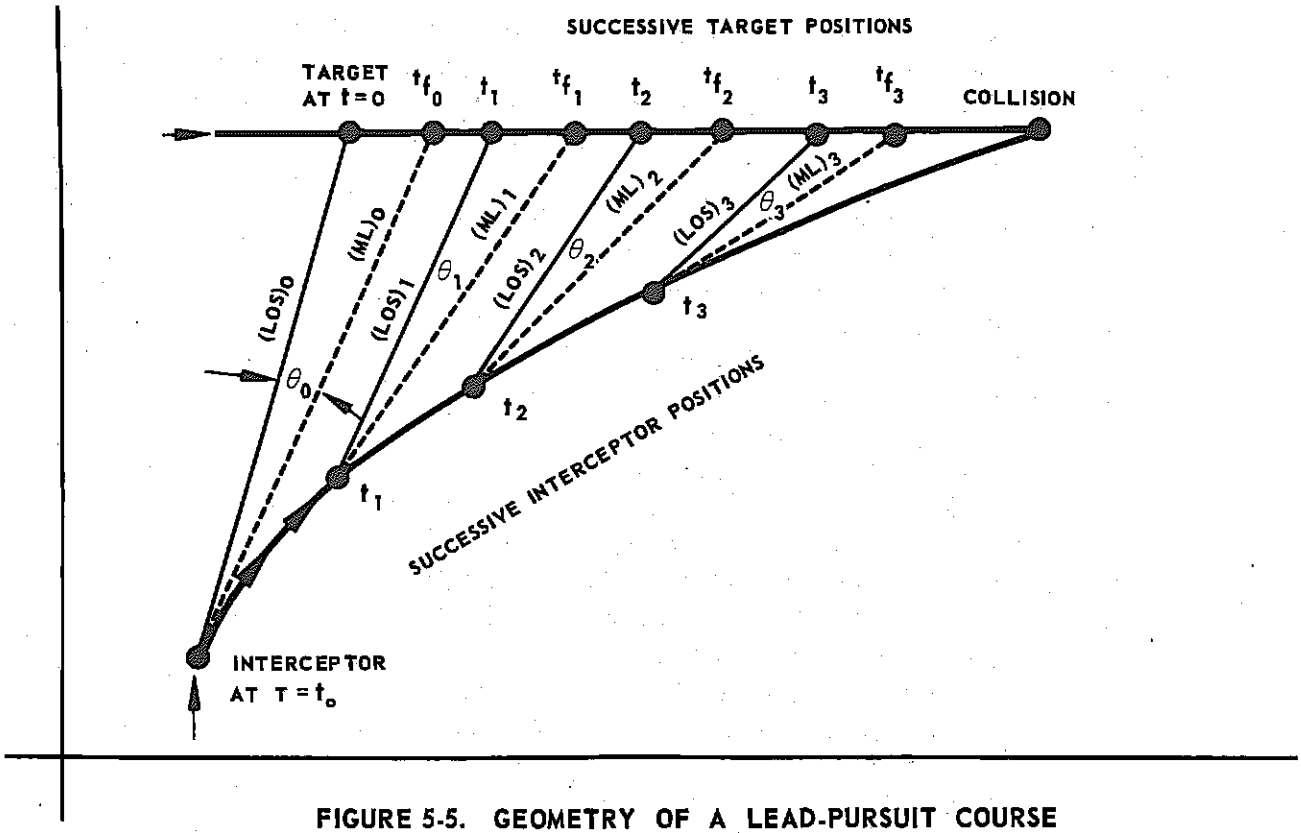

FIGURE 5-5. GEOMETRY OF A LEAD-PURSUIT COURSE

Figure 5-7 shows an attack in which a proportional navigation trajectory is followed. At each instant of time, the interceptor attempts to correct its trajectory to fly on a collision course with the target. Since the target velocity vector is no longer assumed to be constant, the interceptor velocity vector cannot be constant. As long as the target continues to maneuver, the interceptor must also maneuver in order to approach the ideal collision course.

A lead collision course is illustrated in Figure 5-8. If the target velocity vector does become constant, the interceptor then approaches the pure interceptor collision course at a rate that is dependent upon the proportionality constant. In the lead collision course, the interceptor is flown along a straight line course to the missile firing point. At the missile firing point, the interceptor should be on a missile collision course. This requires changing the interceptor-target prediction angle during the flight. The firing point is chosen to satisfy the conditions that (1) the interceptor is flying a missile collision course at launch, (2) the launch

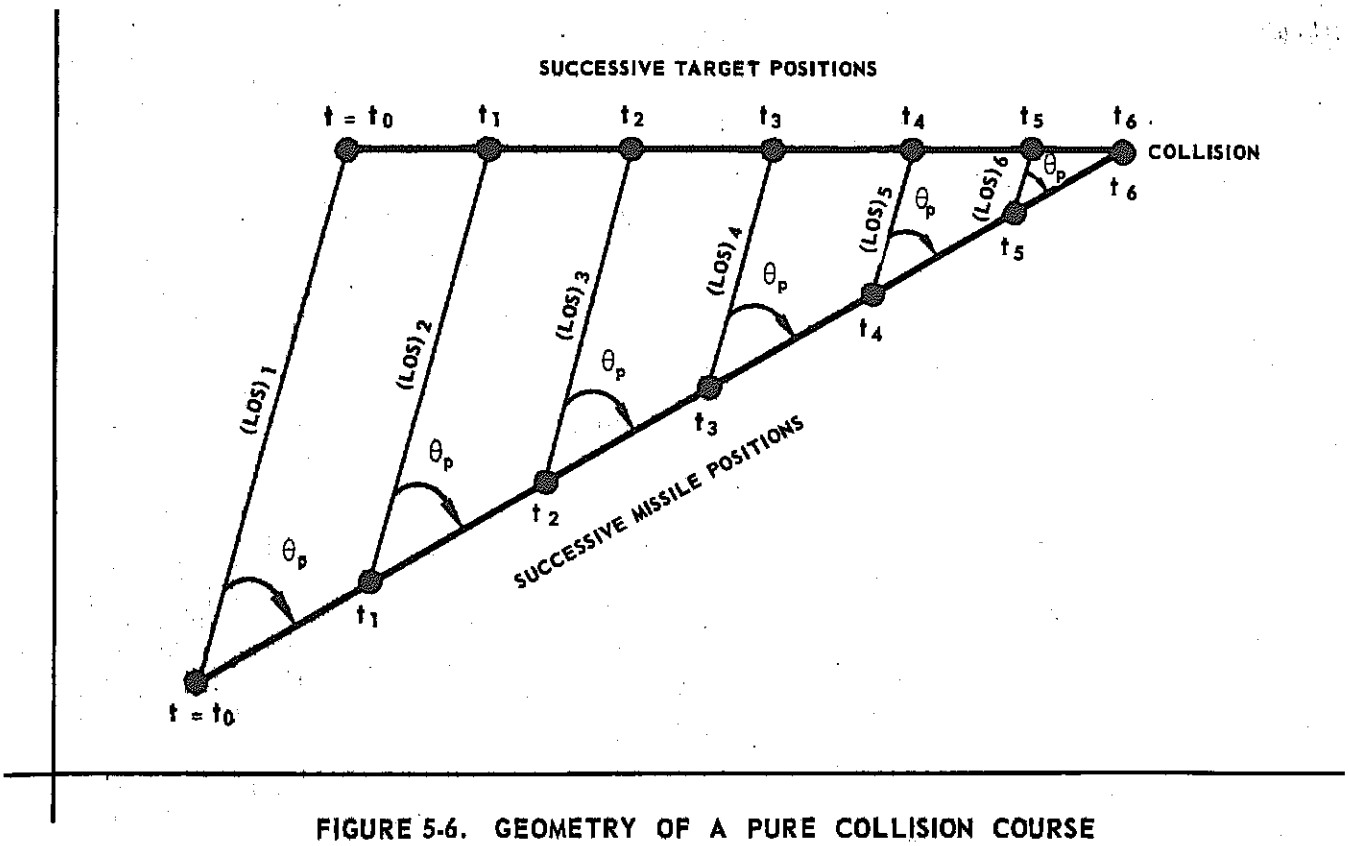

FIGURE 5-6. GEOMETRY OF A PURE COLLISION COURSE

point is at the proper range for greatest missile effectiveness, and (3) adequate separation between target and interceptor remains at target kill for interceptor safety commensurate with adequate target illumination.

The choice of navigation course is determined primarily by the armament to be used. For an airborne fire control system, the navigation course just prior to firing the armament is of greatest interest. When the weapons used are guns, a large number of rounds must be fired for an appreciable period of time for a high probability of kill. A lead-pursuit course represents the best choice since it enables the guns to be trained on the target for the greatest length of time. In the case of rocket armament, the collision course represents a good choice since the probability of kill per projectile is large, and a fairly wide rocket dispersion pattern is attainable. A proportional navigation course is best suited for firing guided missiles. For an assumed system, the guided missile armament may be an accurate, small-warhead type. The missile, in this case, must be launched to actually collide with the target. It is known that a pursuit-type course demands high lateral acceleration of the missile in the near

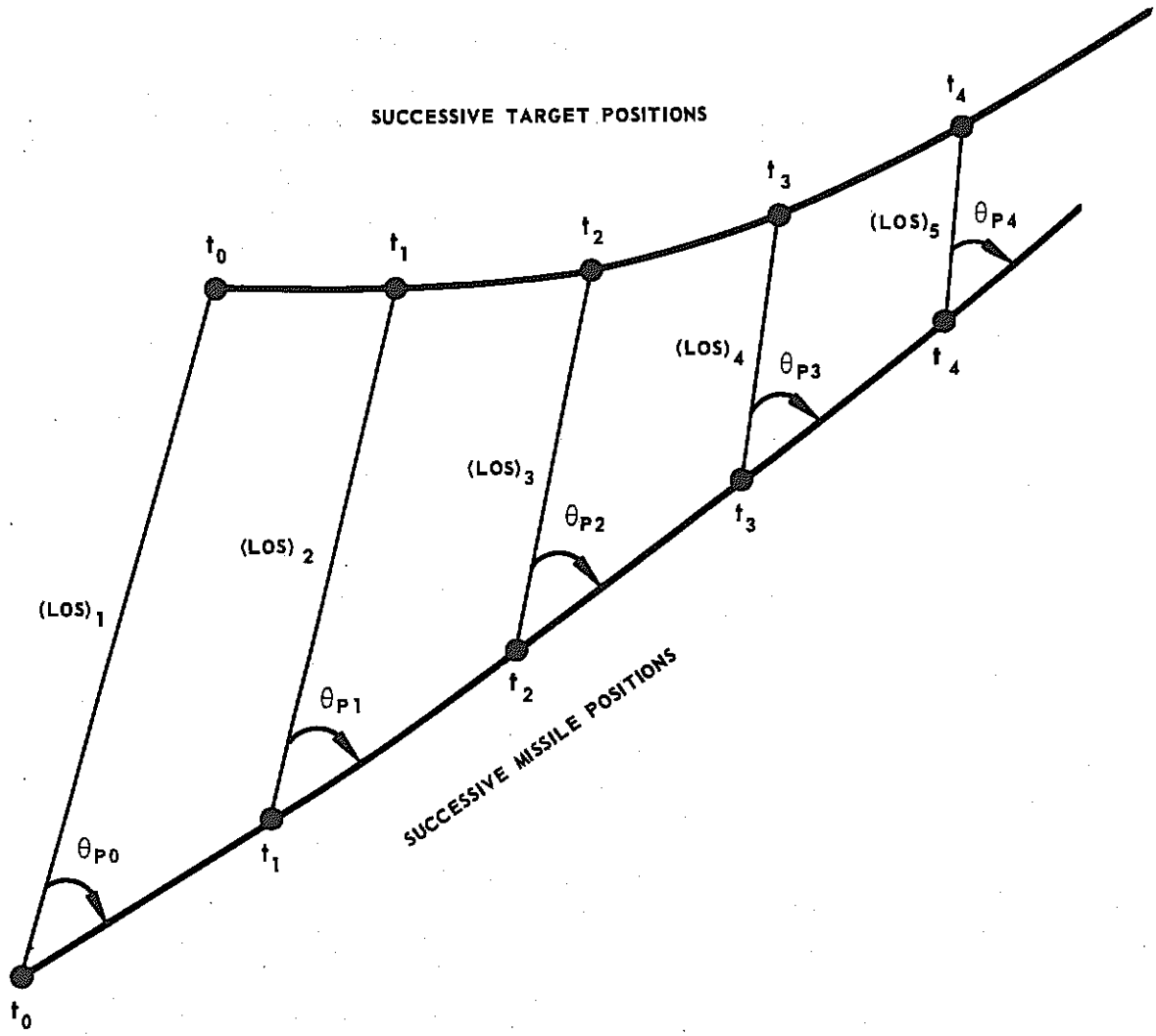

FIGURE 5-7. GEOMETRY OF A PROPORTIONAL NAVIGATION COURSE

vicinity of collision with the target. If the acceleration required is greater than can be produced by the missile, large misses may result. Even if the missile does develop the required lateral acceleration, the effect of noise in the system may still saturate the missile control system and thereby create large misses. A missile collision course does not require high accelerations at any time along the trajectory, provided that the missile has a speed and lateral acceleration advantage over the bomber target. This condition normally exists and makes the collision-type course advantageous for use with missile armament. In order to attain a missile collision course, the interceptor should be flown on a near

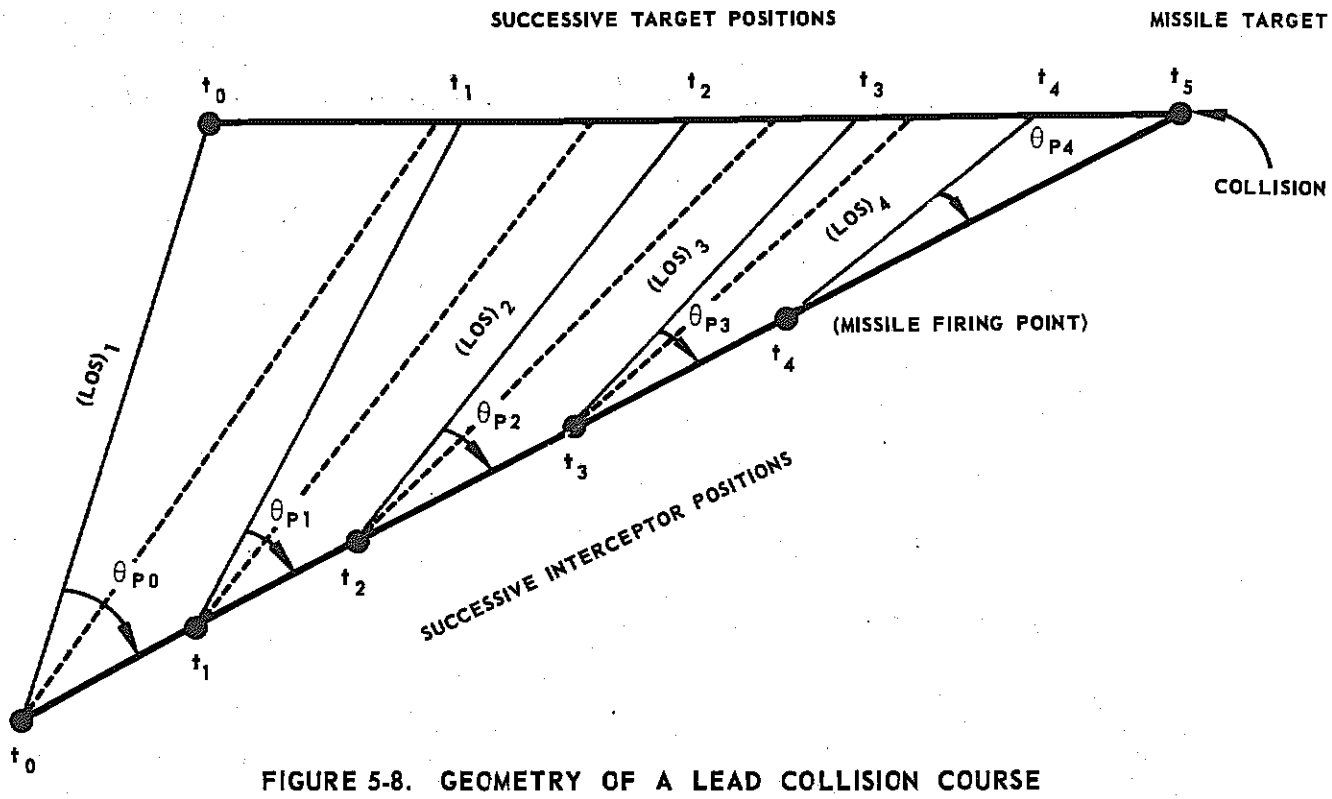

FIGURE 5-8. GEOMETRY OF A LEAD COLLISION COURSE

missile collision course at the time of launch. A missile collision course and an interceptor collision course differ since the missile normally has a speed advantage over the interceptor and is launched from the interceptor. Differences in the magnitudes of the missile and interceptor velocity vectors require that their directions differ in the collision course geometry. This situation can readily be seen in Figure 5-9, where the missile and interceptor velocity vectors differ, but the target velocity vector remains constant. In the figure, a 2:1 missile speed advantage over the target is assumed. If launched from the same point, the missile prediction angle θ_{pm} is clearly less than the interceptor bearing θ_{pi}. In a lead collision course, if the firing point is t_o, the interceptor must have a bearing θ_{pm}, which is clearly <u>not</u> an interceptor constant bearing course - hence, on such a course, the interceptor bearing must vary.

Proportional navigation offers a system in which the missile (or interceptor) does not require range information or particular space

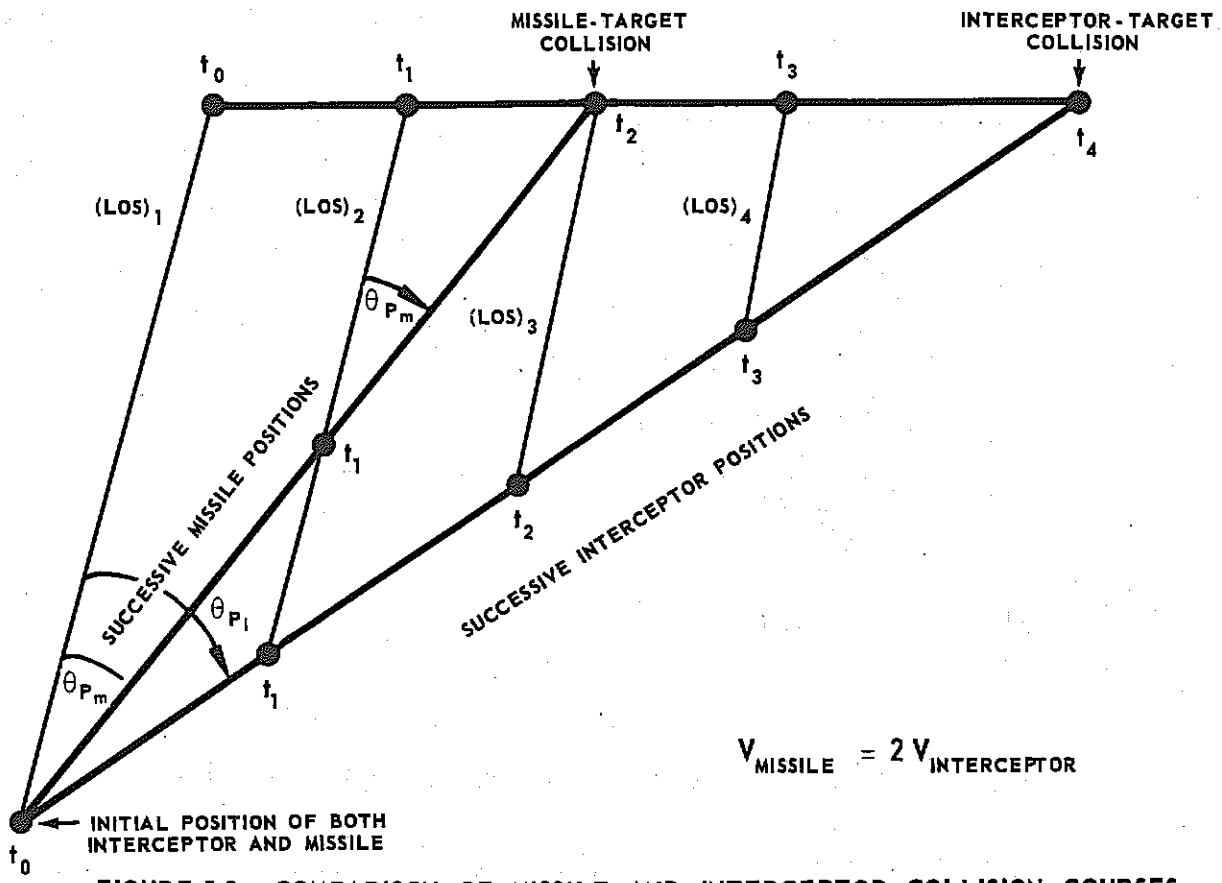

FIGURE 5-9. COMPARISON OF MISSILE AND INTERCEPTOR COLLISION COURSES

reference, but maneuvers in response to the time rate of rotation of the LOS. Mathematically, this condition may be represented by

$$\dot{\gamma} = \lambda \dot{\sigma} \tag{5-30}$$

where γ is the angle that the velocity vector makes with a space reference, σ is the angle that the LOS makes with the reference, and λ is the navigation constant. In an idealized collision course, the LOS does not rotate and, hence, $\dot{\sigma}$ is equal to zero. Consequently $\dot{\gamma}$ equals zero, which means that the missile (or interceptor) does not maneuver and the trajectory is a straight line -- which would eventually result in collision if the various vectors remained constant. If there is deviation from a collision course at any time, the LOS rotates and the interceptor is accelerated laterally so as to reduce $\dot{\sigma}$. In a pursuit course γ equals σ , and λ equals 1. A pure collision course requires that $\dot{\sigma}$ equal zero. In order for λ to

approach infinity, while $\dot{\gamma}$ remains constant, $\dot{\sigma}$ must approach zero. Thus, although a constant bearing course never requires the missile (or interceptor) to execute lateral accelerations greater than those of the target, theoretically it requires infinite gain in the guidance system. Conversely, the pursuit course employs a simple guidance system but always ends in a tail chase that requires high lateral accelerations near the termination of the pursuit. If the interceptor flies a pursuit course and launches its armament well before high lateral accelerations are required, the missiles will be launched on a near missile pursuit course rather than on the desired missile collision course, thus introducing launching error and reducing the probability of target kill. It can be assumed from the preceding arguments that a missile system would employ a proportional navigation system. The proportional navigation system represents a compromise between the collision course requiring very high gain, and the pursuit course requiring unity gain. In proportional navigation, it is possible to adjust the guidance system gain, λ, in such a way that the maximum lateral acceleration requirement is readily met.

SECTION 6 — FIRE CONTROL COMPUTING SYSTEMS

The computing system relates the tracking and steering portions of the fire control system by receiving tracking and ballistic data and furnishing the interceptor control system and missile auxiliaries with required signal inputs. The computer provides the computed prediction angle and navigates the interceptor on the basis of that information. A general block diagram of the over-all computing system and related blocks appears in Figure 5-10. The antenna tracking loop accepts an input which is the direction of the LOS in inertial space, and develops outputs which include the orientation and angular velocity of the scan axis. The computer then develops the control signals from which the aircraft navigation system is driven. Note that although errors which occur in the computer are not checked by the tracking loop, computer dynamics do not affect the tracking. In the system shown in Figure 5-10 the target is tracked, the prediction angle is computed from the tracking data, and the missiles are aimed. Other arrangements than that shown in Figure 5-10 may be used, but the arrangement shown is commonly employed and will, therefore, be described. The computer system could be mechanized in other ways; for example, it could include the whole fire control system in an over-all tracking loop. The tracking and navigation functional loops could then be separated within the computer. Alternatively, the computing system could compute angular rate of the LOS based on the prediction angle, following which the autopilot would interrogate the tracking loop

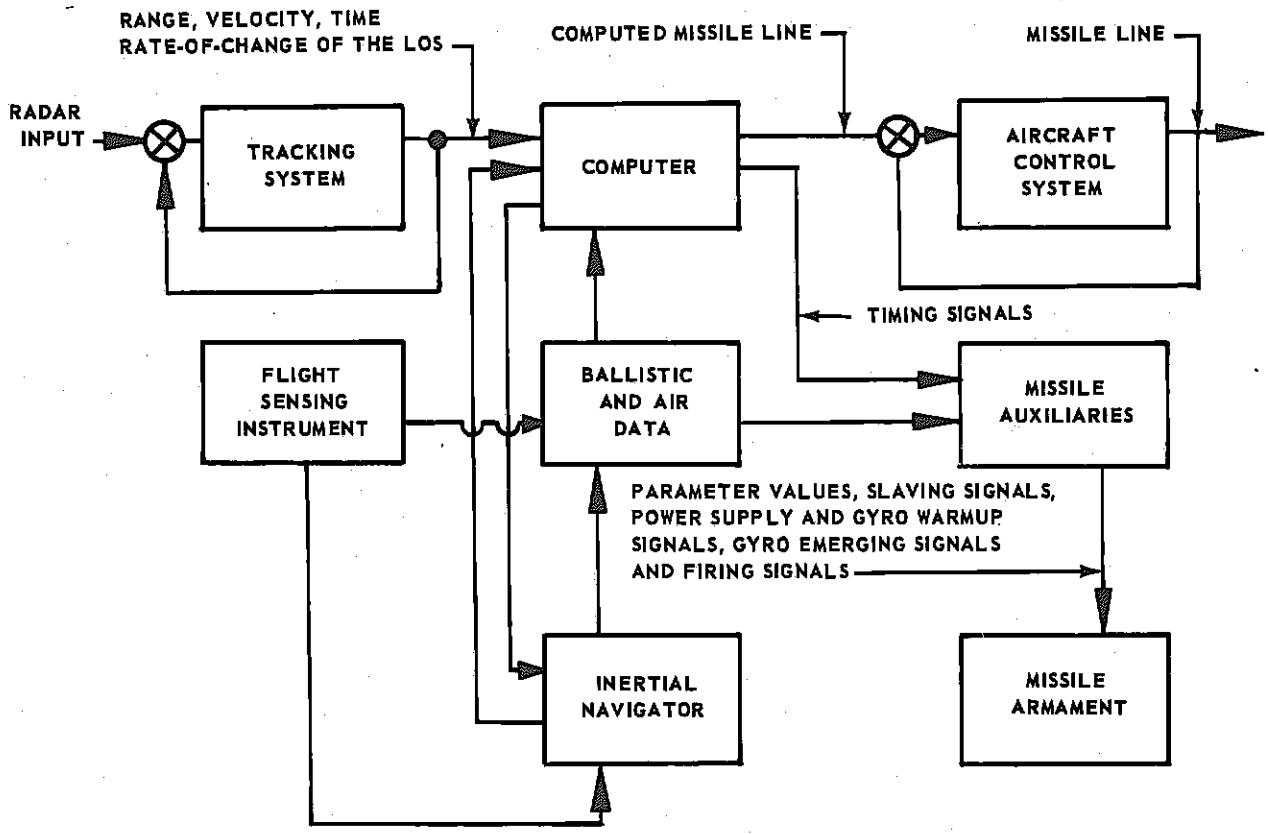

FIGURE 5-10. COMPUTING SYSTEM AND RELATED BLOCKS

to determine the correctness of the prediction values. Various hybrids of these two basic types of computing systems can also be developed.

In the illustrated system, the computer derives the prediction angle given in Equation 5-29. Some of the inputs to the computer include: the angular velocity of the scan axis, gravity, and interceptor velocity. These inputs and auxiliary inputs such as range and air density are operated on and result in the computed prediction angle at the output.

Equations for the design of the lead computer have already been derived in this chapter. Equation 5-5 shows the future range to be expressed as a series of vectors involving the present range, present target velocity (extrapolated over the time of the flight), and the double

integral of target acceleration over the time of flight. If the double integral of Equation 5-5 is replaced by an infinite series in powers of the time of flight, the future range is expressible as an infinite series of vectors. Thus,

$$\bar{R}_f = \bar{R}_o + \bar{v}_o t_f + \bar{a}_o \frac{t_f^2}{2} + \cdots\cdots \tag{5-31}$$

where

$\bar{R}_o$ = target range at firing

$\bar{v}_o$ = target velocity at firing

$\bar{a}_o$ = target acceleration at firing

If an approximation to the series is made by eliminating all terms but the first,

$$\bar{R}_f = \bar{R}_o \tag{5-32}$$

Equation 5-32 is called the zero order approximation to the future range, and leads to a zero order lead computation. If the approximation includes two terms such as

$$\bar{R}_f = \bar{R}_o + \bar{v}_o t_f + \frac{\bar{a}_o t_f^2}{2} \tag{5-33}$$

a first order lead computation results. A second order lead computation results when

$$\bar{R}_f = \bar{R}_o + \bar{v}_o t_f + \frac{\bar{a}_o t_f^2}{2} \tag{5-34}$$

The angular velocity and acceleration of the LOS resulting from target motion are given by

$$\bar{\omega}_i = \frac{\bar{r}_e \times \bar{v}_o}{R_o} \tag{5-35}$$

where $\overline{\omega}_i$ is the angular velocity of the present LOS with respect to inertial space, $\overline{r}_e$ is the unit vector along the present LOS, $\overline{v}_o$ is the target velocity at launch, and R_o is the target range at launch.

$$\dot{\overline{\omega}}_i = \frac{\overline{r}_e \times \overline{a}_o}{R_o} + \frac{\dot{\overline{r}}_e \times \overline{v}_o}{R_o} - \overline{r}_e \times \overline{v}_o \frac{\dot{R}_o}{R_o^2} \tag{5-36}$$

Substituting Equations 5-34, -35, and -36 into the basic equation for lead, Equation 5-8 yields

$$\begin{aligned}
\overline{\theta}_\ell &= \overline{r}_\ell \times \overline{r}_f = \overline{r}_e \times \frac{\overline{R}_F}{R_F} \\
&= \frac{\overline{r}_e R_o}{R_F} \times \left(\frac{\overline{R}_o}{R_o} + \frac{v_o t_f}{R_o} + \frac{\overline{a}_o t_f^2}{R_o^2} \right) \\
&= \frac{R_o}{R_F} \left\{ \overline{\omega}_i t_f + \frac{t_f^2}{2} \left[\dot{\overline{\omega}}_i - \frac{\dot{\overline{r}}_e \times \overline{v}_o}{R_o} + \overline{r}_e \times \overline{v}_o \frac{\dot{R}_o}{R_o^2} \right] \right\}
\end{aligned} \tag{5-37}$$

Equation 5-37 is the lead angle for a second order computation. The corresponding equation for a first order computation is

$$\overline{\theta}_e = \frac{R_o}{R_F} \overline{\omega}_i t_f \tag{5-38}$$

Note that average missile velocity is

$$v_{avg} = \frac{R_F}{t_f} \tag{5-39}$$

so that Equation 5-37 can be written

$$\overline{\theta}_\ell = \frac{R_o \overline{\omega}_i}{v_{avg}} \tag{5-40}$$

Note that the only quantities needed for a lead computer yielding a first order solution are the vector angular velocity of the LOS, the magnitude of the present range, and the average magnitude of the missile velocity. These quantities are either known already or are readily measurable and determined by the fire control system radar.

The quantities measured should be determined with respect to the coordinate system in which the fire control problem is expressed. In practice, the earth and associated air mass coordinates are assumed to be stationary for the short time that the missile is in flight, and angular velocity relative to inertial space can, therefore, be measured. The angular velocity of the LOS can be measured as the rate of change of the angle of the scan axis relative to a gyro-maintained reference direction. Before this information can be used for interceptor control, it must be referred to the interceptor frame of reference.

Although computers using higher order series than the first may appear to be desirable, there is a limit upon the accuracy of measurement of acceleration and other quantities needed for the higher order computations. This limit is set primarily by tracking noise. In order to measure rate of change of the scan axis (angular velocity), time differentiation must be employed. Differentiation emphasizes noise by accentuating the high frequency terms. Unless target accelerations are appreciably greater than the differentiated noise (so that the signal-to-noise ratio is large), an attempt to take target acceleration into account is not warranted. It is therefore assumed for the proportional navigation system that the targets are traveling at constant velocity. Deviations in either target or interceptor velocity vectors would then be corrected in a point-by-point manner. At any instant of time, however, a first order equation is being solved.

In addition to target motion, errors in the prediction angle are introduced by sources which produce curvature of the projectile trajectory. These forces include gravity, aerodynamic lift, drift, drag, thrust, etc. When the interceptor carries guided missile armament these effects are of consequence only during the unguided portion of missile flight. A homing missile is normally unguided during its boost period, which is a fraction of the total flight time. It will be shown that the magnitude of the tracking error at the instant the missile begins to guide (i.e., when the missile antenna gyro is uncaged) is within the allowable rms error, providing the missile time of flight is sufficiently long. In this case, a curvature correction computation is unnecessary. Errors due to the listed

forces can be reduced by including fixed corrections for principal terms such as gravity. Since the length of time of boost is known, the curvature due to gravity can be predicted with reasonable accuracy, and the required correction can be programmed into the computer memory. It can similarly be shown that the magnitude of the error resulting from jump at launch is not great enough to warrant the inclusion of a jump correction computer. When the aircraft and missile velocity vectors are not aligned, the missile tends to jump from the weapon line toward the airspeed vector through an angle called the velocity jump. The two velocity vectors are close in most cases, and the time of unguided flight of the missiles is short so that the miss caused by the jump is within the rms allowable tolerance. A fixed correction for jump may be included, based on an average expected misalignment of the airspeed vector and the initial missile velocity vector.

As a result of noise in the measured angular rate and other input data, a degree of smoothing is required to improve the signal-to-noise ratio and to reduce saturation effects, particularly in the aircraft control system. If smoothing (filtering) is carried out in coordinates that are not stabilized, the roll, pitch, and yaw of the interceptor introduce additional errors in the computer output. Smoothing, therefore, must take place in stabilized coordinates before being transformed into aircraft coordinates for control purposes.

The effect of computing system design on various navigation courses will be investigated. As previously indicated, a straight-line course is suited for rockets and missiles that are released in nearly instantaneous salvos. Assuming that the target velocity vector remains constant, the course then flown by the interceptor may be such that at the time of launching the interceptor is flying a missile collision course (i.e., an interceptor "lead collision" course). As described earlier, a lead collision course differs from a pure collision course by an angle which depends on the increase (after firing) of the missile velocity over the interceptor velocity. Thus, while the angle between the LOS and the interceptor velocity vector remains constant throughout a pure collision course, the lead angle continually changes in the lead collision course. This results in a single point, in a lead collision course, where a firing solution is possible. A lead pursuit course requires little or no vectoring from the ground (GCI) station, since the firing point is not critical. A lead or pure collision course, however, requires ground vectoring since the firing range is critical. The lead or pure collision course has

a desirable characteristic in that the armament is launched at a point which is optimum for armament effectiveness and interceptor safety.

For the equations derived in this chapter, it has been assumed that the available input data are noise free. In a practical case the input information and resulting output information from the computer are noisy. The effect of noise on the over-all system behavior and methods for discriminating against it are discussed in a later chapter.

SECTION 7 — ATTACK COMPUTER REQUIREMENTS FOR A PROPOSED SYSTEM

The attack computer must provide the horizontal and vertical signal for control of the aircraft and launching data for the missiles and missile auxiliaries. The attack computer calculates a course such that: (a) the missile will have the time of flight calculated by the time-of-flight computer, and (b) the guidance system in the missile sees zero heading error at the time it takes over.

The type of computation recommended for a proposed system is one that makes straight-line extrapolation of present velocity. Thus, if the target maneuvers, the fighter also must maneuver in order to continue to satisfy the linear extrapolation requirements.

It is assumed that other computing equipment, not described here, will bring the aircraft into the appropriate vicinity of the target aircraft. It is also assumed that the altitude of the interceptor is approximately the altitude of the target. If this latter assumption is not valid, a climbing or diving attack is required. For a proposed system, it is assumed that the attack computer actually consists of two computers, one for horizontal control of the aircraft, the other for vertical control. Mechanization for only the horizontal control computer will be described. When it is within the limits of computation, the attack computer takes over the solution of the attack problem from the other computational units.

At the proper moment prior to missile release, the attack computer sends a "warm-up" signal to the missile hydraulic system and arms the firing circuit in the missiles. Missile arming requires that the radar be locked onto a target. Afterwards, the computer provides steering information necessary to fire the missile at a range yielding the correct flight time and giving zero heading error at the instant of launch. The elevation channel of the attack computer determines the correct angle for

the interceptor to turn through if the target and interceptor are not at the same altitude at the time of missile launch. For this situation, the interceptor performs a climbing or diving attack as required. For the climb-up attack it is important that sufficient time be allowed for final azimuth steering after the climb, and also that the angle demanded for climbing be not so great as to cause the aircraft to stall. The diving attack is even more difficult to accomplish because the missile requires a minimum aerodynamic range to compensate for launching errors. Because there is increased drag on the missile and interceptor at low altitudes, there is a maximum effective missile range. Minimum aerodynamic range and maximum effective range set boundaries on the minimum and maximum flight times of the missile. If the total distance from interceptor to ground to missile is less than the distance from interceptor to target to missile, it is possible for the missile to lock onto the ground. Velocity tracking systems in both the missile and the aircraft radars should be capable of discriminating against this effect by use of ground-clutter rejection circuitry.

The minimum and maximum range boundaries affect the mechanization of the computer. At the appropriate intervals prior to launch, the missile gyros must be up to speed and the servos energized. Proper signals must be sent to the antenna servos to lock the missile antenna correctly in the azimuth and elevation directions as indicated by the interceptor tracking radar. If the missile gyros are uncaged after launch, the target angle seen by the missile will be different from that seen by the interceptor tracking system at launch. For this situation, the angle difference must be determined by computation and the missile antenna "look" angle pre-adjusted. At or near the computed launch time the appropriate missiles must be fired according to schedule. After the missiles have been launched, the computer should turn the fighter toward the direction from which the target has been coming so that the interceptor will clear the target debris. The radius of curvature of this turn should not be too great when using semiactive missiles since the interceptor's radar antenna must continue tracking and illuminating the target until target kill. After missile launch, the interceptor attack computer must send steering information to put the fighter into a controlled turn and roll. After a computed time-until-missile-impact, the attack computer terminates the controlled turn and relinquishes aircraft control to the other computing equipment. As indicated, the design of an attack computer for firing guided missiles is much simpler than the computer design necessary for firing rockets. For missile launching two principal computed quantities are needed: first, the missile must be launched at an appropriate

range so that there is sufficient time for the flight to allow the missile to correct launching errors and yet not exceed the maximum permissible aerodynamic and radar ranges; second, for reasons previously given, the missile should be fired close to a missile collision course.

SECTION 8 — DERIVATION OF ATTACK COMPUTER EQUATIONS

This section derives the attack computer equations for an illustrative system. It is an example of the general procedure discussed previously in this chapter. It will be assumed that there is a finite time between the launch of the missiles and the uncaging of the missile gyros (the interval termed the "boost period"). During boost the missile computation equipment cannot operate because the missile gyros remain caged. The attack computer equations must provide steering and launching information so that the fighter will fly a straight line course to the proper launching point and launch the missile in such a way that when the gyros are uncaged the missile will have a zero heading error. A vector diagram of the attack computer equations appears in Figure 5-11. The equations which describe the vector diagram are

$$\bar{R} + \bar{v}_t T = \bar{v}_a (T - t_f) + \bar{v}_a t_b + \bar{d} + (\bar{v}_a + \bar{v}_m)(t_f - t_b) + \bar{M}$$

$$= \bar{v}_a T + \left[\bar{v}_m (t_f - t_b) + \bar{d}\right] + \bar{M} \qquad (5\text{-}41)$$

where the following symbols are used:

- T = time from present until missile collision
- t_f = time of flight of the missile
- t_b = time interval between the launching of the missile and uncaging of the missile gyros, i.e., "boost time"
- $\bar{v}_a$ = present velocity of the interceptor
- $\bar{v}_t$ = present velocity of the target
- $\bar{R}$ = present vector range to the bomber
- $\bar{d}$ = vector distance the missile actually travels relative to the interceptor in the time interval t_b
- $\bar{d}_c$ = computed vector distance the missile travels relative to the interceptor in time t_b
- $\bar{v}_m$ = the vector velocity of the missile relative to the interceptor at the end of boost

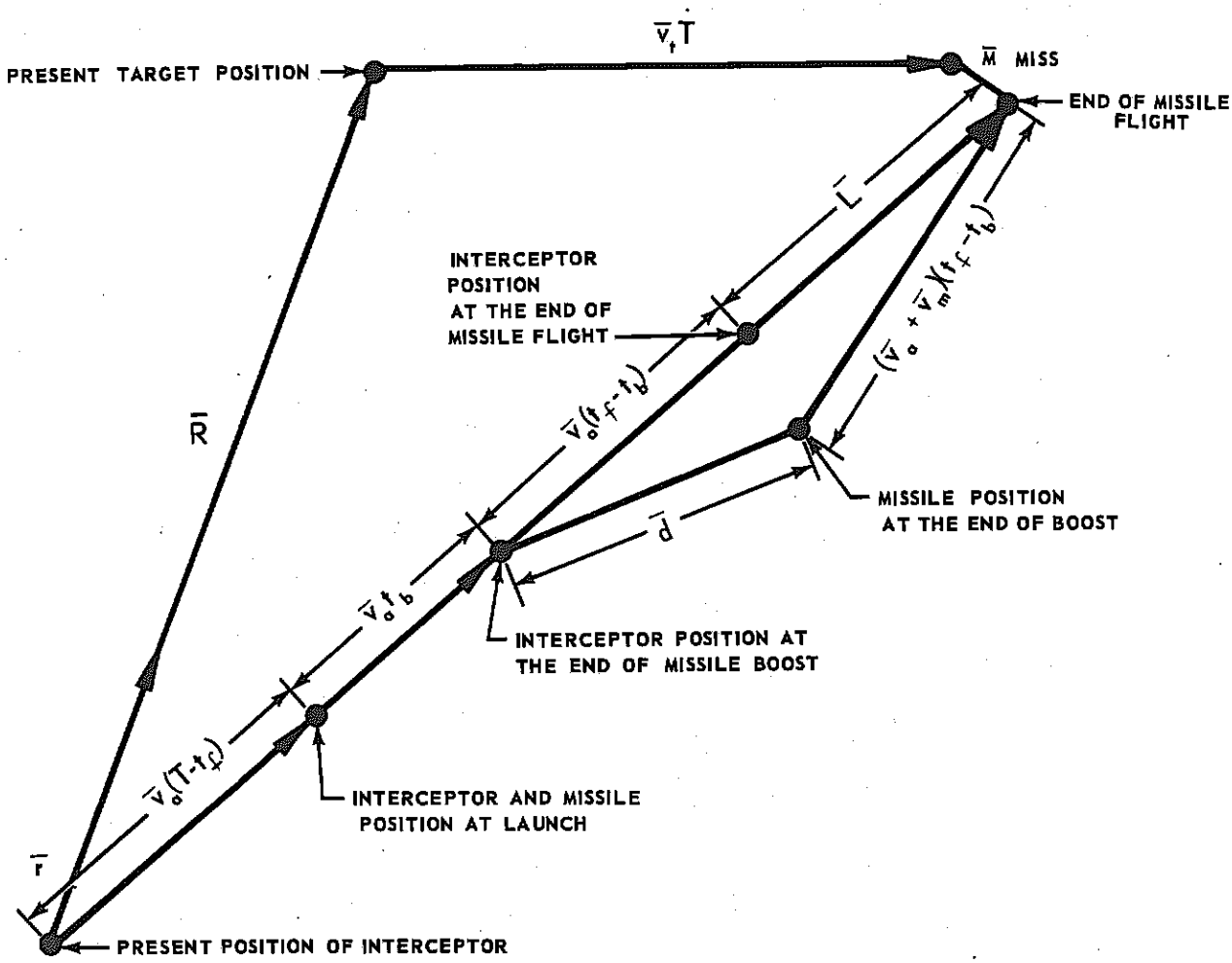

FIGURE 5-11. COMPUTER EQUATION VECTOR DIAGRAM

$\bar{v}_{mc}$ = the computed value of $\bar{v}_m$

$\bar{M}$ = vector miss as seen by the missile at the end of boost

$\bar{L}$ = distance the missile travels relative to the interceptor in time t_f

Similarly,

$$\bar{R} + \bar{v}_t T = \bar{v}_a T + \bar{L} + \bar{M} \tag{5-42}$$

Equating Equations 5-42 and 5-41 shows that

$$\bar{L} = \bar{v}_m (t_f - t_b) + \bar{d} \tag{5-43}$$

Equation 5-43 is immediately evident from the vector diagram and can also be justified as follows.

Since $\bar{d}$ represents the relative travel of the missile during t_b, and $\bar{v}_m(t_f - t_b)$ the relative travel of the missile during $t_f - t_b$, then the total relative travel of the missile during the time t_f must be the sum of $\bar{d}$ and $\bar{v}_m\ (t_f - t_b)$. Equation 5-42 can be solved for the miss, or

$$\bar{M} = \bar{R} + (\bar{v}_t - \bar{v}_a)T - \bar{L} \tag{5-44}$$

The attack computer must determine the interceptor velocity vector $\bar{v}_a$ required to make the miss $\bar{M}$ equal to zero, when $\bar{L}$ is set at some prescribed value. By definition,

$$\bar{v}_t - \bar{v}_a = \dot{\bar{R}} = \frac{d}{dt}(\bar{r}R) = \bar{r}\frac{dR}{dt} + R\frac{d\bar{r}}{dt} \tag{5-45}$$

where $\bar{r}$ is a unit vector directed along $\bar{R}$. But

$$\frac{d\bar{r}}{dt} = \bar{\omega}_t \times \bar{r} \tag{5-46}$$

where $\bar{\omega}_t$ is the angular velocity of the LOS measured in interceptor coordinates. The coordinate system used is shown in Figure 5-12,

where

$\bar{L}$ = a unit vector directed along the interceptor longitudinal axis
$\bar{J}$ = a unit vector normal to $\bar{c}$ and in the plane of the wings
$\bar{k}$ = a unit vector normal to $\bar{c}$ and $\bar{j}$
$\bar{r}$ = a unit vector directed along the radar scan axis
$\bar{a}$ = a unit vector normal to $\bar{r}$ and in the plane formed by $\bar{r}$ and $\bar{k}$
$\bar{e}$ = a unit vector normal to $\bar{r}$ and $\bar{a}$

The coordinates $\bar{i}$, $\bar{j}$, and $\bar{k}$, are fixed so that $\bar{i}$ and $\bar{j}$ vectors lie in the plane of the wings of the aircraft and the vector velocity of the aircraft, $\bar{V}_a$, lies along the $\bar{i}$ direction. The vector $\bar{k}$ is normal to these two

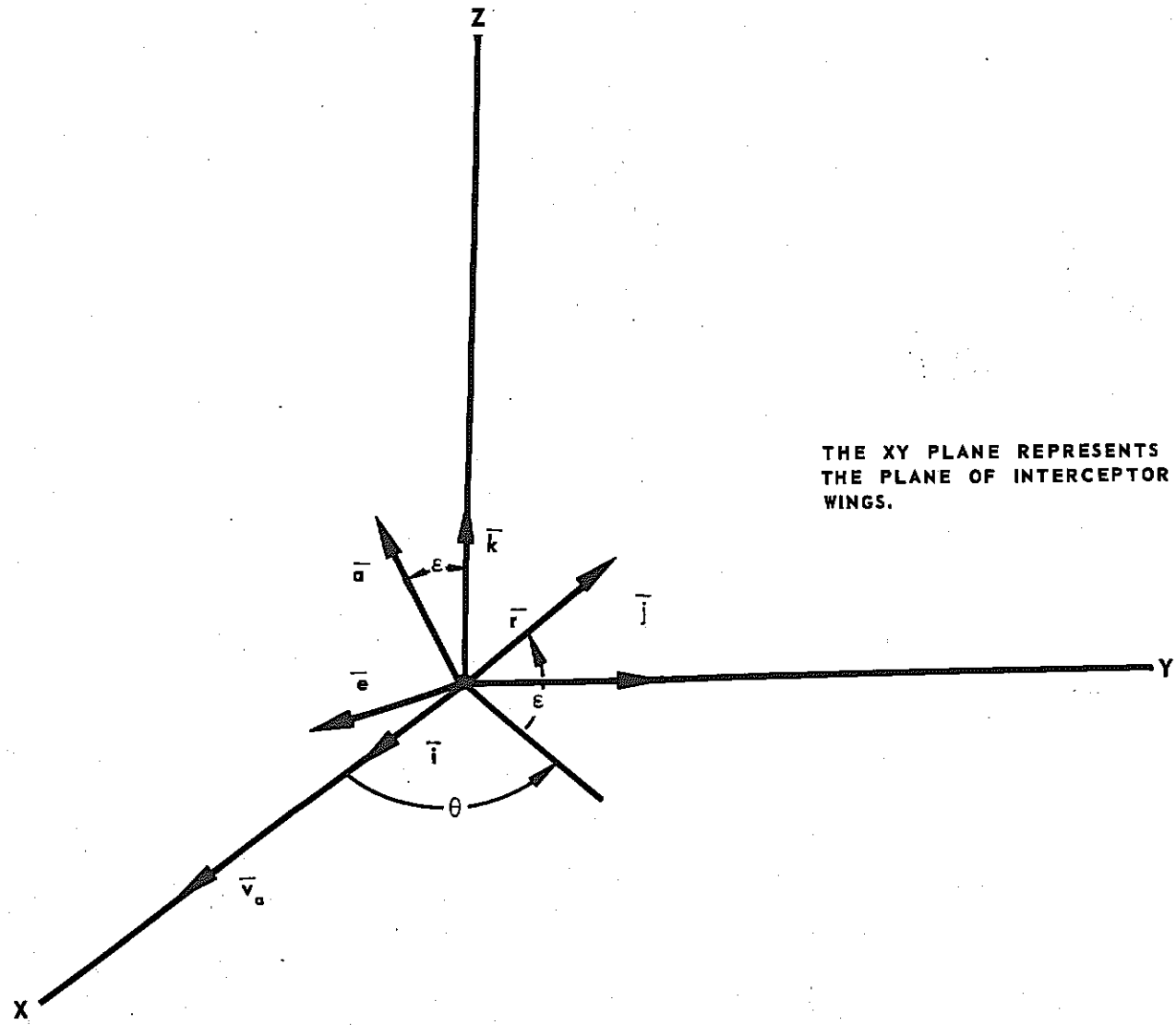

FIGURE 5-12. INTERCEPTOR AND RADAR COORDINATE SYSTEM

vectors. The scan axis is assumed to be along the LOS. The scan axis forms a plane with the vector $\bar{k}$.

$\bar{r}$ = a unit vector directed along the scan axis
$\bar{a}$ = a unit vector directed along the azimuth axis in the radar coordinate system
$\bar{e}$ = a unit vector directed along the elevation axis in radar coordinates

Unit vector $\bar{i}$ is directed along the roll axis of the interceptor, $\bar{j}$ is directed along the pitch axis of the interceptor, and $\bar{k}$ is directed along the yaw axis of the interceptor.

The $\bar{i}$, $\bar{j}$, and $\bar{k}$ vectors define the interceptor coordinate system, and the $\bar{r}$, $\bar{a}$, and $\bar{e}$ vectors define the radar coordinate system. The plane defined by $\bar{r}$, $\bar{k}$, and $\bar{a}$ makes an angle θ with respect to the velocity vector v_a (the vector $\bar{i}$). The azimuth axis makes an angle ϵ with $\bar{k}$ in the plane defined by the azimuth axis and the scan axis. Similarly, the vector $\bar{r}$ makes an angle ϵ with the plane of the wings.

Since the angular velocity vector $\bar{\omega}_t$ is normal to $\bar{r}$, it must be in the plane defined by $\bar{a}$ and $\bar{e}$. Hence, in the radar coordinate system, the angular velocity vector of the LOS can be written

$$\bar{\omega}_t = \bar{e}\omega_e + \bar{a}\omega_a \tag{5-47}$$

where ω_e is the component of the angular velocity about the elevation axis, and ω_a is the component of the angular velocity about the azimuth axis.

Substituting Equations 5-45 and 5-46 in 5-47 yields

$$\bar{v}_t - \bar{v}_a = \bar{r}\dot{R} + R(\omega_e \bar{e} \times \bar{r} + \omega_a \bar{a} \times \bar{r})$$

$$= \bar{r}\dot{R} + \bar{a}R\omega_e - \bar{e}R\omega_a \tag{5-48}$$

Substituting Equation 5-48 into 5-44 yields

$$\bar{M} = \bar{r}(R + \dot{R}T) + \bar{a}R\omega_e T - \bar{e}R\omega_a T - \bar{L} \tag{5-49}$$

The vector miss $\bar{M}$ can now be resolved into components along $\bar{r}$, $\bar{a}$, and $\bar{e}$, yielding

$$\bar{M}\cdot\bar{r} = R + \dot{R}T - \bar{L}\cdot\bar{r} \tag{5-50}$$

$$\bar{M}\cdot\bar{a} = R\omega_e T - \bar{L}\cdot\bar{a} \tag{5-50A}$$

$$\overline{M}\cdot\overline{e} = R\omega_a T - \overline{L}\cdot\overline{e} \tag{5-50B}$$

If trajectory curvature and jump effects are neglected, the distance $\overline{L}$ is along the same direction as $\overline{v}_a$, the interceptor velocity vector. Except for the angle of attack, the interceptor velocity vector and the longitudinal axis of the interceptor are aligned. The missiles are launched parallel to the longitudinal axis of the interceptor, hence, except for the angle of attack error, $\overline{L}$ again lies along the vector $\overline{v}_a$. The aircraft must assume an angle of attack in order to produce any lateral acceleration. Even in uniform velocity flight, there is an angle of attack developed to overcome the effects of gravity and wind forces. If these effects are neglected, the components of $\overline{L} \cong \overline{i}L$ along the various axes are

$$\overline{L}\cdot\overline{r} = L\cos\theta\cos\epsilon \tag{5-51}$$

$$\overline{L}\cdot\overline{a} = -L\sin\epsilon\cos\theta \tag{5-51A}$$

$$\overline{L}\cdot\overline{e} = L\sin\theta \tag{5-51B}$$

Equations 5-51, -51A, and -51B neglect the effects of jump and curvature. Substituting Equations 5-51, -51A, and -51B in Equations 5-50, -50A, and -50B yields

$$\overline{M}\cdot\overline{r} = R + \dot{R}T - L\cos\theta\cos\epsilon \tag{5-52}$$

$$\overline{M}\cdot\overline{a} = R\omega_e T + L\sin\epsilon\cos\theta \tag{5-52A}$$

$$\overline{M}\cdot\overline{e} = R\omega_a T - L\sin\theta \tag{5-52B}$$

The time T from the present until the missile hits the target is defined such that the component of miss along the scan axis is zero, i.e., such that

$$\overline{M}\cdot\overline{r} = 0 \tag{5-53}$$

The angles through which the aircraft velocity vector $\overline{v}_a$ must be turned so that the other components of the miss will be zero, can be determined by dividing the last two equations in Equations 5-52, -52A, and -52B by the space distance the missile will travel from now until it hits.

The missile travels part of this distance while still in the interceptor. The total distance is approximately $v_a T + L$, where it is assumed that L is along $\bar{v}_a$. Letting α_e and α_a be the angles through which the velocity vector must turn, it follows that

$$0 = R + \dot{R}T - L \cos\theta \cos\epsilon \tag{5-54}$$

$$\alpha_e \cong \frac{\bar{M}\cdot\bar{a}}{v_a T + L} = \frac{R\omega_e T + L \sin\epsilon \cos\theta}{v_a T + L} \tag{5-54A}$$

$$\alpha_a \cong \frac{\bar{M}\cdot\bar{e}}{v_a T + L} = \frac{R\omega_a T - L \sin\theta}{v_a T + L} \tag{5-54B}$$

The largest angle which can separate the aircraft velocity vector and the radar scan axis is the angle of attack α plus the "look" angle of the radar antenna. The distance $v_a T + L$ differs from R by the cosine of this angle so that $v_a T + L$ is approximately equal to R, especially for small look angles. In Equations 5-54, -54A, and -54B, the distance $v_a T + L$ will be replaced by R. This change does not affect the absolute accuracy of this system because the control signals developed are in a direction to null these angles. Thus, the constant that corresponds to the range which transforms miss distance normal to the scan axis into angular deflections is simply a sensitivity factor and affects the slope of the control characteristic rather than its crossover point. The gain of the servo loop in which these equations appear as part of the loop transfer function is therefore changed, but the nulling point or crossover is not. Hence, without loss in accuracy Equations 5-54, -54A, and -54B can be written as follows:

$$0 = R + \dot{R}T - L \cos\theta \cos\epsilon \tag{5-55}$$

$$\alpha_e = \omega_e T + \frac{L}{R} \sin\epsilon \cos\theta \tag{5-55A}$$

$$\alpha_a = \omega_a T - \frac{L}{R} \sin\theta \tag{5-55B}$$

The angles α_e and α_a are measured with respect to the antenna scan axis and, if there were no need for smoothing, these would be satisfactory steering signals. Unfortunately, the measured quantities ω_a and ω_e are noisy and must be smoothed. If the smoothing time constants are comparable to or greater than the time required for the aircraft to roll through an appreciable angle, then crosstalk will be introduced by the time lag resulting from the smoothing. This tends not only to add error, but also introduces control stability problems because of high roll rates. For example, if the aircraft suddenly banks to turn, the $\bar{e}$ and $\bar{a}$ vectors will rotate, but because of smoothing, the information out of the computer will still be in terms of the original $\bar{a}$ and $\bar{e}$ vectors just before banking. This problem may be solved by resolving the angles α_e and α_a through a bank-angle resolver in order to obtain angles in the vertical and horizontal planes. Mathematically this amounts to rotating the coordinate system in which α_e and α_a are measured through an angle ψ to a new coordinate system which lies in a plane normal to the roll axis, $\bar{i}$, of the aircraft. The horizontal coordinate lies in a plane parallel to the earth and the vertical coordinate lies along a line through the center of the earth. This is an earth or inertial coordinate system and these coordinates are invariant with respect to bank or roll angle. The coordinate transformation is

$$\alpha_h = \alpha_a \cos \phi + \alpha_e \sin \phi \tag{5-56}$$

$$\alpha_v = -\alpha_a \sin \phi + \alpha_e \cos \phi \tag{5-56A}$$

Once these angles have been resolved into the vertical angle α_v and the horizontal angle α_h as shown in Equations 5-56 and -56A, the gravity drop correction may be added to the vertical component.

Before writing down the final equations and mechanizing the computer, it is important to estimate the error that will arise as a result of assumptions in the computation and errors attributable to measuring instrumentation. The initial missile errors at the time of uncaging must be calculated, since it is this angular error which the missile must correct during the missile flight time. The angular error is the miss divided by the space distance the missile has left to go at the time of uncaging. From Figure 5-11, this angular error is

$$\delta = \frac{M}{(v_a + v_m)(t_f - t_b)} \tag{5-57}$$

As indicated previously, the vector distance the missile travels relative to the interceptor in the interval t_b differs from the corresponding computed vector distance. Further, the vector velocity of the missile relative to the interceptor at the time the missile uncages differs from the velocity assumed by the attack computer. Let the total relative travel of the missile in time t_f as assumed by the attack computer be $\overline{L}'$. Then

$$\overline{L}' = \overline{d}_c + v'_m (t_f - t_b) \tag{5-58}$$

where v'_m is the missile velocity at the end of boost assumed by the computer. Adding and subtracting Equation 5-58 from Equation 5-41 yields

$$\overline{R} + \overline{v}_t T = \overline{v}_a T + \overline{v}_m (t_f - t_b) + \overline{d} + \overline{M} + \overline{d}_c + v'_m (t_f - t_b)$$
$$- \overline{d}_c - v'_m (t_f - t_b) \tag{5-59}$$

or

$$\overline{R} + (\overline{v}_t - \overline{v}_a)T - \overline{d}_c - \overline{v}'_m (t_f - t_b) = \overline{M} - (\overline{d}_c - \overline{d})$$
$$+ (\overline{v}_m - \overline{v}'_m)(t_f - t_b) \tag{5-59A}$$

From Fig 5-11, the computer solves the equation

$$\overline{R} + (\overline{v}_t - \overline{v}_a)T - \overline{L}' = \overline{M} = 0 \tag{5-60}$$

or

$$\overline{R} + (\overline{v}_t - \overline{v}_a)T - \overline{d}_c - v'_m (t_f - t_b) = 0 \tag{5-60A}$$

instead of the ideal equation

$$\overline{R} + (\overline{v}_t - \overline{v}_a)T - \overline{d}_c - \overline{v}'_m (t_f - t_b) - \overline{d} = 0 \tag{5-61}$$

Equation 5-61 can be derived by combining Equations 5-42 and 5-43 and setting $\overline{M} = 0$.

As a consequence of Equations 5-60 and -60A, Equation 5-59A may be set equal to zero and the resulting value for M substituted in Equation 5-57 yielding

$$\delta = \frac{d_c - d - (v_m - v'_m)(t_f - t_b)}{(v_a + v_m)(t_f - t_b)} \tag{5-62}$$

The magnitude of the terms d_c and $\dot{d}$ can be compared. The effect of gravity on trajectory curvature during the unguided portion of the missile flight (that is, the portion during boost before the missile guidance actually takes over) is

$$S'_b = \frac{1}{2} g t_b^2 = \frac{1}{2}(32)(2)^2 = 64 \text{ ft.} \tag{5-63}$$

where a boost time of 2 seconds is assumed for sake of definiteness.

At most, the launch and boost time is about 2 seconds, which, if the effect of gravity on the value assumed for d_c is neglected, yields a maximum error value of 64 feet for d_c. A reasonable estimate for the minimum value of the denominator of Equation 5-62 is about 10,000 feet, since at least this distance must be allowed for launching errors corrected by the missile. It therefore follows, that if $v'_m \cong v_m$,

$$\delta < \frac{64}{10{,}000} \cong 1/3^\circ$$

thus, a gravity or drag of approximately 1g will introduce a one-third degree initial launching error for the worst case. One-g drag will slow the missile down by a factor of 64 feet per second in two seconds so that the second term in Equation 5-62 introduces a maximum error on the order of

$$\delta < \frac{32 \times 2}{v_{a_{min}} + 5000} \cong \frac{64}{10{,}000} \cong 1/2^\circ$$

The effect of the magnitude of gravity and drag can be neglected, since a well-designed missile should be able to accept ± 5 degrees of initial launching error and compensate for it within 10,000 feet. The effects of gravity and drag can also change the direction of $\overline{d}$ and $\overline{v}_m$.

The curvature resulting from gravity drop depends on the missile characteristics. It can be shown that the angular correction is $k_g \frac{L}{gR}$, where k_g has values less than .1 for small air-to-air missiles. This correction may be added to the vertical angle α_v in Equations 5-56 and -56A, which then become

$$\alpha_h = \alpha_a \cos \phi + \alpha_e \sin \phi \tag{5-64}$$

$$\alpha_v = -\alpha_a \sin \phi + \alpha_e \cos \phi + k_g \frac{L}{gR} \tag{5-64A}$$

Changes in interceptor velocity may also cause errors in the direction of $\overline{d}_c$.

In this connection it should be pointed out that the changes in interceptor velocity have been neglected. With the velocity changes expected, it can be shown that the maximum error due to this source is less than one-half degree.

Another correction which must be taken into account at launch is the jump angle. As mentioned before, this angle is proportional to the initial angle between the missile launch line and the missile velocity vector. The change in heading of a missile as a result of jump can be shown to be

$$\Delta \theta_j = k_j \alpha_o \tag{5-65}$$

where α_o is the angle of attack at launch. The proportionality factor k_j is a function of airspeed and air density, and for small missiles may be on the order of 0.5. When this number is set into Equation 5-67 the correction term in the elevation angle (Equation 5-55) is then $\frac{0.5\alpha L}{R}$. Alpha (α) may vary by as much as $\pm$ten degrees and k_j by from 0.1 to

0.2, so that a change in $\Delta\theta_j$ on the order of $\pm 1\text{-}1/2$ degree can be expected.

When the jump correction is added to the elevation angle in Equations 5-55, -55A, and -55B, Equations 5-55, -55A, and -55B become

$$0 = R + \dot{R}T - L \cos\theta \cos\epsilon \tag{5-66}$$

$$\alpha_e = \omega_e T + \frac{L}{R} \sin\epsilon \cos\theta + k_j \alpha \frac{L}{R} \tag{5-66A}$$

$$\alpha_a = \omega_a T - \frac{L}{R} \sin\theta \tag{5-66B}$$

The final equations to be mechanized on the computer are, therefore, from Equations 5-64, -64A, and 5-66, -66A, and -66B

$$0 = R + \dot{R}T - L \cos\theta \cos\epsilon \tag{5-67}$$

$$\alpha_h = \alpha_a \cos\phi + \alpha_e \sin\phi \tag{5-67A}$$

$$\alpha_v = -\alpha_a \sin\phi + \alpha_e \cos\phi + k_g \frac{L}{R} \tag{5-67B}$$

where

$$\alpha_e = \omega_e T + \frac{L}{R}(\sin\epsilon \cos\theta + k_j \alpha) \tag{5-68}$$

$$\alpha_a = \omega_a T - \frac{L}{R} \sin\theta \tag{5-68A}$$

if all the preceding errors are assumed to be random (with zero mean) and independent of each other. The rms error is the square root of the sum of the errors and will be approximately $2\text{-}2\frac{1}{2}$ degrees. This number is well within the allowable maximum missile launching error of ± 5 degrees. It should be pointed out that all of the mentioned errors could, in theory, be eliminated by having the missile under guidance and control through boost. This would require that the missile antenna tracking loop not only track through the boost period, but also that aerodynamic control be included in the missile design. The standard control surfaces cannot be used because

the time constants and control parameters of the system are adjusted for velocities approximating that of the missile velocity after boost. The control surfaces will be virtually ineffective at lower speeds, particularly in the subsonic region. Missile direction control may be accomplished by the use of jet vanes which direct the flight of the missile during the boost period. The additional complication introduced by such a control system makes the effort seem not worthwhile - particularly in view of the relatively small errors introduced as a consequence of uncontrolled flight during boost. After the missile guidance system takes over control, no further correction of ballistic errors is required from the fire control system computer.

Another set of errors arises as a result of computer mechanization. The magnitude of this set of errors can be determined by differentiating Equations 5-66, -66A, and -66B with respect to the variable in question. The principal mechanization error is attributable to angular rate, ω_a, if it is assumed that the missile velocity vector lies approximately in a plane containing the target and the interceptor at the time of launch. If, however, the interceptor is above or below the target just prior to the time of launch, it can be assumed that the interceptor will perform a climbing or diving attack as required. The missile then is not launched until at least an approximate coplanar condition exists. The errors in α_a, which are a consequence of measurement errors in ω_a, can be represented as

$$d\alpha_a = \frac{\partial \alpha_a}{\partial \omega_a} d\omega_a = t_f \, d\omega_a \tag{5-69}$$

Thus, from Equation 5-69, the error attributable to measurement of the angular velocity of the LOS will be $d\alpha_a$ times the time of flight of the missile. For a time of flight of the missile of approximately 30 seconds, if the error in α_a is to be kept less than one-half degree (a factor of one-tenth the maximum launching error allowed), then $\Delta\omega_D$ must be less than 1/10 mil per second. This specification requires a precision radar similar to the one described in Chapter IV.

In addition to errors in angular rate, control system errors are introduced by the rate gyros, resolvers, potentiometers, servos, etc. As a first approximation to the rms error from these sources, assume

± 1/2 degree rms error for each. When the errors from the various sources are again combined, the resultant error amounts to approximately ± 2-3 degrees.

One of the outputs of the attack computer represents the antenna angle of the launched missile at the time of uncaging. This angle is derived from the interceptor antenna angle and from computation in the attack computer. A planar vector diagram of the situation at missile firing appears in Figure 5-13.

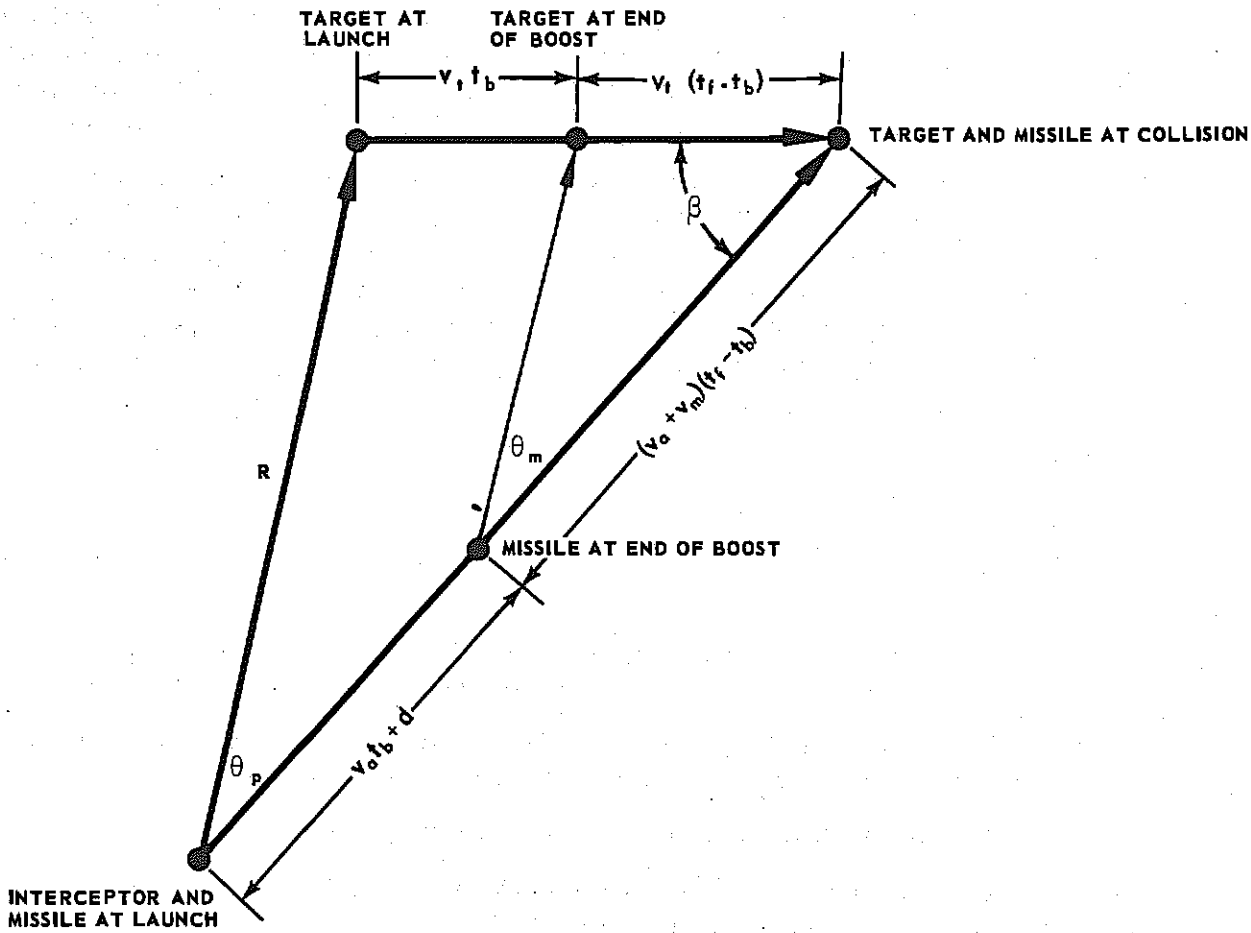

FIGURE 5-13. VECTOR DIAGRAM FOR DETERMINING MISSILE ANTENNA LOOK ANGLE AT THE END OF BOOST

This figure assumes a missile collision course in one plane, with the missile and target velocity vectors remaining constant. If either or both vectors change as a result of changes in speed, direction, or both, the computer simply computes a new course based on a similar diagram by a method of successive straight-line approximations. From the figure it follows that

$$\frac{v_a t_f + d + v_m(t_f - t_b)}{\sin(\theta_p + \beta)} = \frac{v_t t_f}{\sin \theta_p} \tag{5-70}$$

θ_m is the target azimuth at missile uncaging (i.e., at the end of boost) and θ_p is the angle of the target at firing. Also from the figure it follows that

$$\frac{v_t(t_f - t_b)}{\sin \theta_m} = \frac{(v_a + v_m)(t_f - t_b)}{\sin(\theta_m + \beta)} \tag{5-71}$$

Let $\theta_m = \theta_p + \gamma$ and solve. To a close approximation it follows that

$$\theta_m \cong \left(\frac{R}{R + d}\right) \theta_p \tag{5-72}$$

Equation 5-72 is mechanized on the computer.

SECTION 9 — MECHANIZATION OF THE ATTACK COMPUTER AS AN ANALOG COMPUTER

The attack computer mechanizes the three equations derived previously, which are, from Equation 5-66, -66A, and -66B

$$0 = R + \dot{R}T - L \cos \theta \cos \epsilon \tag{5-73}$$

$$\alpha_e = \omega_e T + \frac{L}{R}(\sin \epsilon \cos \theta + k_j \cdot \alpha) \tag{5-74}$$

$$\alpha_a = \omega_a T - \frac{L}{R} \sin \theta \tag{5-75}$$

where

R = present range to target
$\dot{R}$ = present range rate
L = distance missile will travel relative to the interceptor
T = time from present until missile impact
ω_a = angular velocity of LOS about the azimuth axis
ω_e = angular velocity of LOS about elevation axis
θ = radar azimuth angle
ϵ = radar elevation angle
α = interceptor angle of attack
α_a = angle about the azimuth axis through which the interceptor must be turned
α_e = angle about the elevation axis about which the interceptor must be turned

In review, observe that to a first approximation the missile travels straight out along the interceptor velocity vector. T represents the time until the missile and target are at the same range from the fighter. The range miss is resolved along the present LOS and set equal to zero in order to calculate T, which is the time until impact. The time T is needed, along with the time of flight t_f to determine when the missile aiming and warm-up sequence must start. The T equation is Equation 5-73. Equations 5-74 and 5-75 determine the angle through which the interceptor must turn in order for the missile to travel a straight line and hit the target. $R\omega_a T$ represents the distance the target will travel perpendicular to the present LOS, since ω_a is the angular velocity of the target about the azimuth axis. $L \sin \theta$ is the distance the missile travels perpendicular to this line. The difference between the two quantities, $R\omega_a T$ and $L \sin \theta$ is the linear miss perpendicular to the present LOS, in the plane normal to the azimuth axis. The angle which the aircraft must turn through is determined by taking the miss distance and dividing it by the range R. Division by R determines that the computer has constant sensitivity with range, but division by R does not affect the accuracy of the computer. The angle about the elevation axis through which the fighter must be turned can similarly be determined. These angles are then resolved through the bank angle ψ to get angles which are relative to the vertical and horizontal planes. After this transformation, the gravity-drop correction is added to the vertical angle and the signals are

rectified and smoothed. The smoothing is done after the resolution in order to avoid crosstalk and stability problems during banking. Steering can be done prior to lock-on while the system is in the track-while-scan mode. The parameters required by the attack computer are R, $\dot{R}$, ω_a, ω_e, θ, E, and L (the distance the missile will travel relative to the interceptor). From Equations 5-43 and 5-58, it follows that L and L' are

$$L = \bar{v}_m (t_f - t_b) + \bar{d} \tag{5-76}$$

$$L' = v'_m (t_f - t_b) + \bar{d}_c \tag{5-77}$$

The computer actually uses Equations 5-76 and -77 in the manner previously explained. The time of flight, t_f, depends upon the design of the missile.

If the missile is capable of tracking a target at ranges greater than the altitude line, (as is, for example, a pulse-doppler type), then the minimum time of missile flight is independent of the altitude. If the missile range is limited because of the altitude of the target, then the minimum time of flight will be limited by the altitude above local terrain indicated by the radar. Assume that the missile is capable of tracking features and is therefore unaffected by terrain clearance. A reasonable value to assume for the minimum time of flight of the missile is 10 seconds, and for the boost time, t_b, 2 seconds. Assuming that the missile travels in the same direction during its launching period as it does after boost, the value of L will be the velocity of the missile relative to the interceptor multiplied by the time of flight (less the time of boost), as well as d, the distance traveled during the boost period. The distance d traveled during the example boost period has a value given by

$$d = \frac{1}{2} at^2 = \frac{1}{2} (50)(32)(4) = 3200 \text{ feet} \tag{5-78}$$

Assuming a missile velocity of Mach 5 after boost and a minimum time of flight of 10 seconds, the minimum value of L will then be

$$L_{min} = (5000)(8) + 3200 = 43200 \text{ feet}$$

It should be possible to fire the missile for values of t_f less than 10 seconds if the situation warrants it. This requires a manual override by the pilot. The computer should be mechanized so that the system will accept various times of flight either prior to, or during, flight. A t_f computer is therefore required to determine L. A T computer is also necessary to solve Equation 5-73. When T and t_f are available, the difference is used to obtain $T - t_f$, which is the time remaining before launch. This difference is used to actuate the various switching operations necessary in preparing, arming, and firing the missile. In addition, other automatic switching operations must be done. The T servo has a maximum value to prevent it from operating until the interceptor is within a specified angle of a collision course. This prevents the T servo from experiencing servo transients during the navigational and approach phases of the attack. When the interceptor is within a specified angle of a collision course, the T computer is energized and the attack computer begins its sequence of operations. After launching ($T = t_f$), the attack computer puts the interceptor into a controlled turn toward the target to clear the impact area while keeping the target illuminated. If the attack computer continued to function after missile impact, the interceptor escape maneuver would radically change ω_a, ω_e, and $\dot{R}$ so that T would change violently. Nevertheless, it is necessary that the computer continue to function until T = 0 when the missile hits. To prevent violent transients from occurring in the T computer, all of the inputs to this computer can be removed just prior to launching. The T computer can then run as a clock until the attack computer switches control back to the navigational computer.

A block diagram of the attack computer mechanized as an analog computer is shown in Figure 5-14.

Equations 5-67, -67A, -67B, -68, -68A, and -72 have been mechanized as an analog computer in Figure 5-14. The T computer obtains radar inputs R and $\dot{R}$ and the resolver output $L \cos \theta \cos \epsilon$ to solve for

$$T = \frac{L \cos \theta \cos \epsilon - R}{\dot{R}} \qquad \text{from Equation 5-73.}$$

This value of T is multiplied by the radar outputs ω_a and ω_e in potentiometer multipliers to yield respectively $\omega_a T$ and $\omega_e T$. The radar inputs

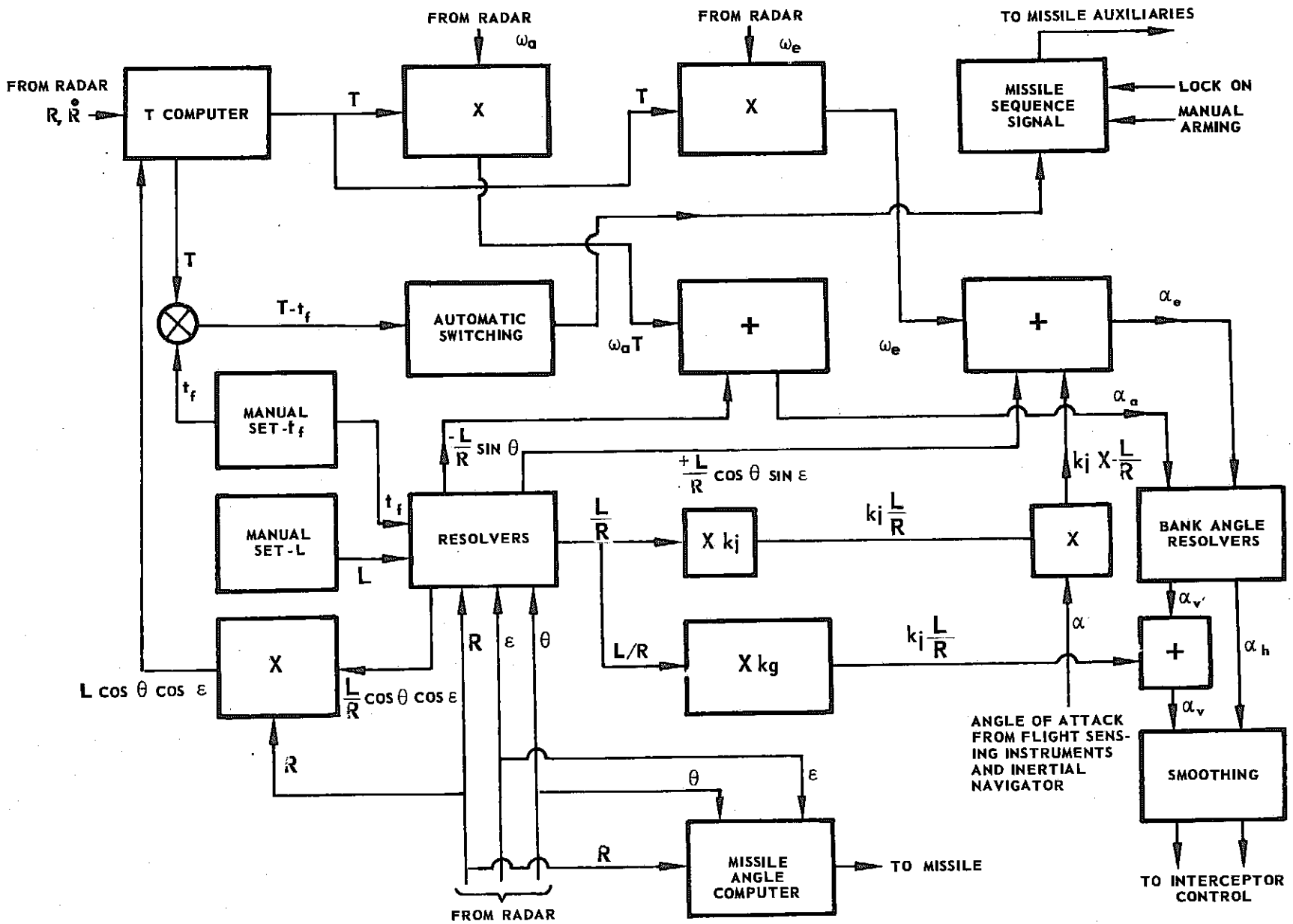

FIGURE 5-14. ANALOG COMPUTER BLOCK DIAGRAM FOR THE DESCRIBED SYSTEM

R, ϵ, and θ, and the preset distance L, are applied to resolvers which develop the outputs $\frac{L}{R}$, $-\frac{L}{R}\sin\theta$, $\frac{L}{R}\cos\theta\sin\epsilon$, and $\frac{L}{R}\cos\theta\cos\epsilon$. The output $-\frac{L}{R}\sin\theta$ is added to $\omega_a T$ in a summing amplifier to yield α_a. $\frac{L}{R}$ is multiplied by the given values k_j and k_g to yield $k_j\frac{L}{R}$ and $k_g\frac{L}{R}$. $k_j\frac{L}{R}$ is further multiplied by the angle of attack α to yield $k_j\alpha\frac{L}{R}$, which is added to $\frac{L}{R}\cos\theta\sin\epsilon$ and $\omega_a T$ in a summing amplifier to yield α_c. α_a and α_e are inputs to the bank angle resolvers which develop α_v' and α_h. $k_g\frac{L}{R}$ is added to α_v' to yield α_v. α_v and α_h are smoothed and applied to the interceptor control system. The given value of t_f is subtracted from T, yielding the time to launch, $T - t_f$, which controls the automatic switching unit that actuates the missile warm-up, parameter, and firing signals. The missile antenna look-angle computation is mechanized in the missile antenna angle computer from radar data inputs, R, θ, and ϵ, and the resulting output is sent to the missile.

The equations necessary for control of the interceptor and arming and launching of the missile (Equations 5-73 through 5-75) have been mechanized as an analog computer in the previous section. It is, of course, also possible to mechanize these equations for use in a digital computer. Some of the technical differences between the two types of computers have already been discussed. The principal state-of-the-art differences involve problems of miniaturization. Digital computers are not, in general, as well suited to the solution of specific problems as are analog computers, but the accuracy obtainable from digital computers makes them preferable. The development of digital computers of size, weight, and complexity comparable to corresponding analog computers can be expected. It must be remembered that, if an all-digital computer is used, not only must the attack computation be performed, but also the automatic navigation computation, which includes guiding the interceptor from take-off to the attack phase, carrying out the attack according to guidance signals from the tracking radar, guiding the interceptor back to the landing area, and guiding the interceptor to landing and touchdown. The basic equations describing the navigation phase are the same for both analog and digital computers, differing only in the form used.

The entire computation must be completed in a time that is short in comparison to the time constants of the interceptor in order that the interceptor flight path will not be distorted by time delays in the computation. In other words, the navigation calculations should be completed in a fraction of a second or the computation results would be obsolete by the time that they could be used. One of the difficult problems in attempting to compute rapidly with a digital computer is that the accuracy to which a complex operation can be carried out is a function of the time allowed for the specified operation. Complex mathematical operations require that the computer have not only a considerable number of arithmetic units but also an appreciable memory. Time required for performing the operation involves not only the number of elements in the computer arithmetic and control units, but also the speed of access to the memory. Any degree of accuracy can be theoretically computed in a digital computer if sufficiently large arithmetic and control units are used. Excessive time, however, is required for the operation unless an infinitely large, quick-access memory is included. Switching of the source of information which occurs in this problem can be accomplished through appropriate design of the control unit. For example, missile launch computations begin when a specific target range is reached. The computer determines this range by comparing the actual target range with a range which is recorded in the memory unit.

As has been mentioned, another disadvantage of the digital method of computing is that the required information is usually in analog form. Furthermore, the information sent to the other fire control system areas must also be in analog form. This imposes the requirement for analog-to-digital input units and digital-to-analog output units, in addition to all the regular computing equipment. It may be concluded from this discourse that if the disadvantages of large size and excessive computing time can be solved by subminiaturized and transistorized digital computers, the advantages of reliability and accuracy available from digital computers can be realized.

SECTION 10 — THE DIGITAL MECHANIZATION OF THE ATTACK COMPUTER

The fire control system computer can be mechanized by digital as well as analog components. As pointed out in earlier discussions comparing analog and digital computers, the digital computer consists of arithmetic and memory units which are suitably programmed to carry out the desired operations. The whole digital computer program can be

subdivided into several individual programs. Three divisions of the computer program correspond to the major phases of operation, namely, navigation, attack, and landing. A complete block diagram of the proposed fire control computing system employing digital computer components is shown in Figure 5-15.

The digital computer mechanization is essentially complete once the computer has been programmed. The attack computer consists of three principal subcomputers; these are (1) the ballistics computer, (2) the steering computer, and (3) the launching computer. The programs for these various computers follow:

(a) THE BALLISTICS PROGRAM

Inputs to the ballistics computer include:

R	= radar range to the target; from the radar	
h	= altitude of interceptor	from the aerodynamics, computer, and flight sensing instruments, and the inertial navigator
α	= angle of attack	
V	= interceptor true air-speed	from the aerodynamics, computer, flight sensing instruments, and the inertial navigator
ρ	= air density	
v_s	= speed of sound	
L	= relative distance of missile travel	stored in the computer memory
k_i	= constants	
d	= missile ballistics parameter	
s	= missile ballistics parameter	
t_f	= missile time of flight	manually set
k_j	= jump proportionality constant	
k_g	= gravity drop proportionality constant	

The outputs are:

L	= missile travel relative to interceptor	outputs to the steering program
α	= interceptor angle of attack	
J	= jump correction	
C	= curvature correction	

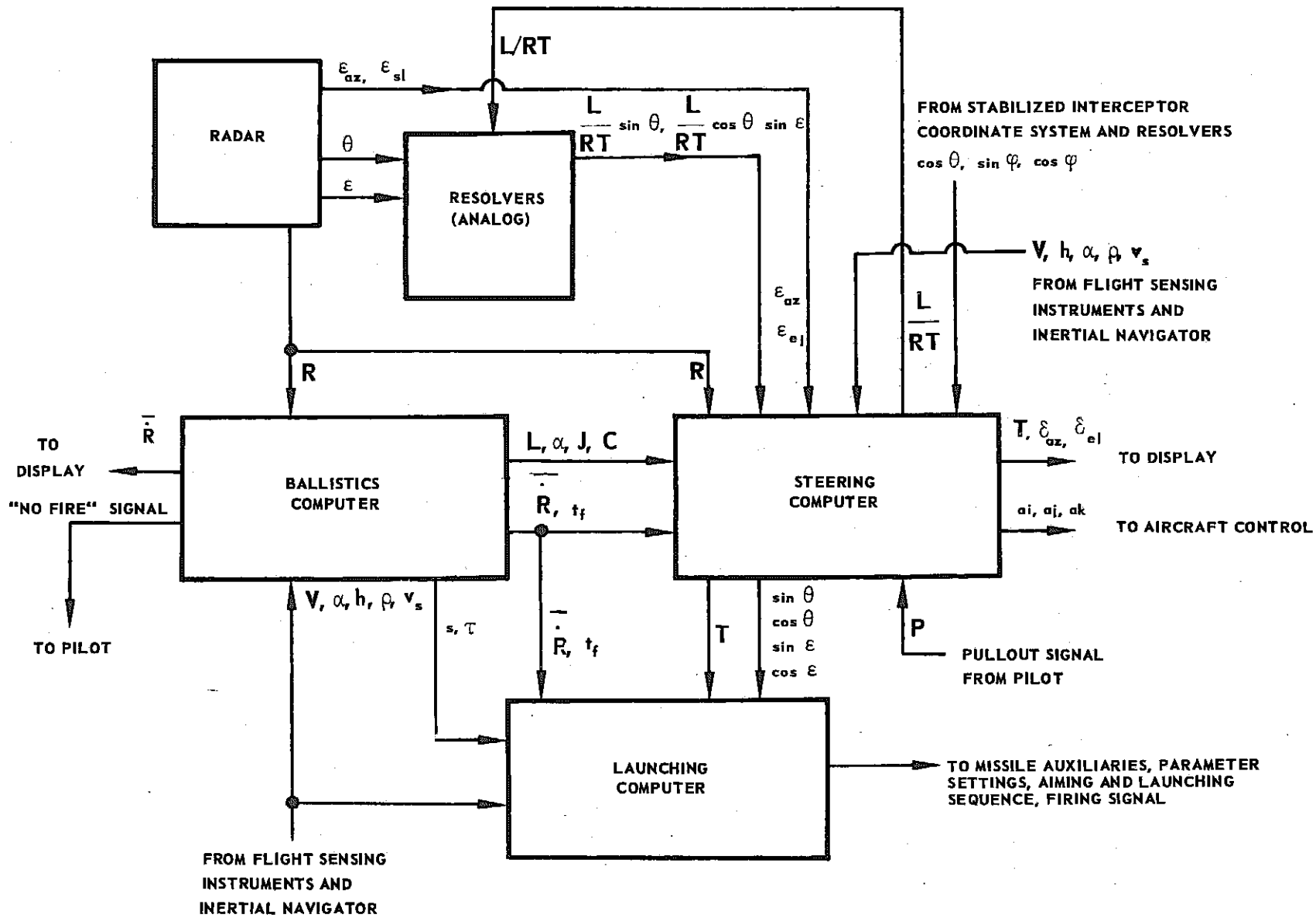

FIGURE 5-15. BLOCK DIAGRAM OF A DIGITAL COMPUTER FOR THE PROPOSED SYSTEM

"no-fire" signal	output to the pilot's display
$(d_2)_n$ = missile ballistics parameter (at instant n)	outputs to the launching program
τ_n = missile attenuator parameter (at instant n)	
t_f = missile time of flight	to steering and launching programs
$\bar{\dot{R}}$ = smoothed radar range rate	to steering and launching programs and radar display

Equations:

(1) $$\dot{R}_n = \frac{R - R_n^{-1}}{\Delta t}$$

(2) $$\bar{\dot{R}}_n = k^{-1}\,\dot{R}_n^{-1} + k_o\,\bar{\dot{R}}_n^{-2}$$ — output to steering program, launching program, and radar display

(3) $$\tau_n = C_1 \quad h < H$$
$$= C_2 \quad h \geq H$$ — output to launching program

(4) $$(t_{f_{min}}) = t_b + N\tau_n$$

(5) $$(L_{max})_n = k_1 + \frac{k_2}{(\rho a)_n} + k_3\left(\frac{1}{(\rho a)_n}\right)^2$$

(6) $$(L_{min})_n = -d_n + s_n\,(t_{f_{min}})$$

(7) $$(L_o)_n = \frac{(R_o)_n\, s_n + \bar{\dot{R}}_n\, d_n}{s_n - \bar{\dot{R}}_n}$$

(8) If $(L_o)_n - (L_{max})_n$ $\begin{cases} \geq 0, \text{ go to } 12 \\ < 0, \text{ go to } 9 \end{cases}$

(9) $\ell_n = (L_o)_n$

(10) $(t_F)_n = \dfrac{(L_o)_n + d_n}{s_n}$

(11) Go to 14

(12) $\ell_n = (L_{max})_n$

(13) $(t_F)_n = \dfrac{(L_{max})_n + d_n}{s_n}$

(14) If $\ell_n - (L_{min})_n$ $\begin{cases} \geq 0 \text{ go to } 16 \\ < 0 \text{ go to } 15 \end{cases}$

(15) "No-fire" signal | output to pilot's display

(16) $L_n = \ell_n$ | output to steering program

(17) $(t_f)_n = (t_F)_n$ | output to steering program and launching program

(18) $J_n = k_j \, a \dfrac{L_n}{R_n}$ | output to steering program

(19) $C_n = k_g \dfrac{L_n}{R_n}$ | output to steering program

(20) Go to steering program

The ballistics program equations are the following: Equation 1 defines the derivative of the range as the first difference of the range. Equation 2 defines the smoothed radar range rate and the equation corresponds to the transfer function of the smoothing filter. The smoothed

range rate is an output to the steering program, the launching program, and the radar display. Equation 3 defines a missile attenuator parameter which depends on the altitude; H is a preassigned altitude for change of missile parameters, and τ_n is an output to the launching program. Equation 4 defines the minimum time of flight: t_b is the boost time and N is the minimum number of missile time constants allowable in order for the launching error to be cancelled; the missile parameter τ in this case is the "missile time constant." Equation 5 defines the maximum missile travel relative to the interceptor, and depends upon the ballistic parameter ρv_s, which is the product of air density and the speed of sound. Equation 6 is the minimum missile travel relative to the interceptor and depends upon the missile ballistic parameters and the minimum time of flight. Equation 7 defines a quantity for comparison with L_{max} and L_{min} in order to determine whether or not to fire the missiles. L_o depends on the initial range, the smoothed range rate and the missile ballistics parameters. Equation 8 is a decision statement. If $L_o > L_{max}$, then go to Equation 12 which defines a new quantity for L_{max}, namely, ℓ. A new quantity t_f is defined by Equation 13 which depends on L_{max} and the missile ballistics parameters. Finally, Equation 14 is a comparison statement to find out whether or not $\ell = L_{max}$ is greater or less than L_{min}. If, in this case $\ell = L_{max} > L_{min}$, go to Equation 16, where L is set equal to ℓ and is an output to the steering program. Similarly, t_f is set equal to t_F and is an output to the launching and steering programs. Returning to the statement of Equation 8, if $L_o < L_{max}$, go to Equation 9, which defines $\ell = L_o$. Equation 10 defines t_f in terms of L_o and the ballistics parameters. Equation 11 says go to Equation 14 where the comparison between ℓ and L_{min} is again made. If $\ell_n > L_{min}$, the procedure is as before; however, if $\ell_n < L_{min}$, then go to Equation 15, which is the "no-fire" signal. This signal goes to the pilot's display and tells him not to fire the missiles since the distance the missile will travel does not lie within the allowable bounds. Equation 18 yields the jump correction, and Equation 19 the curvature correction due to gravity drop. Both of these corrections go to the steering program. Equation 20 indicates to go to the steering program.

(b) THE STEERING PROGRAM

The inputs to the steering program include:

$\bar{R}$	= smoothed radar range rate	From the Ballistics Program
L	= missile travel relative to the interceptor	
t_f	= missile time of flight	
α	= interceptor angle of attack	
J	= jump correction	
c	= curvature	
R	= radar range	from the radar
θ	= aircraft pitch angle	from resolvers in the interceptor coordinate system
ψ	= aircraft roll angle	
v	= interceptor velocity	from the aerodynamic program
$\bar{\dot{v}}$	= smoothed rate of change of v	
$\frac{L}{RT} \sin\theta, \frac{1}{RT} \cos\theta \sin\epsilon$		inputs from the analog units
$\epsilon_{AZ}, \epsilon_{EL}$	= components of the tracking error in the azimuth and elevation planes	inputs from the radar
P	= pullout selection	manual control
K_i, C	= constants stored in the computer memory	

The outputs include:

$\sin\theta \cos\theta, \sin\epsilon, \cos\epsilon$	= trigonometric functions of the azimuth and elevation angle	to the launching program
a_i	= interceptor acceleration along the velocity vector	to aircraft control program
a_j	= interceptor horizontal turning acceleration	
a_k	= interceptor vertical turning acceleration	
T	= time from the present to missile impact	output to launching program and display

δ_{AZ}, δ_{EL} = pilot's azimuth and elevation steering indications, respectively } to pilot's display

$\frac{L}{R\,T}$ } output to the antenna angle resolvers

Equations:

(1) $(\sin\theta)_n = \dfrac{\left(\frac{L}{R\,T}\ \sin\theta\right)_n}{\left(\frac{L}{R\,T}\right)_{n-1}}$

(2) $(\cos\theta)_n = \left[1 - (\sin\theta)_n\right]^{1/2}$

(3) $(\sin\epsilon)_n = \dfrac{\left(\frac{L}{R\,T}\ \cos\theta\ \sin\epsilon\right)_n}{\left(\frac{L}{R\,T}\right)_{n-1}\ (\cos\theta)_n}$

(4) $(\cos\epsilon)_n = \left[1 - (\sin\epsilon)_n^2\right]^{1/2}$

} output to the launching program

(5) $T_n = \dfrac{L_n\ (\cos\theta)_n\ (\cos\epsilon)_n - R_n}{\bar{R}_n}$ } outputs to the launching program and the display

(6) $\left(\frac{L}{R\,T}\right)_n = \dfrac{L_n}{R_n T_n}$ } output to angle resolvers

(7) $(a_v)_n = C\ (V_{max} - V_n) - \bar{\dot{V}}_n$ } output to the aircraft control program

(8) If $(P)_n = \begin{cases} 1, \text{ go to } 19 \\ 0, \text{ go to } 9 \end{cases}$

(9) $$(t_f)_n = -T_n - k_o \begin{cases} \geq 0, \text{ go to } 10 \\ < 0, \text{ go to } 1 \end{cases}$$

(10) $$(M_H)_n = R_n T_n \left\{ \left[(\epsilon_{AZ})_n (\cos\theta)_n (\cos\psi)_n \right] - \left[(\epsilon_{EL})_n + \left(\frac{L}{RT}\right)_n (a_n) (\cos\epsilon)_n \right] \left[(\sin\epsilon)_n (\sin\theta)_n (\cos\psi)_n \right] \right\}$$

(11) $$(M_V)_n = - R_n T_n \left\{ \left[(\epsilon_{AZ})_n (\cos\theta)_n (\sin\psi)_n \right] - \left[(\epsilon_{EL})_n + \left(\frac{L}{RT}\right)_n (a_n) (\cos\epsilon)_n \right] \left[(\sin\epsilon)_n (\sin\theta)_n (\sin\psi)_n + (\cos\epsilon)_n (\cos\psi)_n \right] \right\} - C_n (\cos\theta)_n$$

(12) $$(\overline{M}_H)_n = k_4 (M_H)_n + k_5 (\overline{M}_H)_{n-1} + k_6 (\overline{M}_H)_{n-2}$$

(13) $$(\overline{M}_V)_n = k_7 (M_V)_n + k_8 (\overline{M}_V)_{n-1} + k_9 (\overline{M}_V)_{n-2}$$

(14) $$(a_j)_n = \frac{k_{10} (\overline{M}_H)_n}{V_n T_n + L_n}$$

(15) $$(a_k)_n = \frac{k_{11} (\overline{M}_V)_n}{V_n T_n + L_n}$$

outputs to aircraft control program

(16) $$(\delta_{AZ})_n = \frac{(\overline{M}_H)_n}{V_n T_n + L_n} (\cos\psi)_n - \frac{(\overline{M}_V)_n}{V_n T_n + L_n} (\sin\psi)_n$$

(17) $$(\delta_{EL})_n = \frac{(\overline{M}_H)_n}{V_n T_n + L_n} (\sin\psi)_n + \frac{(\overline{M}_V)_n}{V_n T_n + L_n} (\cos\psi)_n$$

to radar display

(18) Go to launching program

(19) If T_n $\begin{cases} \geq 0, \text{ go to } 20 \\ < \text{go, to navigation program} \end{cases}$

$$\left.\begin{array}{ll} (20) & (a_k)_n = A_1 \\ (21) & (a_j)_n = A_2 \end{array}\right\} \text{to aircraft control program}$$

(22) Go to ballistics program

A description of the equations in the steering program follows. Equation 1 derives $\sin\theta$ from the analog inputs. Equation 2 defines $\cos\theta = \sqrt{1 - \sin^2\theta}$. Equation 3 derives $\sin\epsilon$ from the analog inputs, and Equation 4 finds $\cos\epsilon = \sqrt{1 - \sin^2\epsilon}$. Equations 1 through 4 are all outputs to the launching program. Equation 5 is identical with Equation 5-73 and is the equation for the time T. Equation 5 is an output to the launching program and the radar display. Equation 6 takes the analog input and supplies it as an output to the angle resolvers. Equation 7 yields the acceleration along the interceptor velocity vector in terms of the velocity, maximum velocity, and smoothed rate of change of the velocity of the interceptor. Equation 7 is an output to the aircraft control program. Equation 8 is a manual control and is a decision function made by the pilot. If the pilot decides to pull out, P has the value 1; if he decides not to pull out (no signal), P has the value 0. If P = 0, go to Equation 9. Equation 9 is a decision function which determines which program to go to, depending on the time remaining until missile impact. k_o is a given constant. If $t_f > T + k_o$ then go to Equation 10. If $t_f < T + k_o$, the program is repeated. Equation 10 gives the horizontal component of the miss in stabilized interceptor coordinates. Equation 11 gives the vertical component of the miss in the same coordinates. In Equation 11, the curvature correction term has been included. Equation 12 gives the smoothed horizontal component of the miss from the transfer function equation of the smoothing filter and, similarly, Equation 13 gives the smoothed component of the vertical miss. Equation 14 gives the horizontal turning acceleration for the interceptor which is proportional to the smoothed horizontal miss divided by the distance traveled by the missile. Equation 15 gives the corresponding vertical turning acceleration for the

interceptor, and is proportional to the smoothed vertical miss divided by the missile travel. These two acceleration components are outputs to the aircraft control program. Equations 16 and 17 are Equations 14 and 15 rotated through the roll angle ψ by the bank angle resolver. Equations 16 and 17 are outputs to the display. Equation 18 states "go to the launching program." Equation 19 is the alternate choice from the comparison statement 8, in which the pilot decides to pull out. If $P = 1$, then the program jumps from Equation 8 to Equation 19. Equation 19 is a comparison statement on the time remaining to impact, T. If $T > 0$, then go to 20; if $T < 0$, which means that the missile has already collided with the target, then proceed to the navigation program. Equation 20, which is used when the missile has not as yet collided, gives the value of the horizontal turning acceleration. Similarly, Equation 21 gives the value of the vertical turning acceleration. These quantities are preset constants for the pullout maneuver. Equation 22 says "go to the ballistics program."

(c) THE LAUNCHING PROGRAM

The launching program will not be outlined in detail because the outputs depend on the specific nature of the armament used. The inputs are d_2, r, t_f, $\bar{R}$ from the ballistics program, $\sin\theta$, $\cos\theta$, $\sin\epsilon$, $\cos\epsilon$ and T from the steering program; v, h, ρ and v_s from the aerodynamics and flight sensing instruments, and computer constants. The outputs are numbers needed by the missile auxiliaries and mechanisms. The outputs to the missile auxiliaries include missile parameter settings, missile antenna slaving signals, missile firing signals, missile launching-door-mechanism signals, missile power supply and gyro warm-up and actuating signals, etc.

The preceding programs plus the block diagram in Figure 5-15 complete the design of the digital mechanization for the computer.

CHAPTER VI

INFRARED FIRE CONTROL SYSTEMS

SECTION 1 — INTRODUCTION

The fundamental process of infrared signal detection is illustrated in Figure 6-1. Basically, the operation of a typical infrared system involves the following functions: A fraction of the infrared energy radiated by the target is collected and focused on the detector by an optical system. The detector produces a noisy electrical signal which is filtered by the detector and, again, by the frequency characteristics of the output amplifier. The resulting amplified signal, which is used as a basis for the scope (display) presentation, contains elevation and azimuth information. In general, the overall performance of the infrared system is limited by the noise inherent in the detector used.

The following sections of this chapter discuss (1) the components of the typical infrared system, (2) the basic functional types of infrared systems, (3) the external factors which affect system efficiency, and (4) a method of evaluating infrared systems.

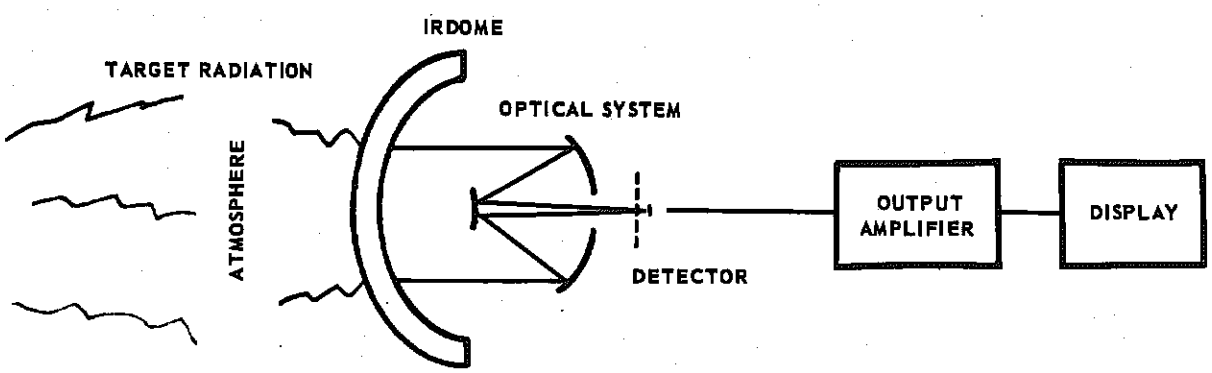

FIGURE 6-1. FUNCTIONAL INFRARED SYSTEM

SECTION 2 — BASIC COMPONENTS OF INFRARED SYSTEMS

(a) INFRARED DETECTORS

Nearly all the passive infrared systems designed for use in an airborne environment employ thermistor, photoconductor, or photovoltaic cells. Thermistors belong to a class of radiation detectors called thermal detectors. In a thermal detector the radiation is absorbed and transformed into heat, producing a temperature rise in the device. The rise in temperature affects a specific characteristic of the detector used, the magnitude of which is a measure of the amount of radiation incident on the detector. A typical thermistor (bolometer) circuit is shown in Figure 6-2.

Photoconductors and photovoltaic cells are a variety of quantum detectors. In these cells the incident photons change the detector characteristic directly. In the photoconductor, the characteristic which varies is the electrical resistance of the cell, whereas, for the photovoltaic cell, a voltage is generated directly. The circuit configuration of the quantum detectors is the same as that of the thermistor. For thermistor operation, the change in temperature due to photon absorption produces a change in the electrical resistance of the cell.

Key characteristics of infrared detectors include detectivity, spectral response, time constant, resistance, and size. The detectivity is defined as the ratio of the square root of the area of the detector to the noise-equivalent input, which in turn is defined as the input power that produces an rms electrical output equal to the rms electrical noise. The spectral response is that region of the electromagnetic spectrum within which the detector is sensitive.

Thermistors, are polycrystalline compounds of metallic oxides, chiefly cobalt oxide, nickel oxide and manganese oxide. When intended for use as radiation detectors, these materials are prepared in thin films or "flakes" to minimize heat capacity per unit of receiver area. Mounted on good heat-conducting backings, these flakes can be made to follow rapid changes in radiation. Their spectral response is essentially flat from the ultraviolet to the far infrared region of the electromagnetic spectrum.

Photoconductor materials include lead sulfide, lead telluride, lead selenide, indium antimonide, and germanium. Cells made from these

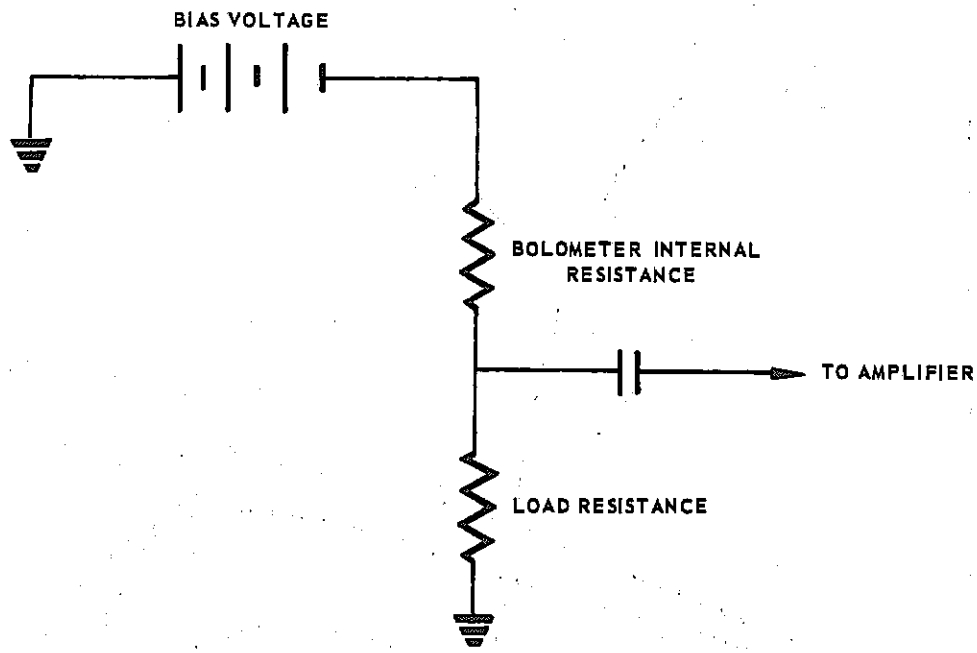

FIGURE 6-2. BOLOMETER (THERMISTOR) CIRCUIT

materials are called "intrinsic detectors" because their operation depends on the excitation of electrons from their valence band to their conduction band. However, electronic excitation can also be achieved if impurities such as gold and zinc are added to the photoconductive material. The so-called impurity detectors consisting of gold-doped germanium and zinc-doped germanium are examples of this class of photoconductors. The spectral detectivity of photoconductors is much greater than that of thermistors; their spectral response, however, is confined to narrow bands in the electromagnetic spectrum making their use highly dependent on the spectral characteristics of the radiation to be detected. Figures 6-3 and 6-4 show the relative detectivity of some infrared detectors.

Next in importance to the spectral detectivity and response is the time constant of a detector. The response of a detector is comparable to that of a simple RC network with its associated time constant. The RC time constant is defined as the time required for the response of the detector to decay to 1/e of its maximum value. In this respect, thermistors are slow, their time constants ranging from hundreds of microseconds to a few milliseconds. Photoconductors, on the other hand, are faster and

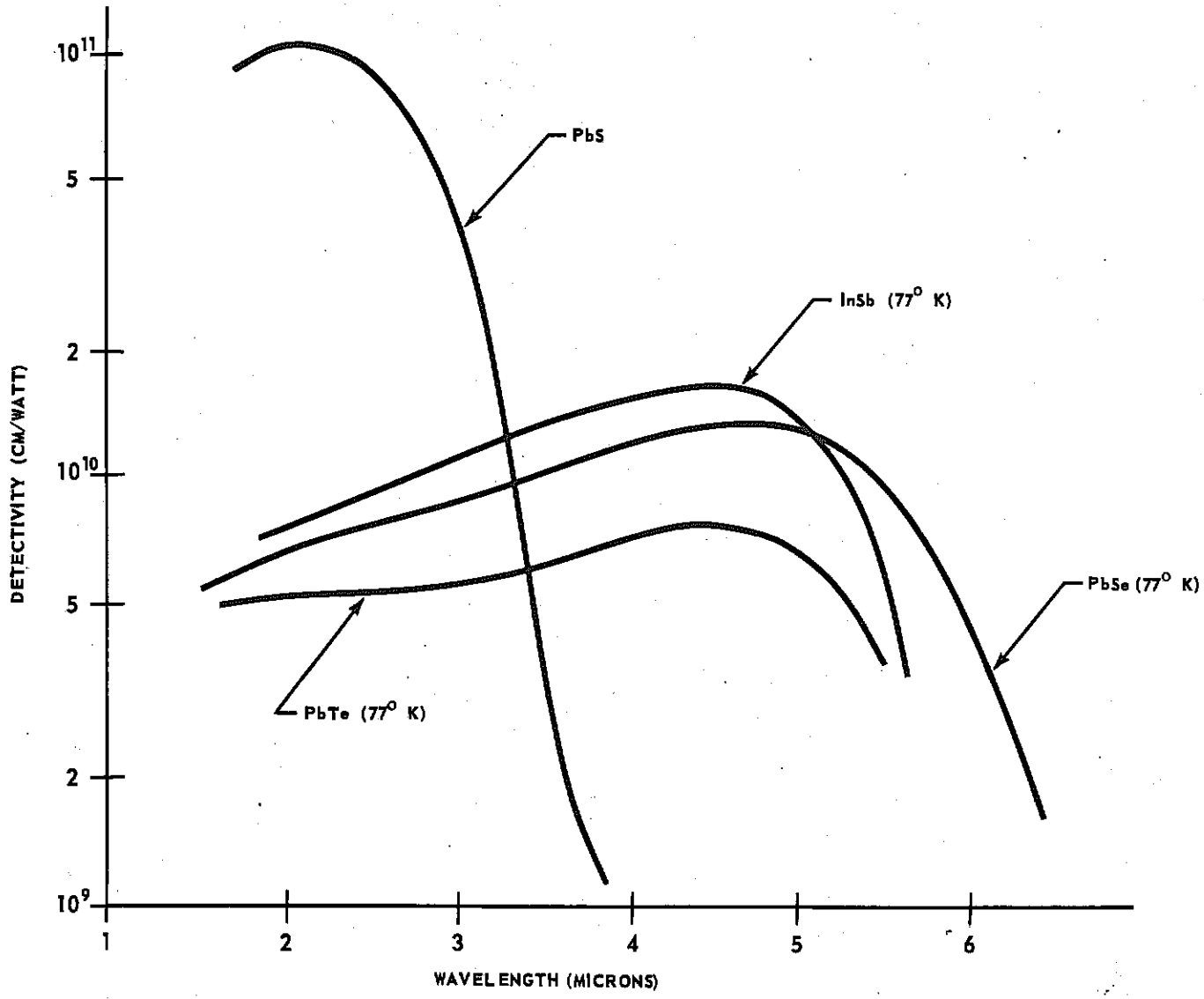

FIGURE 6-3. DETECTIVITY OF COMMON DETECTORS

are therefore preferred over thermistors for high speed scanning applications. An equally important property of infrared detectors is the inherent noise level, which usually limits the performance of the system in which the detector is used. In the case of a thermistor, the output signal is generated by a change in the level of the bias current flowing through it. Variation of bias-current level is due to changes in electrical resistance. The larger the bias voltage applied to the thermistor, the greater will be the increment of change in output current level and, hence,

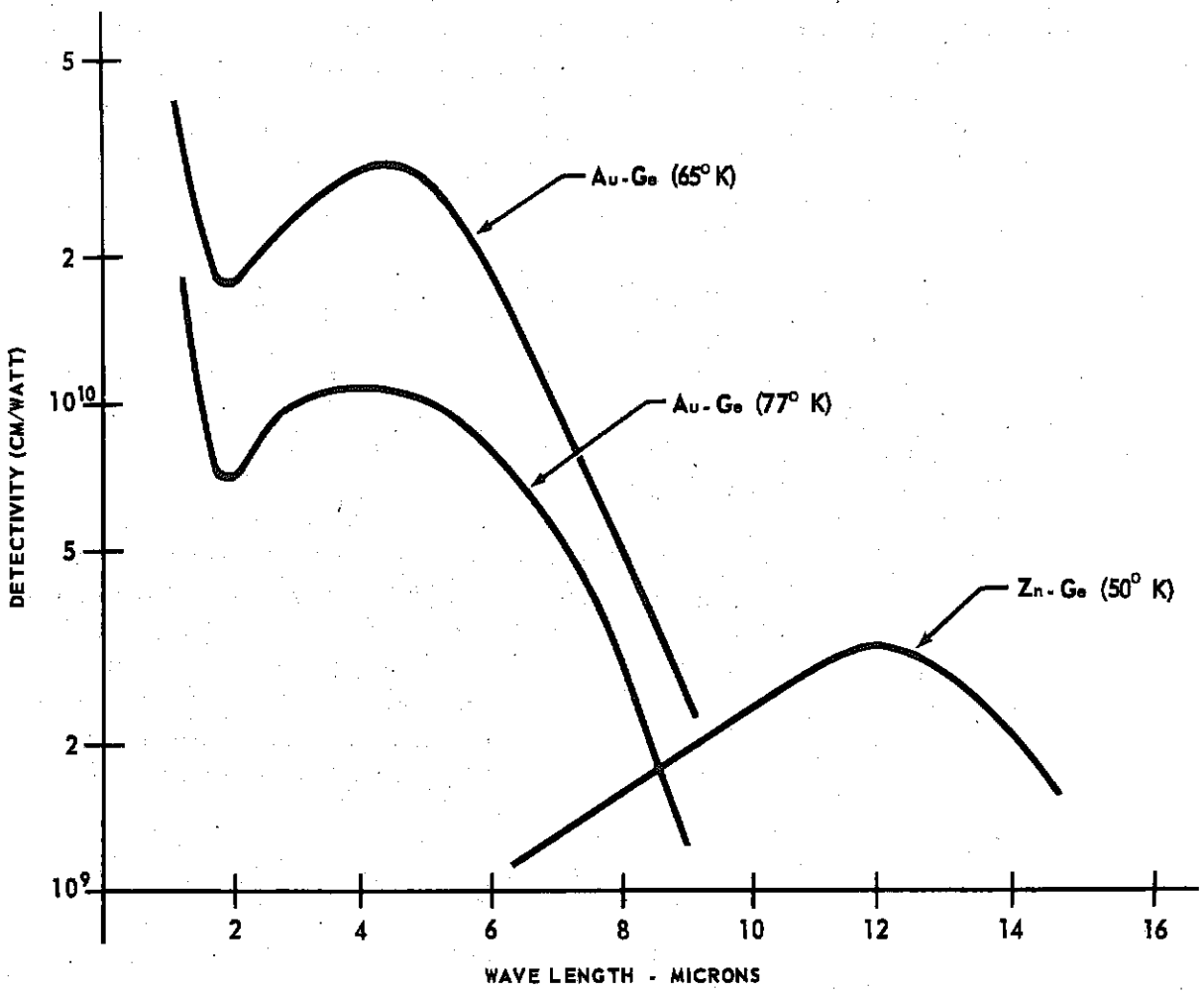

FIGURE 6-4. DETECTIVITY OF DOPED-GERMANIUM DETECTORS

the greater the detector output signal. The limiting noise in thermistors is called "Johnson Noise." It results from thermal fluctuations within the detector and is a direct function of its electrical resistance (R) and temperature (T) as,

$$N_J = 4KTR \qquad (6\text{-}1)$$

where K is Boltzmann's constant (1.38×10^{-23} watt sec/^{o}K)

Photoconductors are limited by noise current caused by voltage fluctuation within the detector. The spectrum of this noise varies inversely with the frequency, f, and directly with the square of the current, I, flowing through the detector as,

$$N_c = \frac{CI^2}{f} \qquad (6\text{-}2)$$

where C is a constant and is therefore independent of I and f.

Noise current differs markedly from Johnson noise since the latter has a flat frequency spectrum, whereas noise current is primarily a low frequency phenomenon.

What a detector truly measures is the difference between the radiation energy incident on it and the radiant energy level of the detector itself. It is logical to expect that the cooler the detector can be maintained the greater the amount of energy it will measure. However, this gain in measurable energy is achieved at the expense of longer time constants. In selecting a cooled detector, the importance of greater sensitivity versus speed of response must be weighed. Common detector cooling temperatures are liquid carbon dioxide (temperature 193°K), liquid nitrogen (temperature 77°K) and liquid oxygen (temperature 80°K).

Most infrared systems used for detection of airborne targets employ high speed scanning systems. These systems use photoconductors almost exclusively. Table 1 shows the characteristics of the various infrared detectors which may be used.

Thus far only photoconductive- and photovoltaic-type cells have been considered. A third type of quantum detector called a photoelectromagnetic (PEM) cell has been developed. A PEM cell consists of a strip of photoconductive material placed in the air gap of a small permanent magnet. Radiation which impinges on the detector does so in a direction perpendicular to both the magnetic field and the major axis of the strip. Radiation incident to the top of the strip produces hole-electron pairs near the surface. The electron carriers diffuse downward into the material and result in the magnetic field deflecting the holes and electrons in opposite directions, thus producing photocurrent. Since the cell resistance is usually less than 100 ohms, it is therefore necessary to use a transformer to increase the input impedance level and realize the full signal-to-noise ratio of the detector.

The detectivity, D*, is defined as a quantity which is the ratio of the square root of the area of the detector to the noise-equivalent input (NEI). It is frequently the system designer's problem to maximize D* for a specific system application. The magnitude of D* varies with the frequency at which radiation falling on the detector is chopped (modulated). The optimum chopping frequency in turn can be determined from the following relationship:

$$f_{c_{opt}} = \frac{1}{2\pi\tau} \qquad (6\text{-}3)$$

where τ = detector time constant

TABLE I INFRARED DETECTOR CHARACTERISTICS

Detector	Type	NEI watt 10^{-11}	D* cm/watt 10^{+9}	sec	Z ohm	A mm^2	T^oK	λ Cut-off
PbS	PC	10	10	100	10^5	100	300	3
PbS	PC	3.8	26	5000	$5x10^2$	100	193	3.75
PbS	PC	3.2	31	7000	10^6	100	77	4.2
PbSe	PC	6.0	3.3	25	30	4	77	5.5
PbTe	PC	3.0	5.6	20	10^7	1.5	77	5.5
InSb	PC	2.3	1.0	1	100	$5x10^{-2}$	77	5
InSb	PV	650	0.03	2	2000	3.6	77	5
Ge-Au	PC	5.0	4.0	1	$3x10^6$	4	77	6.5

If the system is operated below the optimum frequency (see Figure 6-5), it is penalized since cell noise power varies as $\frac{1}{f}$. If operated above this frequency, the noise power falls off but the loss in electrical signal power decreases according to $\frac{1}{f^2}$ at frequencies appreciably greater than $f_{c_{opt}}$.

The general problem confronting the designer is not the optimization of operation of a specific type of cell, but rather the choice of cell with an optimum detectivity for the intended application. The choice must be based on the empirically-determined relationship which has been found to exist among the many cells tested. Cells with long time constants are generally more sensitive than corresponding cells of equivalent quality but shorter time constants. This relationship, known as McAlister's law, is defined as

$$S\tau = K \tag{6-4}$$

where S is the detector sensitivity[1], τ is the time constant and K is a constant.

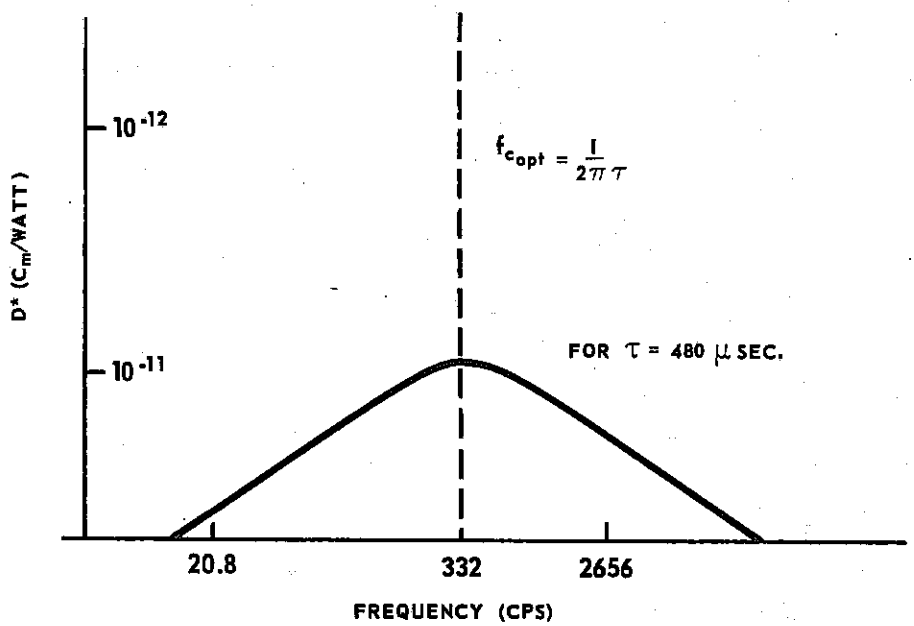

FIGURE 6-5. VARIATION OF DETECTIVITY AT SPECTRAL PEAK WITH FREQUENCY FOR A TYPICAL PbS DETECTOR

1. Defined as the noise equivalent input (NEI) for a 1 cm^2 detector over a 1 cycle bandwidth, which means that $D^* = \frac{1}{S}$

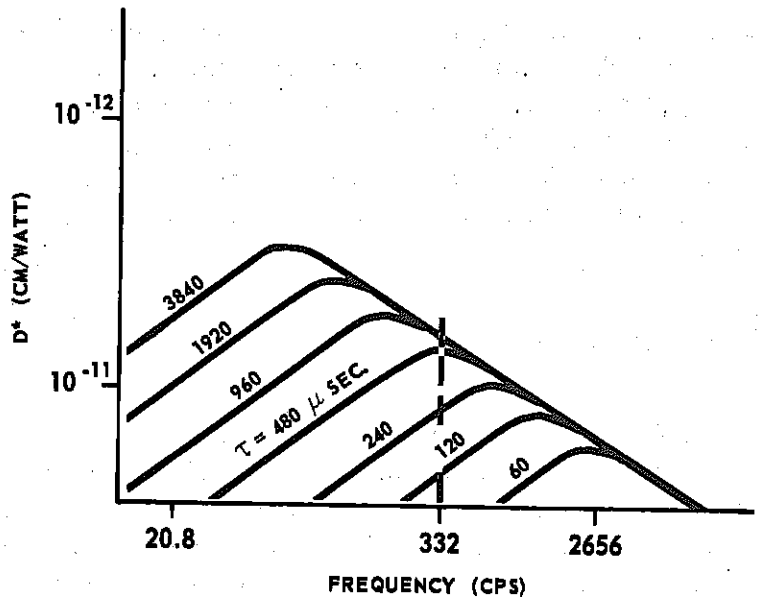

FIGURE 6-6. VARIATION OF DETECTIVITY

This relationship holds fairly well when

60μ sec. $< \tau < 600\mu$ sec.

Figure 6-6 shows how D* varies with f_c for detectors which obey McAlister's law.

(b) THE OPTICAL SUBSYSTEM

The optical subsystem collects incoming radiation from the target and focuses this radiation on the detector. The optical subsystem functio in the infrared system is analogous to that of the antenna in a radar receiving system. The output of the optical detector depends solely on the amount of electromagnetic energy received from the target. In order to obtain high signal-to-noise ratios and derive maximum information from the detector output, strong target signals are required. To accomplish this there are four major requirements that the optical system must fulfill; namely, it must have (1) high resolving power, (2) large field of view, (3) small focal ratio, and (4) high optical efficiency.

(1) Resolving Power and Field of View

The optical subsystem must have resolving power consistent with the type of target to be detected. This requires that the optical system

be capable of focusing as much target radiation as possible on the detector while rejecting background radiation. Assuming the optical surfaces of the system to be designed and shaped to provide perfect imagery, resolving power is, then, limited by diffraction. This limitation is determined by the diameter of the optical system primary objective (D) and by the wavelength of the radiation being received (λ). The minimum angle of resolution is expressed as:

$$\theta_{min} = \frac{1.22}{D} \lambda \text{ radians} \tag{6-5}$$

These resolution considerations apply only when the medium in the focal plane has a resolving power at least equal to that of the optical system. In an infrared system the detecting medium and the infrared detector are synonymous. The resolving power of a detector (α) is a function of its size and of the focal length of the optical system (F). For a square detector of side A

$$\alpha = \frac{A}{F} \tag{6-6}$$

where α can alternatively be interpreted as either the resolving power or the field of view of the detector. In any system the value of α is considerably greater than that of θ; consequently the detector size and, hence, the field of view of the detector, is the factor which limits the system resolving power.

The detector field of view may be defined in terms of the solid angle (ω_d) subtended by the detector at the primary objective. For a rectangular detector of sides A and B

$$\alpha = \frac{A}{F} \tag{6-6}$$

$$\beta = \frac{B}{F} \tag{6-7}$$

$$\omega_d = \alpha \beta = \frac{AB}{F^2} \tag{6-8}$$

(2) Effective Focal Ratio

The radiation-collecting ability of the optical subsystem depends upon the ratio of the diameter of the primary objective to that of the image formed. This is more conveniently described as the ratio of the focal length of the system (F) to the objective diameter (D). This ratio is known as the "effective focal ratio" and is measured in terms of "f/n" numbers.

$$f/n = \frac{F}{D} \tag{6-9}$$

(3) Optical Efficiency

Target radiation passing through the optical subsystem is attenuated. In a refractive system, the extent of attenuation depends on the frequency of the radiation and the transmission characteristics of the various components of the optical subsystem. These components are made of materials such as germanium, arsenic trisulfide, potassium bromide and silicon. These materials do not attenuate radiation uniformly, but are characterized by a complex series of peaks and dips. The selection of the proper material, therefore, depends to a great extent on the spectral region in which the infrared system is to operate.

In addition to good transmissivity, consideration must be given to other features such as cost, susceptibility to corrosion and decomposition (especially that due to poisonous decomposition). Nonavailability of these materials in large sizes is also important since it prevents the development of systems with large apertures.

In a reflective system, the optical materials (listed in Table I) are usually coated with highly reflective surfaces. Aluminum coating material is most practical and gives reflectivity greater than 95% over most of the infrared band.

The optical efficiency of a system is determined by the product of all the reflectivity and transmissivity coefficients of the optical subsystem components. For example, in the case of the frequently applied folded reflective system shown in Figure 6-7, the optical efficiency is

$$e = r_p \, r_s \, t_d \, t_r \tag{6-10}$$

where

r_p = reflectivity of primary mirror

r_s = reflectivity of secondary mirror

t_d = transmissivity of the detector window

t_r = transmissivity of the reticle or chopper

If transmission efficiency of the infrared dome is included in Equation 6-10, it causes a reduction in the value of e.

(4) Optical Chopping

When target radiation is focused on an infrared detector having an electrical output, the output signal is in the form of voltage. The amplitude of the voltage is proportional to the radiation energy striking the detector. Depending on the time constant of the detector, the variations in voltage will correspond to the changes in radiation incident on the detector. The rate of variation frequently is in the range from 0 to 10 cycles per second. As previously stated the detector measures a difference between target radiation focused on it and the detector's own radiation level. Detector radiation level is defined by emissivity and temperature according to the Stefan Boltzmann Law (see Equation 6-12). The amplitude of the output voltage (which has typical values in the order of microvolts) must be amplified in order to be usable. Direct current (dc) amplifiers capable of raising such low magnitude signals to useful levels are characterized by instability, noise, and drift. Inclusion of "radiation

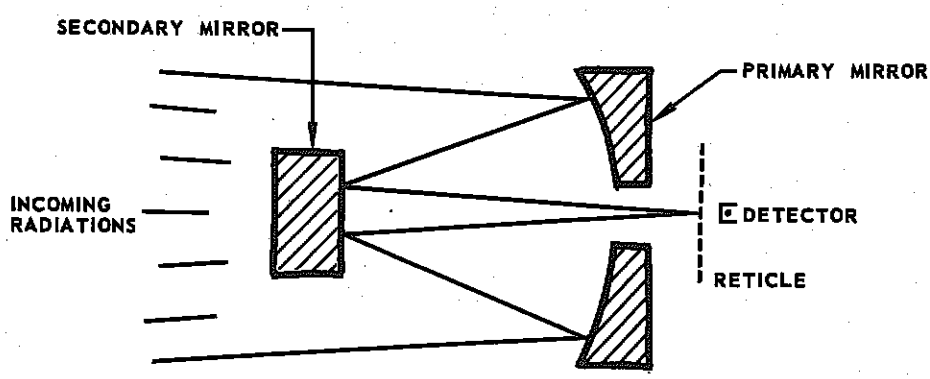

FIGURE 6-7. FOLDED REFLECTIVE SYSTEM

chopping" provides a means for deriving an alternating current detector output signal that can be amplified and processed by well established techniques. The process of "radiation chopping" is performed by a reticle which rotates in the path of radiation. The face of the reticle is etched or photo-engraved in patterns alternately opaque and transparent to infrared (see Figure 6-8). These patterns serve two purposes, that of modulating the signal and, at the same time, that of providing means for discriminating against unwanted background signals. Since reticles are only approximately 50 percent opaque, this quality affects the optical efficiency of the system accordingly. Designers have endeavored, because of this poor optical efficiency, to eliminate the need for a reticle. As a result of this effort, strip detectors (see Figure 6-9) have been developed for use in infrared systems. With a strip detector, modulation is accomplished by sweeping the collected radiation over the sensitive strips, which are finitely separated. The numerous reticle configurations are not discussed in this brief review; however, the choice of a particular reticle is determined by the system function, as well as by the characteristics of the infrared detector. The optimum chopping frequency (f_c) is a function of the detector time constant, (see Equation 6-3 and Figures 6-5 and 6-6).

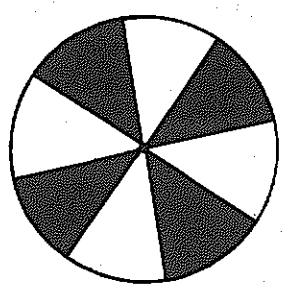

FIGURE 6-8. TYPICAL RETICLE

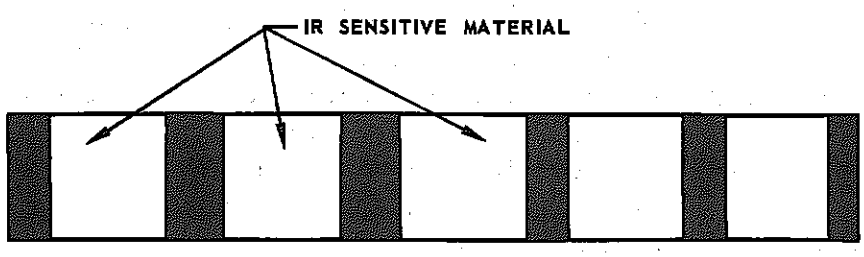

FIGURE 6-9. STRIP DETECTOR

(c) INFRARED DOMES

Infrared domes (irdomes) are generally considered an integral part of the optical subsystem, but, because of the relative importance of these components, they are considered separately here. The purpose of the irdome is to protect the infrared system from the elements. A few irdome materials and their properties are listed in Table II. These materials are adequate for domes on most subsonic and transonic carriers. For the case of a supersonic carrier, far more severe environmental conditions are encountered, as for example, when the velocity of the carrier increases. Under this condition stagnation temperature increase imposes a limit on the usefulness of any dome material as a result of thermal breakdown. The stagnation temperature effect encountered at high Mach number can be counteracted by the process of dome cooling. Dome cooling can be effected by providing a thermally conductive path from the dome front, where the temperature is highest, to the base of the dome, where the temperature is considerably lower. This thermal path may be constructed of strips with high heat conductivity placed from the apex to a ring about the base of the dome. This results in a poor optical arrangement because of the loss of effective aperture area. Another method for cooling the dome is by forcing gas (under pressure) out of a series of small holes at the dome apex. By this means a thin layer of gas is formed; the rearward flow of this gas over the dome provides an intrusive boundary layer which absorbs the energy that would otherwise heat the dome. With proper quantities of gas supplied, the dome remains at approximately the same temperature as the cooling gas. Relatively small amounts of gas are needed for adequate cooling. For example, a 6-inch diameter dome mounted on a vehicle traveling at Mach 7 at an altitude of 60,000 feet could be cooled with a gas supply of approximately two pounds per minute.

An optimum infrared system would have no irdome and, hence, no dome-reradiation to degrade system performance. Research on a domeless system being conducted by the Naval Supersonic Laboratory uses a technique which is similar to the developments in the intrusive boundary layer method described previously for dome cooling. Instead of gas being forced out the apex of the dome, however, the gas is forced through curved jets around the circumference of the optical unit itself. An artificial boundary layer that protects the optical unit at any velocity and angle of attack can be formed by regulating the velocity of the gas flow through the curved jets. The transmissivity of this type of system is considerably higher than for comparable systems employing irdomes.

TABLE II IRDOME MATERIALS

Material	Cutoff (Micron)	Spectral Transmissivity	Degrading Property
Sapphire ($AL_2\ 0_3$)	5	0.85	
Periclase (Mg0)	7	0.80	
Potassium Bromide (KBr)	20	0.90	Hygroscopic
Servofrax ($AS_2\ S_3$)	12	0.70	
Fused Silica ($Si\ 0_2$)	4	0.90	
Silicon (Si)	7	0.55	

SECTION 3 — TYPES OF INFRARED SYSTEMS

(a) SEARCH SYSTEMS

The primary function of the air-to-air infrared search system is target detection. This may be accomplished by using the largest practical field of view in order to detect the greatest number of targets. Interceptor fire control systems may use infrared search systems to detect attacking aircraft; however, infrared search-track systems are better suited to such applications.

The major problems encountered in the development of an infrared search system arise as a result of the requirement to search a large field of view with speed, resolution, and sensitivity for target detection. If a single detector is used, the system resolution requirements should be great enough to permit detection of distant targets. To scan a large field of view in a relatively short time, the amplifier bandpass must be wide. Increase in amplifier bandpass, however, is accompanied by an increase in noise level, which degrades system resolution. Multiple detectors allow coverage of a large field of view in a period which is inversely proportional to the number of detectors employed. The matching of detector characteristics is not a particularly critical requirement, since a search system need only indicate the presence of targets.

(b) TRACK SYSTEMS

Tracking systems may be classified in two categories, according to the method used in processing the input signals, namely, chopped or unchopped, and manual or automatic. Chopped systems are generally operated automatically. The chopper or reticle in the tracking system performs two functions: (1) It selectively chops the incoming target radiation so as to discriminate against the background radiation. In the space domain, this amounts to a space filter which attenuates the frequency components contributed by the background with respect to those contributed by the target. The reticle may also provide target positional information that can be used by the control system to orient the tracker. (2) In the unchopped system, the target indication which is presented on the pilot's display is used to position the tracker by manual controls.

(c) SEARCH-TRACK SYSTEMS

Search-track systems incorporate characteristics of both search and track systems. Such systems must, in general, be capable of searching broad fields of view and tracking a target with reasonable accuracy. Two types of search-track systems exist. The first system type consists of an array of detectors used for the search phase, and a single detector (one of those in the array or a separate one) for the track phase. The same optical system is used for both the search and track phases. The second type of search-track system uses only one detector.

SECTION 4 — FACTORS AFFECTING THE INFRARED SYSTEM

(a) ATMOSPHERIC TRANSMISSION

The amount of radiation reaching the detector depends upon the intensity and spectrum of the source, the spectral response of the detector, and the transmission of the intervening media. Intervening media include the optical system described previously and the atmospheric path. The effect of the atmosphere on the target radiated energy is a combination of attenuation and scattering. The attenuation is due mainly to the amount of precipitable water vapor and carbon dioxide in the path of radiation. The scattering is due to haze (fog, clouds, smoke, and dust) which may be present in the radiation path. Transmission through water vapor and carbon dioxide has been approximated empirically for various path lengths.[2]

2. See Proceedings of IRIS-ONR-#1 and #2 in Vol #1 - 1956

At altitudes greater than 40,000 feet, water vapor absorption and haze scattering are negligible. At lower altitudes, atmospheric absorption may be very critical, especially where the radiated energy occurs at wavelengths corresponding to the water vapor and carbon dioxide absorption bands, as is the case in the detection of jet plume radiation. A very rough transmission spectrum is shown in Figure 6-10. Transmission through haze varies in an exponential manner, mainly as a function of visibility.

$$\frac{I}{I_o} = e^{-\alpha \lambda w} \qquad (6\text{-}11)$$

where I = fractional transmission

w = path of radiation

$\alpha \lambda$ = attenuation coefficient due to haze

$$\alpha \approx \frac{3.92}{V}$$

where V, the visibility, is the distance at which a dark object can just be distinguished against the horizon. Ozone absorption is another impediment to infrared radiation. Since it occurs primarily in the main ozone layer at an altitude of 80,000 feet, it need only be considered if the energy to be detected traverses this layer.

Because of its pernicious nature, the effect of haze attenuation should be taken into account in attempting to design for long IR detection ranges.

(b) TARGET RADIATION

Target radiation is the most important factor required for the determination of infrared detection range. The radiation of a jet-propelled target emanates mainly from three sources:

(1) Tail pipe
(2) Exhaust gas
(3) Aerodynamic heating

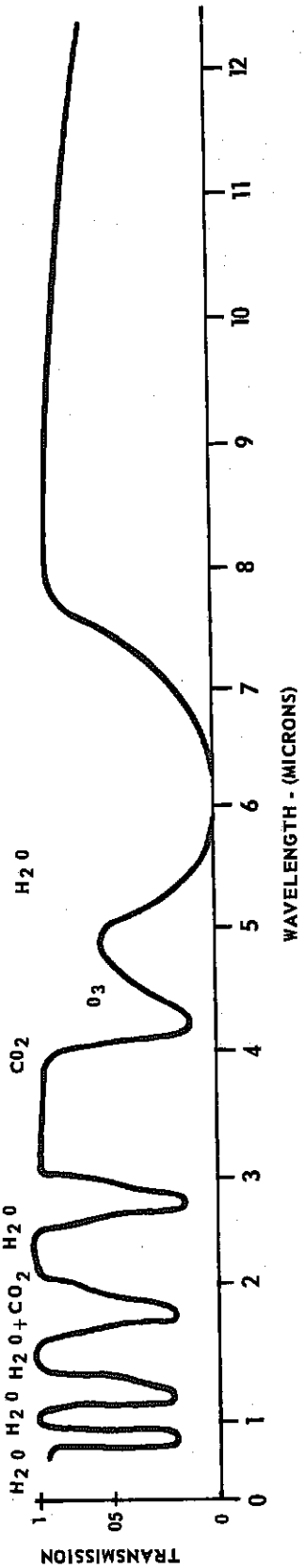

FIGURE 6-10. ATMOSPHERIC TRANSMISSION IN THE INFRARED

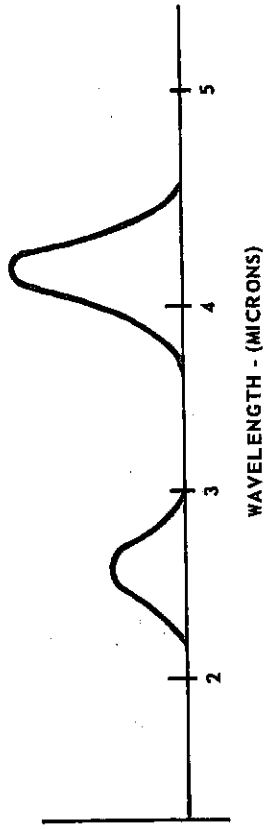

FIGURE 6-11. PLUME RADIATION

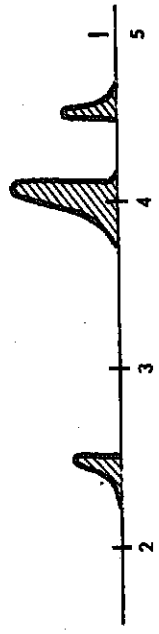

FIGURE 6-12. DETECTIBLE PLUME RADIATION

For rear hemisphere detection, the hot metal parts around the tail pipe and the exhaust nozzle supply the major portion of detectible energy. Radiation from the listed sources is comparable to that of gray bodies, since both obey physical laws which allow their computation with a fair degree of accuracy. For example, assume the average temperature of a tail pipe (T) to have an emissivity (ϵ). The total emissive power is expressed by the Stefan-Boltzmann law:

$$W = \epsilon \sigma T^4 \tag{6-12}$$

where σ = Stefan-Boltzmann constant = 5.67×10^{-12} watts $cm^{-2} {}^{o}K^{-4}$.

The intensity of radiation or steradiancy = $\frac{W}{\pi} \frac{\text{watts cm}^2}{\text{steradian}}$. Assume the area of the source to be A cm, the total radiated power is $\frac{WA}{\pi}$, which represents the power radiated over the entire spectrum. The detectible power $W(\lambda)$ is a function of the spectral radiation of the target (J_λ), the spectral response of the detector (D_λ), the spectral transmission of the atmosphere (T_λ) and the spectral transmission of the optical system (O_λ) or

$$W(\lambda) = \int_{\lambda_1}^{\lambda_2} J_\lambda \, T_\lambda \, D_\lambda \, O_\lambda \, d_\lambda \tag{6-13}$$

$W(\lambda)$ is usually approximated by assuming constant values over narrow bands for the various transmission coefficients. Forward hemisphere detection depends mainly on the amount of energy radiated by the jet exhaust plume. This plume does not radiate as a gray body but as a selective radiator, which means that the energy is radiated in discrete bands. For the case of a jet plume, these bands coincide with the emission bands of water vapor and carbon dioxide, which are the main constituents of the plume. The water vapor emission band is centered about 2.7 micron wavelength and that of carbon dioxide about 4.3 microns. Unfortunately these two spectral bands correspond to regions where atmospheric absorption is quite severe. By superimposing the plume emission spectrum (Figure 6-11) over the atmospheric transmission spectrum (Figure 6-10), the detectible energy is reduced to the extent that it makes forward hemisphere detection a very difficult task (see Figure 6-12). The ratio of detectible energy in the 4.3 micron region to that in the 2.7 micron region is about 5. If boron is added to

the fuel, that ratio might be somewhat improved, since the boron emission band is centered about 4.8 microns. Speeds greater than Mach 2 require afterburner operation. At speeds greater than Mach 3, the temperature of the exhaust gases decreases sharply due to the ram pressure which causes an increase in the ratio of pressure before gas expansion (P_1) to the pressure after gas expansion (P_2). For isentropic expansion

$$\frac{T_1}{T_2} = \frac{(P_1)^{\frac{\gamma-1}{\gamma}}}{P_2} \tag{6-14}$$

where

T_1 = temperature of gas before expansion

T_2 = temperature of gas after expansion

γ = gas constant

At a speed of Mach 3, $\frac{P_1}{P_2}$ is approximately 27, assuming γ of 1.3

$$\frac{T_1}{T_2} = 2.15$$

so that the exhaust temperature is about half that of the gases in the afterburner. At speeds less than Mach 2, the use of the afterburner may greatly increase the target radiation, depending on the wavelength of operation of the detection system. In the short wavelength region (2μ to 3μ), afterburners increase the detectible energy by a factor of about 20, and in the long wavelength region (3μ to 5μ) the increase is about 10 times.

SECTION 5 — INFRARED SYSTEM EVALUATION

The performance of an air-to-air infrared system is most often evaluated on the basis of its ability to detect targets. In turn, the detecting ability may be optimized by an evaluation of the detection against a given target. No method exists whereby infrared detection range can be

predicted with any degree of accuracy. Even in a case where all the parameters involved are known exactly, the effect of atmospheric absorption on target radiation introduces substantial errors. A still larger source of errors could also be created by the omission of a seemingly unimportant parameter. The method presented herein represents a combination and modification of methods that have been developed for determining an infrared range equation. The amount of target radiation (W_d) focused on an infrared detector is a function of the available flux density (F), the diameter of the aperture of the optical system (D), and the optical efficiency of system (e).

$$W_d = \frac{\pi D^2 eF}{4} \text{ watt/steradian} \tag{6-15}$$

In turn, $F = \frac{J \tau}{R^2 \pi}$, where J is the energy radiated by the target in watts, τ is the spectral atmospheric transmission, and R is the target range. W_d can therefore be expressed as

$$W_d = \frac{D^2 eJ \tau}{4R^2} \tag{6-16}$$

The output signal of the detector (S_d) is a function of its responsivity (ρ) expressed in volt/watt

$$S_d = \rho W_d \text{ volts} \tag{6-17}$$

The detector noise (N_d) which in general limits the performance of the system is a function of the detector output amplifier and width

$$N_d = n_1 \sqrt{\Delta f} \text{ volts} \tag{6-18}$$

where n_1 is the noise per unit cycle bandwidth. The signal to noise ratio of the system is then

$$\frac{S_d}{N_d} = \frac{\rho W_d}{n_1 \sqrt{\Delta f}} = \frac{\rho D^2 eJ \tau}{4 n_1 R^2 \sqrt{\Delta f}} \tag{6-19}$$

The noise equivalent input (NEI) is defined as the ratio of unit cycle bandwidth noise to the product of detector responsivity and detector area (A_d)

$$NEI = \frac{n_1}{\rho A_d} \quad \frac{\text{watts}}{\text{cm}^2 \text{ cycle}} \tag{6-20}$$

NEI is sometimes referred to as the detector effective sensitivity.

The resolution of the system (r) is a function of detector size and focal length F_ℓ. It is represented by the angles subtended by the width and breadth of the detector at the primary optics of the system. Assuming a square detector

$$r = \frac{\sqrt{A_d}}{F_\ell} = \frac{\sqrt{A_d}}{D\frac{f}{n}} \text{ radians} \tag{6-21}$$

where f/n is the focal ratio of the optical system.

$$\frac{f}{n} = \frac{F_\ell}{D} \tag{6-22}$$

Since the detector's field of view (also called the instantaneous field of view) covers r^2 (radians squared), the total field of view ($\alpha\beta$) is covered by $\frac{\alpha\beta}{3300r^2}$ elements, where $\alpha\beta$ is expressed in degrees. Assuming a scanning rate of P frames per second or pr^2/sec with a scanning efficiency (η), the total field of view will be covered in $\frac{\alpha\beta}{3300pr^2\eta}$ seconds. This expression is called the total frame time (t_f). If M detectors are used, the frame time is reduced to $\frac{t_f}{M}$ and

$$r^2 = \frac{\alpha\beta}{3300p\eta Mt_f} = \frac{A_d}{D^2\left(\frac{f}{n}\right)^2} \tag{6-23}$$

or

$$A_d = \frac{D^2 (f/n)^2 \alpha\beta}{3300 p \eta M t_f} \tag{6-23A}$$

Substituting A_d into the expression for NEI

$$NEI = \frac{3300 n_1 p \eta M t_f}{\rho D^2 \left(\frac{f}{n}\right)^2 \alpha\beta} \tag{6-24}$$

and

$$\frac{S_d}{N_d} = \frac{825 e J \tau p \eta M t_f}{(NEI) \left(\frac{f}{n}\right)^2 \alpha\beta r^2 \sqrt{\Delta f}} \tag{6-25}$$

from which

$$r = 15 \times 10^{-5} \sqrt{\frac{e J \tau p \eta M t_f}{\frac{S_d}{N_d} (NEI) \left(\frac{f}{n}\right)^2 \alpha\beta \sqrt{\Delta f}}} \text{ n. mi} \tag{6-26}$$

where

e = optical efficiency
J = target radiation (watts/ster)
τ = atmospheric transmission
P = number of frames scanned per second
η = scanning efficiency
M = number of detectors
t_f = frame time (seconds)
Sd/Nd = signal to noise ratio of detector
NEI = noise equivalent input (watts/cm^{2}cps)
f/n = focal ratio of the optical system
α = azimuth coverage (degree)
β = elevation coverage (degree)
Δf = amplifier bandwidth (cycles)

CHAPTER VII

ANALYSIS OF THE FIRE CONTROL SYSTEM

SECTION 1 — INTRODUCTION

The block diagram of the essential elements of the fire control system is shown in Figure 7-1. During the attack phase, the fire control system must perform two fundamental operations. First, it must supply the angle information to the interceptor in order to turn the interceptor onto a proper lead collision course for missile launch. Secondly, the fire control system must make a continuous determination of the time remaining until missile impact and supply this information to the armament and armament auxiliaries. The first information yields a required output which is referred to as the steering information; the second determination yields the so-called time to go information. Mathematically, the outputs

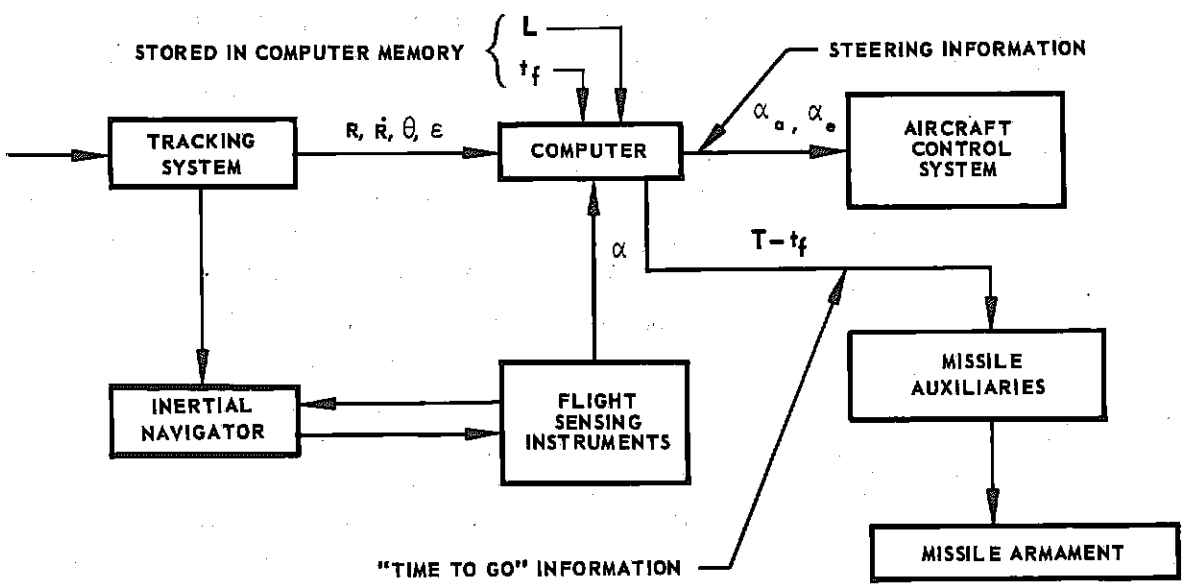

FIGURE 7-1. ESSENTIAL ELEMENTS OF THE COMPLETE FIRE CONTROL SYSTEM

required are the steering information α_a, which is the angle about the azimuth axis through which the fighter must be turned; and α_e, or the angle about the elevation axis through which the fighter must be turned. Similarly the output required for the time to go until impact is T. The inputs to the fire control system shown in Figure 7-1 include R, the present range to the target; $\dot{R}$, the present range rate; L, the distance the missile will travel relative to the fighter; θ, the azimuth of the radar; ϵ, the elevation angle of the radar; and α, the angle of attack of the interceptor. The quantities, R, $\dot{R}$, θ, and ϵ are supplied by the fire control system radar. The quantity L is a preset constant whose value depends upon the missile used, and α is a parameter measured by the aircraft instrumentation. Numerous other input and output signals exist but the aforementioned are basic. For the sake of convenience, the computer equations derived in Chapter 5 are repeated here and numbered 7-1 through 7-3.

$$O = R + \dot{R}\,T - L \cos\theta \cos\epsilon \tag{7-1}$$

$$\alpha_a = \omega_a T - \frac{L}{R} \sin\theta \tag{7-2}$$

$$\alpha_e = \omega_e T + \frac{L}{R} (\cos\theta \sin\epsilon + k_j \alpha) \tag{7-3}$$

Figure 7-1 is essentially an open-ended servo system since the error in the angle through which the interceptor has turned is not used in a feedback servo loop to correct the input. However, when the interceptor does turn through the specified angle, the weapon aiming error should be essentially equal to zero, or be at least within the tolerable launching error of the missile. A sketch of the estimated missile aiming error as a function of the time to go is shown in Figure 7-2. The proper time for missile firing is at $T = t_f$, which is the optimum time of flight of the missiles. Notice in Figure 7-2 that there exists an acceptable firing period, t_f, where the launching errors are within the allowable tolerance of the missile. The missile may be fired in a straight line lead-collision course which is best suited for projectiles that are fired in almost instantaneous salvos. A diagram of a typical lead collision attack is shown in Figure 7-3. A detailed discussion of this type of course is found in Chapter 5. In this type of course, the line of sight from the interceptor to the target is continuously rotating. There is actually only one point on the interceptor trajectory which is at the ideal range (corresponding to $T = t_f$) for missile firing. This point is extended into an

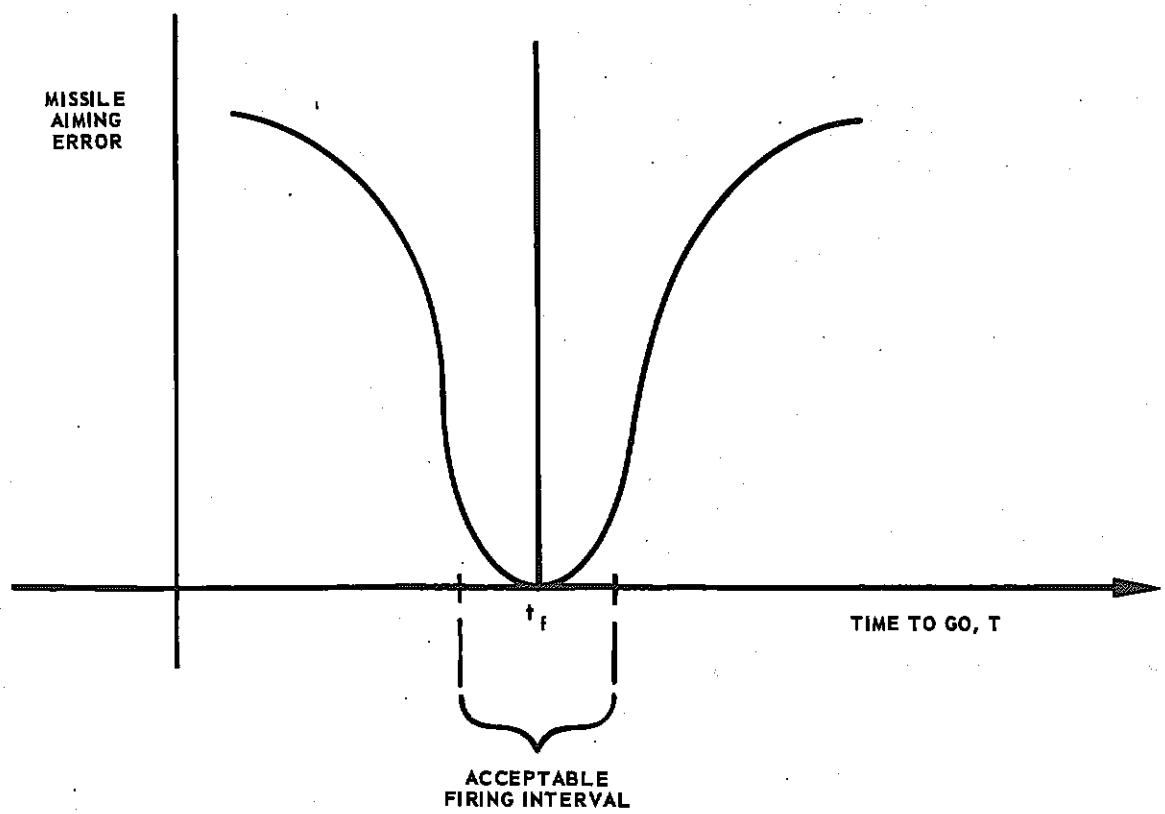

FIGURE 7-2. MISSILE AIMING ERROR AS A FUNCTION OF TIME TO GO TO IMPACT

interval as shown in Figure 7-2 because of tolerances on missile launching error. The width of the interval also depends on advantage of missile velocity over interceptor velocity, because it is this difference in velocity which causes a pure missile collision course to differ from a pure interceptor collision course. If the missile velocity advantage over the interceptor is small, the curve in Figure 7-2 becomes broad and enlarges the acceptable firing interval. This argument follows qualitatively since the smaller the missile velocity advantage, the closer the interceptor lead collision course approaches a pure collision course. This results in a lower angular rate of the line of sight during the attack phase.

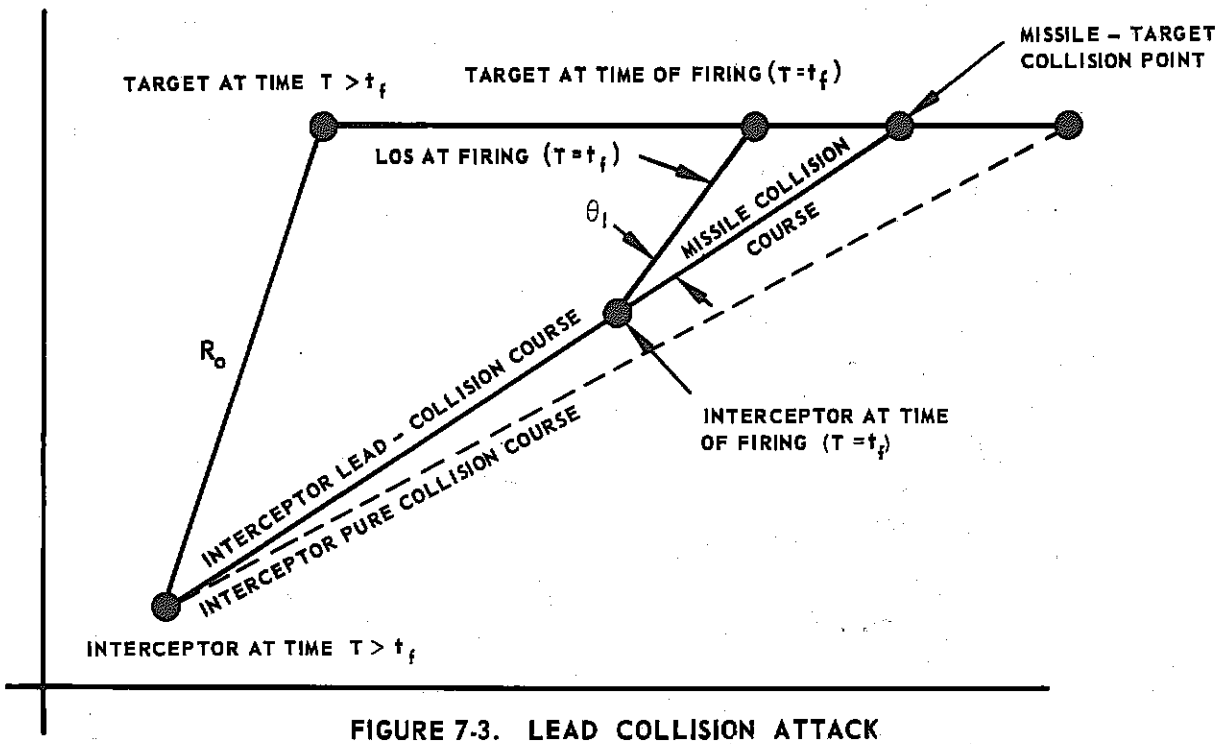

FIGURE 7-3. LEAD COLLISION ATTACK

Since the basic block diagram of a system has been described, it is necessary to choose optimum parameters in order to maximize the probability of weapon kill. Methods for finding solutions to equations which yield some of the fundamental parameters are outlined in this chapter. The actual system is complex and requires that many simplifying assumptions be made in order for the analysis to be conveniently developed. The quantitative results provide starting points for the experimental design. Final parameter optimization of the calculations is determined experimentally. The various analyses to be described are divided according to the blocks shown in Figure 7-1. Many of the more complex analytical problems are associated with the tracking system.

SECTION 2 — TRACKING SYSTEM RADAR ANALYSIS

(a) INTRODUCTION

The block diagram of an example tracking system design is shown in Figure 7-4.

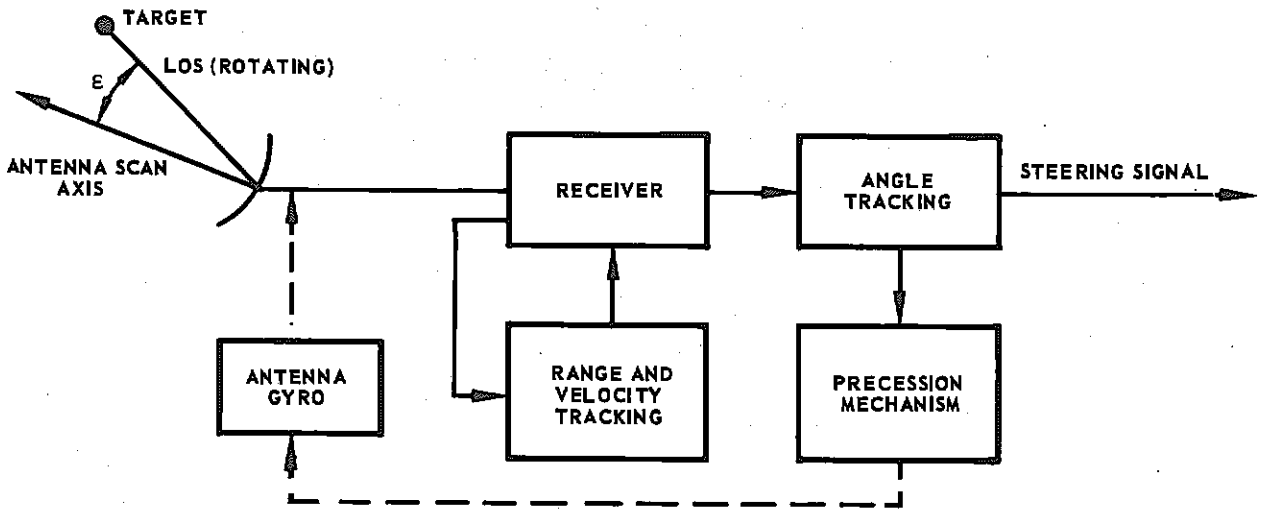

FIGURE 7-4. OVERALL TRACKING SYSTEM LOOP

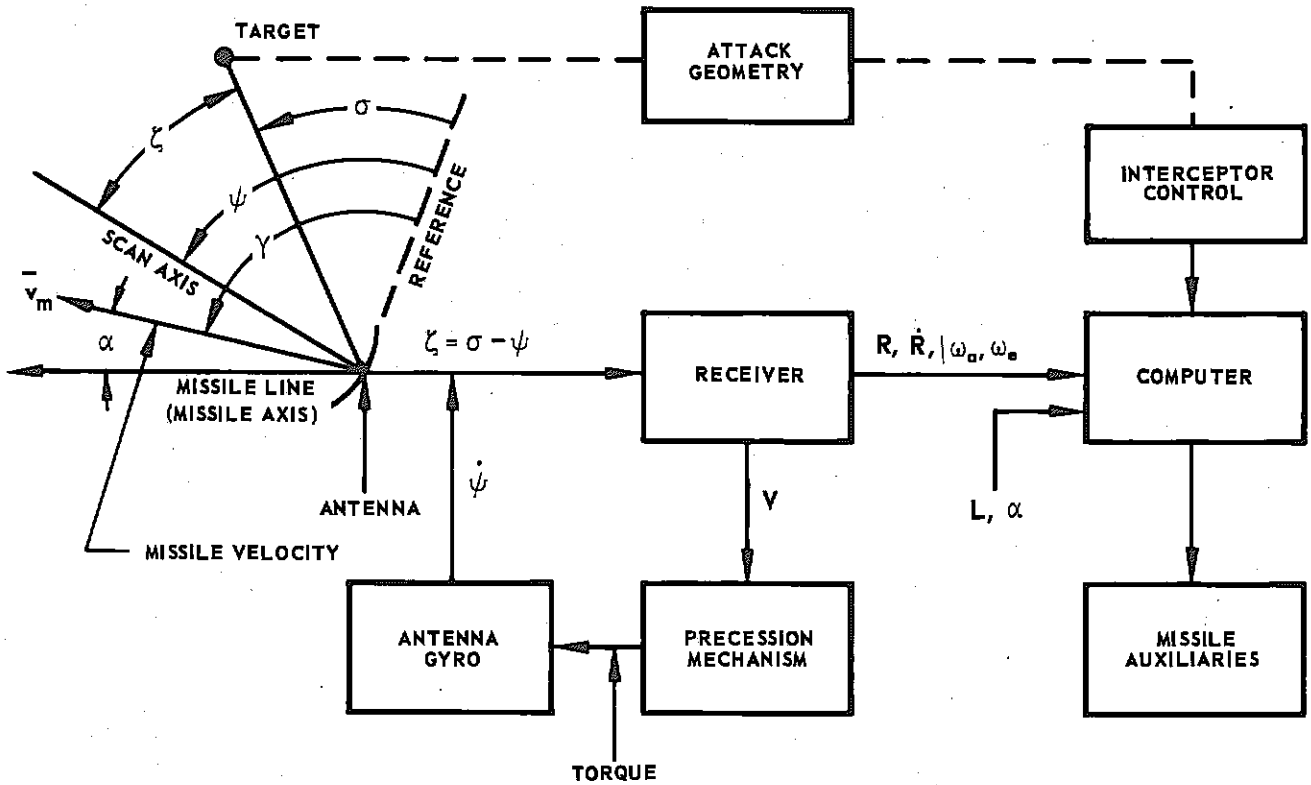

FIGURE 7-5. FUNCTIONAL BLOCK DIAGRAM OF TRACKING SYSTEM

For the present a conical scanning system is assumed. Later in this chapter a description is given of a possible monopulse lobing system for use in place of conical scan. As indicated in Figure 7-5, the fundamental outputs of the radar are range, velocity, and the angular velocity components in the azimuth and elevation planes. Range is measured by the range tracking circuit, range rate is measured by the velocity tracking circuit, and the components of the angular turning rate of the line of sight are measured by the angle tracking system of the radar. In connection with the basic tracking loop, a discussion of auxiliary loops such as AGC and AFC is included.

(b) THE ANTENNA TRACKING LOOP

The antenna tracking loop aligns the scan axis (for a conically scanning system) with the line of sight. The blocks entitled receiver, prececession mechanism, gyro, and antenna, in Figure 7-5, are the components of the antenna tracking loop.

A detailed block diagram of the antenna tracking loop appears in Figure 7-6.

The incoming signal, which contains the position information (the angle between the line of sight and the scan axis), is carried as amplitude modulation on the pulsed carrier because of conical scan. This train of rf pulses passes into the duplexer and first detector where the rf is mixed with the local oscillator frequency to obtain an intermediate frequency. The IF signal is amplified in the IF amplifier and detected by the second detector to obtain train of video pulses. The video pulses, still amplitude modulated by the scan modulation, are amplified in the video amplifier and gated in range by the range gate, the latter having been developed by the range tracking servo. The output of the video amplifier goes directly to the velocity tracking loop. The output video and the voltage controlled oscillator output are differenced to yield a frequency-at-or-near the center frequency of the velocity gate filter. The velocity gate filter gates the signal in velocity. The output of this filter, or gate, goes to velocity track and also to the error detector as shown. The error detector demodulates the scan modulated video signal and amplifies the demodulated scan signal for use by the error phase detector. The latter, in turn, compares the phase of the scan signal with the interceptor radar antenna reference voltages in order to sense the direction and magnitude of the vector characterizing target position. The output of the phase detector resolves this error detector output into two signals, namely, the azimuth and elevation errors.

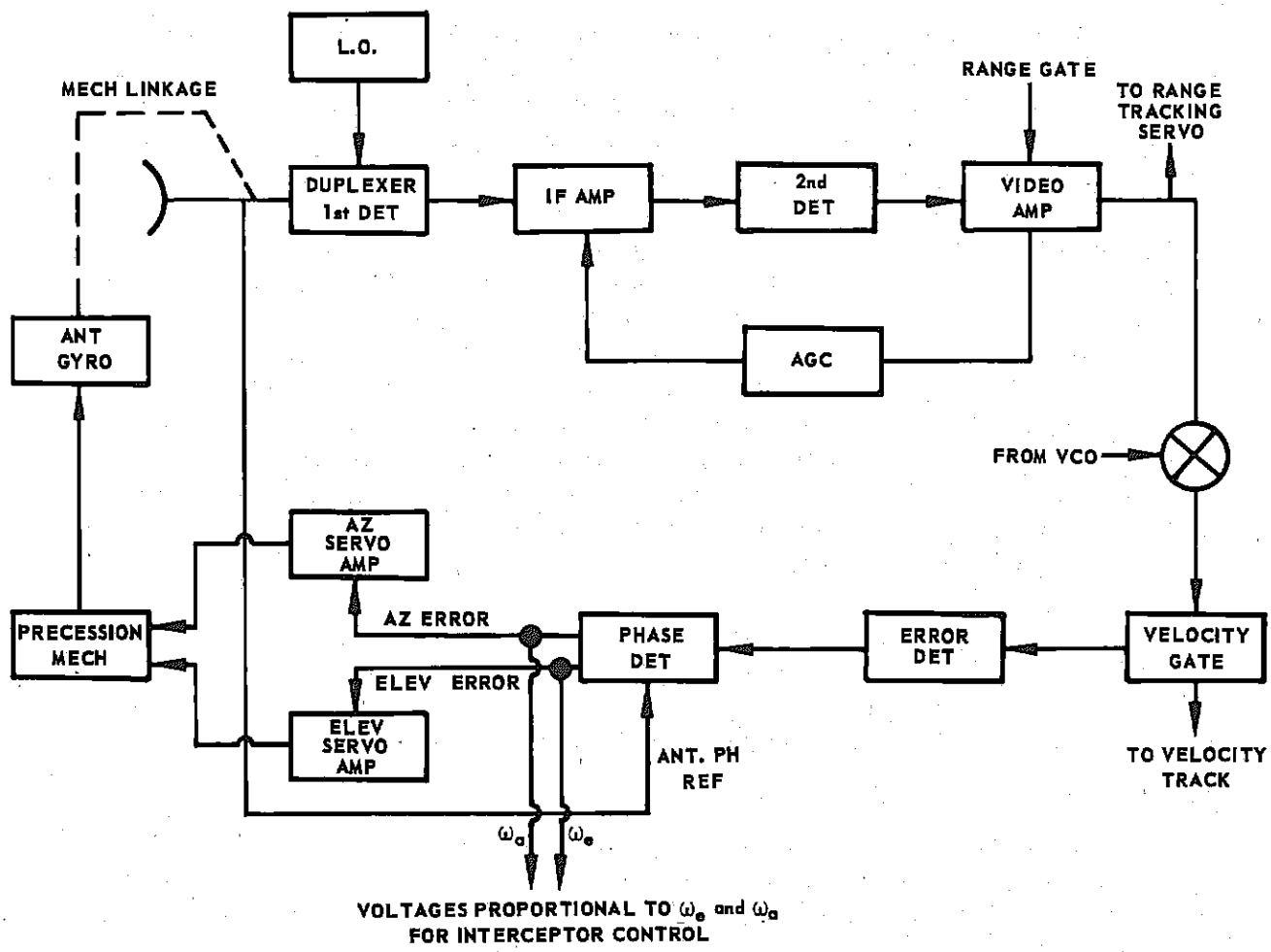

FIGURE 7-6. BLOCK DIAGRAM OF ANTENNA TRACKING LOOP

The azimuth error, which is a slowly varying dc signal, is used to control the precession mechanism in azimuth. Similarly, the elevation error output of the phase detector is amplified by the elevation servo power amplifier and used to control the elevation precession mechanism.

The precession mechanism develops torque which precesses the antenna gyro in a direction which aligns the scan axis of the antenna with the line of sight. The antenna gyro spin axis should be aligned with the antenna scan axis and the gyro coupled to the antenna.

The output of the video amplifier drives the AGC unit which in turn develops AGC voltage for control of the IF amplifier gain. Since the azimuth and elevation error voltages are proportional to the components of the angular rate of the scan axis, they are also proportional (except for the tracking error) to the angular rate of the LOS. The computer inputs ω_a and ω_e can be taken off as shown, from the phase detector output. Alternately, these outputs may be directly measured by potentiometers mounted on the antenna or antenna gyro. Conical scanning may be produced by offsetting the antenna paraboloid with respect to the gyro spin axis and scanning the paraboloid or, alternately, the paraboloid, or dish, can remain fixed and the feed offset with respect to the dish plane. In the latter case, conical scan is produced by spinning the feed. Angle information may be obtained by other means such as phase shift scanning, interferometer radar and monopulse radar. A discussion of these schemes will be included in this chapter. A diagram of the geometry used in connection with the antenna is shown in Figure 7-7.

In a conically scanning system, if the scan axis is not aligned with the target line of sight the received signal is amplitude modulated by a periodically varying wave whose fundamental harmonic is the scan frequency, ω_s. This scan modulation contains the angular information required for tracking, as shown in Figure 7-8.

In Figure 7-8a, σ is the angle between the line of sight and an inertial reference; ψ is the angle between the scan axis and the same inertial reference. The difference in these angles $\sigma - \psi$ is the tracking error. The vector $\rho e^{\gamma\phi}$ is drawn perpendicularly from the scan axis to the target. A plane perpendicular to the scan axis and containing this vector represents the scan plane. A horizontal (left, right) axis and a vertical (up, down) axis are defined in this plane. The angle ϕ is measured relative to the left-right axis. The range to the target is approximately R. The magnitude ρ is proportional to ζ for small ζ and large R, in fact

$$\rho \cong R\zeta \tag{7-4}$$

Figure 7-8b indicates that the maximum intensity returned occurs when the line of sight and the beam axis are closest, and that the minimum intensity occurs when the line of sight and the beam axis are farthest apart. Since the returned intensity varies periodically at the scan frequency, the amplitude of the returned r_f signal also must vary periodically.

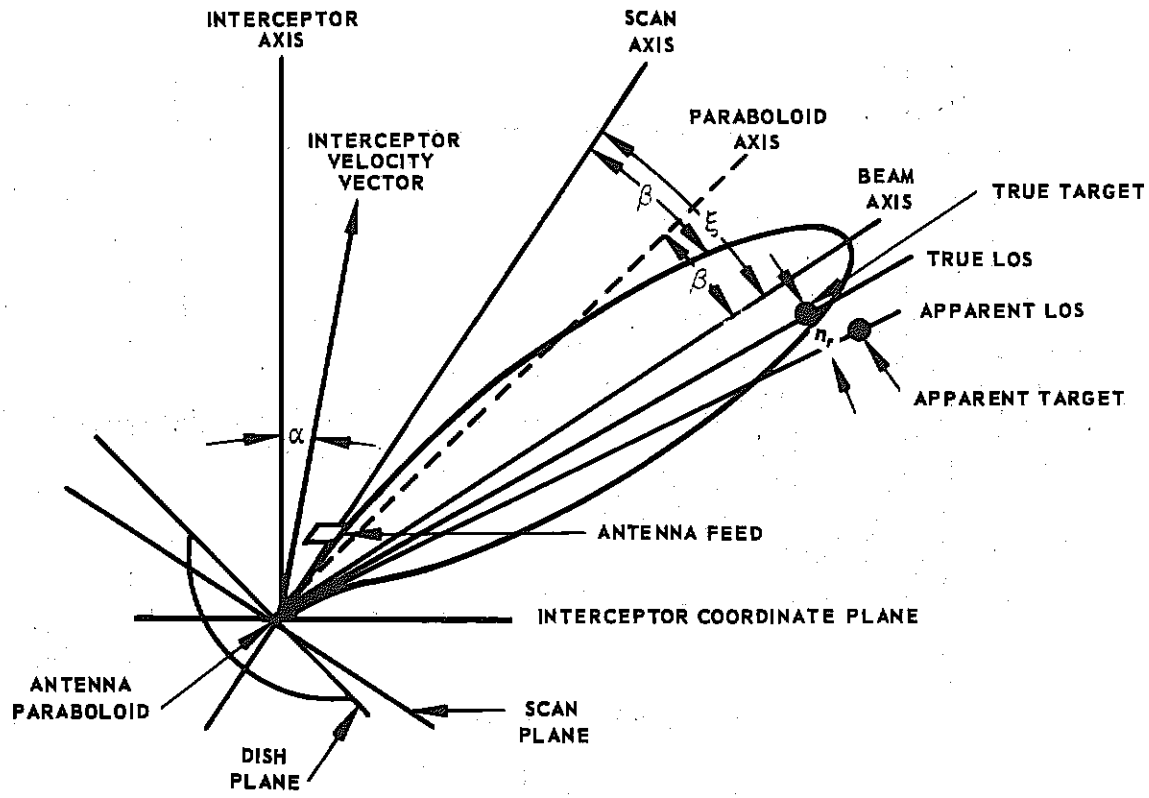

FIGURE 7-7. ANTENNA REFERENCE ANGLES AND GEOMETRY

Let the antenna beamwidth be β, and ξ the squint angle. It can be shown that the maximum linear range in slope of the first harmonic versus error angle occurs when the beamwidth is roughly twice the squint angle. Thus

$$\beta \cong 2\xi \tag{7-5}$$

If the approximation of 7-5 holds, the crossover point on the lobes in Figure 7-8b is approximately the lobe half-power point. Thus, when the target lies on the beam axis, maximum modulation return occurs; when it lies on the scan axis, minimum return occurs. In Figure 7-9, the plot of 7-8b is redrawn in cartesian coordinates. In Figure 7-9 the solid line denotes the beam pattern at an instant when the signal return is at

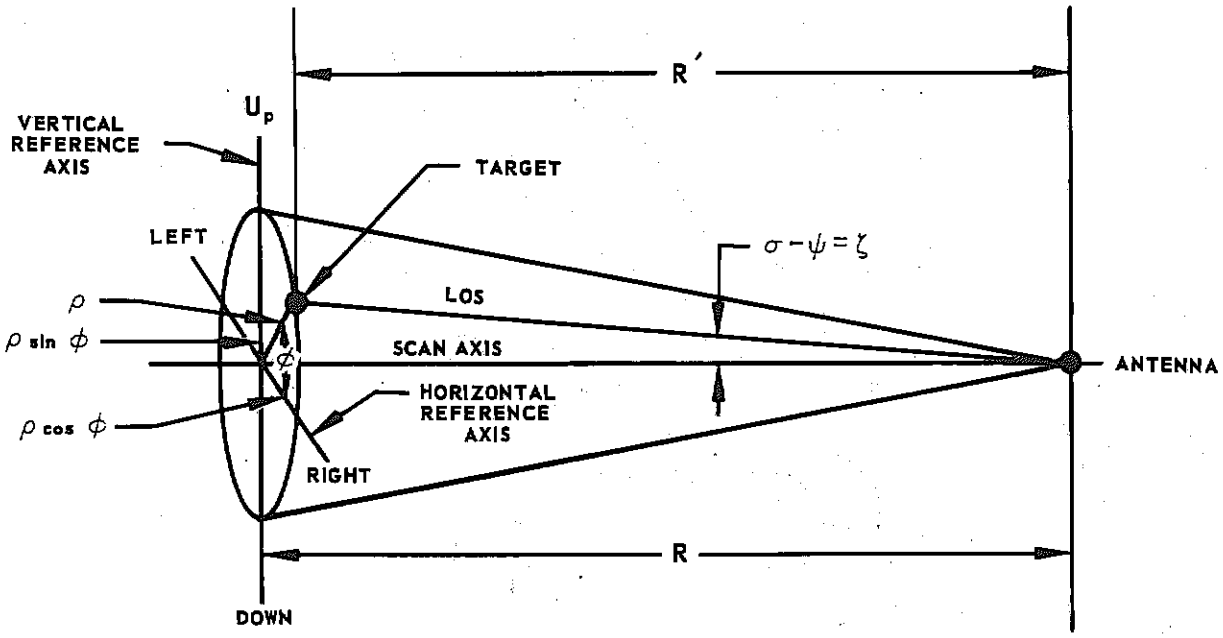

(a) SCAN PLANE GEOMETRY

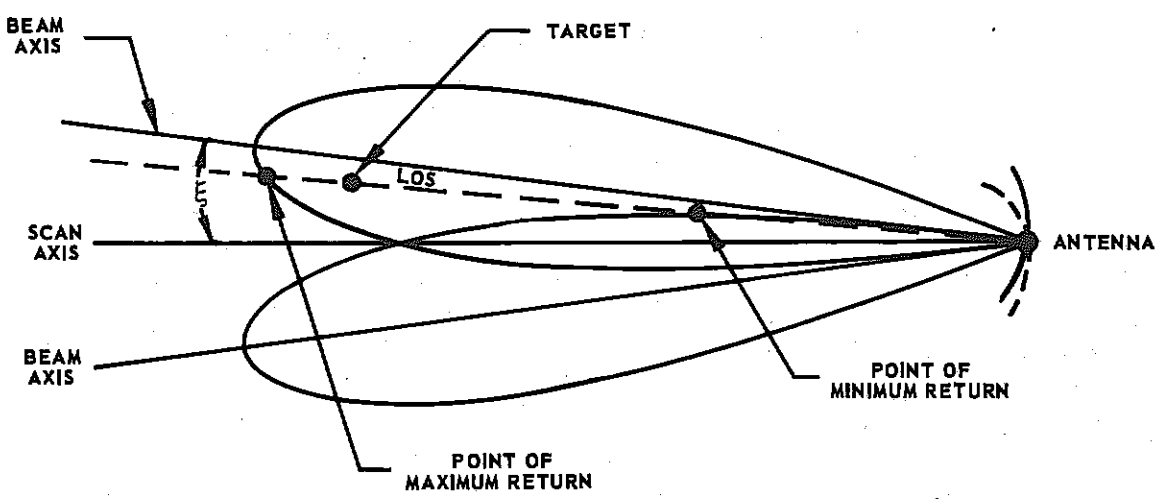

(b) ANTENNA PATTERN GEOMETRY

FIGURE 7-8. SCAN PLANE GEOMETRY AND ANTENNA PATTERN

maximum, namely point a, and the dashed line is the position of the beam one-half scan cycle later when the signal is at a minimum, namely point b. Since only the motion of the beam axis relative to the line of sight is of interest, consider the beam axis to remain stationary and the line of sight to move from x to y in one half of a fixed scan cycle. In other words, the returned intensity is the same as if the target moved from T to T' in one half of a scan cycle. Thus, A is the average return over a scan cycle, where A is the rf amplitude at the crossover C.

If the target travel, ab, is small compared to A, the rate of change of intensity is nearly linear from T to T' and CT = CT'. Let the change in returned rf signal voltage a to b be a fraction, 2m (the modulation range), of the average return A. The return thus varies periodically from (A + mA) to (A - mA), which is the definition of amplitude modulation of an rf carrier. If 2m is much less than A and if the rf carrier

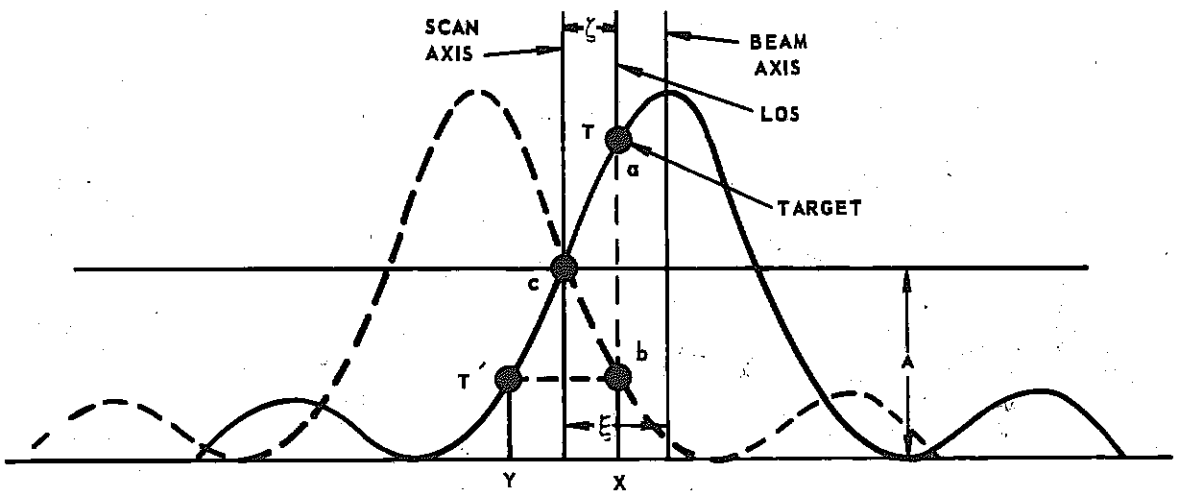

LEGEND:

——— BEAM PATTERN AT INSTANT WHEN SIGNAL RETURN IS AT MAXIMUM, POINT a

– – – – POSITION OF BEAM ½ SCAN CYCLE LATER WHEN SIGNAL RETURN IS AT A MINIMUM, POINT b

FIGURE 7-9. ANTENNA PATTERN GEOMETRY IN CARTESIAN COORDINATES

is a continuous wave of frequency ω_c and amplitude A, the returned rf voltage is

$$E = A\left[1 + m\cos(\omega_s t + \phi)\right]\cos\omega_s t \qquad (7\text{-}6)$$

where

ω_c is the rf carrier frequency

ϕ is the phase of the scan modulation

m is the modulation index

Of course, the actual radar carrier is a pulsed rf wave, not a continuous wave. Ordinarily, when the pulse repetition frequency is much greater than the scan frequency, the envelope of the video pulse train is the same as the envelope of equation 7-6. Equation 7-6 may be written as

$$E = A\cos\omega_c t + A_s(t)\cos\omega_c t \qquad (7\text{-}7)$$

$A_s(t)$ is the scan component of the modulating function

$$A\left[1 + m\cos(\omega_s t + \phi)\right] \qquad (7\text{-}8)$$

and is defined by

$$A_s(t) = V_s\cos(\omega_s t + \phi) \qquad (7\text{-}9)$$

where

$$V_s = A \cdot m \qquad (7\text{-}10)$$

$A_s(t)$ in Equation 7-9 is referred to as the error signal. The phase of the target vector in the scan plane, relative to the left-right axis, is ϕ. The maximum return or peak of the sine wave occurs when the beam axis lies in the plane of the line of sight and the scan axis, and when the angle between the line of sight and the beam axis is a minimum. The minimum return or trough of the sine wave occurs when the beam axis lies in the same plane, but with a maximum angle between the line of sight and the beam axis. If a reference sine wave is also generated and reaches its maximum when the beam axis intersects the left-right horizontal reference

axis in Figure 7-8a, then the phase of the error signal relative to this reference wave is ϕ. Two references can be generated by coils, nominally mounted at the ends of the left-right, up-down axis in the scan plane. The reference coils are not actually at the ends of these axes unless the scan axis and the interceptor axis coincide. The modulating function of Equation 7-8 and the effect of nonlinearties in producing harmonics of the scan frequency is discussed in the appendix. It is shown that a plot of the modulation factor m, versus error angle, ζ, is a discriminator-like curve whose peaks occur at the squint angle from crossover. Refer to Figure 7-10.

Figure 7-10 is a plot of the first harmonic modulation factor only; higher harmonic plots are similar in shape but of greatly reduced slope. Let the slope of $m(\zeta)$ in the region about $\zeta = 0$ be b_o. It is shown that

$$b_o = \frac{V_o'}{A} \tag{7-11}$$

where

$$V_o' = \frac{dV(0)}{d\theta}$$

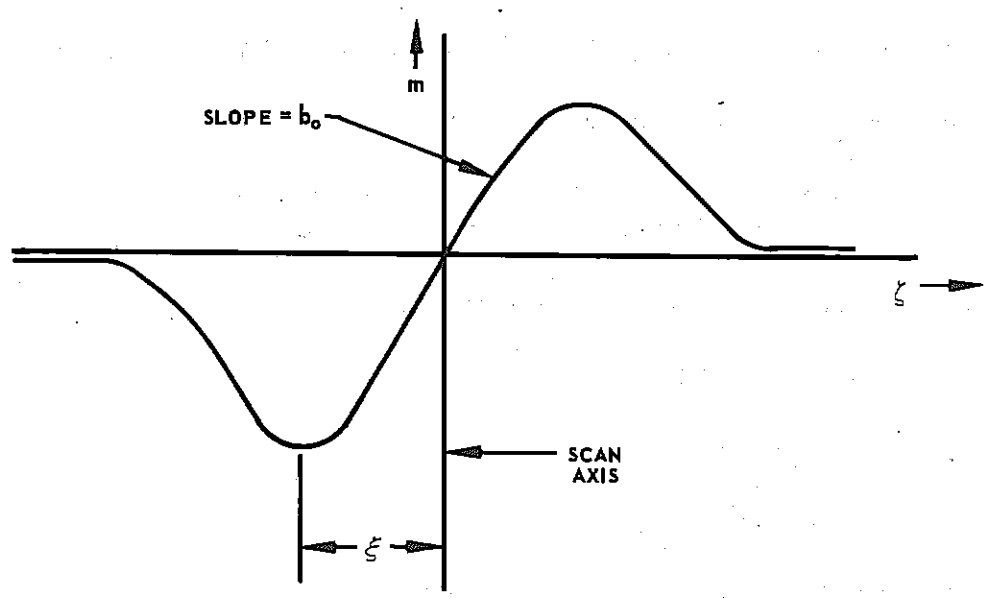

FIGURE 7-10. DISCRIMINATOR-LIKE CURVE RESULTING WHEN MODULATION INDEX, m, IS PLOTTED AGAINST ERROR ANGLE, ζ

is the rate of change of the returned rf voltage with angular displacement θ from the scan axis. Then, from Figure 7-10 and Equations 7-4 and 7-11,

$$m = b_o \zeta = b_o \rho/R = V_o' \rho/AR \tag{7-12}$$

From Equation 7-10, the amplitude of the scan component is

$$V_s = Am = \frac{V_o' \rho}{R} \tag{7-13}$$

Thus the amplitude of the error signal is proportional to the displacement, ρ, of the target from the scan axis. Note that although m is independent of the rf amplitude A, V_s is directly proportional to A because V_o' is directly proportional to A. The amplitude modulated scan signal to be used for analysis is therefore,

$$E(t) = A\left[1 + m\cos(\omega_s t + \phi)\right]\cos\omega_c t; \tag{7-14}$$

$$\zeta << \xi$$

where

$m = \frac{b_o \rho}{R}$ modulation factor

ρ = magnitude of the scan plane target vector

ϕ = phase of the scan plane target vector

b_o = a constant equal to the slope of $m(\zeta)$ near $\zeta = 0$ and is a function of fixed antenna and radar parameters only

A = amplitude of the rf return voltage for $\zeta = 0$

ω_s = scan frequency

ω_c = carrier frequency

ζ = error angle $= \sigma - \psi$

ξ = squint angle

Although the block diagram of the angle tracking loop has been outlined in Figure 7-6, the principal parameters of the system have not yet

been decided upon. Functionally, the system in Figure 7-6 can be reduced to the simple system shown in Figure 7-11 where it is assumed that the radome error is zero, that no crosstalk exists between channels, and that the elevation and azimuth channels are identical.

$$\mathcal{L}[\psi] = F(s)\mathcal{L}[(\sigma - \psi)] = \frac{\mathcal{L}[\sigma]F(s)}{1 + F(s)} = Y_o\mathcal{L}[\sigma] \qquad (7\text{-}15)$$

where the Laplace transform of

$$f(x) = \mathcal{L}[f(x)]$$

Assuming that all of the error lies in one channel, i.e., $\phi = 0$ (when ϕ is measured from the azimuth plane) and that the error signal amplitude is directly proportional to the angle ζ, F (s) is the open loop transfer function of the servo system. A fundamental requirement in determining F(s) is that the missile armament must have minimum rms miss error under a variety of attack geometries. A secondary requirement is that the tracking rms error angle between the line of sight and the scan axis be a minimum. To accomplish these, F(s) must give optimum transient and steady state response in the presence of random disturbances and unavoidable circuit non-linearities.

Analysis of the angle tracking servo is complicated by the dependence of the antenna loop parameters on the interceptor control system. The angle loop cannot be isolated from the rest of the system as in the range and velocity tracking cases. For this reason, the interceptor navigation equations are considered first. Perturbations of the trajectory occur as a result of random disturbances, which phenomena may be classified under the general heading of noise. Noise encountered in a tracking system is of several types and may be classified according to the range between the interceptor and the target. At long ranges, the video signal-to-

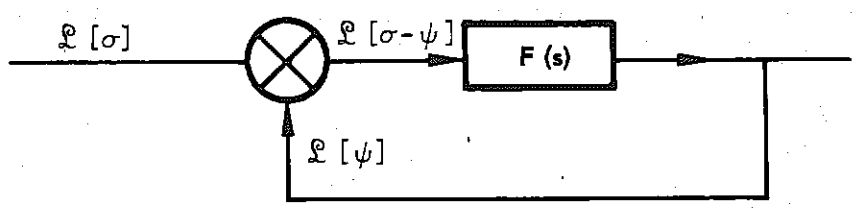

FIGURE 7-11. SINGLE CHANNEL OF ANTENNA LOOP

noise ratio (S/N) is low. In this case, the noise sources are primarily vacuum tube and semiconductor. At short ranges, the signal-to-noise ratio is high but because of target scintillation the signal from the target varies in a random manner. In addition, there are inaccuracies at all ranges due to errors in the antenna and other parts of the system. For the purposes of analysis, all of the noise sources are consolidated into a "noise angle" to be added to the bearing of the line of sight.

In the absence of noise, the fundamental equations during the attack phase are given in Equations 7-1 through 7-3. To simplify these equations assume that attack navigation occurs in one plane only, that is $\epsilon = 0$. Then only Equations 7-1 and 7-2 are of importance and become

$$O = R - L \cos \theta + \dot{R}\, T \tag{7-16}$$

$$a_a = \dot{\sigma}\, T + \frac{L}{R} \sin \theta \tag{7-17}$$

In Equation 7-17, the variable ω_a in equation 7-2 which is the angular velocity of the line of sight about the azimuth axis is replaced by σ, which is the angular rate of the line of sight when the scan axis and the line of sight are all contained in one plane, in this case, the azimuth plane. As can be seen, if the distance the missile travels relative to the interceptor, L, is set equal to zero in Equations 7-16 and 7-17, the angular rate of the angle through which the interceptor must be turned is equal to the angular rate of the line of sight. This is a special case of the proportional navigation equation.

$$\dot{\gamma} = \lambda \dot{\sigma} \tag{7-18}$$

where λ, the navigation constant, is equal to unity. As indicated in Chapter 5, a lead collision course becomes very nearly a pure interceptor course in the vicinity of missile launch and is exactly that at the instant of launch. Since a collision course is a special case of a proportional navigation course, it is convenient to consider the effect of the antenna servo and the long range noise problem on the navigation equation 7-16, 7-17 and also Equation 7-18, where the latter vicinity of launch holds approximately.

Now consider the effect of noise on the navigation equations. When the effective noise angle rate $\dot{\eta}$ is added to $\dot{\sigma}$, Equation 7-17 and 7-18 become

$$\alpha a = (\dot{\sigma} + \dot{\eta})\, T + \frac{L}{R} \sin \theta \tag{7-19}$$

$$\dot{\gamma} = \lambda(\dot{\sigma} + \dot{\eta}) \tag{7-20}$$

At very long ranges, the angular rate is nearly zero, that is, the angle σ is nearly constant. Thus, at long ranges $\dot{\sigma}$ may be set equal to zero in equations 7-19 and 7-20. The long range navigation equations may now be derived. At long ranges, noise generated in the receiver is of consequence. Representing the thermal noise by a sum of sine waves of constant amplitude, c_n, and random phases, ϕ_n,

$$\eta = \sum_{n=1}^{\infty} c_n \cos(\omega_n t + \phi_n) \tag{7-21}$$

where the values of ϕ_n are uniformly distributed from 0 to 2π. The mean power developed across a one-ohm resistor by any one of the sine waves in Equation 7-21 is $\frac{c_n^2}{2}$. Assuming the power in this sine wave to occupy a narrow spectral region Δf and letting G(f) represent the spectral density in watts per cycle (the noise power density), the mean power developed by the <u>nth</u> sine wave is $G(f_n)\,\Delta f$. Setting the expressions equal yields

$$c_n^2 = G(f_n)\Delta f \tag{7-22}$$

The total noise power developed across a one-ohm resistor by the sum of the sine waves in equation 7-21 is the mean square value of η or

$$\overline{\eta^2} = \int_0^{\infty} G(f)\, df \tag{7-23}$$

where

$$\int_0^{\infty} G(f)\, df = \lim_{N \to \infty} \sum_{n=1}^{N} G(n\Delta f)\Delta f \tag{7-24}$$

The integral of the noise power spectral density over all frequencies is evidently the total noise power. From Equation 7-20, with $\sigma = 0$, the mean square turning rate of the interceptor velocity vector is

$$\overline{\dot{\gamma}^2} = \lambda^2 \overline{\dot{\eta}^2} = \lambda^2 \overline{\left[\sum \omega_n c_n \sin(\omega_n t + \phi_n)\right]^2} = \lambda^2 \int_0^\infty \omega^2 G(f)\, df \tag{7-25}$$

when in the vicinity of launch. In the more general case, the mean square turning angle is given by

$$\overline{\alpha_a^2} \cong \overline{\dot{\eta}^2} T^2 + \overline{\alpha_f \dot{\eta}} T + \overline{\alpha_f^2} \tag{7-26}$$

where

$$\alpha_f = \frac{L}{R} \sin\theta \tag{7-27}$$

In the special case where the angle α_f is statistically independent of the noise angle rate $\dot{\eta}$ and assuming $\bar{\dot{\eta}} = 0$, Equation 7-26 becomes

$$\overline{\alpha_a^2} = \overline{\dot{\eta}^2}\, T + \overline{\alpha_f^2} \tag{7-28}$$

Similarly the turning rate in the azimuth plane in the general case can be written as

$$\dot{\alpha}_a = \dot{\sigma} + \dot{\eta} + \dot{\alpha}_f \tag{7-29}$$

At long ranges, the mean square value of $\dot{\alpha}_a$ reduces to

$$\overline{\dot{\alpha}_a^2} = \overline{\dot{\eta}^2} + \overline{\dot{\alpha}_f^2} \tag{7-30}$$

where it has been assumed that $\dot{\eta}$ and $\dot{\alpha}$ are statistically independent. In view of the dependence of both $\dot{\gamma}$ and $\dot{\alpha}_a$ (mean square values) on the mean square value of $\dot{\eta}$, conclusions may be drawn as to the manner the spectral density G(f) must vary with frequency. In order for the mean square values of $\dot{\gamma}$ and $\dot{\alpha}_a$ to be finite, at high frequencies G(f) must fall off according to $\frac{1}{\omega^4}$ or faster. If G(f) is essentially constant over the frequency band of interest as is the case for thermal noise, the $\frac{1}{\omega^4}$ variation can be obtained by inserting two RC filters in cascade between $\dot{\gamma}$ and $\dot{\sigma}$. Since the transform of the voltage output of the filter is the transform of the input voltage multiplied by the filter transfer function, the output power spectral density must be the input spectral density multiplied by the magnitude of the transfer function squared, or

$$G_o(f) = G_i(f) \left| Y(jw) \right|^2 \tag{7-31}$$

where $G_i(f)$ is the input spectral density, $G_o(f)$ the output spectral density, and $Y(s)$ is the filter transfer function. Hence where $G_i(f)$ represents the input spectral density, $G_o(f)$ the output spectral density, and $Y(s)$ is the filter transfer function. Hence

$$\overline{\dot{\gamma}_o^2} = \lambda^2 \int_o^\infty \omega^2 G_o(f)\, df = \lambda^2 \int_o^\infty \omega^2 G_i(f) \left|Y(j\omega)\right|^2 df \tag{7-32}$$

Let

$$Y(s) = \frac{1}{S\tau + 1} \qquad \text{where } \tau = RC \tag{7-33}$$

which is the transfer function for an RC low pass filter.

Thus

$$\left|Y(j\omega)\right|^2 = \frac{1}{1 + 4\pi^2 f^2 \tau^2} \tag{7-34}$$

where $\omega = 2\pi f$, and assuming for simplicity that the input spectral density is a constant, ω_o,

$$\overline{\dot{\gamma}^2} = \lambda^2 \frac{w_o}{2\pi} \int_o^\infty \frac{\omega^2 d\omega}{1 + \omega^2 \tau^2} \tag{7-35}$$

Equation 7-35 also applies to the general case in 7-30 if $\dot{\gamma}$ is set equal to $\dot{\eta}$ so that Equation 7-35 replaces $\overline{\dot{\eta}^2}$ in Equation 7-30. Equation 7-30 then can be written

$$\overline{\dot{a}_a^2} = \frac{w_o}{2\pi} \int_o^\infty \frac{\omega^2 d\omega}{1 + \omega^2 \tau^2} + \int_o^\infty \frac{G(\dot{a}_f)}{2\pi} \frac{d\omega}{1 + \omega^2 \tau^2}$$

$$= \int_o^\infty \frac{w_o + G(\dot{a}_f)}{2\pi} \cdot \frac{d\omega}{1 + \omega^2 \tau^2} \tag{7-36}$$

where $G(\dot{a}_f)$ is the spectral density of $\dot{a}_f$.

Assuming that the angle α_f has a spectral density characteristic that falls off at least as rapidly as $\dot{\eta}$, then the integrand in Equation 7-36 is similar to that shown in Figure 7-12.

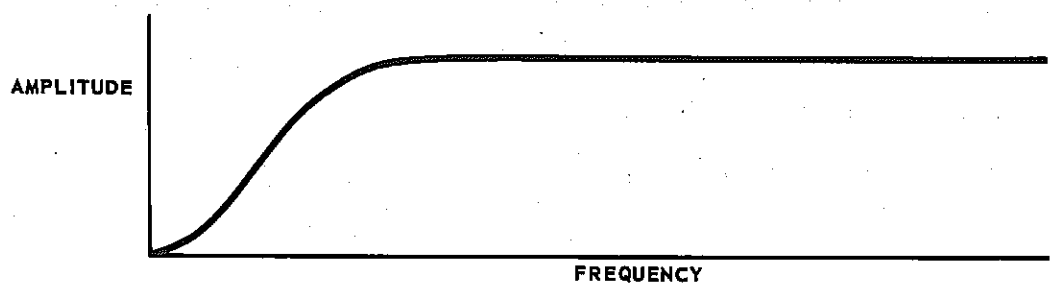

FIGURE 7-12. ATTENUATION CHARACTERISTIC BEFORE FILTERING

Since this function does not fall off at high frequencies, another RC filter or equivalent must be added in cascade, so that $\overline{\dot{\gamma}^2}$ is of the form

$$\overline{\dot{\gamma}^2} = \lambda^2 \frac{w_o}{2\pi} \int_0^\infty \frac{\omega^2 d\omega}{(1+\omega^2\tau_1^2)(1+\omega^2\tau_2^2)} \tag{7-37}$$

τ_1 and τ_2 are the respective time constants of the two filters. A sketch of behavior of the integrand in Equation 7-37 is shown in Figure 7-13.

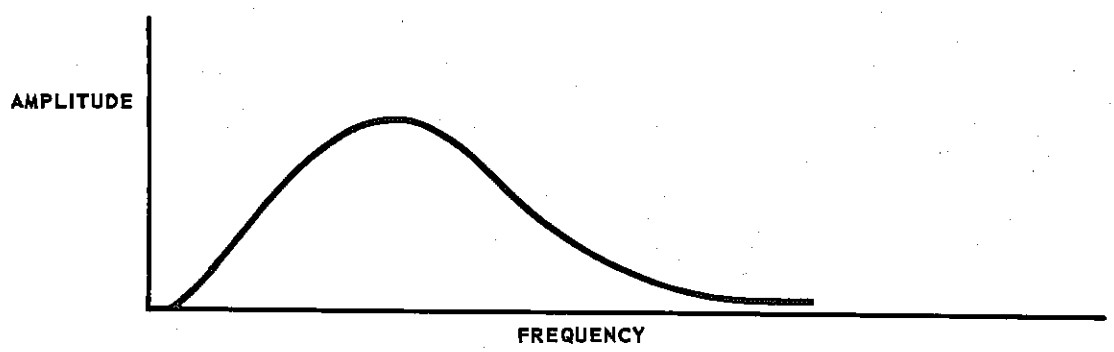

FIGURE 7-13. ATTENTUATION CHARACTERISTIC AFTER FILTERING

Figure 7-14 is a block diagram relating $\dot{\gamma}$ and $\dot{\sigma} + \dot{\eta}$, and similarly Figure 7-15 is a block diagram relating α_a and $(\dot{\sigma} + \dot{\eta})$ T + α_f.

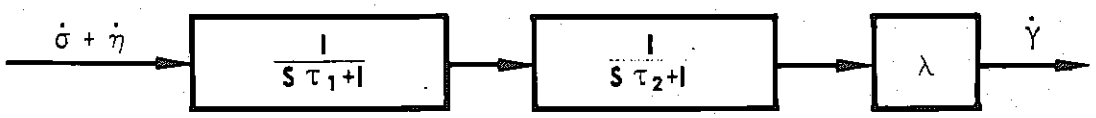

FIGURE 7-14. BLOCK DIAGRAM RELATING $\dot{\gamma}$ AND $\dot{\sigma} + \dot{\eta}$

The differential equation resulting from Figure 7-14 is

$$\tau_1 \tau_2 \dddot{\gamma} + (\tau_1 + \tau_2)\ddot{\gamma} + \dot{\gamma} = \lambda(\dot{\sigma} + \dot{\eta}) \tag{7-38}$$

and the differential equation resulting from Figure 7-15 is

$$\tau_1 \tau_2 \dddot{\alpha}_a + (\tau_1 + \tau_2)\ddot{\alpha}_a + \dot{\alpha}_a = \dot{\sigma} + \dot{\eta} + \dot{\alpha}_f \tag{7-39}$$

Therefore it appears that at long ranges at least two major time lags will be necessary between the antenna and the interceptor control surfaces to prevent noise saturation of the controls. One of these lags can be provided by the closed loop antenna servo. If the antenna precession rate is made proportional to the angular error η, the closed loop looks like a low pass RC filter. Thus

$$\dot{\psi} = \frac{\zeta}{\tau}(\sigma - \psi) \tag{7-40}$$

where $\frac{1}{\tau}$ is the proportionality factor. Equation 7-40 may be rewritten

$$\tau\dot{\psi} + \dot{\psi} = \sigma \tag{7-41}$$

or

$$\mathcal{L}\left[\psi(t)\right] = \psi(s) = \frac{\sigma(s)}{1 + S\tau} \tag{7-42}$$

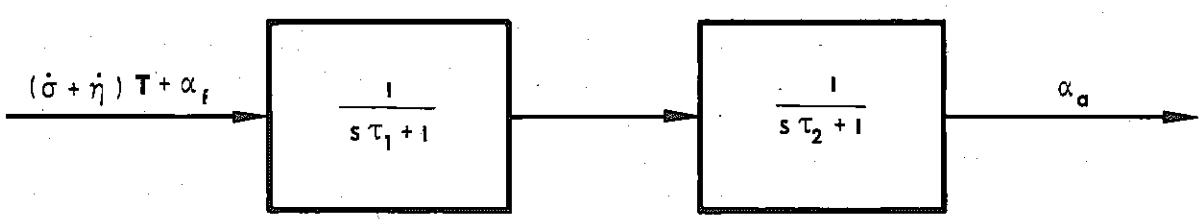

FIGURE 7-15. EFFECT OF FILTERING ON INPUT AZIMUTHAL RATES

Thus the transfer function between the line of sight angle σ and the scan angle ψ is just that of a low pass filter of RC time constant τ. If the antenna loop is to provide only one of the required time constants of the control system, either the computer or the interceptor control system must provide the other. Although certain lags are present in the computer, the second filtering operation will be provided by smoothing the output variables of the antenna tracking loop before application to the computer. There will be additional lags in the interceptor-control system. These lags can all be grouped into a single lag which can be approximated by an RC filter of time constant τ'. The main lag in τ' is inserted deliberately between the antenna loop output and the computer.

It has been shown previously that the RMS error in the angle through which the interceptor must turn can be considerably reduced by employing two time lags in the tracking and interceptor control systems. The nature of noise at short ranges is now being investigated to determine if additional system changes must be made. At short ranges the important noise sources are due to scintillation and antenna imperfections.

Scintillation (which is the variation in the return signal caused by changing target attitude with time) is of three types: (1) amplitude scintillation, where the amplitude of the returned signal varies randomly, (2) angular scintillation, where the direction of the scan axis varies in a random manner as a result of variations in the apparent direction of arrival of the wavefront of the received signal, and (3) range and range derivative scintillation due to the finite depth of the target. Angular scintillation, which results as a consequence of the finite angle at short ranges subtended by the target, varies inversely with range and eventually, at short ranges where the signal-to-noise ratio is high, overrides all other noise sources. Experiments show that the bandwidth of the amplitude scintillation spectrum seldom exceeds 100 cps. Much of the undesirable effect of random variation in the signal envelope due to amplitude scintillation can be avoided by using a scan frequency appreciably higher than 100 cps. This is considerably higher than is conventional but is obtainable in a small, well-balanced antenna. In the case of the large antennas, it is possible to simulate this high rate by electronic techniques.

Electronic lobing of fixed antenna can yield very high effective scan rates. Random amplitude variations constitute amplitude scintillation. The scan component amplitude itself is a function of the rf amplitude. Although m, the percent modulation, is a constant, from Equation 7-13, the amplitude of the scan component is $V_s = Am$, where A is the

unmodulated rf amplitude. If, because of amplitude scintillation, A is a random function of time, A(t), then V_s is also a random function of time, $V_s(t)$. From Equation 7-14, the scan modulated signal in the presence only of amplitude scintillation becomes

$$E(t) = A(t) \cos \omega_c t + V_s(t) \cos(\omega_s t + \phi) \cos \omega_c t \qquad (7\text{-}43)$$

The spectrum of the envelope in this case is shown in Figure 7-16. The scan frequency component and its sidebands lie within the relatively narrow servo pass band. When the scan axis is on the target, note that m = 0 so that noise in the servo passband cannot prevent ζ from approaching zero but merely affects the manner of approach. The amplitude scintillation spectrum A(t) has relatively little power in the servo pass band (the shaded portion) because of the high scan frequency. Since the scintillation noise is not zero when the error signal is zero, the antenna cannot hold ζ equal exactly to zero. Note that there is a relatively large amount of amplitude scintillation power in the error amplifier pass band. Non-linearities in this amplifier decrease the absolute signal level and therefore increase the antenna loop tracking time constant even if only the noise peaks are clipped. The servo pass band is much narrower than error amplifier pass band because of subsequent filtering in the loop.

A theory of angular scintillation may be derived * on the assumption that the target is composed of large number, N, of independent random

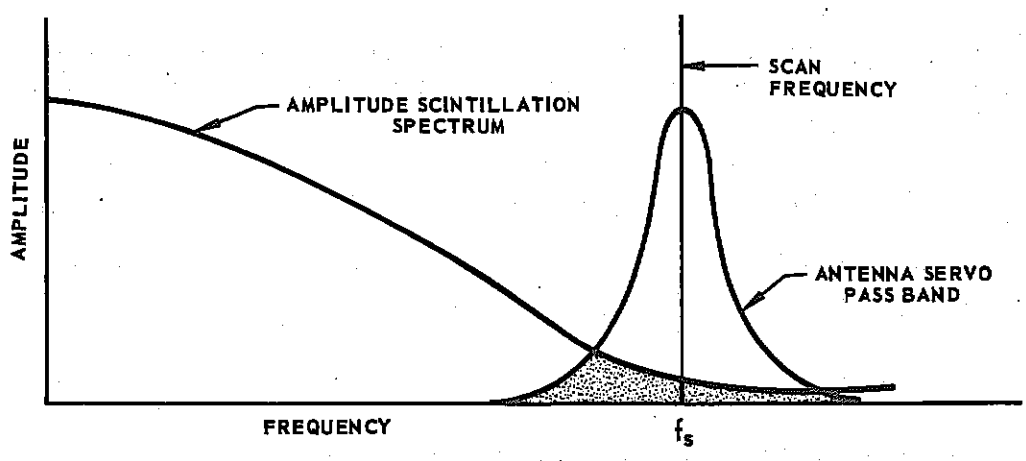

FIGURE 7-16. AMPLITUDE SCINTILLATION SPECTRUM

* "Angular Scintillation of Radar Targets" by R. H. Delano (Proc. of Inst. of Radio Eng.)

radiators. A simplified version of such a theory is developed in the appendix. The basic assumptions of the theory are (1), that the percent modulation is small so that $V_s(t)$, is much less than A(t) and (2), that the scintillation bandwidth B_A is small so B_A is much less than ω_s. The error signal is denoted by E_s and has a value

$$E_s = E_a - E_b = \frac{b_o}{R} \sum_{n=1}^{N} A_n d_n e^{j\phi_\eta} \cos(\theta_n - \theta_r) - Ab_o \zeta e^{j\phi_\zeta} \quad (7\text{-}44)$$

where

E_a = angular scintillation component relative to the mean center of echo

E_b = restoring signal

b_o = slope of the error curve

A_n = rf amplitude of the nth radiator

θ_n = rf phase of the nth radiator

A = resultant rf vector = $\sum_{n=1}^{N} A_n e^{j\theta\eta}$

θ_r = rf phase of A

For practical purposes, the mean center of echo may be considered the centroid of a plane target and the origin of coordinates. The reference axis is the left-right axis in the scan plane where

d_n = displacement of the nth radiator from the origin

ϕ_n = angular displacement of the nth radiator from the reference left-right axis in the scan plane

ζ = error angle relative to the mean center of echo

ϕ_ζ = angular displacement of the scan axis relative to the reference left-right axis in the scan plane

A convenient configuration to consider consists of a long narrow target whose long dimension lies along the left-right axis and whose transverse dimension is negligible. Such a configuration simulates the broadside view of a bomber. For this case,

$$\phi_n = \phi_\zeta = 0 \text{ (or } \pi) \tag{7-45}$$

$$E_s = E_a 1 - Ab_o \zeta \tag{7-46}$$

where

$$E_a 1 = \frac{b_o}{R} \sum_{n=1}^{N} A_n d_n \cos(\theta_n - \theta_r) \tag{7-47}$$

If the antenna tracking loop is assumed to be a linear servo such as described by Equation 7-41, it is possible to determine the affects of angular scintillation on antenna tracking. The tracking equation of such a system in one plane is

$$\dot{\psi} = a_o E_s = a_o \left[E_{a_1} + b_o A(\sigma_T - \psi) \right] \tag{7-48}$$

where ψ is the angular coordinate of the scan axis and σ_T is the angular coordinate of the center of the target area. Equation 7-48 may be written

$$\dot{\psi} + a_o b_o A \psi = a_o E_{a1} + a_o b_o A \sigma_T \tag{7-49}$$

If A were a constant, the equation would describe a linear circuit with time constant $\frac{1}{a_o b_o A}$. Actually A, the amplitude scintillation term, is varying almost as fast as the angular scintillation term E_a. It has been shown * that a good approximation to Equation 7-49 is

$$\dot{\psi} + a_o b_o \overline{A} \psi = a_o E_{a1} + a_o b_o \overline{A} \sigma_T \tag{7-50}$$

where A is a constant equal to the mean of A. Setting

$$\tau = \frac{1}{a_o b_o \overline{A}} \tag{7-51}$$

* Ibid

Equation 7-49 becomes

$$\tau\dot{\psi} + \psi = \frac{E_{al}}{b_o \overline{A}} + \sigma_T = \sigma_T + \frac{Y_T}{R} \tag{7-52}$$

where

$$Y_T = \sum_{n=1}^{N} \frac{d_\eta A_\eta}{\overline{A}} \cos(\theta_n - \theta_r) \tag{7-53}$$

Y_t is the effective displacement of the center of radiation from its mean position and the mean square value of Y_T is given by

$$\overline{Y_T^2} = \frac{1}{2\overline{A}^2} \sum_{n=1}^{N} A_n^2 d_n^2 \cos^2 \phi_n \tag{7-54}$$

If all the A_n are equal then

$$\overline{Y_T^2} = \frac{\overline{A^2}}{2\overline{A}^2} \overline{(d_n \cos \phi_n)^2} = \frac{2}{\pi} \overline{(d_n \cos \phi_n)^2} = \frac{2}{\pi} \overline{d_n^2} \tag{7-55}$$

where

$$\overline{(d_n \cos \phi_n)^2}$$

is the squared radius of gyration in the plane considered; for a long thin target of length ℓ it is equal to $\frac{\ell^2}{12}$. Suppose Y_T has a spectrum of the RC filter type, namely,

$$G_{Y_T}(f) = w_o \Big/ \left[1 + (f^2/B_a^2)\right] \tag{7-56}$$

where the angular scintillation bandwidth B_A is much larger than the servo bandwidth. Then

$$\overline{Y_T^2} = \int_o^\infty \frac{df}{1 + (f^2)/B_a^2} = w_o B_a (\pi/2) \tag{7-57}$$

whence

$$w_o = \frac{\overline{4d_n^2}}{\pi^2 B_a} \tag{7-58}$$

and since

$$\mathcal{L}(\psi) = \frac{\mathcal{L}\left[\sigma_T + (Y_T)/R\right]}{1 + S\tau} \tag{7-59}$$

and letting $\sigma_T = \theta$, then

$$\overline{[\psi(f)]^2} = \frac{1}{R^2}\int_0^\infty \frac{w_o}{1 + (f^2)/B_a^2} \quad \frac{df}{1 + 4\pi^2 f^2 \tau^2} \tag{7-60}$$

Since

$$2\pi\tau \gg 1/B_a \tag{7-61}$$

Equation 7-60 can be approximated by

$$\overline{\psi^2} = \frac{w_o}{R^2}\int_0^\infty \frac{df}{1 + 4\pi^2 f^2 \tau^2} = \frac{w_o}{2\pi\tau R^2}(\pi/2) = \frac{\overline{(d_n)^2}}{\pi^2 B_a \tau R^2} \tag{7-62}$$

The spectrum of $\dot{\psi}$ may be found in the same manner. From Equation 7-59

$$\mathcal{L}(\dot{\psi}) = \frac{S\mathcal{L}(Y_T/R)}{1 + S\tau} \tag{7-63}$$

or

$$\overline{\dot{\psi}^2} = \frac{1}{2\pi R^2}\int_0^\infty \frac{w_o}{1 + (\omega^2)/4\pi^2 B_a^2} \quad \frac{\omega^2 d\omega}{1 + \omega^2\tau^2} \tag{7-64}$$

Therefore, by analogy with Equation 7-35, the spectrum of $\dot{\psi}$ does not fall off until the angular scintillation spectrum falls off. By analogy with the procedure developed in Equation 7-37, and employing Equation 7-59, it follows that

$$\mathcal{L}[\dot{Y}] = \frac{\lambda\mathcal{L}\left[\dot{\sigma} + (d/dt)(Y_T/R)\right]}{(S\tau + 1)(S\tau' + 1)} \tag{7-65}$$

or

$$\tau\tau'\ddot{Y} + (\tau' + \tau)\ddot{\gamma} + \dot{\gamma} = \lambda\left[\dot{\sigma} + \frac{d}{dt}\left(\frac{Y_T}{R}\right)\right] \tag{7-66}$$

In this equation, τ' is the recommended additional lag between the antenna tracking loop and the computer. By comparison with Equation 7-38,

$\frac{y_t}{R}$ is the "noise" angle η, so that in this case

$$\eta = \frac{Y_T}{R} \tag{7-67}$$

The discussion to this point has tacitly assumed that the antenna closed loop transfer function is analogous to that for an RC low-pass filter. It has been shown that as far as noise and scintillation in the overall interceptor control loop is concerned, this type of servo is adequate since the closed loop appears like a simple time lag. This servo, in combination with another time lag external to the antenna control system, prevents noise saturation of the interceptor controls. The possibility of saturation in the antenna loop is now investigated.

It can be seen from Equation 7-63 that one of the fundamental parameters which must be determined is the antenna loop time constant τ. In addition, the exterior tracking system lag τ' must also be determined. These time constants should be determined in order to minimize the rms error in the antenna tracking loop and also eventually to minimize the rms miss of the missile armament. The antenna tracking loop is subject to target loss, where loss is interpreted to mean that the servo can no longer track the target. For practical purposes, the antenna servo never "loses" the target if a reasonably wide antenna beamwidth is used because, if the scan axis wandered over an angular range of the order of twice the squint angle, the rms launching error of the missile armament would far exceed its allowable value. It seems reasonable that τ should be as small as possible, consistent with noise bandwidth considerations. A small τ implies a high gain servo which requires a large value of volts per degree error for the precession rate signals applied to the antenna gyro. The requirement of a large ratio of volts per degree error demands that amplifiers preceding the antenna precession mechanism have a wide dynamic range in order to prevent saturation by large error signals. Even if this condition is satisfied, a more fundamental limitation remains - namely, that the precession rate demanded by the dc error signals out of the precession must not exceed the maximum precession rate that the gyro is capable of developing. Results show that the magnitude of the error signal is not as much the limiting factor as is the amount of scintillation. This fact can be demonstrated analytically. It has been shown that the random variable Y_T is normally distributed; stated mathematically the probability density of Y_T is

$$P(Y_T) = \frac{1}{\sqrt{2\pi \overline{Y_T^2}}} e^{\frac{-Y_T^3}{2\overline{Y_T^2}}} \tag{7-68}$$

where $P(Y_T)\, dY_T$ is the probability of getting some particular value of Y_T. The variable Y_T is normally distributed because it arises as a consequence of the sum of contributions to the angle from numerous independent scatters. Consequently the distribution of Y_T is normal by the central limit theorem. A plot of $P(Y_T)$ is shown in Figure 7-17.

A property of a normally distributed function is that when the function is passed through a linear filter the output still is normally distributed but with a new standard deviation.

It therefore follows from Equation 7-59 that $\dot{\psi}$ is normally distributed with a mean square value given by Equation 7-60. The probability that $\dot{\psi}$ will lie between two values, a and b, is

$$P(a \leq \dot{\psi} \leq b) = \int_a^b P(\dot{\psi})\, d\dot{\psi} \tag{7-69}$$

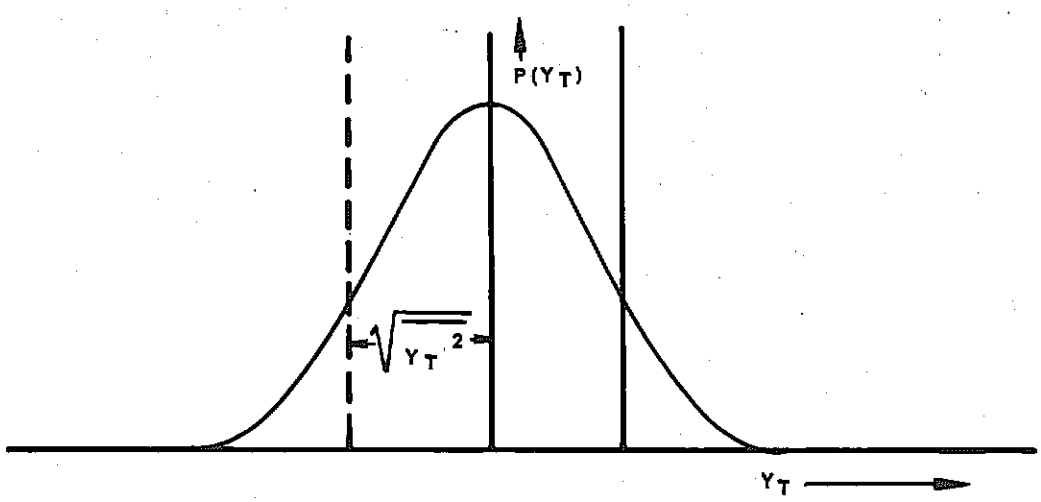

FIGURE 7-17. PROBABILITY DISTRIBUTION OF Y_T

The antenna is capable only of moving at some maximum precession rate, $\dot{\psi}$ maximum. There is a finite probability, P_o, of precession rates greater than maximum being demanded. This probability is given by

$$P_o = 2\int_{\dot{\psi}\,MAX}^{\infty} P(\dot{\psi})d\dot{\psi} \tag{7-70}$$

To keep the rms miss within allowable limits, it is necessary to restrict P_o to less than some value of $P_{min.}$ Usually, in order to do this, the mean square value of $\dot{\psi}$ must be limited, which may be done conveniently by passing the signal plus angular scintillation through a low pass filter. If this filter has a time constant τ'', the Laplace transform of Equation 7-40 becomes

$$\mathcal{L}(\psi) = \frac{\mathcal{L}\left[\sigma_T + (Y_T/R) - \psi\right]}{S\tau(S\tau'' + 1} \tag{7-71}$$

or

$$\tau\tau''\ \ddot{\psi} + \tau\ \dot{\psi} + \dot{\psi} = \sigma_T + \frac{Y_T}{R} \tag{7-72}$$

The problem of servo stability and transient overshoot is now considered. Even if instability does not result when the loop gain exceeds unity, excessive transient overshoot must be avoided since overshoots increase the radome problem and the rms error. Suppose the rms miss is optimized in the region where the loop is critically damped. There are then no transient oscillatory frequencies in the response and hence no sinusoidal overshoots. The value of τ'' required for critical damping may be found as follows. From Equations 7-15 and 7-70, it follows that

$$F(s) = \frac{1}{S\tau(S\tau'' + 1)} \tag{7-73}$$

The block diagram of the antenna servo described by Equation 7-73 is given in Figure 7-18.

$$\frac{\mathcal{L}(\psi)}{\mathcal{L}\left[\sigma_T + (Y_T)/R\right]} = Y_o(s)\ \frac{F(s)}{1 + F(s)} = \frac{1}{S^2\tau\tau'' + S\tau + 1} = \frac{\omega_o^2}{(S + \alpha_d)^2 + \beta_o^2} \tag{7-74}$$

where

$$\alpha_d = \frac{1}{2\tau},\ \omega_o^2 = \frac{1}{\tau\tau''},\ \text{and}\ \beta_o^2 = \omega_o^2 - \alpha_d^2$$

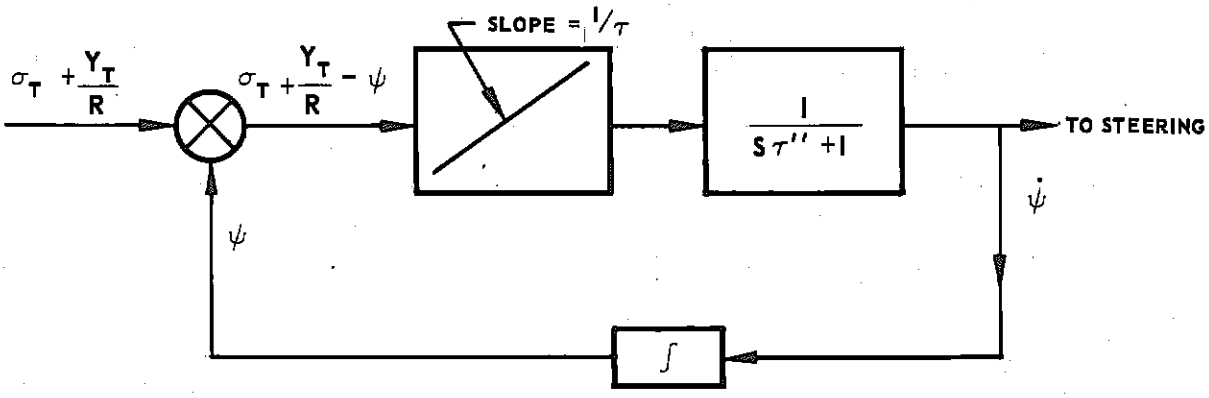

FIGURE 7-18. BLOCK DIAGRAM OF SINGLE INTEGRATOR PLUS LOG ANTENNA SERVO

If the sinusoidal oscillatory terms are to be damped out, $\beta_o = o$, from which $\omega_o^2 = \alpha_d^2$ or

$$\tau'' = \tau/4 \text{ (for critical damping)} \tag{7-75}$$

for this case, Equation 7-74 becomes

$$Y_o(s) = \frac{F(s)}{1 + F(s)} = \frac{\omega_o^2}{(S_T + \alpha_d)^2} = \frac{1}{\left[(S\tau/2) + 1\right]^2} \tag{7-76}$$

and the Laplace transform of the angular turning rate becomes

$$\mathcal{L}[\dot{Y}] = \frac{\lambda \mathcal{L}\left[\dot{\sigma} + (d/dt)(Y_T/R)\right]}{[S\tau/2) + 1]^2 (S\tau' + 1)} \tag{7-77}$$

While the insertion of an rc filter in the loop, as shown in Figure 7-18, is the simplest solution to the saturation problem in the antenna servo, it may not be the best solution. An alternative might be one in which the angular acceleration of the scan axis is proportional to the error angle and to the rate of change of the error angle with time. Such a servo satisfies a differential equation of the form

$$\frac{d^2\psi}{dt^2} = a_1(\sigma - \psi) + a_2\frac{d}{dt}(\sigma - \psi) \tag{7-78}$$

where

$$\sigma = \sigma_T + \frac{Y_T}{R} = \sigma_T + \eta \tag{7-79}$$

In operational notation,

$$\frac{\mathcal{L}[\psi]}{\mathcal{L}(\sigma - \psi)} = \frac{1}{S^2}(a_1 + a_2 S) \tag{7-80}$$

where

$$a_1 = \frac{1}{\tau_1 \tau_2}$$

$$a_2 = \frac{1}{\tau_2}$$

Thus

$$F(S) = \frac{1 + S\tau_1}{S^2 \tau_1 \tau_2} \tag{7-81}$$

$$Y_o(S) = \frac{1 + S\tau_1}{S^2 \tau_1 \tau_2 + S\tau_1 + 1} \tag{7-82}$$

Again it can be seen that the mean square value of $\dot{\psi}$ falls off no more rapidly at high frequencies than the angular scintillation spectrum with the filter function $Y_o(s)$ described in Equation 7-81. The effect of this term can be cancelled at high frequencies by introducing a lag of $\frac{1}{S\tau_3 + 1}$ in the open loop. If τ_3 is much less than τ_1 this does not appreciably affect the performance of this servo. The open loop transfer function of such a servo is

$$F(S) = \frac{1 + S\tau_1}{(S^2 \tau_1 \tau_2)(1 + S\tau_3)} \tag{7-83}$$

and the closed loop transfer function is

$$Y_o(S) = \frac{1 + S\tau_1}{(S^2 \tau_1 \tau_2)(1 + S\tau_3) + 1 + S\tau_1} \tag{7-84}$$

If approximately the same noise power is passed by this closed loop as in the previous case, then the closed loop servo bandwidth must be approximately the same. Certain advantages, including more rapid response time and greater velocity memory, can be attained by the latter described servo with time lag. These advantages can be obtained even with the same noise power being passed, while still avoiding excessive overshoot. The degree of advantage gained is probably outweighed, however, by the additional complexity involved in this latter servo. The fundamental parameters which must be determined are τ and τ''. As previously indicated, τ'' is simply equal to $\frac{\tau}{4}$ so that τ is actually the fundamental parameter. τ is determined so that the value of P_o as given in Equation 7-70 is less than some value of Po_{min}. This number, τ, is chosen arbitrarily but amounts to an rms variation (of the scan axis direction about the line of sight as a mean) of about 1/10 of the separation of the peaks of the error curve in Figure 7-10. In other words, the rms deviation on one side of crossover is about 1/10 of the squint angle. Accordingly, for a beam-width of about 3 degrees the squint angle should be about one-half the beamwidth or about 1-1/2 degrees. The rms error is then about .15 degrees. Gyros capable of developing angular rates on the order of 10 degrees per second are not unreasonable, so this number may be used for $\dot{\psi}$ max in Equation 7-70. Once Po_{min} has been set, the width of the distribution curve for $P(\dot{\psi})$ is determined. Assuming it to be normal, from Equation 7-63 the relationship between Y_T, $\dot{\psi}$ and τ is known. From a knowledge of the distribution of $\dot{\psi}$, the distribution of Y_T can be found. If the variance of the distribution of Y_T, when found analytically by the method described, is less than that encountered in practice or measured experimentally from the targets that are desired to be tracked, then the system must be modified by either increasing τ or $\dot{\psi}$ max for a given

Po_{min}. When these parameters are so adjusted that the width of the calculated Y_T distribution is no less than that of the measured or expected Y_T distribution and the value of $\dot{\psi}$ max is not exceeded for the antenna gyro used, then the appropriate value of τ has been found. The values of τ which satisfy these conditions lie between 0.1 and 1.0 seconds. The value of τ actually is the reciprocal of the product of the unattenuated value of receiver gain multiplied by the precession rate in degrees per second per volt (in the linear range of the gyro precession characteristic). Typical values for this linear precession rate would be 1/10 of a degree per second per volt. In order to derive values of τ between 1/10 and 1/100, the value of the receiver gain must vary from 10 to 100 volts per degree error angle.

It is advisable for the value of τ to vary according to the tactical situation, i.e., some sort of attenuator should be included in the open loop gain of the entire tracking servo to adjust to the optimum value for the given flight conditions.

SECTION 3 — THE VELOCITY TRACKING LOOP

One of the fundamental outputs of the tracking system to the computer is the angular velocity of the line of sight, which has been discussed. The other fundamental outputs include the range and the velocity of the target as a function of time. The velocity tracking loop to be discussed does not measure absolute velocity. In order to obtain absolute velocity measurements, an auxiliary absolute velocity reference must be included. The case considered here is one in which a velocity gate is needed for improving the angle tracking signal-to-noise ratio and discriminating capability. The additional equipment needed to make absolute velocity measurements for use by the computer has been discussed in Chapter 4.

(a) INTRODUCTION TO VELOCITY TRACKING

The type of radar assumed is a pulse-doppler radar, although most of the analysis applies to other types of doppler systems, as well. One way of partially separating the desired target signal from noise, jamming and extraneous targets, may be accomplished by tracking this signal in velocity. Because of the doppler effect the received signal from a target having a finite velocity relative to the interceptor will be different from that transmitted. If the carrier frequency is represented by a term of the form

A sin $(\phi(t))$, the received angle $\theta(t)$ has been changed, i.e. modulated, with reference to the transmitted angle $\phi(t)$. This angle modulation carries the desired velocity information. It is not necessary to have information about $\phi(t)$ to track $\theta(t)$, although this knowledge is necessary if an absolute measurement of velocity (or range and its time derivatives) is to be made. Thus, if the input to a servo is $\theta(t)$ and the servo output is also $\theta(t)$, perfect angle tracking has been achieved. In order to avoid confusion with the spatial angles of the target relative to the missile, the angles $\theta(t)$ and $\psi(t)$ will henceforth be called phase angles.

Thus, a servo which will track the phase angle $\theta(t)$ is defined as a phase-locked servo or phase-locked loop. Frequency will be herein defined as the rate of change of phase, i.e.

$$f(t) \equiv \frac{1}{2\pi} \frac{d\,\theta(t)}{dt} \tag{7-85}$$

A servo which will track $\omega(t) = \dot{\theta}(t)$ is defined as a frequency-locked loop. The phase-and frequency-locked loops are the most important servos to consider from a practical design viewpoint.

Certain general requirements can be imposed on velocity tracking loops which are used in fire control applications. Perfect tracking requires that the difference between servo input and output, or error, be zero. This in turn requires infinite open loop servo gain. Receiver noise also tends to limit the allowable gain. Since high loop gains tend to cause the servo to follow the noise, the useful output of the velocity gate is very noisy. The principal purpose of the velocity tracking loop is to reduce the noise and interferring signals associated with the target signal; it may seem that at low S/N ratios, low loop gain is desirable. The servo loop gain must be sufficient to follow the expected accelerations of the target signal in the absence of noise and the servo loop must be selective in order to discriminate successfully between undesired signals and noise. This selectivity depends upon the width of the velocity gate in the servo loop, i.e., the range of velocities the gate will pass. If the loop gain is so low that the servo will not follow the noise at low S/N ratios, then the servo error voltage which represents the target signal-plus-noise velocity at the velocity gate input will be as noisy as without feedback. If noise fluctuation causes the composite signal to exceed the equivalent maximum (or minimum) velocity which the gate is capable of handling, the target is said to be lost. Also, the target may fluctuate back into the gate, so that it may not be lost permanently.

Since target loss prevents the interceptor radar from tracking the target, it is highly desirable that the probability of loss be as small as possible. One way to insure this is to make the gate wide enough so that at low S/N ratios the number of noise fluctuations which can exceed the gate width is very small. Widening the gate width however, reduces the servo selectivity and tends to defeat the purpose of the system. If the gate is narrowed, the loop gain must be increased so that the error fluctuations are reduced, thereby keeping low the probability of loss. Increasing the gain defeats the other basic servo requirement; namely, keeping the velocity gate output S/N ratio high and consequently, a compromise is necessary.

The servo requirements also are affected by the nature of the input since the input signal is not only noisy, but also frequently affected by undesired signals whose velocities are in the general vicinity of the target. The servo design is also affected by the manner in which the missile is mechanized and by practical limitations of the state of the art.

(b) GENERAL PROBLEMS

Consider first, the return from a single <u>ideal</u> target in the absence of noise. The doppler frequency return depends on the target - radar geometry. The transmitted signal can be represented as

$$E_t(t) = B(t) \sin\phi(t) = B(t) \sin(\omega_c t - \phi_c) \qquad (7\text{-}86)$$

where

$B(t)$ = amplitude function = product of a train of unit amplitude video pulses and a constant amplitude CW - rf wave.

ω_c = Constant rf carrier frequency

ϕ_c = Constant initial phase of the carrier

$$\phi(t) = \omega_c t - \phi_c \qquad (7\text{-}87)$$

If the signal is reradiated from a perfect reflector, the received signal (at the antenna) is identical in form to the transmitted signal, but distinguishable only by a time delay, a phase change at reflection, and considerable attenuation in amplitude. The received signal is therefore

$$E_r(t) = A(t) \sin \theta (t) = A(t) \sin\left[\omega_c(t-2\tau_1) + \phi_r - \phi_c\right] \tag{7-88}$$

where

$A(t)$ = Amplitude function = function of the transmitter and receiver antenna patterns and orientations in space, the cross-section and reflection coefficient of the target, etc.

ϕ_r = Phase shift at reflection

τ_1 = time for a transmitted pulse to travel to the target

$$\tau_1 = \frac{R_1}{c} \tag{7-89}$$

where

R_1 = range of the target from the radar

c = velocity of propagation in space = velocity of light

Let the constant phase portion of the received phase angle be

$$\phi = \phi_r - \phi_c \tag{7-90}$$

Then Equation 7-88 becomes

$$E_r(t) = A(t) \sin\left[\omega_c t - \frac{2R_1\omega_c}{c} + \phi_1\right] \tag{7-91}$$

If $v_1(t)$ is the (time-varying) velocity of the target relative to the radar,

$$R_1(t) = \int_0^t v_1(t)\,dt \tag{7-92}$$

if $v_1(t)$ is a constant velocity v_1, then

$$R_1(t) = v_1 t + R_{o1} \tag{7-93}$$

v_1 is positive if $R_1(t)$ is increasing with t, negative if the radar is closing on the target. The change in frequency due to relative velocity is

$$\omega_1(t) = \dot{\theta}(t) - \omega_c = \frac{-2\dot{R}_1\omega_c}{c} = -\frac{2v_1(t)\omega_c}{c} \tag{7-94}$$

If $v_1(t) = v_1$ = constant,

$$f_1 = \frac{-2v_1 f_c}{c} \tag{7-95}$$

Equation 7-95 is the familiar form of the so-called "doppler shift" or doppler frequency. Doppler frequency is generalized here to include time-varying velocities, so that the doppler frequency for this case is defined as

$$f_1(t) = -\frac{2\omega_c v_1(t)}{c} \tag{7-96}$$

It is of interest to determine the approximate time function and frequency spectrum of the various expected input waveforms. The waveform and spectrum of the return from a single ideal target appears in Figure 7-19.

In Figure 7-19, the doppler shift $f_d = \frac{\omega_d}{2\pi}$ is positive relative to the carrier because it is assumed that the interceptor is closing on the target. If t is measured from the instant that the pulse is transmitted

$$B(t) = A_o \sum_{k=1}^{\infty} \left[\mu(t - kT) - \mu(t - \delta - kT)\right] \tag{7-97}$$

where T = pulse repetition period

δ = pulsewidth

A_o = rf carrier amplitude

$$A(t) = G_o B(t - \tau) \tag{7-98}$$

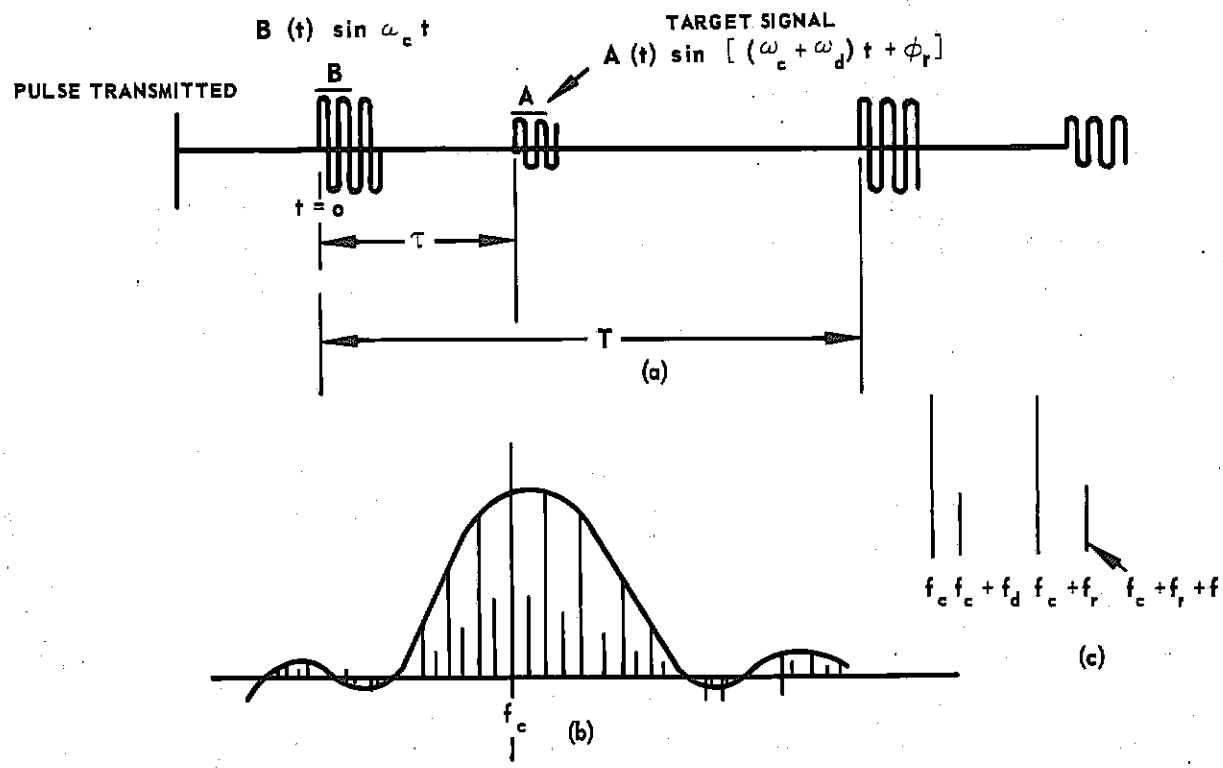

FIGURE 7-19a, b, c. WAVEFORM AND SPECTRUM FOR A SINGLE IDEAL TARGET

where

τ = time delay between the main bang and the target signal.

G_o = attenuation factor dependent on antenna patterns and orientations, target characteristics, etc.

Clearly, the range between the interceptor and target is a function of τ. If a high repetition rate is used, it is possible for additional pulses to be transmitted before the first pulse is returned from the target. This effect introduces range ambiguity but does not affect the uniqueness of the velocity measurement, since the latter depends solely on doppler shifts. The corresponding frequency spectrum is shown in Figure 7-19b and detailed in Figure 7-19c. The received signal spectrum, which is shifted by f_d, is narrower than the transmitted spectrum. Receiver noise is added to this waveform so that the video waveform and spectrum might appear as shown in Figure 7-20.

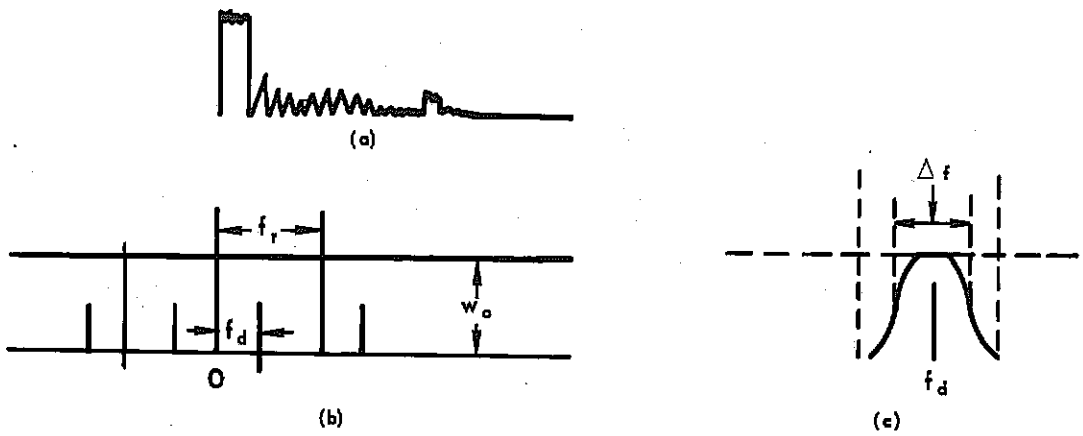

FIGURE 7-20. VIDEO WAVEFORM AND SPECTRUM

The noise spectrum is usually quite broad compared to f_r and usually is centered about each line of the signal spectrum, so that the overall spectrum, although complex, generally is still broad. Nonlinear operations, such as detection, introduce signal-noise intermodulation as well as additional noise-noise modulation, complicating the spectrum further and generally degrading the S/N ratio. Since the doppler component f_d is the desired signal, the velocity gate selects it from the noise spectrum (shown flat in Figure 7-20b for convenience). Noise and undesired signals lying in the vicinity of the gate are also passed by an amount proportional to the gatewidth Δf as shown in Figure 7-20c.

The input signal is also complicated by returns from targets other than the desired one. Because of antenna sidelobes, the ground reflections from all directions appear in the return. If the target is at a range less than the interceptor altitude, the target signal will arrive before the first elements of ground clutter. The input signal might then be as in Figure 7-21.

The frequency spectrum shown in Figure 7-21b arises because the highest velocity of the ground relative to the interceptor is v_i; similarly, the lowest velocity is $-v_i$. The ground return spectrum in reality is complex and is illustrated by the block of frequencies in Figure 7-21b. If the

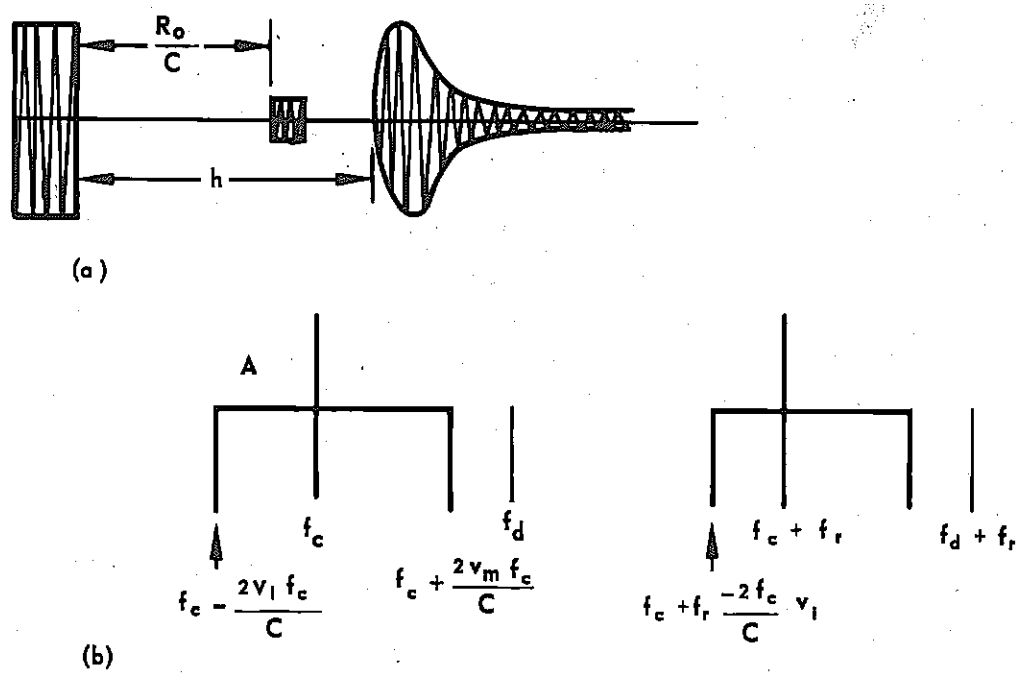

FIGURE 7-21a, b. INPUT SIGNAL WITH GROUND CLUTTER

target is such that its relative velocity to the interceptor is closing, its spectrum lies outside of the ground return spectrum. If the target has zero velocity relative to the ground or is opening in relation to the interceptor, the target spectrum lies in the ground clutter. One of the most significant advantages of doppler systems over conventional pulsed systems is the ground clutter rejection property of the former on closing targets. Such systems are especially useful as a defense against low flying targets. Note that in the pulse-doppler system depicted, the repetition frequency f_r must be sufficiently high to present a clutter-free region for the target doppler frequency, otherwise, the ground clutter rejection capability is lost. It is therefore required that

$$f_r > \frac{4v_i f_c}{c} \tag{7-99}$$

In the absence of other effects, the received pulse train is amplitude modulated by the lobing modulation which carries the target spatial angle information. The received signal due to this effect alone is represented in Figure 7-22.

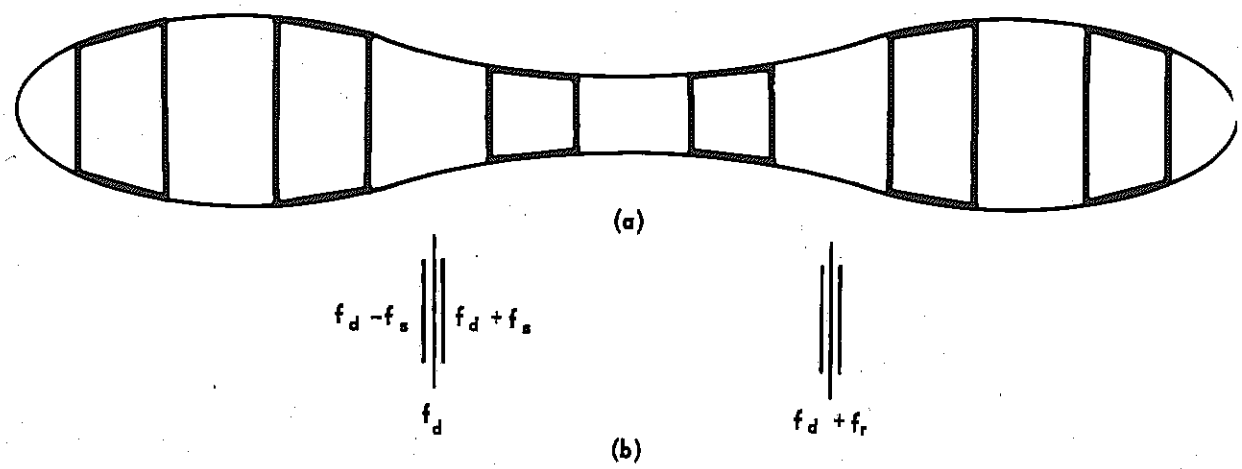

FIGURE 7-22a, b. SCAN MODULATED VIDEO AND SPECTRUM

Each component of the doppler shifted pulse spectrum, therefore, is amplitude modulated with corresponding amplitude modulated sidebands as in Figure 7-22b. The lobing sidebands carry the useful information for guiding the interceptor and the minimum velocity gatewidth corresponds to the lobing frequency.

All of the input signals are random to some extent because of scintillation. Because no physical reflector is perfect, the received signal from any target scintillates, i.e., varies in a random manner. A physical reflector is usually composed of many small specular reflectors which are variously oriented and moving relative to each other. The return from these sources combines to give a signal wave which varies randomly in amplitude and angle. Amplitude and angular scintillation tend to add noise amplitude and phase modulation sidebands to the received spectrum. Range scintillation introduces noise, pulse position, modulation sidebands. Velocity scintillation introduces noisy frequency modulation sidebands. Even in the absence of receiver noise, both the amplitude and the argument of the received waveform $A(t) \sin \sigma(t)$ are noisy.

Finally, the input may be jammed by high power noise (which is spread over a wide spectrum), undesired apparent targets, false lobing signals, etc. The velocity tracking system also must distinguish the desired target from other potential targets and chaff.

It is apparent therefore, that the received signal is a complex function of time and frequency. This chapter considers the design of a velocity tracking loop starting with the least complicated input signal. The necessary design modifications, which are imposed by the effect listed, are analyzed insofar as practical.

Practical limitations strongly affect the velocity tracking loop design. For example, if the target is lost during flight, it may be desirable to search for it in velocity. This procedure requires a threshold setting device which determines whether or not an apparent signal is actually a target, as well as requiring a relock circuit which switches from search to track. Experience has shown that the search and relock feature requires at least 10 db greater S/N ratio than would be necessary in the tracking mode alone. If the radar is capable of tracking jamming signals and target signals, a search scheme is mandatory, since in the jam-track mode, the target signal may drift completely out of the gate. Under these conditions when the jamming ceases, the target would be lost. Except for this effect, it would be very desirable to be able to track the target at all times.

Although it is desirable to have narrow velocity gates (on the order of tens of cycles/sec), high "skirt" slopes in decibels per octave are required for discrimination against undesired signals (particularly main bang sidebands). From stability considerations the phase slope in the passband of the gate should be small. These requirements are conflicting and so a compromise is called for. A high degree of relative stability between transmitter and local oscillator (LO) is necessary for internal synchronization. This can be provided by frequency locking the LO to the transmitter by means of an AFC circuit.

A major consideration in the design is the problem of drift compensation. Circuits such as the voltage controlled and reference oscillators, and integrators will drift causing the frequency or phase crossover reference in the loop to change. If the reference frequency differs appreciably from the center frequency of a narrow gate, the tracking capability of the loop is degraded unless the gate is widened. In any case, loop tracking must follow the drifts, resulting in less available capability for tracking the target.

The effect of nonlinearities generally is to degrade the S/N ratio. The signal amplitude must therefore be kept within the dynamic range of the system, as far as possible. In a frequency or phase tracking system, this

is accomplished by deliberately limiting the signal preceding the discriminator. Such limiting also keeps the discriminator output independent of input amplitude variations since many discriminators are amplitude-sensitive. Unfortunately, limiting may also degrade the S/N ratio. Amplitude control also may be provided by automatic gain control (AGC). Although there may be AGC preceding the velocity loop input, if the signal amplitude varies over wide extremes within the loop, AGC is again required.

(c) DETAILED DESIGN CONSIDERATIONS

One basic pulse-doppler radar design requires that a narrow velocity gate be placed about a target doppler signal so that this gated signal can be used in the fire control angle tracking system. Since the signal frequency as defined in Equation 7-96 is proportional to the target velocity, the velocity gate logically is a filter whose velocity width is proportional to its frequency bandwidth. One method for tracking the input doppler signal is by varying the filter center frequency in accordance with the input frequency while maintaining a constant bandwidth. A scheme which is easier to implement, yet accomplishes the same purpose, uses a fixed center frequency gate and heterodynes the desired input signal frequency into the gate by means of a local oscillator whose frequency is controlled by a servo. A generalized block diagram of a phase angle tracking servo based on this principle appears in Figure 7-23.

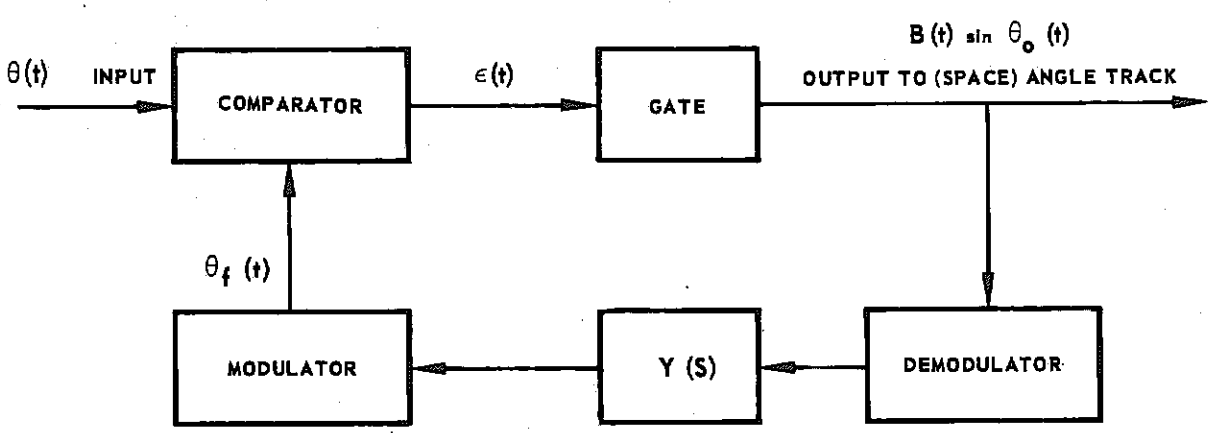

FIGURE 7-23. BLOCK DIAGRAM OF A PHASE ANGLE TRACKING SERVO

The input is A(t) sin θ(t). The loop is to operate on the phase angle θ(t), so the comparator yields ϵ (t) which is a function of the difference between the input and fed back phase angles, θ (t) - θ_f (t). After gating, the useful output to the (space) angle tracking system is B(t) sin θ_o (t) which is similar to the input signal, with much of the undesired interference and noise gated out.

SECTION 4 — IDEAL SERVO ANALYSIS IN THE ABSENCE OF NOISE

The two tracking servos considered are the phase-locked and frequency locked types. In both, the comparator is considered to be an ideal mixer whose output is the product of the two inputs and whose modulator is an ideal voltage controlled oscillator (VCO) with output frequency proportional to the input control voltage. The demodulator in the phase-locked case is an ideal phase detector whose output is proportional to the phase shift of the input relative to the phase reference. In the frequency-locked case, the demodulator is a frequency discriminator whose output is proportional to the difference between the input frequency and the crossover. The crossover is set at the velocity gate center frequency. For an initial case, it is assumed that the system is tracking well. The effect of the gate on the servo transfer function is at first neglected. With these modifications, Figure 7-23, for the phase-locked case, becomes Figure 7-24.

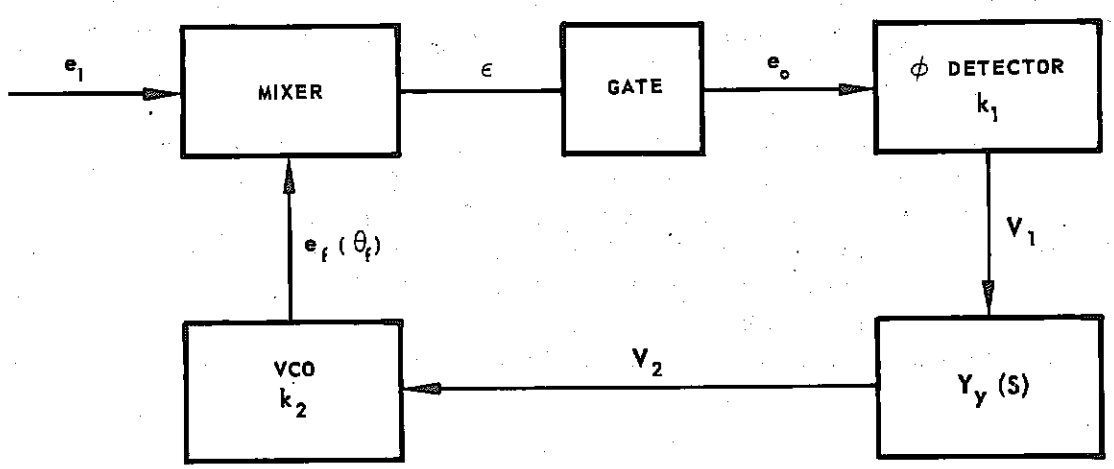

FIGURE 7-24. BLOCK DIAGRAM OF PHASE LOCKED SERVO

Although the input is actually pulsed, only the CW doppler component is important for tracking, and therefore the input is considered a CW sine wave at the doppler shifted carrier frequency. The input amplitude is assumed constant in order to simplify the analysis. The servo equation

$$e_i(t) = A \cos\theta(t) = A \cos\left[(\omega_c + \omega_d)t + \phi_d\right] \tag{7-100}$$

assumes that the gate is appreciably narrower than the PRF so that in the absence of noise and interference, the gate output is an amplitude modulated sine wave where the amplitude modulation (AM) carries the space angle information. In general there is gain and gain control associated with the filtering action of the gate. The demodulator develops a voltage which is proportional to the difference between $\theta_o(t)$ and a reference phase, or to the difference between $\theta_o(t)$ and a reference frequency, depending on the demodulator used. Voltages proportional to higher derivatives of the difference between B(t) and a reference also can be used. The demodulator output voltage is operated upon by a transfer function Y(S) which contains a frequency invariant gain term. The form of Y(S) is set by tracking requirements, especially the servo memory desired and stability considerations. The voltage output of Y(S) controls a modulator which develops a phase $\theta_f(t)$ of frequency such as to heterodyne the input target signal frequency into the gate. Some of the auxiliary functions such as the rear reference scheme, limiting and/or AGC, search and lock-on are not shown in the basic velocity tracking system of Figure 7-23.

Most of the design parameter determinations require analysis, but some can be set by deductive reasoning. The IF gate center frequency should be high enough to give good image rejection and Q, yet, not so high that the required bandwidths and skirt attenuation cannot be attained. The mixer output frequency must be at the center frequency of the velocity gate for perfect tracking. Let this center frequency be f. The VCO output will be assumed to be a constant amplitude cosine wave whose frequency in the absence of a control voltage is ω_o below the input. Therefore

$$e_f(t) = A_f \cos\theta_f(t) \tag{7-101}$$

where

$$\dot{\theta}_f = \omega_f - k_2 V_2(t) \tag{7-102}$$

$$\theta = \omega_f t - k_2 \int_0^t V_2(t)\, dt \tag{7-103}$$

$$\omega_f = \omega_c - \omega_o \tag{7-104}$$

where ω_c is the signal carrier frequency, and ω_f is the VCO frequency in the the absence of a control voltage.

The gate passes only the difference frequency, so that

$$e_o(t) = B(t) \cos(\theta - \theta_f) \tag{7-105}$$

where B(t) is proportional to AA_f. The input to the phase detector is assumed to have constant amplitude. Since B(t) must carry the angle information, some sort of limiting action is necessary preceding the phase detector to satisfy this assumption. Define ϵ_θ as the phase on the phase detector input. Thus

$$\epsilon_\theta = \theta - \theta_f \tag{7-106}$$

Both the gate and the phase detector are aligned at the crossover frequency ω_o. The phase detector output is therefore

$$V_1(t) = k_1 (\epsilon_\theta - \omega_o t) \tag{7-107}$$

also

$$V_2(t) = \int_0^t V_1(\alpha) g_\phi(t - \alpha) d_\alpha \tag{7-108}$$

where

$$g_\phi(t) = \mathcal{L}^{-1}\left[Y_\phi(S) \right] \tag{7-109}$$

Taking Laplace transforms of Equations 7-106, -107, -108, and -109 yields the loop equations:

$$\epsilon_\theta(S) = \theta(S) - \theta_f(S) \tag{7-110}$$

$$V_1(S) = k_1\left[\epsilon_\theta(S) - \frac{\omega_o}{S^2}\right] \tag{7-111}$$

$$V_2(S) = Y_\phi(S)V_1(S) \tag{7-112}$$

$$\theta_f(S) = \frac{\omega_f}{S^2} + \frac{k_2}{S} V_2(S) \tag{7-113}$$

Equations 7-110 through 7-113 may be combined to give

$$\theta_f(S) = \frac{\omega_f}{S^2} + \frac{k_1 k_2}{S} Y_\phi(S)\left[\epsilon_\theta(S) - \frac{\omega_o}{S^2}\right]$$

$$= \frac{\omega_f}{S^2} + Y_1(S)\left[\theta(S) - \theta_f(S) - \frac{\omega_o}{S^2}\right] \tag{7-114}$$

where

$$Y_1(S) = \frac{k_1 k_2}{S} Y_\phi(S) \tag{7-115}$$

Thus

$$\theta_f(S) = \frac{\frac{\omega_f}{S^2} + Y_1(S)\left[\theta(S) - \frac{\omega_o}{S^2}\right]}{1 + Y_1(S)} \tag{7-116}$$

$$\epsilon_\theta(S) = \frac{\theta(S) - \frac{\omega_f}{S^2} + Y_1(S)\frac{\omega_o}{S^2}}{1 + Y_1(S)} \tag{7-117}$$

Making use of Equation 7-101 and the fact that

$$\theta(S) = \frac{\omega_c + \omega_d}{S^2} + \frac{\phi_d}{S} \tag{7-118}$$

Allows Equations 7-113 and 7-114 to be written

$$\theta_f(S) = \frac{\frac{\omega_c - \omega_o}{S^2} + Y_1(S)\left[\frac{\omega_c + \omega_d}{S^2} + \frac{\phi_d}{S} - \frac{\omega_o}{S^2}\right]}{1 + Y_1(S)}$$

$$= \frac{\omega_c - \omega_o}{S^2} + \frac{Y_1(S)}{1 + Y_1(S)}\left(\frac{\omega_d}{S^2} + \frac{\phi_d}{S}\right) \tag{7-119}$$

$$\epsilon_\theta(S) = \frac{\frac{\omega_c + \omega_d}{S^2} + \frac{\phi_d}{S} - \frac{\omega_c}{S^2} + \frac{\omega_o}{S^2}\left(1 + Y_1(S)\right)}{1 + Y_1(S)}$$

$$= \frac{\omega_o}{S^2} + \frac{\frac{\omega_d}{S^2} + \frac{\phi_d}{S}}{1 + Y_1(S)} \tag{7-120}$$

In the frequency-locked case, similar equations may be derived. In this case, Figure 7-23 is replaced by Figure 7-25.

The phase-locked loop discussion up to Equation 7-106 also applies in the frequency locked case by replacing V_2 by v_2. The frequency discriminator is sensitive only to rates of change of phase. Define the frequency of the discriminator input as

$$\epsilon_{\dot\theta} = \dot\theta - \dot\theta_f \tag{7-121}$$

The discriminator crossover frequency is ω_o and its output is

$$v_1 - k_1(\epsilon_{\dot\theta} - \omega_o) \tag{7-122}$$

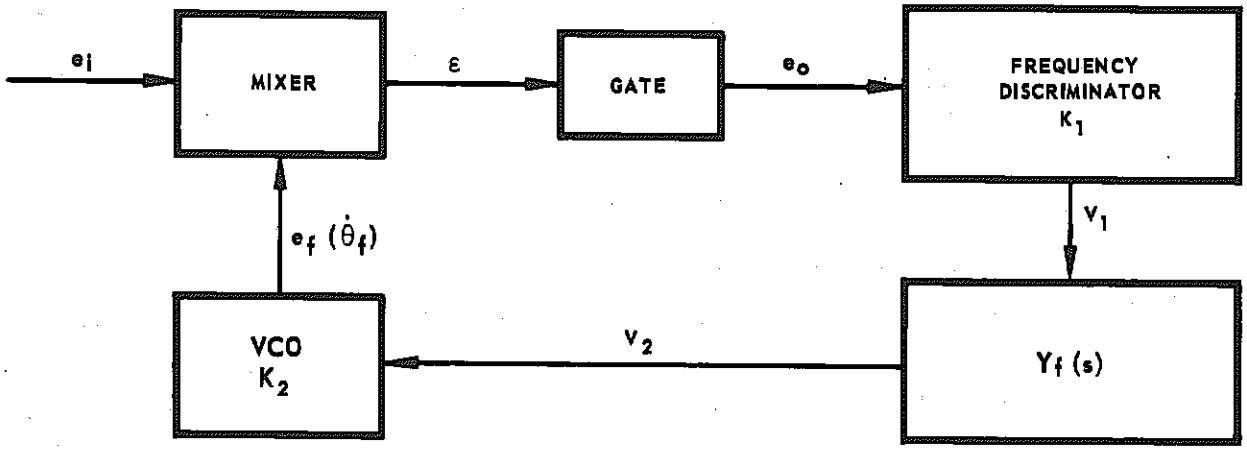

FIGURE 7-25. BLOCK DIAGRAM OF FREQUENCY – LOCKED TRACKING LOOP

also

$$v_2(t) = \int_0^t v_1(\alpha)\, g_f(t-\alpha)\, d\alpha \tag{7-123}$$

where

$$g_f(t) = \mathcal{L}^{-1}\left[Y_f(S)\right] \tag{7-124}$$

The transformed equations are therefore

$$\epsilon_{\dot{\theta}}(S) = \dot{\theta}(S) - \dot{\theta}_f(S) = S\left[\theta(S) - \theta_f(S)\right] = S\,\epsilon_\theta(S) \tag{7-125}$$

$$v_1(S) = K_1\left[\epsilon_{\dot{\theta}}(S) - \frac{\omega_o}{S}\right] = K_1 S\left[\epsilon_\theta(S) - \frac{\omega_o}{S^2}\right] \tag{7-126}$$

$$v_2(S) = Y_f(S)\, v_1(S) \tag{7-127}$$

$$\dot{\theta}_f(S) = S\theta_f(S) = \frac{\omega_f}{S} + k_2 v_2(S) \tag{7-128}$$

Equations 7-125 through 7-128 combine to give

$$\dot{\theta}_f(S) = \frac{\omega_f}{S} + k_2 K_1 Y_f(S)\left[\epsilon_{\dot{\theta}} - \frac{\omega_o}{S}\right] = \frac{\omega_f}{S} + Y_2(S)\left[\dot{\theta}(S) - \dot{\theta}_f(S) - \frac{\omega_o}{S}\right] \tag{7-129}$$

where

$$Y_2(S) = k_2 K_1 Y_f(S) \tag{7-130}$$

Thus,

$$\dot{\theta}_f(S) = \frac{\frac{\omega_f}{S} + Y_2(S)\left[\dot{\theta}(S) - \frac{\omega_o}{S}\right]}{1 + Y_2(S)} \tag{7-131}$$

$$\epsilon_{\dot{\theta}}(S) = \frac{\dot{\theta}(S) - \frac{\omega_f}{S} + Y_2(S)\,\frac{\omega_o}{S}}{1 + Y_2(S)} \tag{7-132}$$

Making use of Equation 7-104 and the fact that

$$\dot{\theta}(t) = \omega_c + \omega_d \tag{7-133}$$

or

$$\dot{\theta}(S) = \frac{\omega_c + \omega_d}{S} \tag{7-134}$$

$$\omega_f = \frac{\frac{\omega_c - \omega_o}{S} + Y_2(S)\left[\frac{\omega_c + \omega_d - \omega_o}{S}\right]}{1 + Y_2(S)}$$

$$= \frac{\omega_c - \omega_o}{S} + \frac{Y_2(S)}{1 + Y_2(S)}\left(\frac{\omega_d}{S}\right) \tag{7-135}$$

$$\epsilon_{\dot{\theta}}(S) = \frac{\frac{\omega_c + \omega_d}{S} - \frac{\omega_c}{S} + \frac{\omega_o}{S}\left(1 + Y_2(S)\right)}{1 + Y_2(S)}$$

$$= \frac{\omega_o}{S} + \frac{\frac{\omega_d}{S}}{1 + Y_2(S)} \tag{7-136}$$

(a) A COMPARISON OF FREQUENCY - AND PHASE-LOCKED LOOPS IN THE ABSENCE OF NOISES

It is interesting to compare the two loops when the open loop transfer functions $Y_1(s)$ and $Y_2(s)$ are set equal. Thus, if

$$Y_1(S) = Y_2(S) = Y(S) \qquad \text{or} \tag{7-137}$$

$$\frac{k_1 Y_\phi(s)}{S} = K_1 Y_f(s) \tag{7-138}$$

it follows from Equations 7-119, -120, and -135 and -136 that

$$\theta_f(S) = \frac{\omega_c - \omega_o}{S^2} + \frac{Y}{1+Y}\left(\frac{\omega_d}{S^2} + \frac{\phi_d}{S}\right) \quad \text{Phase locked} \tag{7-139}$$

$$\omega_f(S) = \frac{\omega_c - \omega_o}{S} + \frac{Y}{1+Y}\left(\frac{\omega_d}{S}\right) \quad \text{frequency locked} \tag{7-140}$$

$$\epsilon_\theta(S) = \frac{\omega_o}{S^2} + \frac{\frac{\omega_d}{S^2} + \frac{\theta_d}{S}}{1+Y} \quad \text{phase-locked} \tag{7-141}$$

$$\epsilon_{\dot\theta}(S) = \frac{\omega_o}{S} + \frac{\frac{\omega_d}{S}}{1+Y} \quad \text{frequency-locked} \tag{7-142}$$

By comparing Equations 7-139, 140, or 141 and 142, it is clear that the transfer function to instantaneous frequency in the phase locked loop is the <u>same</u> as the corresponding transfer function in the frequency locked loop <u>if</u> $\phi = 0$. As can be seen from Equation 7-126, the ideal frequency discriminator is a phase detector in cascade with a differentiator. The constant of integration corresponding to the constant initial phase ϕ_d of the doppler shifted input is lost in the phase locked loop. Since the purpose of the velocity tracking loop is to keep the doppler signal in a frequency gate, the loss of this constant phase is not significant. On the other hand, it is somewhat pointless to follow a phase detector with a differentiator since a number of integrations are needed for memory.

A phase-locked loop might as well be used instead. The significant difference is not whether phase or frequency is the dependent variable in the loop, or the fact that there is an integration inherent in the phase locked loop which is not present in the frequency locked loop, Equation 7-135, but rather the precise nature of the demodulator used. Most demodulators (and modulators) can be represented as multipliers. In effect, a product is taken between the input and some reference. One of the major differences between practical frequency and phase demodulators is that in the practical case, the reference is derived from the input signal, whereas in the latter it is not. The practical phase detectors can be represented as in Figure 7-26.

If the input is

$$e_i = S + N = A \cos(\omega_d t + \phi_d + N(t)) \tag{7-143}$$

and the reference is phase coherent with the signal

$$e_r = S(t) = \cos(\omega_d t + \phi_d) \tag{7-144}$$

such that the reference phase is equal to (or linearly related to) the input phase ϕ_d, then

$$e_1 = e_r e_i = A \cos^2(\omega_d t + \phi_d) + \cos(\omega_d t + \phi_d) N(t)$$

$$= \frac{A}{2}\left[1 + \cos(2\omega_d t + 2\phi_d)\right] + N \cos(\omega_d t + \phi_d) \tag{7-145}$$

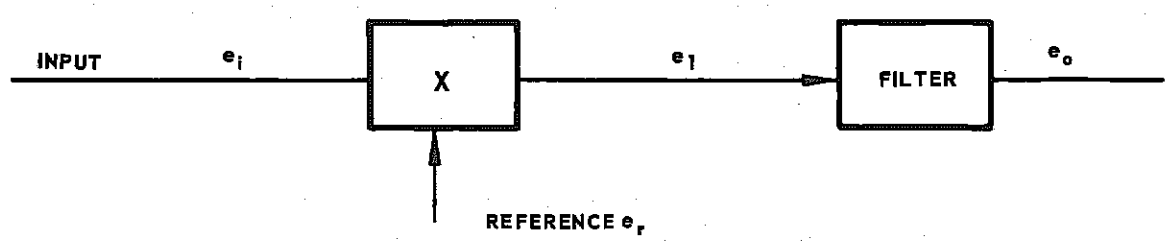

FIGURE 7-26. BLOCK DIAGRAM OF PHASE DETECTOR

After filtering,

$$e_o = S^2 + SN \cong \frac{A}{2} + N'(t) \tag{7-146}$$

where $N'(t)$ is the time function resulting from the portion of the spectrum of the product of $e_r(t)$ and $N(t)$ passed by the filter. In the frequency coherent case, $e_r(t)$ is linearly related to $e_i(t)$ in frequency but unrelated in phase so that

$$e_r(t) = \cos \omega_d t \tag{7-147}$$

$$e_1 = A \cos \omega_d t \left[(\cos \omega_d t \cos \phi_d - \sin \omega_d t \sin \phi_d)\right] + N(t) \cos \omega_d t$$

$$= \frac{A}{2} \cos \phi_d (1 + \cos 2\omega_d t) - \frac{A}{2} \sin \phi_d \sin 2\omega_d t + N(t) \cos \omega_d t \tag{7-148}$$

After filtering

$$e_o \cong \frac{A}{2} \cos \phi_d + N' \tag{7-149}$$

In both of these coherent cases, the noise appears linearly added to the desired output A. In the frequency coherent case, the signal term may be small compared to the noise term, depending on the difference between the input and reference phases .

A typical frequency detector, such as the Foster-Seeley frequency discriminator, can be shown to have the representation of Figure 7-27.

The frequency discriminator actually is a phase detector whose reference is derived from the input and passed through a transfer function $Y(S)$ so that the phase of e_r is proportional to the frequency of e_i. The transform $Y(S)$ therefore contains an integrator in cascade with a frequency selective network, such as an RLC network, whose bandwidth is roughly the discriminator peak-to-peak bandwidth.

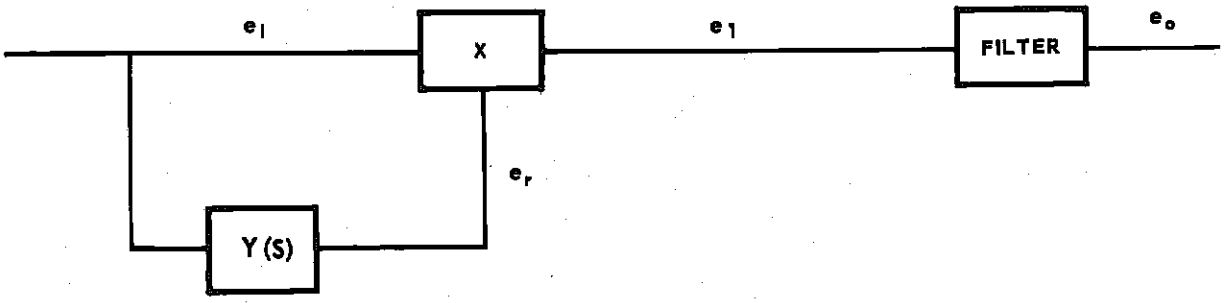

FIGURE 7-27. BLOCK DIAGRAM OF FREQUENCY DISCRIMINATOR

Therefore

$$e_r(S) = e_i\, Y(S) = S\, Y(S) + N\, Y(S) \tag{7-150}$$

and

$$e_1 = e_r e_i = (S + N)^2\, Y(S) = (S^2 + 2\, SN + N^2)\, Y(S) \tag{7-151}$$

contains noise-noise as well as signal-noise beats and is therefore incoherent. The output S/N ratio in the incoherent case is $S^2/(2SN + N^2)$ which, in general, is worse than the coherent output S/N ratio which is simply S/N. Suppose a product demodulator is used with an input signal $\cos(\omega_d t + \phi)$ and a reference signal $\sin(\omega_d t + \phi_r)$. The multiplier is followed by a low pass filter so that the detector output is proportional to $V_1 = k_1 \sin(\phi - \phi_r)$. The phase detector characteristic is shown in Figure 7-28.

From Figure 7-28 it appears that the pull-in range of this detector is $\phi_r \pm 90°$, since for phase errors $2n\pi + 90° < |\phi - \phi_r| < 270° + 2n\pi$, the discriminator slope reverses. Suppose the error is such that the reference frequency is $\omega_d + \delta$ rather than ω_d. The phase detector output is then $V_1 = k_1 \sin(\delta t + \phi - \phi_r)$. An ac control voltage is then developed by the detector, and after modification by $Y_\phi(s)$, drives the VCO. The VCO frequency is sinusoidally modulated so as to reduce the phase error.

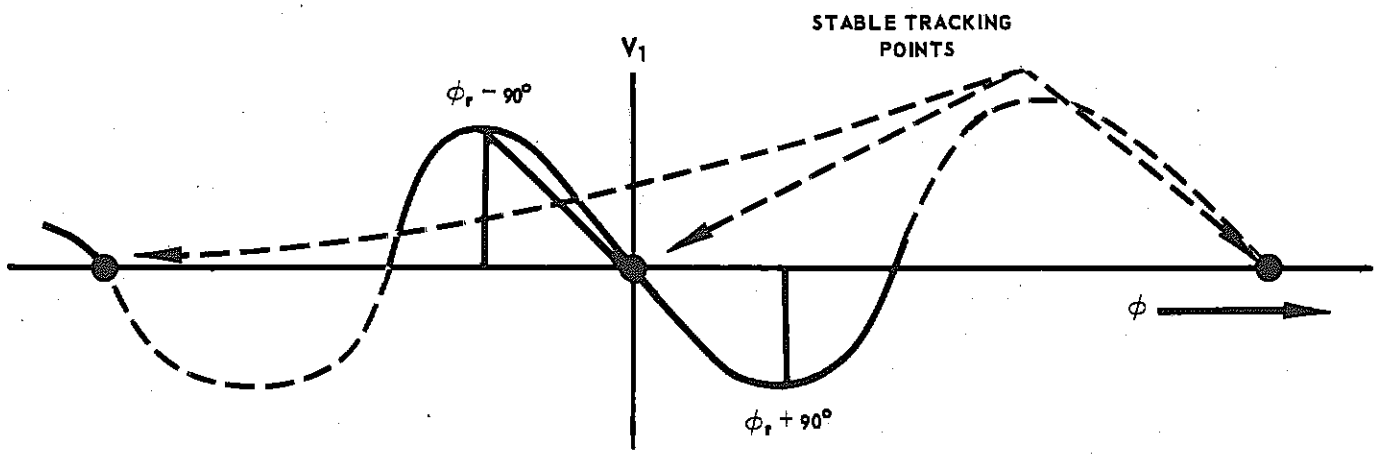

FIGURE 7-28. PHASE DETECTOR CHARACTERISTIC

High rate frequency modulation may cause the deviation to decrease in a practical VCO, thereby limiting the dynamic frequency range. Assuming this effect to be negligible within the frequency range of the gate, the phase-locked system will pull in at least as wide a range of frequencies as will the frequency-locked system. This follows since the phase-locked system can track not only at $\phi = \phi_r$ but also at $\phi = \phi_r + 2n\pi$, where n is an integer. If $n \neq \phi$, a constant phase error of $2n\pi$, is introduced. Since the starting phase of CW waves is of no concern, i.e., does not affect the frequency of the waves, the error signal will lie inside the frequency gate regardless of the constant phase error.

As an example of the pull-in capability of a phase locked loop, consider a constant doppler frequency input with a large initial phase offset $\phi - \phi_r >> 2\pi$.

For convenience in analysis, it is assumed that $\omega_c = \omega_o = \omega_f = 0$, and that $Y_\phi(s) = 1$. From Equations 7-112 and -113

$$\theta_f(s) = \frac{k_2}{2} V1(s) \text{ or } \dot{\theta}_f(t) = k_2 v_1(t) \qquad (7\text{-}152)$$

Letting $\phi_r = 0$, the phase detector response is from Figure 7-28,

$$V_1(t) = k_1 \sin \epsilon_\theta = k_1 \sin(\theta - \theta_f) \qquad (7\text{-}153)$$

Hence

$$\dot{\theta}_f(t) = k_1 k_2 \sin(\theta - \theta_f) \tag{7-154}$$

or

$$\dot{\theta}(t) - \dot{\epsilon}_\theta(t) = k_1 k_2 \sin \epsilon_\theta(t) \tag{7-155}$$

But, in the example, $\dot{\theta}(t) = \omega_d$ and $x(t) = {}_o(t)$, for convenience, Equation 7-155 then becomes

$$\dot{X} + k_1 k_2 \sin X = \omega_d \tag{7-156}$$

The initial condition is $x(t = o) = x_o >> 2\pi$. Equation 7-156 is nonlinear but capable of solution since the homogeneous equation is separable. The homogeneous equation is

$$\dot{X} + k_1 k_2 \sin X = 0$$

or

$$\frac{dX}{\sin X} = - k_1 k_2 d_t \tag{7-157}$$

The complementary solution of Equation 7-156 (i.e., the solution of Equation 7-157) is

$$X = \sin^{-1}\left(\frac{2A_o e^{-k_1 k_2 t}}{1 + A_o^2 e^{-2 k_1 k_2 t}}\right) \tag{7-158}$$

where

$$A_o = \frac{\sin X_o}{1 + \cos X_o} \tag{7-159}$$

A particular solution to Equation 7-156 is

$$X = \sin^{-1} \frac{\omega_d}{k_1 k_2} \tag{7-160}$$

Although the pull-in range for the phase-locked loop is the same as for the frequency-locked loop, the dynamic tracking range may be different depending on how the demodulators are implemented. Consider the typical phase demodulator characteristic (Figure 7-29a) and the typical frequency discriminator characteristics (Figure 7-29b).

Suppose the rates of change of the input doppler frequency are such that a voltage V is required from the demodulator to prevent loss. Then if $V < V_{\phi_{max}} < V_{f_{max}}$, both loops will track; if $V_{\phi_{max}} < V_{f_{max}} < V$, neither loop will track. For the practical cases shown in Figure 7-29, it is possible to make the phase slope equal to k_1 in the vicinity of ϕ_r numerically the same as the frequency slope k_1 in the vicinity of f_o and to make the loop transfer function the same inside the dynamic range. Generally, for these conditions, $V_{f_{max}}$ V_{max}. For the same open loop transfer functions, and with the gate width wide compared to the frequency dynamic range, it can be shown that a higher loop gain is needed to maintain track in the phase-locked case with a demodulator characteristic, as shown in Figure 7-29a, than with the corresponding frequency-locked case with the demodulator characteristic shown in Figure 7-29b. If the velocity gatewidth sets the frequency dynamic range rather than the demodulator characteristic, then the loop gains are identical. Furthermore, a phase detector with a wide dynamic range discriminator characteristic similar to Figure 7-29b (replacing f by ϕ) might be designed. The complete solution may be written

$$X = \sin^{-1} \left[\beta \sqrt{1 - \frac{\omega_d^2}{k_1^2 k_2^2}} + \frac{\omega_d}{k_1 k_2} \sqrt{1 - \beta^2} \right] \tag{7-161}$$

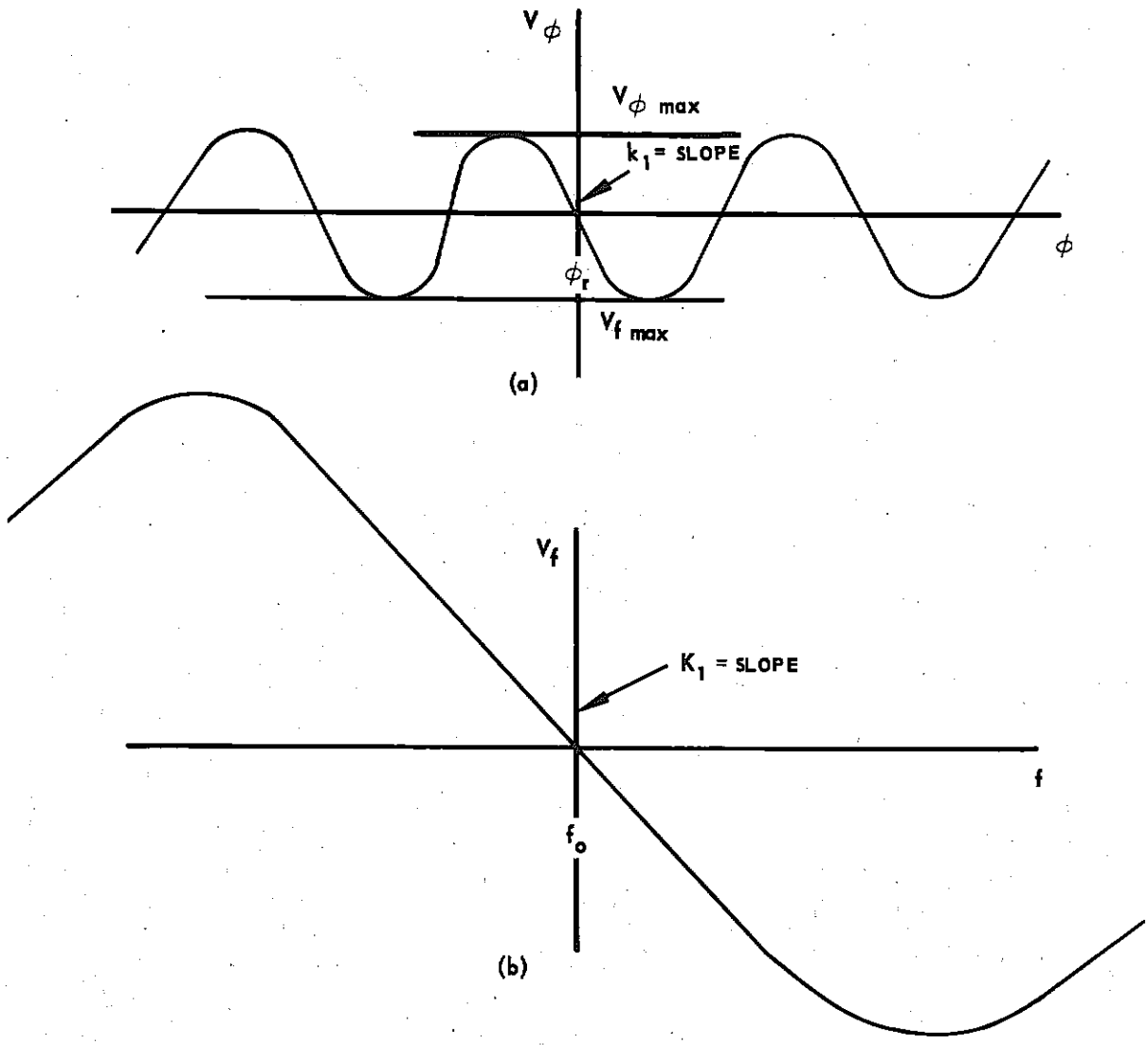

FIGURE 7-29a, b. PHASE AND FREQUENCY DEMODULATOR CHARACTERISTICS

where

$$\beta = \frac{2A_o e^{-k_1 k_2 t}}{1 + A_o^2 e^{-2k_1 k_2 t}} \tag{7-162}$$

Observe that in the steady state, $\lim_{t\to\infty} \beta(t) = 0$ so that the steady state phase tracking error is

$$X(t\to\infty) = \sin^{-1}\frac{\omega_d}{k_1 k_2} \tag{7-163}$$

Note that the initial phase error X_o has been tracked out to the steady state frequency error $\dot{X}(t\to\infty) = 0$ for this case.

The frequency spectrum is a steady state concept, the Fourier series components having constant steady state frequencies. The velocity gate refers to the steady state sinusoidal frequency response of a bandpass filter. If the frequency into the gate is varying, the transient response may be quite different from the steady state response. Similar arguments apply to frequency discriminators. Before the discriminator "realizes" that a constant frequency spectral line is being applied to it, it must "wait" until time is infinite; reasonably good frequency measurements can be made after 10 or so cycles have passed. An average frequency then can be measured by counting the number of cycles and dividing by the time of observation. The average frequency over time, T, is then

$$f \equiv \frac{\text{number of positive going axis crossings in time (T)}}{T} \tag{7-164}$$

Observe that definition Equation 7-164 is in general quite different from the instantaneous frequency, or time rate of change of phase, defined earlier. If the argument of the sine function under consideration can be written $\theta(t) = \omega_o t + \phi$, then the average frequency equals the instantaneous frequency for a sufficiently large value of T.

To illustrate the dynamic range problem, compare frequency and phase locked loops in which has the same open loop transfer function. One might compare the frequency error at the velocity gate input in the two cases where, if the transient frequency versus time function exceeded the gate cutoff frequency, the target would be lost. Hence the maximum frequency error is set by the gate cutoff frequency, thus providing a basis for comparison. Unfortunately, this basis is not valid. Assuming ideal demodulators which are sensitive only to frequency in the

one case and phase in the other, instantaneous frequency excursions outside the gate open the frequency-locked loop but not the phase-locked loop. This follows since the instantaneous phase is the time integral of the instantaneous frequency, and, if the frequency goes to zero instantaneously, the former generally does not. Real loss occurs when the loop is open. In the phase-locked case, this occurs when the frequency rate is such that phase error exceeds the voltage dynamic range of the phase discriminator characteristic. In other words, to maintain track, the error must not demand more voltage from the phase detector than it can provide. This is quite different from the pull-in range, where there is an initial phase offset which is greater than 90 degrees but the voltage dynamic range is not exceeded. Hence, loss of an accelerating target occurs in the phase-locked case when the phase error exceeds 90 degrees offset sufficiently, whereas loss occurs in the frequency locked case, when the frequency error exceeds the discriminator dynamic range or the velocity gate cutoff, whichever is smaller.

(b) SERVO ANALYSIS IN THE ABSENCE OF NOISE

It is necessary to define carefully what is meant by phase tracking in a phase locked loop and frequency tracking in a frequency locked loop. A phase tracking loop is defined here as one in which the phase of the returned doppler is the independent variable in the tracking loop. Similarly, a frequency tracking system is one in which the doppler frequency is the independent variable in the tracking loop. The implication is that in a phase locked loop the discriminator is a phase detector, whereas in the frequency locked loop the discriminator is a frequency discriminator. These names have nothing to do with the number of integrations which take place in the loop. Any number of integrations may take place in either loop. The fundamental difference between phase and frequency tracking is relative accuracy. The phase system is inherently capable of higher tracking accuracies than the frequency system, because the phase system maintains a continuous and essentially instantaneous measure of tracking error, whereas the frequency system determines error by an averaging process. The frequency discriminator must determine that an error exists in frequency before an error voltage can be generated for control. This latter statement indicates that the frequency tracking loop is essentially a device which measures average frequency or the average number of zero crossings of the signal waveform per unit time.

Other factors also affect the servo design. The system should be capable of following any velocities and accelerations which may occur.

The servo is therefore required to be reasonably high gain and capable of following rates of change of the input signal. A step input in acceleration, for example, corresponds to a ramp input in frequency and a parabolic input in phase. In order that the servo follow a ramp input with zero steady state error, two integrators must be employed in the loop. In order that a parabolic input be followed with zero error, three integrators must be employed. The general effect of added integrations in the loop is to increase the tendency towards instability. For the same gain, a three integrator loop will have greater overshoot and longer settling time than the corresponding two integrator servo. With the aid of a simple lead network, a two integrator servo can be stabilized at all gains. On the other hand, a three integrator servo always is unstable for some range of gains, running from zero to some finite value of gain. The three integrator servo is unusual in that it is unstable for low values of gain and stable for large values of gain; on this basis, when the loop gain falls below a critical gain the three integrator servo becomes unstable. Decreases in gain below the critical value can be expected due to amplitude scintillation and transient conditions. The two integrator servo may overshoot so that the mean of the noisy signal will be nearer the edge of the gate during the transient portion of the response. During this response period, the range is greatest (a condition where low S/N ratio exists) and the probability of loss is the greatest. From this viewpoint, the one integrator servo seems to offer advantages because the one integrator servo with a single additional time lag is always stable.

An investigation of the constraints on loop gain, as introduced by dynamic range limitations, is important. Consider the response of both frequency and phase-locked (one and two integrator) servos to a step input and a ramp input in frequency. From Equations 7-115 and 7-130, the open loop transfer function for both phase and frequency locked loops is

$$Y(S) = k_1 k_2 Y_d(S) = K Y_d(S) \qquad (7\text{-}165)$$

where

$Y_d = Y\phi(S)$ for the phase locked case

$= Y_f(S)$ for the frequency locked case

$\omega_c = \omega_o = 0$ for convenience

$K = k_1 k_2$ = frequency invariant loop gain

In the one integrator loop

$$Y(S) = \frac{K}{S} = \frac{1}{St_o} \tag{7-166}$$

where $t_o = \frac{1}{K}$ = loop time constant = (loop gain)$^{-1}$

For the two integrator loop

$$Y(S) = \frac{K(S + a)}{S^2} \tag{7-167}$$

A step input in frequency can be represented as

$$f_i = \left| f_d \right| \mu(t) \tag{7-168}$$

$$\theta_i = \int_o^t f_i(t)\, dt = \left| f_d \right| t\, \mu(t) \tag{7-169}$$

where

$$f_d = \frac{2f_c v}{c} = \frac{2v}{\lambda} \tag{7-170}$$

A ramp input in frequency can be represented as

$$f_i = \left| \dot{f}_d \right| t\, \mu(t) \tag{7-171}$$

$$\theta_i = \int_o^t f_i(t)\, dt = \frac{\left|\dot{f}_d\right| t^2}{2} \mu(t) \tag{7-172}$$

where

$$\dot{f}_d = \frac{2\dot{v}}{\lambda} = \frac{2a}{\lambda} \tag{7-173}$$

First neglect the effect of the velocity gate on the servo tracking function. This assumption is justified if the servo closed loop bandwidth is much less than the velocity gatewidth and if the servo is tracking near the center of the gate. The error for the frequency-locked case is, therefore,

$$\epsilon_f(S) = \frac{f_i(S)}{1 + Y(S)} \tag{7-174}$$

and for the phase-locked case

$$\epsilon_\theta(S) = \frac{\theta_i(S)}{1 + Y(S)} \tag{7-175}$$

The single integrator loop responses for a step input in frequency are:

Frequency locked:

$$\epsilon_f(S) = \frac{f_i(S)}{1 + \frac{1}{St_o}} = \frac{St_o \frac{|f_d|}{S}}{St_o + 1} = \frac{|f_d|}{S + \frac{1}{t_o}} \tag{7-176}$$

$$\epsilon_f(t) = |f_d| e^{-t/t_o} \tag{7-177}$$

Phase locked:

$$\epsilon_\theta(S) = \frac{1}{S}\,\epsilon_f(S) = \frac{\left|f_d\right|}{S\left(S + \frac{1}{t_o}\right)} \tag{7-178}$$

$$\epsilon_\theta(t) = \left|f_d\right| t_o \left(1 - e^{-t/t_o}\right) \tag{7-179}$$

Ramp input in frequency:

Frequency locked:

$$\epsilon_f(S) = \frac{St_o \frac{\left|\dot{f}_d\right|}{S^2}}{St_o + 1} = \frac{\left|\dot{f}_d\right|}{S\left(S + \frac{1}{t_o}\right)} \tag{7-180}$$

$$\epsilon_f(t) = \left|\dot{f}_a\right| t_o \left(1 - e^{-t/t_o}\right) \tag{7-181}$$

Phase locked:

$$\epsilon_\theta(S) = \frac{St_o \frac{\left|\dot{f}_d\right|}{S^3}}{St_o + 1} = \frac{\left|\dot{f}_d\right|}{S^2\left(S + \frac{1}{t_o}\right)} \tag{7-182}$$

$$\epsilon_\theta(t) = \left|\dot{f}_d\right| t_o^2 \left(e^{-t/t_o} - \frac{t}{t_o} - 1\right) \tag{7-183}$$

For the double integrator loop to be critically damped,

$$1 + Y(S) = O = S^2 + KS + K_a = \frac{S^2}{K_a} + \frac{S}{a} + 1 \tag{7-184}$$

Let $t_o^2 = \frac{1}{K_a}$, $2t_o = \frac{1}{a}$, so that

$$t_o = \frac{2}{K} = \frac{1}{2a} \tag{7-185}$$

$$a = \frac{K}{4} \tag{7-186}$$

The open loop transfer function is, therefore,

$$Y(S) = \frac{K(S + a)}{S^2} = \frac{Ka}{S^2}\left(\frac{S}{a} + 1\right) = \frac{2St_o + 1}{S^2 t_o^2} \tag{7-187}$$

Observe that a conventional lead network need not be used to obtain this transfer junction; instead, the outputs of a single integrator, $2/St_o$, and a double integrator, $1/S^2 t_o^2$, can be added to give the desired operation. Thus, for the two integrator loop with lead (critically damped)

Step input in frequency:

Frequency locked:

$$\epsilon_f(S) = \frac{f_i(S)}{1 + \frac{2St_o + 1}{S^2 t_o^2}} = \frac{S^2 t_o^2 \frac{|f_d|}{S}}{S^2 t_o^2 + 2St_o + 1} = \frac{St_o^2 |f_d|}{(St_o + 1)^2}$$

$$= \frac{S|f_d|}{\left(S + \frac{1}{t_o}\right)^2} \tag{7-188}$$

$$\epsilon_f(t) = |f_d| \left(1 - \frac{t}{t_o}\right) e^{-t/to} \tag{7-189}$$

Phase locked:

$$\epsilon_\theta(S) = \frac{1}{S}\,\epsilon_f(S) = \frac{|f_d|}{\left(S + \frac{1}{t_o}\right)^2} \tag{7-190}$$

$$\epsilon_\theta(t) = |f_d|\, t e^{-t/to} \tag{7-191}$$

Ramp input in frequency:

Frequency locked:

$$\epsilon_f(S) = \frac{S^2 t_o^{\,2} \frac{|\dot{f}_d|}{S^2}}{S^2 t_o^{\,2} + 2St_o + 1} = \frac{|\dot{f}_d|}{\left(S + \frac{1}{t_o}\right)^2} \tag{7-192}$$

$$\epsilon_f(t) = |\dot{f}_d|\, t\, e^{-t/to} \tag{7-193}$$

Phase locked:

$$\epsilon_\theta(S) = \frac{1}{S}\,\epsilon_f(S) = \frac{|\dot{f}_d|}{S\left(S + \frac{1}{t_o}\right)^2} \tag{7-194}$$

$$\epsilon_\theta(t) = |\dot{f}_d|\, t_o^{\,2} \left[1 - \left(1 + \frac{t}{t_o}\right) e^{-t/t_o}\right] \tag{7-195}$$

The equations show that for both double and single integrator loops in a frequency locked servo, a step input in frequency must be less than $\beta = 1/2$ velocity gatewidth for the system to track at all. A step change

in frequency occurs, for example, at lock-on. The phase locked loop has no limitation as to the size of the frequency step, providing sufficient gain exists in the double integrator case. Except for the frequency step input where a limitation exists in the magnitude of the initial step, the limitation is on the loop gain $1/t_o$.

The analysis has neglected the effect of the velocity gate. If the closed loop bandwidth is very much less than the velocity gatewidth, the effect of this gate can be neglected.

On the basis of systems analysis in the absence of noise, it may be concluded that a frequency locked loop is preferable to a phase locked loop. While it is true that the frequency locked loop is preferable for a relatively wide velocity gate and narrow dynamic range phase detector, in the presence of noise the conventional phase detector is appreciably superior to the conventional frequency discriminator. Furthermore, noise analysis will indicate a higher loop gain for optimum operation than heretofore indicated. The phase detector can be made to have a wider dynamic range than $\pm 90^\circ$, and a low noise frequency detector can be built so that neither of these apparent disadvantages is inherent. The frequency discriminator bandwidth should be at least as wide as the velocity gatewidth. If it is not, the signal may be in the gate but outside the discriminator bandwidth, so that little or no restoring force is applied to the signal and the loop is essentially open. If noise is present, the S/N ratio for such a signal would be very low. It is not apparent from the transient responses and required gains that use of two integrators is preferable to one. Although the steady state error is smaller in the double integrator case and the corresponding closed loop bandwidth is narrower than in the one integrator case, the transient response comes closer to the gate boundary in the double integrator case. This makes the loss probability due to noise fluctuations during the transient overshoot greater for the double integrator than for the single integrator case. It is during this initial transient, however, that the S/N ratio is usually the poorest. Another possible disadvantage of two integrators is that if the signal disappears, the loop will "remember" the last known rate of change of acceleration in the frequency locked case (the acceleration in the phase locked case); if the rate of change of acceleration is not maintained during a signal fade, the target may be lost. This same argument is applicable to any time rate of change of range.

The assumption of critical damping for the two integrator loop should be considered. Although response time is improved with slight underdamping, if noise is present and if the noise is considered as "riding" on the signal as a mean, even though the signal itself does not exceed the dynamic range, the signal plus noise may exceed this range. The probability of loss under these circumstances is greater when the signal is closer to the edge of the gate. Because underdamping causes the response and the error to overshoot, the transient response brings the signal closer to loss than in the corresponding critically damped case, thereby increasing the probability of loss during the transient period. Although transient analysis of the system in the presence of noise is possible, but quite difficult, it will not be attempted in this report.

(c) SIMPLIFIED NOISE ANALYSIS OF A FREQUENCY-LOCKED LOOP

The problem here is that of keeping the probability of loss less than some prescribed minimum while optimizing system parameters in order that the S/N ratio out of the velocity gate be a maximum. Since minimizing the probability of loss represents a difficult analysis problem, the loss rate will be minimized instead. The loss rate is defined as the reciprocal of the mean time to loss. The procedure will consist of minimizing the loss rate with respect to the servo parameters, particularly the closed loop bandwidth. A maximum allowable loss rate is then set in order to determine the parameter values. At the same time, the S/N ratio out of the gate for this optimum system also will be determined. The minimum receivable power then will be determined to find the maximum range of the missile.

The following simplifying assumptions are made in the analysis to follow:

1. The system initially is locked on so that the signal is near the center of the gate.
2. The system is linear with respect to the frequency variable.
3. For mathematical convenience, the reference carrier frequency, velocity gate center frequency, and discriminator crossover are all assumed to be at zero frequency. The servo is analyzed with one integrator in the open loop.
4. The S/N ratio is low so that signal-noise intermodulation products are neglected.
5. The mixer input is a single frequency doppler signal in broadband thermal noise.
6. The velocity gate passband is square with half bandwidth (equivalent audio bandwidth) of β. Its effect on the servo transfer function will be neglected since the signal is assumed to be well within the gate.
7. The discriminator is linear in the region of interest and the slope of the discriminator characteristic is proportional to the input signal level (that is, no limiter).
8. In determining the spectrum out of the discriminator, fluctuations in amplitude on the input will be neglected.
9. The frequency of the VCO is linearly proportional to the control voltage in the region of interest. The VCO output voltage amplitude is constant.

10. The noise bandwidth at the VCO output is sufficiently narrow, compared to the mixer input noise bandwidth, so that the noise at the mixer input appears essentially unchanged at the output. A corollary to this assumption is that the input and VCO frequency noise are almost uncorrelated.
11. The mixer input noise is distributed normally about the doppler signal as a mean. From assumption 10, the implication is that the error (that is, mixer output) frequencies are normally distributed about the signal error frequency as a mean.

The servo block diagram and notation to be used for the analysis appear in Figure 7-30. The input voltage contains signal and noise which can be represented as a sine wave with a time-varying argument so that the time rate of change of this argument is proportional to

$$f_i = f_d + f_N \tag{7-196}$$

where

f_i = input frequency
f_d = doppler frequency (that is, the desired signal)
f_N = noise frequency

In the preceding equation, f_N can be thought of as the resultant, or sum, of a large number of random noise frequencies. Therefore, f_N is a normally distributed stochastic process which is stationary in the steady state and is normally distributed by the central limit theorem. In the equations following, f_t is the frequency of the constant amplitude VCO output voltage. Although f_f is noisy, because of filtering in the velocity gate and $Y_f(s)$, (or, more properly, because of filtering by the servo closed loop passband) the noise bandwidth of f_N is narrow compared to that of f_f. Furthermore, f_N is almost uncorrelated. The mixer output, or "error," is then

$$\epsilon = f_i - f_f = f_d + f_f = \epsilon_s + \epsilon_N \tag{7-197}$$

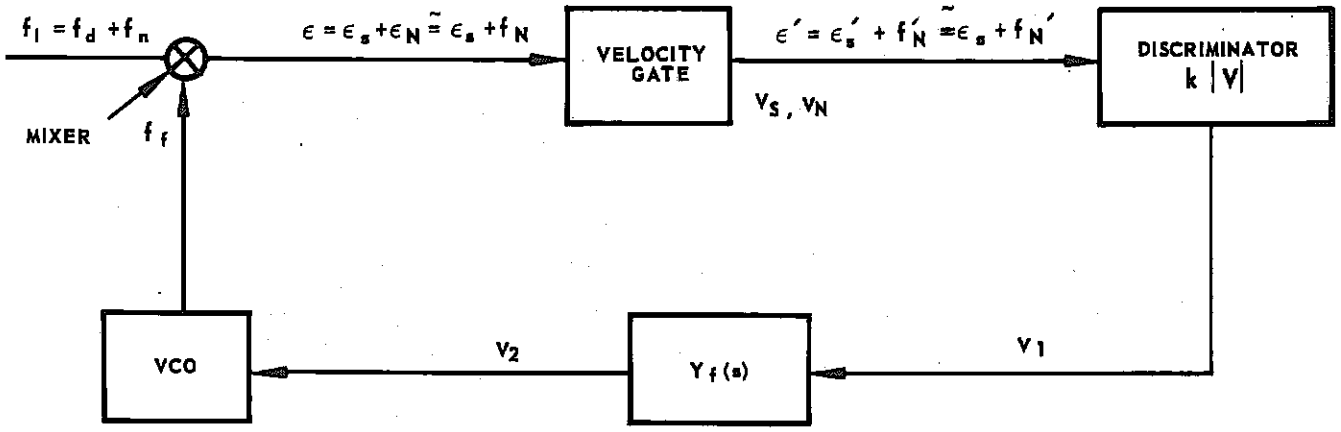

FIGURE 7-30. FREQUENCY-LOCKED SERVO BLOCK DIAGRAM AND NOTATION

where

$$\epsilon_s = f_d - f_f \tag{7-198}$$

$$E_N = f_N \tag{7-199}$$

Note that ϵ_s, the signal error, is noisy because f_f is noisy. It is the signal error ϵ_s that must be minimized since, the velocity servo is required to cause the signal in the gate to approximate the desired doppler signal of frequency f_d. If the gate center frequency is zero, the above condition is satisfied if $\epsilon_s = f_d - f_f$ is minimized rather than $\epsilon = f_i - f_f$, which is the usual servo error. The problem is to synthesize a servo which minimizes ϵ_s according to some criterion, the most common criterion being minimization according to least squares, or in this case minimizing $\overline{\epsilon_s^2}$. This criterion is analyzed although not applied here since the minimum loss rate criterion seems more applicable to this particular problem.

Minimization of the signal error ϵ_s leads to different closed loop transfer functions for signal and noise, as can be seen from the following general analysis.

$$\epsilon_s = f_d - e_f = f_d - \frac{e_i y_o}{1 + y_o} = f_d - \frac{(f_d + f_n)}{1 + y_o} y_o = \frac{f_d}{1 + y_o}$$

$$- \frac{f_n y_o}{1 + y_o} = f_d Y_s - f_n Y_n \qquad (7\text{-}200)$$

where $Y_s = \frac{1}{1 + Y_o}$ = signal transfer function, $Y_n = \frac{Y_o}{1 + Y_o} = Y_o Y_s$ = noise transfer function, and Y_o is the servo open loop transfer function. The noise bandwidth of ϵ_s, much smaller than the noise bandwidth of ϵ_N by assumption, and ϵ_s and ϵ_N are almost uncorrelated. It is important to observe that the fluctuations of ϵ_s cause loss, while the fluctuations of ϵ_N do not. With the assumptions made in this section, the spectrum of f_f will contain a delta function corresponding to f_d after being operated upon by the loop. If the difference between the frequency of this line and f_d lies in the velocity gate, the loop is said to be tracking. Actually, ϵ_s may fluctuate out of the gate and back in again in such a way that the system still is tracking according to the above definition. However, a fluctuation outside the gate when the target is accelerating (that is, $\dot{f}_d > 0$) increases the probability of loss on such a fluctuation (if f_d and the fluctuation are in the same direction). Furthermore, experimental investigations have shown that the target actually is lost most of the time when the signal fluctuates out of the gate. Hence, loss is defined as occurring whenever ϵ_s fluctuates out of the gate i.e., when $|\epsilon_S| > \beta$), regardless of whether or not it fluctuates back in. Although the noise on ϵ_s contributes slightly to the noise on f_f, the noise ϵ_N is the principal contributor. The noise spectrum of f_f will, therefore, be derived only from ϵ_N.

By assumption, the velocity gate has no effect on ϵ_s. If B is the audio bandwidth of the spectrum of f_N, the effect of the velocity gate on $\epsilon_N = f_N$ is to narrow the audio spectral width to β. The output of the velocity gate is, therefore,

$$\epsilon' = \epsilon_s + f_N' \tag{7-201}$$

But if we consider frequencies inside the gate only $f_N' = f_N$

$$f_N' = f_N\left[\mu(f_N) - \mu(f_N - \beta)\right] \tag{7-202}$$

Since no limiter preceding the discriminator has been assumed, the discriminator output is proportional to the amplitude of the input as well as proportional to its frequency. Furthermore, the standard type of frequency discriminator (Foster-Seeley, slope, and others) is nonlinear in that the superposition law does not hold for frequencies even though the slope may be linear. This effect introduces a degradation of the weaker signal. Since signal is less than noise in this case, the signal is degraded by the S/N ratio. If incoherent limiting is used, the degradation is even worse. The commonly used phase detectors, on the other hand, do not introduce nonlinear degradation, and thus represent an argument in favor of phase locked loops. However, it is possible to build frequency discriminators which are very nearly ideal, that is, the voltage output to the sum of two or more frequencies is linearly proportional to their sum. For simplicity this assumption will be made; the effect of practical discriminators is considered later. Now, if V_s is the amplitude of the signal and V_N is the amplitude of the noise at time t, the assumed ideal discriminator develops an output

$$V_1 = k_1\left(\frac{V_s \epsilon_s}{\sqrt{2}} + V_N f_N'\right) = K_s \epsilon_s + K_N \epsilon_N \quad \text{for } \beta \geqslant \epsilon_N \geqslant 0 \tag{7-203}$$

Note that although K_s is a nonrandom constant for V_s = constant, K_N is a random variable.

The voltages V_1 and V_2 are related by

$$V_2(S) = Y_f(S)\ V_1(S) \tag{7-204}$$

For the one integrator case

$$Y_f(S) = \frac{1}{S} \tag{7-205}$$

For the two integrator plus lead case

$$Y_f(S) = \frac{S + a}{S^2} \tag{7-206}$$

An ideal VCO develops a frequency which is proportional to the input control voltage, hence

$$f_f = k_2 V_2 \tag{7-207}$$

The VCO output voltage is then

$$V_f(t) = A_f \cos(\omega_f t + \phi_f) \tag{7-208}$$

From Equations 7-207, -204 and -203 in the region where $0 \leq \epsilon_N \leq \beta$,

$$f_f = k_2\ Y_f V_1 = k_2 Y_f (K_s \epsilon_s + K_N \epsilon_N) = Y_s \epsilon_s + Y_N \epsilon_N \tag{7-209}$$

where

$$Y_s = k_2 K_s Y_f \tag{7-210}$$

$$Y_N = k_2 K_n Y_f \tag{7-211}$$

Observe that

$$Y_N = \frac{Y_s K_N}{K_s} \tag{7-212}$$

But from Equations 7-209, -199 and -198

$$f_f = Y_s(f_d - f_f) + Y_N f_N$$

or

$$f_f = \frac{Y_s f_d + Y_N f_N}{1 + Y_s} = \frac{Y_s}{1 + Y_s}\left(f_d + \frac{K_N}{K_s} f_N\right) \tag{7-213}$$

Similarly

$$f_d - \epsilon_s = Y_s \epsilon_s + Y_N f_N$$

or

$$\epsilon_s = \frac{f_d - Y_N f_N}{1 + Y_s} = \frac{f_d - \frac{K_N Y_s}{K_s} S_N}{1 + Y_s} \tag{7-214}$$

Equation 7-213 shows that the effect of the noise is reduced as K_s/K_N increases. K_s/K_N is related to the S/N ratio. However, since K_N is a random variable, Equations 7-213 and 7-214 are not in a usable form for calculation.

For convenience, neglect the fluctuations in V_1 due to input amplitude fluctuations, since the noise spectral output of the discriminator depends only on frequency variations on the input. The mean output still should depend on the input amplitude. This condition is obtained by assuming that the noise voltage output of the discriminator is proportional to the rms noise amplitude and the instantaneous noise frequency. Since the noise input voltage amplitude and frequency are independent, Equation 7-203 becomes

$$V_1 = k_1\left(\frac{V_S \epsilon_s}{\sqrt{2}} + \sqrt{\overline{V_N^2}}\, f_N'\right) = K_s \epsilon_s + \sqrt{\overline{K_N^2}}\, \epsilon_N \tag{7-215}$$

for

$$\beta \geq \epsilon_N \geq 0$$

Equations 7-213 and 7-214 then become, respectively,

$$f_f = \frac{Y_s}{1 + Y_s}\left(f_d + \sqrt{\frac{\overline{K_N^2}}{K_s}}\, f_N\right) = Y_o\left(f_d + \frac{f_N}{\gamma}\right) \tag{7-216}$$

$$\epsilon_s = \frac{f_d}{1 + Y_s} \quad \frac{Y_s}{1 + Y_s}\sqrt{\frac{\overline{K_N^2}}{K_s}}\, f_N = \frac{Y_o}{Y_s}\, f_d + \frac{Y_o f_N}{\gamma} \tag{7-217}$$

where

$$Y_o = \frac{Y_s}{1 + Y_s} \tag{7-218a}$$

$$Y_s = k_2 K_s Y_f = \frac{k_1 k_2 V_s}{\sqrt{2}}\, Y_f \tag{7-218b}$$

$$\gamma^2 = \frac{K_s^2}{\overline{K_N^2}} = \frac{k_1^2 V_s^2}{2k_1^2\, \overline{V_{N_1}^2}} = \frac{V_s^2}{2\overline{V_N^2}} \tag{7-218c}$$

γ^2 is, therefore, the power S/N ratio at the gate output.

Rice, * shows that for normally distributed noise of mean zero, variance σ^2 and spectral density G(f), the expected number of positive-going crossings per second of a level I is

$$\lambda = \left[\frac{\int_o^\infty f^2 G(f)\, df}{\int_o^\infty G(f)\, df}\right]^{\frac{1}{2}} e^{-\frac{I^2}{2\sigma^2}} \tag{7-219}$$

* S. O. Rice, Math Anal of Random Noise, from "Noise & Stochastic Processes" by Wax, Dover, 1954, P. 193.

where

$$\sigma^2 = \int_0^\infty G(f)/df \tag{7-220}$$

The term lambda, λ , is the loss rate, since the reciprocal of the mean time to loss is simply the expected number of losses per second. It already has been shown that ϵ_s is (approximately) normally distributed. Since Equation 7-219 assumes a normal distribution with zero mean, the concern will be with the variable $\epsilon_s - \overline{\epsilon_s}$. Loss occurs if the signal exceeds the velocity gate cutoff frequency β. Therefore, $I = \beta - \overline{\epsilon_s}$. In Equation 7-219 the spectral density G(f) is $\theta_{\epsilon_s - \overline{\epsilon_s}}(f)$. Since f_d is nonrandom, and $\overline{f_N} = 0$, from Equation 7-217,

$$\overline{\epsilon_s} = \frac{Y_o}{Y_s} f_d \tag{7-221}$$

Hence

$$\epsilon_s - \overline{\epsilon_s} = \frac{Y_o f_N}{\gamma} = Z \tag{7-222}$$

Let the spectral width of f_N be sufficiently wide so that the spectral density of f_N is a constant w_o over the velocity gatewidth $0 \leq f_N \leq \beta$. Hence,

$$G_Z(f) = \frac{G_{f_n}}{\gamma^2} \left| Y_o(j\omega) \right|^2 = \frac{w_o}{\gamma^2} \left| Y_o(j\omega) \right|^2 \tag{7-223}$$

At this point it is necessary to consider $Y_o(j\omega)$. For the single integrator case, from Equations 7-210 and 7-205,

$$Y_s = k_2 K_s Y_f(s) = \frac{k_2 K_s}{s} = \frac{1}{sto} \tag{7-224}$$

where the S/N ratio is varied by varying the noise power, while holding constant the signal amplitude and K_s. The time constant t_o is, therefore, associated with the integrator which is divided by the open loop gain. Hence,

$$Y_o(S) = \frac{Y_s}{1 + Y_s} = \frac{1}{1 + Sto} \tag{7-225}$$

From Equation 7-221, the steady state average error is

$$\overline{\epsilon}_s(t \to \infty) = \lim_{s \to 0} S\overline{\epsilon}_s(S) = \lim_{s \to 0} \frac{sY_o(S)}{Y_s(S)} f_d(s) = \frac{S^2 t_o}{1 + St_o} f_d(S)\Big|_{S \to 0} \tag{7-226}$$

Suppose the target is undergoing a constant acceleration ω relative to the interceptor. From Equation 7-95, the maximum doppler shift is

$$f_d = \frac{2f_c v}{c} = \frac{2f_c}{c} \int_o^t a\,dt = \frac{2f_c}{c} at = k_o t \tag{7-227}$$

$$\therefore f_d(s) = \frac{k_o}{s^2} \tag{7-228}$$

and

$$\overline{\epsilon}_s(t \to \infty) = \frac{t_o k_o}{1 + st_o}\Bigg|_{s \to 0} = k_o t_o \tag{7-229}$$

Similarly, from Equations 7-227 and 7-229,

$$G_Z(f) = \frac{w_o}{\gamma 2} \frac{1}{1 + \omega^2 t_o^2} \tag{7-230}$$

$$\sigma^2 = \int_o^\beta G_Z \ (f)\ df \cong \int_o^\infty G_Z\ (f)\ df$$

$$= \frac{w_o}{\gamma^2} \int_o^\infty \frac{df}{1 + \omega^2 t_o^2} = \frac{w_o}{2\pi t_o \gamma^2} \int_o^\infty \frac{dx}{1 + X^2}$$

$$= \frac{w_o}{2\pi t_o \gamma^2} \left[\tan^{-1}(\infty) - \tan^{-1}(0) \right] = \frac{w_o}{2\pi t_o \gamma^2} \frac{\pi}{2} = \frac{w_o}{4 t_o \gamma^2} \qquad (7\text{-}231)$$

where $G_Z\ (f) \cong 0$ at $f = \beta$ so that the upper limit β can be replaced by infinity to give an approximate result.

Similarly,

$$\int_o^\beta f^2 G_Z(f) df = \frac{w_o}{(2\pi t_o)^3 \gamma^2} \int_o^{2\pi t_o \beta} \frac{X^2 dX}{1 + X^2}$$

$$= \frac{w_o}{(2\pi t_o)^3 \gamma^2} \left. (X - \tan^{-1} X) \right|_o^{2\pi\beta t_o}$$

$$\cong \frac{w_o}{(2\pi t_o)^3 \gamma^2} \left[2\pi\beta t_o - \frac{\pi}{2} \right]$$

$$= \frac{w_o}{16\pi^2 t_o^3 \gamma^2} (4\beta t_o - 1) \qquad (7\text{-}232)$$

From Equation 7-229

$$I = \beta - \overline{\epsilon_s} = \beta - k_o t_o \qquad (7\text{-}233)$$

Hence, substituting Equations 7-233, -232 and -231 in Equation 7-219,

$$\lambda = \left[\frac{\dfrac{w_o}{16\pi^2 t_o^3 \gamma^2}(4\beta t_o - 1)}{\dfrac{w_o}{4t_o\gamma^2}} \right]^{\frac{1}{2}} \exp - \frac{(\beta - k_o t_o)^2}{\dfrac{w_o}{2t_o\gamma^2}}$$

$$= \left(\frac{4\beta t_o - 1}{4\pi^2 t_o^2} \right)^{\frac{1}{2}} \exp - \frac{2 t_o \gamma^2}{W_o} (\beta - k_o t_o)^2 \qquad (7\text{-}234)$$

But it is assumed that $\beta \gg \frac{1}{t_o}$; hence,

$$\lambda \cong \frac{1}{\pi} \sqrt{\frac{\beta}{t_o}} \exp \frac{-2\, t_o \gamma^2}{w_o} (\beta - k_o t_o)^2 \qquad \beta t_o \gg 1 \qquad (7\text{-}235)$$

Now the procedure is to minimize the loss rate, λ, with respect to t_o. This can be done approximately by maximizing the exponent with respect to t_o. Thus,

$$-k_o^2 t_o (\beta - k_o t_o) + (\beta - k_o t_o)^2 = 0$$

$$\beta - k_o t_o = 2 k_o t_o$$

$$t_o = \frac{\beta}{3k_o} \qquad (7\text{-}236)$$

The corresponding closed loop bandwidth is

$$\beta_c = \frac{1}{2\pi t_o} \qquad (7\text{-}237)$$

It now remains to find the voltage S/N ratio needed to maintain track in this optimized system.

From Equation 7-235,

$$\gamma^2 \cong \frac{w_o}{2t_o(\beta - k_o t_o)^2} \quad n \quad \frac{1}{\pi\lambda}\sqrt{\frac{\beta}{t_o}} \tag{7-238}$$

It remains to determine w, the <u>noise frequency</u> spectral density. It is shown in Threshold Signals* that the frequency spectral density of Gaussian noise after passage through a square passband of width B is

$$G(f) = 2\pi B\int_0^\infty dx \cos\frac{2fx}{B}\ \frac{\sin^2 x - x^2}{x^2 \sin^2 X}\ \ln\left(1 - \frac{\sin^2 x}{x^2}\right) \tag{7-239}$$

This integral is accomplished numerically with the following results

$\frac{f}{B} = y$	$\frac{G(f)}{4\pi B} = G(y)$
0	.955
.1	.816
.2	.698
.3	.586
.4	.501
.5	.428
.6	.373
.7	.329
.8	.295
.9	.266
1.0	.242

Table 7-1 Numerical result of Equation 7-239

In this simplified analysis, w_o is considered uniform across the velocity gatewidth β. The equivalent constant noise density w_o is found from the above table by equating noise power over $B = \beta$. This procedure is valid since w_o is actually the spectral density of f_N', which means the spectral density of that portion of f_N lying in the region

* Lawson and Uhlensbeck, MIT Radio Laboratory Series No. 24, McGraw-Hill, p. 374

$0 \leq f_N \leq \beta$. Thus,

$$w_o = \frac{1}{\beta} \int_o^{\beta} G(f)df = 4\pi\beta \int_o^1 G(y)\ dy \qquad (7\text{-}240)$$

Hence, from Equations 7-238 and 7-240, if β = 1000 cps, a target is accelerating at a 10g rate compared to the interceptor, and a loss rate specified as .01 sec^{-1}, the optimum $t_o \cong 1/20$ sec and the S/N ratio γ in the gate must approximate unity.

The loss rate also is greatly dependent on t_o, particularly for small values of t_o. A plot of λ versus t_o is represented by Figure 7-31. Thus, small experimental errors in measurement of S/N ratio or loop gain will have a great effect on measured loss rate.

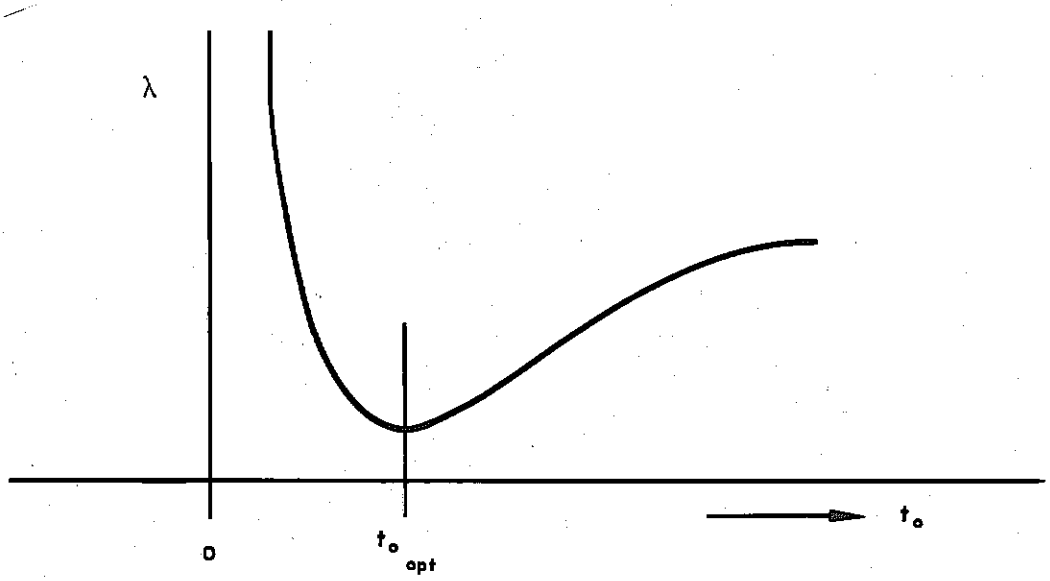

FIGURE 7-31. TYPICAL PLOT OF LOSS RATE VERSUS SERVO LOOP TIME CONSTANT

In the absence of noise, the maximum time constant is

$$t_o = \frac{\beta}{k_o} \qquad (7\text{-}241)$$

The loss rate for this case is

$$\lambda = \frac{1}{\pi}\sqrt{\frac{\beta}{t_o}} \tag{7-242}$$

Hence, the effect of noise is to increase the loop gain from the minimum requirements for steady state tracking at the edge of the gate. Furthermore, the steady state error is the largest error permissible in frequency response to a ramp input. The loss rate increases from the optimum, t_o, as the gain, $1/t_o$, decreases since the mean of the noise (i.e., the signal) is close enough to the edge of the gate to cause many crossings. The loss rate increases as the gain, $1/t_o$, increases from the optimum. This occurs because the noise distribution about the signal is excessively wide, and even though the mean is near the center of the gate, a large number of crossings occur, providing $\beta_{t_o} >> 1$, (that is, providing the gatewidth is still large compared to the loop gain in sec^{-1}). Equations 7-234 and 7-235 are incorrect for $\beta_{t_o} >> 1$. In this case, Equation 7-231 becomes

$$\sigma^2 = \frac{w_o}{2\pi t_o \gamma^2}\left(\tan^{-1} 2\pi\beta t_o - \tan^{-1} 0\right)$$

$$\cong \frac{w_o}{2\pi t_o \gamma^2}\, 2\pi\beta t_o = \frac{w_o \beta}{\gamma^2} \tag{7-243}$$

and Equation 7-232 becomes

$$\int_o^\beta f^2 G_Z(f)\, d f = \frac{w_o}{(2\pi t_o)^3 \gamma^2}\left[2\pi\beta t_o - \tan^{-1} 2\pi\beta t_o\right]$$

$$\cong \frac{w_o}{(2\pi t_o)^3 \gamma^2}\left[2\pi\beta t_o - 2\pi\beta t_o + \frac{(2\pi\beta t_o)^3}{3}\right] = \frac{w_o \beta^3}{3\gamma^2} \tag{7-244}$$

and the loss rate becomes , from Equation 7-219

$$\lambda \cong \left[\frac{w_o\beta^3}{3\gamma^2} \cdot \frac{\gamma^2}{w_o\beta}\right]^{\frac{1}{2}} \exp - \frac{(\beta - k_o t_o)^2}{\frac{w_o\beta}{\gamma^2}}$$

$$= \frac{\beta}{\sqrt{3}} \exp \frac{-\gamma^2(\beta - k_o t_o)^2}{w_o\beta} \qquad \beta t_o << 1 \qquad (7\text{-}245)$$

Note that if $\beta t_o << 1$ and γ^2 = constant, as $t_o \longrightarrow 0$, the loss rate becomes independent of the loop gain and dependent (linearly dependent, since w_o = constant x β) only on the velocity gatewidth, because this now is the limiting factor on the noise width and the noise power.

It is interesting to investigate the variation of λ with the gatewidth β. If the system is tracking near the edge of the gate, the loss rate increases with increasing β because more noise is passed by the wider gate. However, for $\beta > k_o t_o$, $\beta > \frac{w_o}{\gamma 2}$, and $\beta t_o >> 1$, the loss rate decreases with increasing β because, despite additional noise, the signal can fluctuate without loss over a wider region.

(d) THE RANGE TRACKING SERVO

The range tracking servo uses a range gate to discriminate against noise and extraneous targets by means of time discrimination or multiplexing.

Range gating improves the signal-to-noise ratio of the scan modulated video. This improvement makes tracking more accurate and the interceptor control signals less noisy. One of the required inputs to the computer is the absolute range from the target to the interceptor and this range measurement is provided by the range tracking loop. A determination of optimum parameters for the loop follows a procedure similar to that used in the analysis of the velocity tracking loop. The functional block diagram of the system is shown in Figure 7-32.

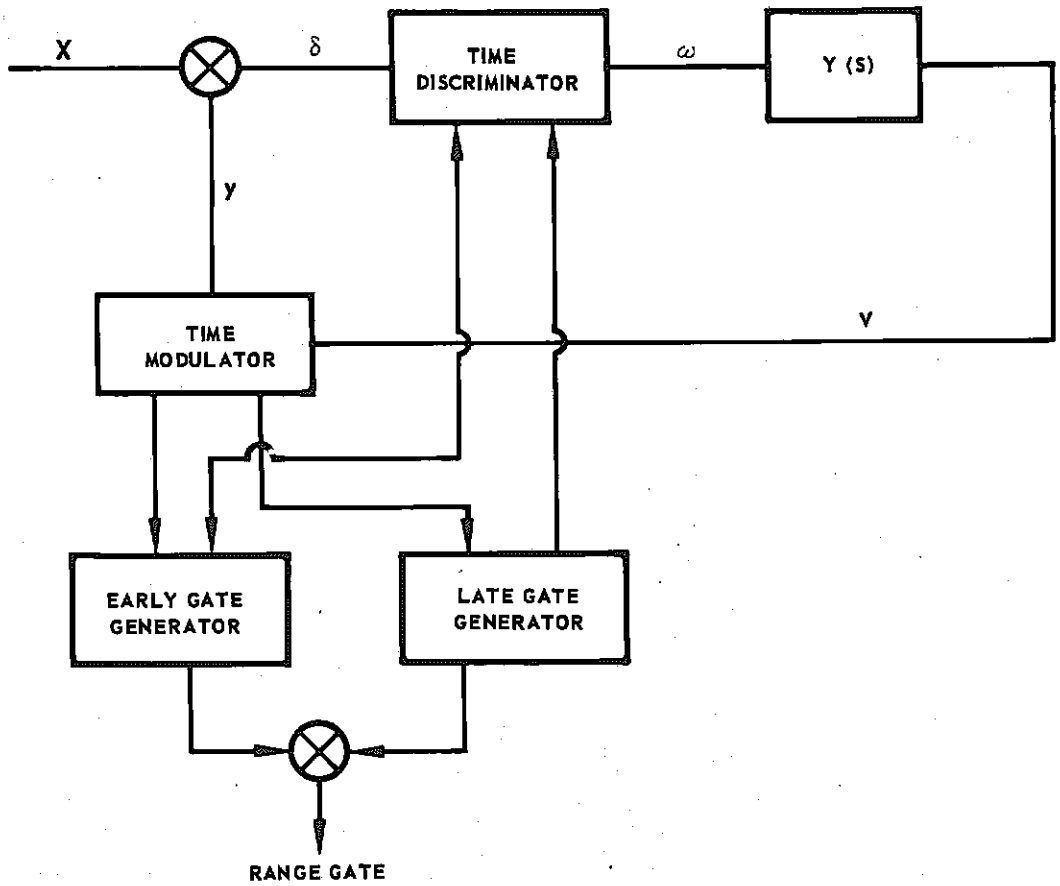

FIGURE 7-32. FUNCTIONAL BLOCK DIAGRAM OF THE RANGE TRACKING UNIT

Note that the range tracking unit is very similar to the general functional diagram of the tracking unit of Figure 7-23. The comparator in the velocity tracking case becomes the differencer in the range tracking case, and the demodulator becomes the time discriminator. Both demodulators are followed by a servo operator Y(S), and both drive a modulator. In the velocity tracking case, the modulator is a voltage controlled oscillator, (VCO), while in the range tracking case it is a time modulator. There is a difference in the gating arrangement. In the velocity tracking case, the gate follows the comparator and, therefore, is within the tracking loop. In the range tracking case, the input video, contrastingly, has already been range gated so that the gating occurs external to the tracking loop. The output of the time modulator is a voltage which is proportional to the delay of the range gate from the position of zero range, i.e., from the

synchronizing pulse. This voltage is a measure of the absolute range of the target from the interceptor. The input represents the position of the center of the video pulse measured from the main bang. The range error δ is given by

$$\delta = x - y \tag{7-246}$$

and is applied to the time discriminator from which there will be an output w given by

$$w = k_1(\underline{S}\,\delta + N) \tag{7-247}$$

Note that the slope of the discriminator characteristic w versus δ is proportional to the absolute signal level $\underline{S}$, whereas the noise is not. This is by direct analogy with the discussion relating to the different transfer functions for signal and noise as contained in the velocity tracking section. The effect of noise on the discriminator characteristic is to make the output fluctuate from the average discriminator characteristic which is shown in Figure 7-33. Since the average value of the noise is $\overline{n} = 0$, then $\overline{w} = k_1\underline{S}\delta$ represents an equation of a straight line. This curve is represented by the straight line b in Figure 7-33. The true discriminator characteristic is more of the form of curve a, which takes into account the nonlinearities of the system. To simplify the analysis, it is assumed that the discriminator characteristic is linear over the range of interest, i.e., curve b in Figure 7-33 will be used. Following a similar argument presented in connection with the velocity tracking servo, the servo operator transfer function Y(S) is assumed to be a single integral or

$$Y(S) = \frac{k_2}{S} \tag{7-248}$$

The split gate comparator, or the time discriminator, and the terminology for the comparator are shown in Figure 7-34.

In Figure 7-34, t_g is the half gatewidth and t_p is the pulsewidth. The output of the time discriminator is the quantity w. After w is operated on by Y(S), the output of Y(S) is V. The time modulator is assumed to be a linear transducer relating the time displacement, y, of the gate to the control voltage, V, out of the transfer function Y(S). Let this relationship be

$$Y = k_3 V \tag{7-249}$$

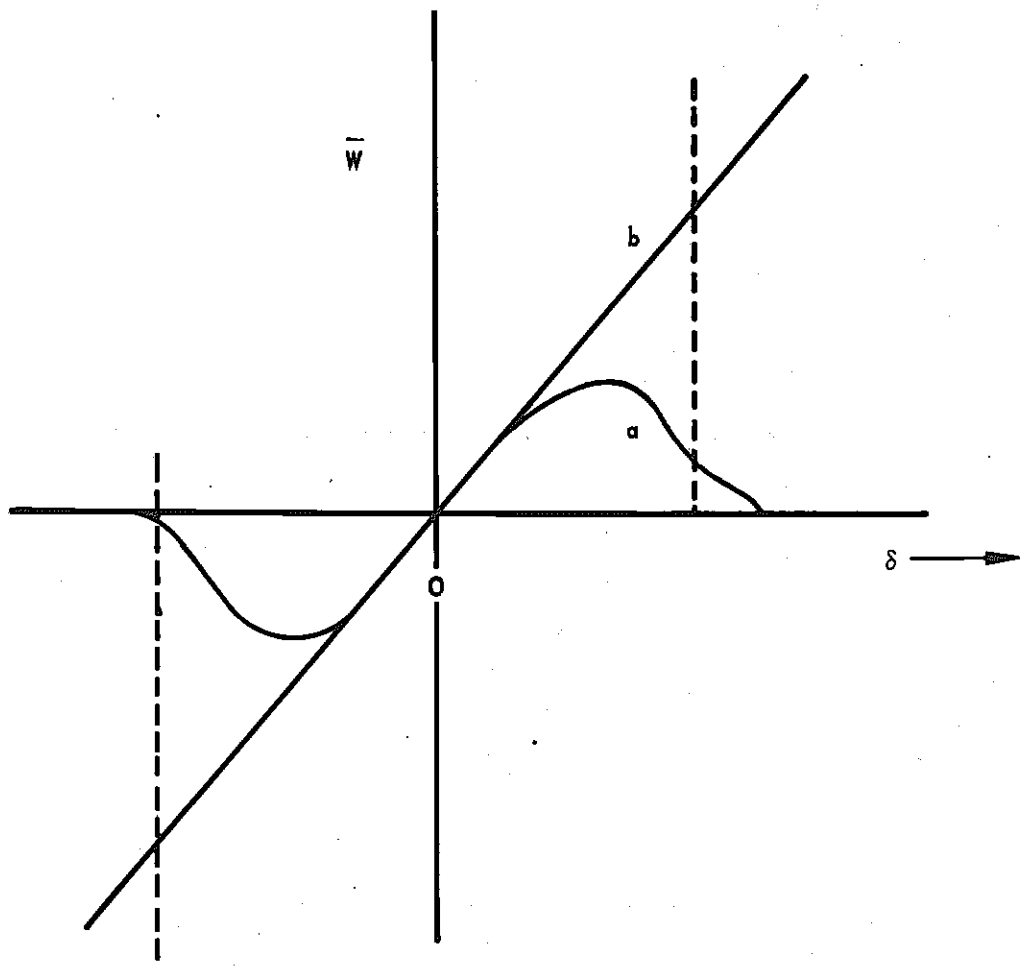

FIGURE 7-33. (a) ACTUAL ERROR SIGNAL VOLTAGE Vs ERROR (b) LINEAR APPROXIMATION TO (a)

If Equations 7-246 through 7-249 are combined, there results,

$$\therefore y = k_3 V = \frac{k_3 k_2}{S} w = \frac{k_3 k_2 k_1}{S} \left[\underline{S}\,\delta + N \right]$$

$$= \frac{k_3 k_2 k_1 S}{S} \left[\delta + N/\dot{S} \right] = \frac{1}{st_o} \left[x - y + \frac{N}{\underline{S}} \right] \qquad (7\text{-}250)$$

or

$$y = \frac{X + \frac{N}{S}}{1 + st_o} \tag{7-251}$$

or

$$t_o\dot{y} + y = X + \frac{N}{S} \tag{7-252}$$

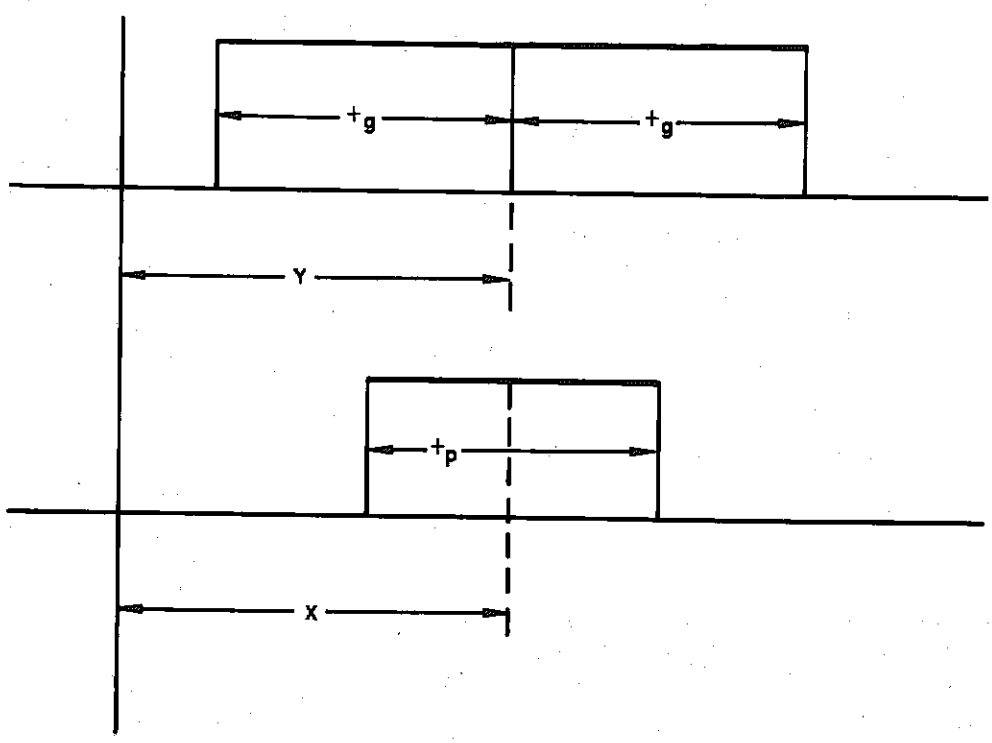

FIGURE 7-34. SPLIT GATE COMPARATOR

where

$$t_o = \frac{1}{k_3 k_2 k_1 S} \tag{7-253}$$

The servo equation is 7-252. The parameter to be optimized is t_o, the servo time constant. In order to find the steady state displacement for a step input in position of the target, consider an input described by

$$\dot{X} = \mu(t) V_m \tag{7-254}$$

or

$$X(s) = \frac{V_m}{s^2} \tag{7-255}$$

The error in this case is

$$\delta = x - y = -\frac{X + \frac{N}{\underline{S}}}{1 + st_o} + X = X\left(\frac{st_o}{1 + st_o}\right) - \frac{N/\underline{S}}{1 + st_o} \tag{7-256}$$

and the steady state error for the mean, where it is assumed that $\overline{N} = 0$, is

$$\overline{\delta}(t \longrightarrow \infty) = \lim_{s \longrightarrow 0} s \cdot \frac{1}{s^2} \cdot \frac{st_o}{1 + st_o} = t_o V_m . \tag{7-257}$$

Since the noise and signal are independent and the differential equation of the servo is linear, the standardized variable $S - \overline{\delta}$ is given by

$$\left| S - \overline{\delta} \right| = \pm \frac{N/\underline{S}}{1 + st_o} \tag{7-258}$$

and the spectrum of this normalized variable is

$$G_{s - \overline{\delta}}(f) = \frac{\overline{N^2}}{\underline{S}^2} \cdot \frac{1}{1 + \omega_o^2 t_o^2} \tag{7-259}$$

Note the inverse dependence of the spectral density of $\underline{S}^2$, where $\underline{S}$ is the signal. This constant of proportionality is the inverse of the slope of the control function or discriminator characteristic and thus implies that there is less random error when the slope is large; that is, the effect of the noise goes down as the signal goes up. Equation 7-259 gives the spectral density of the error measured from the mean in terms of the noise spectrum. The noise considered here is that which is leaving the comparator circuit; that is, it is the noise which is left when the signal plus noise is integrated in each half of the double gate and the two integrals subtracted. The time discriminator may be instrumented by using two parallel switches, one being gated on by the early gate and the other by the late gate, so that the early gate adds to the summing element and the late gate subtracts therefrom (see Figure 7-35).

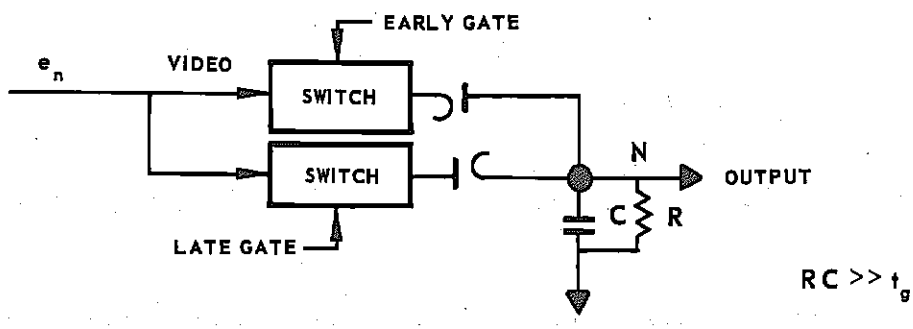

FIGURE 7-35. RANGE GATE COMPARATOR

The averaging time constant RC in Figure 7-35 is long compared to t_g, the half-gate width. For noise alone, each time the gate is turned on, a quantity of charge q_k is deposited on or subtracted from the capacitor C. This quantity is given by

$$q_k = b \int_0^{t_g} e_n^2 \, dt - b \int_{t_g}^{2t_g} e_n^2 \, dt \qquad (7\text{-}260)$$

where b is a constant and e_n is the noise voltage in the IF. A square law detector has been assumed and the integrals of Equation 7-260 are taken over the squared noise voltages. If the signal is much smaller than the noise, then the signal-noise intermodulation products can be neglected in evaluating the mean square value. The standard deviation of the variable

in Equation 7-260 is denoted by σ_q. The voltage N appearing across R will be a function of time as shown in Figure 7-36.

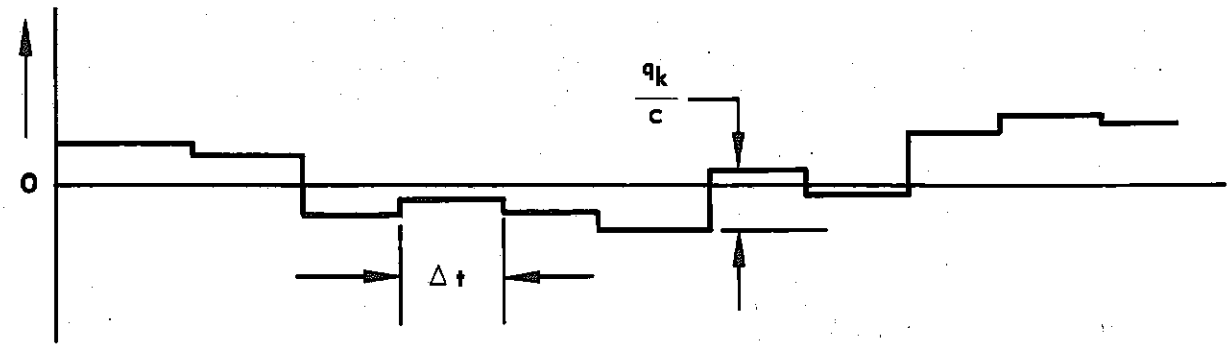

FIGURE 7-36. NOISE OUTPUT OF INTEGRATOR

The time between the steps in this curve is Δt, which is the reciprocal of the repetition frequency. The change in N at each step is $q_{n/c}$. The voltage at any time is determined as the weighted sum of all the voltage increments ever added to C, or

$$N(t) = \sum_{k=-\infty}^{t/\Delta t} \frac{q_k}{c} \exp\left(-\frac{t - k\Delta t}{T_o}\right) \tag{7-261}$$

N(t) is normally distributed by the central limit theorem, and it has a variance given by

$$\overline{N^2} = \sigma_N^2 = \sum_{k=-\infty}^{t/\Delta t} \frac{\sigma_q^2}{C^2} \exp\left(-\frac{2(t - k\Delta t)}{T_o}\right) \tag{7-262}$$

Approximating this sum by an integral yields

$$\overline{N^2} \cong \int_{-\infty}^{t} \frac{\sigma_q^2}{C} \exp\left(-\frac{2(t - \tau)}{T_o}\right) \frac{d\tau}{\Delta t} \cong \frac{\sigma_q^2}{C^2} \frac{T_o}{2\Delta t} \tag{7-263}$$

Equation 7-263 is the mean square value of N. In Figure 7-36, the current pulses, which can be represented as I_n, are discrete random pulses. Assume no correlation between pulses, which is a good approximation if the IF bandwidth is large compared to the repetition frequency, and also

assume that the amplitudes are normally distributed by the central limit theorem. When the sum in Equation 7-262 was replaced by an integral in Equation 7-263, in effect the discontinuities in N were brought very close together, thus decreasing their amplitudes proportionally. A similar assumption may be made for I_n by letting the pulses get very close together but still with no correlation. Such a waveform has a very wide spectrum, essentially constant. Let the spectral density for I_n be a constant, w_o, up to a very high frequency. Then, from Figure 7-36, the voltage is related to the noise current by

$$N(S) = i(S)\left(\frac{R/cs}{R + \frac{1}{cs}}\right) = \frac{i(S)R}{ST_o + 1} \tag{7-264}$$

The noise spectral density is then given by

$$\therefore G_N(f) = \frac{G_i(f)R^2}{\omega^2 T_o^2 + 1} = \frac{w_o T_o^2}{c^2\left[\omega^2 T_o^2 + 1\right]} \tag{7-265}$$

where the noise current spectral density is assumed to be a constant w_o out to high frequencies. The corresponding mean square noise voltage is

$$\overline{N^2} = \int_o^\infty G_N(f)\,df = \frac{w_o T_o}{2\pi c^2}\int_{-\infty}^{\infty}\frac{d(\omega T_o)}{1 + \omega_o^2 T_o^2} = \frac{w_o T_o}{4c^2} \tag{7-266}$$

However, from Equation 7-263

$$\overline{N^2} = \frac{\sigma_q^2}{c^2}\,\frac{T_o}{2\Delta t} \tag{7-267}$$

Equating Equations 7-266 and 7-267 yields a result for w_o the spectral density for the noise current, in terms of σ_q^2, the variance of the charge on the summing capacitor. Thus,

$$w_o = \frac{2\sigma_q^2}{\Delta t} \tag{7-268}$$

Substituting Equation 7-268 into Equation 7-265 yields

$$G_N(f) = \frac{2\sigma_q^2 \; T_o^2}{c^2 \Delta t \; (1 + \omega T_o)} \tag{7-269}$$

The variance of the mean square error, substituting Equation 7-267 into Equations 7-259 and integrating over all frequencies, then becomes

$$\sigma_\delta^2 = \int_{-\infty}^{\infty} G_{S-\overline{\delta}}(f)\, df = \frac{1}{\underline{S}^2} \int_{-\infty}^{\infty} \frac{\sigma_q^2 \; T_o^2}{2\pi c^2 \; t_o 2\Delta t} \; \frac{d(\omega\, t_o)}{1 + \omega_o^2 t_o^2}$$

$$\cong \frac{\sigma_q^2 \, T_o^2}{4 c^2 t_o \Delta t \, \underline{S}^2} \tag{7-270}$$

This mean square error is expressed in terms of the slope S of the control function which can be converted to an IF signal level. If V_s is the peak IF signal level, then the control voltage output for a given displacement δ is

$$e_s = S\delta = bV_s^2 \delta \frac{K_1}{c} \sum_{k=1}^{t/\Delta t} \exp\left[-\frac{1}{T_o}(t - k\Delta t)\right] \tag{7-271}$$

where a square law second detector has been assumed and the optimum condition $t_p = t_g$ is assumed. The factor K_1 is added so that the change in slope of the actual control function can be taken into account. Thus, from Equation 7-271, the slope S is

$$S \cong K_1 \frac{bV_S^2}{c} \; \frac{T_o}{\Delta t} \tag{7-272}$$

Now Equation 7-270 can be written in terms of known parameters by substituting Equations 7-271 and 7-272 back into Equation 7-270, except

for σ_q. This quantity has been calculated by Rice.* The results of this calculation are given as a graph in Figure 7-37. The range of greatest interest is that in which $.5 \leq t_g \Delta f_i \leq 2$, where $t_g \Delta f_i$ is the product of the gatewidth and IF bandwidth preceding the range tracking servo. In this region the following is a good approximation

$$\sigma_q \cong t_g \Delta f_i w_o \tag{7-273}$$

The IF bandwidth Δ_{fi} is assumed to be square and wo is the noise density in the IF, including a factor to take into account the receiver noise. Thus, it follows that

$$\sigma_\delta^2 = \frac{t_g \Delta_{fi}^2 w_o^2 \Delta t}{4 t_o b^2 V_s^4 K_1^2} \tag{7-274}$$

Once the mean square error has been found, the optimum time constant can be determined from the minimum loss rate criterion in exactly the same fashion as in the velocity tracking loop analysis. The velocity track loop analysis showed that the optimum relationship between the time constant and the magnitude of the step in velocity as given by Equation 7-236

$$t_o = \frac{\beta}{3k_o}$$

Similarly, for the tracking case,

$$t_{o\ opt} = \frac{m}{3V_m} \tag{7-275}$$

for a single integrator servo. The term δ_m is the maximum allowable deviation of the center of the range gate from the center of the target. This deviation is just the pulsewidth for the case where the pulsewidth equals the gatewidth. The loss rate criteria used here is the same as that used for the velocity tracking analysis; that is, the expected number of crossings per second of a given level, X, is defined as the loss rate for this level and given by Equation 7-276

*Rice, S.O., "Filtered Thermal Noise-Fluctuation Energy as a Function of Interval Length," Journal of the Acoustical Society of America April, 1943, p. 216.

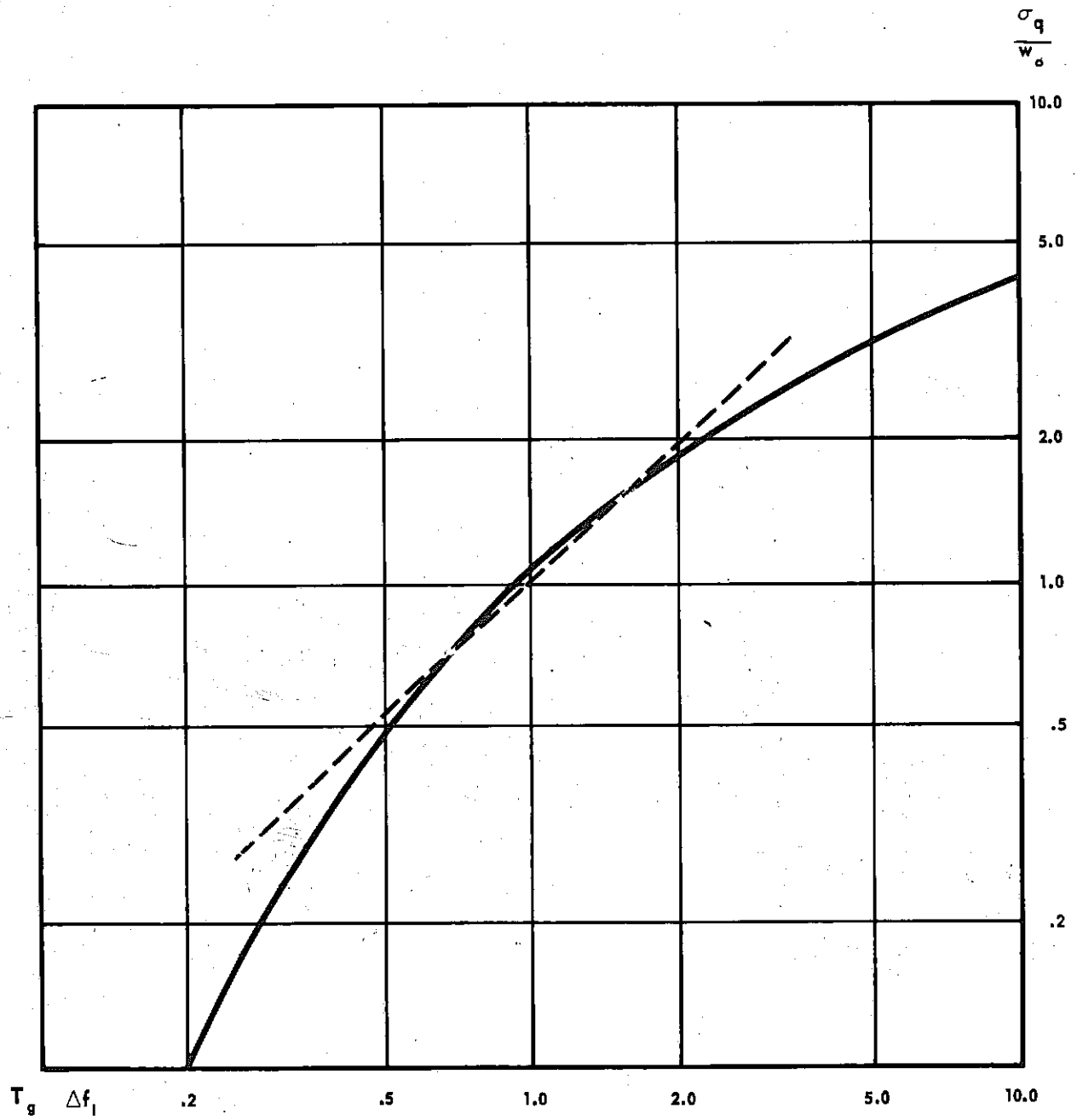

FIGURE 7-37. STANDARD DEVIATION OF CHARGE INCREMENTS T_0 INTEGRATOR CIRCUIT

$$\lambda = Me^{-\frac{(x - x_1)^2}{2\sigma^2}} \tag{7-276}$$

where the variable X is normally distributed with mean zero and a known standard deviation σ. Let the power spectrum of X be uniform from zero frequency to fc and zero at all higher frequencies. In this case M can be written in terms of the cutoff frequency, f_c, or

$$M = \frac{f_c}{\sqrt{3}} \tag{7-276a}$$

The square band equivalent of the power spectrum has a cutoff frequency

$$f_c = \frac{\pi}{2t_o} \tag{7-276b}$$

where the actual spectrum is given by

$$G(f) = \frac{w_o}{1 + \omega^2 t_o^2} \tag{7-277}$$

Equating the total power in the square band equivalent to $\int_o^\infty G(f)df$, or

$$P = w_o f_c = \int_o^\infty \frac{w_o}{1 + \omega^2 t_o^2} df = \frac{w_o \pi}{2t_o} \tag{7-278}$$

It therefore follows that $f_c = \frac{\pi}{2t_o}$, which is Equation 7-276b. Substituting Equation 7-275 into Equation 7-277 and Equation 7-277 into Equation 7-276 and observing that $X - X_1$ is $\delta_{max} - v_m t_o$, where the latter is the steady state displacement of the gate relative to the target pulse for a step input in velocity, it yields the expression for the loss rate,

$$L = \frac{\pi}{2\sqrt{3}t_o} \exp - \frac{(\delta_m - v_m t_o)^2}{2\sigma_\delta^2} \tag{7-279}$$

The optimum t_o which minimizes this loss rate is Equation 7-275. Equation 7-279 can be reduced to a more easily calculated form. The average received power in the IF is

$$P_i = \frac{t_p}{\Delta t} \frac{V_s^2}{2} \tag{7-280}$$

and the gating duty factor is defined by

$$k_g = \frac{t_g}{\Delta t} \tag{7-281}$$

Also, the maximum permissible error may be defined as a fraction of the pulsewidth by

$$\delta_m = K_2 t_p \tag{7-282}$$

Using Equations 7-280 through 7-282 and Equations 7-275 and 7-276, and substituting back into Equations 7-279 yields

$$L \cong .4 \frac{v_m}{t_p} \exp \left[- .2 \frac{P_i^2 t_p \Delta t}{w_o^2 v_m} \right] \tag{7-283}$$

Two other important parameters to be considered are the pulsewidth and the gatewidth and their relationship to each other. The split gate arrangement is shown in Figure 7-38.

The total signal and noise in each half of the gate is integrated and the sum of the two halves is then subtracted in the comparator. This voltage is supplied to the gate positioning circuit in such a manner as to tend to reduce the error to zero. Since the velocity at which the gate moves over is proportional to the error, there must be some error before the gate will move. Therefore, if the target pulse is moving with a constant velocity there must be a constant amount of lag or error in order for the gate to move at the same velocity as the pulse. This constant lag is proportional to the velocity and inversely proportional to the slope of error signal, that is, to the restoring force per unit of lag. It is possible to add higher order derivatives to the control system. For example, one

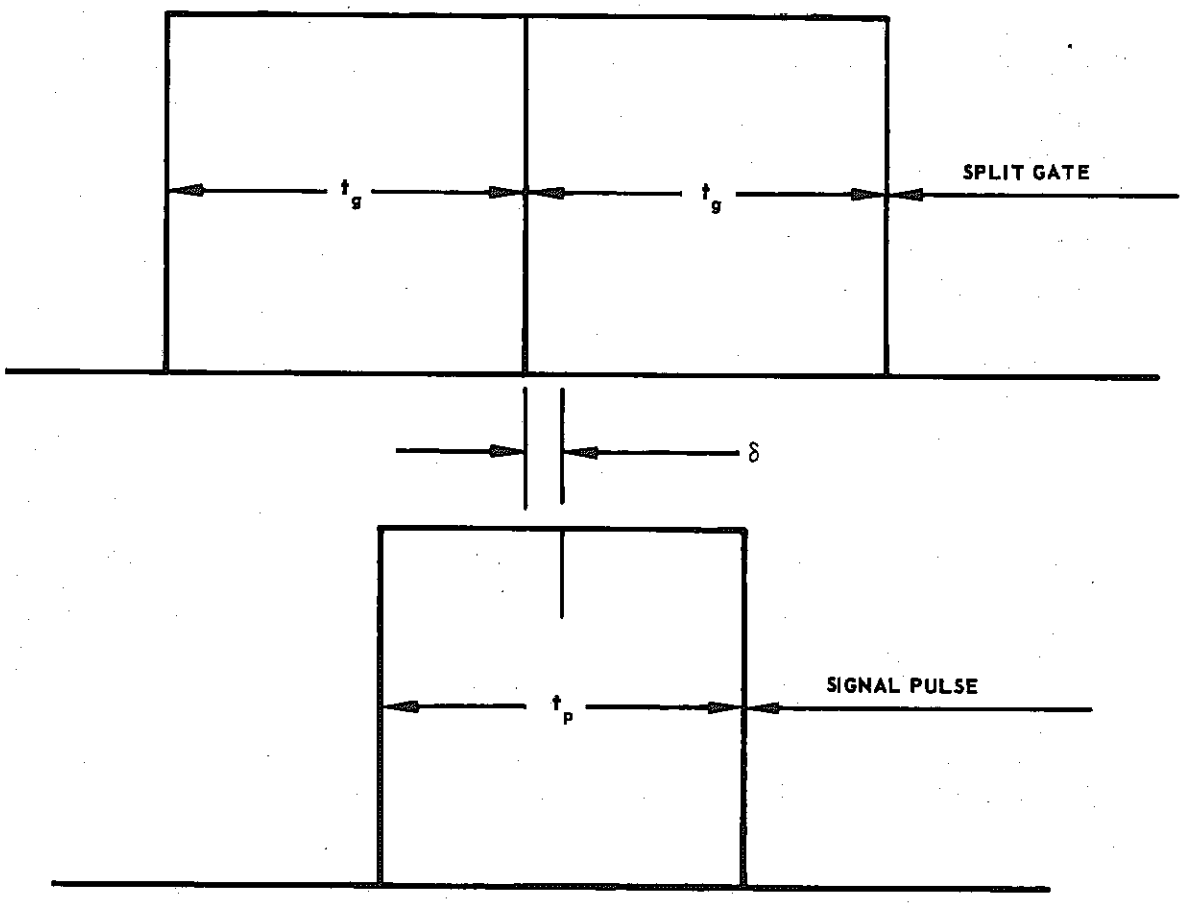

FIGURE 7-38. REPRESENTATION OF SPLIT GATE AND TARGET SIGNAL

could devise a circuit in which a target moving with constant acceleration is followed with fixed lag. Such a servo would follow a constant velocity target with zero lag. This type of servo requires two integrators in the open loop and becomes subject to the difficulties mentioned in connection with the two integrator servo.

The fixed displacement in the steady state, due to constant velocity, can be subtracted from the separation of the target and gate due to noise so that the steady state position of the gate will be in an equilibrium position. From this position, the effects of noise can be calculated. If

only a small amount of noise is added to the signal, then the noise will be of uniform average intensity throughout the range sweep. Therefore, on the average, there will be as much noise in the first half of the gate as in the second half. The average effect of the noise is zero since it cancels when the integrals over the two halves of the gate are subtracted. At any given instant, however, the noise in the two halves of the gate will be different. Therefore, when the subtraction is made instantaneously, there will be a voltage remaining. These successive differences on successive pulses create a noise voltage which tends to move the gate in a random manner about its equilibrium position. As long as the signal is large compared to the noise, this effect is still small, and the gate will be closely centered with only slight deviations due to the noise. As the signal-to-noise ratio decreases, the spread of random error increases. It is possible for the noise over several pulses to force the gate sufficiently off center so that the target gate and target pulse are not aligned. When this happens, the spread of errors becomes unlimited; if there is no restoring force, target loss occurs. The spread of errors in position of the range gate can be calculated from the system parameters and a knowledge of the noise existing at the input to the receiver. When the spread is known, it may be determined at any instant what percentage of errors is likely to cause target loss. It also is possible to determine the probability that the target will be outside the range gate. Target loss is certain if a sufficient time period elapses since there is always a finite probability that errors will add in the same direction. The time that it takes for this to happen is determined by the spread of the errors. If the spread is large, only a short time may elapse before loss occurs. The spread of errors is a function of signal-to-noise ratio, a high S/N ratio corresponding to a small spread. The reciprocal of the average time to loss of the target, as previously mentioned, is defined as the loss rate. When this rate is known, it is possible to define the range in order to evaluate the S/N ratio as a function of range and, therefore, loss rate as a function of range.

Consider the effect of the ratio of the pulsewidth to half-gatewidth, as shown in Figure 7-39a. Here, the total gatewidth $2t_g$ is less than the signal width, t_p. For this case, the graph of control voltage out of the time discriminator in the absence of noise is shown. In this case, the peak control voltage is small and there is a flat dead space in the center of the servo action. By increasing t_g up to $1/2\ t_p$, as shown in Figure 7-39b, the dead space is eliminated and the total range of errors, over

which there is some control voltage, has been increased. The peak control voltage has been increased, but so has the noise in the same proportion; therefore, there is no gain in this direction.

The increased control range is a definite advantage, however, since this is directly related to the point of target loss. Thus, even though the S/N ratio remains constant, the gate is permitted to wander more and the loss rate will be correspondingly lower. In Figure 7-39c, $t_g = t_p$. Here there is no more improvement since the control range has been increased appreciably without dead space. By this means, a lower loss rate can be obtained, providing the signal-to-noise ratio has not been decreased. Evidently there is about twice as much signal and roughly twice as much noise, so an improvement occurs. The slope of the control curve or discriminator characteristic is approximately twice what it was in Figure 7-39b. As was previously pointed out, the fixed error for a target traveling at a constant velocity is inversely proportional to the slope of the discriminator characteristic and, therefore, this fixed error is smaller for Figure 7-39c than for Figure 7-39b. With a smaller fixed error due to target motion, there is more room for random gate motion due to noise. This happens because the equilibrium position is not so close to the edge of the gate and the edge of the discriminator characteristic. A lower loss rate is then attainable for a given S/N ratio as the case shown in Figure 7-39c as opposed to that shown in -39d and -39b.

Suppose that t_g is greater than t_p, as shown in Figure 7-40. The control range is increased here, but neither the slope through the origin nor the peak control voltage has been increased. The fixed error due to target motion and the maximum signal are the same as in Figure 7-39c, but there is more noise and more room for error target loss. This situation appears to have no particular advantage over the case in Figure 7-39c. However, from the viewpoint of rejecting multiple targets and extraneous jamming it is desirable that the range gate be as narrow as possible. From these considerations it can be concluded that the situation shown in Figure 7-39c (i.e., $t_g = t_p$) is probably the optimum.

Another factor to be optimized is the IF bandwidth preceding the range track servo. In the double gate time discriminator, the total signal-plus-noise in each half of the double gate is integrated and the results subtracted. This provides an error voltage which corrects the position of the gate. The noise amplitude in each gate will depend on the system gain and the bandwidth of the IF. The gain is unimportant since

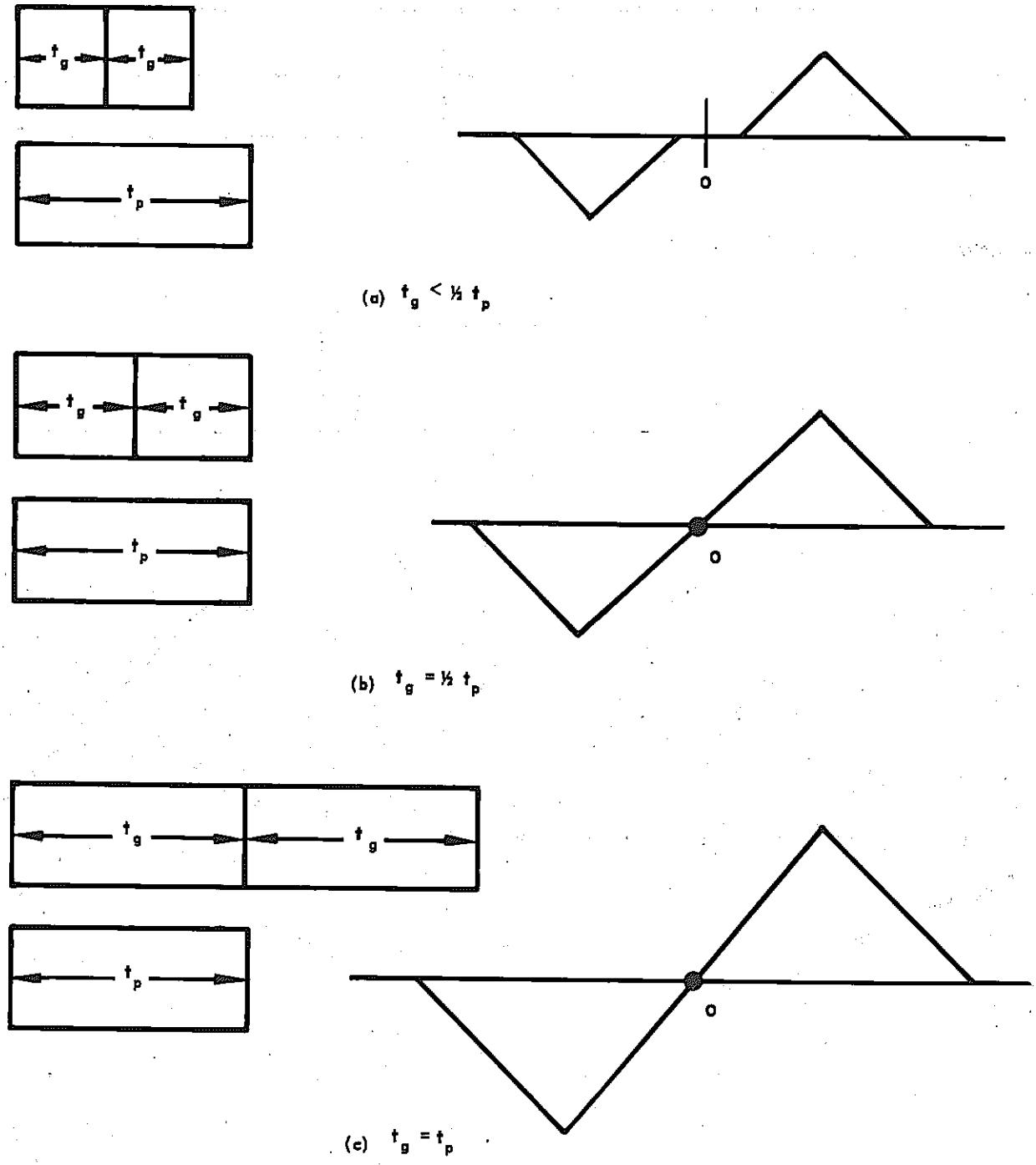

FIGURE 7-39. EFFECT OF VARYING THE GATEWIDTH COMPARED TO THE PULSEWIDTH ($t_p \leq t_g$)

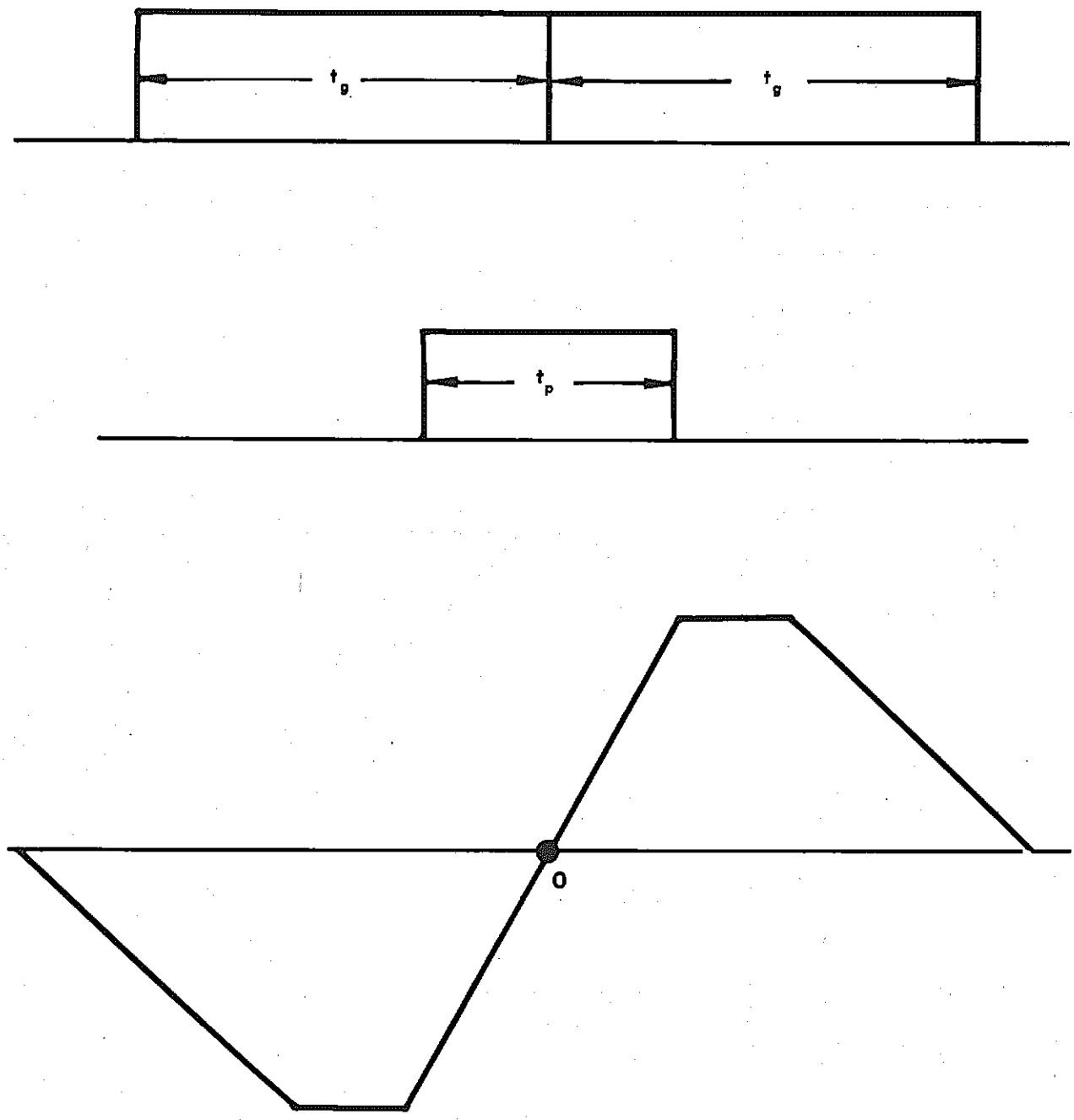

FIGURE 7-40. EFFECT OF VARYING THE GATEWIDTH COMPARED TO THE PULSEWIDTH ($t_P \geq t_g$)

it changes both the signal and the noise by the same amount, but the IF bandwidth Δf_i is important since the amount of noise passed by an amplifier is directly dependent on its bandwidth. Thus, the greater the bandwidth, the more noise is passed, and this has the effect of spreading the correction voltage and producing a greater loss rate. From this point of view it is advantageous to narrow the bandwidth as much as possible. However, the IF bandwidth cannot be made much narrower than the reciprocal of the pulsewidth because of pulse distortion. A suitable amount of distortion, in which the peak of the pulse is reached at roughly the trailing edge of the pulse occurs when $t_p \Delta f_i \cong 2$. The noise in this case is small, yet the peak amplitude has not been reduced. This condition is probably optimum for visual indication since the peak signal amplitude is important for pilot scope readout. However, the analysis shows that for automatic tracking, the optimum occurs when $t_g \Delta f_i \cong \frac{1}{2}$, which is approximately one-quarter the bandwidth used in a typical visual system. The reason for this is that a reduction in bandwidth reduces noise power linearly, while it merely spreads the signal over more time while reducing its amplitude at less than a linear rate. Thus, with wide gates most of the signal reaches the integrator while at the same time noise is reduced. However, this process cannot be carried out indefinitely and, therefore, the optimum is as indicated.

The analysis has shown that the optimum servo time constant is approximately one-third the ratio of the maximum range error to the magnitude of the step input in velocity. This conclusion can be justified since the time constant is inversely proportional to the slope of the discriminator curve. For example, if the target were suddenly moved to one side, the speed of response would be proportional to the restoring force which, in turn, is proportional to the slope of the error curve. Since there is a shift of the equilibrium point when the target is moving with constant velocity, this shift is proportional to the time constant because it is inversely proportional to the slope of the error curve. If the shift is held to a small value, the equilibrium point does not move close to the edge of the gate, where the target can be lost, allowing the number of losses per second to be small. In order to hold the fixed lag to a small value, a short time constant must be used. A circuit with a short time constant is roughly equivalent to a low pass filter of large bandwidth. With a large bandwidth more noise is passed; hence, it must be concluded that a long time constant means less noise. The implication is that some compromise must be reached. If the circuits involved in

limiting the bandwidth to noise were linear, then the bandwidth of the system bandwidth would be a combination of the different bandwidths. Since the IF bandwidth is optimized in order to pass the pulse with little distortion and with minimum noise, it is necessary that the servo bandwidth be optimized. The servo bandwidth is inversely proportional to the servo time constant, t_o. The compromise optimum time constant for a constant velocity target is, from Equation 7-275,

$$t_{o\ opt} = \frac{\delta_m}{3v_m}$$

The condition for maximum range determination now can be made. The expected time before loss is related to the probability of the range gate going beyond the point of target loss. Also, the time to loss is related to the servo time constant as shown. The relationship between the loss rate and the time constant, as well as the other parameters of this system, has been calculated in Equations 7-279, and 7-283. The dependence of the loss rate on the important parameters is given as

$$L = \frac{1}{t_o} \exp\left[- \frac{kP_i^2}{w_o^2 \Delta f_i \Delta f_s k_g} \right] \tag{7-284}$$

where

t_o = servo time constant

P_i = average received signal power

w_o = noise density in the IF

Δf_i = IF bandwidth

Δf_s = the equivalent servo bandwidth which is proportional to $1/t_o$

k_g = gate duty factor = $t_g/\Delta t$

Δ_t = time between pulses = reciprocal of the PRF

k = constant $\cong$ unity

It is assumed that the video bandwidth will not affect appreciably the noise properties of the circuit; it also is assumed that the optimization

conditions on Δf_i, t_g, t_p, and t_o have been met. Further assumption is made that the various pass bands and pulses are rectangular and that the signal-to-noise ratio is low. Notice from Equation 7-284 that the loss rate varies as the exponential of the square of the power signal-to-noise ratio and, therefore, is a very rapid function of the signal-to-noise ratio. An equivalent system bandwidth can be seen to be

$$\Delta f = \frac{1}{k}\sqrt{\Delta f_i \Delta f_s k_g} \tag{7-285}$$

which is the geometric mean of the IF and servo bandwidths with modifications present in k_g and k. Note that the noise is reduced by the square root of the gating factor. When the system parameters are known, the loss rate can be found, or, conversely, the minimum receivable power for a given loss rate can be found. Thus,

$$P_{r\,min} = P_i = w_o \Delta f \sqrt{\ln \frac{1}{Lt_o}} = w_o \Delta f L_T \tag{7-286}$$

where P_i is replaced by the minimum receivable power, $P_{r\,min}$. The quantity

$$L_T = \sqrt{\ln \frac{1}{t_o L}} \tag{7-287}$$

is the tracking loss since it is the factor which modifies the noise power in order to obtain minimum receivable signal power. This tracking loss is related to the servo time constant and to the loss rate.

The maximum radar range can be calculated from the usual radar range equation. This relationship, which is based on purely geometrical considerations, gives the received power in terms of the transmitted power, antenna gain, target area, distance, and receiver characteristics and is

$$R = \frac{1}{2\sqrt{\pi}}\left[\frac{P_t G^2 \lambda^2 \sigma}{4\pi P_{r\,min}}\right]^{\frac{1}{4}} \tag{7-288}$$

where

R = range
P_t = average transmitted power
G = antenna gain
σ = target effective scattering area
$P_{r\,min}$ = minimum average receivable power
λ = wavelength

Everything is known or determinable in this equation except $P_{r\,min}$. This quantity can be determined from the loss rate criterion and is given by Equation 7-286. Substituting Equation 7-286 into Equation 7-288 yields

$$R = \frac{1}{2\sqrt{\pi}} \left[\frac{P_t G^2 \lambda^2 \sigma}{4\pi w_o \Delta f L_T L_P} \right]^{\frac{1}{4}} \tag{7-289}$$

The factor L_p includes system losses such as plumbing losses and scanning losses. The term w_o is the noise density in the IF and includes the receiver noise figure. Equation 7-289 gives a relationship between the loss rate and the range in terms of the system parameters. From this it is possible to determine the range in terms of probability of loss. The following previously determined optimum conditions should be set into the radar range equation:

$$t_g = t_p$$
$$t_g \Delta f_i = 1/2$$
$$t_o = \delta_m / 3v_m$$

where δ_m = constant times t_p. Since $\Delta f_i = \frac{1}{2t_g} = \frac{1}{2t_p}$, the IF bandwidth must be inversely proportional to the pulselength and also to the servo time constant. Therefore, the servo bandwidth depends on t_p. Hence, the range of an optimized system is approximately directly proportional to some positive fractional power of the pulselength; therefore, the longest range is obtained by using the longest possible pulses.

The procedure and calculations in this section have evolved the following design criteria. First, the optimum time constant is related to pulselength and maximum target velocity and is given by $t_o = \delta_m/3v_m$. Second, there is an optimum IF bandwidth which is given by $t_g \Delta f_i = \frac{1}{2}$. Third, the optimum ratio of pulsewidth to half-gatewidth is given by

$$t_g \cong t_p$$

Fourth, for the smallest loss rate and greatest range the longest possible pulse length should be used. These items serve as a guide to the design of a system for maximum range. In general the circuit which limits the maximum range of the radar is not the angle tracking servo but usually is either the range or velocity tracking servo. The limitation on range from the velocity tracking servo can be calculated in the same way as has been done for the range tracking servo. The minimum receivable power is related to the loss rate in an analogous expression to that in Equation 7-286. The loss rate for the optimum time constant in the velocity tracking system already has been calculated and consequently the minimum receivable power can be calculated. From this, the range can be determined from Equation 7-288.

(e) MISCELLANEOUS CONSIDERATIONS

The previous sections have dealt with the three principal loops of the fire control system radar, namely, the antenna, range, and tracking loops. The important system parameters have been evaluated and optimized for determining maximum range and accuracy. Many other problems must be solved in connection with the design of a tracking radar. These are of lesser importance but still must be determined.

(1) Blind Range

When the range from interceptor to target is small, the main bang tends to enter the range gate if the pulsewidth and gatewidth are wide enough. The range gate then tends erratically to track both the main bang and the signal, according to the relative amplitudes and phases of the two pulses. The scan modulation on the main bang feeds into the angle channels introducing spurious information. These problems come under the heading of the blind range problem. The blind range problem is not so important a consideration in interceptor radars as in missiles which

must actually hit the target. This problem is further reduced when using long range missiles.

(2) Multiple Target

The multiple target range tracking problem represents a similar situation in which two or more targets are sufficiently close in either range or velocity to lie in the same gate, causing the gate to attempt to track both of them. Generally, the range gate follows erratically some intermediate point between the two, depending on the apparent center of echo, until range resolution finally is accomplished. The video signal is subject to fluctuations in amplitude due to contamination by noise. If the video signal-to-noise ratio is sufficiently low for the signal to be below the AGC threshold, (i.e., where the AGC is inoperative) the probability is high of the range gate jittering off the target due to noise, particularly if there is inherent gate drift in the absence of signal. If, in addition to noise, the signal fluctuates or fades, the probability of target loss is greatly increased. Amplitude scintillation represents a random fluctuation of this type. Other types of noises which affect range, velocity, and angle tracking are clutter, atmospheric reflections, chaff, etc.

(f) RANGE AND VELOCITY TRACKING COMPARISON

Many of the problems which occur in the design of range tracking servos also occur in the design of the velocity tracking servo. It is convenient to compare the problems of the two servo systems. A CW system discriminates against ground clutter at any altitude in the forward hemisphere attack, and this is one of the main advantages of velocity tracking over range tracking. If the target has a velocity relative to the interceptor which is greater than the velocity of the ground relative to the interceptor, the signal from that target will have a larger doppler shift than the ground clutter signals. Thus, even if targets are in the ground clutter, so far as the range signal is concerned, they may not be in the ground clutter so far as the doppler shift is concerned.

Range tracking systems have no anti-clutter properties. If the target range is equal to or greater than the altitude of the interceptor, the probability of tracking the target may be quite low. A problem common to both range and velocity tracking servos is the resolution of multiple targets. The velocity tracking system is capable of velocity resolution only. The resolution capability is directly proportional to the velocity gatewidth. Similarly the range tracking system is capable of range resolution only.

The range resolution capability is directly proportional to the range gate-width. Unfortunately, simultaneous optimum range and velocity resolution are incompatible. Velocity resolution and ground clutter discrimination degrade with improved range resolution. Similarly, range resolution and range discrimination degrade with increasing velocity resolution.

The tracking, search, and lock-on ranges for pure range tracking systems and pure velocity tracking systems are analogous in every respect. This similarity is a result of the duality of frequency (velocity) and time (range) in CW and pulse systems, respectively. The maximum ranges for a pure CW and a pure pulse system with equivalent parameters are comparable. The velocity tracking system does have an advantage inasmuch as no apparent minimum range exists. This advantage is not significant in the case of interceptors. The size and weight of both systems are comparable. Velocity gating is useful against some jamming techniques which are effective against pulse radar, such as chaff. Velocity radars, on the other hand, are more susceptible to CW and FM/CW jamming and microphonics. A pure CW system suffers from the problem of simultaneous transmission and reception of rf energy. There is no such problem in a pulsed system because of time multiplexing.

A CW or velocity tracking system has a tactical advantage in being able to track low-flying targets. Since an absolute range measurement generally is required for computation, a pure CW system cannot be used and some auxiliary range measuring equipment is necessary, such as provided in a pulse doppler radar. The inability of the pulsed radar to track low-altitude targets appears to be a disadvantage unless early warning techniques are perfected to the point where a low flying target can be attacked near head-on. Pure CW radar is most effective against single targets. Multiple target resolution also represents a serious problem because it is tactically easy and common for a group of targets to fly at the same speed. The relative velocities of the interceptor-targets change, even though the target-ground relative velocity is a constant. The rate of change of relative velocity and range is maximized at short ranges. Although two equally close-spaced targets are resolved in velocity at relatively short ranges, the angular error remaining at the instant of resolution, in general, is too great to allow the interceptor to approach a missile collision course in the remaining time. Restated, velocity resolution occurs too late to give a sufficiently high probability of weapon kill because of the angular error remaining at the instant of resolution. If resolution in range occurs at all, it occurs in general at or near actual launching of the armament so that adequate time remains for cancellation of the launching error.

(g) EXTRACTION OF ANGLE INFORMATION FROM SCAN MODULATION

An important function of the error detector is extraction of the antenna scan modulation from the video. The phase of the scan signal must not be shifted before comparison with the phase references, since such a shift will cause the angle information to be in error by the amount of the shift. When a signal is received by the antenna, the scan modulation has a phase ϕ_r with respect to the interceptor space references. If, in passing through the receiver, the phase of the error signal relative to the x-axis reference is shifted to ϕ_r^1, the apparent angular position of the target will be ϕ_r^1 which is in error by the amount of the shift $\phi_r^1 - \phi_r$. Fortunately, if the phase shift ϕ_r^1 is constant, it can be compensated by shifting the reference axis by the same amount. The apparent position of the target then differs from shifted reference axis by ϕ_r, thus compensating for the error. If the scan frequency does not remain constant during the time of flight the variation of scan frequency ω_s causes a variable phase shift that cannot be easily compensated. To avoid excessive pitch - yaw, crosstalk and angle error, the phase shift in the receiver, produced by variable scan frequency, must not exceed certain limits. This requirement prevents the error amplifier bandwidth from being narrower than certain optimum limits, which establishes a minimum noise bandwidth and a minimum unsaturated output range of the error amplifier. Phase shift of the error signal is serious because an error which should appear entirely in the up-down channel appears as an error in both channels (crosstalk). The scan axis then points in the wrong direction and the rms error is increased. Phase shift produces varying crosstalk when the interceptor rolls, combining effects which result in a helical trajectory. Phase shift in conjunction with saturation of the error signal makes these effects a function of signal level for large signals. Another problem results from the nonlinear output of the error amplifier. First, the response of the receiver to the error is nonlinear, i.e., as a result of conical scanning the percent modulation is not linear with the angular error $\sigma - \psi$. Because the major portion of the gain in the antenna loop is obtained in the error amplifier and a high gain is required to stay within the allowable error, saturation occurs. The bias about which this signal swing occurs is not symmetrically located with respect to the clipping level because the bias point for optimum gain and linearity for small error signals is not symmetrically located. The clipping is thus

asymmetrical, introducing unbalance. A more serious defect of clipping is the crosstalk introduced.

(g) AUTOMATIC GAIN CONTROL CONSIDERATIONS

The receiver must operate satisfactorily over a very wide range of signal levels. The automatic gain control maintains the IF output nearly constant by adjusting the IF amplifier gain. Action by the AGC maintains the receiver signal levels at the middle of their linear range of operation, preventing saturation of the various amplifiers and strong clipping of the signal, which may destroy the scan modulation altogether. This operation is essential to maintain constant gain for the range, velocity, and angle tracking servos. With constant gain, these servos will have constant response time. Constant response occurs since the response time of the angle servo is a primary time lag in the interceptor guidance system and variations in this time constant strongly affect the accuracy of the interceptor guidance. In AGC design, there are several rigid requirements: (1) the servo must be adjusted to give nearly equal response for positive and negative changes in signal level, (2) it must respond rapidly enough to prevent overloading and yet not so rapidly as to distort the scan modulation, (3) excessive overshoot must be avoided since this may overdrive the AGC circuit, (4) saturation and clipping in the servo, which introduce objectionable time delays and nonlinear response, must be minimized, and (5) AGC voltage must not be developed by the main bang. The video is gated in order to minimize these effects. The AGC is inoperative below the point at which it is controlled more by noise than by signal. The AGC contributes to the total phase shift of the scan signal inasmuch as the amount of shift depends on the amount of AGC feedback voltage at the scan frequency. Furthermore, this phase shift is sensitive to the scan frequency and the IF signal level. Any feedback at the scan frequency introduces phase shift so the feedback attenuation is kept as high as possible in the region of the scan frequency. The AGC time constant should not be too short because of the adverse effect of angular scintillation which is increased by rapid AGC response. Because there is a correspondence between small signals and instantaneous centers of radiation far removed from the mean center of radiation, a fast AGC tends to overemphasize these large scintillations, whereas a low AGC tends to average them out.

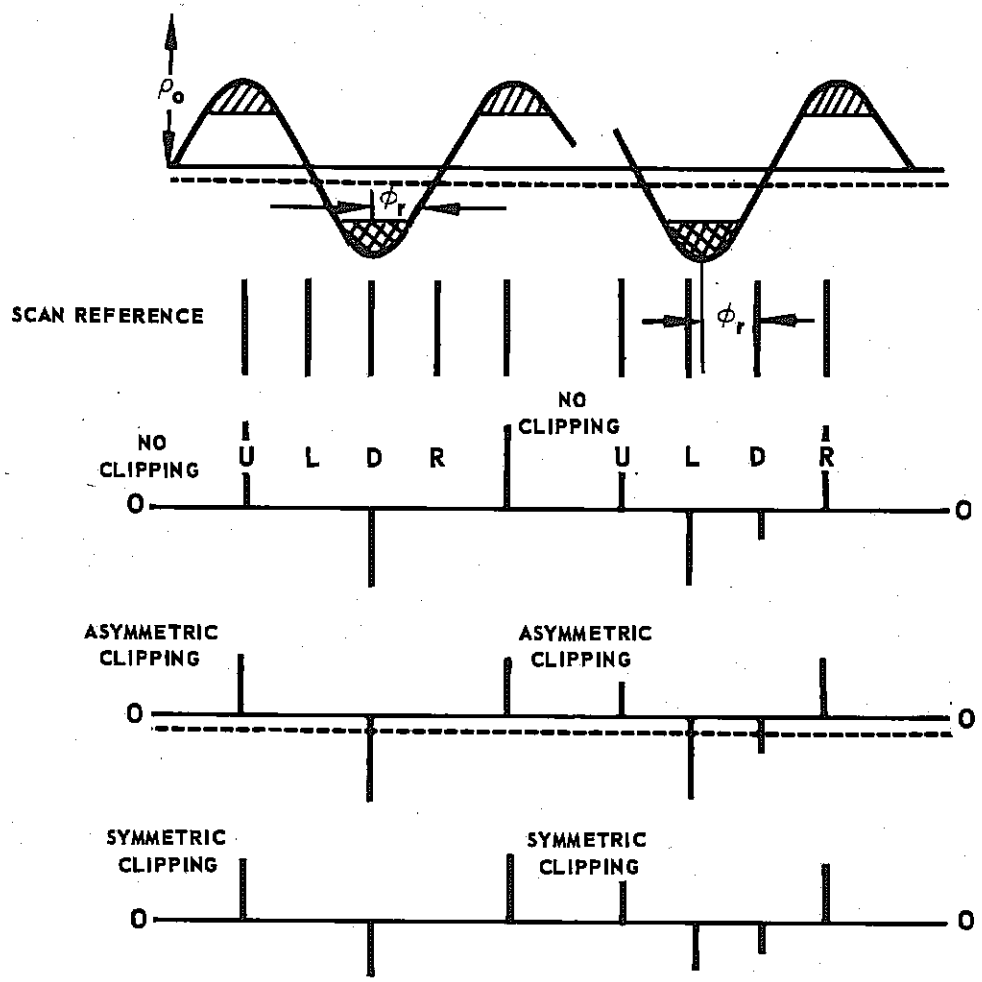

FIGURE 7-41. PHASE DETECTOR OPERATION

(h) PHASE DETECTOR OPERATION

The error resolver usually is a phase detector, which operates on the signal from the error amplifier in order to develop signals in two channels. Essentially, the circuit is composed of two bidirectional switches commutated by the reference voltages. Mathematically, the operation amounts to multiplication of the signal voltage by the reference voltages. Operation of the phase detector is illustrated in Figure 7-41. The up-down and left-right voltages are in push-pull. The switch output charges a condenser and this output is maintained until the next commutation, one scan cycle later. Ideally, the phase detector behaves like a peak, or box car detector yielding a push-pull dc output.

The case in which no clipping of the error signal exists will be considered first. In Figure 7-41, two successive scan cycles in which the signal phase of the second scan cycle has shifted relative to the first are shown. Referring to Figure 7-41a, on the first scan cycle a maximum signal is developed in the up-down channel and zero signal is developed in the left-right channel — a situation corresponding to the scan plane diagram shown in Figure 7-42.

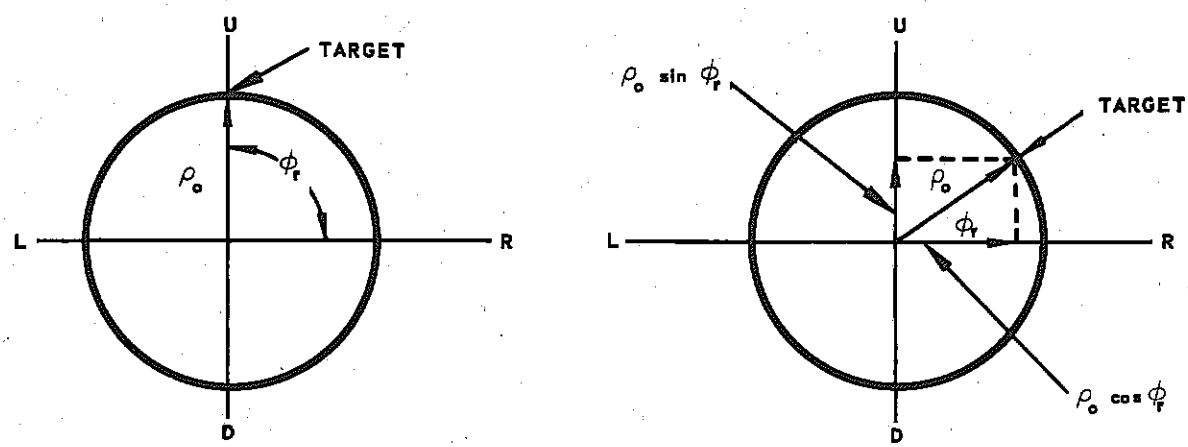

(a) TARGET IN ONE CHANNEL ONLY (b) TARGET IN BOTH CHANNELS

FIGURE 7-42a, b. SCAN PLANE GEOMETRY FOR SINGLE TARGET

The phase ϕ_r of the target vector is 90 degrees with respect to the left-right reference axis. The total vector magnitude ρ_o thus lies in the up-down channel and is thus equivalent to an up precession signal. The

geometry for scan cycle number two is shown in Figure 7-42b when signals exist in both channels. A voltage in the left-right channel gives a right voltage which is slightly larger than the up voltage in the up-down channel. The vector sum of the right voltage component $\rho_o \cos \phi_r$ and up voltage component $\rho_o \sin \phi_r$ is the total vector $\rho_o e^{j\phi_r}$. This vector has a magnitude ρ_o, the amplitude of the sine wave error signal, and a phase ϕ_r, the phase of the error signal relative to the left-right reference voltage.

It is quite important in the design of the error phase detector and the error amplifier as well, that the dynamic range of the amplifiers be sufficient to prevent appreciable signal clipping. In evaluating the effect of signal clipping in the absence of noise and scintillation, consider symmetric clipping. The clipped portion of the signal is shown by the shaded regions of the sine wave in Figure 7-41. Figure 7-42 shows that for scan cycle number one the only effect is a reduction of the total signal in the up-down channel with no resulting phase shift. The scan plane geometry is shown in Figure 7-43.

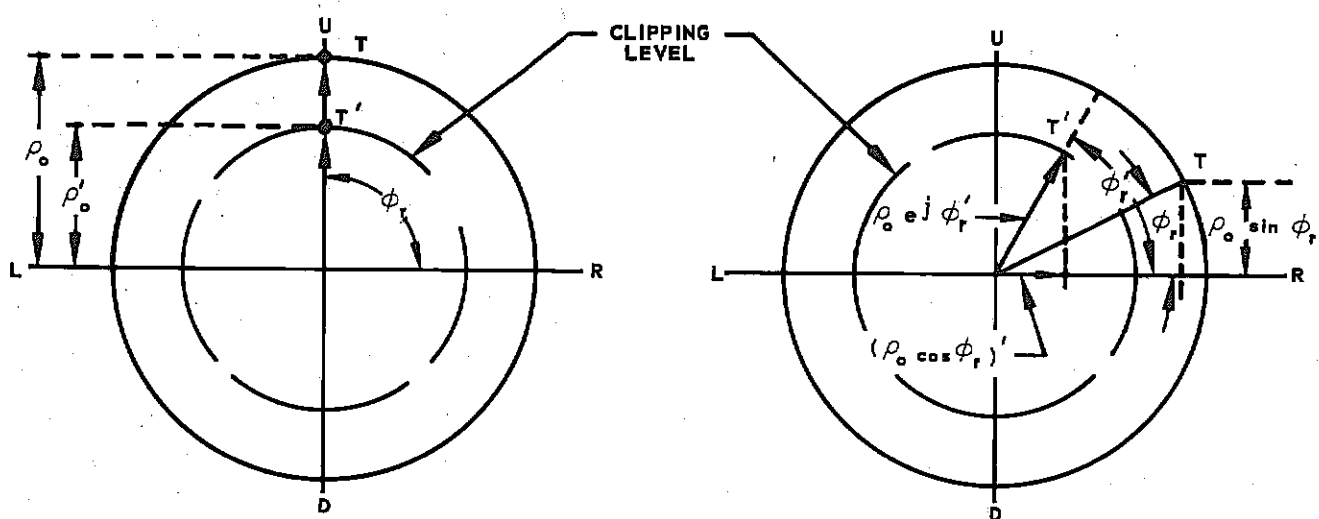

(a) TARGET IN ONE CHANNEL ONLY (b) TARGET IN BOTH CHANNELS

FIGURE 7-43a, b. SCAN PLANE GEOMETRY WITH SYMMETRIC CLIPPING

The symmetric clipping level reduces the true signal magnitude ρ_o to the apparent level ρ_o' with phase ϕ_r unchanged. For scan cycle number two, Figure 7-41b shows the up-down channel voltage to be unchanged while

the left-right channel voltage is reduced. The apparent signal is then changed in magnitude and shifted in phase as seen in Figure 7-43b. The left-right component $\rho_o \cos \phi_r$ is clipped and appears to be $\rho_o \cos \phi_r'$. The up-down component is unclipped and the vector scan of these two components gives a resultant vector $\rho_o' e^{j\phi r'}$ which is reduced in magnitude from the true signal $\rho_o e^{j\phi'}$ and is shifted in phase by $\phi_r' - \phi_r$. If both components were clipped, ϕ_r' would equal 45 degrees regardless of the true value of ϕ_r. Thus, the antenna attempts to track an apparent target T' rather than the true target T. In effect this is crosstalk since the same result is obtained when change in one channel produces a change in the other. Furthermore, this crosstalk interacts with other sources of crosstalk to cause additional crosstalk, so the cumulative effect of clipping cannot be clearly determined. As the errors reduce, a point is reached where neither component is clipped and the system behaves properly. If, at the time clipping ceases, sufficient time does not remain to reduce the error in order to permit tolerable launching of the armament, the miss may be appreciable.

Even if the signal is not clipped, the effect of noise clipping in the phase detector presents a serious problem when sufficient angular scintillation noise is superimposed on the signal. Angular scintillation appears as narrow band noise centered about the scan frequency. For simplicity, a long thin target can be considered a suitable approximation to the broadside view of a bomber, and for such a target, scintillation noise may be represented as a scan frequency carrier, amplitude-modulated by narrow band noise. To make this physically reasonable, it is necessary to consider the multiple sources which give rise to scintillation as random scatterers (that is, reflectors that give returns that are random in phase and amplitude) uniformly distributed over the surface of the long thin targets. The mean center of the echo is then the center of the target. As shown in Figure 7-44, the apparent center of echo appears to jitter or scintillate back and forth across the target because of the random addition of rf return vectors; however, the rate is slow compared to ω_s.

For convenience, it may be assumed that scan axis perfectly tracks the instantaneous center of echo. Although this would require infinite antenna loop gain, the behavior is similar for a finite gain servo. If the target remains stationary, aligned as it is with one of the angle channels, as shown in Figure 7-44, the scan axis will follow the tip of a vector

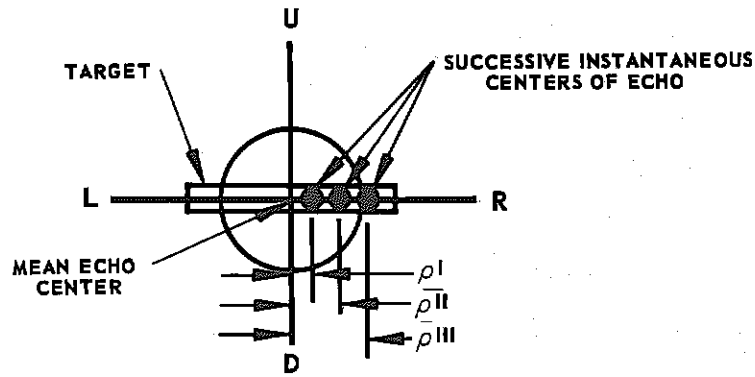

FIGURE 7-44. ANGULAR SCINTILLATION IN LONG, NARROW TARGET

ρ_o which varies in amplitude as a function of time. In other words, the vector $\rho_o e^{j\phi r}$, joining the scan axis and the line of sight, is amplitude-modulated. Furthermore, the phase is unchanged unless the instantaneous center goes to the left of the mean, in which case the phase reverses instantaneously. This effect does not invalidate the amplitude modulation concept, since phase reversals occupy a negligible portion of the total time. Since the rates of change of the magnitude ρ_o are random but slow compared to ω_s, the scintillation can be represented by a scan frequency carrier amplitude modulated by narrow band noise. The geometry corresponding to the case shown in Figure 7-44 is shown in Figure 7-45. A typical waveform is shown in Figure 7-46. Assuming symmetric clipping of the modulated waveform, the clipped portion of the wave contains no accurate amplitude information and no phase information except in a narrow region about successive zeros. If the scan axis is aligned with the mean center of echo, and the target remains stationary (as shown in Figure 7-44), clipping actually is beneficial because the scan axis is pointing in the right direction and the noise is simply a tracking error versus time. Since clipping limits the noise, it must also reduce the rms tracking error. In general, however, clipping is detrimental; for example, if the target moves in azimuth only, the mean vector should increase, causing the servo to track more rapidly; however, the clipped vector will not change appreciably. This results in poor tracking such that if the target accelerates rapidly enough it may be lost. In the more general case in which the target lies in more than one channel, both

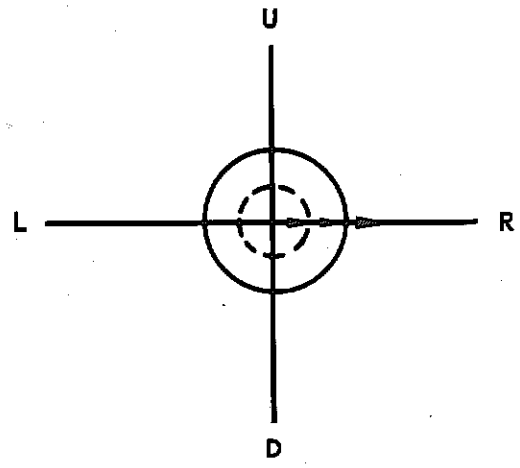

FIGURE 7-45. GEOMETRY OF ANGULAR SCINTILLATION WITH CLIPPING

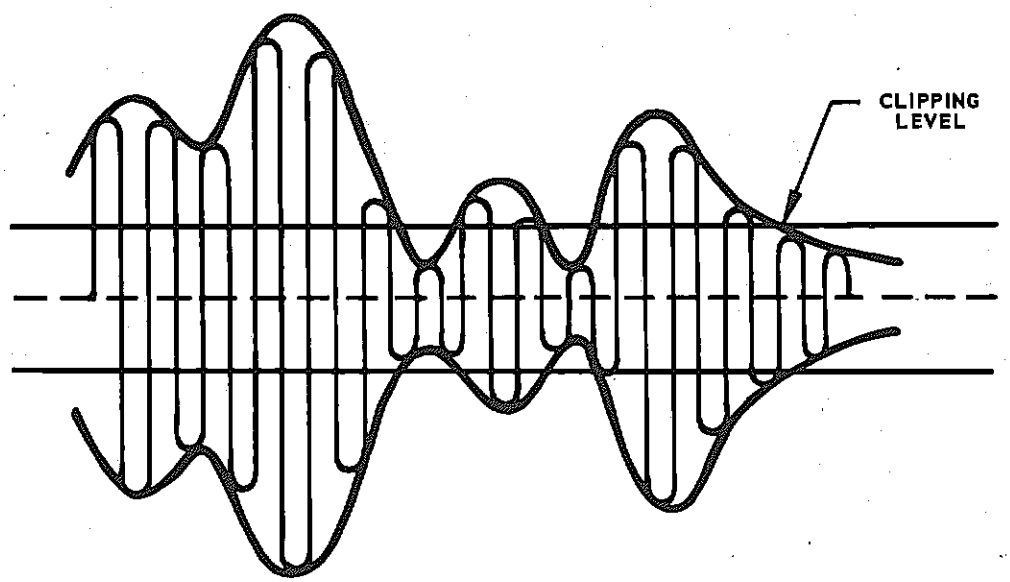

FIGURE 7-46. ANGULAR SCINTILLATION WAVEFORM

components are amplitude-modulated. In this case, clipping results in crosstalk in which there are components of the tracking error perpendicular to the long dimension of the target. These serve to increase the probability of tracking error in the narrow dimension of the target. If the center of the target is not aligned with the scan axis, the scan frequency carrier is both amplitude-and phase-modulated. (See Figure 7-47.)

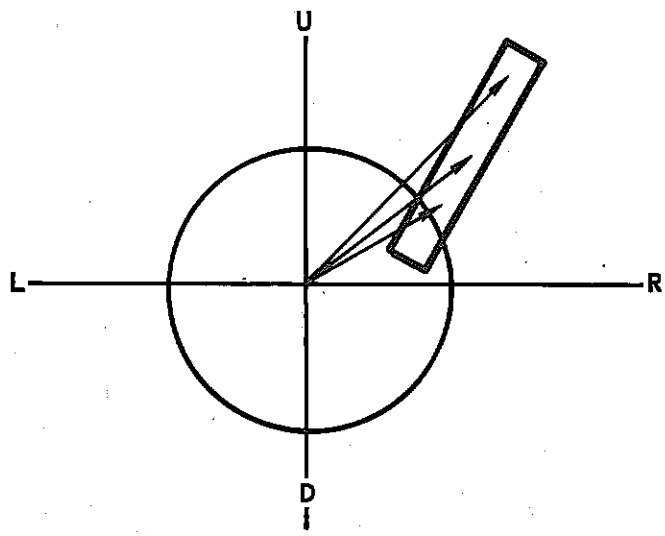

FIGURE 7-47. ANGULAR SCINTILLATION GEOMETRY WHEN CENTER OF TARGET IS NOT AT ORIGIN OF SCAN COORDINATES

Clipping in this case results in poor tracking and modulated crosstalk. Angular scintillation is a serious effect only at short range. At long ranges, the target appears as a point source and thermal wideband noise is the perturbing effect at these ranges. Since the error amplifier is not narrow banded about the scan frequency, the error voltage appears as noise at low signal-to-noise ratios and as slightly perturbed signal at high signal-to-noise ratios. Thus clipping at high signal-to-noise ratios is similar to clipping alone. The effect of clipping at low signal-to-noise ratios is to degrade this ratio even further.

Nonlinearities in the precession amplifier, precession mechanism and in the gyro antenna head itself also can produce undesirable effects similar to those described. Some of the nonlinearities which are likely

to occur include unbalance, hysteresis, dead space, and saturation. The effect of certain types of unbalance is to precess the antenna away from the target until the error signal which is generated cancels the quiescent differential unbalance and the new quiescent scan axis position does not then point at the target. The resultant angular error affects the interceptor guidance in a manner similar to target maneuver. Nonlinearities produce crosstalk even though the boresight error is zero. Boresight error is defined as the angular error between the interceptor line-of-sight and the antenna scan axis when the scan error signal indicates zero. Unequal nonlinearities in the two channels produce unequal precession rates, causing the interceptor to fly the wrong course and results in increased rms miss. Nonlinearities in the region of zero error are more harmful than those in the region of large error because the error, presumably, is smaller at the end of the trajectory, allowing less time for correction. In general, any degree of unbalance between the two channels will produce some degree of crosstalk. Dead space is a region about zero error where no torque is produced as a result of a finite error signal. Dead space is common in mechanical systems due to friction and backlash, and again the resultant effect is increased target miss. Hysteresis also arises from several sources, such as dead space and magnetic effects. Hysteresis causes unbalance and crosstalk resulting in increased tracking error and miss. Because of nonlinear and hysteresis effects, which are common in mechanical precession systems such as the tracking loop, an auxiliary regulatory loop is desirable about the precession mechanism and antenna head.

(i) ANTENNA BEAM DISTORTION

One of the more serious problems in the radar system is the problem of microwave beam distortion. The microwave beam is distorted generally by the antenna system and in particular by the radome. As a consequence of radome error, the apparent line of sight to the target does not lie along the true line of sight. Radome error is illustrated in Figure 7-48. The apparent line of sight is at an angle σ_r with respect to the reference. The error angle between the true line of sight and the apparent line of sight is η_r. From Figure 7-48,

$$\sigma_r = \sigma + \eta_r \tag{7-290}$$

If it is assumed that η_r varies only with the angle, γ, between the true line of sight and the interceptor axis, the equation may be written as

$$d\eta_r = \frac{d\eta_r}{d\gamma} \cdot d\gamma \tag{7-291}$$

If the radome error slope $d\eta_r / d\gamma$ is a constant, K, the equation is

$$\eta_r = K\gamma \tag{7-292}$$

Thus the radome error varies linearly with the angle between the interceptor axis and the line of sight. The error angle η_r appears not only in the plane of the offset angle γ, but also in the plane perpendicular to the offset; this effect is known as radome crosstalk. Considered practically, crosstalk arises due to the apparent line of sight shifting in the plane containing the true line of sight and the interceptor axis, as well as in the plane perpendicular to it, because of asymmetrical refraction effects. Figure 7-49 shows a typical plot of η_r versus γ and the variation of η_r with γ for a given roll angle ϕ. If the radome were a perfect electrical surface of revolution about the interceptor axis, Figure 7-49 would be the same for any ϕ. Unfortunately, both the error curve and the crosstalk curve vary with ϕ. If η_r changes for a constant γ, the effect is similar to boresight error. The change in η_r, and hence the error signal,

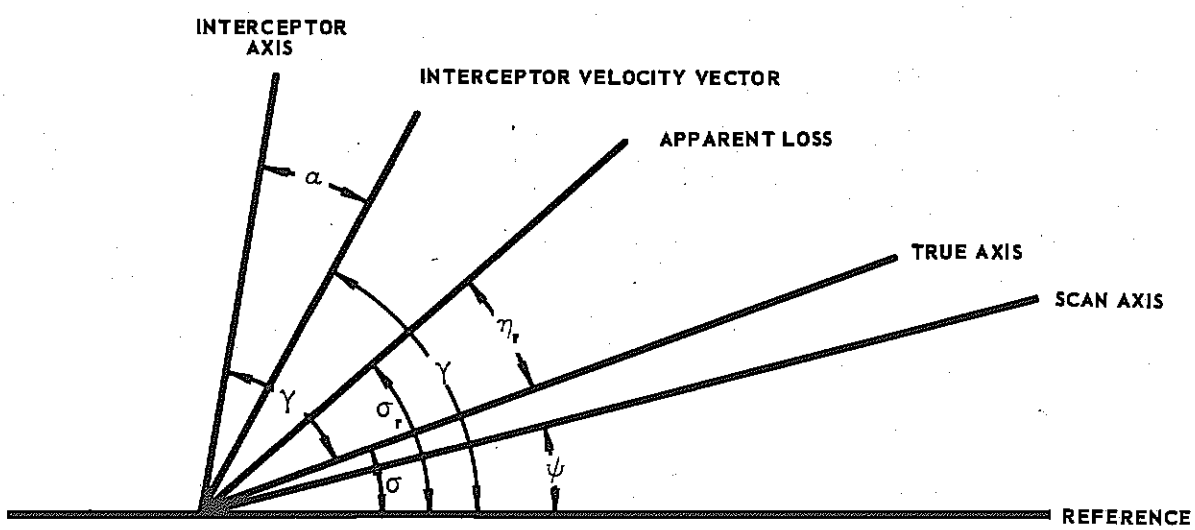

FIGURE 7-48. SPACE GEOMETRY INCLUDING RADOME ERROR

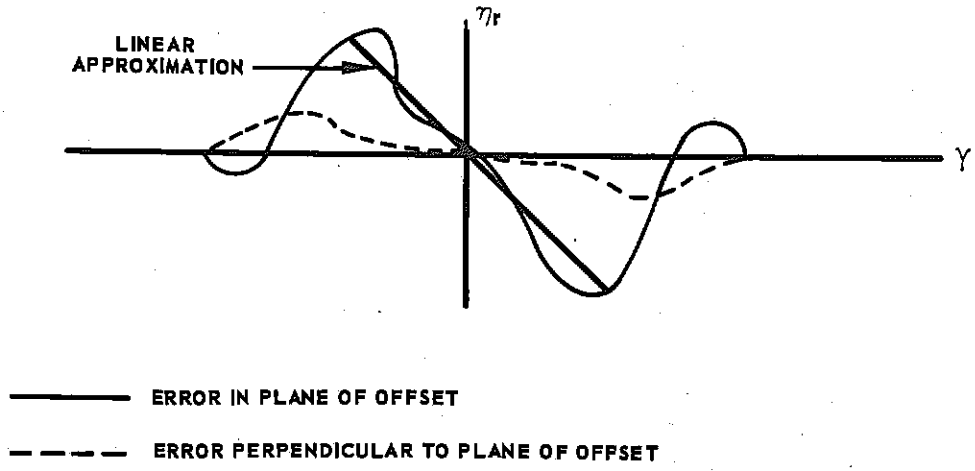

FIGURE 7-49. RADOME ERROR ANGLE, η_r, VERSUS ANGLE BETWEEN MISSILE AXIS AND TRUE LINE OF SIGHT γ, FOR SANDWICH-TYPE OGIVE RADOME

is periodic at the roll rate. The crosstalk does not bear a constant relationship to the error, hence the resultant error is both amplitude and phase modulated with roll. If the true line of sight changes direction during the roll, the resultant vector is modulated in an even more complex manner, equivalent to the effect produced by angular scintillation. The net effect of radome error is an apparent increase in angular scintillation noise resulting at least in increased angle error.

Crosstalk and nonlinearities can occur in the antenna gyro, and also in the gyro and antenna head. Actual cross connections can occur or equivalent crosstalk can be generated by unequal gains in the pitch and yaw channels. If the precession mechanism is considered to be a two-channel torque transformer, the gains in both channels will depend on the position of the scan axis. Unequal gains result in improper steering and thus demand a new error voltage vector that is not the same amplitude or direction as that called for in the absence of crosstalk and nonlinearity. Misalignment of the reference coils, especially at large angle errors, can only cause crosstalk and reduction in gain. Unequal pitch and yaw channel gains produce unequal precession rates and hence steering crosstalk. As has been pointed out, lags in interceptor coordinates adversely affect this crosstalk effect. Any smoothing which follows the tracking system should be done in inertial coordinates in order to minimize the effects of crosstalk and nonlinearities.

CHAPTER VIII

EVALUATION OF FIRE CONTROL RADARS

SECTION 1 — INTRODUCTION

(a) GENERAL EVALUATION CONSIDERATIONS

The purpose of this chapter is to supply the radar systems engineer with the necessary background for evaluating the effectiveness of the airborne radar armament control system.

The general problem to be solved is that of utilizing airborne radar systems in one-or two-man interceptors. The environment is considered as all-weather and the radar serves as the electronic controller for determining the presence of a target; further, the radar set can be used to control the aircraft steering from the time of lock-on until the aircraft armament is fired.

The typical aircraft equipped with armament control radar is under the control of a ground radar which directs the search to a specific limited search sector. The limits placed upon the general area to be searched by the interceptor radar have an important effect on the aircraft's probability of detection, lock-on, and successful completion of the interception.

Advanced interceptor systems attempt to mechanize the entire interceptor problem, retaining for the operator only the function of performing tactical decisions. Performance of the radar-equipped interceptor in the past has been generally unsatisfactory when measured in terms of the ultimate design objective of destroying an airborne target. This chapter will present techniques suitable for evaluating the radar-controlled armament problem. The survey will present some of the general considerations related to the evaluation of radar fire control systems. The mathematical means for evaluating the designs also will be discussed.

A major objective of the radar evaluation problem is the development of a radar set to operate as an integral part of the overall fire control system, and alignment of this fire control radar to the specific requirements of the weapon system.

The first portion of this survey was concerned with the radar design objectives and the techniques for deriving them. It was shown that the particular mission, in turn, determined the weapon system requirements. Some of the various mission environments in which the radar system might operate are (1) high altitude interception, (2) low altitude interception, (3) high altitude escort, (4) low altitude escort, and (5) bombing missions.

The basic purpose of the flight test program is to evaluate the design and performance of the radar system and to demonstrate its performance and capabilities. This objective is accomplished by evaluating system performance under flight conditions. Flight testing also provides a means for determining environmental, launching, accuracy, and reliability limitations.

Equipment to be flight tested generally is checked for system compatibility and functional testing in a roofhouse test lab. Appreciable differences exist in the roofhouse and flight test environments, as for example, the amount of ground clutter, the motion of vehicle, the noise, temperature, vibration, etc., which are generally markedly different in the two environments.

Aircraft testing permits evaluation of the airborne system with real targets. Major tests which should be performed during flight test include search and lock-on range determination, performance of search and tracking servos, and system evaluation using built-in self test functions.

An inflight automatic checkout system can be provided for checking out key parts of the fire control system, especially the various missile functions. Upon successful completion of the countdown the armament may be launched.

Evaluation of the fire control radar system is expressed primarily in terms of effectiveness in determining information relating to target presence or nonpresence. Secondly, the measure of the fire control system effectiveness is based on its tracking ability. The subject of this section will be the techniques used to determine the effectiveness of detection and tracking capability. The results may serve to indicate how evaluation techniques can be improved to permit more effective utilization of radar signal energy.

The history of radar dates back to 1939 when detection and tracking of airborne targets were demonstrated to be practical. Since that period, radar sets have been improved continually in an effort to keep pace with new demands for the detection of higher velocity targets. High velocity targets, in turn, often meant detection of targets with less reflective surface. It also has been required that the fire control radar be engineered with a capability for locking onto and tracking this same high speed target. To achieve radar improvement, it has been necessary to increase the ranges of detection. Because of the high velocities of contemporary aircraft, a large volume of space has to be inspected by increasing the rate of volume swept by the radar antenna, and hence increasing the area of radar observation.

In present airborne fire control radars, the search process culminates when the radar operator, who may also be the interceptor pilot, makes the decision that a target has been detected. The acuity of this determination may vary drastically from operator to operator. Schemes for speeding and improving the radar operator's ability to discern suspect target blips would add considerably to the useful range of detection. The period between the search and track modes is used for decision making; first, that a target is present; second, that the target is the correct one; and last, that the target can be locked onto. The lessening of this decision time would represent a considerable improvement in the overall radar effectiveness.

The next area to be considered in radar system evaluation is the tracking mode, which continues until the armament is fired, or in the case of the semiactive radar missiles, until such time as the missile hits or misses the target.

For the search phase, improvements in radar effectiveness must evolve through an increase in the range at which high altitude, high velocity, small-reflecting-surface targets can be detected. Similar improvement is required of the radar system to search a larger volume of space more intensively and to lessen the aircraft's dependance on ground radar instruction. Sufficient radar detection ranges permit time for the aircraft to be positioned with respect to the target in an effort to optimize the maneuver tactics.

Tracking consists of steering the aircraft in proper relationship to the airborne target flight path. Tracking must consider range and bearing to the target, noting range and bearing deviations by comparison with

reference signals. A range unit is set to proper range by operation of an "action" switch at the range of the target when first observed during search mode of operation. From that time, the range rate error voltage seeks to prevent the range gate from losing the target in range, while signal fading and target acceleration make the tracking problem even more difficult. In general, the positioning problems must be solved by improvement in the tracking servo systems.

To improve the effectiveness of the radar fire control system in range of detection quickly resolves into a problem of detecting a signal in noise. The returned signal is proportional to the average power transmitted and to the sensitivity of the receiving system. The noise present in the radar receiver output is due to receiver input noise. Requirements of the fire control system limit range-of-detection improvements through integration processes because of the short time available and the quantity of information required.

SECTION 2 — EFFECTIVENESS OF AN INTERCEPTOR FIRE CONTROL RADAR

The effectiveness of a radar system used to detect and track a target can be measured primarily in terms of the ultimate mission of destroying the target. No single radar parameter can establish effectiveness or excellence of one radar fire control system over another. The radar variables which most positively effect the interceptor proficiency will be chosen and the results analyzed.

In general, the radar will be effective only when evaluated in view of other major combat factors involved in the interception problem; such factors as fighter and target velocities and altitude, target radar-cross section, interceptor and target "g" factor, missile or rocket aerodynamic and guidance ranges, and ground radar vectoring information must be considered. These, and other variables, will dictate the essential radar requirements of detection range, search volume, and tracking accuracies, all of which determine detailed radar parameters such as power output, duty cycle, search frame-time, receiver sensitivity, time from search to lock-on, and many other factors to be examined in considerable detail throughout this review.

Modern interceptors, operating at velocities above Mach 1, are penalized by the radar systems designed basically for use in slower aircraft, since the antenna now has less time to observe the target as the

attack proceeds. An attempt will be made to incorporate the findings of analyses in radar and related fields to provide a measure of the desired radar performance.

The radar tracking function provides accurate single-target coordinate information. The accuracy of the tracking data is a criterion of the radar performance. Some of the sources of tracking error include the servo-lag errors, noise errors, alignment errors, servo-gain errors, drift errors, gear errors, bias errors, unbalanced forces, striction and friction forces. Search and tracking radar modes may be affected to differing degrees by the errors listed but, in addition, the search and track modes will be equally influenced by target effects such as glint and scintillation, by the receiver thermal noise, and by propagation effect. There are those errors which effect both search and track modes of the radar, and errors such as the servo tracking errors which pertain exclusively to the tracking mode.

The radar system can be properly evaluated in terms of the complete weapon system effectiveness. To intercept a target successfully, the entire attack control system, target, airborne intercept (AI) radar, fire control computer, auto-pilot, and interceptor must be suitably brought into play through use of a computer. This computer accepts input data, takes into account the dynamics of the problem to be solved, and finally provides signals used to steer the aircraft toward the target. The attack phase begins with the lock-on of the target by operation of the interceptor's radar. The control system computer then calculates a course to be flown by the interceptor in order to fire the armament at the correct time. The computer provides control signals to the auto pilot, which activates aircraft control surfaces and places the aircraft on the calculated course. Finally, the computer must calculate the proper time and manner of firing the interceptor armament. Radar data required for the airborne computer includes azimuth and elevation angles, range and range rate, and antenna angular rates. The remainder of required data concern aircraft and weapon information.

For rocket firing, a collision course is mechanized by the computer. This course steers the interceptor in such a manner as to null the angular rate-of-change of the line-of-sight from the interceptor to the target. The airborne radar supplies the computer azimuth and range data of the line-of-sight to the target. Additionally, it provides range rate, from which the computer predicts the next incremental target position. The radar antenna gimbals define the angular position of the line-of-sight to the

target. The angular rate data are derived from rate gyroscopes mounted on the antenna.

The airborne radar maximum lock-on range and the accuracy of the tracking are the characteristics of most importance. In the tactical situation, the fire control problem must be solved in a very short time, especially in the forward-hemisphere approach. The random perturbations of radar azimuth and elevation must be averaged out. The radar data must be accurate, and proper smoothing must be supplied. Large radar tracking errors make necessary an increase in the amount of smoothing required if the pilot's ride is to be limited to tolerable values of g. This increased filtering or smoothing, however, results in a time delay which reduces the ability of the aircraft to counter target maneuvers.

Factors affecting the radar lock-on range are, in many cases, the same as those which affect the radar detection range, since lock-on can occur only after radar detection. Other factors which cause the lock-on ranges to be appreciably smaller than detection ranges include operator decision time, time required to manipulate controls to initiate lock-on, and increased signal required by the radar circuits to initiate automatic tracking. In going from search to track, the volume scanned is reduced, decreasing the scanning loss and providing most of the additional signal needed to initiate lock-on. The major time difference between search and lock-on ranges is contributed by the speed of the operator decision and control-manipulation.

Two general schemes are deduced for improvement of the lock-on range, namely, increasing the detection range and reducing the difference between detection and lock-on ranges. Detection range can be improved by any of the following methods: increasing radar transmitted power (a doubling of power accounting for an approximate 19 percent increase in range), increasing size of the radar reflector (limited by aircraft dimensions), reducing the radar noise figure by use of improved front-end crystals and circuits, reducing the scanning loss by reducing the volume scanned, improving the operator's performance by limiting target area to be examined, and by improving radar display. Finally, the range of detection is estimated to be deteriorated almost half from test performance by the problems of reliability and serviceability.

Evaluation studies indicate the need for improved lock-on circuitry to operate on a lower signal-to-noise ratio to detect and lock on, after

gaining signal strength due to reduction of volume searched (reduction in scanning loss).

(a) RADAR RANGE CONSIDERATIONS

The range of radar detection is not a sharply defined quantity and, hence, it is chosen to describe it as a cumulative probability of detection, that is, the probability that the radar will have detected the target by the time the interceptor has closed to a given range.

The process of lock-on is accomplished after detection and is similarly described in terms of cumulative probability of lock-on. The reasons for the use of probability theory in determining detection and lock-on criteria are based on the following considerations: the noise generated in the radar receiver, the fluctuating character of the radar echo, and the somewhat unpredictable behavior of the radar operator. These items exist even though the radar set has known, constant characteristics.

One method employed in evaluating radar detection performance specifies consideration of the following: interceptor and target aircraft, angle of approach, respective altitudes, speeds of the two aircraft, the terrain over which the flight is made, and use or non-use of ground control information. Seven to ten attempted intercept runs provided information on which to base a calculation of cumulative probability of detection (CPD) for the conditions indicated above.

The conclusions resulting from evaluation tests of a specific airborne radar detection were given as follows:

(1) Detection performance can validly be measured in terms of probability.
(2) Detection range of the radar over land is sensitive to the absolute altitude of the interceptor.
(3) Detection range is insensitive over water at medium altitudes.
(4) For the case of the propeller-driven target aircraft, the advantage of the increased target reflection from nose-on is offset by the increased closing rate inherent in the nose-on approach.
(5) Lock-on performance of AI radars is sensitive to altitude changes over land, and to low altitudes over water.

An interesting evaluation of lock-on capability was demonstrated when a target aircraft was first locked on by the radar-equipped aircraft and then the opening speed increased until lock-on was broken. The results indicated that a stronger signal was required to initiate and hold lock-on than was required for detection. The test required all other factors to be equal and indicated that greater signal power was required for lock-on than for detection.

To determine the expression for maximum radar range in terms of the various parameters of importance, consider the following: the rf echo power available at the output terminals of the receiving antenna, P_r, can be calculated in terms of the following parameters:

P_t = the rf power radiated by the transmitting antenna
G = gain of the transmitting antenna (relative to an isotropic radiator)
σ = scattering cross section of the target
A = the cross section of the receiving antenna
R_1 = the transmitter-to-target receiver distance
R_2 = the target-to-receiver distance

The relationship between these parameters is

$$P_r = \frac{P_t}{4\pi R_1^2} \cdot G \cdot \frac{\sigma}{4\pi R_2^2} \cdot A \qquad (8\text{-}1)$$

The first factor in Equation 8-1 is the power per unit area normal to the line of sight if the transmitting antenna radiates equally in all directions. The second factor, G, is the transmitting antenna gain which is the ratio of the power in the main beam to that in the same direction of the antenna radiating isotropically. The third term $\frac{\sigma}{4\pi R_2^2}$ is the power density at the receiving antenna per unit illuminated power density of the target in terms of the effective scattering cross section σ of the target. The last factor is the intercepting area at the receiving antenna. For the case where a common antenna is used for transmitting and receiving

$$R_1 = R_2 = R \qquad (8\text{-}2)$$

For the case considered, the receiving area A, and the gain G are related as shown by the expression

$$G = \frac{4\pi A}{\lambda^2} \tag{8-3}$$

Substituting Equations 8-2 and 8-3 into Equation 8-1 results in

$$P_r = \frac{PA^2\sigma}{4\pi\lambda^2 R^4} \tag{8-4}$$

The maximum radar range is thus given by

$$R_{max} = \left(\frac{P\sigma}{4\pi P_{r\,min}}\right)^{\frac{1}{4}} \left(\frac{A}{\lambda}\right)^{\frac{1}{2}} \tag{8-5}$$

$P_{r\,min}$, the minimum receivable signal power, depends upon the device which is to use the information. If the signal is to be displayed on an oscilloscope indicator, the minimum receivable power is limited by the radar operator's ability to distinguish small signals from noise. In other words, one operator will require less signal to observe a given intensity on the radar scope than a less observant operator. Consequently, the range of detection in a given set of circumstances will differ from one operator to another. In an automatic sensing or alerting device, $P_{r\,min}$ is determined by the setting of a threshold above which an indication is given. $P_{r\,min}$ can be reduced and R_{max} increased by lowering the threshold setting. Reduction of the threshold, however, increases the probability of false indication such as is caused by noise. In all problems of thresholding, some compromise must be made between the number of allowable false alarms and the possibility of missing the target. The term $P_{r\,min}$ in an automatic tracking or automatic lock-on scheme is set by the capability of the tracking or search-stop device. In the tracking case, some criterion such as minimum probability of loss of track must be set for optimizing the servo. On such a basis, $P_{r\,min}$ and, hence, R_{max}, can be evaluated. The transmitted power, P_t, the receiving antenna area, A, and the transmitter wave length, λ, have been defined. The remaining

quantity σ is the cross-sectional area of the target, and may be considered as the area normal to the transmitted beam. The energy of this beam would have to be extracted and scattered uniformly over all directions in order to produce the same signal at the receiver as the actual target. This value may be greater or less than the geometrical cross section, but usually is of the same order as the geometrical cross section. The term σ depends upon many factors such as the size, shape, orientation, material composition of the target, wavelength and polarization of the receiving and transmitting antennas, and the scattering angle. In reality, the cross-sectional area fluctuates as a function of time. Changes in aspect, orientation, and vibration of complex targets give rise to these fluctuations or scintillations. These fluctuations or scintillation effects have been discussed in Chapter III. Reviewing briefly the results, two mathematical models used to represent these scintillation effects are (1) a source consisting of many independent random scatterers whose rf return voltages and phases add in a random manner to give a stochastic return signal, and (2) a model in which only a few specular reflectors combine to give a complex diffuse signal return. Factors not represented in Equation 8-5, but which affect maximum range, are those factors that cause losses in signal energy; e.g., atmospheric absorption and other propagation effects. Atmospheric absorption is not of particular importance at X-band frequencies, except during conditions of heavy condensation.

The term R_{max} generally is defined in terms of a given σ; that is a given range is specified for a given cross-section area target. Using this definition, the factor which again remains to be defined is $P_{r_{min}}$ The term $P_{r_{min}}$ is determined by the amount of noise with which the desired signal must compete.

There are three principal types of noise in radar systems: (1) target noise, (2) environment noise, and (3) receiver noise. Target noise is associated with the echo signal. The echo signal may be considered in terms of stochastic processes as a result of the statistical nature of the fluctuations of σ. Although the fluctuations and scintillations do affect the behavior of the system by limiting the effectiveness with which certain data may be obtained, they do not determine the lower limit of usable signal. These effects may be considered as the detailed properties of the echo signal. For example, in a tracking system, it may

actually be desirable to track the noisy signal rather than to discriminate against it. Environmental and receiver noises appear as extraneous signals which compete with the echo signal and should therefore be discriminated against. Environmental noise includes all the extraneous external radiations entering the receiver. This includes items such as undesired targets, ground clutter, various types of natural and man-made interference, and countermeasures.

Even if all other noises were reduced to negligible quantities, the third type of noise, that is, receiver noise, is always present. Receiver noise is the ultimate limiting factor in the determination of $P_{r_{min}}$. Receiver noise has a broad, flat spectrum which is referred to as "white" noise. The amount of noise generated within a specific receiver is expressed in terms of a noise figure.

The receiver noise power,

$$\eta = (NF)kTB \tag{8-6}$$

is referred to the receiver input. The receiver noise figure power ratio is (NF), B is the receiver IF bandpass, k is Boltzmann's constant and equals 1.38×10^{-6} ergs per degree Kelvin, and T is the absolute temperature. Room temperature is approximately 300 degrees Kelvin.

The signal at the point where the target is to be identified or tracked is S and is equal to

$$S = L P_{r_{min}} G_r \tag{8-7}$$

The major losses in the term L are microwave losses between the receiver input and the antenna. The noise N, at a point corresponding to the location where the signal S is measured, is related to the noise power P_n by

$$N = G_r P_n \tag{8-8}$$

The required signal-to-noise ratio at the point where the signal is to be identified in the presence of noise

$$\frac{S}{N} = \frac{LP_{r\,min}}{(NF)kTB} = \frac{LP\sigma A^2}{4\pi R^4_{max}\lambda^2(NF)kTB} \tag{8-9}$$

The signal power is related to the noise for a given point in the manner of a constant, i.e., one which depends upon the way in which the signal is processed and the noise discriminated against. In the case of the search radar with simple scope presentation, this so-called constant is approximately one. If the minimum receivable power is equal to the rms noise power it is considered that a standard operator should have a high probability of noticing the target presence. It can be shown that for the case of range tracking radar it is possible to design the tracking servo so that the signal-to-noise constant is approximately one tenth. This demonstrates that, by proper design of automatic tracking servos, the minimum receivable power can be reduced by as much as one-tenth as compared to a system with a human operator. A reduction of the signal-to-noise factor by ten in the minimum receivable power is equivalent to an increase of 1.78 in the maximum range, as indicated in Equation 8-5. This considerable increase in range demonstrates the validity of the statement made previously to the effect that the automatic tracking radar range almost always exceeds range of the search radar. That statement is also supported by the fact that a pulse-to-pulse integration process continues during the tracking function. In the search case, only a finite number of pulses are returned. The more pulses returned per look, the lower the minimum signal power necessary; this results from the fact that when pulses are added (integrated), the random noise effect tends to cancel, while the echo signal returns (which are nonrandom) tend to add. This integrating or filtering process is well known and commonly used in radars to improve signal-to-noise ratios. The effect of integration and filtering on signal-to-noise ratio is discussed in Chapter VII.

(b) INCREASING THE RADAR RANGE

To increase the radar range, the parameters of the radar range equation are examined and means are suggested for improvement in the overall range. Fluctuation factors are neglected in the range equation.

Radar range is given by

$$R_o = \left(\frac{PG^2 \lambda \sigma}{(4\pi)^3 \; kTB\,(NF)L} \right)^{\frac{1}{4}} \qquad (8\text{-}10)$$

where

R_o = range for $\frac{S}{N}$ of 1
P = peak transmitted pulse power
G = antenna gain

λ = wavelength
σ = target cross section
k = Boltzmann's constant
T = absolute temperature
B = IF bandwidth
(NF) = Noise figure of receiver ratio of receivers's noise power to noise power of pure resistance element at temperature T
L = loss factor

The final term L includes many losses such as those due to waveguide, radome, and TR, as well as atmospheric losses. Scanning loss, which is the ratio of the minimum detectable signal (MDS) power when the radar antenna is scanning, to MDS when the radar antenna is pointed directly at the target, is also included in the L term. Other losses such as degradation due to field conditions and poor maintenance may be included in L.

Any of the terms in the numerator, if increased in magnitude, would improve the radar range and, similarly, reduction of the values of the denominator terms would improve radar range. A frequently selected wavelength, X-band, is desirable since it is relatively free of atmospheric and rain absorption and provides narrow beamwidths with the apertures available in interceptor aircraft, thus permitting reasonably accurate tracking.

Doubling the transmitter power theoretically increases range by about 19 percent. This increased power is limited by the waveguide breakdown and the power available from magnetrons.

Increasing the antenna diameter increases the range directly but requires a larger interceptor to carry a larger antenna.

Reduction of the receiver noise figure by 4.0 db's would increase the range by a factor of 1.26.

It is estimated that improving the radar design for greater reliability and ease in maintenance would increase operational detection ranges as much as 45 percent.

Scanning losses account for an average of 13 db loss over the entire antenna pattern. If the antenna reflector motion were eliminated, the scanning loss would be reduced to that due to the conical motion only, and the detection range could be increased by a factor of about 1.8.

SECTION 3 — EVALUATION BY THEORETICAL ANALYSIS

(a) PULSE-DOPPLER RADAR EVALUATION SUMMARY

Pulse-doppler radar has effectively overcome the ground clutter problem of the pulse radar. Ground clutter not only masks targets during search, but is responsible in many cases for lock-on being broken at ranges corresponding to the range of the ground clutter. Airborne moving target indication (AMTI) used in many search radars is only partially effective in reducing ground clutter and, additionally, has a deteriorating effect on range performance.

Pulse-doppler radar, operating at higher pulse repetition frequencies (PRF's), produces higher average power output than a comparable pulse radar.

The principle of operation of the pulse-doppler radar depends on the doppler frequency-shift phenomena associated with relative motion between signal source and moving object. The doppler effect is given by

$$f_r = \frac{C + V}{C - V} f_t \qquad (8\text{-}11)$$

where for pulse-doppler radar

f_t = transmitted frequency

C = propagation velocity
V = target velocity
f_r = frequency of returned signal

The doppler frequency shift is the difference between transmitted and received frequencies as given by

$$f_d = f_t - f_r = \frac{2V}{C-V} f_t \text{ or since } C >> V \tag{8-12}$$

$$f_d = \frac{2Vf_t}{C} = \frac{2V}{\lambda} \tag{8-13}$$

where λ is the wavelength of transmitted signal.

To obtain pulse-doppler information, the frequency difference between the transmitted and received signal from a radar target is obtained by heterodyning. The maximum doppler frequency is given by

$$f_d(\max) = 1/2 \text{ PRF} \tag{8-14}$$

Because potential radar targets may have very high closing speeds during head-on approach, the selected PRF must be high, i.e., on the order of ten times as high as PRF's of conventional pulse radars. The high PRF permits radar range determination at only very short distances. To circumvent this condition, several PRF's are transmitted and a unique range, corresponding to an unambiguous range, is obtained. In the pulse-doppler radar, the returned signal frequency shift is determined by use of signal in the receiver which is referenced to the transmitted signal.

A block diagram of a basic pulse-doppler radar is shown below:

The transmitter may consist of an rf amplifier capable of a high duty cycle. The output of the transmitter sends rf energy to the antenna while receiving coherent rf drive from the receiver. Pulse modulation is applied to the power amplifier from a hard-tube pulse generator at the high PRF rates required by the system. For the power amplifier, rf drive is from the receiver and forms the basis for system coherence. The transmitter produces rf energy which passes through the duplexer and out the antenna. Because of the high PRF required, the TR tubes must have the keep-alive electrode pulsed to reduce the ionization time between pulses.

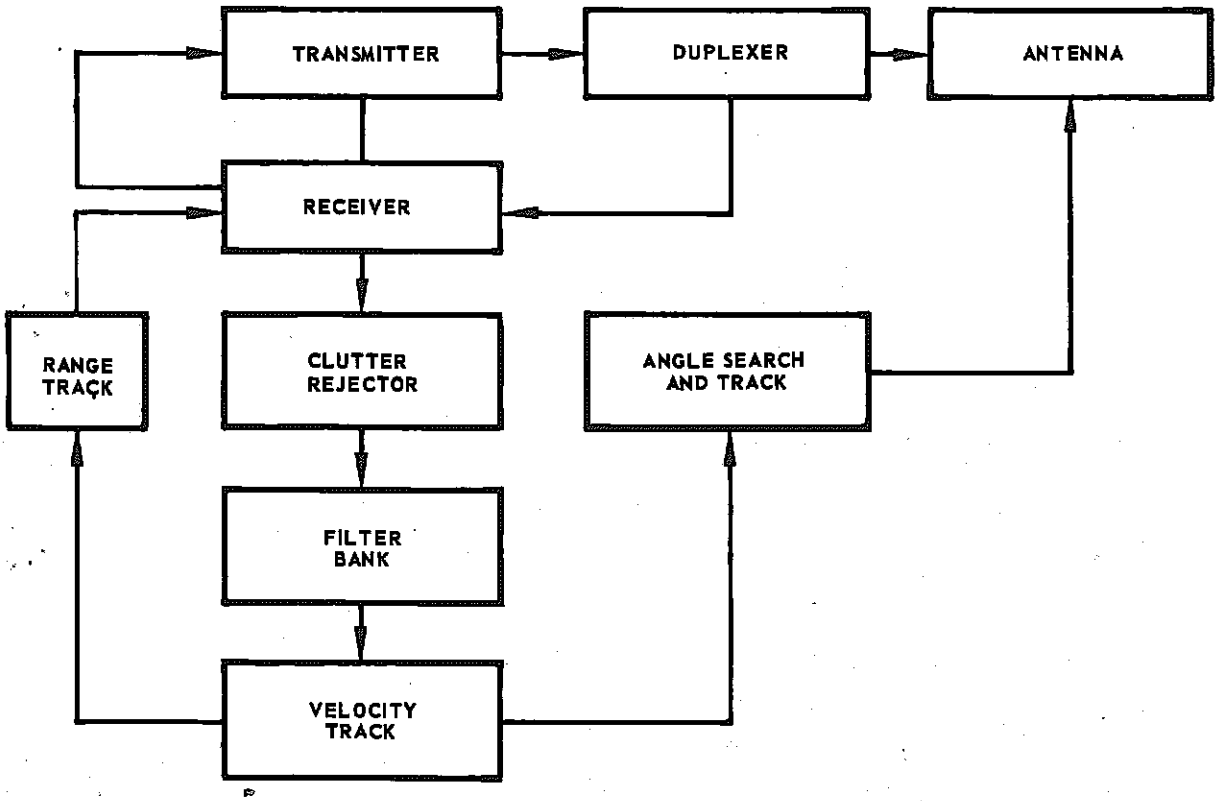

FIGURE 8-1. BASIC PULSE DOPPLER RADAR BLOCK DIAGRAM

Between transmitted pulses, the antenna can receive return echo pulses. Radar echo passes through the duplexer and into the mixer, where a local oscillator signal of exceptionally high frequency stability heterodynes the incoming signal to an IF frequency. The same oscillator also is heterodyned with the output of a coherent oscillator to provide the coherent rf transmitter drive. In tracking mode, the IF amplifier stages are range-gated so that target echoes appear only at coincidence of the range gate and target echo. The IF signal is applied to the detector stage, which also receives a signal from the coherent oscillator for reference purposes. The output of the detector stage goes to the clutter rejector, which acts on the video to remove the altitude line and the main beam clutter. The altitude line and main-beam clutter are removed by suitable filters. For main-beam clutter elimination, a clutter computer selects the filter bandwidth and positions the clutter region at the filter frequency.

The video remaining after elimination of main-beam clutter and altitude line goes to a bank of doppler bandpass filters. The filter bank consists of a number of filters designed to pass doppler frequencies in the range of interest corresponding to the radar target velocities. The filter bank outputs are switched sequentially to determine whether the signal exceeds a threshold bias in the threshold detector. When the filter containing echo signal is identified, target velocity information is available for range, tracking, and indicator display. The target angular position is determined by the antenna azimuth position.

After detection of the target in one of the doppler filter detector channels, the velocity information is known and more precise velocity can now be obtained so that a velocity gate can be positioned to track the target accurately. Target velocity is tracked by means of a feedback loop which causes a variable frequency oscillator to shift in frequency to maintain the echo signal in a narrow bandpass filter. The frequency of the variable frequency oscillator is thus a measure of target velocity. Tracking in angle can be performed in a manner similar to the conical scanning technique of the conventional pulse radar, where the conical scanning antenna causes a returned echo signal to contain amplitude modulation. Whenever the target within the radar beamwidth differs from electrical boresight, an angular tracking error, which is proportional to amplitude modulation contained in the returned signal, is derived and drives the antenna servo in a direction to reduce the tracking error.

The pulsed transmission of the pulse-doppler radar permits the receiver to be turned off during the transmission period. The output of the modulated amplifier consists of a square wave envelope of sine waves. Coherency of the transmitted signal is maintained.

The square wave pulse modulation is at a repetition rate (f_r) consisting of an infinite number of sine wave frequencies f_r, $2f_r$, $3f_r$ . . . . n_{f_r}. The modulating process may be considered as a process of amplitude modulation at the frequencies f_r, $2f_r$ . . . . . n_{f_r}. The power amplifier output consists of signals of the amplitude modulation $(1 + \sin \omega_1 t)$ $\sin \omega_o t$ $(1 + \sin \omega_2 t)$ $\sin \omega_o t$, $(1 + \sin \omega_3 t)$ $\sin \omega_o t$. Expansion of these terms gives the sum-difference terms.

$$\sin \omega_o t + \sin \omega_o t \sin \omega_n t = \sin \omega_o t + 1/2 \sin (\omega_o + \omega_n)t$$

$$+ 1/2 \sin (\omega_o - \omega_n) t \qquad (8\text{-}15)$$

Modulation of the carrier frequency with square wave modulation produces upper and lower sidebands at frequencies displaced at increments equal to integral multiples of the modulation frequency.

In evaluating the performance of the pulse-doppler radar, the closing velocity and ground clutter effects are of utmost consideration. In the normal pulse-doppler system there exists a clutter-free region for the case of the head-on target. This is due to a sufficiently high pulse repetition frequency. To determine if the returned target signal lies in the ground clutter signal region, the two signal frequencies are compared. The frequency of the ground clutter signal is $f_o \pm 2 \frac{V}{\lambda}$. The ground clutter effect can be eliminated by a computer in the fire control system which selects an appropriate rejection bandwidth. Ground return clutter power is compared with the target signal power by the ratio of cross-sectional area of the clutter σ_c to the cross-section of the target, σ.

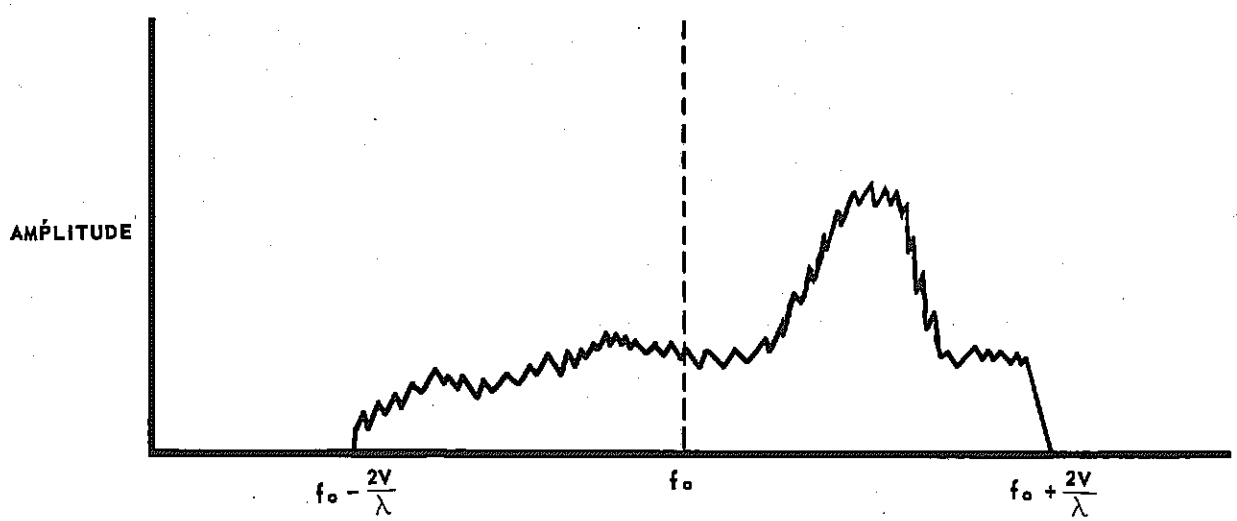

FIGURE 8-2. GROUND RETURN CLUTTER

This ratio $\frac{\sigma_c}{\sigma}$ determines the degree that the target signal is obscured. The ground clutter cross-sectional area is computed from the following equation:

$$\sigma_c = Kh \frac{C}{2} \tau \beta \quad \sec \theta \tag{8-16}$$

where

K = constant determined by terrain characteristics
θ = antenna depression angle
C = velocity of light
τ = radar pulselength
β = antenna beamwidth
h = elevation

Ability to see targets in the ground clutter is determined from the probability of look-through as,

$$P_{LT} = \frac{\sigma}{\sigma_c} \tag{8-17}$$

The probability of look-through as a function of $\frac{\sigma}{\sigma_c}$ is shown in Figure 8-2.

Probability of detection in the presence of ground clutter is obtained by

$$P_C = P_d P_{LT} \tag{8-18}$$

where P_d is the probability of detection without clutter and P_{LT} is the probability of ground clutter look-through.

(b) RANGE PERFORMANCE

The range equation used for the conventional pulsed radar is modified for the pulse doppler radar as follows:

$$R_o = \left[\frac{P_{ag} \delta^2 \lambda^2 \sigma G^2 L}{(4\pi)^3 (NF) k T \Delta f} \right]^{\frac{1}{4}} \tag{8-19}$$

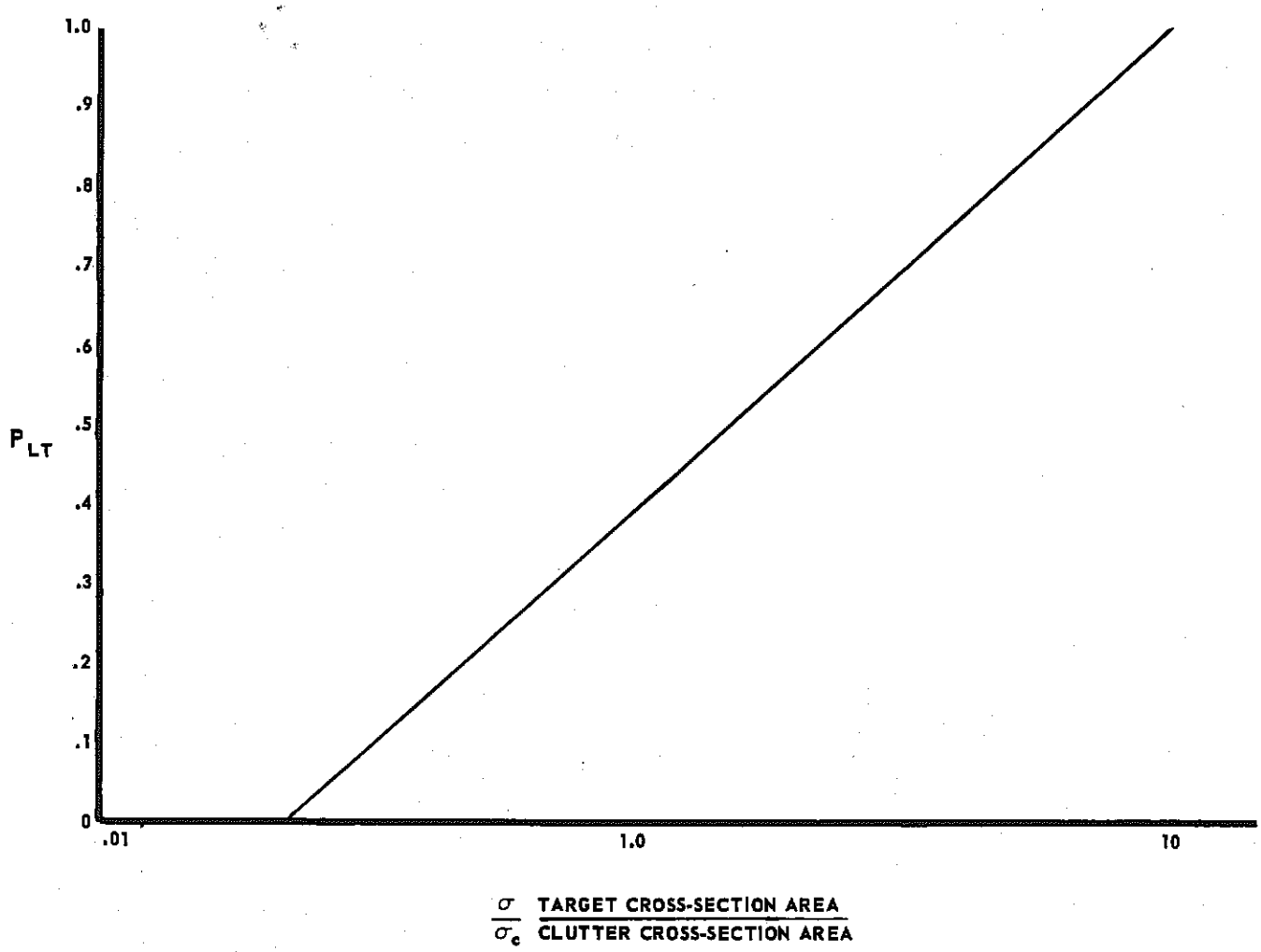

FIGURE 8-3. PROBABILITY OF LOOK-THROUGH

where

R_o = range for $\frac{S}{N} = 1$
P_{ag} = transmitter average power
L = loss factor, including eclipsing loss
Δf = noise bandwidth
(NF) = noise figure
λ = wavelength

σ = cross section target area
G = antenna gain
kT = Boltzmann's constant x noise temperature
δ = transmitter duty cycle

Eclipsing results from the echo signal being obscured due to the receiver being blanked out during transmission time. Eclipsing loss can be approximated by $1-\delta$. Reduction of eclipsing is accomplished by switching the pulse repetition frequency.

Probability of Detection

The probability techniques discussed in connection with conventional pulse radar are equally applicable to the pulse-doppler radar probability of detection. False alarm probability for the pulse doppler can be obtained from the equation.

$$\tau_{fa} = \frac{n}{BW \cdot N} \qquad (8\text{-}20)$$

τ_{fa} = false alarm time
n = false alarm number
BW = bandwidth of a filter
N = number of filters

(c) THE PULSE-DOPPLER RADAR PHASE JITTER

As pulse-doppler radars have come into more common usage, the problem of evaluating the practical system has assumed a position of greater importance. The physical system behaves in a manner quite different from the radar set as described in the design objectives. The practicality of the system is determined by its deterioration from the theoretical values.

For the pulse-doppler radar, random fluctuations in phase of the returned radar signal have a degrading effect on the filters used to select the range of expected doppler shift. The doppler filters cannot reject both the signals which fall outside of the frequencies and the signals which they were designed to pass. Filter rejection ability is decreased. The fluctuation in phase also results in a loss of resolution as well as a loss in system accuracy.

The originators of the phase fluctuations are the radar system, the airframe, and the aircraft environment. The ultimate limitation upon a pulse-doppler radar system is caused by the atmospheric turbulence, which is the major factor causing phase jitter, the other factors being negligible. Phase jitter is due to fluctuations in the length of the optical path to the target as caused by atmospheric turbulence. Air turbulence causes the index of refraction of air to fluctuate, accounting for the phase jitter. The worst condition of air turbulence is found inside thunderstorms and cloud formations.

Atmospheric jitter is mainly a low frequency phenomenon and the system, for a given degree of degradation, tolerates a larger rms jitter than "white noise." Low frequency components of signal shift the position of the comb-filter teeth and affect the accuracy rather than resolution. The radar system parameters must finally be adjusted to obtain improved performance from the comb filters.

(d) CONTINUOUS WAVE (CW) RADAR

Velocity information may be obtained by means of a CW radar which functions as described in the following paragraphs.

A target is illuminated by a search CW radar for a duration equal to the time the radar beam is pointed at the target. For purposes of analysis, the amplitude of the transmitted signal is assumed to be of constant amplitude A, and frequency is represented by f. The spectrum has the form $\frac{\sin \pi(f_a - f)\tau}{\pi(f_a - f)\tau}$ and is illustrated below centered about f_a:

The bandwidth, $\frac{1}{\tau}$, centered about f_a contains 90 percent of the total energy in the spectrum. Because of the beam shape and target characteristics, the received pulse may be amplitude- and phase-modulated. The center frequency of the returned signal will be shifted from the carrier by an amount proportional to the doppler frequency shift. Doppler frequency is given by:

$$f_d = \frac{2V}{\lambda} \qquad (8\text{-}21)$$

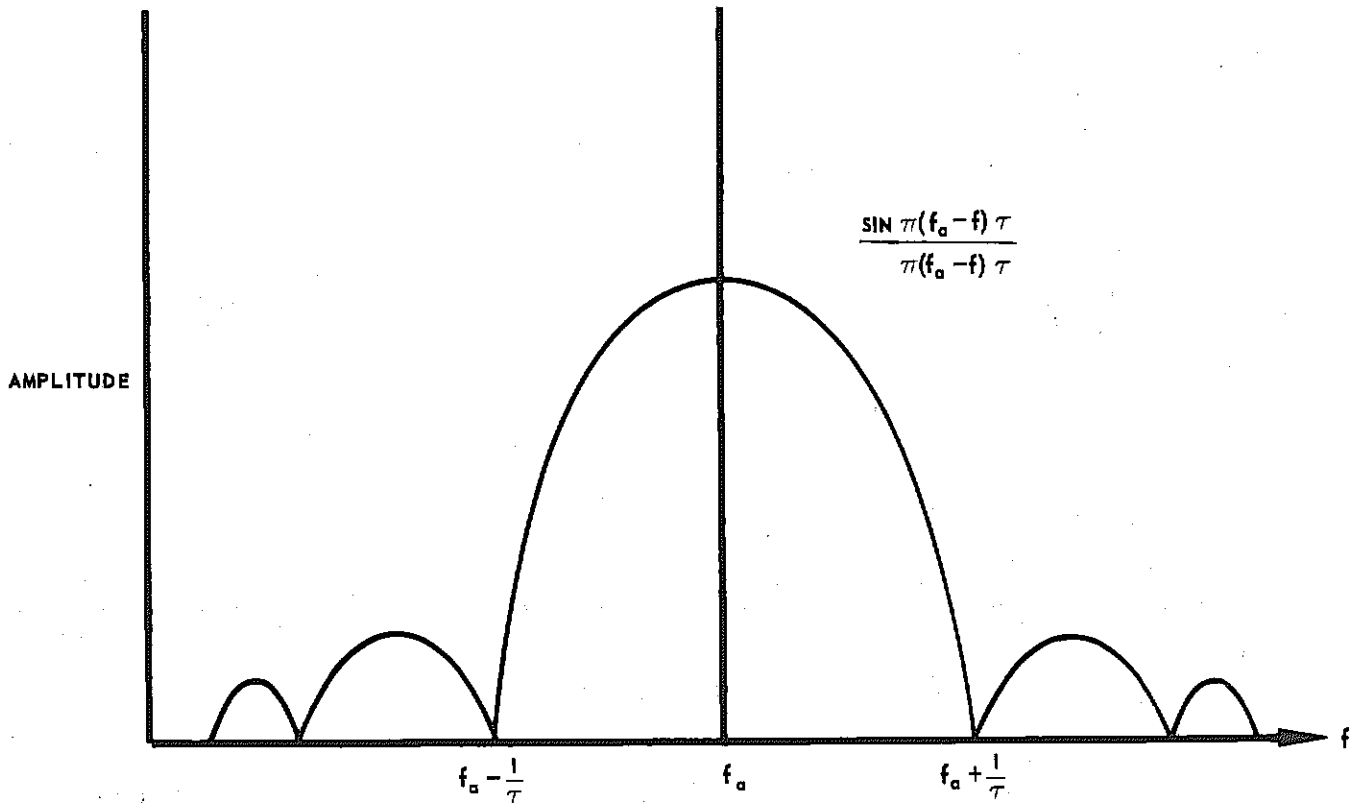

FIGURE 8-4. CW RADAR SPECTRUM

where

V = the relative radial velocity
λ = the wavelength

The polarity of the doppler shift is positive for targets approaching the radar, and negative for receding targets. The amount of shift is proportional to the relative velocities of the moving targets. The spectrums of return from three types of targets are illustrated in the figure below.

The amount of frequency separation between fixed and moving targets permits the use of filters to eliminate fixed targets.

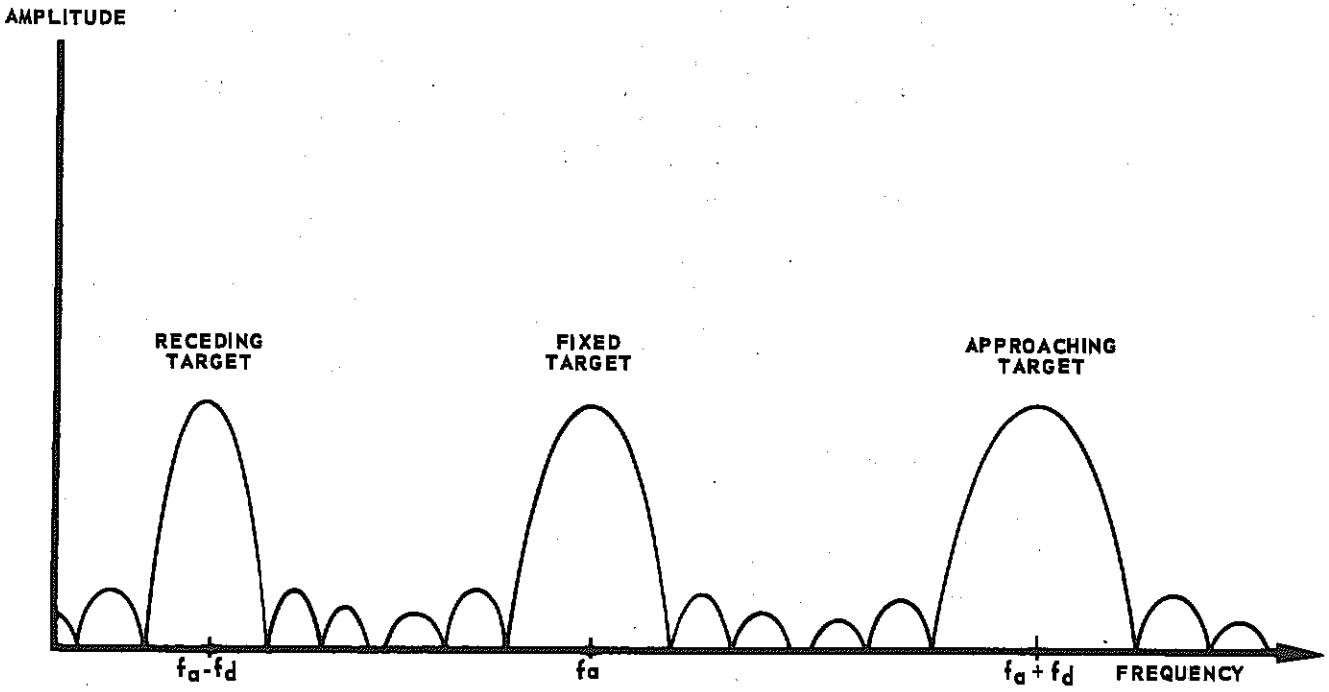

FIGURE 8-5. CW RETURN SPECTRUM

The IF bandwidth must be sufficiently wide to pass the maximum excursions of the doppler frequency corresponding to expected velocities. The IF bandwidth is substantially greater than the maximum expected doppler frequency which allows IF noise to pass along with any signal present. In order to increase signal-to-noise ratio, the signal is passed through a narrow-band filter. To cover the entire range of expected doppler frequencies requires filters of bandwidth $\frac{1}{\tau}$. Alternatively, some scheme of sweeping a filter over the doppler band of frequencies may be used. A scanning technique is limited at the highest scanning frequency by the requirement that the filter must have an integrating effect; that is, the scan must stay on a target long enough to provide integration of the signal, yet be fast enough to provide the required data rate.

Integration or filtering can be performed at either IF or video frequencies. Filtering at IF frequencies has the advantage over video since it maintains the target direction information inherent in the doppler frequency shift.

Video signal is obtained by beating the IF signal with a reference oscillator at the same IF center frequency. (See Figure 8-6.) The

polarity of the doppler shift is lost in the heterodyning process; the spread of frequencies covering only half the spread at IF may be covered with one-half the number of filters required at IF frequencies. Even though doppler-shift polarity is lost at video while the noise which was present in the lost signal remains, the noise adds to the video and results in a lower signal-to-noise ratio.

Integration or predetection integration at IF requires twice the number of filters needed for video integration. The narrow bandwidth filters required at IF impose the further restriction of selection of a lower intermediate frequency. Filters of 100 bandwidth, capable of operating at an IF of 100, would be suitable for such a scheme.

The required system stability is obtained by using a highly stable (crystal controlled) IF oscillator and a cavity for maintaining the transmitter tube stable during the time required for transmission and reception.

Ground clutter in the airborne CW radar is translated as a distance equivalent to the doppler frequency corresponding to the radial velocity between the aircraft and the illuminated ground surface. The velocity varies according to the antenna direction, being greatest when the beam is pointed forward, and approximately zero when directed broadside. Spread of the doppler frequency varies as a function of aircraft speed, radar beamwidth, and beam angle with respect to the aircraft. Ground clutter moves in frequency as the antenna scans, obscuring targets having lower doppler frequencies than those due to the clutter. The ground clutter can be reduced by adjusting the reference oscillator frequency for zero at the maximum amplitude of clutter spectrum.

The major CW radar problem is that of isolating the receiver and transmitter, which operate continuously. Leakage of transmitter power directly into the receiver results in excessive noise being introduced into the receiver, and effectively lowers the receiver noise figure. Means for improving transmitter-receiver isolation consist of using improved duplexer arrangements. The simple technique of using separate transmitting and receiving antennas for isolation does not lend itself to efficient installation in an interceptor aircraft.

A basic block diagram of a CW radar is illustrated in Figure 8-6.

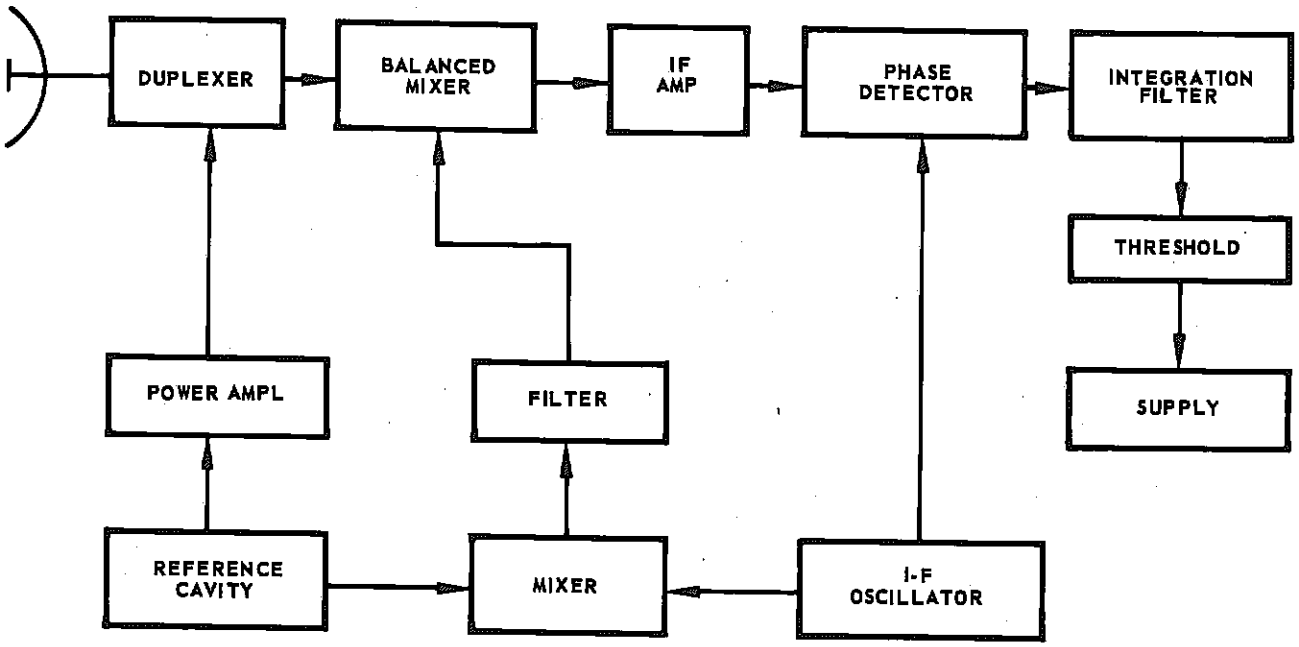

FIGURE 8-6. BASIC VELOCITY (CW) RADAR

(e) SIDE-LOOKING RADAR

Side-looking radars are recent innovations with certain advantages over the conventional radar systems. The side-looking radar uses antennas which are fixed to the airframe of the aircraft. The antenna, generally, is set to point in the direction of the earth's vertical.

The side-looking radar antenna does not scan by an antenna scanning motion; instead, the aircraft forward velocity produces a motion of the radar beam with respect to the illuminated ground surface. The return signals are displayed on an indicator which is photographed to produce a permanent radar map of the strip of terrain over which the aircraft has passed. The photograph is oriented to represent a time ground map in the sense that angles and distances are in true relationship.

The picture detail is determined by the system resolution capability. This resolution is determined in range by the pulsewidth and in azimuth by the antenna beamwidth. A narrow pulse and a long horizontal antenna

would, therefore, give maximum resolution. Because of the geometry of the aircraft, long antennas can conveniently be installed parallel to the fuselage.

This arrangement permits a large number of radar pulse hits on the target per beamwidth with a resultant improvement in target detection. In the conventional pulse-modulated radar, detection of high speed targets causes a smearing in the displayed target blip. The side-looking radar effectively overcomes this deficiency.

(f) LOBING TECHNIQUES

Lobing techniques are used to determine the direction of arrival of the wavefront from a target. By determining this, the position of the target in space can be determined relative to the position of the interceptor in space. A technique for determining direction of return by simultaneously comparing two or more lobes may be employed. The general term used to describe simultaneous lobing is "monopulse." Monopulse is a method for precision direction finding of a pulsed source of radiation. In either sequential or simultaneous lobing, the angle of arrival is determined by comparing the signals received on two or more noncoincident antenna patterns. These patterns are usually mirror images about an axis, which is called the scanning axis in the sequential lobing case. Rapid beam switching or conical scanning is severly limited in tracking accuracy because of the angular jitter caused by pulse to pulse fading of the return signal. In other words, the effect of amplitude scintillation is severe in a conical scanning type, antenna lobing scheme. Although the effect of amplitude scintillation on tracking accuracy can be smoothed by integrating over a sufficiently large number of scans, this results in undesirable lags in the tracking loop. Also, if the fading signal has a strong component near the scanning frequency (as in the case of propeller modulation) the misalignment signal contains components very near to the conical scan frequency. Simultaneous lobing compares antenna patterns, but is distinguished from sequential lobing by the fact that the angle of arrival can be measured continuously and instantaneously by comparing the antenna patterns simultaneously. Therefore, the amplitude scintillation errors present in sequential lobing measurements are not present in simultaneous lobing, since only the instantaneous relative amplitudes of the signals received from a given direction are measured.

Although sequential lobing techniques used for obtaining angle of arrival depend solely on comparison of amplitudes, simultaneous lobing

can compare amplitude, phase, or both. However, the advantages of simultaneous lobing are obtained at the expense of added complexity in the system. It is usually necessary to have at least two receiver channels for monopulse systems, as compared to a single channel for the sequential lobing scheme. An important fact to remember in monopulse methods is that since the information is received on two antenna patterns simultaneously, even though the absolute amplitudes and phases of the received signal may vary with changing characteristics of the source of propogating medium or target, their relative values are functions only of the angle of arrival.

There are 3 basic types of monopulse radar systems.

(1) Phase Comparison-

The difference in direction of arrival is measured by the delay in arrival at the phase sensing receiving antennas. The phase of one of the signals is delayed from that in the other and this delay is a measure of the direction of arrival as shown in Figure 8-7.

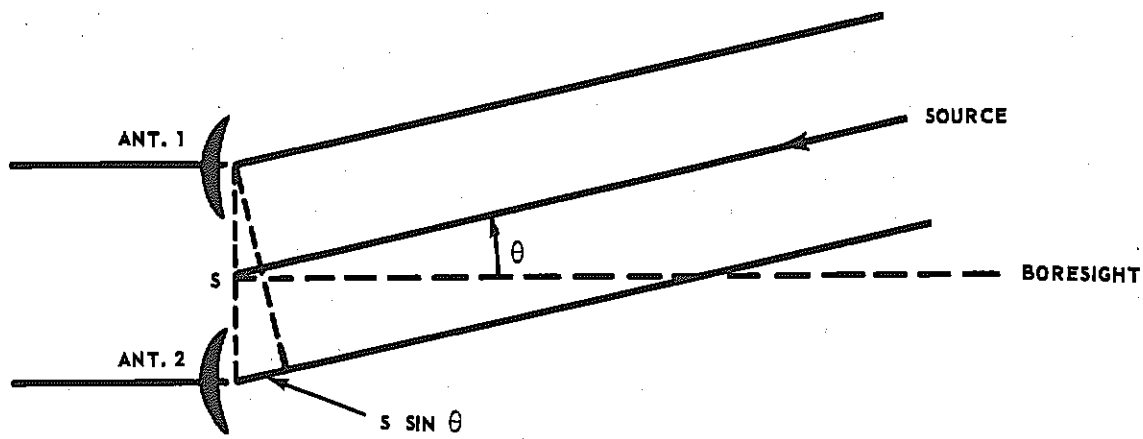

FIGURE 8-7. PHASE COMPARISON MEASUREMENT

The phase difference is related to the angle of arrival by

$$\phi = \frac{2\pi}{\lambda} S \sin\theta \qquad (8\text{-}22)$$

By heterodyning the rf signals against a common local oscillator, the signals are converted to an intermediate frequency with the relative phases, as well as amplitudes, preserved.

(2) Amplitude Comparison -

In a typical amplitude comparison monopulse system, the angle of arrival is sensed by a pair of amplitude patterns whose main beams are squinted off the boresight by a displacement of the feeds. Note that a single channel is possible here, since in amplitude comparison of signals received from isolated pulse sources, the angle information is contained solely in the relative amplitudes of the signals received on the pulse returned by the two feeds. Hence, the pulses received may both be passed through a common receiving channel, if one of them is delayed in time by at least its own length. This is the reason for the delay network in the single channel. This, in effect, is a type of time multiplexing.

(3) Sum and Difference Comparison -

A third type of monopulse system is shown in Figure 8-8. Whether the received signals are obtained from an amplitude or phase sensing antenna, their difference is an odd function about the boresight axis, their sum an even function. The ratio of their difference to the sum

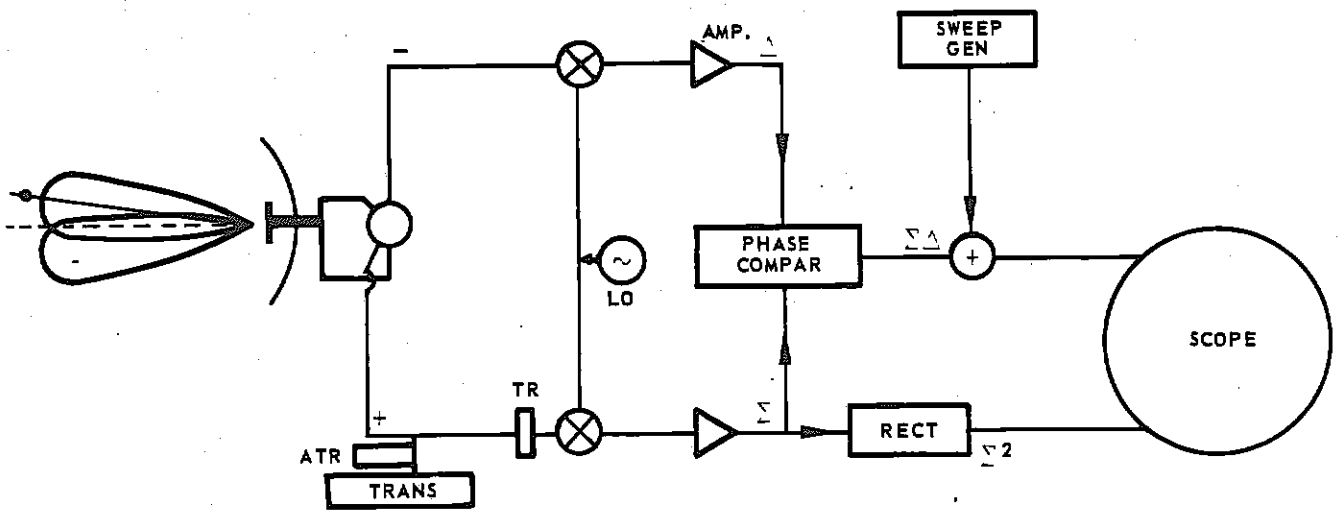

FIGURE 8-8. SUM DIFFERENCE MONOPULSE RADAR

is always independent of the absolute level of the received signal, which is also true of the other two systems described. In Figure 8-8, the angle information is obtained by amplitude sensing, although phase sensing also could have been used. Here a single antenna is used for both transmission and reception.

The conical scanning antenna, which has been used for many years in airborne radars, suffers because of susceptibility to countermeasure techniques. Monopulse techniques have certain advantages over the conical scanning variety.

The waveguide consists of four sections at the feed end. (See Figure 8-9C.) Two patterns are produced by the monopulse antenna, the sum pattern adds the signals from the waveguides, the difference pattern is produced by subtracting signals in the right-left or upper-lower feed horn pairs. The various combinations of signal additions and subtractions are used for obtaining reference signal, azimuth tracking signal, and elevation tracking signal as follows: The sum signal is proportional to the antenna elevation tracking error. The sum pattern is illustrated in Figure 8-9a, and the difference pattern for azimuth or elevation error determination is shown in Figure 8-9b. Signals from the four feeds, A, B, C, and D, are mixed in the "magic - T" ring junctions 1 and 2 (Figure 8-10b) to obtain the sum and differences. At junction 3, the differences A-B and C-D are added to give (A + C) - (B + D). (Refer to Figure 8-10c, which illustrates the action of a "magic-T" junction.) If two signals, E_1 and E_2, are applied simultaneously to the waveguide as indicated (same frequency and same phase), the signals in waveguide 3 and 4 combine so that addition occurs in waveguide 3 and the signals subtract in waveguide 4.

(g) EVALUATION OF RANGE RATE TECHNIQUES

Distinguishing a moving target in the presence of ground clutter is possible by various techniques using the conventional pulse-modulated, FM/CW, or pulse-doppler radars. These techniques make use of range-rate discriminating features which utilize the phase and amplitude changes of the return echo as compared to the return from the ground clutter.

Noncoherent Airborne Moving Target Indicator (AMTI) functions on the basis of comparing successive pulses to determine which echoes are reflected from moving objects as compared to ground clutter motion. The moving target and ground clutter return set up doppler frequencies from

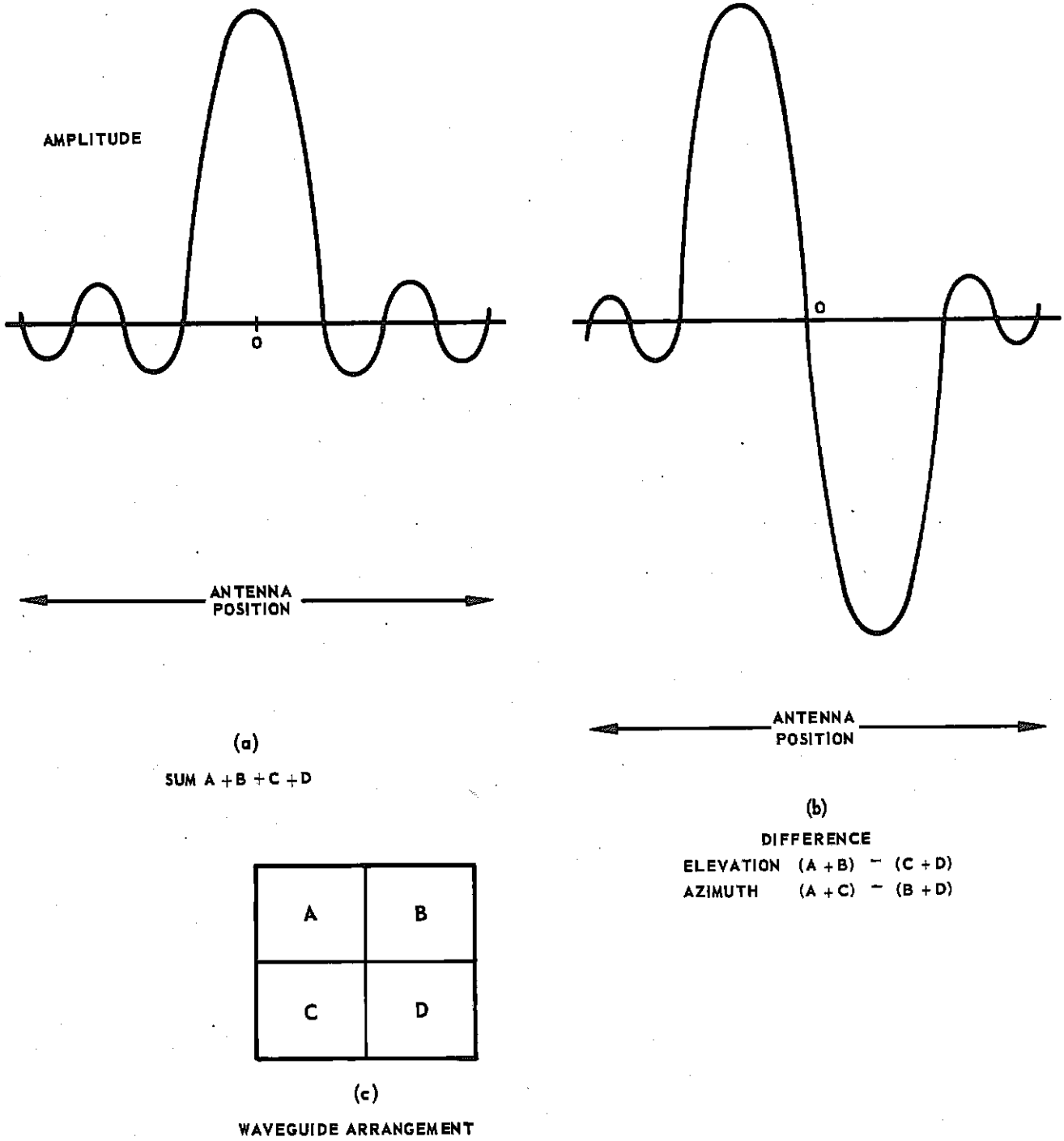

FIGURE 8-9a, b, c. MONOPULSE SUM AND DIFFERENCE PATTERNS

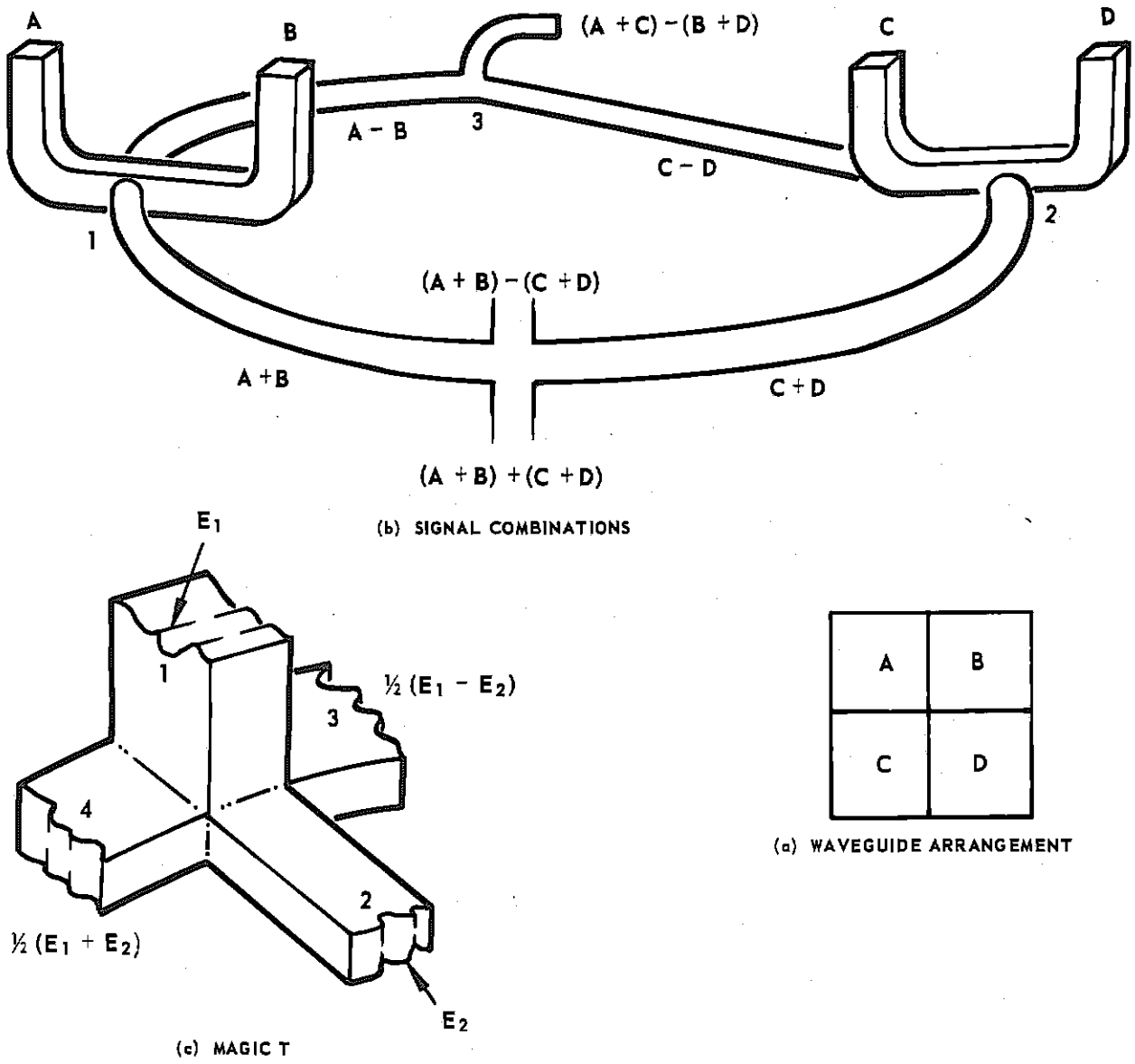

FIGURE 8-10. MONOPULSE WAVEGUIDE MIXING CIRCUIT

the same range, which beat together and provide an echo signal that is displayed on the scope. This AMTI system requires that ground clutter

be present at the same range and bearing as the target. Since clutter can occupy, in many cases, a small area of the total search volume, moving targets will be missed in the uncluttered area.

Moving targets also can be detected by radar systems employing coherent oscillators (COHO). The phase of the returned moving echo varies according to the doppler shift and a fluctuating echo is generated when the echo and COHO oscillator signal are added. Targets which do not move have a constant phase shift compared to the coherent oscillator and do not fluctuate. Moving echoes are retained while the fixed target echoes are eliminated by video cancellation on consecutive pulses. In order to be effective, the moving target indicator circuitry must effectively cancel out the effect of the aircraft's velocity.

Using FM/CW radar, moving targets may be distinguished by means of the doppler shift of continuous wave (CW) signals returned from the moving targets. The most serious drawback of the FM/CW radar is caused by the requirement for isolation of the receiving circuitry from the transmitter, which operates continuously.

Pulse-doppler radar techniques have been developed to overcome the poor performance caused by clutter in the conventional pulse radar at low altitudes. As radar detection range requirements are increased, the clutter problem becomes more important. The range performance of the pulse doppler is superior to the conventional pulse radars primarily because of the higher pulse repetition frequency, which results in a higher average power output. However, the advantages of the pulse-doppler radar are achieved at the expense of greater complexity of equipment.

Pulse-doppler radar uses a technique similar to the FM/CW system to obtain target discrimination in the presence of ground clutter. The return from a moving target, and from ground clutter, differs by some doppler-frequency shift and so can be discriminated in the radar set. The pulse-doppler system, however, is gated and therefore is not limited by transmitted signal fed through to the receiver. The range discrimination provided by range gating reduces the clutter competing with the signal to give greater clutter rejection than is obtainable by use of the CW radar.

(h) TRACKING RADAR

(1) General Considerations

During operation of the fire control radar in tracking mode of operation, the conventional radar tracks a single object by providing range and angle data. Angle tracking consists of keeping the antenna pointed at the target at all times. Conical or monopulse scanning can be used to permit correcting the antenna angular error. Range tracking singles out the target echo in range by bracketing it with a time pulse called the range gate. The range gate, which is generated in the receiver, coincides with the expected range of the target echo, effectively eliminating echoes at all other ranges. Range gating is performed using a split gate consisting of early and late gates. The time discriminator circuitry acts to servo out the error signal in the two half-gates in order to keep the echo pulse within the range gate. The nature of the tracking system is determined by the characteristics of the servo system used. In some applications, aided tracking is employed rather than relying completely on an automatic system. Aided tracking, as used in various airborne fire control systems, uses a computer input to the tracking system (see section on Flight Evaluation Program). In some older, nonairborne types of fire control systems, the aided-tracking was accomplished using manual operation of a handwheel to control the rate at which the range gate moved.

A simple antenna tracking scheme is illustrated in Figure 8-11. The block diagram showing the elementary receiver and electromechanical requirements is shown in Figure 8-11. The noise filter in Figures 8-11 and 8-12 can be represented by the following elementary RC circuit: whose transfer function, using operational notation is

$$Y_1(P) = \frac{1}{RCP + 1} = \frac{1}{\tau_1 P + 1} \qquad (8\text{-}23)$$

The transfer function of the antenna driving motor is obtained as follows: The transfer functions shown in the blocks are obtained for each block as

$$Y_2(P) = \frac{e_1}{Y_1 \epsilon} = K_1 \qquad (8\text{-}24)$$

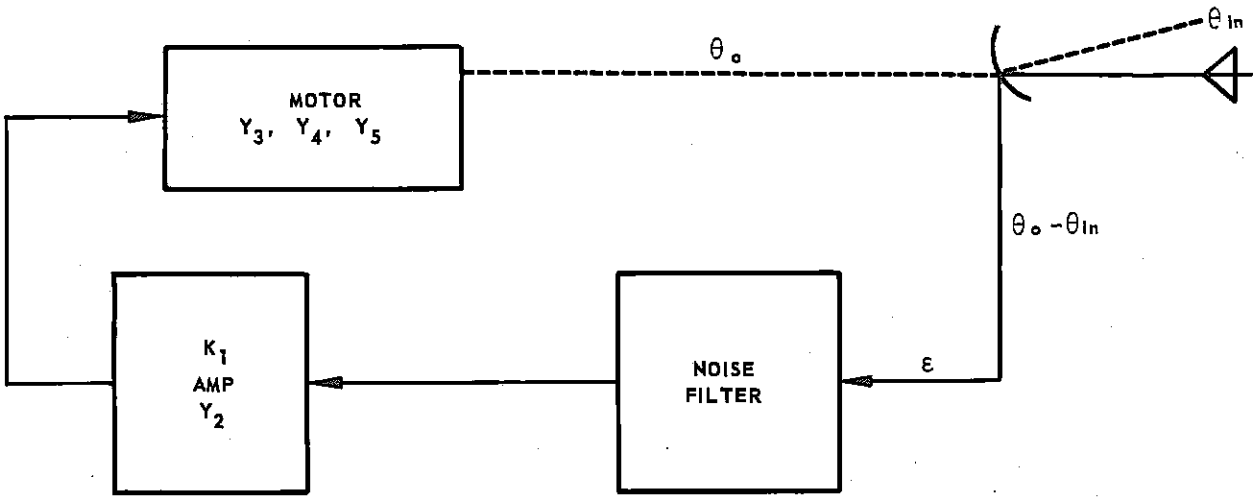

FIGURE 8-11. SIMPLE ANTENNA ANGLE TRACKING SERVO SYSTEM

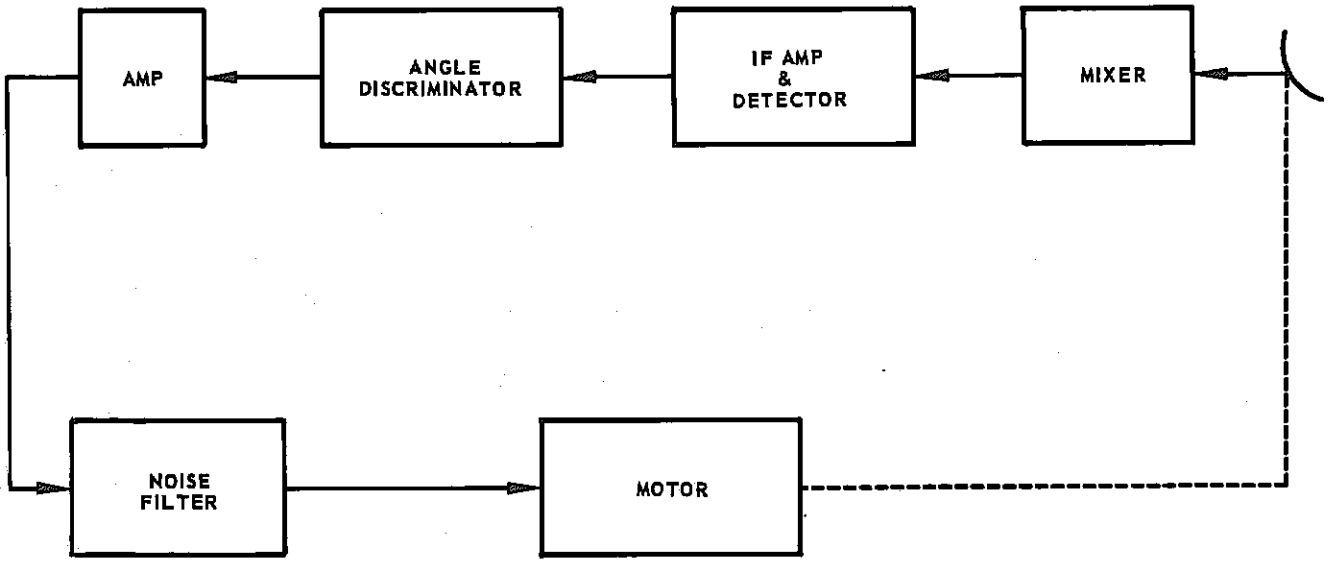

FIGURE 8-12. BLOCK DIAGRAM, RECEIVER-SERVO ANTENNA ANGLE TRACKING SYSTEM

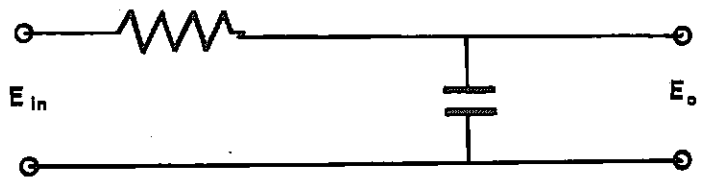

FIGURE 8-13. BASIC NOISE FILTER

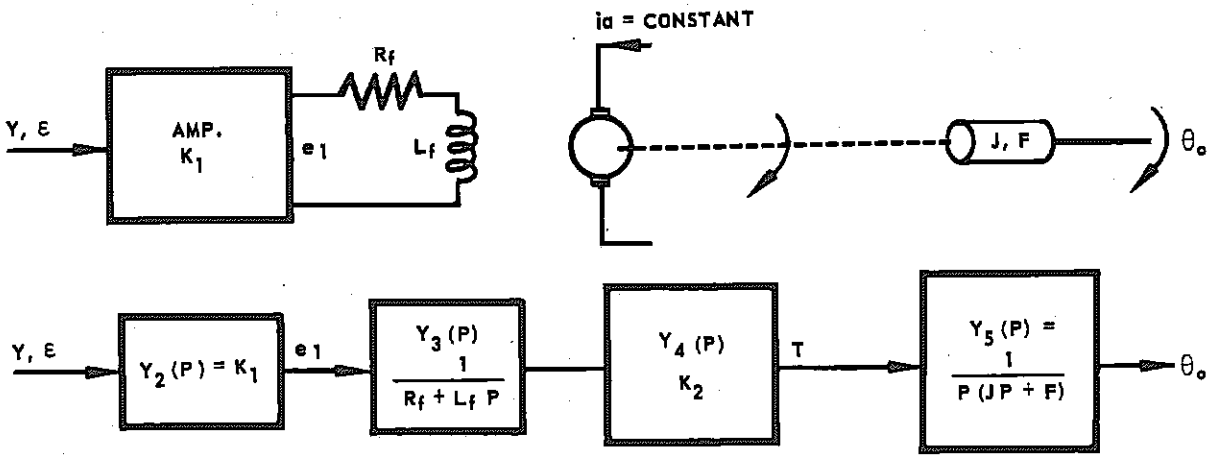

FIGURE 8-14. FUNCTIONAL BLOCK DIAGRAM OF ELEMENTARY TRACKING SERVO SYSTEM

$$Y_3(P) = \frac{i_f}{e_1} = \frac{1}{R_f + L_f P} \tag{8-25}$$

$$Y_4(P) = \frac{T}{i_a} = K_2 \tag{8-26}$$

The term K_2 represents a constant determined by the characteristics of the motor. The final block represents the transfer function of the

combined inertia and damping coefficients of the motor and load J, and F, respectively.

$$Y_5 = \frac{T}{\theta_o} = JP^2 + FP \qquad (8\text{-}27)$$

Combining the blocks results in

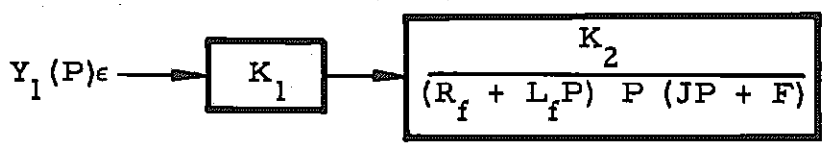

FIGURE 8-15. COMBINING TRANSFER FUNCTIONS OF FIGURE 8-14

Including the noise filter transfer function with the other block of Figure 8-12 results in Figure 8-16.

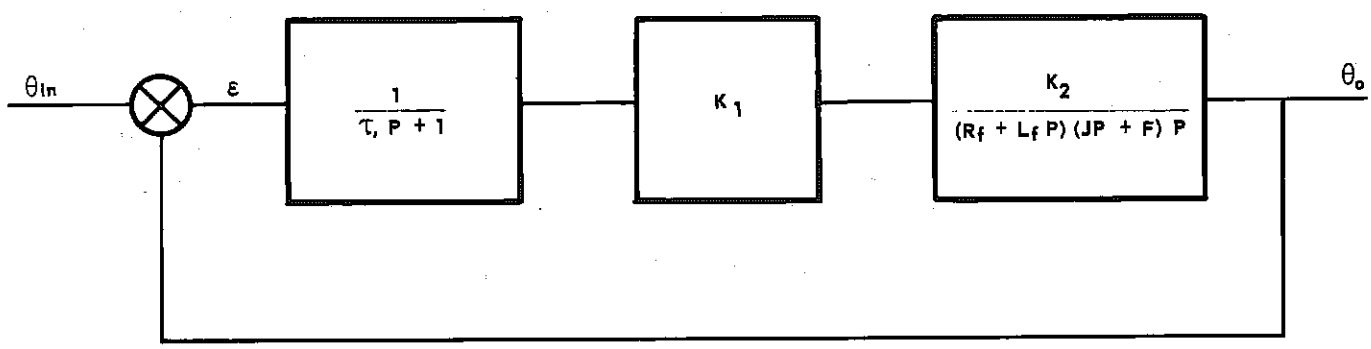

FIGURE 8-16. CLOSED LOOP SYSTEM OF FIGURE 8-12

The complete closed loop transfer function is of the form

$$Y_L = \frac{\theta o}{\theta_{in}} = \frac{A}{1 + AB} \tag{8-28}$$

substituting system notation

$$Y_L = \frac{\dfrac{K_1 K_2}{(T_1 P + 1)(L_f P + R_f)(JP^2 + FP)}}{1 + \dfrac{K_1 K_2}{(T_1 P + 1)(L_f P + R_f)(JP^2 + FP)}} \tag{8-29}$$

Simplifying

$$Y_L = \frac{\theta o}{\theta i} = \frac{1}{(\tau_1 P + 1)(L_f P + R_f)(JP^2 + FP) + K_1 K_2} \tag{8-30}$$

Increasing the amplifier gains reduces the error more rapidly, up to a point determined by stability considerations.

To simplify the illustration, assume the filter transfer function $\frac{1}{\tau_1 P + 1}$, as well as the motor transfer function $\frac{1}{L_f P + R_f}$, equal unity. Solving for the roots of the characteristic equation

$$JP^2 + FP + K_1 K_2 = 0 \tag{8-31}$$

$$P^2 + \frac{F}{J} P + \frac{K_1 K_2}{J} = 0 \tag{8-32}$$

The damping factor equals

$$\zeta = \frac{F}{2\sqrt{JK_1K_2}} \tag{8-33}$$

and the undamped natural resonant frequency is

$$\omega_o = \frac{\sqrt{K_1K_2}}{J} \tag{8-34}$$

If the complete transfer function is considered, the characteristic equation is quartic, (P^4), requiring a more involved scheme for determination of the roots of the polynomial.

The system used for illustration would be inadequate since the delays caused by the noise filter and motor transfer function have not been considered in a practical fashion. Antenna tracking systems used in fire control sets contain noise and require filtering, thereby introducing time delays and phase shifts and complicating the design problem.

SECTION 4 — RANGE OF TRACKING RADAR

Determination of maximum tracking range for a pulse-modulated radar is made difficult by the action of noise on nonlinear servo circuits. It is possible to analyze the tracking process by approximating the nonlinear circuit with linear circuitry.

Range for the case of radar detection was determined from the radar range equation and the probability of detection. For this case, a range R_o was defined as the range at which signal-to-noise ratio was unity. This may be considered reasonable for detection of target by an operator examining the face of an oscilloscope. The operator attempts to detect the target by the time the signal equals the noise, which corresponds to the case of approximately equal peak signal and noise powers. Automatic tracking, however, does not work with the same detection criteria as the human radar operator. For the radar set to track automatically in range and azimuth, complex circuitry is required, and it is necessary to determine a new minimum signal power which will permit automatic tracking in the presence of noise. The problem is to specify the range at which

tracking can begin, and to determine the system tracking performance at low signal-to-noise ratios. An examination of the range tracking capability will suffice to illustrate the requirements for the azimuth and elevation tracking requirements.

Range circuitry is required to provide a continuous indication of range and range rate to the target. Range error generally is sensed by use of a split range gate, one form of which is shown in the figure below:

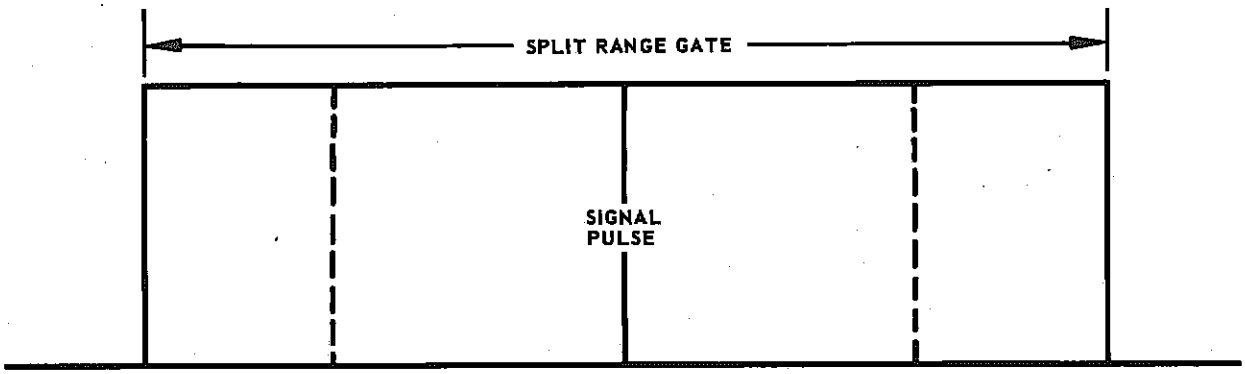

FIGURE 8-17. SPLIT RANGE GATE

The signal pulse is shown superimposed on the split gate. In addition to the signal pulse, noise will be superimposed in the range gates and will be integrated, along with the signal, in the two halves of the range gate. After the process of signal and noise integration, the signal difference in the split gate is obtained by subtraction to give a signal proportional to the position error. An electronic servo system uses the error signal to reposition the range gate, thus reducing the error signal to zero. If the servo system is designed to cause the gate rate of motion to be proportional to the positional error, the system is designated as a velocity-coupled servo. The servo system also may be designed to follow the target when it moves with constant acceleration. This type of servo is defined as an acceleration-coupled servo and will follow a constant velocity target with zero lag. If one assumes a constant velocity or acceleration existing in the respective velocity-coupled and acceleration-coupled servos, each system will come to rest at some displacement from the center of the gate which is proportional to the system lag.

This condition would exist if not for the different effect of noise on each half of the range gate. Noise is purely random so that when the integrated noise in the two half gates is subtracted, there is an appreciable

difference in the output which is not due to target motion. The servo system moves to null the error signal by repositioning the range gate. This effect is repeated on each pulse, generating an error signal which causes an undesirable random positioning of the range gate about the rest or equilibrium position. If the signal-to-noise ratio becomes sufficiently small, the random fluctuations become greater, finally resulting in complete unlimited jitter when the signal is zero. Since noise is random in nature, the probability always exists that noise will cause the target pulse to be completely lost from the range gate. For a large signal-to-noise ratio, range gate lock-on would be broken in the average over a longer interval of time than for the case of a small signal-to-noise ratio. Loss rate is defined by the relationship

$$R_L = \frac{1}{t_{avg}}, \tag{8-35}$$

where t_{avg} is the average time to loss of target for a constant range. Time required to break lock-on is therefore dependent on the signal-to-noise ratio.

The chances for breaking lock-on may be minimized by suitably adjusting parameters which effect this condition. If the total of both halves of the range gate width and the pulsewidth are approximately equal, the resultant servo control voltage (assuming no noise) will be optimum for most conditions.

The IF bandwidth can be reduced to decrease noise power passed on to the video stages. Noise is reduced linearly by bandwidth reduction, spreading the signal over a longer time period, and reducing the signal amplitude at less than the rate of noise reduction. The optimum IF bandwidth is given by the relationship from Chapter 7

$$t_g \Delta f_{IF} = \frac{1}{2} \tag{8-36}$$

where t_g is the width of half the range gate and Δf_{IF} the bandwidth frequency.

The value of approximately 1/2 compares to a value of

$$t_p \Delta f_{IF} = 2 \qquad (8\text{-}37)$$

where t_p is the pulsewidth

This value of 2 represents an optimum condition where the final output is for scope visual presentation. It is seen that the IF bandwidth requirement for automatic tracking is only one-quarter that required for a visual search system.

Optimization of the range servo may be obtained by proper adjustment of the servo time constant. The slope of the error signal, generated as the output of the range gate, is inversely proportional to the servo time constant. The speed of response of the restoring force to a step change in target position is proportional to the slope of the error curve, a large slope giving a fast response which is obtained by means of a short time constant. If the target is moving, the short time constant will quickly restore the error signal to the equilibrium point and prevent loss of target caused by moving past the gatewidth limits. The short time constant servo can, therefore, tolerate greater range gate wander (due to noise) than the longer time constant servo. The fast acting, short time-constant circuit, however, requires a greater bandwidth and passes a greater amount of noise than a similar long time-constant servo. An optimum condition for the range servo time constants is given for the indicated cases as follows:

<u>Velocity Coupling, Optimum</u>

$$t_{sec} \cong \frac{\epsilon}{3V_m} \qquad (8\text{-}38)$$

<u>Acceleration Coupling, Optimum</u>

$$t_{sec} \cong \frac{\epsilon}{5\,a_m} \qquad \text{where} \qquad (8\text{-}39)$$

V_m = target velocity, maximum

a_m = target acceleration, maximum

ϵ = the error at loss of the target

= $Kt_p \simeq 0.8t_p$

The time to loss is related to the servo time constant, since a slow acting servo would not lose the target as rapidly as a fast acting servo, regardless of noise considerations.

The loss rate is given by the expression

$$L \simeq \frac{1}{t_o} \exp \frac{-K^2 P_i^2}{w_o^2 \left(\Delta f_i \, \Delta f_s \, K_g\right)} \tag{8-40}$$

The symbol L is the loss rate and is equal to the reciprocal of the average time to loss of the target. The other symbols are defined as:

t_o = servo time constant
P_i = average received signal power
w_o = noise density in IF
Δf_i = IF bandwidth
Δf_s = equivalent servo bandwidth $\frac{1}{t_o}$
K_g = range gate duty factor $= \frac{t_g}{\Delta t}$
t_g = range gate half pulsewidth
Δt = reciprocal of the repetition rate
K = constant, approximately equals 1

It should be noted that the exponential power is essentially the square of the power signal-to-noise ratio and shows the very rapid decay of the loss rate with increasing singal-to-noise ratio.

An equivalent system bandwidth is defined as $\Delta f_{eq} = \sqrt{\frac{1}{K} \Delta f_i \, \Delta f_s \, k_g}$ and is the geometric mean of the IF and servo bandwidths as modified by K_g and K. Solving the loss rate equation for P_i to determine a minimum receivable power $\left(P_{r\,min}\right)$ at a given loss rate

$$P_{r_{min}} = P_i = W_o \Delta f_{eq} \sqrt{\ln \frac{K^1}{t_o L}} \tag{8-41}$$

$$= W_o \Delta f_{eq} X_T$$

K^1 is a proportionality constant
X_T is the quantity under the square root

Substituting the equation for minimum receivable power into the radar range equation obtains

$$R = \frac{1}{2\sqrt{\pi}} \sqrt[4]{\frac{P_t G^2 \lambda \; 2\sigma}{4\pi w_o \Delta f_{eq} X_T L_P}} \tag{8-42}$$

where

σ = target dimensions
λ = wavelength
G = antenna gain
P_t = transmitted power, peak
L_p = system losses
X_T = tracking loss $\sqrt{\ln \frac{K^1}{t_o L}}$
Δf_{eq} = equivalent system bandwidth
w_o = noise density in IF (including receiver noise figure)

From this equation, range can be derived in terms of probability of loss.

Methods for calculating the maximum range of an automatic tracking radar have been shown in Chapter 7 along with optimum values for performance parameters. Maximum range is attained with an IF bandwidth narrower than indicated by the usual bandwidth equation

$$\Delta f_{B\omega} = \frac{1}{P_{\mu_s}} \tag{8-43}$$

where P_{μ_s} is the pulselength in microseconds. Maximum range is attained with a long servo time constant and very long pulselength.

SECTION 5 — EVALUATION OF TRACKING RADAR

Four sources of error are considered in the evaluation of automatic angle tracking radar and these sources are presumed to add randomly to produce a total angular perturbation of the tracking antenna line-of-sight. These include thermal noise of the receiver input stage, servo jitter, input signal amplitude variation, and beam-pointing error (scintillation error). The reflected power is proportional to the surface area and the directivity and orientation of this surface in the direction of the radar antenna. The target orientation may be considered to be a random variable so that the returned signal is also a random variable.

The problem of tracking a moving target is complicated in airborne radar by the requirement for tracking from a rolling and pitching aircraft. Interceptor motion may have a far greater effect on the antenna line-of-sight than the motion of the target being tracked. This requires that the servo loop for stabilizing the antenna against aircraft motion be considerably wider than that used for automatic tracking.

Since the position of the antenna line-of-sight is used for reference of the automatic tracking, any error resulting from incomplete elimination of pitch and roll causes jitter of the radar antenna. This error should be reduced to a value of the same order of magnitude as the automatic tracking process without antenna stabilization.

The means for determining the servo bandwidth required when the antenna stabilization loop is subjected in roll to a step function order will be shown. The frequency and amplitude of the roll of the aircraft, while under automatic control, are considered, and the gain of the stabilization loop required to reduce the antenna motion to this figure is determined. For the case of an interceptor rolling at 1 radian in 0.4 cps and the desired antenna stabilization error equal to 1 milliradian, the required gain is $\frac{1 \text{ radian}}{1 \text{ milliradian}}$ or $\frac{1000}{1}$ which is 60 db. If this loop gain is reduced at 6 db per octave, a servo bandwidth of 100 cps is required.

The equation describing a typical tracking and stabilization loop is given by:

$$\dot{\theta}_d = \frac{\dfrac{\omega_S}{S\left(1 + \dfrac{\omega_S}{S}\right)} \cdot \dfrac{\omega_C}{S} \quad \dfrac{S + \omega_2}{S + \omega_1}}{1 + \dfrac{\omega_S}{S\left(1 + \dfrac{\omega_S}{S}\right)} \quad \dfrac{\omega_C}{S} \quad \dfrac{S + \omega_2}{S + \omega_1}} \dot{\theta} \tag{8-44}$$

$$+ \frac{\dfrac{1}{1 + \dfrac{\omega_S}{S}}}{1 + \dfrac{\omega_S}{S\left(1 + \dfrac{\omega_S}{S}\right)} \quad \dfrac{\omega_C}{S} \quad \dfrac{S + \omega_2}{S + \omega_1}} \dot{\phi}$$

where

$\dot{\theta}_d$ = the radar antenna angular space rate

$\dot{\theta}$ = the angular rate of change of the line-of-sight in the vertical plane

ϕ = the aircraft bank-angle rate

Aircraft roll rate response to a bank-angle order can be described by the greatly simplified expression

$$\dot{\phi}_{out} = \frac{AS}{S^2 + BS + C} \dot{\phi}_{IN} \tag{8-45}$$

A,B and C are constants determined by the specific aircraft.

By assuming a fixed target position as compared to the antenna motion, the $\dot{\theta}$ coefficient of Equation 8-44 can be neglected and the remainder of the equation reduced to

$$\dot{\theta}_d = \frac{S^2\left(S + \omega_1\right)\dot{\phi}}{S^3 + S^2\left(\omega_1 + \omega_S\right) + S\omega_S\left(\omega_1 + \omega_C\right) + \omega_2\omega_C\omega_S} \qquad (8\text{-}46)$$

Substituting $\dot{\phi}$ from the aircraft transfer function into Equation 8-46 gives

$$\dot{\theta}_d = \frac{S^2\left(S + \omega_1\right) AS}{\left[S^3 + S^2\left(\omega_1 + \omega_S\right) + S\omega_2\left(\omega_1 + \omega_C\right) + \omega_2\omega_C\omega_S\right]\left(S^2 + BS + C\right)} \qquad (8\text{-}47)$$

Integration of Equation 8-47 provides the error angle in the radar antenna as a result of the aircraft roll. A plot of the error angle in milliradians for various stabilizing loop cutoff frequencies is shown in Figure 8-18.

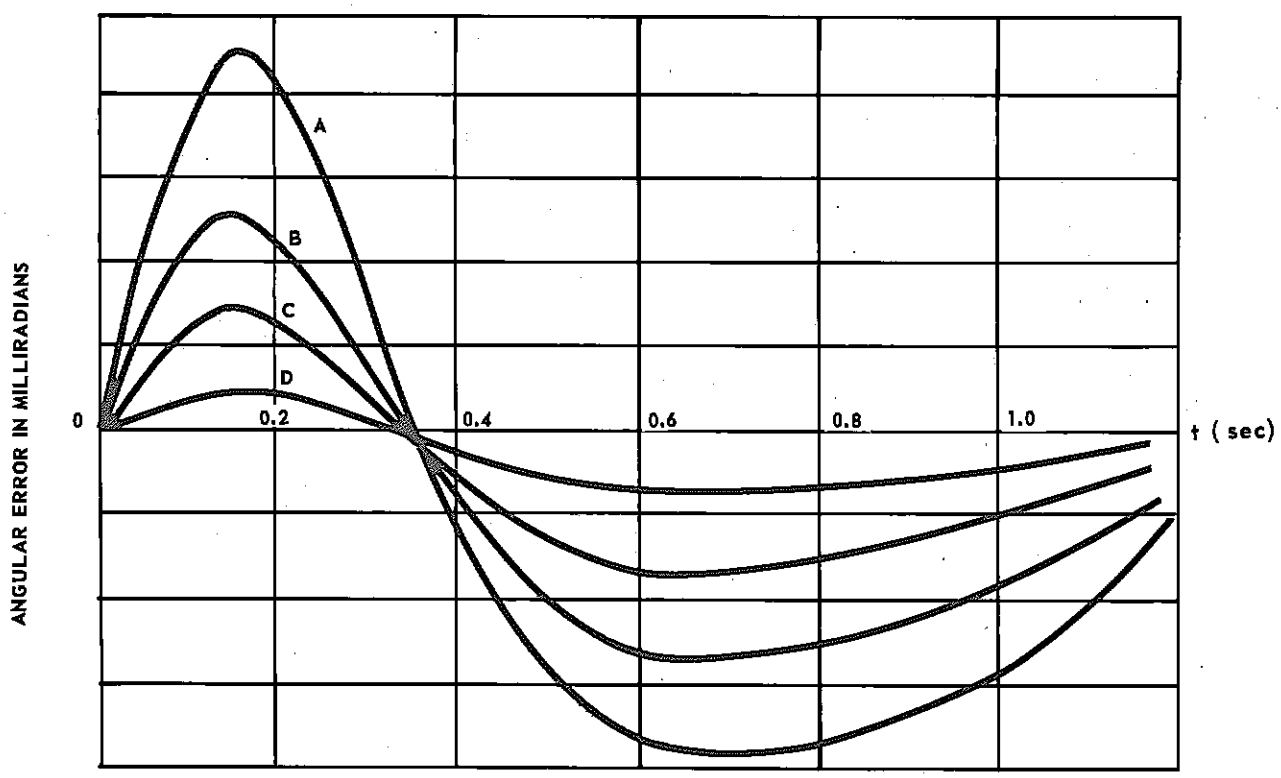

FIGURE 8-18. ANGULAR ERROR DUE TO ROLL TRANSIENT AS A FUNCTION OF STABILIZATION BANDWIDTH

A simplified, automatic tracking servo loop and a radar antenna stabilization servo loop are shown in Figures 8-19 and 8-26, respectively. A rate gyro is used in the stabilization feedback loop to provide rate information with fewer low frequency, unfilterable components of platform noise than the angle-detector output. The rate gyro is also excellent from considerations of backlash in gears, elastic coefficients and static friction.

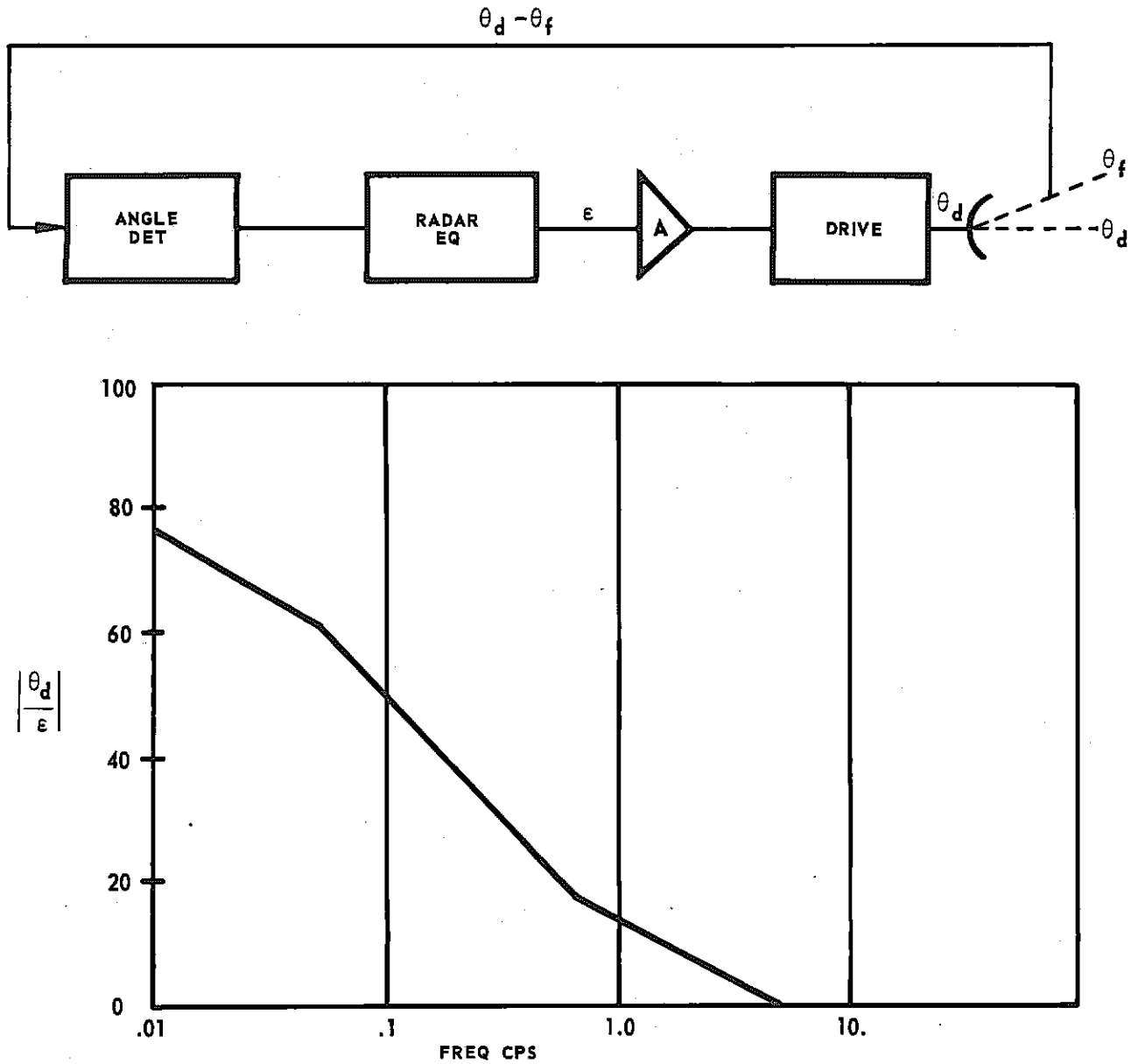

FIGURE 8-19. OPEN LOOP GAIN OF 3 CYCLE RADAR AUTOMATIC TRACKING LOOP SERVO

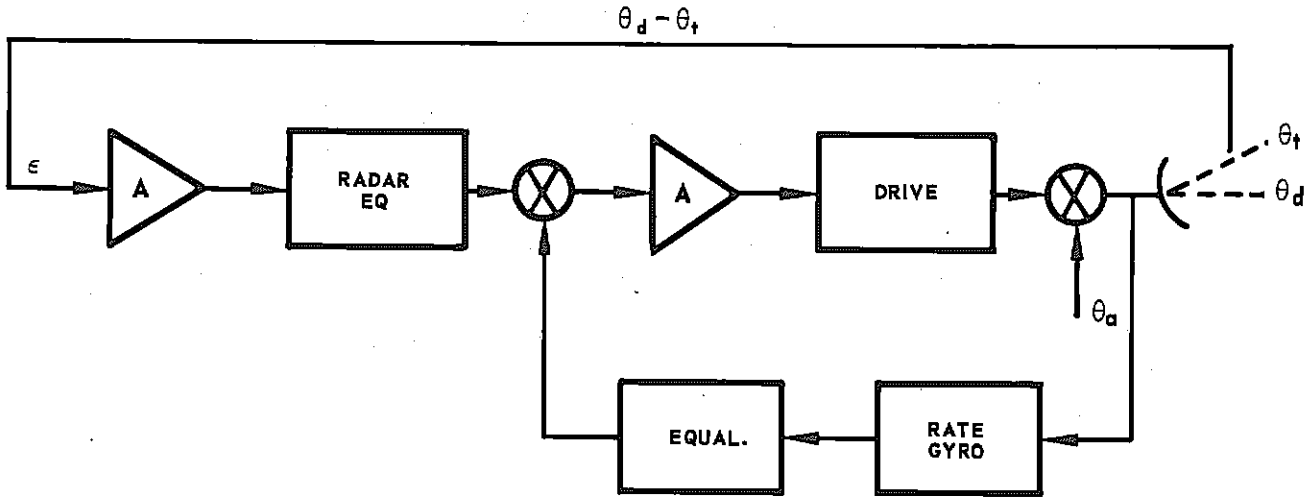

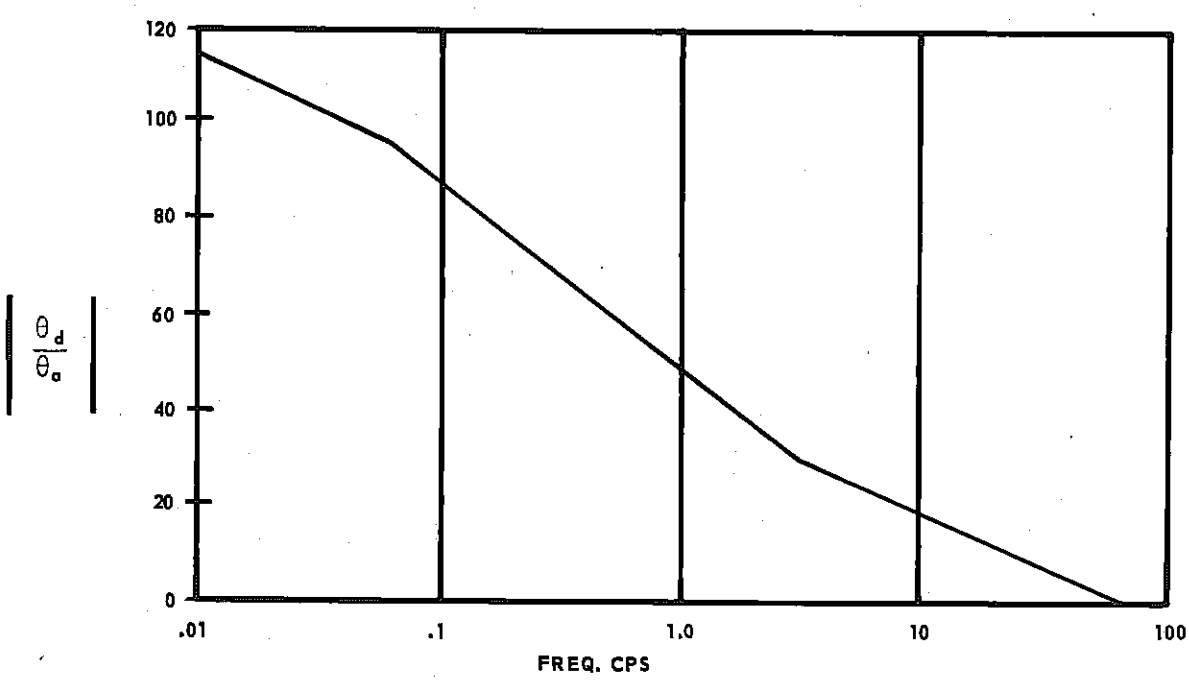

FIGURE 8-20. OPEN LOOP GAIN OF STABILIZATION LOOP WITH THREE-CYCLE TRACKING LOOP CLOSED

SECTION 6 — EFFECT OF NOISE ON DETECTION

Range of detection, as given by the range equation, does not accurately predict range because it does not account for the effect of noise. Noise in the receiver combines with the signal, changing in a random manner so that the basic problem in radar detection is that of discerning a signal in noise. Detecting a signal is based on probability considerations and also on the number of available signal pulses. The number of signal pulses available depends mainly on the pulse repetition frequency, the speed of the interceptor, speed of the target, target size, and the radar mode of operation (whether wide or narrow scan). The range of detection, designated R_o, frequently is considered in terms of a "standard" signal-to-noise ratio equal to one. Many of the predictable parameters, including losses, are contained in the range equation. The radar range is inversely proportional to the fourth root of the signal-to-noise ratio existing at range R, as

$$\frac{R}{Ro} = \left[\frac{\left(\frac{S}{N}\right)_o}{\left(\frac{S}{N}\right)}\right]^{\frac{1}{4}} \tag{8-48}$$

Since by definition the signal-to-noise ratio $\left(\frac{S}{N}\right)_o$ is one, then

$$\frac{R}{Ro} = \frac{1}{\left(\frac{S}{N}\right)^{1/4}} \tag{8-49}$$

Since signal and receiver noise are added randomly in the radar receiver (because of the random nature of noise), the signal can sometimes be detected in the noise, or noise may cause the radar operator to misinterpret a noise signal, or the condition may exist where noise shrouds any signal which may actually exist. The likelihood of interpreting noise as a signal is defined by the "false alarm probability." The false alarm probability may be interpreted as the reciprocal of the number of decisions to be made by the radar operator or $P_F = \frac{1}{N_D}$, where P_F is the false alarm probability and N_D is the number of decisions to be made.

The term N_D can be determined from the geometry of the radar scope. Assume the radar scope to be divided into decision intervals in range increments approximately the time length of the transmitted pulse translated into range units. The azimuth decision intervals are based on the total swept area divided by the antenna beamwidth. To illustrate, assume the following radar parameters:

R_D = range scale 30 miles

ω_B = antenna beamwidth 3.5 degrees

S_R = antenna scan rate 1 scan per second

ω_{ant} = antenna scan width 120 degrees

τ = pulse length 1 microsecond

R_P = range corresponding to pulse length in miles

Range decision increments $R_D = \frac{R_D}{R_p} = \frac{30}{.1} = 300$

Azimuth decision intervals $\frac{\omega_{ant}}{\omega_B}$ sec $= \frac{120°}{3.5}$ sec $= 34.3$

Thus the total decision increment is (34. +) x 300, or 10,200, corresponding to P_F of approximately 10^{-4} decisions per second or a false alarm rate of one per second. Typical values of decision intervals vary from 5000 to 20,000. False alarm probability for a false alarm rate of one false alarm per hour for the example shown would be $\frac{10^{-4}}{3600}$ or 2.78×10^{-6}.

The available noise power is

$$P_n = \frac{\overline{e^2}}{4R} = KT\Delta f \qquad (8\text{-}50)$$

This is designated as the ideal noise power; however, the noise in a system is always larger due to various contributions of various parts of the receiver, antenna, atmospherics, etc. The noise figure ($\overline{NF}$) is the factor by which the actual noise power differs from the ideal noise power.

At room temperature (approximately 300°K) and system bandwidth of 2 megacycles the noise power is

$$P = 1.37 \times 10^{-23} (300)\ 2 \times 10^{6} = .82 \times 10^{-14} \text{ watt}$$

For the system with a noise figure of 10 db, (a ratio of 10) the actual noise power would be $10 \times .82 \times 10^{-14} = .82 \times 10^{-13}$ watt.

Typical false alarm probabilities vary from 10^{-6} to 10^{-9}. When the radar range is set to sweep a smaller volume of space, as during a sector scan, a smaller number of decision intervals is included and, therefore, the false alarm probability number is increased, as is the detection probability.

In considering the false alarm probability, a fixed reference or bias sets the limit which signal or noise must exceed in order to be considered a false alarm. The signal, which is compared to the bias or reference level, results from an integration process either performed in the receiver IF stages and called IF integration, or detected first, then integrated, and finally compared to the bias. If the false alarm probability is increased, the signal-to-noise ratio must be increased to maintain a constant probability of detection.

Minimum detectable signal in a radar receiver is limited by several noise factors, the major ones being noise in circuit elements of input circuits, shot effect in the first tube, and man-made noise. Clutter caused by sea return, rain, clouds, and land masses also tends to reduce the minimum detectable signal.

Noise voltage across a resistor is given by

$$\overline{e^2} = 4\,KTR\Delta f$$

where

$\overline{e^2}$ = mean squared noise voltage
k = Boltzmann's constant = 1.38×10^{-23} joules/degree
Δf = frequency interval under consideration
R = input resistance
T = temperature, degrees Kelvin

In calculating the maximum range of a radar set from the range equation, the practice has been to assume that the minimum detectable signal, (8-51)

$$P_{min} = kT \quad f\overline{NF} \qquad (8\text{-}51)$$

where $\overline{NF}$ is the noise figure

Marcum* explains that errors of ± 30 percent are common in the agreement of the range equation with experimental values. He also indicates that the equation does not even account for the effects of integration of pulses, which are vitally important in target detection.

The range of a radar set is a statistical variable and must be given in terms of probabilities rather than in exact terms such as the range equation.

Because of the statistical nature of noise, there are bound to be periods of large signal-to-noise values, and on a radar screen without high resolution the so-called blip ordinarily cannot be distinguished from noise, at least not during the instant the blip first becomes apparent. The average interval at which noise is mistaken for signal blip is termed the false-alarm time and it will be seen that probability of detection is related to the false-alarm time.

$$\text{Set } \frac{R}{R_o} = \left[\frac{K\ T\ \overline{NF}}{E_R}\right]^{\frac{1}{4}} \qquad (8\text{-}52)$$

---

* Marcum, J.J.: A Statistical Theory of Target Detection by Pulsed Radar RM-754 Rand Corp., Dec. 1957

Where E_R is the received energy per pulse at the range R under consideration

$$\frac{R}{R_o} = \left[\frac{1}{\frac{E_R}{KT\ NF}}\right]^{\frac{1}{4}} = \frac{1}{x^{\frac{1}{4}}} \qquad (8\text{-}53)$$

where the quantity in the denominator of Equation 8-53 is the signal pulse energy in units of the average received noise pulse energy. Illustrating the above equation, suppose that E_R, the signal power, is four times the average noise power, then $x = 4, \frac{R}{R_o} = \frac{1}{4^{\frac{1}{4}}}$ or $\frac{R}{R_o} = .7$. Associated with this signal-to-noise level is a certain probability of detection. Curves will be provided showing the probability of detection P_D for values of $\frac{R}{R_o}$ related to the signal-plus-noise to noise ratio by the given equation assuming some value of false-alarm time.

Pulse integration is defined as the process of summing a common group of signal pulses and using the summed group for detection purposes rather than attempting to detect the individual pulse. In the absence of radar-reflected signal, the same integrating circuitry will act to integrate the existent noise. The phenomenon which permits integration to gain an advantage comes from the random fluctuation of the noise pulses and, in fact, with the integrated pulses $\sqrt{N}$ times the fluctuations voltage of a single pulse. It is the signal-to-noise fluctuation or the deviation about a mean ratio, not the signal-to-noise, which permits integration of pulses to improve probability of detection. The greater the number of pulses integrated, the greater is the signal-to-fluctuation ratio and, hence, the improved probability of detection, but at the expense of longer detection times.

A signal is indicated when the receiver output exceeds a fixed bias level. This signal may originate from a signal plus noise, or from noise alone. The bias level is determined from consideration of the noise alone, that is, the bias is set so that noise exceeds the bias level a certain number of times in an interval. The higher the bias level is set, the

less frequently will noise exceed it. With a given bias level, the problem remains to determine the probability that any value of incoming signal plus noise will exceed this level.

Pulse integration was defined as the addition of pulses. With no additional circuitry, the radar is able to accomplish integration through the persistence of the radar cathode ray tube. Reports show an advantage to be gained by integration performed in the IF stages over integration in the video stages. For moving targets, the integration process becomes less suitable since the integrating techniques require that successive pulses be coherent.

Practical electronic pulse integrators take the form of narrow band audio filters having their center frequency at the pulse repetition frequency or harmonic of the PRF. The greater the number of pulses, the more closely the spectrum clusters about the harmonics of the repetition frequency, allowing the filter to be narrower, excluding more and more noise while retaining the signal energy.

The total number of independent chances for obtaining a false alarm in the false alarm interval T_{fa} is

$$n = \frac{n}{N} = \frac{T_{fa} f_r n}{N} \tag{8-54}$$

where

f_r = pulse repetition frequency
n = number of pulse intervals per sweep
N = number of pulses integrated

If the definition of false alarm is the 0.5 probability that noise will not exceed the bias level, then $(1 - P_n)^{n'} = 0.5$.

A limit is set on the number of pulses which can be integrated because the returned pulses fail to overlap when the target has moved through a distance,

$$d \approx T_p \frac{c}{2} \tag{8-55}$$

T_p = pulse length

c = velocity of light

The effective distance over which the pulses can be assumed to contribute their full amplitude is about one-half this value or

$$d \approx T_p \frac{c}{4} \tag{8-56}$$

If the rate of change of range is v, the time available for integration is

$$T_i = \frac{T_p C}{4v} \tag{8-57}$$

The maximum number of pulses which can be integrated in this time is

$$N_{max} = T_i f_r = \frac{T_p f_r c}{4V} \tag{8-58}$$

The term for radar losses in the range equation can be computed by tabulation of the numerous physical losses in the radar system. Waveguide and duplexer account for approximately a 1 - 2 db loss in transmitted power and in received signal. The radome loss for the case of a well-engineered unit will be from about 1/2 to 1 db. An attempt is made to account for differences between theoretical and practical results by assigning a loss factor due to the radar operator of about 2 - 4 db. Another loss, caused by the fact that not all received pulses between the antenna half-power points are of the same strength, can account for about 1.5 db. The collapsing loss, which is a loss caused by the inclusion of noise sample along with signal plus noise, is defined by

$$L_c = \frac{\left(S_o + N_o\right) + N_1}{\left(S_o + N_o\right)} \tag{8-59}$$

where $\left(S_o + N_o\right)$ is the number of signal plus noise samples and N_1 is the number of additional noise samples.

An IF bandwidth loss is associated with receiver IF bandwidth, which is greater than an optimum, given by

$$N = \frac{\beta \tau}{1.2} \tag{8-60}$$

where β is the IF bandwidth in megacycles per second and τ is the pulse length in microseconds.

The probability of detecting a radar target during the time of a single sweep or scan of the antenna gives rise to what is termed "single-look" probability, blip-scan ratio, or simply a probability of detection curve. This curve, shown in Figure 8-21, indicates the probability of detection

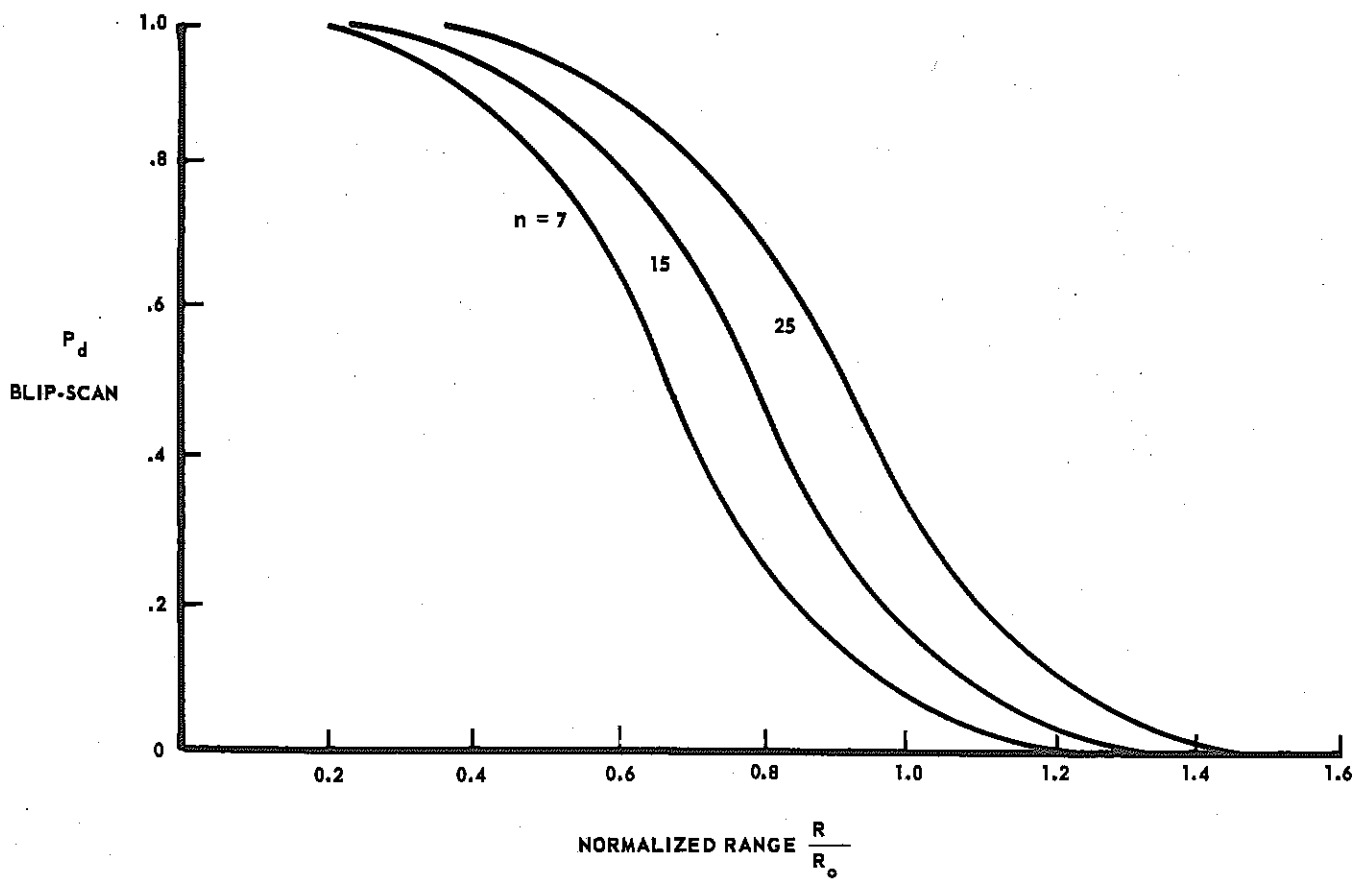

FIGURE 8-21. PROBABILITY OF DETECTION CURVES

of a radar target as a function of normalized range, $\frac{R}{R_o}$. The relationship of the quantities R, R_o, and $\frac{S}{N}$ is $\frac{R}{R_o} = \frac{1}{\left(\frac{S}{N}\right)}$

Several curves are drawn showing generally the number of pulses integrated.

More frequently, the curves showing cumulative probability are provided, (see Figure 8-22) since these curves show the more practical case of detection of targets by the time the ranges have decreased to specific values. The cumulative probability is affected by the radar operator factor and by the target closing rate. A family of curves of cumulative probability of detection is given for various closing rates. The term $\frac{\Delta R}{R_o}$ is the ratio of the change during one sweep of the radar antenna to the range for R_o, the range at unity signal-to-noise ratio. The curves are computed from Figure 8-21, the single-look detection probability, for 25 pulses integrated, and for an operator factor assumed to be 0.5.

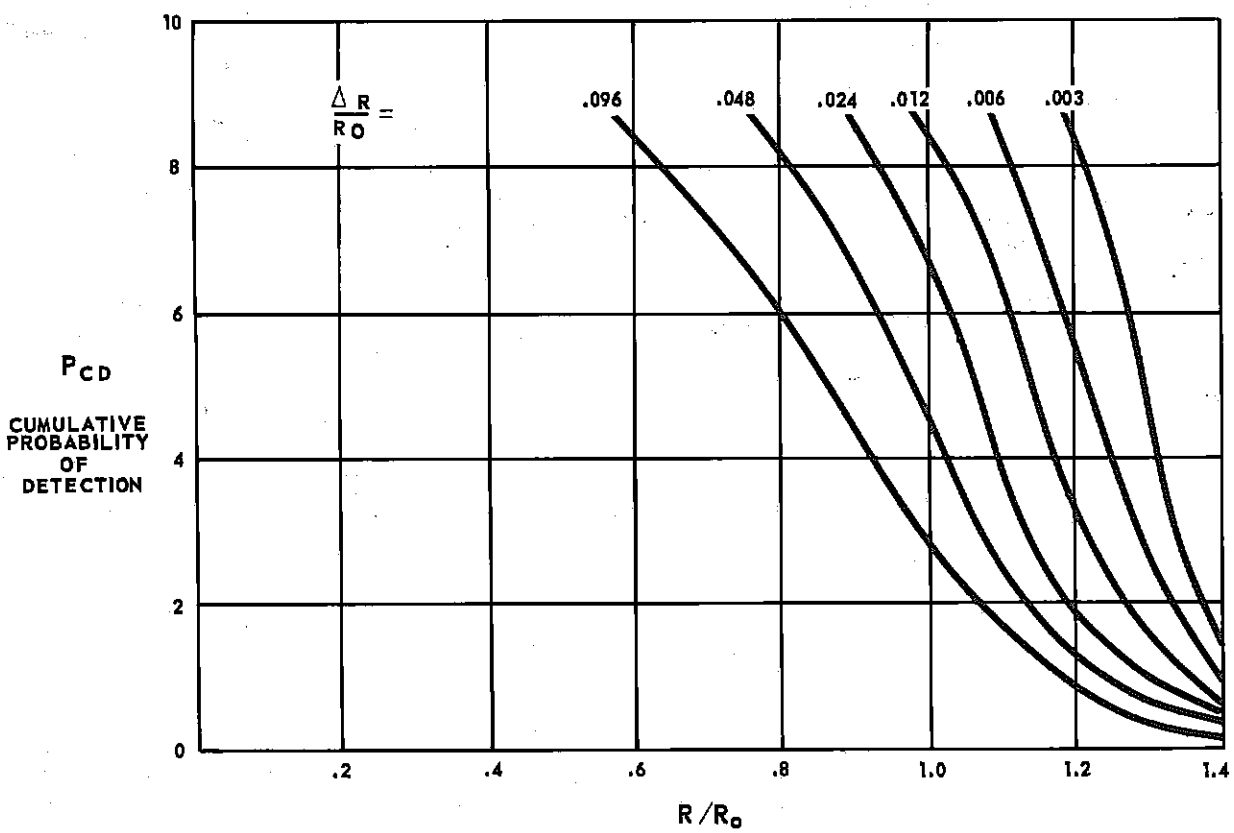

FIGURE 8-22. CUMULATIVE PROBABILITY OF DETECTION

Figure 8-23 permits evaluation of the $\left(\frac{R}{R_o}\right)_2$ term when the change in range between scans is known or can be estimated.

The effect on cumulative probability of changing n, the number of pulses integrated, can be determined by use of Figure 8-24.

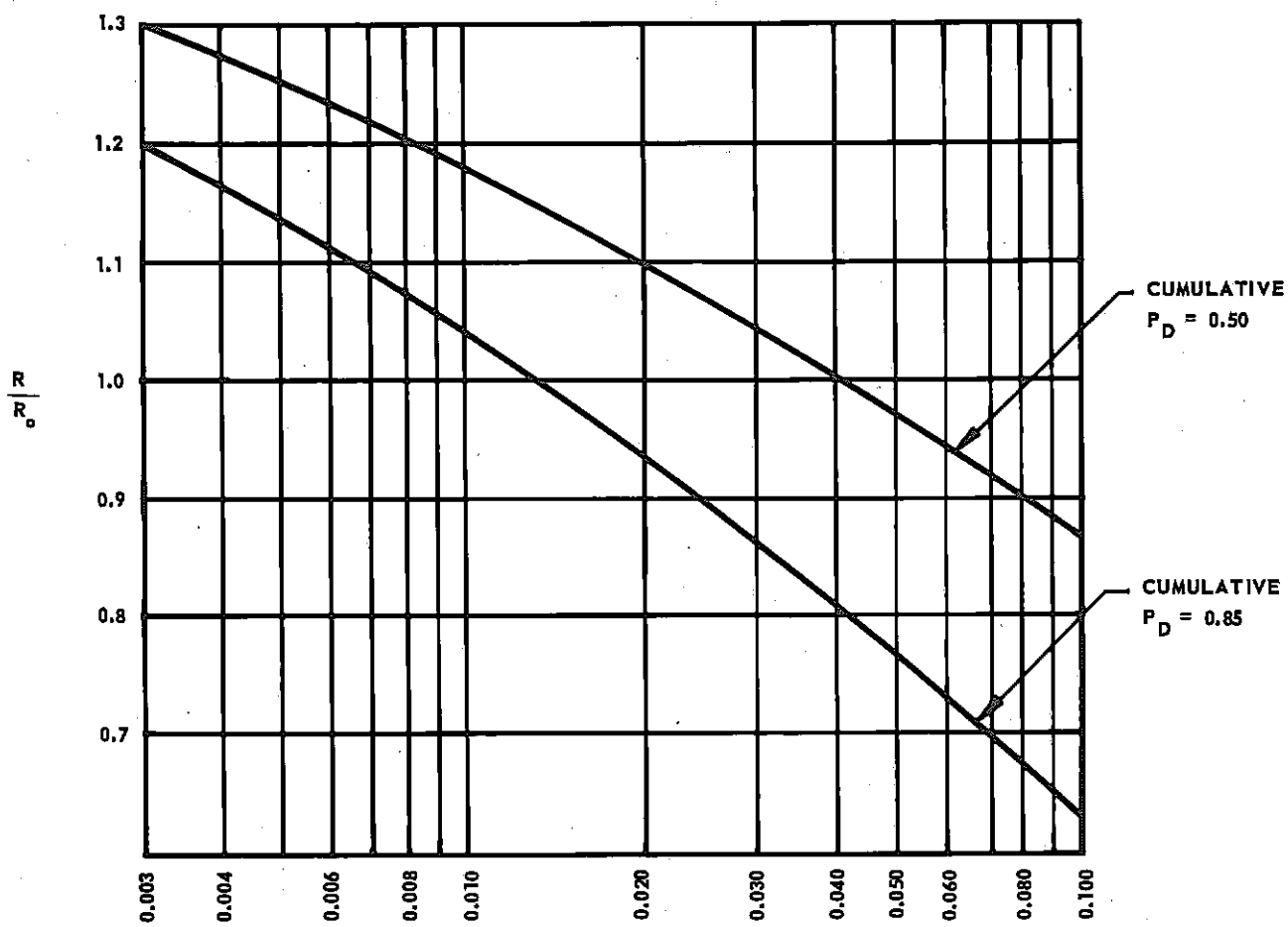

FIGURE 8-23. NORMALIZED CHANGE IN RANGE BETWEEN SCANS, $\frac{\Delta R}{RO}$

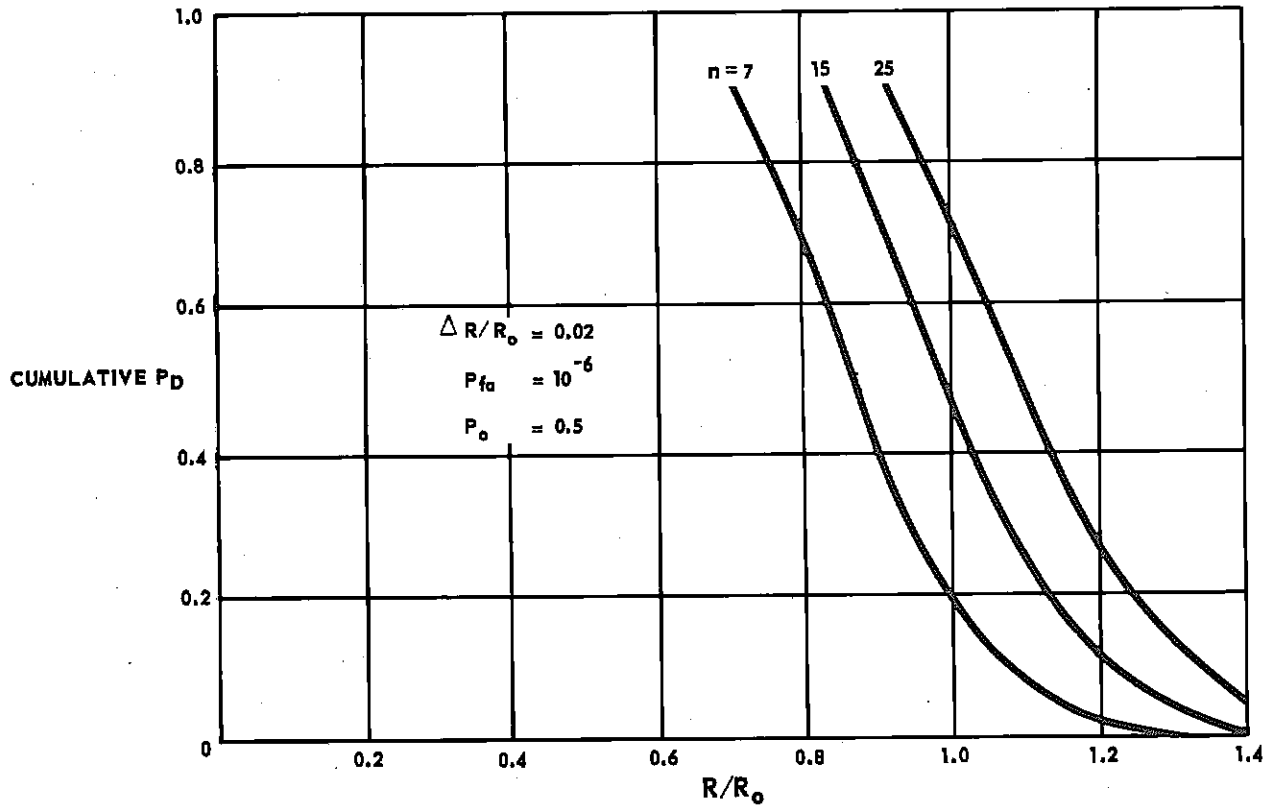

FIGURE 8-24. EFFECT OF PULSES INTEGRATED ON CUMULATIVE PROBABILITY OF DETECTION

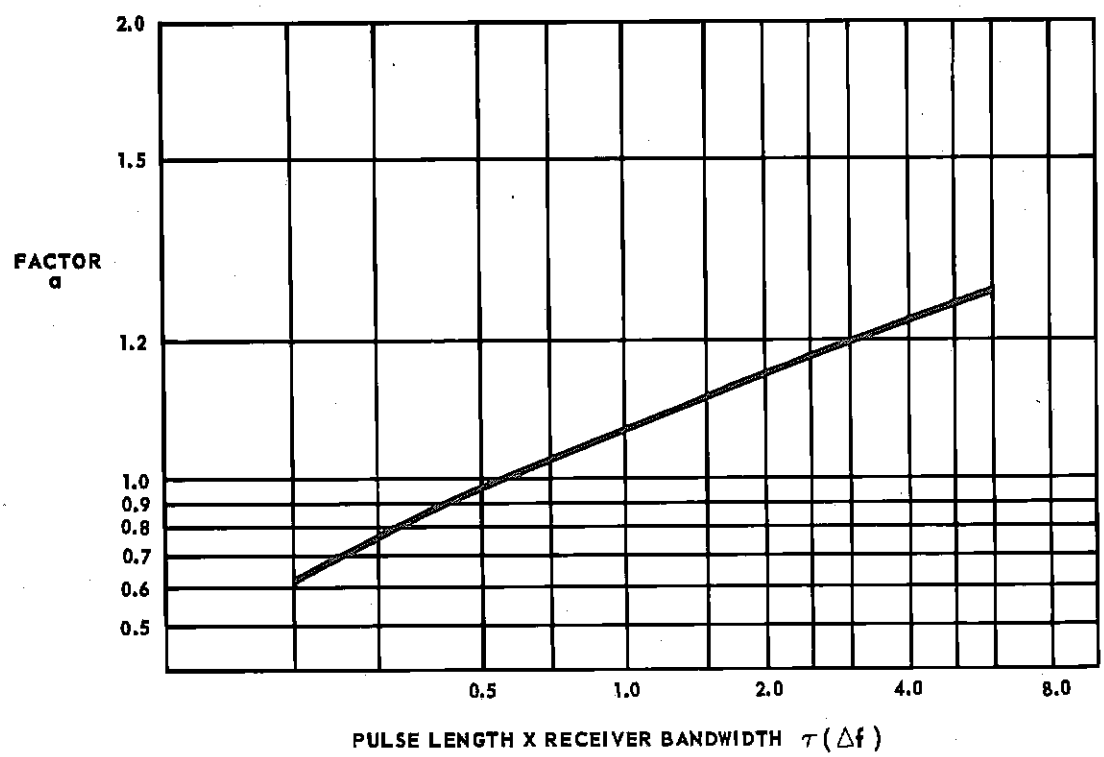

FIGURE 8-25. CORRECTION FACTOR CHART

Zeoli* describes a method for deriving the cumulative probability from experimental flight test data and then using these data to scale to some new radar condition. The scaling technique is applied to some specific cumulative detection probability, say 50 percent, as follows:

$R_{50}(2)$ represents the new range, $R_{50}(1)$ the old range. The term $\dfrac{\left(\frac{R}{R_o}\right)_2}{\left(\frac{R}{R_o}\right)_1}$ is obtained from the $\dfrac{\left(\frac{\Delta R}{R_o}\right)_2}{\left(\frac{\Delta R}{R_o}\right)_1}$ factor from Figure 8-23.

$$R_{50}(2) = \frac{R_o(2)}{R_o(1)} \; \frac{\left(\frac{R}{R_o}\right)_2}{\left(\frac{R}{R_o}\right)_1}_{50} \times \left(\frac{n_2}{n_1}\right)^{0.175} \times \frac{a_2}{a_1} \times R_{50}(1) \qquad (8\text{-}61)$$

The a_2 and a_1 terms appearing in the scaling equation account for changes in pulse length - IF bandwidth product. This factor can be obtained from Figure 8-25.

The advantage of the scaling techniques stems from the fact that the ratio cancels out systematic and bias errors, eliminating those errors which are invariant from the old flight tests to the new situation.

---

* Zeoli G.W. The Prediction of AI Radar Detection Range from Flight Test Data TM No. 379 Hughes Aircraft Co., 15 April 1954.

SECTION 7 — EVALUATION BY GROUND TESTING

(a) RADAR SELF-TEST EVALUATION -- GENERAL

Practical analysis of radar system effectiveness invariably demonstrates the severe degradation of the equipment under field conditions. Many schemes and techniques have been devised to simplify radar evaluation and to improve the determination of radar accuracies. An attempt will be made in this section to describe some of the practical evaluation methods.

Radar system evaluation techniques generally fall in a broad category of equipment self-tests or tests performed with external test sets. Self-testing of the radar system is provided as a part of the radar equipment and usually represents a qualitative go, no-go measurement, while the external testing techniques may represent either a quantitative or qualitative measurement. The test mode selected will generally depend on the time available for testing.

Radar self-tests permit accelerated testing of the equipment but accomplish this at the expense of a general increase in system complexity. Self-testing schemes vary according to the ingenuity of the designer, but those methods which utilize the same circuitry in the same manner as the original circuitry may be rated most successful if a quantitative evaluation results. Such success appears unlikely of attainment, nevertheless, such a goal represents an optimum condition.

A practical evaluation program can be approached through extensive flight evaluation against realistic targets under simulated combat conditions. As a result of such testing, information can be obtained for use in refining fire control system parameters as required. Practical evaluation programs can reproduce the idealized conditions only to a small degree. Difficulties which are not directly concerned with the objectives are encountered during flight tests and make the evaluation very difficult. Subjecting a new radar to the severities of field conditions invariably results in a rash of component failures. After this phase of the checkout, the equipment has to be 'debugged' on the basis of incompatabilities in the various subsystems, such as between the radar and computer, missile auxiliaries, cockpit controls, power supply, and any other subsystem interconnections which make up the particular fire control system. When system compatability has been obtained, the radar set can be evaluated in terms of the complete fire control system.

Assuming that system reliability is sufficiently high to permit flight tests to be completed without equipment failures, the design goals can be evaluated under flight conditions. The mean time between failures is short in a modern fire control system because of the great complexity of the systems. An intolerable condition arises when the fire control system cannot be evaluated during the allowable flight time because of one or more failures occuring during the flight. A great amount of effort is expended to attain the required mean time between failures of the fire control system. Design engineers constantly strive to develop systems and circuitry which do not operate marginally, and which, if failure should occur, will not cause abortion of the mission.

Built-in self-tests can determine, if suitably designed, the functioning of individual units and subsystems and also may provide correlation of the system test to probability of successful weapon launch and kill.

The evaluation of a radar set by means of self-tests is performed to varying degrees in most modern fire control radars. A typical set uses normal operating performance as well as special self-tests to determine if the set is within minimum performance standards.

Various degrees of inspection are provided at suitable periods coincidental with the aircraft operational schedules, such as during preflights, postflight, and during shutdown for engine inspections.

Tests made during the evaluation are conducted with certain units of the fire control system. Units used in one of the E series fire control systems for testing are the (1) flight monitor, (2) preflight monitor control, (3) computer test set, and (4) test multimeter.

The flight monitor, located in the cockpit, is a test unit that can be used to determine the operational suitability of the fire control system. Some of the tests provide known scope patterns while others simply operate lights on the flight monitor. From the results of the tests it can be decided whether the fire control system can be used successfully for attack with the provided weapons. The tests are performed in steps with a rotary switch in the flight monitor unit as known indications are observed in each switch position.

The preflight monitor is another test unit which permits performance of more detailed fire control system checks. These tests are more quantitative than those performed with the flight monitor. The results of

the preflight monitor are presented on the radar scope, the test lights on the preflight monitor, or by indications on the airborne test multimeter. The results of the tests, in addition to presenting quantitative results for determining flight suitability, permit the operator in many cases to isolate any malfunction to a suspected faulty unit.

The computer test set is an item of airborne test equipment used to perform tests on the ballistics computer. From the tests it can be determined whether the ballistic computer is working properly and, if not, any of the required adjustments can be made.

(b) ANALOG AND DIGITAL COMPUTERS IN SYSTEM TEST AND EVALUATION

(1) Use Of Computers For Radar System Test And Evaluation

Experience has shown the effectiveness of computers in the test and evaluation of airborne fire control systems. The speed and dependability of such evaluation techniques provide a promising solution to the problem of evaluating such systems. The computer may be one existing in the aircraft as an integral part of the fire control system, or it may be part of a ground checkout system. The advantages and disadvantages of the relative techniques will become apparent as details of the respective systems are described. The computers may be either analog or digital.

(2) Analog Techniques Of Computations

Many radars utilize analog methods to compute the various radar functions required in the search and track modes of operation. The particular equations to be solved by analog methods depend on the geometry of the attack. The computer performs the computations necessary to enable the pilot to fly collision or pursuit courses while using the radar scope as the readout device. The computer is supplied with information from the radar and air data subsystems for computing the appropriate flight path for target interception.

The computer calculates the steering error and displays this error to the pilot by means of a suitable radar scope presentation. The steering presentation is positioned by an amount and direction proportional to the steering error. Either the pilot or automatic flight control systems

may be used to null out the error by properly centering the indicator error signal. The three dimensional steering equations may be illustrated by use of the simpler two dimensional case as follows:

The geometry of the lead collision attack is shown in Figure 8-26. The equations derived from the geometry of Figure 8-26 are as follows:

$$(V_I T + F) \cos \theta = R + V_B T \cos \alpha \qquad (8\text{-}62)$$

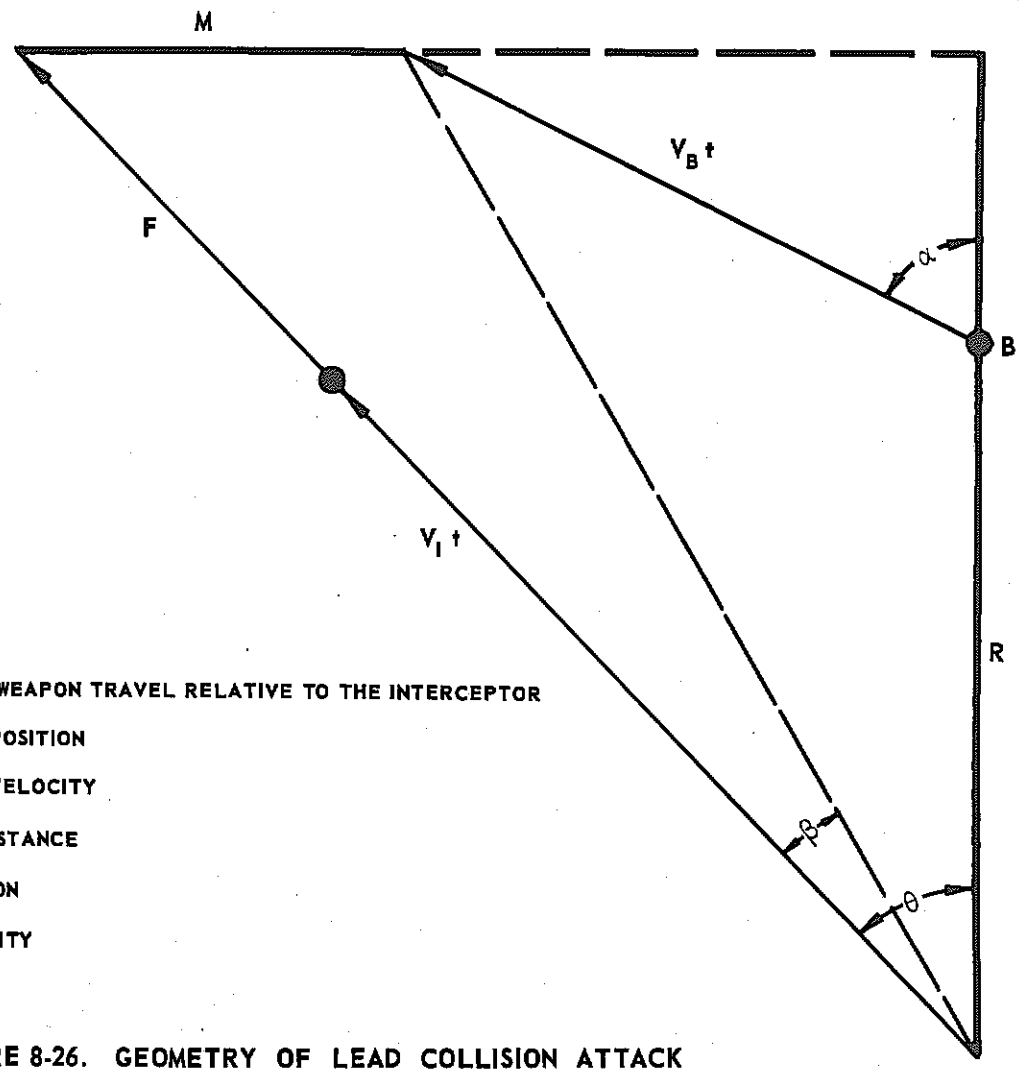

WHERE

R = RANGE

F = THE RANGE OF WEAPON TRAVEL RELATIVE TO THE INTERCEPTOR

I = INTERCEPTOR POSITION

V_I = INTERCEPTOR VELOCITY

M = WEAPON MISS DISTANCE

B = BOMBER POSITION

V_B = BOMBER VELOCITY

t = TIME

FIGURE 8-26. GEOMETRY OF LEAD COLLISION ATTACK

solving for T

$$T = \frac{R - F\cos\theta}{V_I\cos\theta - V_B\cos\alpha} \tag{8-63}$$

from Figure 8-26

$$(V_I T + F)\sin\theta = M + V_B t\sin\alpha \tag{8-64}$$

and

$$M = (V_I\sin\theta - V_B\sin\alpha)T + F\sin\theta \tag{8-65}$$

The bomber range rate may be obtained from inspection of Figure 8-26

$$\dot{R} = V_B\cos\alpha - V_I\cos\theta \tag{8-66}$$

The line-of-sight rate of rotation

$$\omega_C = V_I\frac{\sin\theta - V_b\sin\alpha}{R} \tag{8-67}$$

Solving for $\dot{R}$ by equations 8-63 and 8-66

$$\dot{R} = \frac{F}{T}\cos\theta - \frac{R}{T} \tag{8-68}$$

Solving for $\frac{M}{T}$ from equations 8-67 and 8-65

$$\frac{M}{T} = R\omega_D + \frac{F}{T}\sin\theta \text{ or} \tag{8-69}$$

$$\frac{M}{T} = R\omega_D - R\omega_C \tag{8-70}$$

Reducing the miss term $\frac{M}{T}$ to zero gives

$$R\omega_D = \frac{F}{-T} \sin\theta \tag{8-71}$$

Analog representation of Equation 8-69 is presented in Figure 8-27.

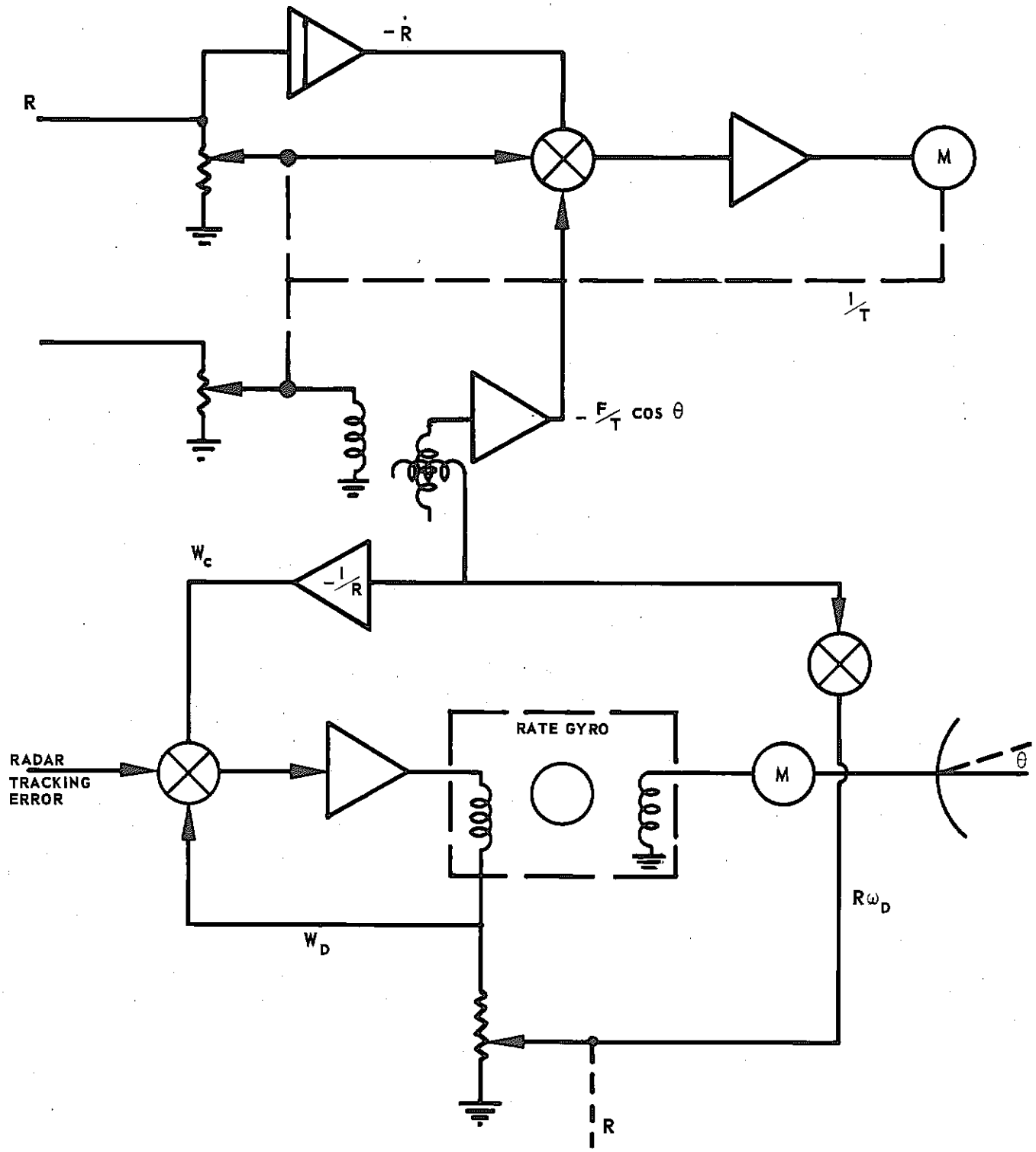

FIGURE 8-27. SCHEMATIC REPRESENTATION OF EQUATION 8-69

(3) Ground Test Evaluation Of Fire Control System By Digital Computers

Weapon system testing time expends a significant portion of the total expected meantime between failures. The requirement for rapid system evaluation is amenable to the technique of digital computer evaluation.

A ground test digital evaluation scheme has been proposed for use in airborne fire control system evaluation.* Such a scheme would be of most value in a complex system where time and manpower are inadequate to enable squadrons to be sufficiently combat-operational in the available time.

The general technique of digital computer evaluation presently is being used in such diversified fields as telephone and missile system checkout. The proposed interceptor fire control system evaluation technique, in many respects, is similar to the missile checkout procedure.

Many of the shortcomings of present day checkout systems may be attributed to the testing techniques. These approaches check only the overall system performance and do not check many key functions which are inconvenient to observe or excite. A more rigorous approach would be to design wiring and instrumentation as part of the weapon system to enable a comprehensive evaluation to be accomplished.

The objectives of the digital computer ground evaluation program are (1) to determine the combat readiness of the weapon system by static and dynamic testing of the individual systems, (2) isolate malfunction(s), and (3) detect gradual decay of the system.

Missile systems presently utilize provisions for detailed testing in order to detect defective and marginal systems. This thorough checkout is required since a malfunction can result in a complete missile loss.

---

* RACO (Rapid Automatic Checkout) Report No. ZM 570, 15 January 1959, Convair, A Division of General Dynamics Corp. - San Diego, California

Evaluation of a missile is continued to the instant of launch to incur the greatest probability of mission success. Present aircraft weapon systems still depend on a pilot's ability to perform a satisfactory mission even though the weapon system develops a malfunction. Considerable increases in complexity in interceptor systems seem to justify the application of automatic evaluation techniques to manned systems.

To implement ground computer evaluation techniques, it is necessary to provide instrumentation devices in the mechanical systems, and isolation circuitry for the electrical systems to afford access to data points. A suggested method for applying calibrated forcing functions to a mechanical device is by use of relays. Wiring from the instrumentation test points is brought to aircraft connector plugs and from there to the external digital evaluator system. The digital computer tests are programmed at a high speed so that the entire evaluation can be accomplished, according to the extent of the programmed text, in a short interval of time.

The aircraft system is prepared for use with the digital evaluator during the aircraft design phase. The test system can be viewed as a data processor for use in evaluation and maintenance if the aircraft weapon system (1) is equipped with the proper instrumentation, (2) has the proper checkout program for logical analysis of the weapon system, and (3) if the test capability test points and memory space are not exceeded.

In addition to the evaluation capability, the digital test system is able to predict impending failure through additional programming of the computer. Failure prediction is feasible if (1) the key parameters which are indicative of failure are monitored, (2) the measurements are related to stored data, and (3) marginal testing concepts are utilized deliberately to degenerate operating conditions.

An interceptor system has been analyzed to determine the ground system computer requirements. For each subsystem of the interceptor at least four objectives would have to be realized, as follows:

(1) Description of the system, objectives and methods of checkout, and instrumentation for obtaining the desired objectives.
(2) A block diagram of the system, showing instrumentation.
(3) Detailed listing of all normally replaceable aircraft modules covered by the checkout.
(4) A logic chart indicating the procedure required for the evaluation and fault finding techniques.

The logic chart contains required data of system operational capability as well as data for malfunction isolation. The logic chart is composed of blocks describing details required for logical analysis of the operational capability as well as fault isolation routines. The blocks may be utilized for (1) Information - conveying the necessary facts to establish logical analysis, (2) Data-to present information from other boxes to continue the flow of logical analysis, (3) Instruction - to program the logic path for the computer to follow, (4) Decision - for use in deciding a passable or reject (go, no-go) condition, (5) Conclusion - result of the logic path followed by the computer, and (6) Displayed Results - the presentation of the results of the other five links in the logic chain.

The logic flow is presented in block-chart form with a description of the operation and path to be followed. The flow chart follows from block to block until the satisfactory operation display is reached, or until a no-go condition is reached. The chart indicates the instruction or decision block required to isolate the malfunction.

Block diagram Figure 8-28 shows a possible arrangement for performance of the system evaluation functions.

Data access (see Figure 8-28) provides great numbers of channels which are the aircraft test-data outputs. The data access channels are selected by the switching matrix, which samples the measurement data. Actual measurement occurs after first converting analog voltage levels or frequency data to digital bits. Comparison circuitry provides the conversion function of analog to digital. The reference memory supplies the required data storage and access point. Magnetic drums are a favored storage device which can provide the required speed, flexibility and storage space, as well as excellent random access capability. The logic analysis and decision functions are performed with digital techniques. Operations are the typical computer arithmetic unit functions of addition, subtraction, multiplication, division, and transferring of data under control of the program contained in the memory. The readout may be accomplished by visual or printed tabulation of test results.

The digital computer lends itself readily to self evaluation by means of parity checking, redundancy, and by logical analyses.

To initiate operation of many aircraft functions requires some sort of forcing function. This feat can be accomplished by use of high speed

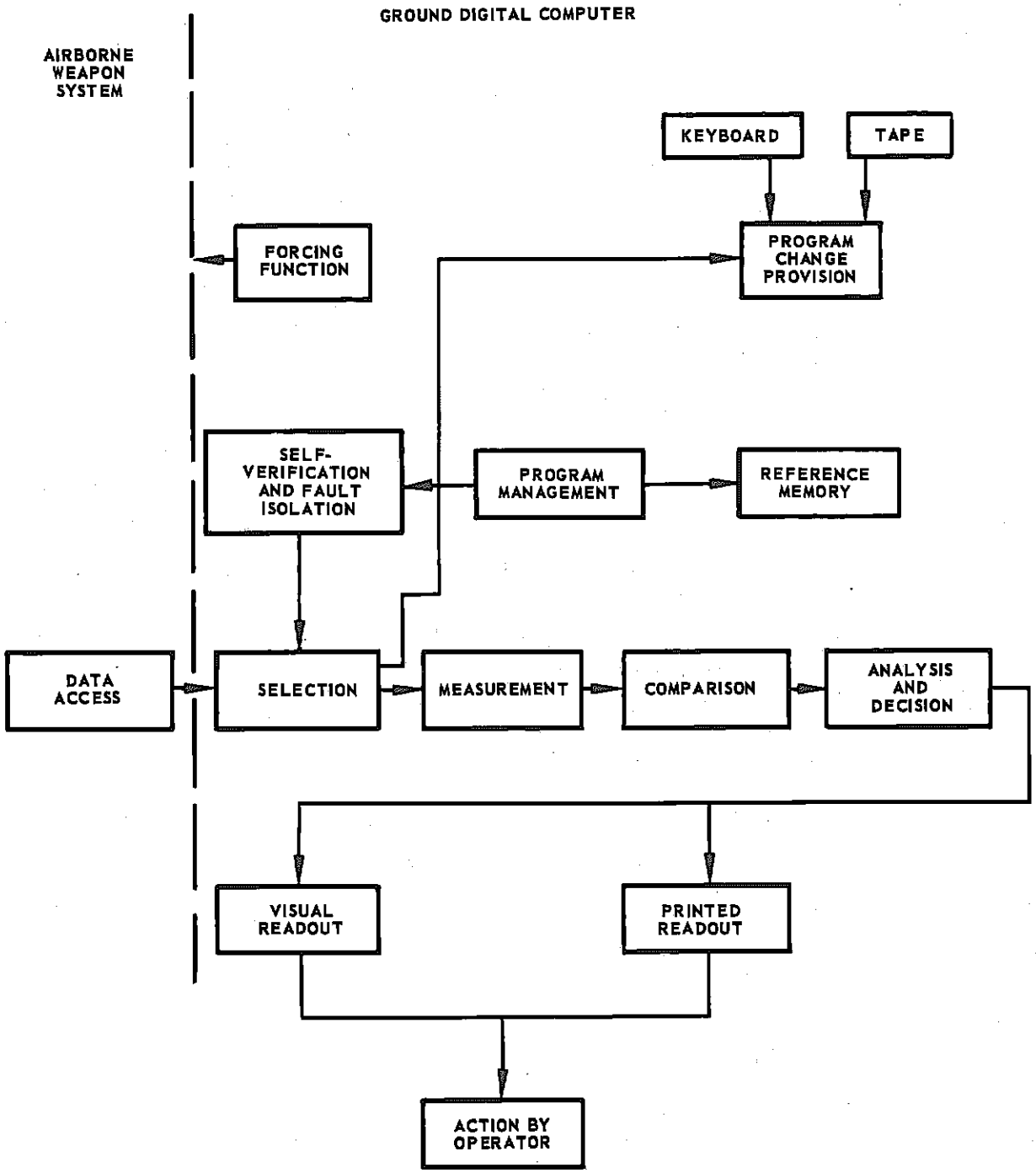

FIGURE 8-28. GROUND DIGITAL COMPUTER EVALUATION FUNCTIONAL BLOCK DIAGRAM

digital-to-analog conversion as commanded by coding contained in the memory drum.

Operation of the proposed ground system digital computer evaluation is accomplished by using a prepared test program. The test routine is fed into the memory of an internally programmed test unit specifically written for the weapon system under test. A digital data tape is located aboard the test aircraft to provide information on the serial number and modifications required to make the aircraft and test system compatible. The test evaluator, which is controlled from an internal program, applies required forcing functions through the switching matrix to the aircraft. Outputs of the test channels are properly switched into the analog-to-digital converter and the output of the converter is applied to the digital register. The result of the computer operation is an evaluation of the aircraft under test. Tolerable limits of the measured quantities are predetermined and incorporated in the computer memory unit. The test results can be presented to the operating personnel by use of standard methods such as scope readout, printed data, and numerical readout.

The approach to test and evaluation as described is applicable if the weapon system has been prepared during the design stages for use with the ground system digital evaluator. Only in this way can the high speed and reliability of such a proposed interceptor evaluation scheme be accomplished.

SECTION 8 — EVALUATION BY AIRBORNE TESTING

(a) AIRBORNE FIRE CONTROL SYSTEMS TESTING

(1) An Example Of A Flight Evaluation Program

The purpose of the flight evaluation program is to determine the causes and frequency of weapon malfunctions. Four factors which contribute to fire control error are (1) inaccuracies caused by the mechanized equations which do not represent the exact fire control equations, (2) inaccuracies in equation mechanization (electrical as opposed to mathematical), (3) pilot and autopilot inaccuracies, and (4) radar scintillation errors. Flight test results do not enable one to determine easily what portion of each error is attributable to each of the four categories.

In addition to the primary objectives of the flight evaluation program, i.e., measurement of the miss of the aim point, other objectives relating

to the fire control system are obtained. Inflight tracking data can be used to substantiate theoretical antenna tracking data. Measurements can be made by photographic techniques with the camera equipment bore-sighted to the radar antenna line of sight. The radome required for use with camera equipment must be optically clear. Tracking performance of the antenna with and without computed tracking can be made.

From a report of the flight evaluation tests, it was determined that without computed tracking a significant lag error existed in the radar antenna line of sight. The lag error was virtually eliminated by use of the computed tracking loop as shown in Figures 8-29 and 8-30.

Results obtained from a particular flight test evaluation indicate bias in both azimuth and elevation channels. The bias was attributed to the following three causes: (1) pilot steering bias, (2) bias due to

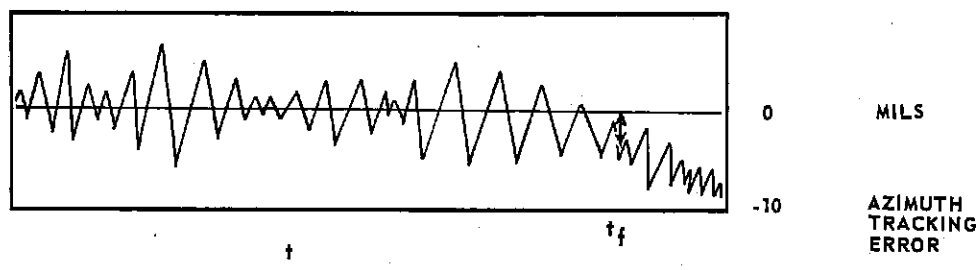

t_f REPRESENTS FIRING TIME

FIGURE 8-29. ANTENNA TRACKING ERROR WITHOUT COMPUTER AIDED TRACKING

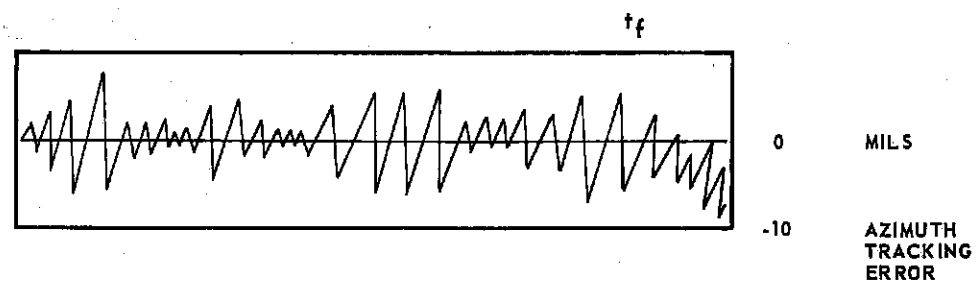

FIGURE 8-30. ANTENNA TRACKING ERROR WITH COMPUTER AIDED TRACKING

instrumented quantities, and (3) bias due to radar computer performance. The most important factors contributing to the overall variances are the same as the three causes of bias, namely, pilot-steering, radar computer, and measurement. In addition, an important variance is attributed to chance variations. Variances due to the radar computer and pilot steering were considered together. Qualitative indications of pilot steering were obtained from the azimuth and elevation steering signal voltages recorded on the oscillograph, and from motion pictures of the radar scope.

Evaluation of the fire control system enables inadequacies in system performance to be determined. Each inadequacy must be subjected to a detailed study to ascertain the necessary measures of redesign to optimize the system's performance.

Examples of several inadequacies in system performance are illustrated. A large dither or oscillating motion was apparent in the radar scope steering dot. The cause was found to be due to an oscillating motion of the antenna resulting from excessive starting friction. A means was achieved for eliminating the starting friction. This consisted of subjecting the antenna to a high frequency (compared to the original oscillation frequency), low amplitude motion in both the azimuth and elevation.

(2) Data Collection

A report of the flight test evaluation consists of data from the pilot's log, and verbal report in addition to that from a multichannel oscillograph and films from the strike cameras. Range quantity is obtained from the radar range voltage. Range rate utilizes the range voltage by smoothing and differentiating this quantity. The rate of interceptor roll is obtained by a potentiometer mounted directly on the computer roll servo, which in turn obtains roll data from the aircraft's vertical gyro. Interceptor angular velocity is obtained from a rate gyro mounted along the vertical axis. Angular velocities about the remaining axes are obtained from integrating gyros.

Cameras are used to obtain position and pilot-attach-display information. Two or more cameras may be required to view the maximum dead-ahead coverage. Pilot attack information can be obtained by another camera mounted to view the radar scope. Camera information is correlated by means of timing pips at each camera exposure.

(3) Practical Flight Evaluation

Several detection and lock-on flight techniques which are acceptable for the evaluation of radar detection and lock-on ranges have evolved from flight test results. The "Race Track" type of flight pattern consists of the test and target aircraft closing head-on. The flight paths describe an elliptical shape, whose dimensions are selected to establish the anticipated detection ranges of the radar set which is being considered. The test run is made and the first appearance of the target echo is recorded. Confirmation of the detected target range and identification is confirmed on the succeeding antenna sweeps. The lock-on range determination is recorded as that range at which the first lock-on can be accomplished.

The second flight path, referred to as the "Rubber Band" type pattern, directs the target aircraft to travel away from the interceptor on a course parallel to and above the interceptor. The target aircraft moves outward, increasing the range separation until the target echo disappears. This range is noted as the maximum detection range tail-on aspect. The target aircraft continues for a time along the same opening path to provide a new set of initial conditions, then decreases airspeed while the interceptor increases airspeed. The new detection range is again determined, using as a criterion the presence of the target echo on several successive sweeps.

Maximum lock-on determination is accomplished by attempting to lock-on at frequent intervals along the opening and closing tracks. The first lock-on occurring during the closing phase and the last lock-on occurring during the opening phase represent the ranges to be recorded.

A third method is similar to the "Rubber Band" method, but different in the following respect. During the opening tail-on aspect maximum detection run, the target is directed to open for a specified time interval and follow this by a reversal of heading. The first appearance of the target echo on the closing heading represents the maximum detection range. Maximum lock-on range is determined as before.

(4) Search Stabilization

The antenna search stabilization function is ruled as satisfactory if an echo from an airborne or surface target is displayed adequately during roll and pitch maneuvers. A procedure for evaluating antenna search stabilization consists of detecting a target at near maximum range and at

a large azimuth angle from the direction of interceptor flight. The interceptor is then rolled and pitched to the maximum limits for which the stabilization is designed. If the target echo remains on the scope, the stabilization is satisfactory.

(5) Range And Angle Tracking

The range and angle tracking capability is determined by the ability to retain range and angle track during high antenna azimuth rates. To accomplish this, the target is positioned near the limit of the antenna azimuth travel, then the relative heading is changed abruptly until the target is positioned at the opposite antenna azimuth limit. The time required for this maneuver is noted and the rate in degrees or radians per second is determined.

(6) Tracking Through Ground Clutter

The ability of a conventional pulse modulated radar set to track through the ground return clutter (altitude line clutter) can be demonstrated for various speed and altitude programs. As an example, the opening rate can be obtained as follows, the target aircraft is positioned at a range less than the altitude line, then instructed to open at various rates compatible with the radar tracking rate of the interceptor's radar. At a range beyond the altitude line, the target aircraft is directed to slow down and the interceptor speed is increased until the desired closing speed is obtained. During each tracking run through the altitude line, the relative stability of the error dot, error circle and the range rate reading on the range circle are recorded. If lock-on is not broken during the pass through the altitude line the test is considered successful and, conversely, if lock-on is broken or switched to the altitude line, the mission is rated unsuccessful.

Evaluation of other capabilities of the airborne fire control system, such as ground mapping and susceptibility to countermeasures are not discussed here but are important aspects which should be determined in any radar system evaluation.

The probability curves for detection and lock-on for various differential altitudes can be plotted on the typical range-versus-percent-probability curves. See Figures 8-31 and 8-32. The conventional pulse radar system will typically show a decrease in maximum detection and lock-on ranges with decreased altitude, Figures 8-31 and 8-32.

The major purpose of a typical fire control evaluation is concerned with the performance of a simulated tactical interception.

In addition to the basic determinations many other considerations enter into the tactical intercept evaluation. For example, manipulating the aircraft controls to effect lock-on might easily be a cause for poor lock-on ranges. Jitter of the steering circle and the dot might similarly affect ability of the pilot or automatic steering system to fly the required intercept course.

At very low altitudes, unsatisfactory lock-on ranges might degrade performance to the point of serious reduction of detection and lock-on ranges.

The myriad of factors unrelated to the primary intercept mission, which tend to inhibit the gathering of valid flight test data, are too numerous

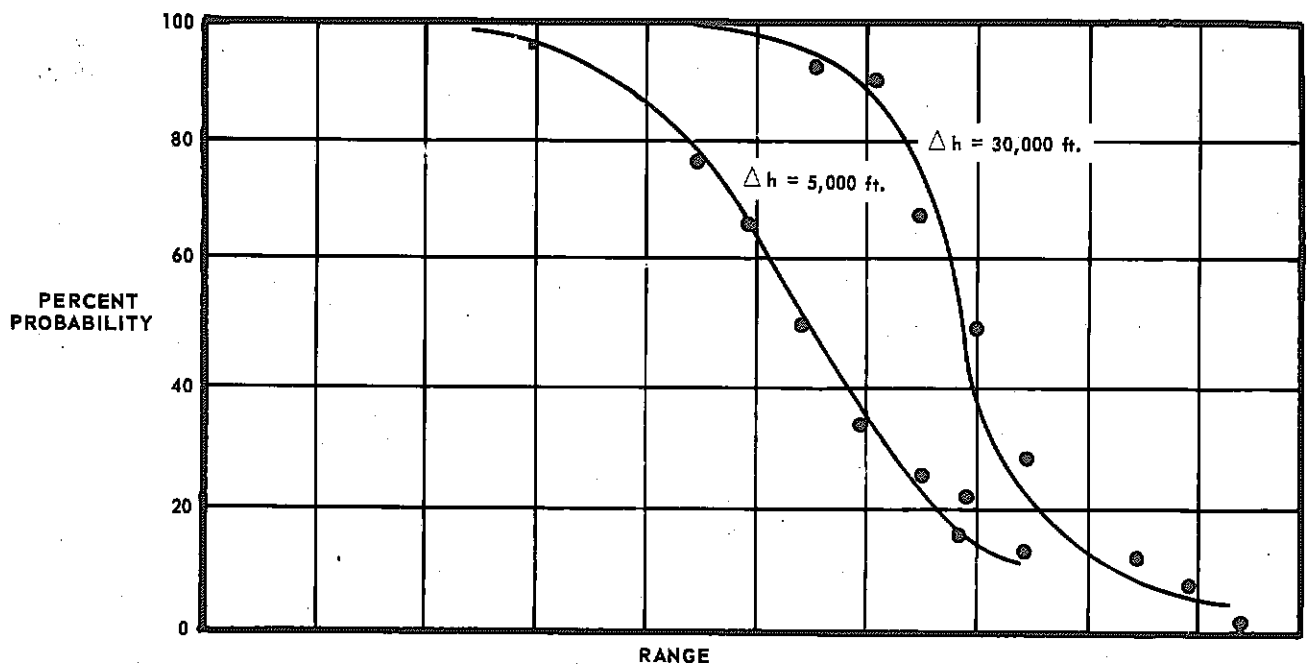

FIGURE 8-31. RANGE OF DETECTION (Opening Condition)

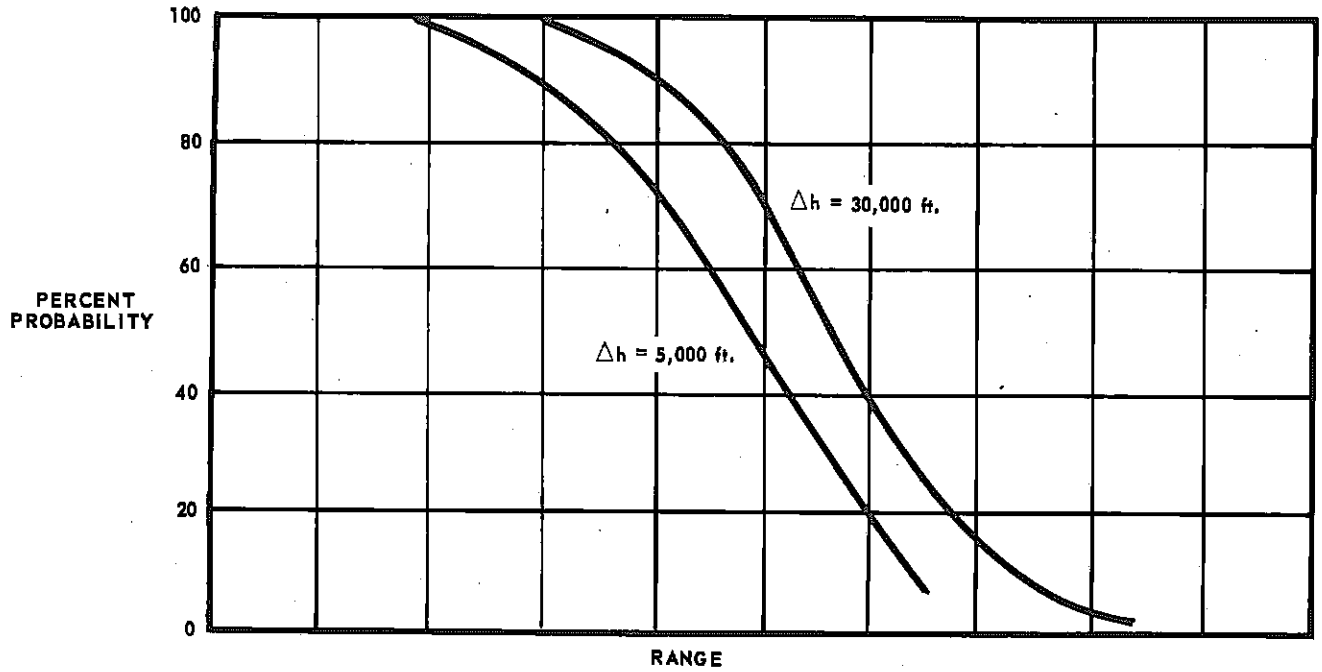

FIGURE 8-32. RANGE OF LOCK-ON (Opening Condition)

to be detailed here but a large number of the deficiencies fall into the following categories:

1) Radar and fire control malfunctions
2) Aircraft malfunctions
3) Maintenance down time
4) Aircraft cockpit control inaccessibilities
5) Modular accessibility difficulty
6) Fire control equipment pressurization problems
7) Problems of equipment alignment in aircraft
8) Equipment temperature problems
9) Radar scope visibility problems
10) Unavailability of spare parts, instructions manuals, etc

(b) DEVELOPMENT OF THE CUMULATIVE PROBABILITY CURVE FROM FLIGHT TEST DATA

The development of a cumulative probability curve, such as that in Figure 8-33, can be derived from flight data. The Y axis represents

the cumulative probability scale or the percentage of total flights that detect by range R.

As an illustration, suppose that a group of 10 aircraft attempt to determine the cumulative probability curve for a specific radar on the same target. The data shown in Table 8-2 represent ranges in order at which each aircraft first detected the target.

The curves can be interpreted as indicating what percentage of the total flights detect the same target for the ranges shown.

The curve obtained by flight evaluation can be compared to the curves obtained by calculation of the cumulative probability from

$$P_{cum} = 1 - \prod_{i=1}^{n} \left(1 - P_{si}\right) \tag{8-72}$$

where P_{si} is the single-look probability, the blip-scan, or simply the probability of detection.

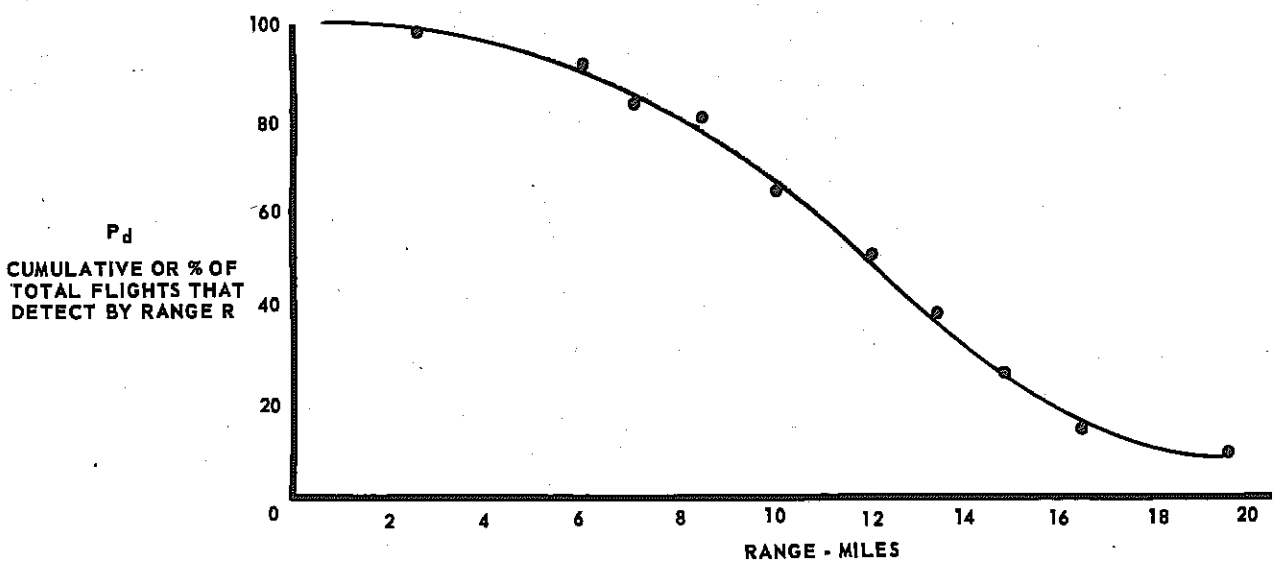

FIGURE 8-33. RANGE - MILES

Table 8-2. Data for Determining Probability Curve

Aircraft	Range of Detection Miles	% Detected
1	19.2	100
2	16.4	90
3	15.6	80
4	14.9	70
5	13.6	60
6	11.8	50
7	11.2	40
8	9.3	30
9	8.4	20
10	5.0	10

(c) FLIGHT TEST EVALUATION OF LABORATORY MODEL PULSE-DOPPLER RADAR

The airborne laboratory model of the pulse-doppler radar, used to evaluate the basic design, obtains data for air-to-air search and detection and collects data on ground clutter effect. The test of detection capabilities is performed against known and controlled targets. The test aircraft is instrumented to record the outputs of the individual velocity gates. Instruments consist of a multichannel recorder and signal translator for recording the doppler signals. Another multichannel recorder records the detected signals from the velocity gates. Means for counting antenna scans to determine the blip-to-scan ratio are included. Other parameters such as transmitter power, component temperatures, etc., are recorded. Sidelobe and mainlobe clutter are recorded from the output of the doppler filters to determine spectral density and terrain characteristics.

Test data, obtained as a result of breadboard flight test, permit evaluation of the theoretical basis on which the equipment was designed.

One of the most meaningful data items to be compiled as a result of flight test is the detection range. A fair number of repeated flights is required to determine an average range for cumulative probability of target detection. If for example, five flights resulted in the following detection ranges in miles, 10, 14, 16, 14, 12, and the fifth flight missed

detection entirely, the cumulative probability would be as shown in Figure 8-34. The P_{dc} for 90% would be about 11 miles.

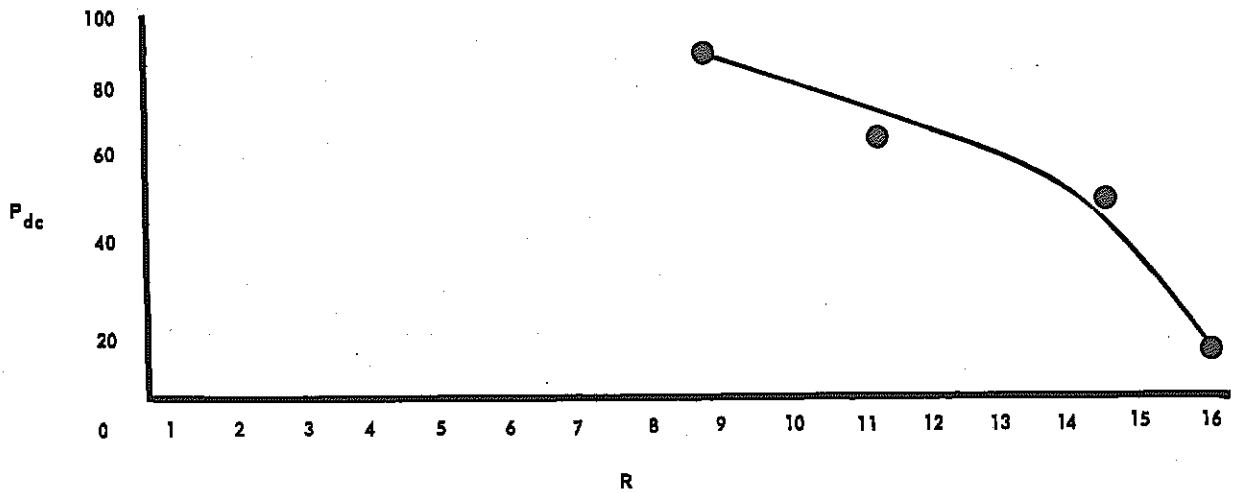

FIGURE 8-34. FLIGHT DETERMINATION OF PROBABILITY CURVE

The flight tested breadboard model provides an experimental basis for determining the characteristics for the more refined prototype model. Drastic discrepancies of the flight test results and theoretically calculated performance would require important changes to be incorporated in the prototype model. At this point an estimate of the characteristics of the prototype model can be made by examining differences to be expected in the parameters of the old and new systems. The differences can be resolved into an equation for the new system, in terms of an expected detection range, as

$$R_{PRO} = A\,R_{BB} \qquad (8\text{-}73)$$

where R_{PRO} = expected detection range of the prototype equipment
A = gain resulting from improved parameters
R_{BB} = detection range of the breadboard equipment

(d) FLIGHT DATA COMPILATION TECHNIQUES

Evaluation of the fire control effectiveness is generally implemented with flight test data obtained from recorders (see section on NADAR),

strike cameras, pilot reports, etc. The flights may be either "dry runs" or "live" firings. Weapon "live" firing is performed over instrumented ranges using tracking camera recording (cine-theodolite) equipment. This equipment records on film the exact azimuth, slant elevation, and bearing of the target, armament, and interceptor.

Evaluation programs are valuable since they permit disclosure of sources of system errors and also enable the system to be adjusted for optimum performance.

Oscillograph recordings of the fire control system parameters are difficult to read, very time consuming, and are themselves sources of inaccuracies. More advanced techniques for recording data make use of punched cards and magnetic tapes. By this means the data can be fed directly into a computer for data reduction computations. The computer can print out the required data, system errors, hit probability density, and other required quantities.

(e) EVALUATION OF RADAR DETECTION FROM FLIGHT DATA

The literature of flight evaluation comparisons with theoretical data of radar detection is sparse, and the confidence with which the limits of search and lock-on can be predicted is subject to large uncertainties. The reports of detection theory by Marcum and others have been briefly described in this review. The question yet unanswered is, "to what degree is there confirmation of refutation of the detection theory by flight data?"

Comparison of the detection theory with practical flight evaluation requires close control of the radar and target parameters. The aircraft closing rate must be maintained relatively constant. This can be done by careful selection of the speed and course of target and interceptor. Antenna gain and system losses remain fairly constant during a single flight. For improved results the approach of the interceptor and target aircraft should be limited to a very narrow angle to limit the amount of fluctuation of the target cross-sectional reflectivity area. These accuracy requirements complicate the entire process.

Selection of a suitable flight range for collection of data represents a difficult problem in itself. A satisfactory solution to the problem was obtained in one case by testing over the ocean at moderate altitudes (approximately 20,000 feet). Under these conditions the target aircraft

can be caused to fly a relatively straight course (1 to 2 degrees) using direction finding instruments to home on a transmitter. The distance between target aircraft and interceptor should be well in excess of the maximum theoretical detection range. Choice of either a head-on or tail-chase approach should be made on the basis, among other factors, of the flight program objective of evaluating the detection of high and low speed targets.

Actual flight data have indicated large changes in radar system parameters from flight to flight. Practical test programs should attempt to maintain key radar parameters relatively constant. Transmitter power output, for example, should be held constant to within 1 to 2 db or better. For those parameters which cannot be controlled, a base reference can be used to convert all values to a common reference. Transmitter peak power, P_p, and receiver noise power, P_N, can be measured before and after each flight, and the flight-derived detection range corrected according to

$$R_c = R_f \left(\frac{P_{P1}}{P_{N1}} \cdot \frac{P_{N2}}{P_{p2}} \right)^{1/4} \tag{8-74}$$

where

R_c is the corrected range

R_f the range obtained from flight test at the reference peak power

P_{P1} the reference peak power

P_{N1} receiver reference noise power

P_{N2} receiver noise power during flight (measured after flight)

P_{P2} peak transmitter power during flight (measured after flight)

The ratio $\frac{P_P}{P_N}$ provides a convenient measurement criterion for estimating the performance capability of the radar system.

The result of comparing flight test data to theoretical calculations for the same conditions is shown in Figure 8-35. No allowance is made

in the theoretical calculation for the effect of the radar operator. Many authors in this field attempt to equalize the two curves based on a loss attributable to the radar operator.

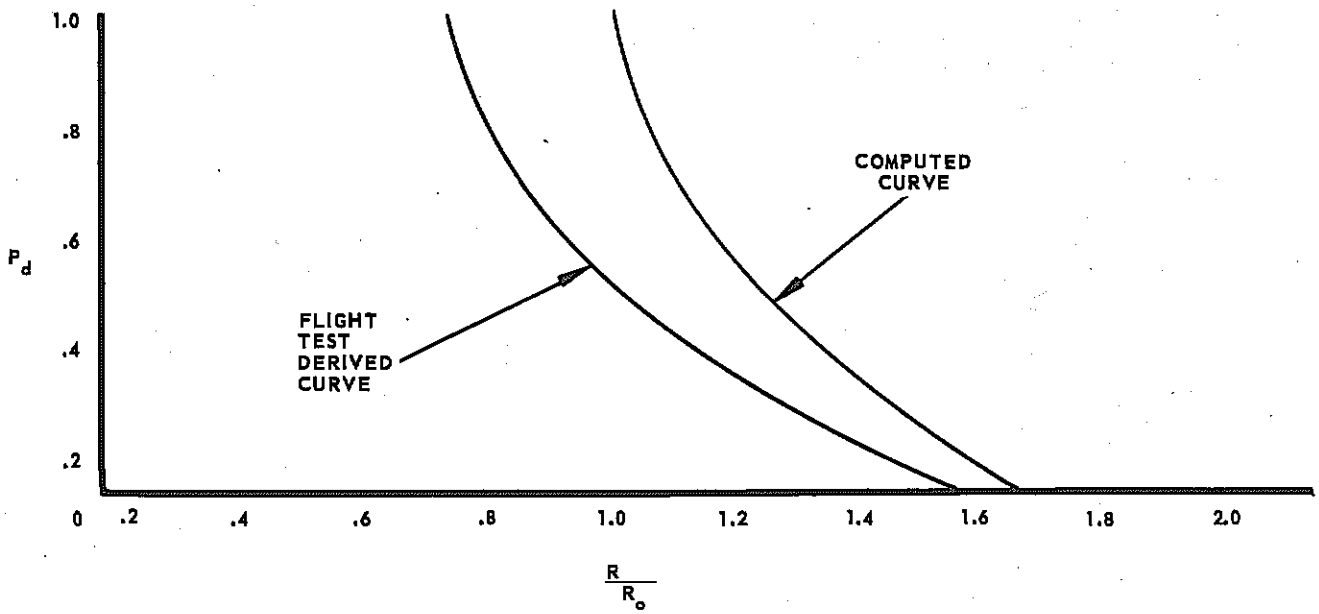

FIGURE 8-35. FLIGHT TEST DERIVED CURVES AND COMPUTED CURVE
(No allowance made in the computed curve for operator factor)

Multichannel data recorders should record at least the following data: range, range-rate, azimuth angle, elevation angle, and receiver automatic gain voltage. The radar operator should record the instant of target detection. This measurement may be mechanized on a channel which records the instant of depression of the search-to-lock-on ("action") switch. The lock-on time should similarly be recorded by means of suitable scope display recording instrumentation.

No account has been made of the operator factor, which plays a key role in the intercept problem. It is reasonable to state that this factor is at least as important as any of the other radar and fire control parameters; however, no attempt is made in this review to analyze the properties of the radar operator or their effect on the detection evaluation problem.

(f) ROLE OF THE AIRBORNE DIGITAL COMPUTER IN ADVANCED FIRE CONTROL SYSTEM EVALUATION

The use of the airborne digital computer for system test and evaluation of advanced fire control systems may prove to have great merit. The digital computer would be used for tactical as well as the automatic-testing functions of the fire control system. The large number of input and output signals, the capability to store large quantities of data on a storage device, and the speed and accuracy of the computational operations make the airborne digital computer proficient for the evaluation application.

Inclusion of system evaluation capability in the airborne tactical computer adds significant weight to the tactical system. A description of the use of a ground-based external computer tester has been shown to provide a comparison of the advantages and disadvantages of the two evaluation schemes.

A complete program of tactical and test data can be stored on the airborne digital computer storage drum. Each of the major sections, test and tactical, is operated independently of the other. The computer provides test routines to determine proper operation prior to flight as well as during flight evaluation runs. This program consists of subsystem and system checking functions. If a test indicates a malfunction, the computer can provide trouble shooting programs for aid in locating the fault.

Space requirements for the evaluation section of the digital computer are relatively severe when compared to space required only for the tactical program. Depending on the extent of the test program, the volume of memory drum space required may be more than double that of the tactical program. The additional memory space, however, makes possible the rapid evaluation of the computer, as well as major portions of the complete fire control system.

The first evaluation test is performed by the self-checking of the digital computer. Upon completion of satisfactory self-tests the computer can be used in system and subsystem testing.

Computer tests may be initiated from cockpit controls or from controls in the subsystem area. Indicator lights or a cathode ray oscilloscope

(radar scope) can be used to indicate normal or abnormal operation of the computer, and can be used to isolate the unit in which a malfunction occurs.

Basic building blocks of a digital computer system are the arithmetic, control, memory, and input-output units. The memory unit provides storage for instructions and numbers. The function of the arithmetic unit is to perform operations on numbers stored in the memory unit. Results of the arithmetic operation are recorded in another section of the memory drum. The control unit reads the instructions on the memory unit, logically interprets the instructions, and causes the arithmetic unit to perform the required operation. The input-output unit provides means for introducing signals from sectors of the fire control system other than the computer. The input signals are converted to digital bits, which are then recorded on the memory drum. Outputs are read (by a transducer) from the memory unit and an appropriate signal is developed for control of various phases of the fire control system.

The self-test feature of the digital computer performs logical operations to check key portions of this unit. The stored contents of the memory drum may be read out and checked against a known correct value. The control and arithmetic unit may be caused to perform the fundamental orders for addition, subtraction, multiplication, and division. The results are again checked against known correct quantities. The input-output unit may be tested during the evaluation of the remainder of the fire control system.

(g) MISSION EFFECTIVENESS

The role of the airborne digital computer may be further enhanced by utilizing portions of the computer program to evaluate intercept mission effectiveness. No estimate of increase in equipment weight or size requirements is available to implement such a program. The airborne computer is utilized to record portions of a nonfiring run, thus eliminating some of the difficulties encountered when using oscillograph recording techniques.

For flight test evaluation, the cockpit display should be recorded by instrumentation to obtain the detection and tracking scope presentation. These data can then be compared with the computer recorded data. Computer data should include key signals from the various fire control subsystems as well as the armament subsystem. An estimate of firing

accuracy would be determined by computer calculation of time between armament firing and impact (see Appendix).

(h) AIRBORNE ATTACK TEST SIMULATION

(1) Simulated Attack Test

In one of the E series radars, most of the fire control system is used and checked out in the performance of the missile auxiliary open-loop self-tests. The system is put into operation by setting a "Test Run" switch to the "run" position. In this position the range gate marker is slewed in range. At the time of firing, the test range slewing is stopped when the "On Target" lamp is lit. The computer is uncaged, the on-target relay is energized to enable the steering dot channel, the on-target relay is energized to enable the range rate reference channels which furnish the range rate signal, and the on-target relay is energized to apply the attack display to the deflection amplifiers and then to the indicator. As the range trace is slewed, the ballistic circuits go through a series of coincidences, a light goes on, a weapon-abort circuit is energized causing the attack run to be switched from missiles to rockets if the salvo selector switch circuit is not functioning properly. An abort condition is indicated by a test light going on momentarily and the elevation bar moving from the right to the left side of the indicator. Higher-than-normal filament voltage is applied to the missile heaters at this time. After a moment, the filament voltage is lowered to a normal operating condition. Locked-on target voltage is applied to energize the rate relay, which causes the pulse repetition frequency to be applied to the master trigger-blocking oscillator. The missile antenna servo and missile range gate servo are also activated.

The attack situation continues with the missile channel lamp being operated. Finally the "fire" signal is operated lighting a "fire" lamp. The range gate slewing is stopped.

The above represents a small but important part of the technique by which self-test of a radar can be accomplished. Only upon satisfactory completion of the entire self-test routine can there by any degree of certainty that the fire control system will function properly in flight.

(2) Nadar, An Airborne Attack Evaluator

The North American Data Airborne Recorder (NADAR) represents one type of airborne recording device used for recording data on

the operational parameters of fire control system. Signals recorded on tape during flight can be played back immediately after the aircraft return from flight. The signals are played on an oscilloscope in the NADAR Ground Playback and Test Console.

The NADAR Recording device records signals from the fire control computer, namely those signals applied to the grids and deflection plates of the pilot's radar scope during the attack run. The tape recording begins when radar lock-on is accomplished. The tape is completed when a "pull-out" or similar signal is received. The recording sequence may be repeated on subsequent attack flights.

The ground playback unit reproduces on an oscilloscope all the recorded information in proper time sequence and amplitude as on the original attack display.

Recording of the airborne radar system signals is made on four channels in the recording head. The four signals recorded are the horizontal deflection signal, vertical deflection signal, the range signal, and the blanking signal.

The recording permits an evaluation of the attack flight and pilot control, and is also valuable in pilot training.

SECTION 9 — RESULTS OF EVALUATION STUDIES

Evaluation studies indicate the following:

1. Lock-on ranges should be increased for the fire control radar used with rockets and guided missile armament.
2. Detection capability at very low and very high altitudes without sensitivity to ground or sea reflections. New radar techniques should be evaluated for improved detection capability.
3. Detection and lock-on ranges should be maximized and equalized to eliminate difference in range between detection and lock-on.
4. Ability to lock-on and remain locked-on at very low and very high altitudes should be improved.
5. Evaluation of the probability of detection and probability of lock-on should be correlated with flight evaluation. Methods of instrumentating these quantities should be improved.

6. Means for reducing operational degradation should be established. Increased reliability, improved performance monitoring, and improved ease of maintenance should be goals to decrease degradation.
7. Airborne radar performance should be improved by one or more of the following methods: use of a larger antenna, reduction of receiver noise, and increasing transmitter power. Another avenue for radar improvement lies in the reduction in scanning loss by limiting the radar search sector. This would require improved GCI vectoring but would result in improved operator performance.

CHAPTER IX

TECHNIQUES OF ESTIMATING WEAPON SYSTEM EFFECTIVENESS

SECTION 1 — WEAPON - TARGET PARAMETERS

Mathematical analysis never can be directly applied to the real world, rather it is applied to a mathematical model which is essentially a set of postulates selected to represent the real world. The validity of the analysis thus is functionally dependent upon the relationship between the postulates and the real world. Thus physical test results are important in order to judge the validity of the analysis.

In order to formulate the mathematical model, an understanding of weapon-target parameters is necessary. The systems engineer must have a reasonable concept of the configuration and operational characteristics of both the weapon and the target. Test results should be carefully scrutinized and in many instances visits to the field are highly beneficial prior to the formulation of the mathematical model.

The evaluation of any system estimates the effectiveness of the system in the accomplishment of an objective. The objective for any weapon system is to destroy or incapacitate the target. Knowledge of the target should be as complete as possible and especially vulnerable areas should be carefully sought out.

The target complex can be made up of single or multiple units which may be homogeneous or of mixed composition. The units may be land, sea, air or even space targets. The targets themselves may be identified by type, speed, location and particular vulnerable areas. Inherent in any potential enemy target is the degree to which it can be identified or detected by visual, electronic, or other means. The detectability of a target encompasses such factors as: use of electronic countermeasures, target size and physical characteristics, and decoys to confuse the detectors. The detection process is composed of acquisition, identification, and evaluation of intentions prior to the designation of a contact as a target.

The total entity of a weapon system consists of an instrument of combat, such as an aircraft or missile, together with all the related equipment, supporting facilities and services required to bring the instrument to bear upon the target or to the place where it can carry out its designated function. Description of a weapon system includes selection of the type of instrument, providing a carrier for the instrument, providing facilities and services so that the weapon will be available at the right time, and providing means for the safety of friendly elements. This latter requirement is obviously difficult in such weapons as ballistic missiles.

The weapon itself may be of a wide variety of types. It may project a warhead from an impulse which may be from a source either external to the weapon or within the weapon itself. The warhead must have a means for determining time to explode (fuzing). There are many types of fuzes such as antidisturbance, pressure, concussion, combination, electronic, time, radio proximity. The range of the weapon is related intrinsically to the study of ballistics. The accuracy of a weapon is usually expressed as a circular error of probability (CEP) which is defined as the radius of a circle centered on the desired point of impact and containing 50% of the expected shots.

The platform is the device for carrying the weapon within firing range to the target. It may take the form of a fixed launcher many thousands of miles from the target in the case of some ballistic missiles. Many launchers incorporate a means for initial guidance of the weapon. The weapon platform is designated by the type of environment in which it is commonly employed and by the environment of the target. Weapon systems can thus be designated as air-to-air, air-to-ground, ground-to-ground, ground-to-air, and subsurface-to-surface. In many cases the platform is highly complex, as in the case of a high speed interceptor. The platform may be fixed, maneuverable, mobile or hardened by extensive armor. It must be reliable and accurately controllable.

The effectiveness of the weapon against the target can be measured by several factors -- time, destructiveness, cost, or military worth. Force effectiveness may be determined for either homogeneous or heterogeneous weapon systems. For heterogeneous systems the principal criterion usually is cost effectiveness. Despite the wide variety of targets, weapons, and platforms, there are certain elements, which are common and basic to the overall problem. Consequently, for any given

physical situation the experienced operations analyst can readily isolate the significant parameters pertinent to the evaluation for a given effectiveness criterion. These parameters are the basis for the mathematical model.

SECTION 2 — WEAPON SYSTEMS ANALYSIS

The interceptor-bomber air battle problem is illustrated in Figure 9-1. In the accomplishment of an interception, interceptors are sent aloft, "scrambled", and directed to maintain a specified heading, altitude, and speed to intercept the target threat. Interceptor heading corrections are performed during the midcourse phase to negate bomber maneuvers and to reduce interceptor positioning errors for the terminal attack. At the offset point arrival, the interceptor pilot performs a turn to the terminal attack heading and commences the search, lock-on, tracking and conversion portion of the mission. At the appropriate time, the armament is launched and the interceptor breaks off the attack.

The analysis under consideration is divided into several areas of study. These areas are:

1. Conditions of engagement which include
   a. Methods of intercept control
   b. Initial positioning
   c. Modes of attack
   d. Tactics - GCI, Bomber and Fighter
2. Radar detection and tracking systems
3. Electronic countermeasures
4. Model development

The two basic mathematical model formulations used to evaluate interceptor-bomber air engagements are <u>barrier</u> formulations and <u>simulation</u> formulations. Sub-model developments are an important part of the model programming and include:

1. Interceptor Positioning for Terminal Attack
2. Detection Sequence
3. Lock-On Sequence
4. Interceptor Tracking and Steering Sequence
5. Bomber Tactics
6. Interceptor Tactics
7. Missile Simulation

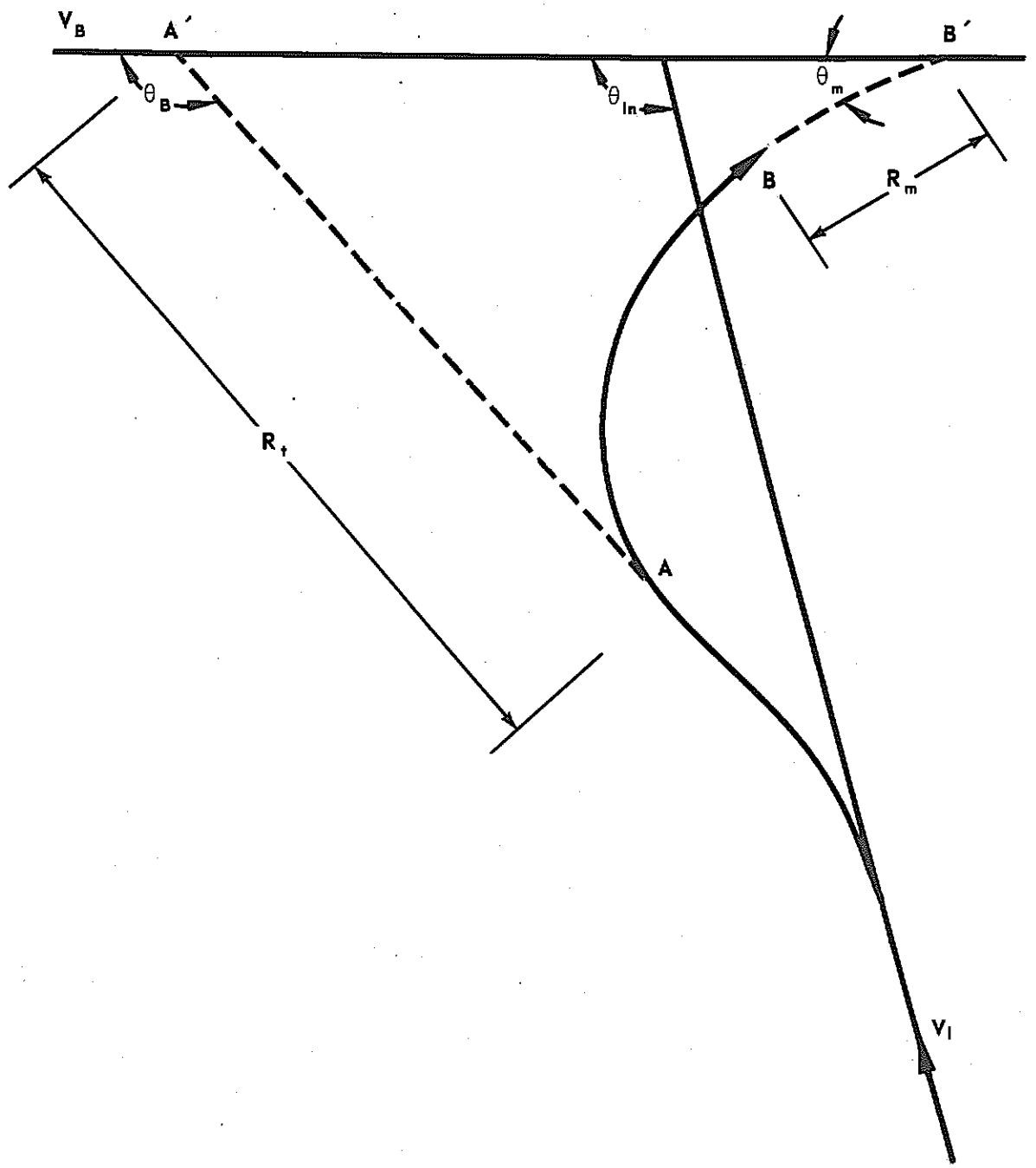

FIGURE 9-1. PURSUIT PATH INTERCEPTOR VS. BOMBER

The barrier model is a three-dimensional analytical method of arriving at an expected value of the probability of an interceptor detecting and converting on a bomber. The barrier model may be used to evaluate cases involving a non-maneuvering bomber. As the fighter flies along a course, with a fixed heading, searching for the bomber, there exists a limit point on that course at which the fighter must detect the bomber in order to convert. The barrier is the locus of points at which the interceptor with the same heading, should react to the presence of the target. The limitations are the scan angle, maneuverability, detection range, lock-on range and lock-on time. The maneuver barrier is the locus of points where the fighter must begin a maximum "g" turn in order to convert on the bomber. This barrier is translated back to allow time from detection through lock-on to the initiation of the conversion turn. The bomber must be within the scan angle to be detected. This scan barrier also is translated back. The composite barrier is the combination of the individual barriers.

The cumulative probability of detection is computed until the fighter reaches the composite barrier. Runs are made to the barrier from each of a group of points which represent a normal distribution about the GCI interceptor positioning point (IPP). The cumulative probabilities of detection from all of the weighted points are combined to give the expected probability of detection and conversion. Barrier formulations are particularly well adapted to the determination of radar and fire control system design parameters.

The interceptor fire control system must initiate the attack within a prescribed limit for success to occur. The interceptor must detect at the greatest possible range in order to allow for identification of the target as well as to provide sufficient time for completion of the remaining attack phase. A finite time is required for the lock-on procedure to be accomplished. The pilot's radar scope presentation at this time changes from the search mode display to the attack mode display, (which is generally in the form of a steering dot). The pilot attempts to maintain the steering dot centered, causing the plane to be directed toward the target. The missile is fired when the weapon armament range is obtained.

The conversion barrier consists of (1) the maneuver barrier which is the locus of points determined by the turn requirements to place the interceptor on a proper course for interception, (2) the scan barriers which are lines marking the radar antenna scan limits, and (3) the delay barrier

which is determined by the minimum length of time required by the fire control system between turning and firing. When the conversion barrier has been found, the delay times permissible for identification, lock-on and system stabilization are determined.

(a) MANEUVER BARRIER

The maneuver barrier is that segment of the conversion barrier defined by the minimum time from turning to armament release. The equations for the maneuver barrier are developed by considering that the interceptor's flight from the initiation of the corrective turn to the aimpoint consists of two portions: a circular turn through a positive angle and a straight line flight of range R, both in ground coordinates. Figure 9-2 shows the approach to the X-axis in ground coordinates at an instant of time prior to the interceptor's initiation of turn. The X-axis and the heading angles are invariant under a transformation to the bomber coordinate system so that the coordinates of the initial point of the straight line are:

$$X_R = -R\left[\cos(\phi - C\zeta) - \frac{1}{n}\right] \tag{9-1}$$

$$Y_R = R\sin(\phi - C\zeta) \tag{9-2}$$

where:

ϕ = the interceptor heading during the detection or search phase

$V_{F/B}$ = speed ratio $\frac{V_F}{V_B}$

C = + 1 if the turn is to the left (as shown)

C = -1 if the turn is to the right

ζ = interceptor turn angle

During the turn the changes in X and Y in bomber space are

$$\Delta X_t = Cr_t\left[\sin(\phi - C\zeta) - \sin\phi\right] + \zeta\frac{V_t}{V_{F/B}} \tag{9-3}$$

$$\Delta Y_t = Cr_t\left[\cos(\phi - C\zeta) - \cos\phi\right] \tag{9-4}$$

where

V_t = turn velocity
V_F = fighter velocity
V_B = bomber velocity
g = gravity

r_t is the radius of turn and can be specified either in terms of the load factor N, which equals the ratio of lift to weight or the roll angle β as

$$r_t = \frac{V_F^2}{g\sqrt{N^2-1}} = \frac{V_F^2}{g \tan \beta} \tag{9-5}$$

Combining, the coordinates of a general maneuver barrier are

$$X(R,\zeta) = \frac{R + \zeta V_t}{N} - R \cos(\phi - C\zeta) + Cr_t \left[\sin(\phi - C\zeta) - \sin \phi \right] \tag{9-6}$$

$$Y(R,\zeta) = R \sin(\phi - C\zeta) + Cr_t \left[\cos \phi - C\zeta) - \cos \phi \right] \tag{9-7}$$

By definition, the maneuver barrier is the locus of last points on relative approach paths at which the interceptor can initiate a doctrine turn to the selected course. Therefore, the value of R is the minimum value, R_{min}, which is necessary in terms of time, for the fire control system. This value can be expressed as

$$R_{min} = V_F (t_s + t_f) + F \tag{9-8}$$

where

t_s = the time interval from completion of the doctrine turn to firing of armament
t_f = the flight time of the armament
F = the range of the armament relative to the interceptor

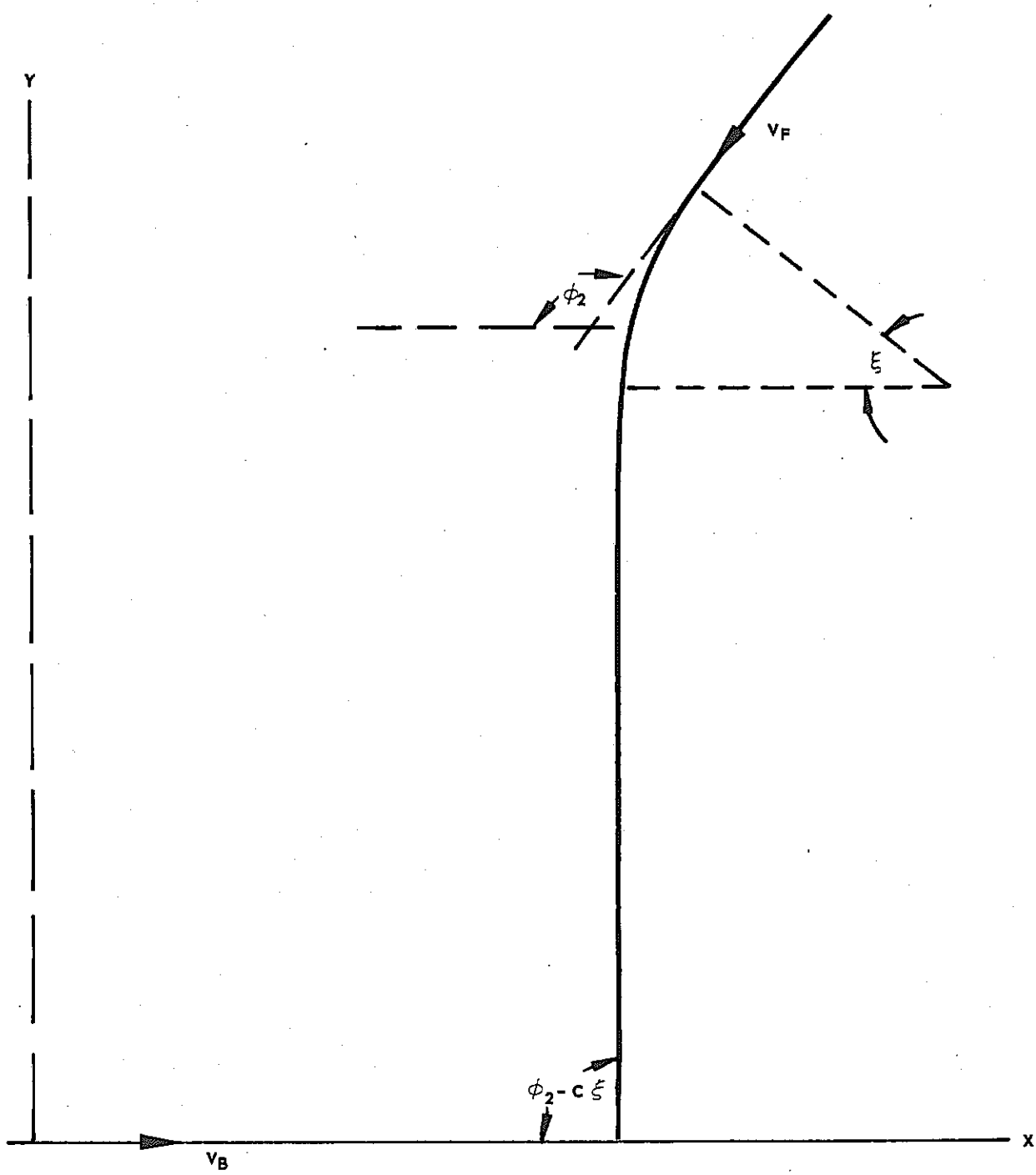

FIGURE 9-2. REPRESENTATIVE INTERCEPTOR APPROACH PATH GROUND COORDINATES

The corresponding detection barrier is obtained by translating the coordinates of the maneuver barrier by the quantities

$$\Delta X = t_d V_F \left(\frac{1}{V_{F/B}} - \cos\phi\right) \tag{9-9}$$

$$\Delta Y = t_d V_F \sin\phi$$

where t_d is the time interval required for the processes between detection and the initiation of the conversion phase. Figure 9-3 shows a typical maneuver barrier. For some relative approach paths, there may be no intersection with the maneuver barrier as in the C = + 1 area of Figure 9-3. To achieve a lead collision course in this region, it is necessary to complete the conversion turn at a distance greater than R_{min} from the aimpoint.

(b) ANTENNA SCAN BARRIER

The scan barrier is that segment of the conversion barrier established by the mechanical train limits of the interceptor search radar antenna. Beyond this barrier, the target cannot appear on the radar scope. The equation of the antenna barrier is:

$$X = -Y \cot(\phi - C\mu) + \frac{F}{V_{F/B}} \tag{9-10}$$

where

μ = the radar scan angle limit angle from the interceptor heading
$F/V_{\frac{F}{B}}$ = the distance between the aim point and the target

An interceptor which reaches the scan barrier without first crossing the maneuver barrier can complete a successful conversion. However, the distance R from the end of the turn to the aimpoint will need to be greater than R_{min}; the distance will be precisely R_{min} only if conversion is begun at the maneuver barrier. The flight time from the beginning of the turn to the aimpoint can be expressed as

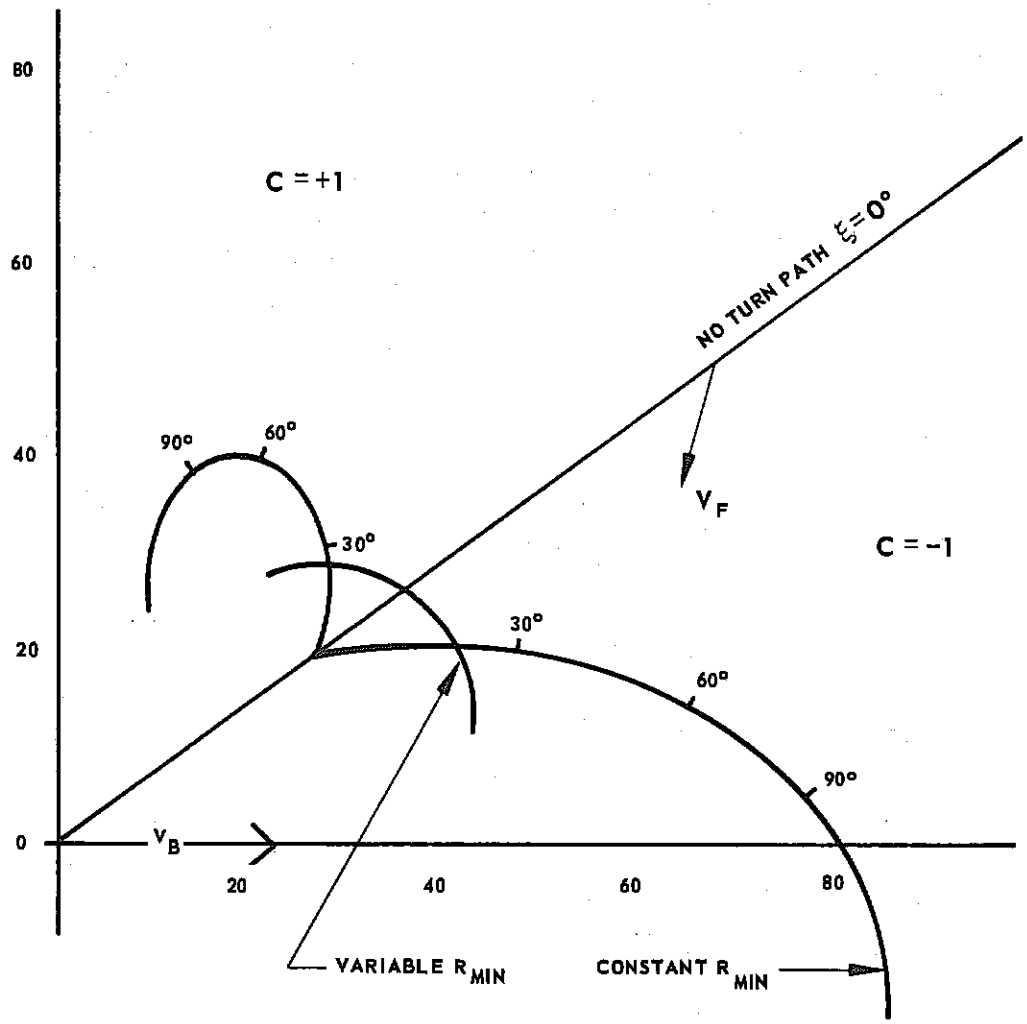

FIGURE 9-3. REPRESENTATIVE MANEUVER BARRIER

$$\Delta t = \frac{R}{V_F} + \zeta \frac{r_t}{V_F} \tag{9-11}$$

(c) SECTOR BARRIER

The sector barrier is that set of points on the conversion barrier by which a turn will be required to establish the selected lead-collision course within a desirable sector of the target. This desirable sector may be specified from considerations of the target armament, the effective radar echo area of the target, the type of detection equipment (i.e. continuous wave radar, pulse doppler radar, infrared, etc.). The fact that an approach path may not be the most effective, however, does not necessarily mean that the interceptor's probability of killing the target is negligible. Crossing the sector barrier is not deemed an abort in the sense that the accumulation of probability is stopped. The sector barrier is not regarded as a true barrier in the sense of the maneuver or scan barriers.

(d) LOCK-ON BARRIER

The lock-on barrier, like the detection barrier, can be obtained by translating the conversion barrier away from the target by a specified time interval. In this case t_L represents the interval between completion of lock-on and initiation of the conversion turn. The section corresponding to the maneuver barrier is

$$X = \frac{R_{min} + \zeta r_t}{N} - R_{min} \cos(\phi - C\zeta) + Cr_t \left[\sin(\phi - C\zeta) - \sin\phi\right] + t_L V_F \left(\frac{1}{V_{F/B}} - \cos\phi\right) \tag{9-12}$$

$$Y = R_{min} \sin(\phi - C) + Cr_t \left[\cos(\phi - C) - \cos\phi\right] + t_L V_F \sin\phi \tag{9-13}$$

where R_{min} is either $R_{nt} - \xi r_t$ or a constant. R_{nt} is the range for the condition of no turn of the fighter. Lock-on must be accomplished at or

before the interceptor arrives at any point on the cumulative curve. A characteristic of the AI radar is the maximum range at which lock-on can be accomplished. This is a circle with center at the target and radius R_L

$$R_L = \left[\left(X - \frac{F}{V_{F/B}}\right)^2 + Y^2 \right]^{1/2} \tag{9-14}$$

The intersection of this circle with the lock-on barrier defines the maximum distance a relative approach path may be off the "no turn" path. An approach outside this corridor would require lock-on at a range greater than the maximum possible.

(e) MAXIMUM TIME BARRIER

The region from which it may be possible for the interceptor to kill the target is closed on the far side by the maximum time barrier. The duration of the terminal engagement might be limited by the fuel load that the interceptor carries and/or the allowable penetration of the target area. If this is specified by a time interval, t_{max}, then translating the detection barrier by the difference between the time it takes from detection to armament release, the t_{max} will define the greatest permissible distance for the interceptor at the time it begins its terminal phase. For head-on approaches, there is usually sufficient time for the engagement regardless of the speed differential. For tail-chases, the maximum time barrier may be highly significant when the relative velocity is low. The equations for this barrier, corresponding to the maneuver limit are:

$$X = R_{min} \left[\cos(\phi - C\zeta) - \cos\phi \right] + \zeta r_t \cos\phi \tag{9-15}$$

$$+ C r_t \left[\sin(\phi - C\zeta) - \sin\phi \right] + t_{max} V_F \left(\frac{1}{V_{F/B}} - \cos\phi \right)$$

$$Y = R_{min} \left[\sin(\phi - C) - \sin\phi \right] - r_t \sin\phi$$

$$+ C r_t \left[\cos(\phi - C) - \cos\phi \right] + t_{max} V_F \sin\phi$$

where R_{min} is $R_{nt} - \zeta r_t$ or a constant. If the flight time from the scan barrier to armament release is

$$\Delta t_s = \frac{R_s}{V_F} + \frac{\zeta r_t}{V_F} \tag{9-16}$$

where R_s and ζr_t have been determined by solving for the intersection of the general maneuver barrier with the scan barrier, then the maximum time barrier is completed by the equations:

$$X - \Delta t_s V_F \left(\frac{1}{V_{F/B}} - \cos\phi\right) = -(Y - \Delta t_s V_F \sin\phi)\cot(\phi - C\mu) + \frac{F}{V_{F/B}} \tag{9-17}$$

Figure 9-4 shows the complete composite barrier. Only if the interceptor begins the terminal phase of the air battle from within this boundary can it have a finite probability of killing the target.

Figure 9-5 presents a simplified schematic of barrier formulation of the terminal air battle.

(f) NORTAM FORMULATION

Instead of barrier formulations, simulation techniques can be used for the analysis of the terminal air battle. One of these techniques is the Nortam (Northrop Terminal Attrition Model) Formulation. This is a three-dimensional mathematical model of a simulated engagement. It employs Monte Carlo techniques with sequential sampling and independent sub-model analysis. A simplified schematic is shown in Figure 9-6.

Each box represents a sub-model. These handle various events of the attack such as initial positioning, bomber maneuver, fighter progression, bomber defensive sequence, detection and lock-on, electronic countermeasures (ECM), fighter counter tactics, conversion and armament launch, etc.

The Initial Positioning Point (IPP) sub-model computes the location of the ideal IPP and the standard deviations of the expected errors in

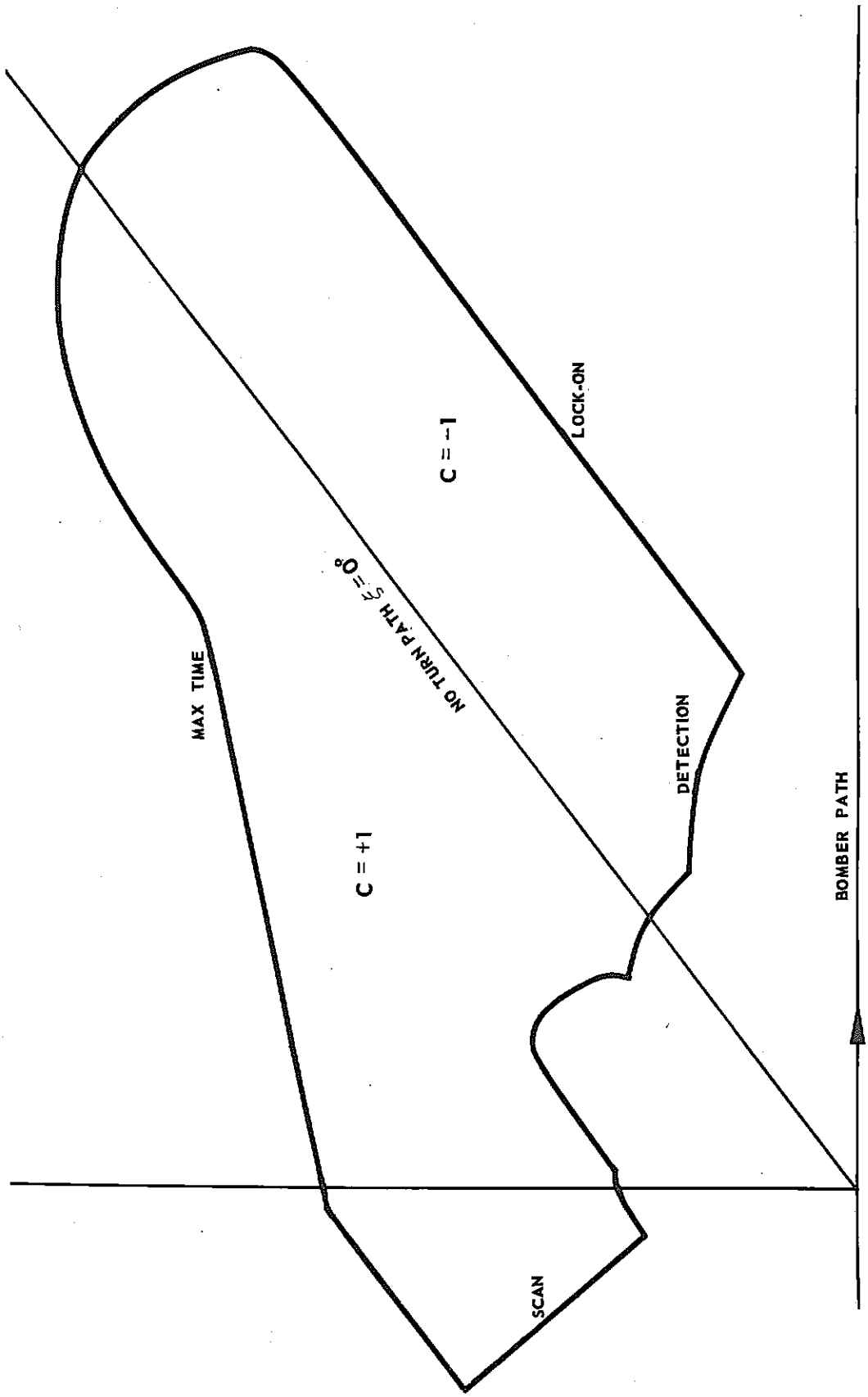

FIGURE 9-4. REPRESENTATIVE COMPOSITE BARRIER

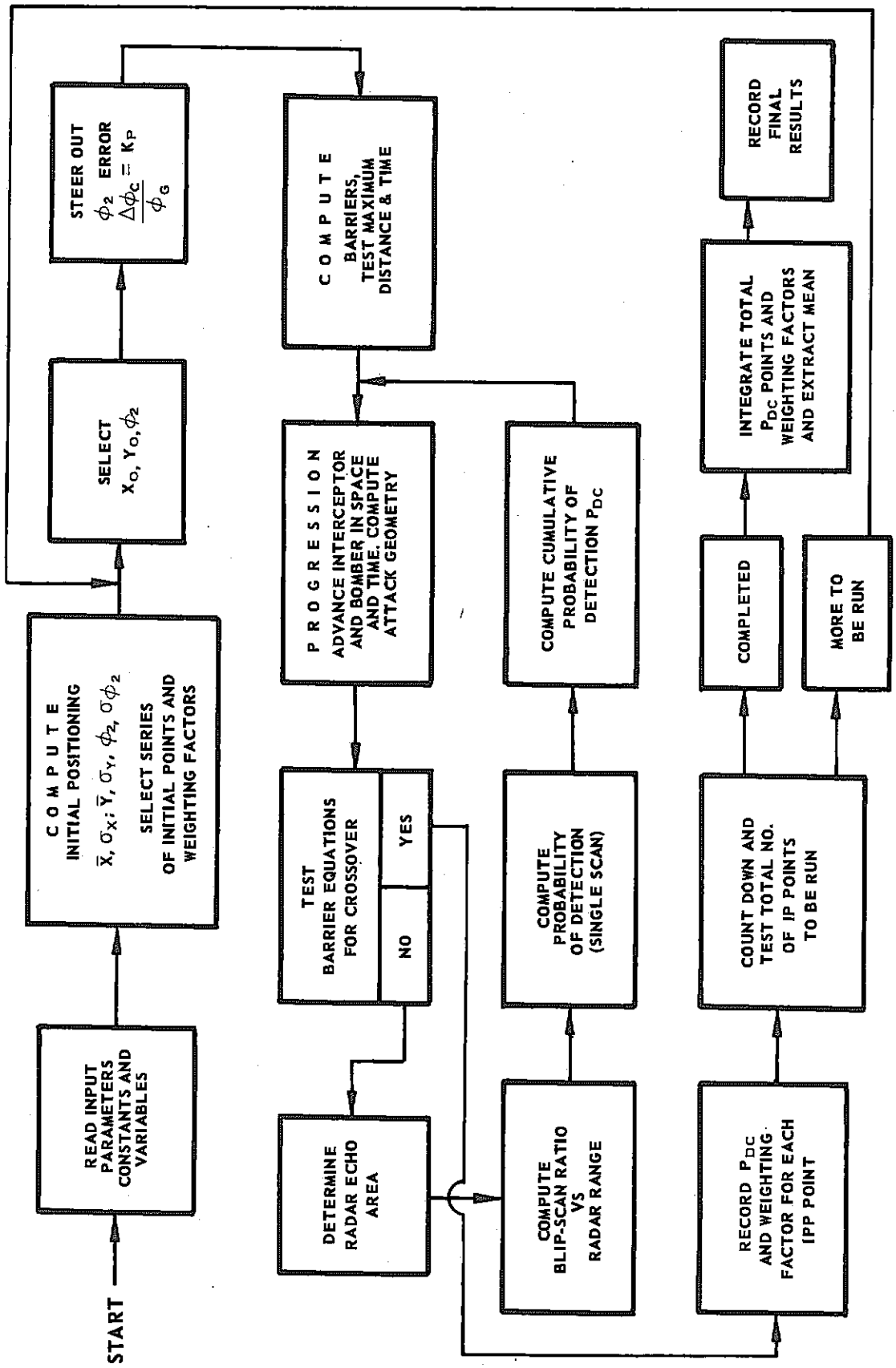

FIGURE 9-5. SIMPLIFIED SCHEMATIC OF BARRIER FORMULATION TERMINAL AIR BATTLE

location and heading. Using the Monte Carlo method with sequential sampling about the IPP, successive passes through the model are made until the probability of detection and conversion can be established within a specified degree of confidence.

A bomber maneuver is controlled by an input code to occur either during the search phase or tracking phase. Also specified is the type maneuver, such as a climb, dive, or turn; and the maneuver can be repeated as desired. In the Progression Box the fighter moves with respect to the bomber through one time interval. The expended time is checked against the maximum allowable time per run. If the maximum allowable time is exceeded, a time abort is declared. Range is checked also for an opening attack. The bomber sequence sub-model checks the status of the bomber at each time interval to determine if it carries armament. The bomber search, detection, lock-on and armament release are handled in a manner similar to that of the fighter except that the bomber does not maneuver to a firing position.

When the fighter is within radar range of the bomber, the detection and sub-model are entered. Here the probability of a target blip appearing on the radar scope during one time interval is computed. This probability is compared with a random number to determine if detection has occured. The fighter progresses after detection until it is within lock-on range and acquires the target.

After lock-on the Geometry Box computes the changes in heading and/or elevation necessary to intercept the bomber on a specified type course-lead collision or pursuit, as well as the amount of time required. The maximum allowable changes in heading and elevation are computed and compared with the required changes. The smaller of the required or allowable changes is steered out in the Progression Box.

The ECM Box is controlled by an input code to select the type ECM desired for evaluation. This may include no ECM, chaff, noise jammers or varying combinations. The probability of break lock is computed and compared with a random number. If lock is broken, the fighter countertactics sub-model is entered. This countertactic is specified by code. The fighter executes the countertactic until lock-on is regained or the attack is aborted.

After lock-on or relock, armament preparation begins. If too much time is lost acquiring lock-on, the attack may be aborted due to

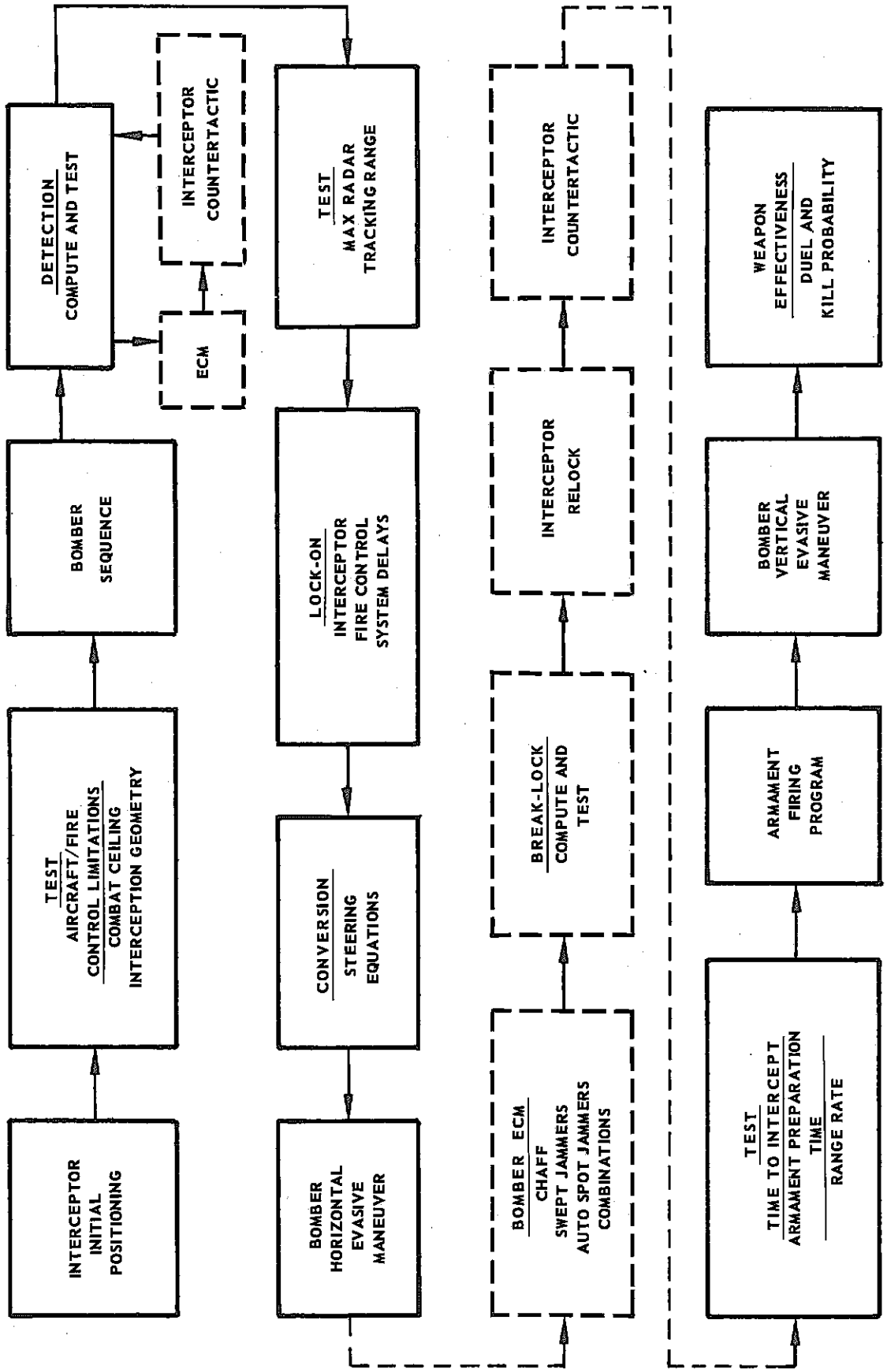

FIGURE 9-6. SIMPLIFIED SCHEMATIC OF NORTHROP TERMINAL ATTRITION MODEL (NORTAM)

insufficient time to prepare the armament. The armament is launched when the bomber is within range, and the fighter breaks off the attack.

(g) COMPARISON OF BARRIER AND SIMULATION TECHNIQUES

Simulation techniques are very flexible in their application. They can be used to evaluate lead pursuit, lead collision or other modes of attack. The mid-course angle and terminal angle of attack can be varied as well as load factor, armament range, radar echo area, ECM, and speeds in order to determine their sensitivity. Pulse and pulse doppler radar can be evaluated in addition to infrared and other tracking systems. Simulation techniques are most effective for determining (1) attrition planning factors for current weapons, (2) combat tactics and doctrine for current weapons, (3) weapon improvement objectives and requirements, and (4) general terminal attrition data for weapon system development planning.

Barrier techniques cost less since they require fewer inputs and less computer time than simulation techniques. However, their effectiveness, without a large increase in complexity and cost is usually limited to a non-maneuvering bomber. Their optimum utility lies in the determination of radar and fire control system design parameters.

(h) MISSILE SIMULATION TECHNIQUES

The above barrier or simulation analysis is completed when the interceptor fires at the target or breaks off the attack. This is not a complete analysis of the weapon system. The weapon itself also must be evaluated in terms of the fire control system. The purpose is to determine the effectiveness of a weapon of given CEP (or to determine the CEP for a given weapon). If the weapon is an air-to-air missile, simulation techniques generally are used to analyze the weapon. The missile is simulated as part of an interceptor fire control system.

A complete simulation can include six degrees of freedom in three dimensions for the missile. Equations for the aerodynamic characteristics of the missile are incorporated into the computer set-up. These include equations for such factors as lift, pitching, yawing and rolling moment, drag, and various empirical coefficients. The simulation should develop the launching envelopes for the specific missile. This is a volume from within which the missile must be fired in order to hit the target. Boundaries are set by such factors as minimum range, maximum

range, look angle of the missile, and ability of the missile to counteract gravity effect. The boundary is an estimate of the effective performance limits of the missile against a given target.

Finally, with a missile of given CEP, the probability of kill P_k against a specific target is determined. This can be obtained by evaluating statistically a number of runs as in Monte Carlo techniques. Another approach is to analytically express the target vulnerable area and by mathematical formulation derive the single shot probability of kill. (The problem can be reversed to provide the required CEP for a given kill probability.)

SECTION 3 — MISSION EFFECTIVENESS

To determine the effectiveness of a given weapon system, several phases of the mission must be investigated. These phases include the ground phase (combat readiness, costs, maintenance, etc.) the takeoff and climb phase (abort rate, vectoring errors, type of control), and the terminal attack phase. In general, the terminal attack phase is the most significant. This phase is composed of four steps - detection, conversion, launch, and kill. The terminal effectiveness of an interceptor is expressed by stipulating a reasonable combat performance in terms of the probability of detection and conversion (P_{DC}), i.e. the probability that an interceptor will detect a hostile aircraft from a position such that the attack course is possible. Missile effectiveness is evaluated by the probability of a kill (P_k). In estimating the effectiveness of an interceptor which attacks along an AI radar-directed course, one of the steps involved is the determination of the probability that the interceptor detects the hostile aircraft in such a position that attack is possible. Thus there must be found probabilities of detection when conversion to an attack is possible for all possible approach paths. The quantity desired, then, is the average expected value of these probabilities. This value of P_{DC} depends upon the following parameters:

1. Vectoring accuracy during search phase
2. Interceptor and target speed
3. Interceptor turn capability
4. Interceptor weapon characteristics
   A. Range versus time of flight
   B. Desired time of flight as a function of altitude

C. Missile preparation time prior to launch
D. Missile launch envelopes

5. Interceptor AI Radar Characteristics
   A. Blip-scan ratio as a function of range
   B. Field of view or scanning limits
   C. Time required to scan entire field of view
   D. Level of radar maintenance
6. Interceptor Fire Control System Requirements
   A. Identification (detection) time
   B. Time to lock-on
   C. Maximum allowable lock-on range
   D. Time required to reduce steering errors
   E. Time to reduce computer transients
7. Target Radar Echo Area

Therefore, the probability of success of a mission may be considered as the product of two probabilities:

1. The probability of detecting and converting on the target sufficiently early for the interceptor to bring its missiles into effective firing position and readiness (P_{DC})
2. The probability of weapon kill (P_K)

Specific techniques for computing these items have been discussed in the preceding section by either barrier or simulation formulations. The probability of weapon effectiveness is greatly dependent upon the characteristics of the weapon itself, including such items as homing accuracy for a missile, ballistic dispersion patterns, susceptibility to countermeasures.

As an example, assuming zero aim bias and the applicability of the normal (or Gaussian) distribution, the following equation gives a good approximation to the probability of a single shot hit on a circular target of radius R.

$$P(R) = 1 - \exp\left[-\frac{R^2}{2\sigma^2}\right] \tag{9-18}$$

where σ is the standard deviation computed from fire control system analysis. The assumption of zero aim bias merely means that the fire

control system is aiming correctly at the center of the target (or target projected position) at the time of missile launch. The errors remaining are then considered to be of a random nature, each with its own standard deviation. The total system standard deviation is then the square root of the sum of the squares of the individual error standard deviations. The CEP usually is specified for armament accuracy. CEP is the Circular Error of Probability and denotes the radius of a circle containing 50% of the single shots. Consequently, in the above formula it would denote a value of R for which P = 0.5. The above formula thus can be rewritten by solving for $\sigma = f(\text{CEP})$ by the substitution of P(R) = 0.5 and R = CEP which yields

$$P = 1 - \exp\left[-\frac{(1.18)^2 R^2}{2(\text{CEP})^2}\right] \tag{9-19}$$

for a circular target of any radius R.

If the probability of destroying a point target with armament of given CEP and known lethal radius (LR) is desired, the above expression becomes

$$P = 1 - \exp\left[-\frac{(1.18)^2 (\text{LR})^2}{2(\text{CEP})^2}\right] \tag{9-20}$$

When the target has a finite radius (TR), the expression is

$$P = 1 - \exp\left[-\frac{(1.18)^2 (\text{LR-TR})^2}{2(\text{CEP})^2}\right] \tag{9-21}$$

It should be noted that as the lethal radius increases, the CEP proportionately increases for the same probability of success. In effect, system accuracy requirements are reduced as expressed in terms of CEP.

If the number of shots is large against a given target, further approximation can derive the following kill probability

$$P_K = 1 - e^{-NP} \tag{9-22}$$

where P is the single shot probability and N is the number of shots. If the number of shots is small, the probability of a hit can be approximated by a binomial distribution.

It should be noted that the above elementary discussion assumed a circular target approximation. More precise results can be obtained by applying numerical integration methods to a geometrical description of the target. However, the increase in computation time is significant since, in general, analytical methods of target area formulation do not exist and numerical approximation techniques must be applied. However, these techniques are suitable for computer mechanization procedures.

SECTION 4 — FORCE EFFECTIVENESS

The previous section outlined the major techniques for the evaluation of weapon effectiveness. In general it should be noted that the complete determination of the effectiveness of a particular type of aircraft with a given armament against a bomber with a particular armament system for even a single altitude, single direction of attack, and fixed intercept velocities is an enormous task. Such investigations generally are carried out with large-scale computing equipment. A limited investigation generates hundreds of pages of data. Finally, the systems analyst still has no more than a cursory indication of the performance of a given system under limited conditions. The synthesis problem which relates to a method of picking optimum parameters has not yet been solved. The analysis problem is only imperfectly solved. Even so, the above limited data for the weapon system must be used as the basis for the study of the integration of this weapons systems with other weapons systems in a force effectiveness analysis. The force itself may be of heterogeneous composition. The general problem of the systems analyst is to minimize cost in achieving a given level of force effectiveness. (Other criteria may be used, such as minimum time, maximum destructiveness, etc.). Since the general problem is basically one of maximization of strategy, two relatively recent systems engineering techniques can be readily applied to force effectiveness studies. These are linear programming and game theory. As an example of the application of linear programming, consider the case where it is desired to assign an optimum force at a minimum cost for a maximum force effectiveness. The problem attempts to allocate a finite amount of available material and labor to the construction of certain weapons: antiaircraft guns, fighter planes, and guided missiles. The total expected value of the number of kills of enemy bombers is to be maximized. The following table gives the requirements (Table 9-1)

TABLE 9-1. MAXIMUM FORCE EFFECTIVENESS PROBLEM

	Units of Material Per 1000	Units of Labor Per 1000	Expected Kills Per 1000
Antiaircraft Guns	3	1	400
Fighters	1	1	300
Missiles	1	3	400
Maximum Total Available	25	50	

The expected kills would be obtained from a weapons systems effectiveness study as shown in the earlier section. Assuming the number of thousands of guns be X, the number of thousands of fighters Y, and the number of thousands of missiles Z, we obtain from the above table the following inequalities

$$3X + Y + Z \leq 25$$

$$X + Y + 3Z \leq 50$$

The inequality expresses the condition where all available material and labor are not used. The expected number of kills is

$$K = 400X + 300Y + 400$$

and this expression is to be maximized. Since only positive numbers of weapons can be built, the inequalities shown following, results.

$$X \geq 0, Y \geq 0, Z \geq 0$$

The solution by standard linear programming techniques is

$$X = 0$$

$$Y = 25/_2$$

$Z = 25/_2$

$K = 8{,}750$ maximum

The generalized linear programming problem can be outlined by the following matrix

TABLE 9-2. LINEAR PROGRAM MATRIX

	U1	U2			Uj			Um	
X1	A11	A12			A1j			A1m	C1
X2	A21	A22			A2j			A2m	C2
Xi	Ai1	Ai2			Aij			Aim	Ci
Xn	An1	Am2			Anj			Anm	Cn
	b1	b2			bj			bm	

For the general minimization problem, the function

$$C = \sum_{i=1}^{n} C_i X_i \tag{9-23}$$

subject to m inequalities of the type

$$\sum_{i=1}^{n} Aij \; X_i \geq b_i$$

and n inequalities of the type

$$X_i \geq 0$$

is to be minimized.

The general maximization problem is to maximize the function

$$K = \sum_{j=1}^{m} b_j U_j \tag{9-24}$$

subject to n inequalities of the type,

$$\sum_{j=1}^{m} A_{ij} U_j \leq C_i$$

and m inequalities of the type

$$U_j \geq 0$$

Every linear programming problem can be converted into a two-person zero-sum game. The zero-sum merely means that the net gains and losses of both persons are equal to zero.

Although much has been written about game theory in the past ten years, the practical applications of this theory are not extensive. The difficulty of properly setting up the matrix of the game often reduces the validity of the solution due to the necessity for many assumptions which are only rough approximations to the real situation.

The practical problems to which game theory is applicable are those in which there is a conflict of interests and the participants have some control over the outcome. The practical problem that can essentially be solved is the two-person zero-sum game. Almost every military situation can be so categorized. The objective of game theory is to find an optimum strategy (defined as a strategy which gives the player the greatest expected value of payoff) and to determine the value of the game (that is, the expected value of the pay-off if players use optimum strategies).

In reducing a game-theory problem to mathematical form, all possible strategies for each player are enumerated and arranged in the form of a matrix as shown below, (Table 9-3).

TABLE 9-3. GAME THEORY MATRIX PROBLEM

		RED				
		1	2	3	4	Row Minima
BLUE	1	+4	-2	-3	0	-3
	2	+1	-1	0	+3	-1
	3	+2	0	+1	+3	0
	4	+3	-2	-4	0	-4
	Column Maxima	+4	0	+1	+3	

The blue player is considered the maximizing player and the red player the opposing or minimizing player. The terms in the matrix could represent the following hypothetical situation. Blue's forces consist of four different interceptors, each with a different type of fire control system 1, 2, 3, 4. Red has available four different ECM equipment, the effectiveness of each ECM equipment against each interceptor being indicated relatively by the terms in the matrix. Thus if blue selects interceptor number one and red selects ECM equipment number one, a relative advantage of -4 accrues to blue. The problem is to determine the optimum strategy for blue. This simple matrix contains a saddle point. This is a point where the max-min equal the min-max. The max-min is the maximum value of the row minima and represents the minimizing of losses by blue. Conversely the min-max is the minimum value of the column maxima and is equivalent for red. The above criterion is called the minimax principle and lies at the basis of game theory solution methods. The saddle point in the above matrix lies at row three, column two at a value 0. So thus blue should play pure strategy row three and red should play pure strategy column two. If the game does not have a saddle point a mixed strategy will be derived at. As theory progresses, additional applications of game theory will be found.

Upon completion of the analysis the systems analyst will recommend an optimum composition of various types of forces for the accomplishment of the mission assignment. However, interpretation of the results should be weighed with evaluation of the assumptions used to develop the results.

APPENDIX A

ASSOCIATED FIRE CONTROL SUBSYSTEMS

APPENDIX A

ASSOCIATED FIRE CONTROL SUBSYSTEMS

The major interest of this volume, although concerned with the fire control system, does not describe in detail many major facets of a complete system. Thorough treatment of these remaining system components is worthy of a separate study, and it will deal with such items as navigation to the target area, takeoff and landing, communication techniques, and identification techniques.

A few of the subsystem details, including requirements and problems, are given in the following paragraphs.

TRACK-WHILE-SCAN SYSTEM

A track-while-scan system may be used advantageously in conjunction with the computer. After the target has been selected by the pilot, the values of angular position and the relative velocity, $\dot{R}$, are stored in the computer. In addition, the measured range must be stored in the computer. One method for tracking in range is by locking onto the apparent target range and then varying the pulse repetition frequency so as to keep the echo pulse positioned at the midpoint of the interpulse interval. True range then can be calculated from a knowledge of true range and the repetition rate. Thus if

$$R = (M + 1/2)\, t_r \qquad \text{(A-1)}$$

where R is the range measured in units of time, M is an undetermined integer, and t_r is the interpulse period; then, since t_r is the reciprocal of f_r, the prf,

$$t_r f_r = 1 \qquad \text{(A-2)}$$

Differentiating the two above equations with respect to time gives

$$\dot{R} = (M + 1/2)\, \dot{t}_r \qquad \text{(A-3)}$$

and

$$t_r \dot{f}_r + \dot{t}_r f_r = 0 \qquad \text{(A-4)}$$

These can be combined with Equation A-1 to give

$$R = \frac{-\dot{R} f_r}{\dot{f}_r} \qquad \text{(A-5)}$$

where $\dot{R}$ is measured by the velocity tracking system and the rate of change of the repetition rate can be found from the repetition rate. Range is therefore found by this simple computation.

In the track-while-scan system, as the system continues to search, the values of azimuth, θ, elevation, ϵ, and range rate, $\dot{R}$, are passed through gates which allow information to flow in the memory circuits from the radar receiver on each scan when the antenna is at the appropriate azimuth and elevation angles. The gates are repositioned on each scan with current and predicted target information. Thus, the outputs from the various gates and memory circuits represent estimates of the target coordinates. These outputs can be supplied to the computer for transmittal as coordinates to the display system and for controlling interceptor functions.

TRACKING ON JAMMING

Another useful technique which can be included in the fire control system is the track on jamming scheme. Electronic jamming has a basic disadvantage since it emits electromagnetic radiation, revealing to the jammed aircraft its angular position. The jamming source can be tracked in angle by detecting the conical scan modulation and using it to operate the interceptor radar antenna angle error servo. In this mode of reception the angle error circuits must not be operated during the transmit time or at ranges where ground clutter is anticipated since homing would be initiated on these signals. This can be accomplished in the pulse doppler radar by using range multiplexing for eliminating transmitted pulses and frequency discrimination for eliminating ground return. The output signal from the tracking system would be treated in the normal manner. A threshold indication device would be used to switch from normal to track on jamming mode. When the normal

tracking modes are disrupted by jamming, this threshold device would then be activated.

IDENTIFICATION SYSTEMS

The identification system includes the ground-to-air identification function and the air-to-air identification function. Air-to-air identification is accomplished using an interrogator-responder in conjunction with the interceptor radar which sends a coded interrogation signal to all aircraft. Upon reception of the coded interrogation, friendly aircraft which are equipped with the proper transponder return a coded reply to the interrogator-responder. The correct reply is received and a characteristic identification is displayed on the radar indicator, completing the friendly aircraft identification process. If the reply is incorrect or if no reply is received the aircraft is identified as suspect.

The ground-to-air identification takes place when a ground station sends out interrogation signals to unidentified targets. Interceptors equipped with a suitable transponder and having the proper code will be identified properly.

COMMUNICATION SYSTEM

Verbal communication is required for air-to-air and air-to-ground communication. In addition, data link is necessary in order to coordinate with a ground control system such as SAGE. Data link messages provide the interceptor with vectoring and target acquisition information. Also included in the communication group is the UHF automatic direction finder for obtaining bearing data from transmitters.

If operation outside the useful range of ground vectoring equipment is desired, the communication ability of the system may be severely restricted. Various methods of propagation can be used, such as meterorite scattering, ionospheric, troposheric, or frequency diversity for communication beyond the line of sight. The principal problem in the reception of any type of communication is in the recovering of useful signals which are below detector noise thresholds. Here modern information theory concepts can be applied. Coding can be so arranged that redundancy is included in the received signal to improve the apparent signal-to-noise ratio for the same channel capacity. The apparent transmitter power can be increased by reducing the bandwidth. Thus the principals on which improvements can be based include a reduction of the apparent communication

bandwidth, decreasing the bit rate (information rate), using much of the intersymbol influence, improving the detector efficiency (since the signal can be made to add directly while the noise adds quadratically with increased redundancy), and using optimum filters. In general, the problem is one of determining the minimum information bandwidth and the maximum transmission rate and operating at maximum channel capacity. To make optimum use of the trade-off between signal-to-noise ratio and bandwidth, a suitable modulation scheme must be used. Frequency modulation techniques may be used with some improvement. Pulse code type of digital transmission may prove to be a more successful method of communication than the classical methods. Much of the results of information theory can be used in pulse code transmission to combat noise (including noise combating codes), and to obtain optimum trade-off between bandwidth and signal-to-noise ratio.

CODING

Since the ground control must provide data messages for many interceptors, each message from the ground is required to be coded; decoding equipment is required onboard the interceptor for accepting and decoding these messages. To instrument such a system, it is necessary not only to accept digital transmission in a binary system, but also the system must accept and synchronize with the synchronizing pulses which identify the beginning of each coded number. The use of redundancy as an anti-jamming method has been discussed as a desirable element in such a system. Redundancy, as used for the detection of errors, is described in Appendix D. The same message can be repeated and compared pulse by pulse. The decision then is made that a pulse or space exists at a specific position only if it appears in a majority of the received messages. Because of the random nature of noise, there is low probability that pulses will be injected or deleted in the same sequential position for repeated messages. For example, a message is repeated N times and the message is to be rejected by the airborne decoder unless all agree the likelihood that an error has been passed is quite small. The larger the value of N, the smaller is the signal-to-noise ratio required to prevent error. Repetition of messages can take place in two ways: (1) the message may be simultaneously transmitted over N frequency channels and the received signals instantaneously compared or (2) the message can be transmitted over one channel and each coded information element repeated N times during the message. The received pulses

are stored and counted at the end of the sequence. The process is equivalent to taking the product of the bandwidth required by the time of transmission.

Although the airborne equipment is capable of operating with low data rates, the transmission system must be able to transmit high data rates in order to communicate with numerous interceptors and to change messages to the interceptor as required. These changes must not be delayed by the transmitter data handling capacity. In case of severe jamming, the messages may be rejected by decoding apparatus, and consequently the accepted messages rate would be less than the transmission rate. If, during jamming, the messages were accepted at the rate of transmission, the probability of erroneous messages would increase.

The message decoder in the interceptor contains circuits which convert the received binary numbers into electrical signals which can be utilized by the fire control system or the pilot. The binary number is generally converted to a dc voltage proportional to the value of the number. Pulses from the synchronizer reset the decoder at the beginning of reception of each new number. In addition, a selector gate routes each decoded number into a proper channel. The selector gate also operates relays which indicate the correct operation of the system up to that point and warn the pilot if the decoder fails to operate. Repeated failure to accept and decode incoming messages indicates that the system is subject to malfunction (or possible jamming).

NAVIGATION

The navigation problem, although not specifically a part of the fire control attack problem, is discussed here. Airborne navigation equipment may utilize ground navigation stations such as TACAN, SHORAN, LORAN, OMNI and DME, as well as airborne inertial navigation systems. Because of the possibility of losing ground vectoring information due to jamming or other reasons, the inclusion of an inertial navigation system is valuable. One possible inertial navigator might utilize a stabilized coordinate system (provided by three gyros) and a gimbal platform with accelerometers set along the orthogonal axis. The three gyros are used to stabilize the platform in the selected coordinate system. The servo system used for platform stabilization may employ integrating accelerometers or rate and acceleration measuring gyros for detection of error and compensation. Synchros mounted on the gimbal axes of an inertial

navigator permit determination of heading, pitch, and bank angles. The inertial navigation accuracy capabilities are about two miles of positional error per hour of flight. The inertial guidance system may also supply an inertial reference for use by the antenna stabilization loop. This stabilization counteracts the effect of interceptor maneuvers so that the angle tracking radar is required to follow only the space motion of the line of sight to the target.

INERTIAL NAVIGATION

In inertial navigation, horizontal acceleration is used to determine changes in position. Gravity is an accurately known function of position on the earth. Inertial navigation is then performed based on the mechanization of the dynamic equations of motion. The inertial directions depend on the inertial frame of reference.

The principal law on which inertial navigation is based is the law of conservation of angular momentum. Thus, the spin axis of a free gyro maintains a constant initial direction in the absence of external torques. Even if the equipment used for inertial navigation were perfect and not subject to external torque, the inertial navigator would still be subjected to a periodic oscillation (called the Coriolis effect) about the correct flight path. Therefore, unless independent velocity or position measurements are available in flight, accurate navigation by inertial techniques requires a continuously operating system to compensate for unwanted changes in position. Inertial navigation requires the use of sensing devices such as accelerometers and acceleration measuring gyros which respond to direction and magnitude of acceleration. Navigation by inertial methods is used as a substitute or as an aid during periods when ground vectoring or beacon information is inadequate. Limitations in inertial guidance exist as a result of development limitations rather than by any basic theoretical limitations. Directional gyros presently have drift rates on the order of 1 to 10 degrees per hour; using these equipments in an inertial navigator to establish inertial reference directions would cause position error of 60 to 600 nautical miles per flight hour. If the accelerometers have a total sensing range of $\pm$ 1 g and an accuracy of one tenth of one percent, it contributes an average position error of approximately 3 1/2 nautical miles to an inertial navigator.

AUTOMATIC LANDING AIDS

Landing system equipment includes instrument landing system equipment, such as localizer, glide slope, and marker beacon receivers. In addition, automatic ground control approach is supplied from ground control approach (GCA) centers.

AIR DATA SUBSYSTEM

A knowledge of the tactical situation is required during flight in order to launch the missiles properly. The information required is mach number, static pressure, impact pressure, ambient temperature, total temperature, and angle of attack. The computations which use the measured data are performed by the fire control system computer. From measurements of total pressure, static pressure, angle of attack and total temperature, the mach number, the indicated angle of attack, the true pressure and the altitude are determined by computation.

APPENDIX B

EXAMPLE OF A WEAPON SYSTEM INTERCEPTION MODEL

APPENDIX B

EXAMPLE OF A WEAPON SYSTEM INTERCEPTION MODEL *

An illustrative mathematical procedure for simulating an encounter between an interceptor weapon system and a target aircraft is developed to demonstrate capabilities of the weapon system against both passive and maneuvering targets.

The progress of an attack is simulated by the use of digital computer iteration techniques on a set of equations defining the response of the fire control system (FCS), the interceptor pilot, and the aircraft to initial inputs. Starting with inputs as defined by the initial attack geometry, the solution of the set of equations by use of a digital computer provides data for determining capabilities of the weapon system. A block diagram of the interceptor model is shown in Figure B-1.

The various factors involved are assumed to vary along paths constructed of short, straight line segments, with each segment representing 0.1 second. The following simplifying assumptions are made as indicated:

1. The fire control system is essentially noise free.
2. The interceptor
   (a) Thrust, drag and lift coefficient ($C_{L\alpha}$) are proportional to airspeed and altitude.
   (b) The angle of attack is proportional to airspeed load factor and $C_{L\alpha}$.
   (c) The weight is constant.
   (d) There is no sideslip (coordinated maneuvers).
3. Target
   (a) The target maintains constant speed and altitude.
   (b) Target maneuvers are initiated at specified ranges and at specified turn rates.
   (c) The target maneuver is terminated at launch signal.

* Norair Technical Publication TM 3574-59-14 by R.F. Moyer

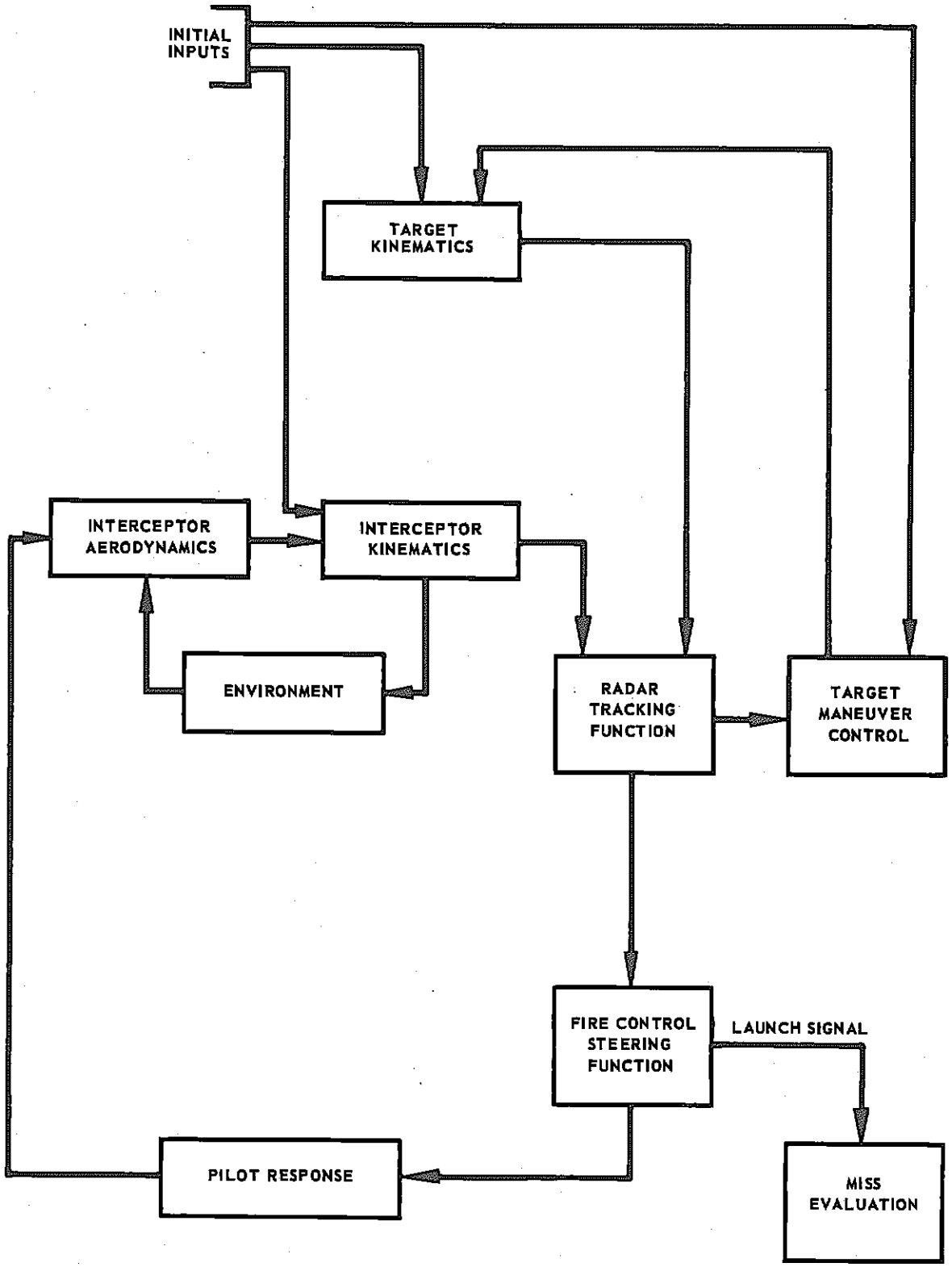

FIGURE B-1. BLOCK DIAGRAM WEAPON AND TARGET MODEL

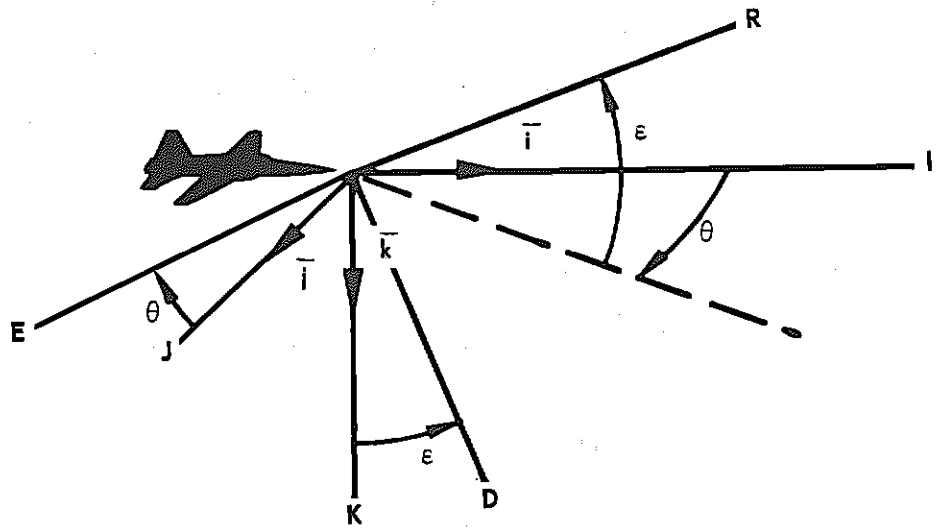

FIGURE B-2. INTERCEPTOR AND RADAR COORDINATE SYSTEM

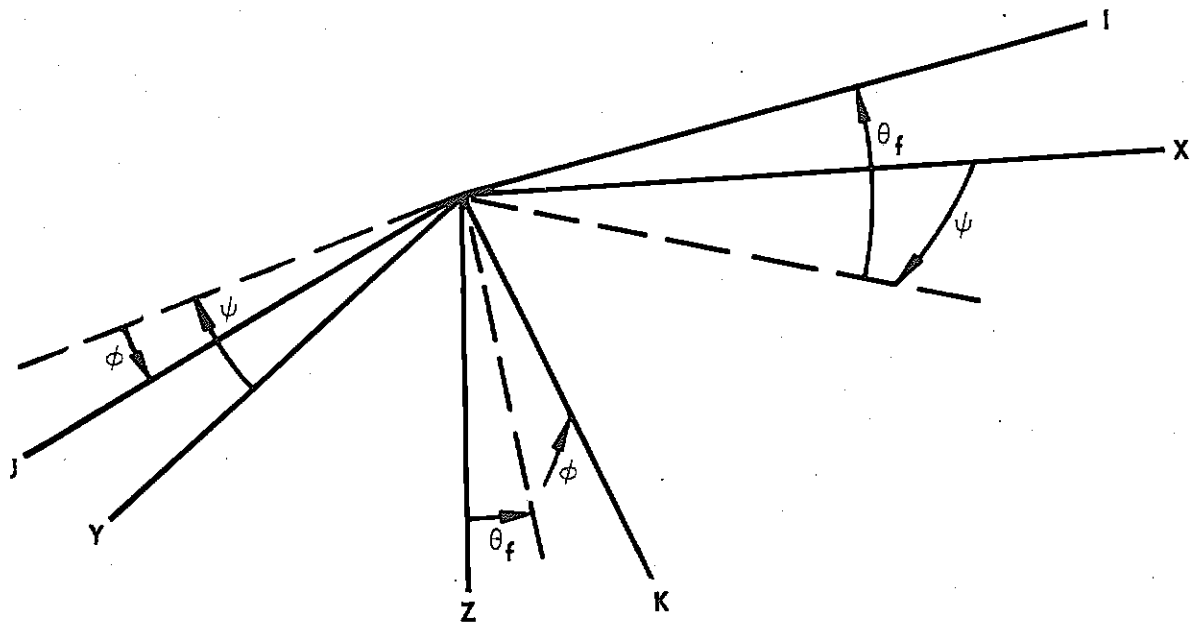

FIGURE B-3. SPACE AND INTERCEPTOR COORDINATE SYSTEM

4. Pilot response
   (a) The load factor is proportional to elevation steering error, but is subject to aircraft limitations.
   (b) Roll angle and turn rate are proportional to azimuth steering error.

COORDINATE SYSTEMS

The interceptor coordinate system, radar coordinate system, and the space coordinate system are used in the derivation of the simulation equations. It is necessary to convert parameters defined in each of these systems to the others to complete the derivations.

The INTERCEPTOR coordinate system (Figure B-2) consists of an I-axis (positive forward) which lies in the vertical plane of symmetry of the airplane along the mean launcher reference line (MLRL), a K-axis (positive downward) which lies in the vertical plane of symmetry perpendicular to the I-axis, and a J-axis (positive to the right) perpendicular to both the I- and K-axes. Unit vectors parallel to these axes are denoted by $\bar{i}$, $\bar{j}$, $\bar{k}$.

The RADAR coordinate system (Figure B-2) consists of an R-axis (positive forward) along the radar line of sight (LOS), an E-axis (positive to the right) perpendicular to the R-axis and in the interceptor's (I-J) azimuth plane, and a D-axis (positive downward) perpendicular to both the R- and E-axes. Unit vectors parallel to these axes are denoted by $\bar{r}$, $\bar{e}$, $\bar{d}$.

Figure B-2 illustrates the relationship between the axes of the interceptor and the radar coordinate systems. The direction of the radar (R-axis) from the interceptor to the target is given by the azimuth angle, θ, and the elevation angle, ϵ.

The space coordinate system (Figure B-3) consists of a horizontal X-axis (positive toward the north), a horizontal Y-axis (positive toward the east) perpendicular to the X-axis, and a vertical Z-axis (positive downward) perpendicular to both the X- and Y-axes. Unit vectors parallel to these axes are denoted by $\bar{x}$, $\bar{y}$, $\bar{z}$.

Figure B-3 illustrates the relationship between the axes of the space and interceptor coordinate systems. The heading of the interceptor is

given in the horizontal plane by the angle, ψ, the flight attitude by the pitch angle, θ_f, and the roll angle, ϕ.

CONVERSION EQUATIONS

The relationship between the unit vectors in the interceptor and radar coordinate systems is defined by Equations B-1 through B-6.

The relationship between the unit vectors in the interceptor and the space coordinate systems is defined by Equations B-7 through B-12.

$$\bar{r} = \bar{i} \cos\theta \cos\epsilon + \bar{j} \sin\theta \cos\epsilon - \bar{k} \sin\epsilon \tag{B-1}$$

$$\bar{e} = -\bar{i} \sin\theta + \bar{j} \cos\theta \tag{B-2}$$

$$\bar{d} = \bar{i} \cos\theta \sin\epsilon + \bar{j} \sin\theta \sin\epsilon + \bar{k} \cos\epsilon \tag{B-3}$$

$$\bar{i} = \bar{r} \cos\theta \cos\epsilon - \bar{e} \sin\theta + \bar{d} \cos\theta \sin\epsilon \tag{B-4}$$

$$\bar{j} = \bar{r} \sin\theta \cos\epsilon + \bar{e} \cos\theta + \bar{d} \sin\theta \sin\epsilon \tag{B-5}$$

$$\bar{k} = -\bar{r} \sin\epsilon + \bar{d} \cos\epsilon \tag{B-6}$$

$$\bar{x} = \bar{i} \cos\theta_f \cos\psi + \bar{j}\left(\sin\theta_f \sin\phi \cos\psi - \cos\phi \sin\psi\right) + \bar{k}\left(\sin\theta_f \cos\phi \cos\psi + \sin\phi \sin\psi\right) \tag{B-7}$$

$$\bar{y} = \bar{i} \cos\theta_f \sin\psi + \bar{j}(\sin\theta_f \sin\phi \sin\psi + \cos\phi \cos\psi) + \bar{k}(\sin\theta_f \cos\phi \sin\psi - \sin\phi \cos\psi) \tag{B-8}$$

$$\bar{z} = -\bar{i} \sin\theta_f + \bar{j} \cos\theta_f \sin\phi + \bar{k} \cos\theta_f \cos\phi \tag{B-9}$$

$$\bar{i} = \bar{x} \cos\theta_f \cos\psi + \bar{y} \cos\theta_f \sin\psi - \bar{z} \sin\theta_f \tag{B-10}$$

$$\bar{j} = \bar{x}(\sin\theta_f \sin\phi \cos\psi - \cos\phi \sin\psi) + \bar{y}(\sin\theta_f \sin\phi \sin\psi + \cos\phi \cos\psi) + \bar{z} \cos\theta_f \sin\phi \tag{B-11}$$

$$\bar{k} = \bar{x}(\sin\theta_f \cos\phi \cos\psi + \sin\phi \sin\psi)$$
$$+ \bar{y}(\sin\theta_f \cos\phi \sin\psi - \sin\phi \cos\psi) + \bar{z} \cos\theta_f \cos\phi \quad \text{(B-12)}$$

TARGET KINEMATICS

Throughout the attack it is assumed that the target aircraft maintains a constant altitude and velocity and is capable of performing a horizontal turn at a specified turn rate, initiating the maneuver at a specified range between the interceptor and the target.

Initially, the position of the target is defined as A_o, B_o, C_o where A_o and B_o are its initial displacements along the X- and Y-axes, respectively. The initial displacement of the target along the Z-axis, denoted by C_o, is equal to the negative of the target altitude. (See Figure B-4.)

Since the instantaneous velocity vector of the target is at an angle β with respect to the X-axis, the displacement of the target position over the time interval Δt is defined by:

$$\bar{V}\Delta t = \bar{x}V_b \Delta t \cos\beta + \bar{y}V_b \Delta t \sin\beta \quad \text{(B-13)}$$

or

$$\Delta A = V_b \Delta t \cos\beta \quad \text{(B-13a)}$$

$$\Delta B = V_b \Delta t \sin B \quad \text{(B-13b)}$$

The target aircraft initially maintains a constant heading (β_o). When the range (R) between the target and the interceptor is equal to or less than a specified maneuver range (R_m), the target performs a horizontal turn at a specified turn rate ($\dot{\beta}$). The kinematics of the target aircraft can be determined by the following equations:

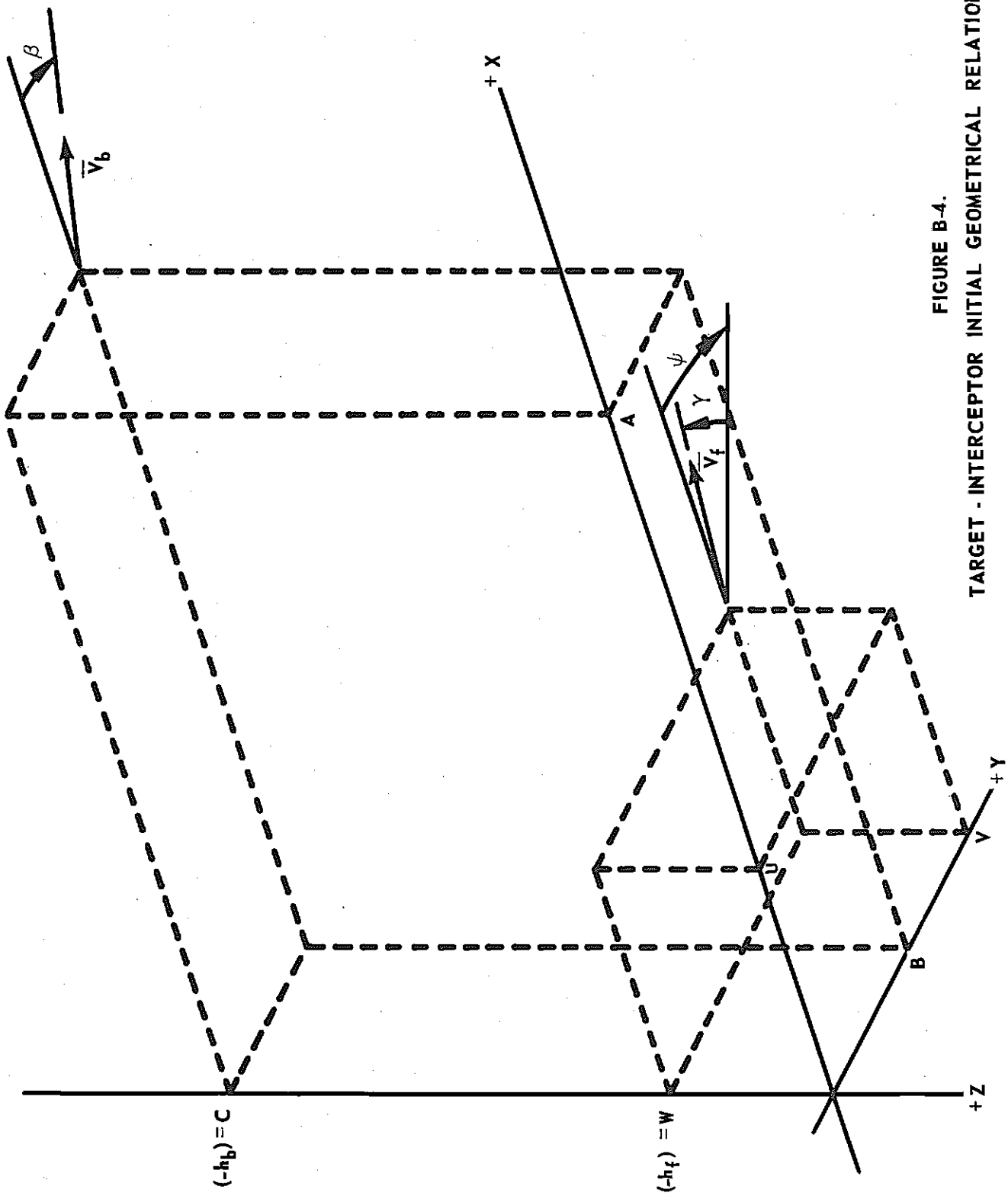

FIGURE B-4.
TARGET - INTERCEPTOR INITIAL GEOMETRICAL RELATIONSHIP

$$A = A_o + V_b \Delta t \cos \beta_o \tag{B-14}$$

$$B = B_o + V_b \Delta t \sin \beta_o \tag{B-15}$$

$$\beta = \beta_o \qquad R > RM \tag{B-16}$$

$$\beta = \beta_o + \beta \Delta t \qquad R \leq RM \tag{B-17}$$

INTERCEPTOR KINEMATICS

The initial position of the interceptor is defined as U_o, V_o, W_o where U_o, V_o, W_o are the initial displacements of the interceptor along the X-, Y-, and Z- axes, respectively. (See Figure B-4.) Since the interceptor is flying at an angle of attack (a) and is assumed to have no sideslip, its displacement in interceptor coordinates during the time interval Δt is:

$$\overline{V}_f \Delta t = iV_f \Delta t \cos a + \overline{k} V_f \Delta t \sin a \tag{B-18}$$

Taking the dot product of the vector displacement $\overline{V}_f$ (Equation B-18) with the three unit vectors, $\overline{x}$, $\overline{y}$, $\overline{z}$, (Equations B-7, B-8, B-9) yields the components of the interceptor displacements in the space coordinate system:

$$\Delta U = V_f \Delta t \sin a \left[\cos\psi (\cos \theta_f \cot a + \sin \theta_f \cos \phi) + \sin \psi \sin \phi \right] \tag{B-19}$$

$$\Delta V = V_f \Delta t \sin a \left[\sin\psi (\cos \theta_f \cot a + \sin \theta_f \cos \phi) - \cos Y \sin \phi \right] \tag{B-20}$$

$$\Delta W = -V_f \Delta t \sin a \left(\cos \theta_f \cos \phi - \sin \theta_f \cot a \right)^* \tag{B-21}$$

* Since the Z-axis is negative up and pitch angle is positive up, the change in vertical displacement is negative when the pitch angle (θ_f) is positive.

The location of the interceptor after any given time interval is obtained by iteration, using:

$$U = U_o + \Delta U \tag{B-22}$$

$$V = V_o + \Delta V \tag{B-23}$$

$$W = W_o + \Delta W \tag{B-24}$$

TARGET-INTERCEPTOR RELATIVE RANGE AND VELOCITY

The position of the interceptor for successive values of time depends upon the maneuvers of the interceptor. These maneuvers are determined by the pilot's response to the steering signals from the FCS and the aerodynamics of the interceptor. The FCS steering signals, in turn, are determined by the relative position and motion of the target with respect to the interceptor.

ANTENNA ANGLES

Figure B-5 illustrates the relative position of the target from the interceptor along the radar LOS, R, and the projection of the range on the interceptor coordinate axes. The azimuth antenna angle (θ) and the elevation antenna angle (ϵ) define the relative position of the radar axes with respect to the interceptor axes. The azimuth and elevation antenna angles and the range may be determined with Equations B-25, -26, and -27.

$$\theta = \text{arc tan}\left(\frac{R_J}{R_I}\right) = \text{arc sin}\left(\frac{R_J}{\sqrt{R_I^2 + R_J^2}}\right) \tag{B-25}$$

$$\epsilon = \text{arc sin}\left(\frac{-R_K}{R}\right) \tag{B-26}$$

$$R = \sqrt{R_I^2 + R_J^2 + R_K^2} \tag{B-27}$$

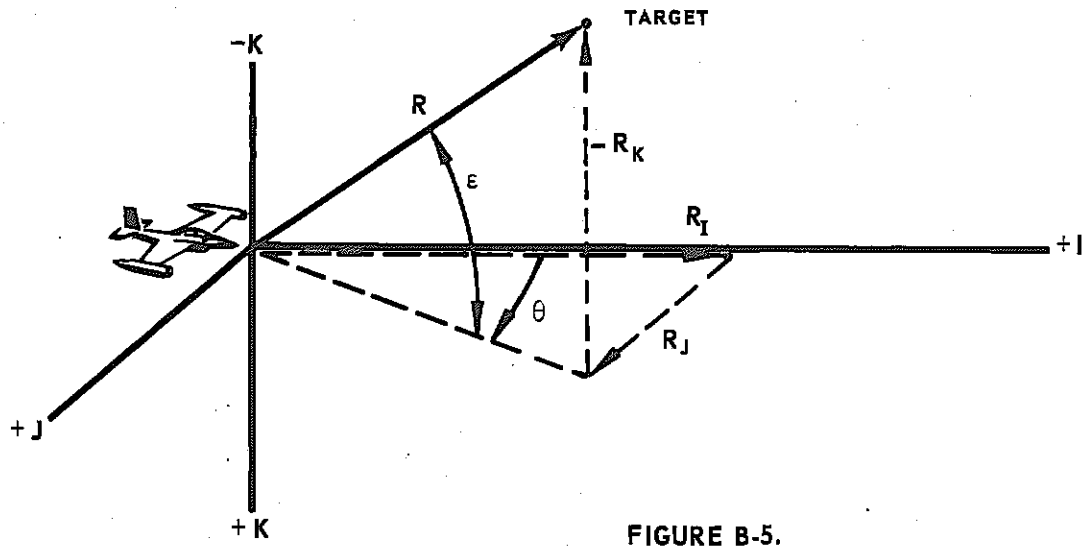

FIGURE B-5.
RANGE COMPONENTS IN THE INTERCEPTOR

1. RELATIVE RANGE

Figure B-6 illustrates the relative positions of the interceptor and the target in the space coordinate system. The range vector in the space coordinate system is defined by Equation B-28.

The dot product of the range vector (Equation B-28) with the three-unit vectors $\bar{i}$, $\bar{j}$, $\bar{k}$ (Equations B-10, B-11, and B-12) yields the components of range in the interceptor coordinate system (Equations B-29, B-30, and B-31).

$$\bar{R} = \bar{x}(A - U) + \bar{y}(B - V) + \bar{z}(C - W) \qquad \text{(B-28)}$$

$$R_I = (A - U)\cos\psi\cos\theta_f + (B - V)\sin\psi\cos\theta_f - (C - W)\sin\theta_f \qquad \text{(B-29)}$$

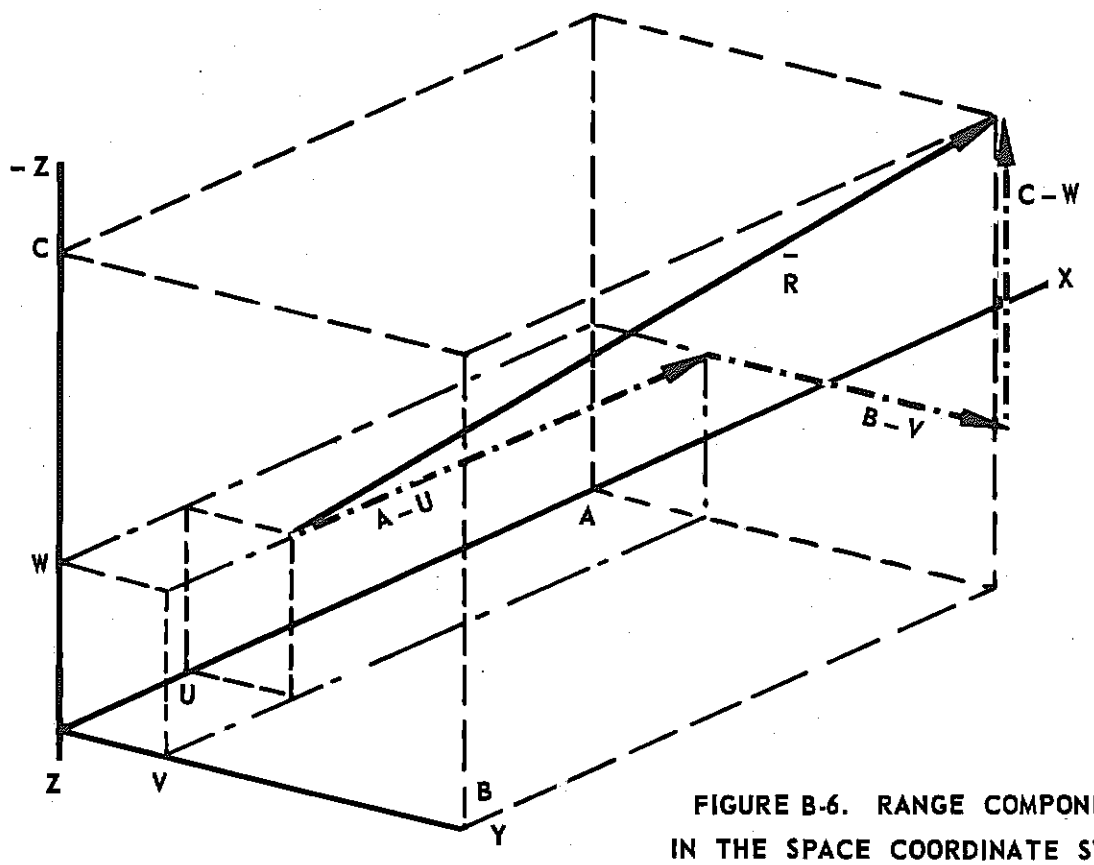

FIGURE B-6. RANGE COMPONENTS IN THE SPACE COORDINATE SYSTEM

$$R_J = (A - U)(\cos\psi \sin\theta_f \sin\phi - \sin\psi \cos\phi)$$
$$+ (B - V)(\sin\psi \sin\theta_f \sin\phi + \cos\psi \cos\phi)$$
$$+ (C - W) \cos\theta_f \sin\phi \qquad \text{(B-30)}$$

$$R_K = (A - U)(\cos\psi \sin\theta_f \cos\phi + \sin\psi \sin\phi)$$
$$+ (B - V)(\sin\psi \sin\theta_f \cos\phi - \cos\psi \sin\phi)$$
$$+ (C - W) \cos\theta_f \cos\phi \qquad \text{(B-31)}$$

2. RELATIVE VELOCITY

The relative velocity of the target with respect to the interceptor is defined as

$$\overline{V}_R = \overline{V}_b - \overline{V}_f \tag{B-32}$$

Taking the dot product of the target velocity $\overline{V}_b$ (Equation B-13) with the three unit vectors $\overline{i}$, $\overline{j}$, $\overline{k}$ (Equations B-10, B-11, and B-12), simplifying and subtracting the interceptor velocity $\overline{V}_f$ (Equation B-18) yields the relative velocity of the target with respect to the interceptor in the interceptor coordinate system (Equations B-33, -34, -35).

$$V_{R_I} = V_b \cos(\beta - \psi) \cos \theta_f - V_f \cos \alpha \tag{B-33}$$

$$V_{R_J} = V_b \cos(\beta - \psi) \sin \theta_f \sin \phi + V_b \sin(\beta - \psi) \cos \phi \tag{B-34}$$

$$V_{R_K} = V_b \cos(\beta - \psi) \sin \theta_f \cos \phi - V_b \sin(\beta - \psi) \sin \phi - V_f \sin \alpha \tag{B-35}$$

The dot product of $\overline{V}_R$ (Equation 36) with the three-unit vectors $\overline{r}$, $\overline{e}$, $\overline{d}$ (Equations B-1, B-2, and B-3) yields the relative velocity of the target with respect to the interceptor in the radar coordinate system (Equations B-37, B-38, and B-39).

$$\overline{V}_R = V_{R_I} \overline{i} + V_{R_J} \overline{j} + V_{R_K} \overline{K} \tag{B-36}$$

$$V_{R_R} = \dot{R} = (V_{R_I} \cos \theta + V_{R_J} \sin \theta) \cos \epsilon - V_{R_K} \sin \epsilon \tag{B-37}$$

$$V_{R_e} = R\omega_d = -V_{R_I} \sin \theta + V_{R_J} \cos \theta \tag{B-38}$$

$$V_{R_d} = -R\omega_e = (V_{R_I} \cos\theta + V_{R_J} \sin\theta) \sin\epsilon + V_{R_K} \cos\epsilon$$

$$R\omega_e = -(V_{R_I} \cos\theta + V_{R_J} \sin\theta) \sin\epsilon - V_{R_K} \cos\epsilon$$

(B-39)

3. FIRE CONTROL SYSTEM EQUATIONS

Equations derived from the geometry of a lead collision attack are solved by the fire control computer.

The intercept is conducted in two phases. After lock-on has been established, the weapon system enters the first phase of the attack. The pilot steers out the azimuth error during phase I of the intercept. This is accomplished in the mathematical model by setting the elevation steering error equal to zero.

When a prelaunch signal is received, the weapon system enters phase II of the interception. The pilot, during phase II, pulls the interceptor into the climbing attitude necessary to center the steering dot, thus producing proper attitude orientation.

4. ENVIRONMENT

The atmospheric environment is defined by Equations B-40 through B-45. The velocity of sound (M) versus altitude (W) is defined by Equations B-40 and B-41. The density of air (ρ) versus altitude is defined by Equations B-42 through B-45.

$$M = 1117 + 0.0041286\,W \text{ when } W > -36{,}089 \text{ ft} \qquad \text{(B-40)}$$

$$M = 968 \text{ when } W \leq -36{,}089 \text{ ft} \qquad \text{(B-41)}$$

$$h = \frac{-W}{10{,}000} \qquad \text{(B-42)}$$

$$\sigma = 1.0 - 0.2923982h + 0.0323548h^2 - 0.0014766h^3 \qquad \text{(B-43)}$$

when $W > -30{,}000$ ft

$$\sigma = 0.943867 - 0.2327232h + 0.0133572h^2 - 0.0003044h^3 \quad \text{(B-44)}$$

when $W \leq -30{,}000$ ft

$$\rho = 0.002378\sigma \quad \text{(B-45)}$$

5. INTERCEPTOR AERODYNAMICS

Aerodynamic functions as illustrated in Figure B-7 have been tabulated in the mathematical model. The coefficient of lift (C_L) and the interceptor mach number are determined with Equations B-46 and B-47. The computer then determines the following functions (Figure 7a through 7d) from the tabulated data:

$C_{L\alpha}$	:	Rate of change of coefficient of lift with respect to the angle of attack
C_D	:	Coefficient of drag
T_h	:	Maximum thrust
ΔC_D	:	Added coefficient of drag due to external stores

The total drag on the interceptor (D_I) and the acceleration of the interceptor due to the effects of weight, thrust and drag are determined with Equations B-48 and B-49. After the time interval (Δt), the interceptor velocity may be evaluated using Equation B-50.

$$C_L = \frac{nW_I}{.5\rho V_f^2 S} \quad \text{(B-46)}$$

$$V_{f_M} = \frac{V_f}{M} \quad \text{(B-47)}$$

$$D_I = \frac{1}{2}\rho S V_f^2 (C_D + \Delta C_D) \quad \text{(B-48)}$$

$$\dot{V}_f = \frac{g}{W_I}(Th - D_I - W_I \sin\gamma) \quad \text{(B-49)}$$

$$V_f = V_{f_o} + \dot{V}_f \Delta t \tag{B-50}$$

Similarly, from aerodynamic considerations the interceptor heading (ψ) and climb angle (γ) may be determined by Equations B-51 and B-52. The new angle of attack (α) is derived with Equation B-53. Since the rate of change of the angle of attack is limited, Equation B-55 is also used in the mathematical model. If the inequality (Equation B-55) is satisfied, the program uses the angle of attack as determined by Equation B-53. If the inequality is not satisfied, the program uses the angle of attack determined by Equation B-54. The instantaneous pitch angle of the interceptor (θ_f) is determined from Equation B-56.

$$\psi = \psi_o + \frac{ng\,\Delta t \sin \phi}{V_f \cos \gamma} \tag{B-51}$$

where n is the load factor and g is the acceleration due to gravity.

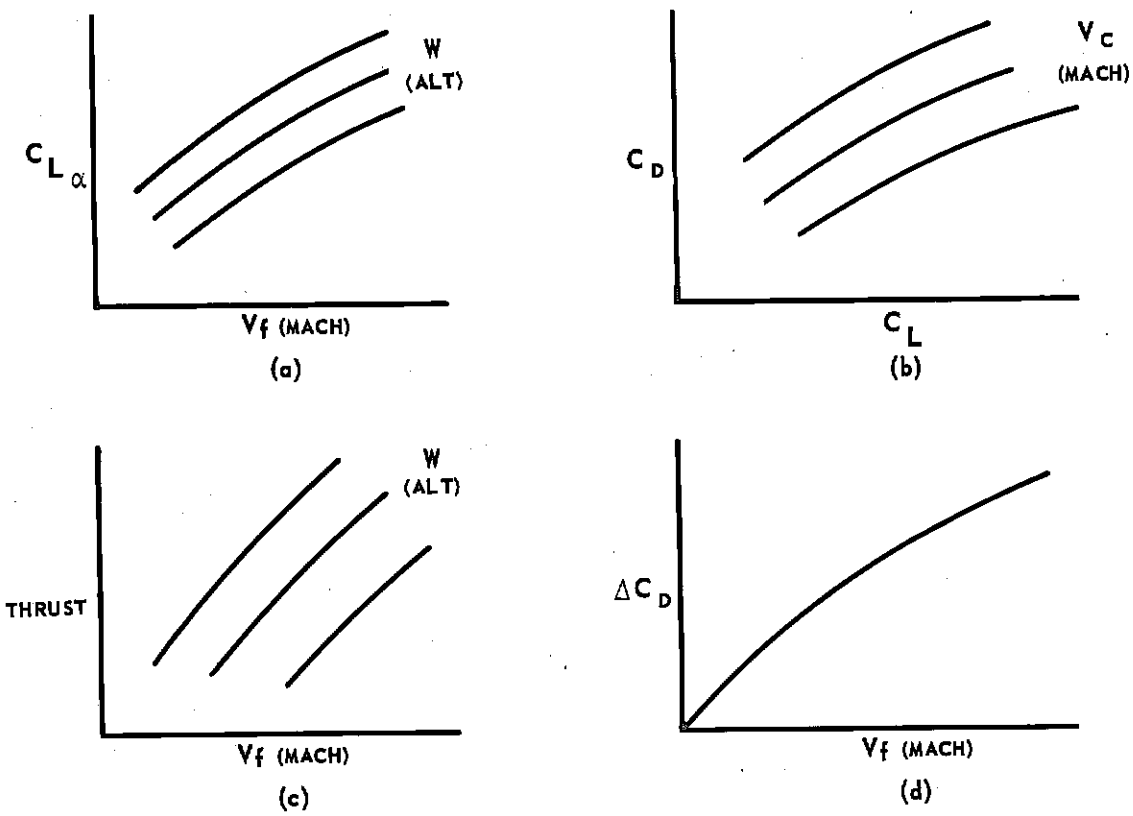

FIGURE B-7. AERODYNAMIC FUNCTIONS

$$\gamma = \gamma_o + \frac{g\Delta t}{V_f} (n \cos \phi - \cos \gamma) \tag{B-52}$$

$$\alpha = 0.0174533 \left(\frac{C_L}{C_{L_\alpha}} \right) \tag{B-53}$$

$$\alpha = \alpha_o + \dot{\alpha}_{max} \Delta t \tag{B-54}$$

$$\dot{\alpha} = \frac{\alpha - \alpha_o}{\Delta t} \leq \dot{\alpha}_{max} \tag{B-55}$$

$$\theta_f = \gamma + \alpha \cos \phi \tag{B-56}$$

Several additional functions have been added to the mathematical model to improve the simulation and the versatility of the system.

6. RELATIVE ROCKET RANGE

The relative range of the armament is a function of time of flight (T_f) and interceptor altitude (W). Relative range is calculated in the model using Equation B-57.

7. JUMP ANGLE

Jump angle of the armament (J_L) is determined from Equation B-58. At launch the armament will weathercock into the relative wind and finally stabilize at the angle J_L with respect to the I-axes of the interceptor. This jump angle in the physical system is calculated with the jump angle computer.

The variable K_J, a function of interceptor altitude and mach number, is developed in the jump angle computer.

$$F = f(T_{fl}\ W_l \ldots .) \tag{B-57}$$

$$J_L = K_J \alpha \tag{B-58}$$

$$K_J = f(V_{fl}\ W \ldots .) \tag{B-59}$$

8. THRUST

Any time during the intercept, if desired, and additional thrust may be applied to the aircraft to evaluate the effect of including an additional thrust. This additional thrust (Th_a) is a constant and is added to the regular thrust of the interceptor (Equation B-60) after the prelaunch signal has been received.

9. PILOT RESPONSE

The steering error (Δ), the amount of error the pilot must steer out to attain the proper lead collision course, is illustrated in Figure B-9-a for an interceptor with a zero roll angle. This indicated error is computed by the fire control system as an azimuth (ΔAZ) and an elevation (ΔEL) component of steering error. Assuming the same total steering error, Δ (Figure B-9-b), an interceptor with a roll angle (ϕ) will cause

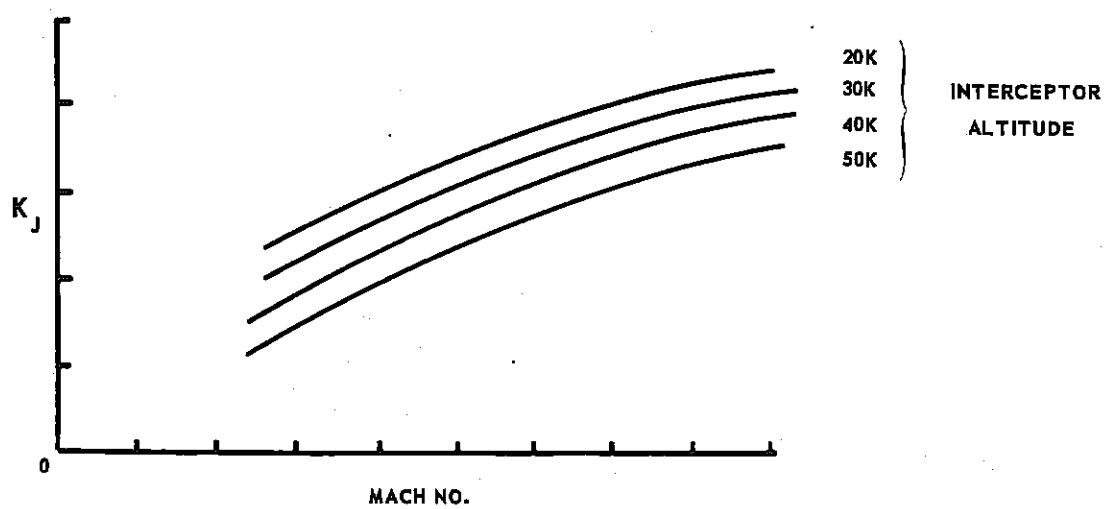

FIGURE B-8. JUMP ANGLE RATIO

the apparent components of steering error to change. The actual components of steering error the pilot must steer out (ΔAZ_ϕ and ΔEL_ϕ) are illustrated in Figure B-9-c and may be calculated from Equations B-61 and B-62.

10. LOAD FACTOR

A load factor (n), required to steer out the true elevation error (ΔEL_ϕ), is developed from Equation B-63. This load factor is limited in the model between the minimum and maximum values an average pilot is expected to withstand under normal conditions. The load factor, in turn, determines the coefficient of lift using Equation B-71. Equation B-65 represents a linear approximation of the maximum coefficient of lift available to the aircraft as illustrated in Figure B-10. If the coefficient of lift resulting from Equation B-64 is greater than the maximum, Equation B-66 is used to compute load factor.

$$Th = Th + Th_a \tag{B-60}$$

$$\Delta AZ_\phi = \Delta AZ \cos\phi + \Delta EL \sin\phi \tag{B-61}$$

$$\Delta EL_\phi = \Delta EL \cos\phi - \Delta AZ \sin\phi \tag{B-62}$$

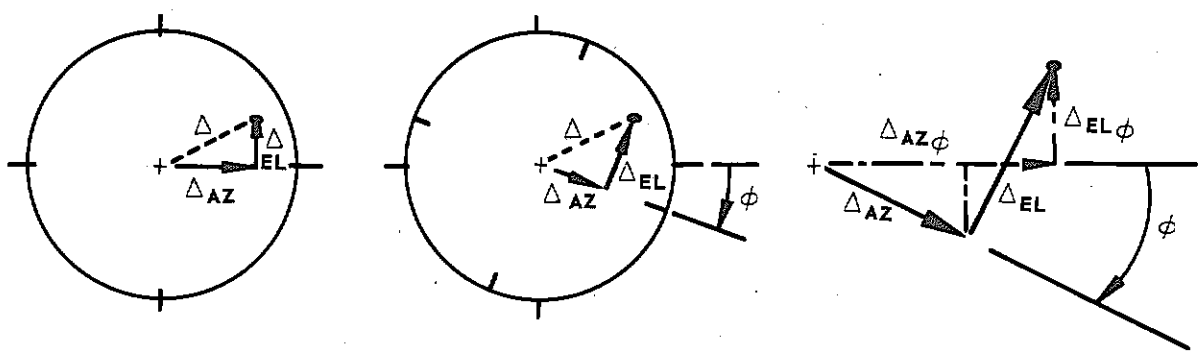

FIGURE 9a FIGURE 9b FIGURE 9c

FIGURE B-9a, b, c. SCOPE RELATIONSHIPS

$$n = (K_6 \Delta EL_\phi + \cos\gamma)/\cos\phi \text{ where}$$
$$n_{min} \leq n \geq n_{max} \tag{B-63}$$

$$C_L = \frac{nW_I}{\frac{1}{2}\rho V_f^2 S} \tag{B-64}$$

$$C_{L_{max}} = K_8 + K_9 h + K_{10} V_{f_M} + K_{11} h V_{f_M} \tag{B-65}$$

$$n = \frac{\frac{1}{2} V_f^2 S C_{L_{max}}}{W_I} \quad \text{if } C_L > C_{L_{max}} \tag{B-66}$$

11. ROLL CONTROL

A technique for controlling the roll angle of the interceptor is required to steer out the azimuth error (ΔAZ_ϕ). The desired roll angle versus time is illustrated in Figure B-11. This desired roll angle is approximated in the mathematical model by Equations B-67 through B-70. Assuming a large azimuth error (ΔAZ_ϕ), the output of Equation B-67 is illustrated in Figure B-12. The actual roll angle (ϕ) is computed in the model using Equation B-70.

$$\dot{\phi} = K_{12} \left|\Delta AZ_\phi\right| \left(\frac{|\phi|}{\phi_{max}} + K_{14}\right) \left(1.0 + K_{14} - \frac{|\phi|}{\phi_{max}}\right) \tag{B-67}$$

$$\text{if } \Delta AZ > K_{13}\phi$$

$$\dot{\phi} = -K_{12} \left|\Delta AZ_\phi\right| \left(\frac{|\phi|}{\phi_{max}} + K_{14}\right) \left(1.0 + K_{14} - \frac{|\phi|}{\phi_{max}}\right) \tag{B-68}$$

$$\text{if } \Delta AZ_\phi < K_{13}\phi$$

$$\dot{\phi} = 0 \qquad \text{if } \Delta AZ_\phi = K_{13}\phi \tag{B-69}$$

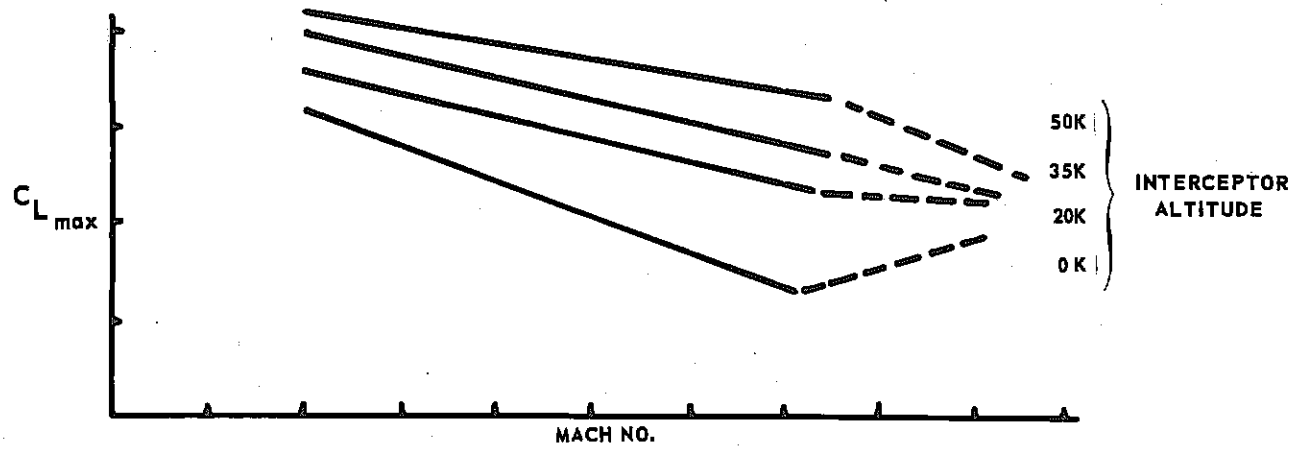

FIGURE B-10. MAXIMUM COEFFICIENT OF LIFT

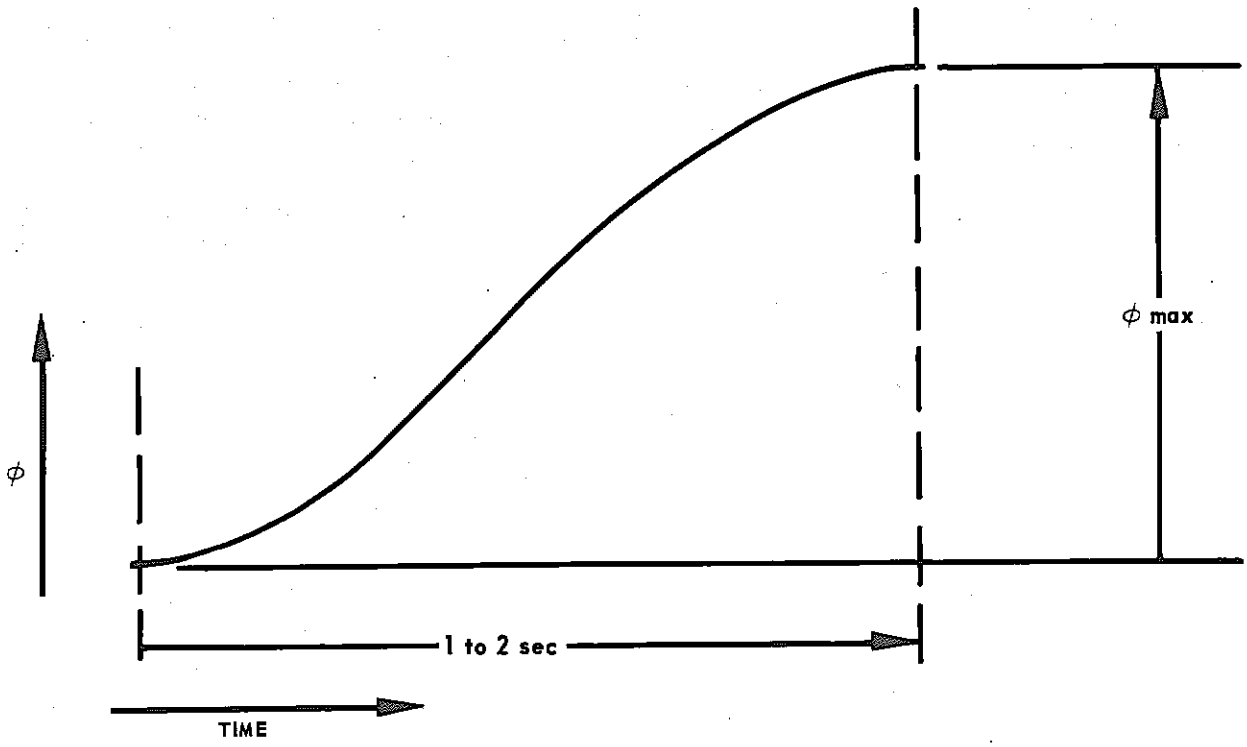

FIGURE B-11. ROLL ANGLE REQUIREMENT

$$\phi = \phi_o + \dot{\phi}\Delta t \qquad \text{where } |\phi| \leq \phi_{max} \tag{B-70}$$

$$T \leq T_f \tag{B-71}$$

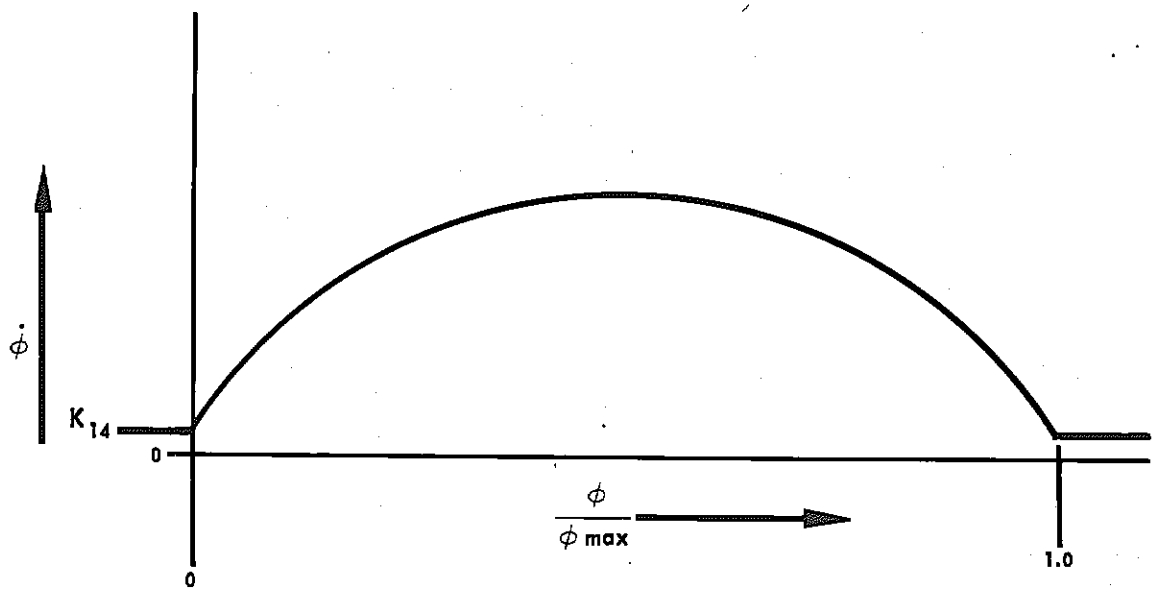

FIGURE B-12. ROLL RATE VERSUS NORMALIZED ROLL ANGLE

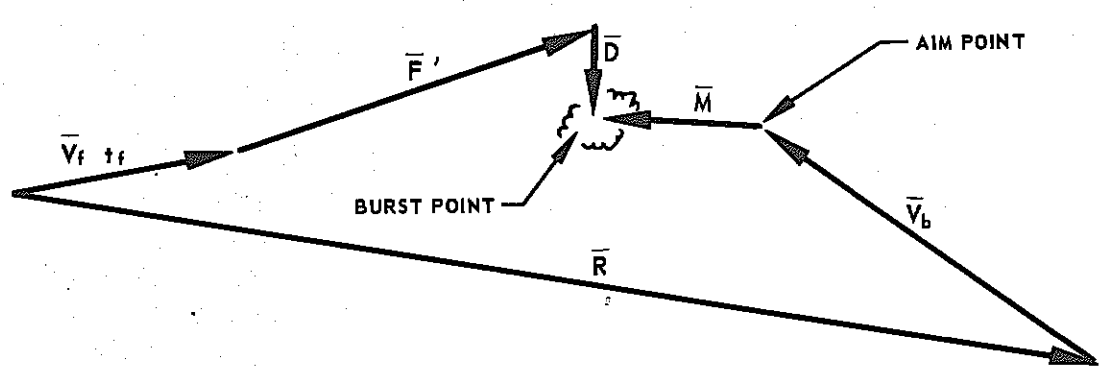

FIGURE B-13. VECTOR MISS DIAGRAM

$$\overline{V_f} t_f + \overline{F'} + \overline{D} - \overline{M} - \overline{V_b} t_f - \overline{R} = 0 \qquad \text{(B-72)}$$

$$\overline{M} = \overline{V_f} t_f + \overline{F'} + \overline{D} - \overline{V_b} t_f - \overline{R} \qquad \text{(B-73)}$$

$$M_I = V_f t_f \cos \alpha + F' \cos J_L - D \sin \theta_f - V_{b_I} t_f - R_I \qquad \text{(B-74)}$$

$$M_J = D \cos \theta_f \sin \phi - V_{b_J} t_f - R_J \qquad \text{(B-75)}$$

$$M_K = V_f t_f \sin \alpha + F' \sin J_L + D \cos \theta_f \cos \phi - V_{b_K} t_f - R_K \qquad \text{(B-76)}$$

12. MISS EVALUATION

The launch signal for the armament occurs when the servo time is less than or equal to the armament time of flight. If the armament is an unguided rocket, the location of the rocket at the time of detonation may be determined from the launch conditions. The correct aim point may also be determined with the target parameters at the time of launch. Figure B-13 illustrates the vector miss diagram where miss is defined as the distance from the aim point to the rocket burst point (Equations B-72 and B-73). The components of the vector miss in the interceptor coordinates at launch time are calculated with Equations B-74, B-75 and B-76. In the mathematical model, these miss distances are resolved into the space coordinate system, the target coordinate system and the radar coordinate system with the coordinate conversion Equations (B-1 through B-12).

If there is any steering error at the time of launch, this error is removed from the radar coordinate miss components. Thus, these new miss distances represent the intrinsic magnitude of weapon system miss with a zero steering error. This system miss also is resolved into the other coordinate systems.

TABLE B-1. Typical Input Data

Initial Target Position (A,B,C)
Initial Target Heading β
Target Maneuver Range R_M
Target Velocity V_B
Initial Interceptor Position (U,V,W)
Initial Interceptor Heading (ψ)
Interceptor Velocity V_f
Miscellaneous Constants as Required

13. SIMPLIFIED FLOW CHART

A simplified flow chart of the interception mathematical model is illustrated in Figure B-14. Although many check and control statements have been omitted, this flow chart outlines the logical steps used in the model.

14. INPUT DATA

Typical inputs to the mathematical model are tabulated in Table B-1.

15. OUTPUT

The mathematical model prints out the following data after every second of real flight time. It also prints out precise data of the time of climb and of the time of launch:

(1) Real time
(2) U,V,W
(3) $\cos(\beta - \psi)$
(4) ϕ_f, γ, ϕ
(5) A,B
(6) β, ψ
(7) T
(8) V_f
(9) n
(10) $\dot{R}$, R
(11) $\Delta AZ, \Delta EL$
(12) θ, ϵ
(13) $R\omega_e$, $R\omega_d$
(14) $(M/T)_{AZ}$, $(M/T)_{EL}$
(15) Thrust, Drag

In addition, at the time of launch the model prints out the jump angle, the computed F-pole, the drop and the various components of miss.

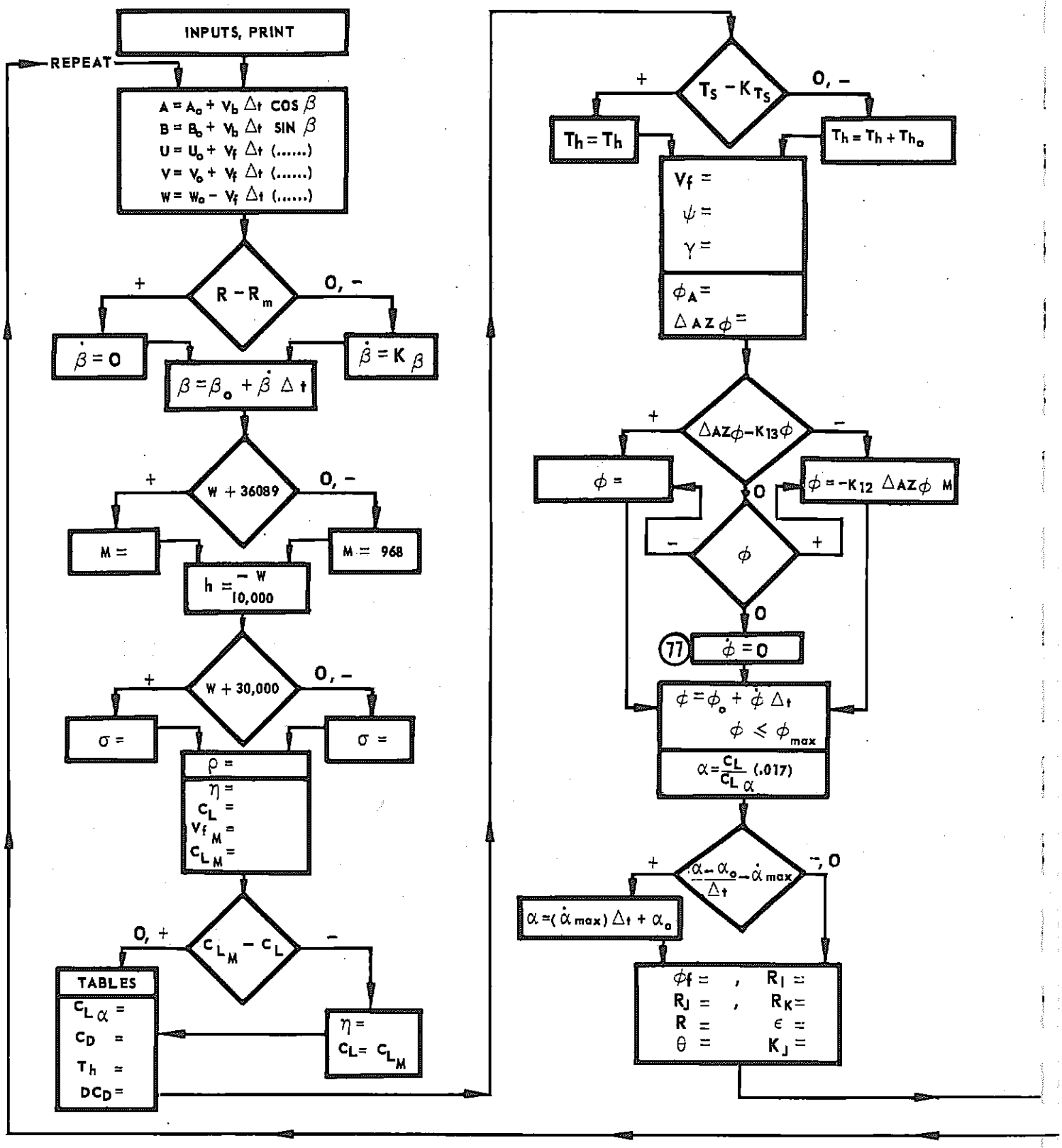

FIGURE B-14. INTERCEPTOR FLOW CHART

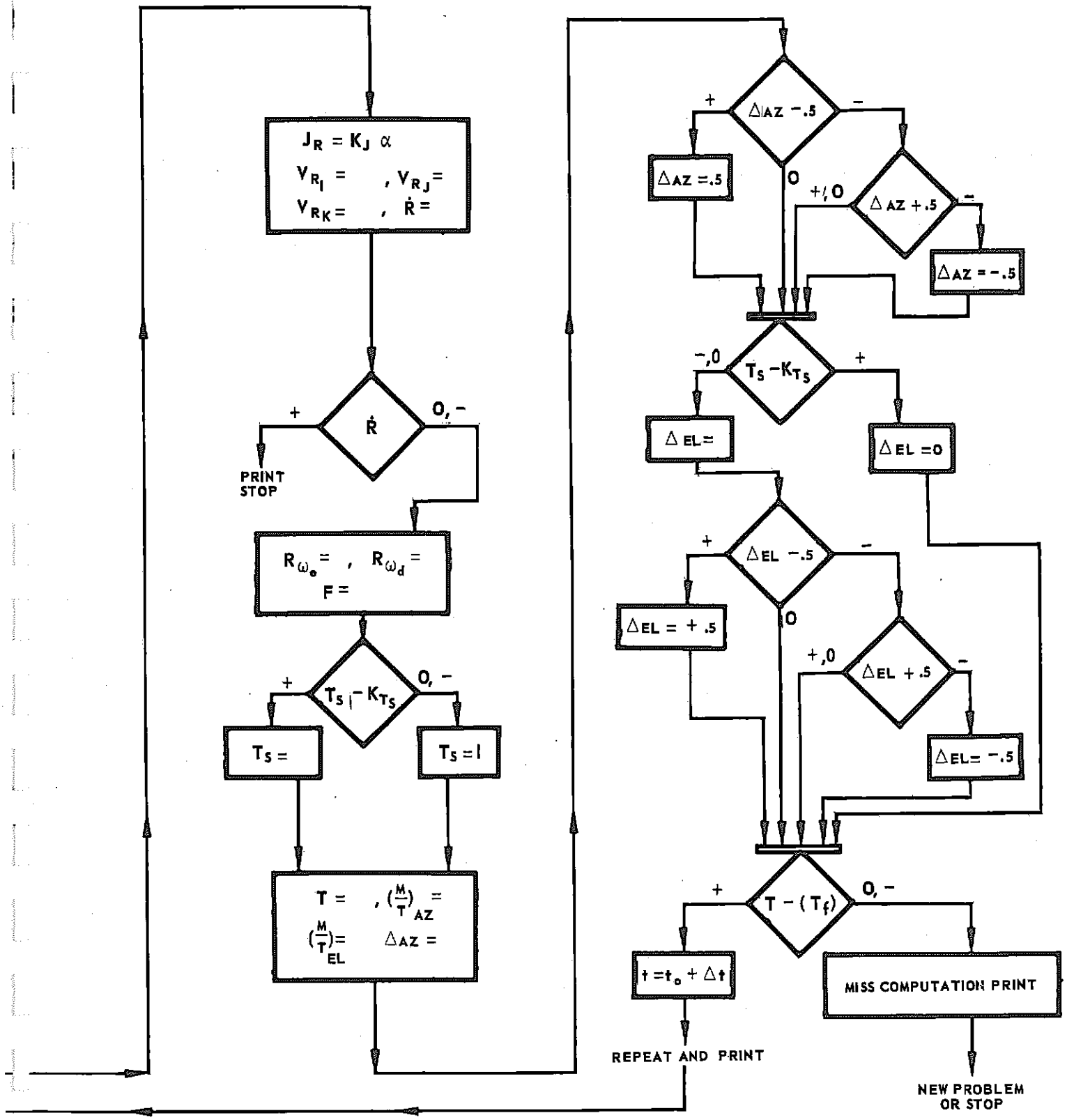
$J_R = K_J \alpha$
$V_{R_I} =$, $V_{R_J} =$
$V_{R_K} =$, $\dot{R} =$
$\dot{R}$
+
0, −
PRINT STOP
$R_{\omega_e} =$, $R_{\omega_d} =$
$F =$
$T_S - K_{T_S}$
+
0, −
$T_S =$
$T_S = 1$
$T =$, $(\frac{M}{T})_{AZ} =$
$(\frac{M}{T})_{EL} =$ $\Delta AZ =$
$\Delta AZ - .5$
+
−
0
$\Delta AZ = .5$
+, 0
$\Delta AZ + .5$
−
$\Delta AZ = -.5$
$T_S - K_{T_S}$
−, 0
+
$\Delta EL =$
$\Delta EL = 0$
$\Delta EL - .5$
+
−
0
$\Delta EL = + .5$
+, 0
$\Delta EL + .5$
−
$\Delta EL = -.5$
$T - (T_f)$
+
0, −
$t = t_o + \Delta t$
MISS COMPUTATION PRINT
REPEAT AND PRINT
NEW PROBLEM OR STOP

APPENDIX C

DISCUSSION OF FIRE CONTROL RADAR ERRORS AND CORRELATION

APPENDIX C

DISCUSSION OF FIRE CONTROL RADAR ERRORS AND CORRELATION*

The fundamental objective of any fire control system is to maximize the system hit probability. There are two types of errors that reduce this probability. One type of error is predictable and the other random. The predictable error is the algebraic sum of the dynamic following error of the system and the known errors in computer calibration. The random error arises from the dispersion of the weapon, random misalignments between elements of the system, and the transmission of noise through the system. The primary noise source in the fire control system is from the radar set.

It is generally assumed that the random error exhibits essentially a Gaussian probability distribution. The hit probability density is defined as the probability that a given armament will hit a target of small area divided by the magnitude of this small area. It can be shown that

$$P_{HD} = \frac{1}{2\pi\sigma^2} e^{-\frac{b^2}{2\sigma^2}} \qquad \text{(C-1)}$$

where

P_{HD} ... Hit probability density

b ... Magnitude of total predictable error

σ ... Mean-square value of total random error

---

* S. Moglewer, Weapon Systems Analysis, Norair Division, Northrop Corporation

where

$$\sigma^2 = \sigma_g^2 + \sigma_a^2 + \sigma_n^2 \qquad \text{(C-2)}$$

σ_g^2 ... Mean-square value of armament dispersion pattern

σ_a^2 ... Mean-square value of system misalignments

σ_n^2 ... Mean-square value of system noise

The predictable error, b, may be calculated by a knowledge of the servo loop and other characteristics of the system and the projected values of target angular velocities and acceleration. Weapon dispersions can be obtained from test results. System misalignments must be derived from specific tests of the system in question.

The tracking problem for a fire control system consists of distinguishing between an apparent change in track due to signal noise and that due to actual tracking changes.

The radar tracking noise effect is perhaps the most significant error in the fire control system for any dynamic problem. Observations of target positions are never completely accurate. For example, the radar range may be in error by ± 20 yds (at 2000 yds, range for an airborne target). Angular errors can vary up to 2.5 mils, corresponding at representative ranges to yardage errors about equal to those for range. These errors in observation will generate corresponding errors in the final aiming orders delivered by the fire control system.

The noise created by radar effects such as scintillation and propagation phenomena is smoothed in an attempt to minimize the induced errors. There are two basic approaches to the problem; one is to consider it as a problem in time series and to compute the autocorrelation function. The assumption is then made that the mean square error is dependent only upon this function.

The input signal to the computer is the sum of the true tracking signal, f(t), and the observational error, g (t). Since prediction of future

position is required, the quantity desired is $f(t + t_f)$ where t_f represents the prediction time. (If f(t) represents a rate, the interest then is in the average value of f(t) over the prediction interval.) Since the prediction is not accurate, denote by $f^* (t + t_f)$ the quantity actually predicted.

It can be shown that:

$$f^* (t + t_f) = \int_{-\infty}^{0} \left| f(S) + g(S) \right| dK(S) \qquad \text{(C-3)}$$

where d K (S) represents the effect of the data smoothing circuit. The problem is one of finding a shape for the function K (s) which will minimize the difference between $f (t + t_f)$ and $f^* (t + t_f)$. The autocorrelation for f(t) is defined as:

$$\phi_1 (\tau) = \underset{T \to \infty}{\text{LIM}} \frac{1}{2T} \int_{-T}^{T} f(t + \tau)\, f(t)dt \qquad \text{(C-4)}$$

This is a measure of the correlation between adjacent values of a series and is thus a measure of the predictability of the target path. Since practically all targets are characterized by continuous trajectories with continuous derivatives, finite values of $\phi_1 (\tau)$ must exist.

In a similar manner the autocorrelation of the observational error g(t) represents the extent to which the error is functional.

$$\phi_2 (\tau) = \underset{T \to \infty}{\text{LIM}} \frac{1}{2T} \int_{-T}^{T} g (t + \tau)\, g(t)dt \qquad \text{(C-5)}$$

For a random noise we should expect $\phi_2 (\tau)$ to vanish rapidly as τ increases from zero. Thus neighboring values of g are quite uncorrelated and only the average input data over some finite past interval are needed in order to have most of the observational errors averaged out. Note that this implies a capacity for memory to the computing function.

It can be shown that

$$\tau^{2} = \phi_1(0) - 2\int_0^\infty \left|\phi_1(t_f + \tau)\right| dK(\tau) + \int_0^\infty dK(\tau)\int_0^\infty \left|\phi_1(\tau - S) + \phi_2(\tau - S)\right| dK(S) \qquad \text{(C-6)}$$

The only quantities on which the mean square noise error is dependent are the autocorrelations ϕ_1 and ϕ_2 of the true target path and observational error, respectively, and the term K which specifies the data smoothing function.

The assumption that the time series is stationary implies the need for the integration to infinity. Since this is impossible in practical equipment, various approximations are required to handle the integration over a finite time interval. However, the extent of the finite time interval is dependent upon the noise structure, therefore requiring memory in the computer. The use of digital equipment for autocorrelation techniques is applicable to the fire control problem, inasmuch as analog computers, even with relatively limited memory capacity, are quite complex. The application of autocorrelation prediction techniques to the airborne fire control problem will have to await the development of the computer "state-of-the-art," even though suitable filters are theoretically realizable and these techniques are inherently strong.

The second approach to the data smoothing problem is to consider it as a filter problem. This assumes that noise appears principally at considerably higher frequencies than true signal. Thus the two can be separated by a low pass filter. The separation, however, is not complete since some components of the signal spectrum extend into the noise region. The smoothing process is accompanied by some mutilation of signal. In addition, there is no inherent prediction in this type of approach. Separate provision must be made for the prediction portion of the computer. Since effective separation between signal and noise depends upon the assumption that the signal components are of quite low frequency with respect to the noise, the presence of high frequency energy is quite serious. When the target maneuvers, the true signal will contain various high frequency components. A conventional airplane is restricted in its maneuvering capability and limited in rate of change of speed. Additionally, there are restrictions on the maximum angle of dive

and climb. Even though a heavy airplane is restricted in elevation changes, violent heading maneuvers are possible by banking sharply.

Although it is theoretically possible to build special filters that take into account the aircraft maneuver restrictions, present commercially available equipment is not nearly so sophisticated.

Since the filter approach contains inherent cutoff of some signal and passing of some noise, solutions of this nature should be expected to contain lag, particularly in the case of maneuvering targets. Thus the filter approach is not theoretically as effective as autocorrelation techniques. However, it is realizable and thus is suitable for present use.

APPENDIX D

NOISE IN FIRE CONTROL SYSTEMS

APPENDIX D

NOISE IN FIRE CONTROL SYSTEMS

The fundamental mathematics underlying the theory of noise is based on the Theory of Probability. Of principal interest in this volume are the concepts of correlation function and spectral density, and the effect of linear (and nonlinear) systems on these quantities.

The autocorrelation function of a function y (t) is defined as the time average

$$R(\tau) = \overline{y(t)y(t+\tau)} = \lim_{T\to\infty} \frac{1}{2T} \int_{-T}^{T} y(t)y(t+\tau)dt \qquad \text{(D-1)}$$

In general, R (τ) is a function of the time interval τ and varies from one member of an ensemble to the next, if y (t) is drawn from a random ensemble of functions. The correlation function can also be defined as

$$R(\tau,t) = \overline{y(t)y(t+\tau)} = \int_{-\infty}^{+\infty}\int y_1 y_2 \, P(y_1, y_2, t) \, dy_1 \, dy_2 \qquad \text{(D-2)}$$

where

$$y_1 = y(t)$$
$$y_2 = y(t+\tau)$$

and p (y_1, y_2, t) is the joint probability distribution of the random variables y_1 and y_2. If this distribution of possible a priori values of the joint variable y_1, y_2 depends on time (as shown), the distribution is said to be nonstationary so that the correlation function in Equation D-2 is a function of time. If the random process has a probability distribution which is independent of time, then the process is said to be stationary, and it turns out that the ensemble coverage in Equation D-2 is independent of time and is equal to the time average in Equation D-1. The latter

is independent of that member in the ensemble over which the average for a stationary process. Note that $R(\tau)$ is an even function in τ and $R(0) = y_2$ is the power (developed across a one-ohm resistor when the mean $\tilde{y} = 0$) in the function.

The spectral density is simply the Fourier transform of the correlation function, and as such is an even function of frequency. Formally, the relationships between the correlation function $R(\tau)$ and the spectral density $G(f)$ are

$$R(\tau) = \int_0^\infty df\, G(f) \cos \omega \tau \qquad \text{(D-3)}$$

$$G(f) = 4 \int_0^\infty d\tau R(\tau) \cos \omega \tau \qquad \text{(D-4)}$$

Note that $R(0) = \overline{y^2} = P$ = power, hence

$$P = \int_0^\infty G(f)\, df \qquad \text{(D-5)}$$

Many physical systems can be represented by the differential equation

$$f(t) = \frac{d^n x}{dt^n} + a_{n-1} \frac{d^{n-1} x}{dt^{n-1}} \cdots + a_2 \frac{dx}{dt} + a_1 x + a_o \qquad \text{(D-6)}$$

The solution of this differential equation is of the form

$$X(t) = \sum_i A_i e^{\alpha_i t} + \int_0^t f(t - r)\, g(r) dr \qquad \text{(D-7)}$$

If $f(t)$ is known exactly, then the integral in Equation D-1 can be carried out and the solution $x(t)$ is known explicitly. Unfortunately, since $f(t)$ is random, the integral in Equation D-7 cannot be carried out explicitly. It follows that $x(t)$ is also random and therefore is not known as an explicit function of time. Only statistical information about the output can be found so that it is necessary to have a knowledge of the statistical

properties of the input. Assume that the input f(t) is noise which has the following properties

$$\overline{f(t)} = \overline{N(t)} = \int_{-\infty}^{\infty} N(t)\, p(N)\, dN = 0 \qquad \text{(D-8)}$$

$$G(f) = w_o \qquad \text{(D-9)}$$

where p(N) is the probability density of the noise N(t), and G(f) is the spectral density, which is a constant w_o, for white noise. The use of a bar over a quantity denotes an ensemble average, as in Equation D-8. Equation D-8 states that the mean of the noise is zero, which is generally true of the types of noise considered, providing the noise has not passed through a nonlinearity. By definition, the spectral density for white noise is a constant. Also, the probability distribution of the noise is Gaussian. From the relationships D-3 and D-4 and from Equation D-9 it follows that the correlation function for white noise is

$$R_N(\tau) = \int_o^{\infty} G_N(f) \cos\omega\tau d\tau = \int_o^{\infty} w_o \cos\omega\tau d\tau = \frac{w_o}{2}\delta(\tau) \qquad \text{(D-10)}$$

From the properties of white noise in Equations D-8 through D-10 and from Equation D-7, the statistical properties of the output can be found. In the special case where the distribution of the input variable is normal, it is known that the output is also normal if the operation is linear. This follows from the property of Gaussian distributions that any linear operation on a normal variable yields a normal variable. Thus, in the present case of white Gaussian noise on the input, it is known that the output x(t) is Gaussian. To determine the output distribution it is required to find the various parameters defining the output distribution. To find the one-dimensional distribution, only the mean and standard deviation are necessary. To find the two-dimensional distribution, it is necessary to know the means and standard deviations for both variables and also the correlation coefficient. Higher distributions can also be found. In any case, the output moments of a linear system with noise on the input can be derived, even if the noise is non-Gaussian. The response of linear systems to non-Gaussian noise is in general non-Gaussian.

The nth moment of the output can be found as follows:

$$\overline{X^m} = \int_{-\infty}^{\infty} X^n(t)\, p(x)\, dx = \int_{-\infty}^{\infty} p(x) \left[\sum_i A_i e^{\alpha_i t} + \int_0^t f(t - r) g(r)\, dr \right]^n dx$$

$$= \overline{\left[\sum_i A_i e^{\alpha_i t} + \int_0^t N(t - r) g(r) dr \right]^n} \qquad \text{(D-11)}$$

Similarly the n by m cross product moment is

$$\overline{x_1^n x_2^m} = \iint_{-\infty}^{\infty} x^m(t_2)\, x^n(t_1)\, p(x_1, x_2)\, dx_1\, dx_2$$

$$= \iint_{-\infty}^{\infty} p(x_1, x_2) \left[\sum_i A_i e^{\alpha_i t_1} + \int_0^{t_1} f(t_1 - r) g(r) dr \right]^n \cdot$$

$$\left[\sum_k A_k e^{\alpha_k t_2} + \int_0^{t_2} f(t_2 - r) g(r) dr \right]^m dx_1 dx_2$$

$$\text{(D-12)}$$

where

$$x(t_i) = x_i;$$
$$t_1 = t; \quad t_2 = t_1 + \tau = t + \tau \qquad \text{(D-13)}$$

and τ is the time separation between samples.

The most important cases are $n = 1$, $n = 2$, and $n = m = 1$. For $n = 1$ it follows from Equation D-10 that

$$\overline{x} = \int_{-\infty}^{\infty} -p(x) \left[\sum_i A_i e^{\alpha_i t} + \int_0^t f(tr) g(r) dr \right] dx \qquad \text{(D-14a)}$$

or

$$\overline{x} = \sum_i A_i e^{a_i t} \int_{-\infty}^{\infty} p(x)dx + \int_0^t g(r)dr \int_{-\infty}^{\infty} f(t - r)p(f)\, df$$

$$= \sum_i A_i e^{a_i t} + \int_0^t \overline{f(t - r)}\, g(r)dr \qquad \text{(D-14b)}$$

Several important properties of random variables have been invoked here; namely, that the average of a nonrandom variable is simply the nonrandom variable itself and the average of a constant times a random variable is the constant times the average of the random variable. Furthermore, it is assumed that the integration over the time variable can be interchanged with the integration over the space variable. Another important property used in Equation D-14b is that the average value of the integral of a function is the integral of the average value of the integrand. This can be seen, since if

$$y(t) = \int_0^t x(a)d\,a \qquad \text{(D-15a)}$$

then

$$\overline{y} = \iint_{-\infty}^{\infty} yp(y_1 x)\, dydx = \iint_{-\infty}^{\infty}\int_0^t x(a)da\,p(y_1 x)dydx \qquad \text{(D-15b)}$$

or, assuming the integrals converge absolutely,

$$\overline{y} = \int_{-\infty}^{+\infty} yp(y)dy = \int_{-\infty}^{\infty} \left[\int_0^t x(a)da\right] p(x)dx \qquad \text{(D-15c)}$$

thus

$$\overline{y} = \int_0^t da \int_{-\infty}^{\infty} x(a)\; p(x)dx = \int_0^t \overline{x}(a)d\,a \qquad \text{(D-16)}$$

Similarly the autocorrelation function of the output is

$$R(\tau,t) = \overline{x(t_1)\ x(t_2)} = \overline{x_1 x_2} = \sum_i \sum_k A_i A_k e^{\alpha_i t_1 + \alpha_k t_2}$$

$$+ \sum_k A_k e^{\alpha_k t_1} \int_0^{t_2} \overline{f(t_2 - r)} g(r) dr + \sum_i A_i e^{\alpha_i t_2} \cdot$$

$$\int_0^{t_1} \overline{f(t_1 - r)} g(r) dr$$

$$+ \int_0^{t_1} \int_0^{t_2} \overline{f(t_2 - r) f(t_1 - s)} g(r) g(s) dr ds \qquad \text{(D-17)}$$

The mean square value of the output can be found from Equation D-17 by simply setting $\tau = 0$. Thus,

$$\overline{x^2(t)} = R(0,t) = \sum_i \sum_k A_i A_k e^{(\alpha_i + \alpha_k)t} + 2 \sum_k A_k e^{\alpha_k t} \cdot$$

$$\int_0^t \overline{f(t - r)} g(r) dr + \iint_0^t \overline{f(t - r) f(t - s)}\ g(r) g(s) dr ds$$

$$\text{(D-18)}$$

$$\overline{x}_1 = \overline{x}(t_1);\ \overline{x}_2 = \overline{x}(t_2);\ \sigma_1^2 = \overline{x^2}(t_1) - \overline{x}^2(t_1) \qquad \text{(D-19)}$$

and

$$\sigma_2^2 = \overline{x^2}(t_2) - \overline{x}^2(t_2);\ \rho(\tau t) = \frac{\overline{x_1 x_2} - \overline{x_1}\,\overline{x_2}}{\sigma_1\ \sigma_2} \qquad \text{(D-20)}$$

In general these moments and parameters are functions of the origin in time $t = t_1$ so that the distribution on the output (if capable of being found) is a transient or a nonstationary distribution. If the system contains dissipation, the output distribution ordinarily will approach a steady-state stationary distribution as $t \to \infty$. For the case of white

Gaussian noise on the input, Equations D-7 through D-10 may be employed to simplify the preceding results appreciably. In fact, for this case,

$$f(t) = N(t); \quad \overline{x} = \sum_i A_i e^{\alpha_i t} \tag{D-21}$$

$$\overline{x_1 x_2} = \sum_i \sum_k e^{\alpha_i t_1 + \alpha_k t_2} A_i A_k$$

$$+ \frac{w_o}{2} \int_o^{t_1} \int_o^{t_2} \delta(t_2 - t_1 + S - r)\, g(r)\, g(s)\, dr ds$$

$$= \frac{w_o}{2} \int_o^{t_1} g(\tau + s) g(s) ds + \sum_i \sum_k A_i A_k e^{\alpha_i t_1 + \alpha_k t_2} \tag{D-22}$$

$$\overline{x^2} = \sum_i \sum_k A_i A_k e^{(\alpha_i + \alpha_k)t} + \frac{w_o}{2} \int_o^t g^2(s) ds \tag{D-23}$$

$$\rho \sigma_1 \sigma_2 = \frac{w_o}{2} \int_o^{t_1} g(\tau + s)\, g(s) ds \tag{D-24}$$

$$\sigma^2 = \frac{w_o}{2} \int_o^t g^2(s) ds \tag{D-25}$$

Note that in evaluating equation D-22, the upper limit of integration after integrating the variable r is t_1, where it is assumed that $t_2 > t_1$. The reason for this is that if s is allowed to run to t_2, then there will be a response for $t < 0$, that is, a response before the excitation is applied, which is physically impossible.

One might find the spectrum corresponding to the correlation function in Equation D-17 by taking the Fourier transform in the usual way. However, this would yield a time-varying spectral density which usually is not useful. The concept of spectral density usually implies a

steady state spectrum and, furthermore, a non-time-varying spectrum. In order to make the correlation function in Equation D-17 useful in determining the spectrum, one must first let $t_1 = t \to \infty$. Thus

$$\lim_{t \to \infty} R(\tau, t) = \iint_0^\infty \overline{f(t_2 - r)\, f(t_1 - s)}\, g(r)g(s)drds$$

$$= \iint_0^\infty R_i(\tau + S - r)\, g(r)g(s)drds \qquad \text{(D-26)}$$

The transient terms vanish in Equation D-26, but $R(\tau, t \to \infty)$ still may be time-varying because of time-varying signals present in the input. In general, then, it is also necessary to take a time average of the steady state correlation function before inverting to find the spectrum. Thus, taking the time average of Equation D-26

$$R(\tau) = \overset{\sim\sim}{R(\tau, t)} = \iint_{-\infty}^{\infty} R_i(\tau + S - r)g(r)g(s)drds \qquad \text{(D-27)}$$

where the wiggly overscore indicates a time average.

The lower limit on the integral in Equation D-27 is $-\infty$ since $g(t) = 0$ for $t < 0$. The steady state spectrum is then found by inverting Equation D-27, or

$$G_o(f) = 4\int_0^\infty R(\tau) \cos \omega \tau d\tau$$

$$= 4\int_0^\infty \cos \omega \tau d\tau \iint_{-\infty}^{\infty} \overset{\sim\sim}{R_i(\tau + s - r)}g(r)g(s)drds \qquad \text{(D-28)}$$

Often only the output spectrum is desired, and if this is the case it is much easier to find the output spectrum directly without first evaluating the correlation function. A formula for the output spectrum in terms of the input spectrum can be found directly from Equation D-28 as follows:

$$G_o(f) = 2\int_{-\infty}^{\infty} e^{j\omega\tau} d\tau \iint_{-\infty}^{\infty} R_i(\tau + S - r)g(r)g(s)drds$$

$$= \int_{-\infty}^{\infty} dsg(s)e^{-j\omega s} \int_{-\infty}^{\infty} R_i(\tau + S - r)e^{j\omega(\tau + S - r)} d(\tau + S - r)$$

$$= Y(-j\omega)\, Y(j\omega)G_i(f) = G_i(f) \quad |Y(j\omega)|^2 \tag{D-29}$$

Note that the input spectrum is simply the transform of the input correlation function and the Fourier transform of the weighting function is the transfer function $Y(j\omega)$. Defining total average power as the integral of the spectral density over positive frequencies only yields

$$P_o(f) = \int_o^{\infty} G_o(f)df = \int_o^{\infty} G_i(f) \quad |Y(j\omega)|^2 \, df \tag{D-30}$$

Also, since R(0) is simply the mean square value of the output, it follows that

$$P_o(f) = R_o(0) \tag{D-31}$$

RESPONSE TO SIGNAL AND NOISE

If the input consists of a nonrandom signal-plus-noise, the various moments can be found from Equations D-14, D-17, and D-18. Thus if

$$f(t) = S(t) + N(t)$$

$$\overline{x} = \sum_i A_i e^{\alpha_i t} + \int_o^t \left[\overline{S(t - r) + N(t - r)}\right] g(r)\, dr \tag{D-32}$$

then

$$= \sum_i A_i e^{\alpha_i t} + \int_o^t S(t - r)g(r)dr \tag{D-33}$$

where

$\overline{s(t)}$ = S(t) if the signal is nonrandom,

and

$$R(\tau,t) = \sum_i\sum_k A_i A_k e^{\alpha_i t_1 + \alpha_k t_2} + \sum_k A_k e^{\alpha_k t_1} \cdot$$

$$\int_o^{t_2} \overline{S(t_2 - r)}\, g(r)dr + \sum_i A_i e^{\alpha_i t_2} \int_o^{t_1} \overline{S(t_1 - r)} g(r)dr$$

$$+ \int_o^{t_1}\int_o^{t_2} \Big[\overline{S(t_2 - r)\, S(t_1 - s)} + \overline{S(t_2 - r)\, N(t_1 - s)}$$

$$+ \overline{S(t_1 - s)\, N(t_2 - r)}$$

$$+ \overline{N(t_1 - r)\, N(t_2 - s)}\Big] g\ (r)g(s)drds \qquad \text{(D-34)}$$

If S(t) and N(t) are uncorrelated and S(t) is nonrandom, then Equation D-34 becomes

$$R(\tau,t) = \sum_i\sum_k A_i A_k e^{\alpha_i t_1 + \alpha_k t_2} + \sum_k A_k e^{\alpha_k t_1}$$

$$\int_o^{t_2} S\,(t_2 - r)g(r)dr + \sum_i A_i e^{\alpha_i t_2} \int_o^{t_1} S(t_1 - r)g(r)dr$$

$$+ \int_o^{t_1} \int_o^{t_2} S(t_2 - r)\, S(t_1 - s)\, g(r)g(s)drds$$

$$+ \frac{w_o}{2} \int_o^{t} g(\tau + s)g(s)ds$$

$$= \overline{x}_1 \overline{x}_2 + \frac{w_o}{2} \int_o^{t} g(\tau + s)g(s)ds \qquad \text{(D-35)}$$

Note that for this case, the covariance becomes

$$\rho\,\sigma_1\sigma_2 = R(\tau_2 t) - \overline{x}_1\overline{x}_2 = \frac{w_o}{2}\int_o^t g(\tau + s)g(s)ds \qquad \text{(D-36)}$$

Hence, the correlation coefficient ρ and the variances σ^2 and σ_2^2 do not depend on the signal. In fact, none of the moments except the mean depend on the signal (provided $\overline{SN} = 0$ and $\overline{S} = S$) as can be seen in Equation D-37.

$$x(t) - \overline{x}(t) = \int_o^t N(t - r)g(r)dr \qquad \text{(D-37)}$$

THE SPECTRUM OF SIGNAL AND NOISE AFTER FILTERING

The steady state spectrum can be found following the technique used in the derivation of Equation D-29. It can be shown that

$$G_o(f) = \left[G_{ss}(f) + 2G_{sn}(f) + G_{nn}(f)\right]\left|Y(j\omega)\right|^2 \qquad \text{(D-38)}$$

The quantity $G_{SN}(f)$ in Equation D-38 is the cross spectral density. If the signal and noise are uncorrelated, as is often the case, $G_{SN}(f) = 0$. In this case, the input spectrum becomes simply

$$G_i(f) = G_{ss}(f) + G_{nn}(f) \qquad \text{(D-39)}$$

One may define an output power signal-to-noise ratio as follows:

$$\frac{S}{N} = \frac{P_s}{P_N} \qquad \text{(D-40)}$$

The meaning of signal-to-noise ratio is not clear, in general, unless additional data as to spectral regions of interest, signal components of interest, etc., are given. In the simplest case, it is merely the ratio of the total signal power to the total noise power over an infinite frequency range.

APPENDIX E

NONLINEAR THEORY OF CONICAL SCANNING

APPENDIX E

NONLINEAR THEORY OF CONICAL SCANNING

The purpose of this appendix is to derive the modulating function and to determine percentage modulation curves of the antenna beam as a function of error angle. Assuming that the antenna beam is a perfect surface of revolution about the beam axis, a scan-modulation theory will be derived based on a two-dimensional model by letting the beam remain fixed while the target moves. The periodic variation in returned intensity will then be represented as a planar motion. A diagram of the three-dimensional geometry appears in Figure E-1.

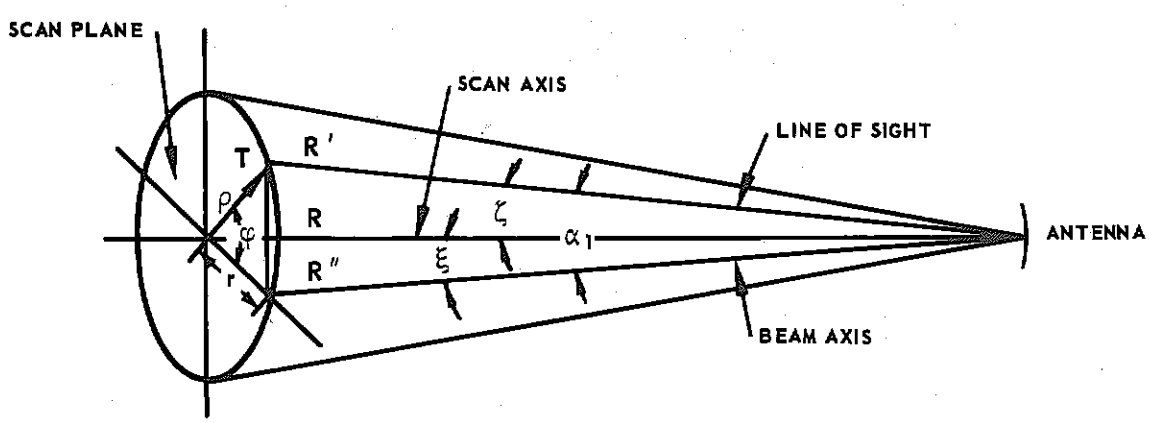

FIGURE E-1. THREE-DIMENSIONAL GEOMETRY OF ANTENNA BEAM

Certain geometrical relationships may be found relating angular displacements at the antenna to distances in the scan plane. It is assumed that the beamwidth is twice the squint angle ($\beta = 2\xi$). The following symbols are used (see Figure E-1).

R = range from antenna to scan plane
R' = range from antenna to target, T
R'' = range from antenna to intersection of beam axis and scan plane

r = distance between scan axis and intersection of beam axis and scan plane
ρ = distance between scan axis and target
s = distance between target and intersection of beam axis and scan plane
ξ = angle between scan axis and beam axis (squint angle)
ζ = angle between scan axis and line of sight (error angle)
a_1 = angle between beam axis and line of sight

The following relationships hold:

$$R' = \frac{R}{\cos \zeta} \qquad R'' = \frac{R}{\cos \xi} \tag{E-1}$$

$$r = R \tan \xi \qquad \rho = R \tan \zeta \tag{E-2}$$

$$s = \sqrt{\rho^2 + r^2 - 2r\rho \cos \phi} \tag{E-3}$$

$$= R\sqrt{\tan^2 \xi + \tan^2 \zeta - 2 \tan \xi \tan \zeta \cos \phi}$$

$$s = \sqrt{R'^2 + R''^2 - 2R'R'' \cos \alpha_1} \tag{E-4}$$

$$= R\sqrt{\sec^2 \zeta + \sec^2 \xi - 2 \sec \xi \sec \zeta \cos \alpha_1}$$

$$\cos \alpha_1 = \cos \zeta \cos \xi + \sin \xi \sin \zeta \cos \phi \tag{E-5}$$

For small ξ and ζ, that is, for $\rho << R$, $r << R$, these formulas become, approximately,

$$R' \doteq R \doteq R'' \tag{E-6}$$

$$r \doteq R\xi \qquad \rho \doteq R\zeta \tag{E-7}$$

$$s \doteq R\sqrt{2 - 2 \cos \alpha_1} \doteq R\alpha_1 \tag{E-8}$$

The beam may be represented in Cartesian coordinates as a plot of the magnitude of the rf voltage as a function of angular displacement, θ, from the scan axis (see Figure E-2a). The scan plane geometry corresponding to this diagram appears in Figure E-2b.

It is convenient to consider the variation of s with ϕ as a variation in the magnitude of r - s along the s-axis. Thus

$$x = r - s \tag{E-9}$$

where x(t) is a measure of the voltage returned as a function of time. Since a constant angular rate, ω_s, of the target relative to the x-axis with the beam fixed gives the same modulating function as a rate ω_s of the beam with the target fixed,

$$\phi = \omega_s t \tag{E-10}$$

In Equation E-10, it is assumed that the initial phase at t = 0 is zero. If the phase $\neq 0$ at t = 0, $\omega_s t$ may be replaced by $\omega_s t + \phi_o$. Substituting Equations E-3 and E-10 in Equation E-9

$$x(t) = r - \sqrt{r^2 + \rho^2 - 2r\rho \cos \omega_s t} \tag{E-11}$$

For $\rho << r$, this reduces to

$$x(t) \doteq \rho \cos \omega_s t \tag{E-12}$$

which is merely the projection of ρ on the x-axis. Figure E-2a relates the rf voltage, V, with angular target displacements along the x-axis. Since x(t) in Equation E-9 is an apparent target motion along the x-axis and since it correctly represents the variation in s during the scan cycle,

$$\theta(t) = \tan^{-1} \frac{x(t)}{R}$$

$$\tan^{-1} \left(\tan \zeta - \sqrt{\tan^2 \xi + \tan^2 \zeta - 2 \tan \xi \tan \zeta \cos \omega_s t} \right) \tag{E-13}$$

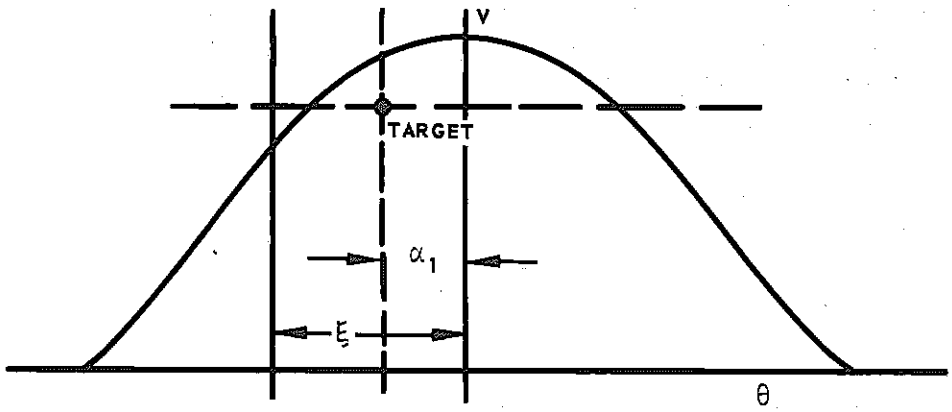

(a) RF RETURN VOLTAGE VERSUS ANGULAR DISPLACEMENT, θ, FROM SCAN AXIS

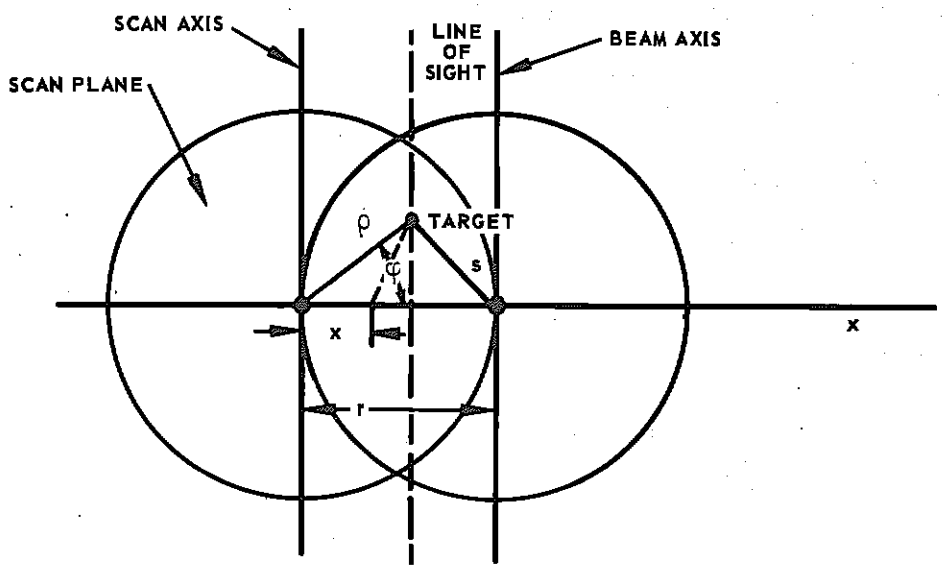

(b) SCAN PLANE GEOMETRY FOR (a)

FIGURE E-2. ANTENNA BEAM AND SCAN PLANE GEOMETRY

But for $\rho < r$, and from Equations E-4, E-3, and E-5

$$x(t) = r\left[1 - \left(1 + \frac{\rho^2}{r^2} - \frac{2\rho}{r}\cos\omega_s t\right)^{1/2}\right]$$

$$= r\left\{1 - \left[1 + \frac{1}{2}\left(\frac{\rho^2}{r^2} - \frac{2\rho}{r}\cos\omega_s t\right) - \frac{1}{8}\left(\frac{\rho^2}{r^2} - \frac{2\rho}{r}\cos\omega_s t\right)^2 + \ldots\right]\right\}$$

$$= r\left[-\frac{1}{2}\frac{\rho^2}{r^2} + \frac{\rho}{r}\cos\omega_s t + \frac{1}{8}\left(\frac{\rho^4}{r^4} - \frac{4\rho^3}{r^3}\cos\omega_s t + \frac{4\rho^2}{r^2}\cos^2\omega_s t + \ldots\right)\right]$$

$$= \rho\left[-\frac{1}{4}\frac{\rho}{r} + \frac{1}{8}\frac{\rho^3}{r^3} + \left(1 - \frac{1}{2}\frac{\rho^2}{r^2}\right)\cos\omega_s t + \frac{1}{4}\frac{\rho}{r}\cos 2\omega_s t + \ldots\right] \tag{E-14}$$

Equation E-9 shows x(t) to have a dc term, a fundamental at the scan frequency and all higher harmonics of the fundamental. Neglecting terms of $0(\rho^2/r^2)$ and higher, Equation E-9 becomes

$$x(t) = \rho\left[\cos\omega_s t - \frac{1}{4}\frac{\rho}{r}(1 - \cos 2\omega_s t)\right] \tag{E-15}$$

Equation E-15 reduces to Equation E-12 for $\rho << r$, as it should. Substituting Equation E-14 in Equation E-13

$$\theta(t) = \tan^{-1}\left\{\tan\zeta\left[-\frac{1}{4}\tan\zeta + \frac{1}{8}\tan^3\zeta + \left(1 - \frac{1}{2}\tan^2\zeta\right)\cos\omega_s t + \frac{1}{4}\tan\zeta\cos 2\omega_s t + \ldots\right]\right\} \tag{E-16}$$

If $\theta(t)$ is expanded in ζ, a series of the following form results:

$$\theta(t) = f_o(\zeta) + f_1(\zeta)\cos\omega_s t + f_2(\zeta)\cos 2\omega_s t + \ldots \tag{E-17}$$

where $f_o, f_1 \ldots f_n$ are functions determined by expanding Equation E-16. If ζ is small, $\tan\zeta \doteq \zeta$ and

$$\theta(t) \doteq \tan^{-1}(\zeta \cos \omega_s t) = \zeta \cos \omega_s t - \frac{\zeta^3}{3} \cos^3 \omega_s t + \ldots$$

$$\doteq \frac{\rho}{R} \cos \omega_s t; \quad \rho << R \qquad \text{(E-18)}$$

Figure E-3 might then be a graphical representation of V(t).

$V(\theta)$ has a shape determined by the antenna and radar parameters (such as wavelength antenna aperture, and so forth) and not by the position of the target. Expanding $V(\theta)$ in a Taylor's series about $\theta = 0$,

$$V(\theta) = V(0) + \theta V'(0) + \frac{\theta^2}{2!} V''(0) + \ldots \qquad \text{(E-19)}$$

Substituting Equation E-17 in Equation E-19 and letting $V^{(n)}(0) = V_o^{(n)}$

$$V(t) = A + F_o\left[\zeta, V_o^{(n)}\right] + F_1\left[\zeta, V_o^{(n)}\right] \cos \omega_s t \qquad \text{(E-20)}$$

$$+ F_2\left[\zeta, V_o^{(n)}\right] \cos 2\omega_s t + \ldots$$

where $V(0) = A$ and $F_o, F_1 \ldots F_n$ are functions determined by expanding Equation E-19 in ζ.

For small values of ζ, the input $\theta(t)$ is nearly sinusoidal (the case shown in Figure E-3). Substituting Equation E-18 in Equation E-19

$$V(t) \doteq V_o + V_o' \frac{\rho}{R} \cos \omega_s t + \frac{V_o'' \rho^2}{2! R^2} \cos^2 \omega_s t + \ldots \qquad \text{(E-21)}$$

$$= A + \frac{V_o'' \rho}{4R} + \frac{V_o' \rho}{R} \cos \omega_s t + \frac{V_o'' \rho^2}{4R^2} \cos 2\omega_s t + \ldots$$

Thus, even if $\zeta << \xi$, it is possible to generate harmonics. With the proper choice of the ratio of squint angle to beamwidth and with proper antenna design, the region about the scan axis on $V(\theta)$ may be quite linear over a fairly wide range. In this case, $V_o'' << V_o'$ and

$$V(t) \doteq A + \frac{V_o'\rho}{R} \cos \omega_s t; \; \zeta << \xi \; V_o^{(n)} << V_o', \; n \geqslant 2 \qquad \text{(E-22)}$$

Let

$$m_k = \frac{F_n \left[\zeta, \; V_o^{(n)} \right]}{A} \qquad \text{(E-23)}$$

where m_k is the modulation factor for the kth harmonic. Equation E-20 then becomes

$$V(t) = A(1 + m_o + m_1 \cos \omega_s t + m_2 \cos 2\omega_s t + \ldots) \qquad \text{(E-24)}$$

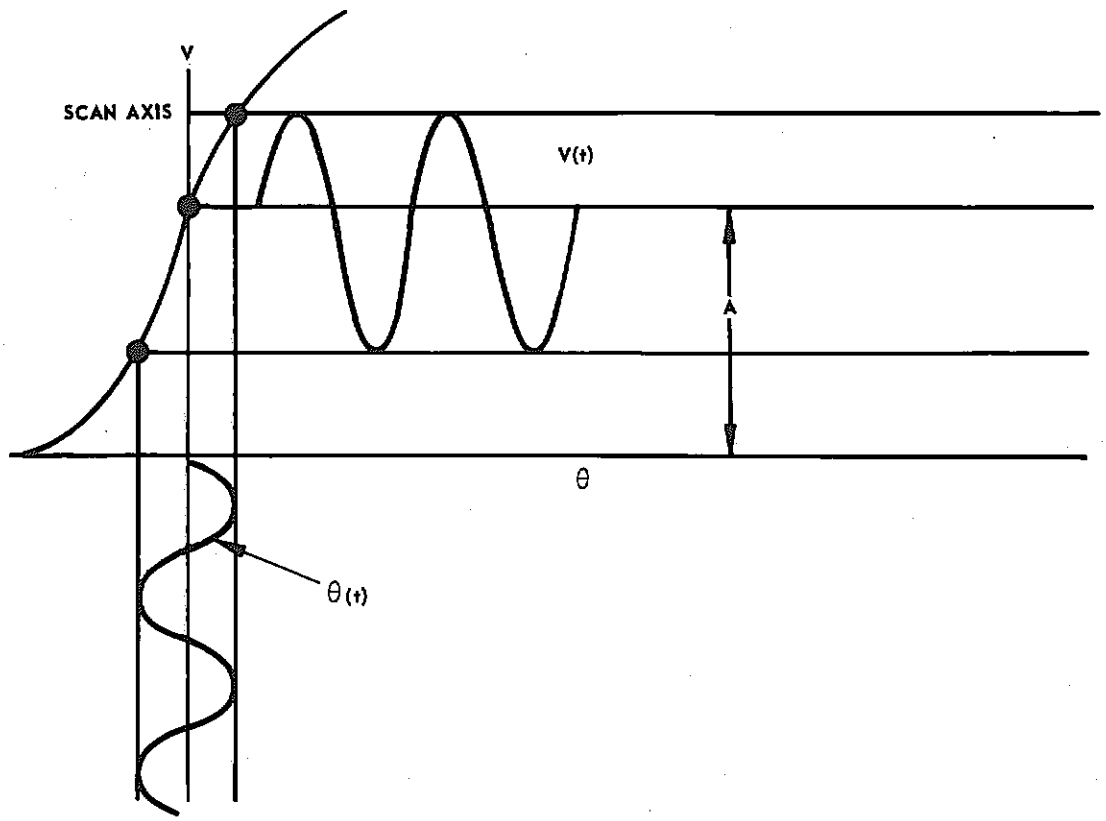

FIGURE E-3. GRAPHIC REPRESENTATION OF DERIVATION OF V(t) FROM θ(t)

From Equations E-18 and E-22, if ζ is small and $V_o^{(n)} << V_o'$, $n \geq 2$,

$$m_1 = \frac{V_o'\zeta}{A} = \frac{V_o'\rho}{AR} \tag{E-25}$$

Equation E-22 can now be written

$$V(t) \doteq A\left[1 + m_1 \cos(\omega_s t + \phi_o)\right] \tag{E-26}$$

where ϕ_o is the initial phase at $t = 0$.

This expression for V(t) is the modulating function used in the body of this report.

A plot of

$$m_1 = \frac{F_1\left[\zeta, V_o^{(n)}\right]}{A}$$

is linear near zero (see Equation E-25) and nonlinear for large values of ζ. Since a plot of $|V(t)|$ versus ζ on either side of crossover is the beam pattern above the 3-db points, and since, except for the dc, the major contribution to this curve is made by the first harmonic term, it is physically reasonable for $m_1(\zeta)$ to be a discriminator-like curve with peaks at approximately the squint angle from crossover.

APPENDIX F

ANGULAR SCINTILLATION THEORY

APPENDIX F

ANGULAR SCINTILLATION THEORY*

Consider a target composed of two point sources (see Figure F-1). Let the reflected rf amplitude from source 1 be A_1 and from source 2 be A_2 and let them be separated by distance a. Each of these rf waves is amplitude-modulated at the scan frequency according to Equation F-17. There is a direction for the scan axis for which zero error signal exists in the angle servo. This direction is the line joining the antenna and the apparent radar center of the target and is the direction along which the antenna would point if the rf phase relation between the two targets were indefinitely sustained. Assume that the resultant of the unmodulated rf signals is much greater than the modulation components so that overmodulation and distortion will not occur. The position of the apparent radar center can now be calculated. From Equation F-17, the resultant received signal is given by

$$E_r = A_1 \left[1 + m_1 \cos(\omega_s t + \phi_1)\right] \cos(\omega_c t + \theta_1)$$

$$+ A_2 \left[1 + m_2 \cos(\omega_s t + \phi_2)\right] \cos(\omega_c t + \theta_2) \qquad \text{(F-1)}$$

where subscripts 1 and 2 refer to sources 1 and 2.

The modulation coefficient depends on the angular displacement of the radiator from the scan axis. For small displacements, this coefficient is

$$m_i = b_o \epsilon_i = \frac{b_o d_i}{R_i} \qquad \text{(F-2)}$$

---

* Hughes Aircraft Company TM-233, "Angular Scintillation of Radar Targets."

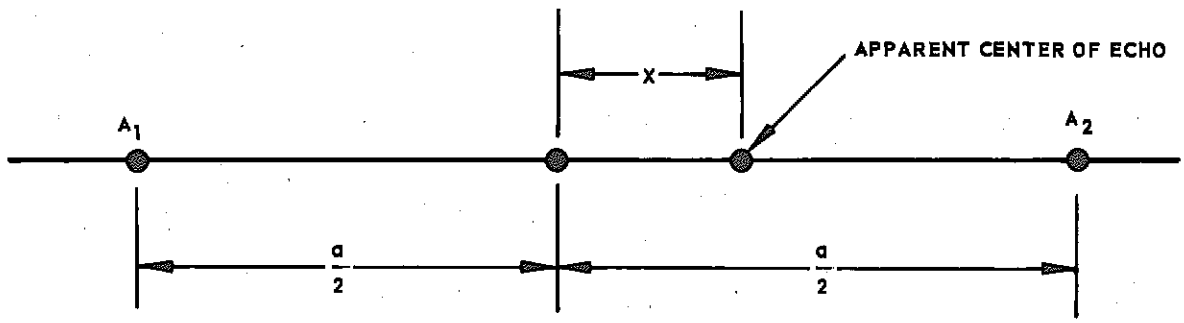

FIGURE F-1. TWO-TARGET SCAN PLANE GEOMETRY

where

d_i = displacement of ith radiator from scan axis

R_i = range from radar to ith radiator

ϵ_i = angular displacement of ith radiator from scan axis

Note that $R_i >> d_i$, in general, hence

$$m_i \doteq \frac{b_o d_i}{R} \tag{F-3}$$

and

$$m_1 = \frac{b_o d_1}{R} = \frac{b_o (a/2 + x)}{R} \tag{F-4}$$

$$m_2 = \frac{b_o d_2}{R} = \frac{b_o (a/2 - x)}{R}$$

Write Equation F-1 as

$$E_r = E_1(t) \cos (\omega_c t + \theta_1) + E_2(t) \cos (\omega_c t + \theta_2) \tag{F-5}$$

Transforming coordinates to a plane which is rotating at an angular rate of ω_c and using the exponential representation of a sinusoid, Equation F-5 becomes

$$E_r = E_1(t)e^{j\theta_1} + E_2(t)e^{j\theta_2} = E(t)e^{j\theta_r} \qquad \text{(F-6)}$$

where E(t) is the magnitude and θ_r the phase angle of the resultant rf vector. It follows that

$$E(t) = E_1(t)e^{j(\theta_1 - \theta_r)} + E_2(t)e^{j(\theta_2 - \theta_r)}$$

$$= E_1(t)\cos(\theta_1 - \theta_r) + E_2(t)\cos(\theta_2 - \theta_r) \qquad \text{(F-7)}$$

Zero error signal exists when the scan component of E(t) (that is, the envelope of E_r) is zero. Thus,

$$E_s(t) = \sum_{i=1}^{2} E_{is}(t)\cos(\theta_i - \theta_r) = 0 \qquad \text{(F-8)}$$

or

$$A_1 m_1 \cos(\omega_s t + \phi_1)\cos(\theta_1 - \theta_r) + A_2 m_2 \cos(\omega_s t + \phi_2)$$
$$\cos(\theta_2 - \theta_r) = 0$$

Transforming coordinates to a plane rotating at ω_s and noting that in this particular case, $\phi_1 = r$, $\phi_2 = 0$,

$$-A_1 m_1 \cos(\theta_1 - \theta_r) + A_2 m_2 \cos(\theta_2 - \theta_r) = 0$$

Substituting Equation F-4 in the above equation

$$A_1\left(\frac{a}{2} + x\right)\cos(\theta_1 - \theta_r) = A_2\left(\frac{a}{2} - x\right)\cos(\theta_2 - \theta_r) \qquad \text{(F-9)}$$

It is instructive to draw a vector diagram of Equation F-8 (Figure F-2).

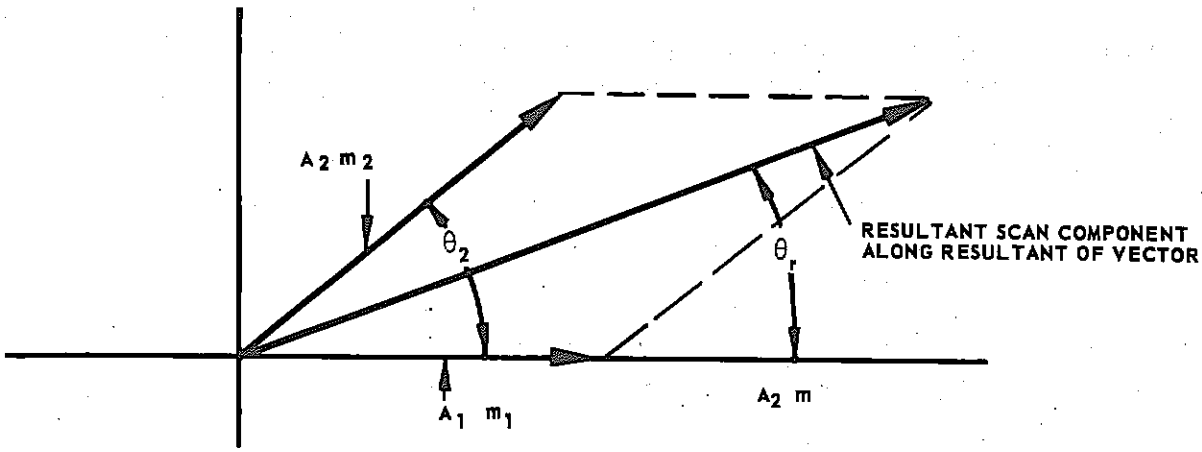

FIGURE F-2. TWO-TARGET VECTOR DIAGRAM OF SCAN COMPONENTS IN R-F PLANE

From Figure F-2, $\theta_1 = 0$. Let $A_2 = kA_1$; then

$$\left(\frac{a}{2} + x\right) \cos \theta_r = k \left(\frac{a}{2} - x\right) \cos (\theta_2 - \theta_r)$$

or

$$\tan \theta_r = \frac{k \sin \theta_2}{1 + k \cos \theta_2} \qquad \text{(F-10)}$$

let $u = \frac{x}{a/2}$, whence

$$u = \frac{x}{a/2} = \frac{1 - k^2}{1 + k^2 + 2k \cos \theta_2} \qquad \text{(F-11)}$$

Since all values of $\theta_2 - \theta_1$ are equally probable, the probability distribution of u may be found. There is a finite probability that the apparent line of sight does not lie between the two targets. For instance, if $\theta_2 = \pi$, Equation F-11 reduces to

$$u = \frac{1 + k}{1 - k}$$

Here $x > a/2$ for all values of $k (k \leq 1)$, and for $k = 1$, $x \to \infty$. In fact, $u \leq 1$ (that is, $x \leq a/2$) only for values of θ_2 defined by

$$\cos \theta_2 \geq -k$$

These effects have serious consequences, since an airplane can be thought of as a long thin target (at certain attitudes), and a long thin target can be represented by two point targets at either end. The probability of a miss is therefore appreciable.

Actually the target can be considered to be composed of N radiators (N reflecting surfaces each contributing an amplitude, A_i, and a phase, θ_i, to the received signal). If N is large, statistical conclusions may be drawn as to the probability of miss and rms error. By analogy with the two-radiator target, the resultant signal is

$$E_r = \sum_{i=1}^{N} A_i \left[1 + m_i \cos(\omega_s t + \phi_i)\right] \cos(\omega_c t + \theta_i) \qquad \text{(F-12)}$$

or

$$E_r = E(t) e^{j\theta_r} \qquad \text{(F-13)}$$

where

$$E(t) = \sum_{i=1}^{N} E_i(t) \cos(\theta_i - \theta_r)$$

and

$$E(t) = A + E_s(t) = \sum_{i=1}^{N} A_i \cos(\theta_i - \theta_r)$$

$$+ \sum_{i=1}^{N} A_i m_i \cos(\omega_s t + \phi_i) \cos(\theta_i - \theta_r) \qquad \text{(F-14)}$$

In the scan plane,

$$E_s = \sum_{i=1}^{N} A_i m_i \cos(\theta_i - \theta_r) e^{j\phi_i} \qquad \text{(F-15)}$$

From Equation F-3 this becomes

$$E_s = \frac{b_o}{R} \sum_{i=1}^{N} a_i d_i e^{j\phi_i} \cos(\theta_i - \theta_r) \qquad \text{(F-16)}$$

Equation F-16 may be interpreted geometrically (see Figure F-3). From Figure F-3, the scan component vector for the ith radiator has an amplitude $A_i m_i = a_i d_i b_o / R$ and a phase ϕ_i. The ith scan component vector is thus $E_i = (A_i d_i b_o / R) e^{j\phi_i}$. To get the resultant scan component vector, all the vector components along the resultant rf vector must be added (see Figure F-4). (Components perpendicular to the resultant add to zero.) From Figure F-4, $E_s = \sum E_{si} \cos(\theta_i - \theta_r) =$

$\sum (A_i d_i b_o / R) e^{j\phi_i} \cos(\theta_i - \theta_r)$, but this is merely Equation F-16, derived from an intuitive geometrical viewpoint.

Within a fairly broad angular region where the A_i are constant,* the mean radar center of echo is the geometrical centroid of the target area. Choose this point as origin of coordinates, that is, that point where

$$\sum_{n=1}^{N} A_n b_o d_n e^{j\phi_n} = 0 \qquad \text{(F-17)}$$

Note that the d_i and ϕ_i are measured from the intersection of the scan axis and the scan plane, whereas d_n and ϕ_n are measured from the mean

* Actually, the A_i change with time, but so slowly compared to the θ_i that little error is introduced by considering the A_i constant from a practical viewpoint.

center of echo (see Figure F-5). The expression for E_s must be re-written in terms of the distances and angles of the radiators from this new origin.

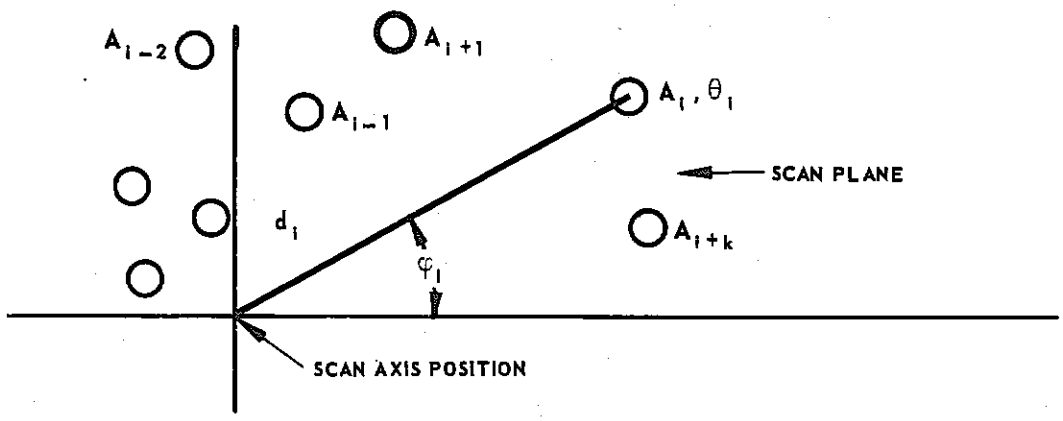

FIGURE F-3. GEOMETRY OF RADIATORS IN SCAN PLANE

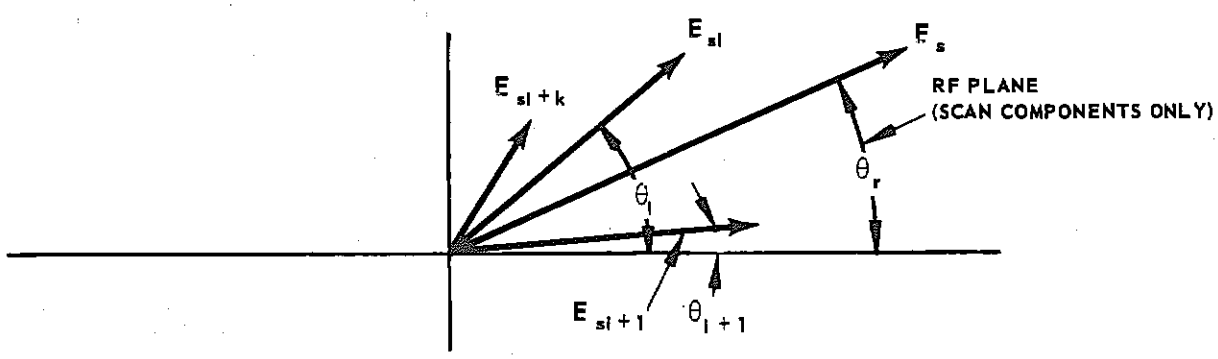

FIGURE F-4. VECTOR DIAGRAM OF SCAN COMPONENTS IN RF PLANE

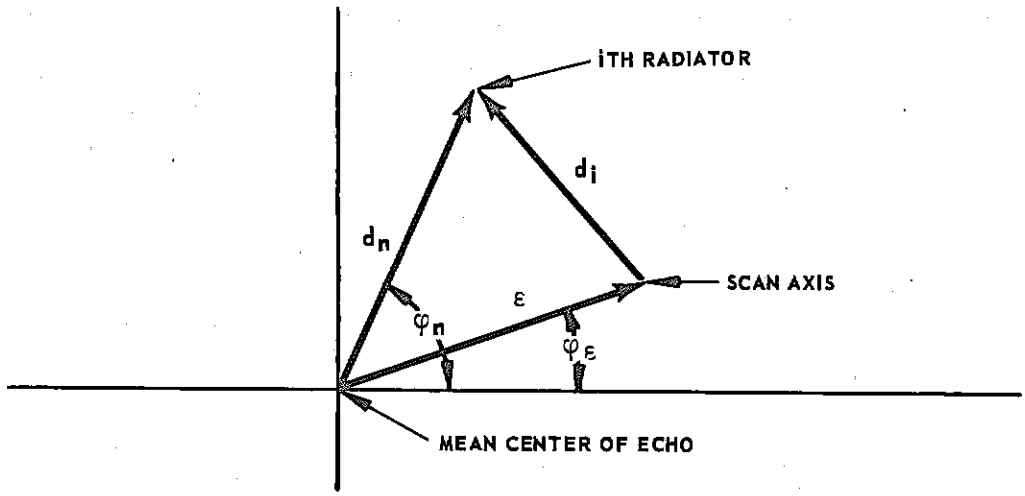

FIGURE F-5. SCAN PLANE GEOMETRY AFTER SHIFT OF ORIGIN

Therefore,

$$E_s = \sum_{n=1}^{N} \left[\frac{b_o A_n d_n}{R} e^{j\phi_n} - A_n b_o \epsilon e^{j\phi_\epsilon} \right] \cos(\theta_n - \theta_r)$$

$$= \frac{b_o}{R} \sum_{n=1}^{N} A_n d_n e^{j\phi_n} \cos(\theta_n - \theta_r) - A b_o \epsilon e^{j\phi_\epsilon} = E_a - E_b$$

(F-18)

The error signal E_s now consists of two terms: E_b, which is that due to the displacement of the scan axis from the mean center of echo, and E_a which is the angular scintillation term. The quantity A is the magnitude of the resultant unmodulated rf vector and has the frequency spectrum of the amplitude scintillation.

APPENDIX G

PREDICTION AND FILTERING PROBLEM

APPENDIX G

PREDICTION AND FILTERING PROBLEM

One of the principal things which the computer must do is predict the future position of the target. This is of particular importance in the case of the rockets and guns. Predicting the future position of a target when the input signal is contaminated by noise and extraneous information requires some sort of filtering. After filtering, the usable signal must approximate the input signal but be advanced in time by the amount of prediction. Several classical approaches have been used to attempt to solve this problem.

The purpose of this section is to develop a method of optimizing filters and feedback networks which operate on a desired signal in the presence of noise. Noise is defined here as any random disturbance introduced at the input or at any other point in the network. Numerous criteria exist for the optimization of networks and computer systems which operate on time series and functions. Probably the best known of these is the rms error criterion which requires minimization of the root mean square difference between the network output and the desired signal. One of the classical methods for minimizing the rms error is the "Wiener" method. This method is quite restricted from a practical viewpoint. Numerous other criteria can be defined and other methods derived. In this section, the rms criterion will be used, but a method by Phillips and Weiss will be developed for the purpose of determining optimum filter transfer functions for prediction in the presence of noise. These transfer functions then can be realized by either analog or digital devices.

First, a brief description of the assumptions and procedure in the Wiener method * is made. A perturbed time function f(t), which is a sum of a true signal S(t) and noise N(t), is assumed. The problem is one of operating on f(t) in order to recover S(t). In addition to the smoothing

* Wiener, N., "Extrapolation, Interpolation and Smoothing of Stationary Time Series" N. Y. Wiley 1949.

problem, it is desirable to find an approximation to the value S(t) at $t \pm \alpha$ where α is the lag or prediction time. The problem is represented in Figure G-1.

The Wiener theory depends on three main assumptions: (1), that the time series f(t) is stationary, (2) the optimization criterion is the minimization of the mean square error

$$\overline{\left[g(t) - S(t + \alpha) \right]^2}$$

(this mean is an ensemble average) and (3), the operator network is a linear, physically realizable, filter. With these assumptions it remains to find the optimum filter. This is done in the Wiener method by representing the mean square error in the following way:

$$\overline{\epsilon^2} = \lim_{T \to \infty} \frac{1}{2T} \int_{-T}^{T} \left| S(t + \alpha) - g(t) \right|^2 dt \qquad \text{(G-1)}$$

The criterion is met when $\overline{\epsilon^2}$ is a minimum. Equation G-1 can be expanded making use of the input-output relationship for the filter. The resulting expression is a function only of the weighting function of the filter to be optimized and the various correlation functions which are possible. The procedure is to minimize this integral expression by means of the calculus of variations. When the condition of physical realizability is included as a constraint in the minimization process, a first order

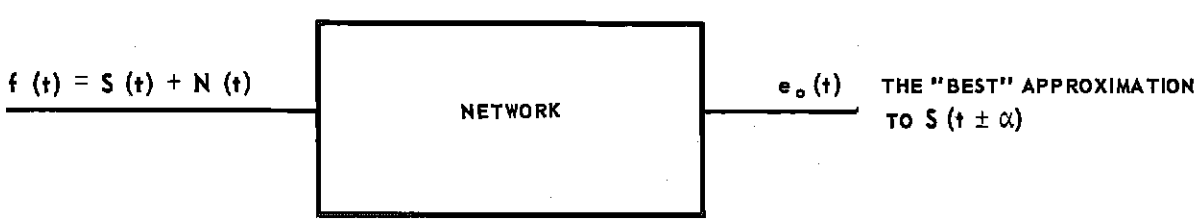

FIGURE G-1. WIENER PROBLEM

integral equation called the "Wiener-Hopf" Integral Equation results. The solution of this integral equation is, in general, quite difficult but yields the optimum physically realizable transfer function and consequently the minimum mean square error. Wiener has carried through the solution of this problem for the cases of prediction and lag.

Consider now the Wiener assumptions. The assumption that the signal and noise are stationary can be easily checked in a physical problem. In general, in the aircraft prediction problem, this assumption is not satisfied. However, even if the signal is not truly stationary it often can be approximated by a stationary series, particularly if the nonstationary variation occurs at a low rate. (For example, the angular modulation on a radar carrier returned from a maneuvering target of this type.) In cases where the assumption (stationary) is inapplicable, an alternative approach must be used.

The input $S(t) + N(t)$ is known over a range which can be defined from, say, $-T$ to $+T$. Although the noise power can be considered as finite for all times, this is certainly not the case for an intelligent signal. These facts restrict the practical applicability of the Wiener theory. Even though the signal which extends from minus infinity to plus infinity can be fitted to $S(t)$ over the range $-T \leq t \leq T$, the Wiener theory averages the error in the range $-\infty$ to $+\infty$, so that the major portion of the error comes from the extension of the function rather than from the desired range. The extension of the Wiener theory to finite intervals is a very difficult mathematical problem. Another difficulty with the least square error assumption is that the principal attention is paid to large errors. In the case of the fire control system, it is more important to make predictions as accurately as possible even though gross errors occur occasionally as a consequence. The final assumption of the Wiener theory, namely, that of linearity, is a restriction of the type of device to be used for smoothing and prediction. The reason for making this assumption is that linear problems are solved more easily than nonlinear problems.

An alternative approach which seems to be better for the fire control problem is that devised by R. S. Phillips and P. R. Weiss.* In this

---

* "Theoretical Calculation on the Best Smoothing of Position Data for Gunnery Prediction," Report 532, Radiation Laboratory MIT, Cambridge, Mass.

method, the signal is assumed to be a definite polynomial function of time (the coefficients being unknown). The filter is to be designed to the requirement that a signal should be passed without distortion. Whatever parameters are left after meeting this requirement are adjusted to best reduce the mean square noise. The Phillips-Weiss theory, therefore, is concerned primarily with tracking errors and the problem is one of smoothing these errors by a filter so as to minimize the errors in prediction. This is precisely the type of problem which is desired to be solved. To illustrate the difference between this method and the Wiener theory, consider the diagram in Figure G-2.

In Figure G-2, both N(t) and S(t) are stationary random series with given probability distributions. They are added and filtered to give the output $e_o(t)$. The problem here is a typical one for the Wiener theory. For the Phillips-Weiss theory, a typical problem is illustrated in Figure G-3.

Here the input noise signal is f(t). What is desired is not f(t), but S(t) where S(t) is the mean of the perturbed signal f(t). For example, if the signal is a constant velocity target which is perturbed by noise, the representation shown in Figure G-3 illustrates f(t) and S(t). The filter is then an operator whose output E(t) approximates S(t) in a least square sense. Note that S(t) is a definite nonstationary function of time whereas f(t) is a stationary random function about the mean S(t). The example illustrated in Figure G-3 is the angular tracking error. The filter is adjusted first to pass the polynomial representing the signal without distortion. The next step is to pass the noise such that N(t) equals f(t).

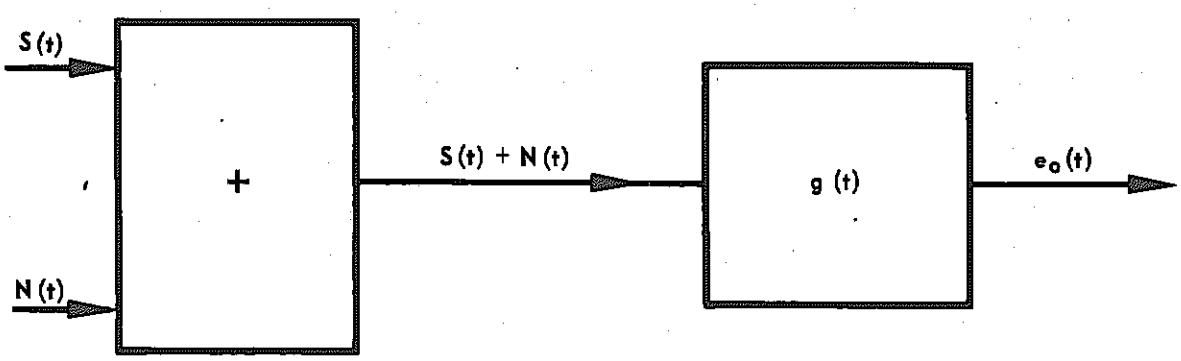

FIGURE G-2. FUNCTIONAL REPRESENTATION OF WIENER PROBLEM

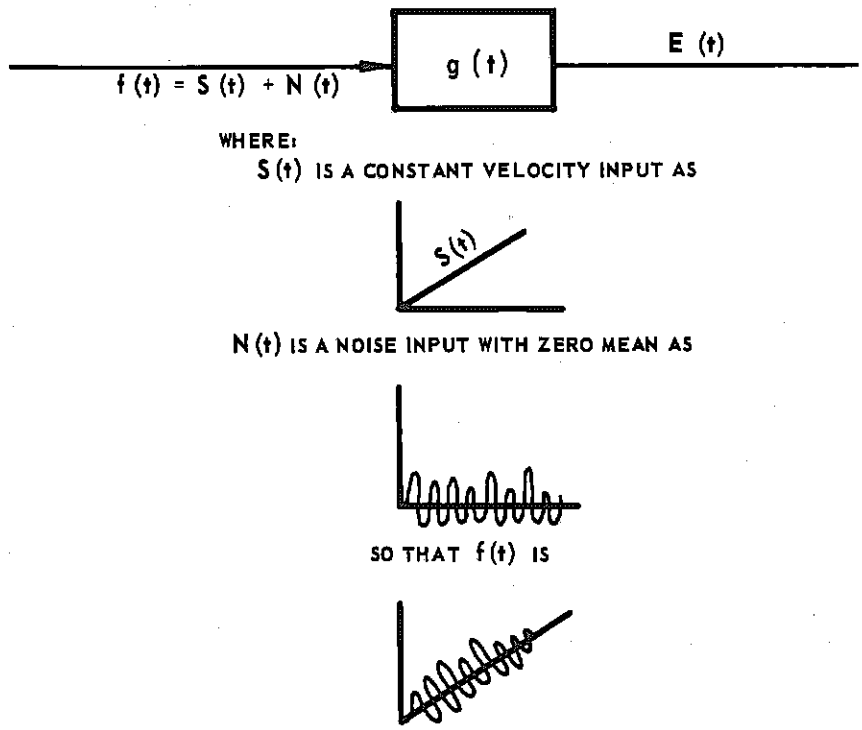

FIGURE G-3. PHILLIPS-WEISS PROBLEM

The filter is then further synthesized assuming noise alone. Thus if g(t) is the weighting function of a smoothing and prediction circuit with smoothing time T, the error in prediction due to tracking error only is

$$\epsilon(t) = \int_0^T f(t-x)\, g(x)\, dx \qquad \text{(G-2)}$$

The mean square error is thus

$$\overline{\epsilon^2} = \lim_{T \to \infty} \frac{1}{2T} \int_{-T}^{T} \left[\int_0^T f(t-x)\, g(x)\, dx \int_0^T f(t-y)\, g(y)\, dy \right] dt \qquad \text{(G-3)}$$

Let t - x = Z. Then

$$\overline{\epsilon^2} = \int_0^T\!\!\int \left[\lim_{T \to \infty} \frac{1}{2T} \int_{-T-x}^{T-x} f(Z)\, f(Z+x-y)\, dZ \right] g(x)\, g(y)\, dxdy \qquad \text{(G-4)}$$

But from Equation G-1 the mean square error can be expanded to yield

$$\overline{\epsilon^2} = \lim_{T\to\infty} \frac{1}{2T} \int_{-T}^{T} \Big[S(t+a)\, S^*(t+a) + e_o(t)\, e_o^*(t) - S(t+a)\, e_o^*(t) - S^*(t+a)\, e_o(t) \Big] dt \qquad \text{(G-5)}$$

where $x^*(t)$ = complex conjugate of $x(t)$.

The auto-correlation function of $y(t)$ is defined as

$$R_{yy}(\tau) = R_{yy}(-\tau) = \overline{y(t)\, y(t+\tau)} = \lim_{T\to\infty} \frac{1}{2T} \int_{-T}^{T} y(t)\, y(t+\tau)\, dt \qquad \text{(G-6)}$$

and the cross correlation function is

$$R_{xy}(\tau) = R_{xy}^*(-\tau) = \overline{x^*(t)\, y(t+\tau)} = \lim_{T\to\infty} \frac{1}{2T} \int_{-T}^{T} x^*(t)\, y(t+\tau)\, dt \qquad \text{(G-7)}$$

Hence

$$\overline{\epsilon^2} = \iint_{o}^{T} R_{ff}(x-y)\, g(x)\, g(y)\, dxdy \qquad \text{(G-8)}$$

The transfer function is related to the weighting function by

$$Y(s) = \int_{o}^{\infty} g(t)\, e^{-st} dt \qquad \text{(G-9)}$$

Expanding $Y(s)$ into power series in s yields

$$Y(s) = M_o - M_1 s + \frac{M_2 s^2}{2!} - \ldots \qquad \text{(G-10)}$$

where

$$M_k = \int_{o}^{\infty} t^k g(t)\, dt \qquad \text{(G-11)}$$

M_k is the kth moment of the weighting function. If the input and output of the filter are related by a linear differential equation with constant coefficients, the transfer function is a rational algebraic ratio of polynomials in S. Thus

$$Y(s) = \sum_{i=o}^{n} \left[a_i s^i \Big/ \sum_{j=1}^{n} b_j S^j \right] \quad (a_o = b_o = 1) \tag{G-12}$$

Equation G-12 may also be written as

$$Y(s) = \sum_{i=o}^{r} \frac{c_i s^i}{i!} + \text{higher order terms} \tag{G-13}$$

If a signal

$$e_i(t) = t^r \mu(t) \tag{G-14}$$

is now applied, the response is

$$e_o(t) = t^r + rc_1 t^{r-1} + (r-2) C_2 t^{r-2} \ldots + C_r + \text{in} \tag{G-15}$$

If the coefficient c_i in Equation G-13 is such that

$$c_i = t_f^i \tag{G-16}$$

then

$$e_o(t) = (t+t_f)^r + \ldots \tag{G-17}$$

The higher order terms vanish exponentially with time because the order of the denominator of Y(s) is greater than the order of the numerator. The first term is an advanced or retarded facsimile of the applied signal according to whether t_f is positive or negative. Thus Y(S) is a transfer function of a network which is distortionless to the signal t^r. It must

therefore be distortionless to every signal t^q (where q is a positive integer less than r and includes zero). Thus, it is concluded that if a signal S(t) (where S(t) is a polynomial of at most degree r) is applied to a distortionless transmission network of order r, then the response will be of the form

$$e_o(t) = f(t+t_f)\ \mu(t) \tag{G-18}$$

Returning to the minimization problem, it is assumed that the signal may be represented by a known polynomial

$$S(t) = k_o + k_1 t + k_2 t^2 + \cdots + k_r t^r \tag{G-19}$$

By comparing Equation G-10, it is clear that

$$C_m = M_m (-1)^m \tag{G-20}$$

and substituting Equation G-11, G-16 and G-20 yields

$$\int_o^T t^n g(t)dt = (-t_f)^n \ ; M = 0, 1, \ldots, r \tag{G-21}$$

Equation G-21 is restrictive on the network functions g(t). The output tracking error must thus be minimized subject to the integral side conditions. See Equation G-21. Minimization problems of this type are called isoperimetric problems in the calculus of variations. The method of solution for this type of problem is called the method of Lagrange Multipliers. According to this method, the minimization of $\overline{\epsilon^2}$ subject to side conditions may be formulated as follows

$$\overline{\epsilon^2} = \iint^T R_{ff}(x-y)\ g(x)\ g(y)\ dxdy$$

$$- \sum_{m=o}^{r} \lambda m \left[\int_o^T t^m g(t)\ dt - (-t_f)^m \right] \tag{G-22}$$

Equation G-22 is the same as Equation G-6 since by Equation G-21 the summation Equation G-22 is zero. The λ_m in Equation G-22 is the so-called Lagrange Multiplier. Proceeding with the minimization, the first variation of Equation G-22 is

$$\delta \overline{\epsilon^2} = \iint_o^T \left[\delta g(x)\ g(y) + \delta g(y)\ g(x) \right] R_{ff}(x-y)\ dxdy$$

$$+ \sum_{m=o}^{r} \lambda_m \int_o^T t^m \delta g(t)\ dt \qquad \text{(G-23)}$$

Since $R_{ff}(x-y)$ is a real even function, Equation G-23 may be rewritten

$$\delta \overline{\epsilon^2} = \int_o^T \delta g(y) dy \left[\int_o^T g(x) R_{ff}(y-x)\ dx - \sum_{m=o}^{r} \lambda_m y^m \right] \qquad \text{(G-24)}$$

It follows that the integrand must be zero, whence

$$\int_o^T g(x) R_{ff}(y-x) dx = \sum_{m=o}^{r} \lambda_m y^m \qquad \text{(G-25)}$$

If

$$\int_o^T g_m(x) R_{ff}(y-x) dx = y^m \qquad \text{(G-26)}$$

then

$$g(x) = \sum_{m=o}^{r} \lambda_m g_m(x) \qquad \text{(G-27)}$$

For, from Equations G-25 to G-27

$$\int_o^T \sum_{m=o}^{r} \lambda_m g_m(x) R_{ff}(y-x) dx = \sum_{m=o}^{r} \lambda'_m y^m \qquad \text{(G-28)}$$

In principle, the problem is now solved. The procedure consists of determining $R_{ff}(y-x)$ from Equation G-28, the $g_m(x)$ from Equation G-26, the λ_n from Equations G-21 and G-26, and g(x) from Equation G-27. In general, every λ_n will be a polynomial in t_f. The difficulty in this theory lies in the solution of the integral Equation G-26. Once the integral equation is solved, the optimum transfer function for prediction is known.

In connection with this method, it should be mentioned that the Phillips-Weiss method is a particular case of a more general problem. For instance, instead of assuming the signal to be a polynomial of the form

$$S(t) = \sum c_k t^k \tag{G-29}$$

S(t) could be approximated by an orthogonal expansion

$$S(t) = \sum_{k=1}^{n} c_k \phi_k(t) \tag{G-30}$$

where the n side conditions are

$$\phi_k(t_f) = \int_0^\infty \phi_k(x) g(x) dx \tag{G-31}$$

The general problem is that of constructing a filter that passes any signal perfectly and minimizes the mean square noise as well. A perfect filter for a signal S(t) is one in which the error in the output is zero for S(t) at the input.

The perfect filter for this signal is therefore defined by

$$S(t+\alpha) = \int_0^T S(t-x) g(x) dx \tag{G-32}$$

Minimizing the mean square noise demands that

$$\overline{N^2(t)} = \lim_{T \to \infty} \frac{1}{2T} \int_{-T}^{T} dt \int_{0}^{T} N(t-x)g(x)dx \int_{0}^{T} N(t-y)g(y)dy \qquad \text{(G-33)}$$

be minimized. The optimum filter is found by minimizing Equation G-33 subject to the constraints imposed by Equation G-32. Again the procedure makes use of the Lagrange Multipliers and the calculus of variations. The general procedure is quite difficult to carry out unless S(t) has a simple form so that the integral Equation G-32 can be solved to give the required constraints.

BIBLIOGRAPHY

Chapter II

1. "An Integrated Electronic and Control System for the Advanced All-Weather Interceptor," Hughes Aircraft Company, 27 March 1950, (Classified)

2. "Guided Missile Engineering," Puckett, A. E., and Ramo, S., McGraw Hill Book Company, Inc., 1959

3. "Aircraft Attrition Study," NAI Report No. 56-298, Aircraft Vulnerability Volume 5, Northrop Corporation, 30 November 1956, (Classified)

4. "A Survey of Air-to-Air Fire Control System," NAI Report No. 57-179, Northrop Corporation, January 1957, (Classified)

Chapter III

1. "Fire Control Principles," Wrigley, W. and Hovorka, J., 1st Editior McGraw Hill Book Company, 1959

2. "An Integrated Electronic and Control System for the Advanced All Weather Interceptor," Hughes Aircraft Company, 27 March 1950, (Classified)

3. "Operations Research, Armament, Launching," Merrill, G. and Goldberg, H., D. Van Nostrand Company

Chapter IV

1. "Fire Control Principles," Wrigley, W. and Hovorka, J., 1st Edition, McGraw Hill Book Company, 1959

2. "Theoretical Calculation on Best Smoothing Data for Gunnery Prediction," Phillips, R. S. and Weise, P. R., Massachusetts Institute of Technology Radiation Laboratory, Cambridge Mass., 1944

3. "An Integrated Electronics and Control System for the Advanced All-Weather Interceptor," Hughes Aircraft Company, 27 March 1950, (Classified)

4. "Guidance," Lock, A. S. and Merrill, G., D. Van Nostrand Company, Inc., 1955

5. "Introduction to Monopulse," Rhodes, D. R., McGraw Hill Book Company Inc., 1959

Chapter V

1. "Fire Control Principles," Wrigley, W. and Hovorka J., McGraw Hill Book Company, 1959

2. "An Integrated Electronic and Control System for the Advanced All-Weather Interceptor," Hughes Aircraft Company, 27 March 1950, (Classified)

3. "A General Description of the Universal Computer," TM 339, Hughes Aircraft Company, 1 June 1954, (Classified)

4. "The Hughes Fire Control System for Navy Interceptors," Hughes Aircraft Company, August 1951, (Classified)

5. "Functional Introduction to Hughes Fire Control Systems," Hughes Aircraft Company, April 1957

Chapter VI

1. "The Detection and Measurement of Infrared Radiation," Smith, R. A., Jones, F. E. and Chasmar, R. P., Oxford at the Clarendon Press, 1957

2. "Proceedings of Infrared Information Symposia," Volume 1 through 4, Office of Naval Research (Classified)

Chapter VII

1. "A Theory of Target Glint or Angular Scintillation in Radar Tracking," Delano, R. H., Proc.IRE, Volume 41, No. 12

2. "Calculation of Range of Automatic Tracking Radars," Muchmore, R. B., TM 193, Hughes Aircraft Company, 1954

Chapter VIII

1. "Proc. of Second Annual Joint Military - Industrial Electronic Test Equipment Symposium," Volume 1, BuShips, Project SETE 230/2.1, New York University

2. "Flight Test Evaluation of the Universal Computer," Report No. 479A-11-F3, Hughes Aircraft Company, (Classified)

3. "Airborne Radar Requirements for High-Speed Combat," Johnson, Emerson, Stillman, Foust, RM-1808, Rand Corp., (Classified)

4. "A Statistical Theory of Target Detection by Pulsed Radar," Project Rand Report RA 15061, Marcum, J. I., 1 December 1947, (Classified)

5. "Radar Range Performance," TM-277, Drukey, D. L., Hughes Aircraft Company, 15 April 1954

6. "Threshold Signals," Lawson and Uhlenbeck, Radiation Laboratory Series, Volume 24, McGraw Hill Book Company Inc.

Chapter IX

1. "Aircraft Attrition Study," NAI 56-298, Volumes 1 through 6, Northrop Corp., March 1957, (Classified)

2. "Terminal Air Battle Study," NAI 57-1240, Volumes 1 through 6, Northrop Corp., 1958, (Classified)

BUREAU OF AERONAUTICS

FLIGHT CONTROL AND FIRE CONTROL SYSTEM MANUALS

VOL I – **"METHODS OF ANALYSIS AND SYNTHESIS OF PILOTED AIRCRAFT FLIGHT CONTROL SYSTEMS"** AE-61-4 I (251 pages, 459 figures; $4.00)

Chapters – Fundamental Concepts, Analysis, Synthesis, Optimum Synthesis Methods, Non-linearities, Machine Methods, Analog Computer, Mathematical Background.

VOL II – **"DYNAMICS OF THE AIRFRAME"** AE-61-4 II (185 pages, 178 figures; $4.25) Addendum to Vol II (27 figures; $1.50)

Chapters – Derivation of the Airframe Transfer Functions, Discussion of Transfer Functions, Discussion of Stability Derivatives, Methods of Obtaining Stability Derivatives.

VOL III – **"THE HUMAN PILOT"** AE-61-4 III (157 pages, 55 figures; $3.50)

Chapters – Fundamental Aspects – Sensing and Actuating Processes of a Human Pilot, Approximate Methods Predicting Responses of a Human Pilot.

VOL IV – **"THE HYDRAULIC SYSTEM"** AE-61-4 IV (224 pages, 63 figures; $4.25)

Chapters – General Considerations, Analysis of the Generalized Hydraulic Servo Actuator, a Generalized Hydraulic Control System, The Fully Powered Hydraulic Control System, The Power Boost Hydraulic Control System, Special Considerations in Hydraulic Control System Design and Analysis, Component Design Factors, Influence of Servomechanisms on the Flutter of Servo-Controlled Aircraft, Methods of Analysis of Servo Flutter Interaction.

VOL V – **"THE ARTIFICIAL FEEL SYSTEM"** AE-61-4 V (152 pages, 103 figures; $3.00)

Chapters – The Control Feel Problem, Design Procedure, Design Criteria.

VOL VI – **"AUTOMATIC FLIGHT CONTROL SYSTEMS FOR PILOTED AIRCRAFT"** AE-61-4 VI (339 pages, 138 figures; $6.00)

Chapters – Automatic Flight Control Systems Past and Present, Components of Automatic Flight Control Systems, Design Methods, Systems Engineering and Other Design Considerations, Appendix.

VOL VII – **"METHODS OF DESIGN AND EVALUATION OF INTERCEPTOR FIRE CONTROL SYSTEM"** AE-61-4 VII (550 pages, 168 figures; $7.50)

Chapters – The Tactical Environment, Design Objectives, Armament, The Radar, The Computer, Infrared Fire Control Systems, Analysis of the Fire Control System, Evaluation of Fire Control Radars, Techniques of Estimating Weapon System Effectiveness, Appendices.

The volumes listed above complete the series of Flight Control and Fire Control System Manuals presently available, and are identical in content to the original contract publications.

To order one or more of these volumes, contact: NORTHROP CORPORATION, NORAIR DIVISION, 1001 East Broadway, Hawthorne, California, Attn. Dept. 3860